# PRINCIPLES OF SOIL AND PLANT WATER RELATIONS

---

## SECOND EDITION

M.B. Kirkham

*Kansas State University, 2004 Throckmorton Plant Science Ctr, Manhattan, USA, 66506*

AMSTERDAM • BOSTON • HEIDELBERG • LONDON
NEW YORK • OXFORD • PARIS • SAN DIEGO
SAN FRANCISCO • SINGAPORE • SYDNEY • TOKYO
Academic Press is an imprint of Elsevier

Academic Press is an imprint of Elsevier
The Boulevard, Langford Lane, Kidlington, Oxford OX5 1GB, UK
Radarweg 29, PO Box 211, 1000 AE Amsterdam, The Netherlands
225 Wyman Street, Waltham, MA 02451, USA
525 B Street, Suite 1800, San Diego, CA 92101-4495, USA

Second edition 2014

Copyright © 2014, 2005 Elsevier Inc. All rights reserved.

No part of this publication may be reproduced, stored in a retrieval system or transmitted in any form or by any means electronic, mechanical, photocopying, recording or otherwise without the prior written permission of the publisher Permissions may be sought directly from Elsevier's Science & Technology Rights Department in Oxford, UK: phone (+44) (0) 1865 843830; fax (+44) (0) 1865 853333; email: permissions@elsevier.com. Alternatively you can submit your request online by visiting the Elsevier web site at http://elsevier.com/locate/permissions, and selecting Obtaining permission to use Elsevier material.

**Notice**
No responsibility is assumed by the publisher for any injury and/or damage to persons or property as a matter of products liability, negligence or otherwise, or from any use or operation of any methods, products, instructions or ideas contained in the material herein. Because of rapid advances in the medical sciences, in particular, independent verification of diagnoses and drug dosages should be made.

**Library of Congress Cataloging-in-Publication Data**
Kirkham, M. B.
Principles of soil and plant water relations / by M.B. Kirkham, Kansas State University, 2004 Throckmorton Plant Science Center, Manhattan.
p. cm.
Includes bibliographical references and index.
ISBN 978-0-12-420022-7
1. Plant-water relationships. 2. Plant-soil relationships. 3. Groundwater flow. I. Title.
QK870.K57 2014
577.5′7--dc23
2014011893

**British Library Cataloguing in Publication Data**
A catalogue record for this book is available from the British Library

For information on all Academic Press publications visit our web site at store.elsevier.com

Printed and bound in USA
14 15 16 17 18 10 9 8 7 6 5 4 3 2 1

ISBN: 978-0-12-420022-7

ELSEVIER
Book Aid International
Working together to grow libraries in developing countries
www.elsevier.com • www.bookaid.org

# Dedication

To my family

# Preface to the First Edition

This textbook is developed from lectures for a graduate class in soil—plant—water relations taught at Kansas State University. Students in the class are from various departments, including agronomy, biology, horticulture, forestry and recreational resources, biochemistry, and biological and agricultural engineering. The book can be used as a text for graduate- or upper-level undergraduate courses or as a self-study guide for interested scientists. The book follows water as it moves through the soil—plant—atmosphere continuum. The text deals with principles and is not a review of recent literature. The principles covered in the book, such as Ohm's law and Poiseuille's law, are ageless. The book has equations, but no knowledge of calculus is required. Because plant anatomy is often no longer taught at universities, chapters review root, stem, leaf, and stomatal anatomy. Instrumentation to measure status of water in the soil and plant is also covered. Many instruments could have been described, but the ones chosen focus on traditional methods such as tensiometry and psychrometry and newer methods that are being widely applied such as tension infiltrometry and time domain reflectometry. Because the humanistic side of science is usually overlooked in textbooks, each chapter ends with biographies that tell about the people who developed the concepts discussed in that chapter.

Although a textbook on water relations might logically include developments in molecular biology, this topic is not covered. Rather, the text focuses on water in the soil and whole plant and combines knowledge of soil physics, plant physiology, and microclimatology. Chapter 1 reviews population and growth curves and provides a rationale for studying water in the soil—plant—atmosphere continuum. Chapter 2, which defines physical units, at first may appear elementary, but many students have not had a class in physics. The definitions in this chapter lay the foundation for understanding future chapters. Chapter 3 goes over the unique structure and properties of water, which makes life possible. Chapter 4, on tensiometry, is the first instrumentation lecture. Other instrumentation lectures include: Chapter 9 on penetrometer measurements; Chapter 10 on measurement of the oxygen diffusion rate in the soil; part of Chapter 11 on applications of tension infiltrometry to determine soil hydraulic conductivity, sorptivity, repellency, and solute mobility; Chapter 13 on time domain reflectometry; Chapter 16 on psychrometry; Chapter 17 on pressure chambers; Chapter 22, which includes ways to measure stomatal opening and resistance; and Chapter 24 on infrared thermometers. Chapters 4 through 13 focus on water in the soil; Chapters 14 through 22, on water in the plant; and Chapters 23 through 27, on water as it leaves the plant and moves into the atmosphere.

Within any one chapter, the notation is consistent and abbreviations are defined when first introduced. When the same letter stands for different parameters, such as *A* for "ampere" or "area" and *g* for "acceleration due to gravity" or "grams", these differences are pointed out.

I express my appreciation to the following people who have helped make this book possible: my sister, Victoria E. Kirkham, professor of romance languages at the University of Pennsylvania, who first suggested on March 12, 1999, that I write this book; Dr Kimberly A. Williams, Associate Professor of Horticulture, who audited my class in 2000 and then nominated me for the College of Agriculture Graduate Faculty Teaching Award, of which I was the inaugural recipient in 2001; Mr Martin Volkmann in the laboratory of Prof. Dr Rienk van der Ploeg of the University of Hannover in Germany, for converting the first drafts of the electronic files of the chapters, which I had typed in MS-DOS using WordPerfect 5.1 (my favorite word-processing software), to Microsoft Word documents, to ensure useable backup copies in case my 1995 Compaq computer broke (it did not); my students, who have enthusiastically supported the development of this book; anonymous reviewers who had helpful suggestions for revisions and supported publication of the book; publishers and authors who allowed me to use material for the figures; and Mr Eldon J. Hardy, my longtime professional draftsman at Oklahoma State University, now retired. His drafting ability is unparalleled. He has redrawn the figures from the original and ensured that they are uniform, clear, and precisely done.

I am grateful to the publishers, Elsevier, including Michael J. Sugarman, Director, for accepting my book for publication, and Kelly D. Sonnack, Editorial Coordinator, for her help during the production of this book. Through my late father, Don Kirkham, former professor of soils and physics at Iowa State University, I have known of the venerable scientific publications of Elsevier since I was a child, and truly am "non solus" with a book.

*M.B. Kirkham*
*Manhattan, Kansas.*
*April 6, 2004.*

# Preface to the Second Edition

The second edition results from an invitation that I received on April 22, 2013, from Elsevier/Academic Press to revise the first edition. The major changes in the new edition include the addition of three chapters: one on dual thermal probes to monitor soil—water content (Chapter 9); one on sapflow (Chapter 21); and one on interception of direct-beam solar radiation by leaves of plants (Chapter 30). The comments made in the Preface to the first edition hold for the second edition. These new chapters result from lectures that I give in my graduate class on soil—plant—water relations. They deal with principles and are not a review of the literature. As for the original chapters, I have ended the new chapters with biographies about the people who developed the concepts in the chapters.

In revising the book, I have interviewed experts on the topics—i.e., Loyd R. Stone about tensiometers (Chapter 5); Gerard J. Kluitenberg about the dual thermal probe technique (Chapter 9); and Kevin P. Price about drones (Chapter 27). I thank each of them for sharing their knowledge with me.

Based on a suggestion of one of the reviewers, I have kept all of the original chapters (27 of them). Changes made in the original chapters, based on comments from the reviewers, are the following: a reorganization of the order of the chapters; a shortening of some of the titles; and an addition of the history of the concept of the soil—plant—atmosphere continuum (added to Chapter 22). Other additions include the following: a problem showing how to convert grams to slugs (Chapter 2); Helmert's equation for calculation of the acceleration due to gravity (Chapter 4); a problem showing how to determine soil water content with time domain reflectrometry probes (Chapter 8); a discussion of the least limiting water range (Chapter 10); a biography of Katherine Esau (Chapter 15); notation of the continuing controversy about the cohesion theory (Chapter 20); a discussion of the normalized difference vegetation index (Chapter 27); and an analysis of the effect of elevated carbon dioxide on water-use efficiency (Chapter 29).

I express my appreciation to the following people who have helped make this new edition possible: Candice Janco, Senior Acquiring Editor of Elsevier/Academic Press, for inviting me to revise the first edition; Sean R. Coombs, Editorial Project Manager, Elsevier, Inc. Science and Technology Books, for his prompt and kind help throughout the revision; Brent E. Clothier and Steven R. Green, both of the Systems Modelling

Group, The New Zealand Institute for Plant and Food Research, Ltd., Palmerston North, New Zealand, for figures provided in the chapter on sapflow (Chapter 21); Soil Measurement Systems, Tucson, AZ, for providing figures of tensiometers (Chapter 5); Eldon J. Hardy, my longtime professional draftsman, for redoing the population figure (Chapter 1); and Marsha K. Landis, Graphic Designer and Web Manager, Kansas State University, for taking pictures of equipment shown in the new edition. I also want to give special thanks to the three reviewers of the draft proposal, who supported publication of the revised edition: Bingru Huang, Professor II, Department of Plant Biology and Pathology, Rutgers University, New Brunswick, NJ; William L. Kingery, Professor and Graduate Coordinator, Department of Plant and Soil Sciences, Mississippi State University; Mississippi State, MS; and Anvar R. Kacimov, Professor and Dean, College of Agriculture and Marine Sciences and Head of the Department of Soils, Water and Agricultural Engineering, Sultan Qaboos University, Al-Khob, Sultanate of Oman.

As for the first edition, I dedicate the second edition to my family whose support made the book possible.

*M.B. Kirkham*
*Manhattan, Kansas.*
*January 1, 2014.*

CHAPTER

# 1

# Introduction

## 1.1 WHY STUDY SOIL–PLANT–WATER RELATIONS?

### 1.1.1 Population

Of the four soil physical factors that affect plant growth (mechanical impedance, water, aeration, and temperature) (Shaw, 1952; Kirkham, 1973), water is the most important. A classic analysis was done by Boyer (1982) to determine the reasons for crop losses over a four-decade period in the United States. He found that drought causes 40.8% of crop losses and excess water causes 16.4%. Insects and diseases amount to 7.2% of the losses. Thus, soils that are too dry or too wet are the major reasons for lost productivity.

People depend upon plants for food. Because water is the major environmental factor limiting plant growth, we need to study soil–plant–water relations to provide food for a growing population. What is our challenge?

The earth's population is growing exponentially. The universe is now considered to be 13,000,000,000 (13 thousand millions or 13 billion) years old (Zimmer, 2001). The earth is thought to be 4.45 billion years old (Allègre and Schneider, 1994). The earth's oldest rock is 4.03 billion years old (Zimmer, 2001). Primitive life existed on earth 3.7 billion years ago, according to scientists studying ancient rock formations harboring living cells (Simpson, 2003). Human-like animals have existed on earth only in the last few (less than 8) million years. In Chad, Central Africa, six hominid specimens, including a nearly complete cranium and fragmentary lower jaws, have been found that are 6–7 million years old (Brunet et al., 2002; Wood, 2002). The earliest fossil in Europe, which belongs to the genus *Homo*, was found in Spain and has been dated to 1.1–1.2 million years ago, which suggests that the first settlement of Western Europe was related to demographic expansion out of Africa (Carbonell et al., 2008).

*Principles of Soil and Plant Water Relations*
http://dx.doi.org/10.1016/B978-0-12-420022-7.00001-X

Copyright © 2014 Elsevier Inc. All rights reserved.

In 8000 BC, at the dawn of agriculture, the world's population was 5 million (Wilford, 1982). At the birth of Christ in 1 A.D., it was 200 million. In 1000, the population was 250 million (National Geographic, 1998a) (Figure 1.1). By 1300, it had grown larger (Wilford, 1982). But by 1400, the population had dropped dramatically due to the Black Death, also called the bubonic plague (McEvedy, 1988), which is caused by a *bacillus* spread by fleas on rats. The Black Death raged in Europe between 1347 and 1351 and killed at least half of its population. It caused the depopulation or total disappearance of about 1000 villages. Starting in coastal areas, where rats were on ships, and spreading inland, it was the greatest disaster in western European history (Renouard, 1971). People fled to the country to avoid the rampant spread of the disease in cities. The great piece of literature, *The Decameron*, published in Italian in 1353 and written by Giovanni Boccaccio (1313—1375), tells of 10 people who in 1348 went to a castle outside of Florence, Italy, to escape the plague. To pass time, they each told a tale a day for 10 days (Bernardo, 1982).

By 1500, the world's population was about 250,000,000 again. In 1650, it was 470,000,000; in 1750, it was 694,000,000; and in 1850, it was 1,091,000,000. At the beginning of the nuclear age in 1945, it was 2.3 billion. In 1950, it was 2,501,000,000; in 1970, 3,677,837,000; and in 1980,

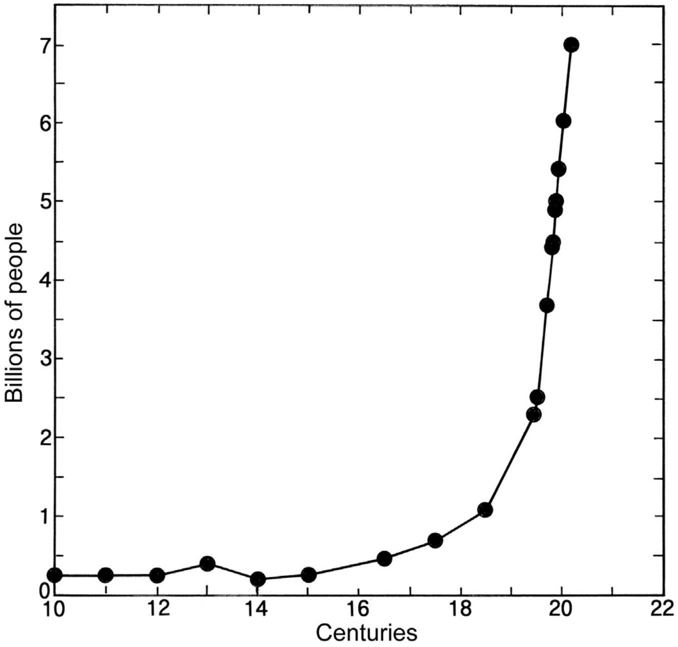

**FIGURE 1.1** The human population growth curve. *Drawn by author from data found in literature.*

4,469,934,000. In 1985, it was 4.9 billion and in 1987 it was 5.0 billion (New York Times, 1987). In 1999, the world's population reached 6 billion (National Geographic, 1999). On October 31, 2011, the United Nations Population Fund estimated that the seventh billion person was born in the world (McGurn, 2011).

Note that it took more than six million years for humans to reach the first billion; 120 years to reach the second billion; 32 years to reach the third billion; and 15 years to reach the fourth billion (New York Times, 1980). It took 12 years to add the fifth to sixth billion (1987–1999), and 12 years to add the next billion (sixth to seventh billion; 1999–2011). The population is projected to reach 9.3 billion by 2050 (Chin et al., 2011). If fertility rates drop until women have about two children each, the population will stabilize at 10.8 billion (National Geographic, 1998b).

The population may also fall due to plagues (Weiss, 2002), such as the one that devastated Europe in the fourteenth century. Current potential plagues may result from acquired immune deficiency syndrome, thought to be caused by a virus; influenza, another viral infection—for example, there may be a recurrence of the 1918 pandemic (Gladwell, 1997); sudden acute respiratory syndrome, a deadly infectious disease caused by a coronavirus (Lemonick and Park, 2003); hospital infections, which cannot be treated with any known antibiotics; and mad-cow disease, which is formally called bovine spongiform encephalopathy (BSE). BSE is called Creutzfeldt-Jakob (also spelled as Creutzfeldt-Jacob) disease, when it occurs in humans (Hueston and Voss, 2000). It is thought to be caused by *prions*, which were discovered by Stanley Prusiner (born in 1942), director of the Institute for Neurodegenerative Diseases at the University of California, San Francisco (the discovery won Prusiner both the Wolf Prize (1996) and the Nobel Prize (1997) in medicine). Prions are a new class of protein, which, in an altered state, can be pathogenic and cause important neurodegenerative diseases by inducing changes in protein structure. Prions are designed to protect the brain from the oxidizing properties of chemicals activated by dangerous agents such as ultraviolet light.

### 1.1.2 The "Two-Square-Yard Rule"

The population is limited by the productivity of the land. There is a space limitation that our population is up against. Many of us already have heard of this limitation, which is a space of two square yards per person. The sun's energy that falls on two square yards is the minimum required to provide enough energy for a human being's daily ration. Ultimately, our food and our life come from the sun's energy. The falling of the sun's energy on soil and plants is basic. We want to make as many plants grow on those two square yards per person as possible, to make sure we have enough to eat.

Let us do a simple calculation to determine how much food can be produced from two square yards, using the following steps:

1. Two square yards is 3 ft by 6 ft or 91 cm by 183 cm.

$$91 \text{ cm} \times 183 \text{ cm} = 16{,}653 \text{ cm}^2 \text{ or, rounding, } 16{,}700 \text{ cm}^2.$$

2. The solar constant is 2.00 $\text{cal/cm}^2\text{/min}$, or, because one langley = 1 $\text{cal/cm}^2$, it is 2.00 langleys/min. The langley is named after Samuel Pierpoint Langley (1834–1906), who was a US astronomer and physicist who studied the sun. He was a pioneer in aviation.
   The solar constant is defined as the rate at which energy is received upon a unit surface, perpendicular to the sun's direction in free space at the earth's mean distance from the sun (latitude is not important) (Johnson, 1954). The brightness of the sun varies during the 11-year solar cycle, but typically by less than 0.1% (Lockwood et al., 1992).
3. 16,700 $\text{cm}^2 \times 2.00 \text{ cal/cm}^2\text{/min} = 33{,}400$ cal/min.
4. 33,400 cal/min × 60 min/h × 12 h/day = 24,048,000 cal/day, or, rounding, 24,000,000 cal/day. We multiply by 12 h/day, because we assume that the sun shines 12 h/day. Of course, the length the sun shines each day depends on the day of the year, cloudiness, and location.
5. There is 6% conversion of absorbed solar energy into chemical energy in plants (Kok, 1967). This 6% is for the best crop yields achieved; 20% (Kok, 1967) to 30% (Kok, 1976) conversion is thought possible, but it has not been achieved; 2% is the conversion for normal yields; and under natural conditions, $\leq 1\%$ is converted (Kok, 1976). The solar energy reaching the earth's surface that plants do not capture to support life is wasted as heat (Kok, 1976). Let us assume a 6% conversion:

$$24{,}000{,}000 \text{ cal/day} \times 0.06 = 1{,}440{,}000 \text{ cal/day}.$$

6. The food "calories" we see listed in calorie charts are in kilocalories. So, dividing 1,440,000 cal/day by 1000, we get 1440 kcal/day, which is not very much.

We recognize that the earlier calculation of productivity from two square yards is simplified, and more complex and thorough calculations of productivity, which consider geographic location, sky conditions, leaf display, and other factors, have been carried out (e.g., De Wit, 1967). Nevertheless, the 1400 kcal/day is a useful number to know. It would be a starvation diet. One could live on it, but the calories probably would not provide enough for active physical work, creative intellectual activity, and reproduction. Women below a minimum weight cannot reproduce

(Frisch, 1988). Civilization would advance slowly with this daily ration. People begin to die of starvation when they lose roughly a third of their normal body weight. When the loss reaches 40%, death is almost inevitable.

Triage is a system developed during World War I. It is the medical practice of dividing the wounded into survival categories to concentrate medical resources on those who could truly benefit from them and to ignore those who would die, even with treatment, or survive even without it. This practice has been advocated to allocate scarce food supplies. If we can grow more food, then this system does not need to be put into effect. In this book, we seek a better understanding of movement of water through the soil—plant—atmosphere continuum, or SPAC (Philip, 1966), because of the prime importance of water in plant growth.

We focus on principles rather than review the literature. Many references are given, but no attempt is made to cite the most recent papers. Articles explaining the principles are cited. They often are in the older literature, but we need to know them to learn the principles. No knowledge of calculus is required to understand the equations presented.

In this book, we divide the movement of water through the SPAC into three parts: (1) water movement in the soil and to the plant root; (2) water movement through the plant, from the root to the stem to the leaf; and (3) water movement from the plant into the atmosphere. We then combine all parts when we look at electrical analogues for water movement through the soil—plant—atmosphere continuum (Chapter 22). However, before we turn to principles of water movement in the SPAC, let us first consider plant growth curves.

## 1.2 PLANT GROWTH CURVES

### 1.2.1 The Importance of Measuring Plant Growth and Exponential Growth

The world population growth curve (Figure 1.1) is an exponential curve. What do plant growth curves look like? Because water is the most important soil physical factor affecting plant growth, it is important to quantify plant growth to determine effects of water stress. In any experiment dealing with plant—water relations, some measure of plant growth (e.g., height, leaf area, biomass) should be obtained. Plant growth curves also exemplify quantitative relationships that we seek to understand basic principles of plant—water relations. If we can develop equations to show relationships, then we can predict what is going to happen. Equations describing plant—growth curves demonstrate how we can quantify, and thus predict, plant growth.

We first consider the growth of the bacterium *Escherichia coli*. In the early nineteenth century, when plants and animals were being classified, the bacteria were arbitrarily included in the plant kingdom, and botanists first studied them (Stanier et al., 1963; pp. 55–56). Even though bacteria are not plants or animals, we can follow their growth to understand plant growth curves.

Under ideal conditions, a cell of *E. coli* divides into two cells approximately every 20 min; for the sake of simplicity we assume that it is exactly 20 min. Let us consider the propagation of a single cell. Our purpose is to find a relation between the number $N$ of cells at some moment in the future and the time $t$ that has elapsed. At the start of our observations, at the time 0 min, there is one cell. When 20 min have elapsed there are two cells. When 40 min have elapsed there are $2 \times 2 = 2^2$ cells. When 60 min have elapsed there are $2 \times 2^2 = 2^3$ cells; that is, when three time intervals of 20 min each have passed, there are $2^3$ cells. We observe a pattern developing: when $m$ time intervals each of 20 min have passed, at the time $t = 20m$ min, there are $2^m = 2^{t/20}$ cells. Thus, if $N$ denotes the number of cells present at the moment when $t$ minutes have elapsed, then the relation we seek is given by the equation

$$N = 2^{t/20}. \tag{1.1}$$

Because the time $t$ appears in the exponent of the expression $2^{t/20}$, this equation is said to describe *exponential growth* of the number $N$ of cells (De Sapio, 1978, pp. 21–23).

A famous book called *On Growth and Form* by D'Arcy Wentworth Thompson contains the following statement (Thompson, 1959; vol. 1, p. 144): "Linnaeus shewed that an annual plant would have a million offspring in twenty years, if only two seeds grew up to maturity in a year." Linnaeus is, of course, Carolus Linnaeus (born Karl von Linné) (1707–1778), the great Swedish botanist. We can show that what Linnaeus said is true by adapting the preceding equation, as follows:

$$X = 2^{20}, \tag{1.2}$$

where $X$ is the number of offspring from the plant in 20 years.

To solve this equation, we need to use logarithms. John Napier (1550–1617), a distinguished Scottish mathematician, was the inventor of logarithms. (See the Appendix, Section 1.3, for his biography.) To solve equations using logarithms, we need to know the fundamental laws of logarithms, which are as follows (Ayres, 1958, p. 83):

1. The logarithm of the product of two or more positive numbers is equal to the sum of the logarithms of the several numbers. For example,

$$\log_b(P \cdot Q \cdot R) = \log_b P + \log_b Q + \log_b R \tag{1.3}$$

2. The logarithm of the quotient of two positive numbers is equal to the logarithm of the dividend minus the logarithm of the divisor. For example,

$$\log_b(P/Q) = \log_b P - \log_b Q \tag{1.4}$$

3. The logarithm of a power of a positive number is equal to the logarithm of the number, multiplied by the exponent of the power. For example,

$$\log_b(P^n) = n \log_b P \tag{1.5}$$

4. The logarithm of a root of a positive number is equal to the logarithm of the number, divided by the index of the root. For example,

$$\log_b P^{(1/n)} = (1/n) \log_b P. \tag{1.6}$$

In calculus, the most useful system of logarithms is the *natural system* in which the base is a certain irrational number $e = 2.71828$, approximately (Ayres, 1958, p. 86). The natural logarithm of $N$, $\ln N$, and the common logarithm of $N$, $\log N$, are related by the formula

$$\ln N = 2.3026 \log N. \tag{1.7}$$

To solve our equation, we take the logarithm of each side:

$$\log\left(2^{20}\right) = \log X$$

Using logarithm Rule No. 3, we get

$$20 \log 2 = \log X$$

Solving (and reading out all the digits on our hand calculator):

$$\begin{aligned}\log X &= 20(0.30103) = 6.0205999\\ X &= 1,048,576.\end{aligned}$$

Linnaeus was right.

### 1.2.2 Sigmoid Growth Curve

The S-shaped, or sigmoid, curve is typical of the growth pattern of individual organs, or a whole plant, and of populations of plants (Figure 1.2). It can be shown to consist of at least five distinct phases: (1) an initial lag period during which internal changes occur that are preparatory to growth; (2) a phase of ever-increasing rate of growth; (because the logarithm of growth rate, when plotted against time, gives a straight line during this period, this phase is frequently referred to as the log period of growth or “the grand period of growth”); (3) a phase in

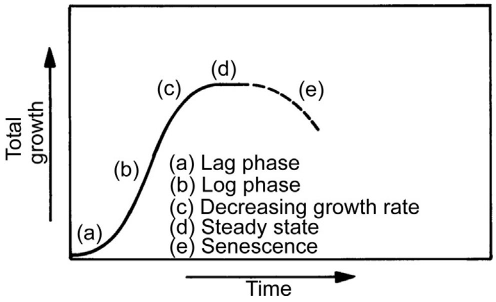

**FIGURE 1.2** Five phases in the sigmoid growth curve. *From Mitchell (1970, p. 95). Reprinted by permission of Roger L. Mitchell.*

which growth rate gradually diminishes; and (4) a point at which the organism reaches maturity and growth ceases. If the curve is prolonged further, a time will arrive when (5) senescence and death of the organism set in, giving rise to another component of the growth curve (Mitchell, 1970, p. 95).

### 1.2.3 Blackman Growth Curve

Since about 1900, people have used growth curves to analyze growth. Significant relationships of a mathematical nature, however, are difficult to apply to such a complex thing as growth (Hammond and Kirkham, 1949). One well-known theory of plant growth is the compound interest law of Blackman (1919). He related plant growth to money in a bank. When money accumulates at compound interest, the final amount reached depends on:

1. The capital originally used;
2. The rate of interest; and
3. The time during which the money accumulates.

Comparing these factors to plants
1 = the weight of the seed;
2 = the rate at which the seed material is used to produce new material;
3 = the time during which the plant increases in weight.
Blackman related the three factors into one exponential equation,

$$W_1 = W_0 e^{rt}, \tag{1.8}$$

where

$W_1$ = the final weight
$W_0$ = the initial weight
$r$ = the rate of interest
$t$ = time
e = the base of natural logarithms (2.718…).

The Blackman equation works best for early phases of growth (the log phase of growth in the sigmoid growth curve). In the later growth stages, the decreasing relative growth rate has appeared to make impossible the application of this theory to the entire growth curve. Blackman attempted to do this, nevertheless, by using the average of all the different relative growth rate values as the $r$ term in Eqn (1.8). He called this term the "efficiency index" of plant growth.

Hammond and Kirkham found that the growth curves (dry weight versus time) of soybeans [*Glycine max* (L.) Merr.] and corn (*Zea mays* L.) were characterized by a series of exponential segments, which were related to the growth stages of the plants. The exponential equation for all segments had the form:

$$w = w_o e^{r(t-t_o)}, \tag{1.9}$$

where

$w$ = weight of the plant at time $t$
$w_o$ = weight of the plant at an arbitrary time $t_o$
$r$ = relative growth rate
e = base of natural logarithms (2.718…).

Taking the natural logarithm of each side, we get

$$\ln w = \ln w_o + \ln e^{r(t-t_o)}$$

$$\ln w_o + [r(t - t_o)x\ 1]$$

$$\ln w_o + r(t - t_o).$$

Converting to common logarithms by dividing each term by 2.303, we get

$$\log w = \log w_o + [r(t - t_o)]/2.303.$$

Now let

$$y = \log w$$

$$a = \log w_o$$

$$b = r/2.303$$

$$x = t - t_o.$$

We get $y = a + bx$, which is the equation of a straight line.

The differential form of Eqn (1.9), $w = w_o e^{r(t-t_o)}$, is

$$dw/(w dt) = r \tag{1.10}$$

where $r$, the relative growth rate, is the increase in *weight* per unit weight per unit time. It is obtained by multiplying the slope, $b$, of the line by 2.303.

Hammond and Kirkham (1949) plotted the common logarithm of dry weight versus time and found that soybeans have three growth stages, I, II, and III. The analysis showed that the plants produce dry matter at the greatest relative rate during period I; at a smaller rate during period II; and at a still smaller rate during period III. That is, the slopes declined with age (slope $= r/2.303$). They saw that the dates of change in the growth curves from period I to period II were also the dates when the plants began to bloom. The dates of the second change in the growth curve, or the change from period II to period III, were the dates when the plants reached maximum height. The soybeans grew on two different soils, Clarion loam and Webster silt loam. The soybean plants in the Clarion soil bloomed and reached maximum height about a week earlier than the soybeans on the Webster silt loam soil. The growth curves clearly showed this difference (Figure 1.3). Growth curves, therefore, can be used to see the effect of the soil environment on plant growth. Hammond and Kirkham (1949) did not give a reason for the difference in rate of growth on the Webster and Clarion soils, but it probably was related to one of the four soil physical factors that affect plant growth: water, temperature, aeration, or mechanical impedance. For corn, they found four periods of growth (Figure 1.4). The additional period in corn apparently was related to the difference in time of appearance of male and female flowers in corn. The physiological changes associated with the breaks in the curves were connected with tasseling, silking, and cessation of vegetative growth. The last break occurred after the corn plants had reached maximum height. In sum, the data for soybeans and corn showed that a quantitative analysis

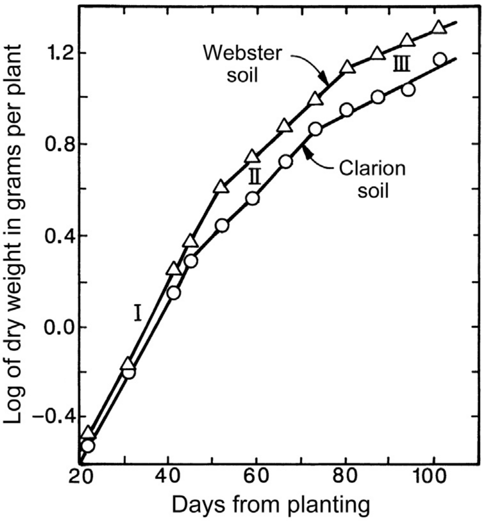

**FIGURE 1.3** Logarithmic dry matter accumulation curves of soybeans grown in the field in Iowa on Webster and Clarion soils. *From Hammond and Kirkham (1949). American Society of Agronomy, Madison, Wisconsin. Reprinted by permission of the American Society of Agronomy.*

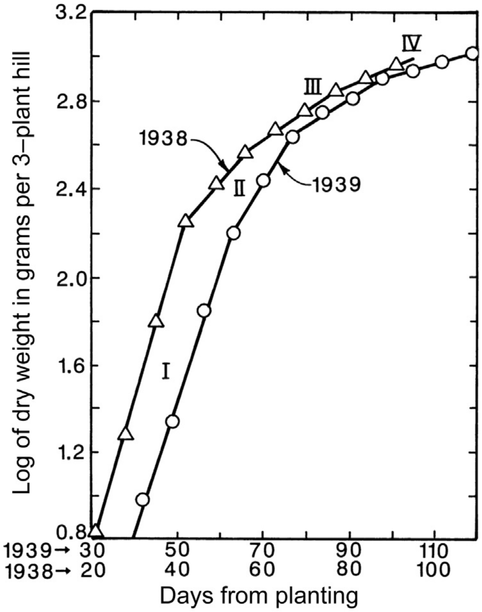

**FIGURE 1.4** Logarithmic dry matter accumulation curves of Iowa 939 corn in 1938 and 1939. *From Hammond and Kirkham (1949). American Society of Agronomy, Madison, Wisconsin. Reprinted by permission of the American Society of Agronomy.*

of the complete growth curve can be accomplished if the overall growth is partitioned into segments based on the growth stages of the plants.

The equations for plant growth show that we can develop significant mathematical relationships for a quantitative analysis of plant growth. This is probably because plant growth is governed by basic chemical and physical laws. From these relationships, we can predict plant growth.

## 1.3 APPENDIX: BIOGRAPHY OF JOHN NAPIER

John Napier (1550—1617), a distinguished Scottish mathematician, was the inventor of logarithms. The son of Scottish nobility, Napier's life was spent amid bitter religious dissensions. He was a passionate Protestant. His great work, *A Plaine Discouery of the Whole Reuelation of Saint John* (1594), has a prominent place in Scottish ecclesiastical history as the earliest Scottish work on the interpretation of the scriptures. He then occupied himself by inventing instruments of war, including two kinds of burning mirrors, a piece of artillery, and a metal chariot from which a shot could be discharged through small holes. Napier devoted most of his leisure to the study of mathematics, particularly to developing methods of facilitating computation. His name is associated with his greatest method, logarithms. His contributions to this mathematical invention are contained in two treatises: *Mirifici logarithmorum canonis descriptio* (1614; translated into English in 1857) and *Mirifici logarithmorum canonis constructio*, which was published two years after his death (1619) and translated into English in 1889. Although Napier's invention of logarithms overshadows all his other mathematical work, he has other mathematical contributions to his credit. In 1617, he published his *Rabdologiae, seu numerationis per virgulas libri duo* (English translation, 1667). In this work, he describes ingenious methods of performing the fundamental operations of multiplication and division with small rods (Napier's bones). He also made important contributions to spherical trigonometry (Scott, 1971).

## References

Allègre, C.J., Schneider, S.H., 1994. The evolution of the earth. Sci. Am. 271 (4), 66–75.

Ayres Jr, F., 1958. Theory and Problems of First Year College Mathematics. Schaum Publishing, New York.

Bernardo, A.S., 1982. The plague as key to meaning in Boccaccio's "Decameron." In: Williman, D. (Ed.), The Black Death. The Impact of the Fourteenth-Century Plague. Center for Medieval and Early Renaissance Studies, State University of New York at Binghamton, Binghamton, New York, pp. 39–64.

Blackman, V.H., 1919. The compound interest law and plant growth. Ann. Bot. (Old Series) 33, 353–360.

Boyer, J.S., 1982. Plant productivity and environment. Science 218, 443–448.

Brunet, M., Guy, F., Pilbeam, D., Mackaye, H.T., Likius, A., Ahounta, D., Beauvilain, A., Blondel, C., Bocherens, H., Boisserie, J.-R., De Bonis, L., Coppens, Y., Dejax, J., Denys, C., Duringer, P., Elsenmann, V., Fanone, G., Fronty, P., Geraads, D., Lehmann, T., Lihoreau, F., Louchart, A., Mahamat, A., Merceron, G., Mouchelin, G., Otero, O., Pelaez Campomanes, P., Ponce De Leon, M., Rage, J.-C., Sapanet, M., Schuster, M., Sudre, J., Tassy, P., Valentin, X., Vignaud, P., Viriot, V., Zazzo, A., Zollikofer, C., 2002. A new hominid from the Upper Miocene of Chad, Central Africa. Nature 418, 145–151.

Carbonell, E., Bermúdez de Castra, J.M., Parés, J.M., Pérez-González, A., Cuenca-Bescós, G., Ollé, A., Mosquera, M., Huguet, R., van der Made, J., Rosas, A., Sala, R., Vallverdú, J., García, N., Granger, D.E., Martinón-Torres, M., Rodríguez, X.P., Stock, G.M., Vergès, J.M., Allué, E., Burjachs, F., Cáceres, I., Canals, A., Benito, A., Díez, C., Lozano, M., Mateos, A., Navazo, M., Rodríguez, J., Rossell, J., Arsuaga, J.L., 2008. The first hominin of Europe. Nature 452, 465–469.

Chin, G., Marathe, T., Roberts, L., 2011. Doom or vroom? Science 333, 538.

De Sapio, R., 1978. Calculus for the Life Sciences. WH Freeman and Co, San Francisco.

De Wit, C.T., 1967. Photosynthesis: its relationship to overpopulation. In: San Pietro, A., Greer, F.A., Army, T.J. (Eds.), Harvesting the Sun. Academic Press, New York, pp. 315–320.

Frisch, R.E., 1988. Fatness and fertility. Sci. Am. 258 (3), 88–95.

Gladwell, M., September 29, 1997. The dead zone. New Yorker, 52–65.

Hammond, L.C., Kirkham, D., 1949. Growth curves of soybean and corn. Agron. J. 41, 23–29.

Hueston, W.D., Voss, J.L., 2000. Transmissible Spongiform Encephalopathies in the United States. CAST Report No. 136. Council for Agricultural Science and Technology, Ames, Iowa.

Johnson, F.S., 1954. The solar constant. J. Meteorol. 11, 431–439.

Kirkham, D., 1973. Soil physics and soil fertility. Bull. Rech. Agron. Gembloux Fac. Sci. Agron. l'État (New Series) 8 (2), 60–88.

Kok, B., 1967. Photosynthesis—physical aspects. In: San Pietro, A., Greer, F.A., Army, T.J. (Eds.), Harvesting the Sun. Academic Press, New York, pp. 29–48.

Kok, B., 1976. Photosynthesis: the path of energy. In: Bonner, J., Varner, J.E. (Eds.), Plant Biochemistry. Academic Press, New York, pp. 845–885.

Lemonick, M.D., Park, A., May 5, 2003. The truth about SARS. Time, 48–53.

Lockwood, G.W., Skiff, B.A., Baliunas, S.L., Radick, R.R., 1992. Long-term solar brightness changes estimated from a survey of sun-like stars. Nature 360, 653–655.

McEvedy, C., 1988. The bubonic plague. Sci. Am. 258 (2), 118–123.

McGurn, W., October 25, 2011. And baby makes seven billion. Wall Street J., A17.

Mitchell, R.L., 1970. Crop Growth and Culture. Iowa State University Press, Ames.

National Geographic, 1998a. Population 193 (1), 6–8.

National Geographic, 1998b. Millennium in maps. Population. Map insert for 194 (4).

National Geographic, 1999. Global population reaches a milestone. 196 (4), (unpaged).

New York Times, March 16, 1980. Population of the earth is said to be 4.5 billion. Section I, page 2.

New York Times, July 12, 1987. Zagreb baby hailed as 5 billionth person. Section I, page 5.

Philip, J.R., 1966. Plant water relations: some physical aspects. Annu. Rev. Plant Physiol. 17, 245–268.

Renouard, Y., 1971. Black death. Encyclopaedia Britannica 3, 742–743.

Scott, J.F., 1971. Napier (Neper), John. Encyclopaedia Britannica 15, 1174–1175.

Shaw, B.T., 1952. Soil Physical Conditions and Plant Growth. Academic Press, New York.

Simpson, S., 2003. Questioning the oldest signs of life. Sci. Am. 288 (4), 70–77.

Stanier, R.Y., Doudoroff, M., Adelberg, E.A., 1963. The Microbial World, second ed. Prentice-Hall, Englewood Cliffs, New Jersey.

Thompson, D.'A.W., 1959. On Growth and Form, second ed., 2 vols.. Cambridge University Press, Cambridge (First published in 1917.).

Weiss, R., 2002. War on disease. Nat. Geog. 201 (2), 2–31.

Wilford, J.N., 1982. The people boom. Off the chart! Condensed from the *New York Times*, October 6, 1981. Reader's Digest 120 (717), 114–115.

Wood, B., 2002. Hominid revelations from Chad. Nature 418, 133–135.

Zimmer, C., 2001. How old is…. Nat. Geog. 200 (3), 78–101.

CHAPTER

# 2

# Definitions of Physical Units and the International System

## 2.1 DEFINITIONS

In soil—plant—water relations, we will be using units based on physical definitions. Therefore, we need to review the definitions. We will define the following: force, weight, work, energy, power, pressure, and heat. The definitions come from Schaum (1961), but they can be found in any physics textbook.

### 2.1.1 Force

*Force* is a push or pull exerted on a body. If an unbalanced force acts on a body, the body accelerates in the direction of the force. Conversely, if a body is accelerating, there must be an unbalanced force acting on it in the direction of the acceleration. The unbalanced force acting on a body is proportional to the product of the mass and of the acceleration produced by the unbalanced force.

#### *2.1.1.1 Newton's Laws of Motion*

For completeness, we now review these three laws, even though the second law is the one we are interested in for the definition of force. (See the Appendix, Section 2.4, for a biography of Newton.)

1. A body will maintain its state of rest or of uniform motion (at constant speed) along a straight line unless compelled by some unbalanced force to change that state. In other words, a body accelerates only if an unbalanced force acts on it.
2. An unbalanced force $F$ acting on a body produces in it an acceleration $a$ which is in the direction of the force and directly

http://dx.doi.org/10.1016/B978-0-12-420022-7.00002-1

Copyright © 2014 Elsevier Inc. All rights reserved.

proportional to the force, and inversely proportional to the mass $m$ of the body.
In mathematical terms, this law states that $ka = F/m$ or $F = kma$, where $k$ is a proportionality constant. If suitable units are chosen so that $k = 1$, then $F = ma$.

3. To every action, or force, there is an equal and opposite reaction, or force. In other words, if a body exerts a force on a second body, then the second body exerts a numerically equal and oppositely directed force on the first body. These two forces, although equal and oppositely directly, do not balance each other, because both are not exerted on the same body.

#### *2.1.1.2 Units of Force*

In the equation $F = ma$, it is desirable to make $k = 1$; that is, to have units of mass, acceleration, and force such that $F = ma$. To do this, we specify two fundamental units and derive the third unit from these two.

1. In the *meter-kilogram-second* or *mks absolute system*, the fundamental mass unit chosen is the kilogram and the acceleration unit is the m/s$^2$. The corresponding derived force unit, called the *newton* (nt or N), is the unbalanced force that will produce an acceleration of 1 m/s$^2$ in a mass of 1 kg.
2. In the *centimeter-gram-second* or *cgs absolute system*, the fundamental mass unit is the gram and the acceleration unit is the cm/s$^2$. The corresponding derived force unit, called the *dyne*, is that unbalanced force that will produce an acceleration of 1 cm/s$^2$ in a mass of 1 g.
3. In the *English gravitational system*, the fundamental force unit is the *pound* and the acceleration unit is the ft/s$^2$. The corresponding derived mass unit, called the *slug*, is the mass that when acted on by a 1 lb force acquires an acceleration of 1 ft/s$^2$.

Thus the following indicate three consistent sets of units that may be used with the equation $F = ma$ ($F = kma$ with $k = 1$):

- **mks system:** $F$ (newtons) $= m$ (kilograms) $\times a$ (m/s$^2$)
- **cgs system:** $F$ (dynes) $= m$ (grams) $\times a$ (cm/s$^2$)
- **English system:** $F$ (pounds) $= m$ (slugs) $\times a$ (ft/s$^2$)

### 2.1.2 Mass and Weight

The mass $m$ of a body refers to its inertia, and the weight $w$ of a body is the pull or force due to gravity acting on the body which varies with location. (Inertia is the tendency of matter to remain at rest if at rest, or, if moving, to keep moving in the same direction, unless affected by some outside force.) Weight $w$ is a force with a direction approximately toward the center of the earth.

If a body of mass $m$ is allowed to fall freely, the resultant force acting on it is its weight, $w$, and its acceleration is that due to gravity, $g$. Then in any consistent system of units the equation $F = ma$ becomes

$$w = mg.$$

Thus

$w$ (newtons) $= m$ (kilograms) $\times g$ (m/s$^2$)
$w$ (dynes) $= m$ (grams) $\times g$ (cm/s$^2$)
$w$ (pounds) $= m$ (slugs) $\times g$ (ft/s$^2$).

It follows that $m = w/g$. For example, if a body weighs 64 lb at a place where $g = 32$ ft/s$^2$, its mass is $m = w/g = 64$ lb/(32 ft/s$^2$) $= 2$ slugs. If a body weighs 49 N at a place where $g = 9.8$ m/s$^2$, its mass $m = w/g = 49$ N/(9.8 m/s$^2$) $= 5$ kg.

**Problem**: How many grams are there in one slug?

We remember that one pound = 454 g. We abbreviate pound as lb and gram as g.

One slug of mass = 32 lb of mass = 32 × 454 g of mass = 14,528 g of mass. The conversion was made by Don Kirkham (personal communication, February 15, 1994).

### 2.1.3 Work

A force does work on a body when it acts against a resisting force to produce motion in the body. Consider that a constant external force $F$ acts on a body at an angle $\theta$ with the direction of motion and causes it to be displaced a distance $d$ (Figure 2.1). Then the work $W$ done by the force $F$ on the body is the product of the displacement $d$ and the component of $F$ in the direction of $d$. Thus

$$W = (F \cos \theta)d.$$

If $d$ and $F$ are in the same direction, $\cos \theta = \cos 0° = 1$ and $W = Fd$.

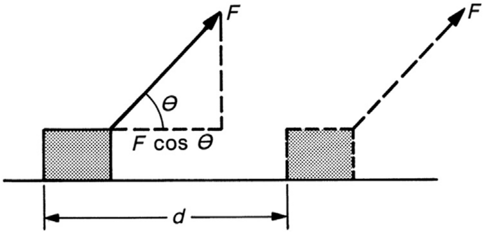

FIGURE 2.1 Illustration for definition of work. *Adapted from Schaum (1961, p. 49). This material is reproduced with permission of The McGraw-Hill Companies.*

#### 2.1.3.1 *Units of Work*

Any unit of work equals a unit of force × a unit of length.

- One *foot-pound* (ft-lb) of work is done when a constant force of 1 lb moves a body a distance of 1 ft in the direction of the force.
- One *newton-meter* (Nm), called 1 joule (J), is the work done when a constant force of 1 N moves a body a distance of 1 m in the direction of the force. Because 1 N = 0.2248 lb and 1 m = 3.281 ft,

$$1 \text{ joule} = 1 \text{ newton} - \text{meter} = 0.7376 \text{ ft} - \text{lb}$$

$$1 \text{ ft} - \text{lb} = 1.356 \text{ joules.}$$

One *dyne-cm*, called 1 *erg*, is the work done when a constant force of 1 dyne moves a body a distance of 1 cm in the direction of the force. Since $1 \text{ N} = 10^5$ dynes and $1 \text{ m} = 10^2$ cm,

$$1 \text{ joule} = 10^7 \text{ ergs.}$$

### 2.1.4 Energy

The *energy* of a body is its ability to do work. Because the energy of a body is measured in terms of the work it can do, it has the same units as work.

The *potential energy* (PE) of a body is its ability to do work because of its position or state. The potential energy of a mass $m$ lifted a vertical distance $h$, where $g$ is the acceleration due to gravity, is

$$\text{PE} = mgh.$$

In the mks system: PE (joules) = $m$ (kg) × $g$ (m/s$^2$) × $h$ (m). In the cgs system: PE (ergs) = $m$ (grams) × $g$ (cm/s$^2$) × $h$ (cm).

Because $mg = w$, we may also write: $\text{PE} = mgh = wh$.

### 2.1.5 Power

*Power* is the time rate of doing work. Average power = (work done)/(time taken to do this work) = force applied × velocity of body to which force is applied, where the velocity of the body is in the direction of the applied force.

#### 2.1.5.1 *Units of Power*

The unit of power in any system is found by dividing the unit of work in that system by the unit of time. Thus two units of power are the J/s (or watt, abbreviated W) and the ft-lb/s. Other practical units of power are the kilowatt and the horsepower.

- 1 W = 1 J/s
- 1 kilowatt (kW) = 1000 W = 1.34 horsepower
- 1 horsepower (hp) = 550 ft-lb/s = 33,000 ft-lb/min = 746 W.

The power of car engines is given in units of horsepower. My car has a 221-horsepower engine. Work done = power × time taken. Hence the total work done in 1 h, when the rate of doing work is 1 kW, is 1 kilowatt-hour (kWh). The total work done in 1 h, when the rate of doing work is 1 horsepower, is 1 horsepower-hour (hph). Every month, I receive a bill for electricity, and the meter readings on the bill, taken from the meter for my apartment, are in units of kilowatt-hours. This is a unit of work.

### 2.1.6 Pressure

*Pressure* or $p$ is a force per unit area

$$p = \frac{(\text{force } F \text{ acting perpendicular to an area})}{(\text{area } A \text{ over which the force is distributed})}$$

or

$$p = F/A.$$

Some units of pressure are the $\mathrm{lb/ft^2}$, $\mathrm{lb/in^2}$, $\mathrm{N/m^2}$, and $\mathrm{dyne/cm^2}$. The $\mathrm{dyne/cm^2}$ is a unit that we will use often in plant–water relations.

$$1 \times 10^6\ \mathrm{dyne/cm^2} = 1\ \mathrm{bar}.$$

However, a bar is not an SI unit. The SI unit is the Pascal, and 10 bars = 1 MPa or 10 bars = 1 MPa. We will talk about the SI system of units in Section 2.2.

### 2.1.7 Heat

*Heat* is a form of energy. The three units most commonly used in measuring the quantity of heat are defined as follows.

1. **One calorie** (cal) = the quantity of heat required to raise the temperature of 1 g of water by 1 °C.
   Because the calorie was originally defined as stated earlier, it has been recognized that the energy requirement for raising the temperature of 1 g of water by 1° depends slightly on the temperature, with a variation of about half a percent over the interval from 0° to 100 °C. For work requiring an accuracy no greater than 1%, the above definition is satisfactory. For the most precise work, it has been agreed to define the calorie in terms of electrical units of energy, so that 1 calorie = 4.1840 J. This is very

close to the amount of energy required to raise the temperature of 1 g of water from 16.5 to 17.5 °C.

2. **1 kilocalorie** or **kilogram-calorie** (kcal or kg-cal) = 1000 cal.
3. **1 British thermal unit** (Btu) = the quantity of heat required to raise the temperature of 1 pound of water by 1°F. 1 Btu = 453.6 × 5/9 cal = 252 cal.

## 2.2 LE SYSTÈME INTERNATIONAL D'UNITÉS

*Le Système International d'Unités*, which is French for "The International System of Units" or SI units, is a listing of decisions promulgated since 1889 on units of measurement. The General Conference on Weights and Measures (CGPM) meets regularly to update the units. The document was originally written in French, and consequently the name of the system has a French name. CGPM stands for the French *La Conférence Générale de Poids et Mesures*. The goal of the CGPM is "to make recommendations on the establishment of a *practical system of units of measurement* suitable for adoption by all signatories to the Meter Convention" (United States Department of Commerce, 1977, p. 1). Another goal, in my opinion, is to have standard units worldwide, so that anybody reading an article in the world now or in the future will know exactly what the unit is. This allows replication of experiments. It is important that people understand published works even after the death of the authors of these works. I investigated buying a chlorophyll meter, also called an SPAD meter. The acronym stands for "soil plant analysis development" (Loh et al., 2002). I decided against buying the meter, because it does not read out in SI units. It reads out in SPAD units. The units will be used only as long as the meter can be bought. Someone 100 years from now could not replicate or understand experiments with an SPAD meter, unless the meter is used then. Graphs of absorption spectra of chlorophyll *a* and chlorophyll *b* (Steward, 1964, p. 51) can be replicated 100 years from now, because they are expressed in standard units for absorption coefficients and wavelengths.

The tenth CGPM (1954), by its Resolution 6, and the fourteenth CGPM (1971), by its Resolution 3, adopted as base units of this "practical system of units," the units of the following seven quantities: length, mass, time, electric current, thermodynamic temperature, amount of substance, and luminous intensity. The eleventh CGPM (1960), by its Resolution 12, adopted the name *International System of Units*, with the international abbreviation SI, for this practical system of units of measurements and laid down rules for the prefixes and the derived and supplementary units.

SI units are divided into three classes: base units, derived units, and supplementary units (Taylor, 1991, p. 1). The base units and their abbreviations are (United States Department of Commerce, 1977, p. 6; Taylor, 1991, pp. 3—5) (Table 2.1):

- length = meter (m)
- mass = kilogram (kg)
- time = second (s)
- electric current = ampere (A)
- thermodynamic temperature = kelvin (K)
- amount of substance = mole (mol)
- luminous intensity = candela (cd)

The derived units are combinations of the base units. Examples of SI derived units expressed in terms of base units are (United States Department of Commerce, 1977, p. 6; Taylor, 1991, p. 6) (Table 2.2):

- area = square meter ($m^2$)
- volume = cubic meter ($m^3$)
- speed, velocity = meter per second ($m/s$)
- acceleration = meter per second squared ($m/s^2$)
- wave number = 1 per meter ($m^{-1}$)
- density, mass density = kilogram per cubic meter ($kg/m^3$)

Other derived units with special names are given by the United States Department of Commerce (1977) and Taylor (1991).

The class of supplementary units contains two purely geometrical units: the SI unit of plane angle, the *radian*, and the SI unit of solid angle, the *steradian*. (A radian is an arc of a circle equal in length to the radius or

**TABLE 2.1** SI Base Units[1]

| | **SI Unit** | |
|---|---|---|
| **Quantity** | **Name** | **Symbol** |
| Length | Meter | m |
| Mass | Kilogram | kg |
| Time | Second | s |
| Electric current | Ampere | A |
| Thermodynamic temperature | Kelvin | K |
| Amount of substance | Mole | mol |
| Luminous intensity | Candela | cd |

[1] *From Taylor (1991, p. 5).*

**TABLE 2.2** Example of SI Derived Units Expressed in Terms of Base Units[1]

| | **SI Unit** | |
|---|---|---|
| **Quantity** | **Name** | **Symbol** |
| Area | Square meter | $m^2$ |
| Volume | Cubic meter | $m^3$ |
| Speed, velocity | Meter per second | m/s |
| Acceleration | Meter per second squared | $m/s^2$ |
| Wave number | Reciprocal meter | $m^{-1}$ |
| Density, mass density | Kilogram per cubic meter | $kg/m^3$ |
| Specific volume | Cubic meter per kilogram | $m^3/kg$ |
| Current density | Ampere per square meter | $A/m^2$ |
| Magnetic field strength | Ampere per meter | A/m |
| Concentration (of amount of substance) | Mole per cubic meter | $mol/m^3$ |
| Luminance | Candela per square meter | $cd/m^2$ |

[1] *From Taylor (1991, p. 6).*

the angle at the center of a circle formed by two radii cutting off such an arc, equal to 57.295+ degrees.) Another supplementary unit is the *astronomical unit*. This unit does not have an international symbol; abbreviations used, for example, are AU in English, UA in French, and AE in German. The astronomical unit of distance is "the length of the radius of the unperturbed circular orbit of a body of negligible mass moving round the Sun with a sidereal angular velocity of 0.017 202 098 950 radian per day of 86,400 ephemeris seconds" (United States Department of Commerce, 1977, p. 11). In the system of astronomical constants of the International Astronomical Union, the value adopted is

$$1\ \text{AU} = 149{,}597.870 \times 10^6\ \text{m}.$$

**Notes about units:** The appropriate unit should be used for each situation. For example, it would be inappropriate to use astronomical units to report the height of a corn plant, just as it would be inappropriate to use nanometers to report the distance from the earth to the sun. On graphs, sometimes data are reported on an axis as, for example, "$\times 10^3$". This notation is ambiguous, because the reader is not sure whether to multiply the number by 1000 or divide the number by 1000. It is best to use the prefixes to define a unit. The SI prefixes range from a factor of $10^{18}$ (exa) to $10^{-13}$ (atto) (United States Department of Commerce, 1977, p. 10). In addition, plant physiological data should not be normalized and given as a ratio. By normalization, we mean dividing values obtained in an experiment (e.g., value for transpiration or photosynthesis) by a common value. Normalization is used to smooth data (make the data less variable). But it should not be done. The ratio cancels out the units. A reader has no way to compare normalized data with values given in the literature, because no units are given. Units always should be given with data, so the data can be understood now and in the future. Normalized numbers with no units should not be confused with dimensionless numbers with no units. Dimensionless numbers, such as the Reynolds number (which we shall define in Chapter 15), are widely used by engineers. Haynes (2013, p. 2—12) lists dimensionless numbers and states that the SI unit for each of them is one.

## 2.3 EXAMPLE: APPLYING UNITS OF WORK AND PRESSURE TO A ROOT

Let us use our knowledge of the definitions of work and pressure to quantify the work done by a root as it pushes through the soil (Kirkham, 1973). When roots open up the soil, they expend energy. We can obtain a simple mathematical expression for the amount of work a root does as it grows. To make matters easy, let us first assume that, as the root moves along, only its end exerts forces, to push the root through the soil; and let us assume that the end of the root is blunt rather than rounded. By "blunt", let us mean that the end of the root is flat like the end of a solid right circular cylinder. Let us see what happens as we push such a solid cylinder through the soil. As we push the cylinder through the soil with a force, $F$, the resisting force of the soil will also have the value $F$, and, if we push the cylinder a distance, $d$, the work, $W$, done will be the product of the force and the distance, $d$:

$$W = Fd. \tag{2.1}$$

We now wish to get Eqn (2.1) in terms of the soil pressure. If we take $r$ to be the radius of the cylinder that we are pushing in the soil, then the soil pressure $P$ (force per unit area) on the end of the cylinder in contact with the soil will be

$$P = F/\left(\pi r^2\right). \tag{2.2}$$

So we divide both sides of Eqn (2.1) by the factor $\pi r^2$ and in the result substitute $P$ for $F/(\pi r^2)$ to find that Eqn (2.1) becomes

$$W/\left(\pi r^2\right) = Pd \tag{2.3}$$

which may be written in the form

$$W/\left(\pi r^2 d\right) = P. \tag{2.4}$$

But $\pi r^2 d$ is the volume, say $V$, of soil displaced. So we may write Eqn (2.4) as

$$W/V = P \tag{2.5}$$

or

$$W = PV. \tag{2.6}$$

Equation (2.6) says that the work done by the root end as it pushes its way through the soil is equal to the product of root pressure and the volume of soil displaced by the root. Equation (2.6) gives us useful information. The equation says that, if the pressure, $P$, encountered by the roots in a soil of poor structure is twice as great as for a soil in good structure, the roots must do twice as much work to establish the same size root system in the poor soil as in the good soil.

## 2.4 APPENDIX: BIOGRAPHY OF ISAAC NEWTON

The following biographical material on Newton comes from Tannenbaum and Stillman (1959).

Newton was born on December 25, 1642, in Woolsthorpe, Lincolnshire, England. He was premature, and the midwife thought he would not live the night. He did not have the advantage of a happy, loving family. His father was said to be extravagant and wild, but he had no influence on Isaac, because he died more than two months before Isaac was born. His mother, Hannah, remarried to a Reverend Mr. Smith to avoid a life of poverty. After the marriage, Isaac lived in a separate house with his grandmother, but near his mother’s home.

Because Isaac turned out to be a hopeless farmer, his family sent him to Cambridge in 1661. He became engaged to his childhood friend Catherine Storey, but they were never married. After Newton got his undergraduate degree, he wanted to get his master’s degree with the support of a teaching assignment, but the rules of the University of Cambridge were strict and no members of the faculty could marry. Isaac and Catherine remained lifelong friends.

During the time of the great plague, Cambridge University was closed (the doors closed on August 8, 1665), and Newton went home and studied the movement of the planets. This is when the famous “apple” story occurred. There he reasoned that the moon does not fly off into space because the earth and the moon attract each other with a force that is directly proportional to the product of their masses. The same law holds the planets in orbit around the sun. Newton returned to Cambridge after the plague and started to study telescopes. His home headquarters at Cambridge served as his laboratory, because scientists did not have laboratories then.

On October 22, 1669, Isaac was appointed Lucasian Professor of Mathematics after his tutor, Dr. Isaac Barrow (1630−1677), stepped down so Newton could have the chair. As a professor he was expected to give lectures, but few students came to Newton's lectures. After his death, many people read his written versions of the lectures.

In 1671, Isaac was asked to build a telescope for the Royal Society, which had been formed in 1645. Members called themselves the "Invisible College" and they met in bars. The group welcomed Isaac's work on the telescope, and on January 11, 1672, Newton was elected to membership in the Royal Society and was invited to present more of his work, which he did. He also presented his theory of light and color, which some members, especially Robert Hooke (1635−1703), criticized because they had their own theories. Shy and studious Newton was deeply hurt by the criticism. He defended his work in several papers, but then gave up, saying he did not want to "become a slave to defend it." He submitted no more papers for publication to the Society. Newton then wrote the *Principia* (*Philosophiae Naturalis Principia Mathematica*; begun in 1684 and first published in 1687), which was an instant success and made him one of the most famous men at Cambridge.

About 1693, he became involved in an argument with Gottfried Wilhelm Leibniz (1646−1716), a philosopher and mathematician, who had independently discovered calculus in Germany. Leibniz's method of writing calculus was eventually the one that was universally accepted.

While the arguments between Leibniz and Newton were raging over who discovered calculus first, Newton's good friend Charles Montague was elected president of the Royal Society. On March 19, 1696, Montague got the king to make Newton Warden of the Mint. People used to chip pieces off of coins for the valuable metal, so coins got smaller and smaller as they circulated. During Newton's tenure, new coins were made and recoinage was complete in 1699. He was promoted to Master of the Mint, a position that provided a good salary that enabled him to help his poorer relatives. He believed that "they who gave away nothing till they died…, never gave". He also gave freely to many worthy causes such as the fund for building a new library at Trinity College, which was designed by Newton's friend Sir Christopher Wren. Newton also contributed money toward the purchase of a permanent building for the Royal Society.

Newton became president of the Royal Society on November 30, 1703, and remained president until his death. On April 16, 1705, Queen Anne knighted him. Of all his nieces and nephews, only one, Catherine, the daughter of his half-sister Hannah, was intellectually related to him.

Newton gave Catherine the best education available to a woman at that time, and she presided over his London home in his later years. To their home she attracted men such as Jonathan Swift (1667–1745) and Alexander Pope (1688–1744). John Dryden (1631–1700) wrote poems about her. Voltaire (1694–1778) also visited their house and was the first to publish the falling apple story. Newton had an excellent library in his study with over 1800 books, each with his bookplate "Philosophimur," meaning "let us seek knowledge." In the quiet of his study, he could pursue the religious studies that were so important to him.

Newton's last years were peaceful. His old enemies, Hooke and Leibniz, had died. Catherine had married, and her husband, John Conduit, took over the management of the Mint. The Conduits and their daughter lived with Newton, and this daughter inherited all of Newton's papers. Her son was the Earl of Portsmouth, and Newton's papers are known as the Portsmouth Collection. Newton developed gout, and, on the way back from a meeting of the Royal Society, became ill, and died on March 20, 1727. The inscription on his tomb reads, "Let Mortals rejoice/That there has existed such and so great/AN ORNAMENT OF THE HUMAN RACE." Of his own place in history, Newton simply said, "If I have seen farther…, it is by standing on the shoulders of giants."

## References

Haynes, W.M., 2013. Handbook of Chemistry and Physics, ninty fourth ed. CRC Press, Boca Raton, Florida.

Kirkham, D., 1973. Soil physics and soil fertility. Bull. Rech. Agron. Gembloux Fac. Sci. Agron. l'État (New Series) 8 (2), 60–88.

Loh, R.C.W., Grabosky, J.C., Bassuk, N.L., 2002. Using the SPAD 502 meter to assess chlorophyll and nitrogen content of Benjamin fig and cottonwood leaves. Horttechnology 12, 682–686.

Schaum, D., 1961. Theory and Problems of College Physics, sixth ed. Schaum Publishing, New York.

Steward, F.C., 1964. Plants at Work. Addison-Wesley, Reading, Massachusetts.

Tannenbaum, B., Stillman, M., 1959. Isaac Newton: Pioneer of Space Mathematics. McGraw-Hill, New York.

Taylor, B.N., (United States of America Ed.) 1991. The International System of Units (SI). Approved translation of the sixth edition (1991) of the International Bureau of Weights and Measures publication Le Système International d'Unités (SI). NIST Special Publication vol. 330, 1991 Ed. US Department of Commerce, National Institute of Standards and Technology: Washington, DC.

United States Department of Commerce, 1977. The International System of Units (SI). In: NBS Special Publication 330. US Department of Commerce, National Bureau of Standards, Washington, DC.

CHAPTER

# 3

# Structure and Properties of Water

## 3.1 STRUCTURE OF WATER

To understand the nature of water in soil and plants, we need a mental picture of the water molecule. The water molecule (Figure 3.1) is composed of two hydrogen atoms and one oxygen atom. The water molecule is positively charged on one side and negatively charged on the other and is, thus, a dipole. Two hydrogen atoms each share a pair of electrons with a single oxygen atom. The two hydrogen atoms of the water molecule are separated at an angle of 103−106°, measured with the oxygen atom as the apex of the angle and with the two hydrogen protons

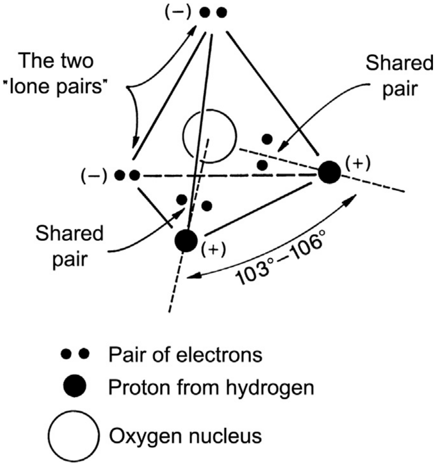
(−) ●●
The two "lone pairs"
Shared pair
(−) ●●
(+)
Shared pair
(+)
103°−106°
●● Pair of electrons
● Proton from hydrogen
○ Oxygen nucleus

**FIGURE 3.1** Tetrahedral charge structure of a water molecule. *From Kirkham and Powers (1972). This material is used by permission of John Wiley & Sons, Inc.*

http://dx.doi.org/10.1016/B978-0-12-420022-7.00003-3

Copyright © 2014 Elsevier Inc. All rights reserved.

as points on the angle sides. The electron pairs shared between the oxygen nucleus and the two hydrogen protons only partially screen (neutralize) the positive charge of the protons. The result is that the proton side of the molecule becomes the positive side of the water molecule (Kirkham and Powers, 1972, p. 2).

There are two concentrations of negative electricity, one concentration above and one concentration below a plane defined by the two hydrogen protons and the oxygen atom. They are called the *lone-pair electrons.* One pair is above the plane and one pair is below. These two lone pairs of electrons do not take part directly in bond formation, as do the electrons shared between the hydrogen and oxygen atoms of the water molecule. The electric charge structure of the water molecule resembles a tetrahedron with the oxygen near the center, two of its corners positively charged due to the partially screened protons of the hydrogen, and the remaining two corners of the tetrahedron negatively charged due to the two pairs of lone-pair electrons. (The word *tetrahedron* comes from the late Greek *tetraedros*, which means four-sided, and is a solid figure with four triangular surfaces.) This arrangement makes the water molecule a dipole, that is, one end of the molecule tends to be positive and the other end tends to be negative (Kirkham and Powers, 1972, p. 3). *Dipole* is a term used in physics and physical chemistry and is anything having two equal but opposite electric charges or magnetic poles, as in a hydrogen atom with its positive nucleus and negative electron. The tetrahedral structure of water can be disrupted by changes in pressure and temperature, as well as high concentrations of salt (Leberman and Soper, 1995). New insights into the structure of water are being made with the development of modern experimental techniques and sophisticated models (Zubavicus and Grunze, 2004), which can require the use of supercomputers (Gerstein and Levitt, 1998).

## 3.2 FORCES THAT BIND WATER MOLECULES TOGETHER

### 3.2.1 Hydrogen Bonding

There are two attractive forces between water molecules: hydrogen bonding and the van der Waals—London force. Hydrogen bonding results from the electrical structure of water molecules that makes them group together in a special way. The negative lone-pair electrons of one water molecule are attracted to a positive partially screened proton of another water molecule (Kirkham and Powers, 1972, p. 3). Thus each corner of the four corners of the water tetrahedron can be attached, by electrostatic attraction, to four other water tetrahedron molecules in solution (Figure 3.2). This type of bonding is called hydrogen bonding.

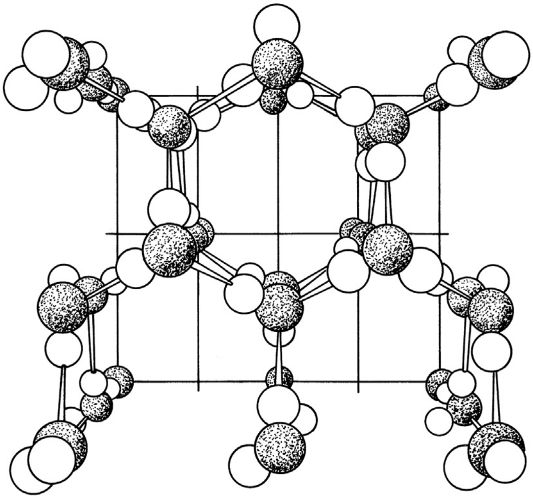

**FIGURE 3.2** Diagram showing approximately how water molecules are bound together in a lattice structure in ice by hydrogen bonds. The dark spheres are oxygen atoms, and the light spheres are hydrogen atoms. *From Kramer (1983). Reprinted by permission of Academic Press.*

Hydrogen bonding is important in binding water molecules together. Hydrogen bonds play a crucial role in the behavior of water, and their spatial patterns and fluctuations characterize the structure and dynamics of the liquid (Luzar and Chandler, 1996). Hydrogen bonds have a binding force of about 1.3–4.5 kcal/mol in water (Kramer, 1983, p. 11). Nobel (1974, p. 46) puts the value of hydrogen bonding at about 4.8 kcal/mol. The energy for hydrogen bonds in ice is 9.6 kcal/mol (Pauling, 1964, p. 456.) (We shall return to this value in Chapter 20, when we calculate the tensile strength of water.) Although neighboring water molecules are predominantly held together in ice by electrostatic forces (hydrogen bonding), there is also a significant covalent component to the bond (Isaacs et al., 1999). Only part of the structure of water due to hydrogen bonding is destroyed by heating, and about 70% of the hydrogen bonds found in ice remain intact in liquid water at 100 °C (Kramer, 1983, p. 12). Postorino et al. (1993) found that at 400 °C almost all hydrogen bonding is broken down.

### 3.2.2 van der Waals–London Force

A van der Waals–London force is one that exists between neutral nonpolar molecules, and, therefore, does not depend on a net electrical charge. The force was first described by van der Waals (1837–1923), a Dutch physicist. (See the Appendix, Section IV, for his biography.) London (1930) used quantum mechanics to obtain a quantitative expression for the van der Waals attractive force. This attractive force occurs because the electrons of one atom oscillate in such a way as to make it a rapidly fluctuating (about $10^{15}$ or $10^{16}$ Hz) dipolar atom, which in turn polarizes an adjacent atom, making it, too, a rapidly fluctuating dipole atom such that the two atoms attract each other. The generated force varies inversely as the seventh power of the distance between the atoms (Kirkham and Powers, 1972, p. 4). An article in *Nature* puts the value as the sixth power (Maddox, 1985). Because this attractive force varies inversely as the sixth or seventh power, it is short-ranged. Quantum mechanics predicts that at distances greater than 100 Å one atom cannot polarize another. ($1\ \text{Å} = 10^{-10}$ m. The unit Ångstrom is named after Anders Jöns Ångström, 1814–1874, a Swedish physicist.) The exact proportion of attraction that we can attribute to the van der Waals–London force is not known. Kramer (1983, p. 11) puts the attractive force at about 1 kcal per mole. It is generally felt that this force contributes little to the attraction of water to itself.

## 3.3 PROPERTIES OF WATER

We now look at the unique physical properties of water. These properties permit life. If life exists on other planets, it probably is based on water rather than on any other molecule, like ammonia. In 1999, when scientists discovered a solar system 44 astronomical units (AUs) from earth, which was the first planetary system ever found around a normal star, aside from our solar system, it was postulated that some of those planets could be located at the right distance from their host star to have liquid water and, hence, life (Showstack, 1999). Life depends on water. The discovery of water on Mars (Haskin et al., 2005) stoked the talk of life on Mars (Kerr, 2004). Jupiter's small inner moon, Amalthea, seems to be mostly porous ice (Anderson et al., 2005). Sensors have found water on the moon (Kaku, 2009). Water molecules have been detected on a planet 370 trillion miles ($584.6 \times 10^{12}$ km) away (Hotz, 2007).

We will list 15 properties of water. The list is extracted from the book by Kramer (1983, pp. 8, 9, and 14), and the definitions of the properties come from the *Handbook of Chemistry and Physics* (Weast, 1964). Other authors have described the unique physical properties of water (Buchan, 1996; Perkowitz, 1999).

### 3.3.1 Specific Heat

Water has the highest specific heat of any known substance except liquid ammonia, which is about 13% higher. The handbook states (Weast, 1964, p. F-57) that if a quantity of heat $H$ calories is necessary to raise the temperature of $m$ grams of a substance from $t_1$ to $t_2$ °C, the specific heat, $s$, is

$$s = H/[m(t_2 - t_1)]$$

The units of specific heat are cal/g/°C. Table 3.1, adapted from van Wijk and de Vries (1966, p. 41), gives the specific heat of water at different temperatures.

From Table 3.1, one sees that the specific heat of water decreases with an increase of temperature up to 35 °C, and then the specific heat increases with further increase in temperature. Paul (1986) noted that the majority of isothermic animals maintain their body temperatures, during non-hibernation, within a few degrees of 36 °C (human temperature = 98.6 °F or 37 °C), because the specific heat of water is a minimum at 35 °C. He said:

> As usual the key to much of life's mystery lies in the extraordinary behaviour of water…. [T]he relationship between the specific heat of water and temperature reveals that at 35 °C the specific heat of water is at its minimum value of 4.1779 J $g^{-1}$ °$C^{-1}$…. An organism functioning at this temperature will find it necessary to generate or dissipate the minimum amount of heat energy in order to maintain its temperature constant. From the point of view of the organism's energy economy this temperature is clearly the most efficient at which to function. It seems likely that since the environmental temperatures on Earth are, with few exceptions, lower than 35 °C, organisms which have been able to set their working temperatures at a point just slightly above the temperature at which the specific heat of water is at its minimum value have thrived.

**TABLE 3.1** Physical Properties of Liquid Water[1]

| **Temperature (°C)** | **Density (g/cm$^3$)** | **Surface Tension (g/s$^2$)** | **Dynamic Viscosity (g/cm/s) × $10^{-2}$** | **Heat of Vaporization (cal/g)** | **Specific Heat (cal/g/°C)** | **Thermal Conductivity (cal/cm/s/°C) × $10^{-3}$** |
|---|---|---|---|---|---|---|
| −10 | 0.99794 | – | – | 603.0 | 1.02 | – |
| −5 | 0.99918 | 76.4 | – | – | – | – |
| 0 | 0.99987 | 75.6 | 1.7921 | 597.3 | 1.0074 | 1.34 |
| 4 | 1.00000 | – | – | – | – | – |
| 5 | 0.99999 | 74.8 | 1.5188 | 594.5 | 1.0037 | 1.37 |
| 10 | 0.99973 | 74.2 | 1.3077 | 591.7 | 1.0013 | 1.40 |
| 15 | 0.99913 | 73.4 | 1.1404 | 588.9 | 0.9998 | 1.42 |
| 20 | 0.99823 | 72.7 | 1.0050 | 586.0 | 0.9988 | 1.44 |
| 25 | 0.99708 | 71.9 | 0.8937 | 583.2 | 0.9983 | 1.46 |
| 30 | 0.99568 | 71.1 | 0.8007 | 580.4 | 0.9980 | 1.48 |
| 35 | 0.99406 | 70.3 | 0.7225 | 577.6 | 0.9979 | 1.50 |
| 40 | 0.99225 | 69.5 | 0.6560 | 574.7 | 0.9980 | 1.51 |
| 45 | 0.99024 | 68.7 | 0.5988 | 571.9 | 0.9982 | 1.53 |
| 50 | 0.98807 | 67.9 | 0.5494 | 569.0 | 0.9985 | 1.54 |

[1] *From van Wijk and de Vries (1966). Reprinted by permission of Prof. Daniel A. de Vries.*

The idea supposes that the evolution of warm-blooded animals and the chemical properties of water are related (Kadler and Prockop, 1987). Paul's suggestion created a series of responses (Calder, 1986; Dunitz and Benner, 1986; Bird, 1987; Kadler and Prockop, 1987; McArthur and Clark, 1987; Stevenson, 1987).

The high specific heat of water stabilizes temperatures and results in the relatively uniform temperature of islands and land near large bodies of water (Kramer, 1983, p. 8). This is important for the growth of crops and natural vegetation.

### 3.3.2 Heat of Vaporization

The heat of vaporization of water is the highest known. The heat of vaporization is defined as the amount of heat needed to turn 1 g of a liquid into a vapor, without a rise in the temperature of the liquid. This term is not in the list of definitions given by Weast (1964), so the definition comes from Webster's New World Dictionary of the American Language (1959). The units are cal/gram and values for the heat of vaporization of water at different temperatures are given in Table 3.1. The heat of vaporization is a latent heat. *Latent* comes from the Latin *latere*, which means to lie hidden or concealed. Latent heat is the additional heat required to change the state of a substance from solid to liquid at its melting point, or from liquid to gas at its boiling point, after the temperature of the substance has reached either of these points. Note that a latent heat is associated with no change in temperature, but a change of state. Because of the high heat of vaporization, evaporation of water has a pronounced cooling effect and condensation has a warming effect (Kramer, 1983, p. 8). The cooling effect from evaporation is important in semiarid regions, such as Kansas (see Chapter 28).

### 3.3.3 Heat of Fusion

The heat of fusion of water is unusually high. The heat of fusion is the quantity of heat necessary to change 1 g of a solid to a liquid with no temperature change (Weast, 1964, p. F-44). It is also a latent heat and is sometimes called the latent heat of fusion. It has only one value for water, because water freezes at one value (0 °C), and it is 79.71 cal/g or the rounded number 80 cal/g.

The high heat of fusion of water is used in frost control. Irrigation water drawn from the ground is often at a uniform temperature above freezing. In Nebraska, for example, groundwater is generally at about 12 °C (Rosenberg, 1974, p. 276), and each gram can supply about 12 cal to the air with which it comes in contact. This thermal effect is small, however, when compared to the liberation of heat that occurs when water freezes (80 cal/g). Irrigation water may contribute more than 90 cal/g (12 cal/g + 80 cal/g) in the process of cooling and freezing (Rosenberg, 1974). Fields may be flooded as a means of protecting crops from frost. Such a measure is extreme and is likely to be ineffective in an advective frost, because winds would remove the liberated heat from the flooded fields rapidly and freeze the unprotected vegetation. (In simple terms, advection means that wind is blowing and bringing hot or cold air into an area. We shall discuss advection when we talk about evapotranspiration in Chapter 28).

Sprinkling is a more effective use of irrigation water in frost protection (Rosenberg, 1974, p. 276). Plants are sprinkled at the onset of freezing temperatures. As water freezes onto the plant parts, the heat of fusion is liberated. As long as the freezing continues, the temperature of the ice will remain at 0 °C. Sprinkling must be continued after the sun comes up the next day or until the temperatures have risen to melt the ice. If sprinkling is discontinued prematurely, heat will be drawn from the plant parts to melt the ice and frost damage may occur. Care must be taken when sprinkling tall plants. Ice loads of great weight will break them (Rosenberg, 1974, p. 276).

### 3.3.4 Heat Conduction

Water is a good conductor of heat compared with other liquids and nonmetallic solids, although it is poor compared to metals (Kramer, 1983, p. 8). Thermal or heat conductivity is not defined by Weast (1964), but it is defined in the 2013 edition of the *Handbook of Chemistry and Physics* (Haynes, 2013, p. 2—66) as the "[r]ate of heat flow divided by area and by temperature gradient." Heat conductivity is defined in the 1959 edition of the *Handbook of Chemistry and Physics* (Hodgman, 1959, p. 2431) as "the quantity of heat in calories which is transmitted per second through a plate one centimeter thick across an area of one square centimeter when the temperature difference is one degree Centigrade." The units, therefore, are cal/s/cm$^2$/(°C/cm) or cal/cm/s/°C. Table 3.1 gives values of thermal conductivity of water at different temperatures. The table shows that at 20 °C, water has a thermal conductivity of 0.00144 cal/s/cm/°C. For comparison, copper, a metal, at 18 °C has a thermal conductivity of 0.918 cal/s/cm/°C (Hodgman, 1959, p. 2431), or about a thousand times greater than water. Table 3.1 shows that thermal conductivity of water increases as the temperature increases, and this fact is presented in many textbooks without explanation. Apparently a widely agreed upon explanation does not exist or it is too complicated to present succinctly (Gerard J. Kluitenberg, Department of Agronomy, Kansas State University, personal communication, October 27, 2010).

Survival of crops in the spring can depend on thermal conductivity. There are cases in which soil surface management can prevent a radiation freeze from occurring in row crops. In the spring of 1993, a number of Kansas farmers reported freeze damage in corn fields that had been cultivated. Uncultivated fields had no damage. In some cases the damaged and undamaged areas were adjacent, apparently in locations where the farmer had stopped cultivating for the day. Disturbing the soil by cultivation reduced the thermal conductivity and prevented stored heat from being released back toward the surface (Gerard J. Kluitenberg, personal communication, June 18, 1993). Both the solid soil and the water channels in the soil were disturbed by cultivation. If continuous water channels were broken, then the heat conducted by water upward from lower in the soil was reduced. Lower levels of the soil profile store heat, and, in the early cool spring months in Kansas, this heat can move upward to the cooler soil surface. Remember that in Nebraska groundwater is generally at about 12 °C. As we shall see later, when we discuss linear flow laws (Chapter 7), Fourier's heat flow law (Kirkham and Powers, 1972, p. 75) is a linear flow law and shows that heat is transported according to a temperature gradient. In Kansas, typically we do not start to worry too much about winter survival of winter wheat (*Triticum aestivum*) until temperatures at the crown level (usually 1–2 in or 2.5–5 cm deep) get below 10 to 12 °F (−12.2 to −11.1 °C). Where there is snow cover, soil temperatures will not get that cold. Where there is no snow cover, soil temperatures will depend on how much moisture is in the ground. Soil moisture holds a lot of heat, so even if we get temperatures of 0 °F (−17.8 °C) or below for a few days, the wet soil should not get that cold and winter wheat probably will not be damaged (James P. Shroyer, Kansas State University, personal communication, January 8, 2010).

### 3.3.5 Transparency to Visible Radiation

Water is transparent to visible radiation. This allows light to penetrate bodies of water and makes it possible for algae to photosynthesize at considerable depths (Kramer, 1983, p. 8).

### 3.3.6 Opaqueness to Infrared Radiation

Water is nearly opaque to longer wavelengths in the infrared range. Thus, water filters are good heat absorbers (Kramer, 1983, p. 8). A practical use of water to absorb heat was observed in Israel by Kirkham (1985), who said, "An unusual use of water is illustrated… at the Dead Sea, in Israel, where experiments are underway to get energy from the sun's heat. The salt water in these ponds is heated very hot by the sun, transferred by pipe to a nearby building; exposure to very cold water produces steam, which becomes a potential source of energy." The good absorption of heat by water helps to make this energy production in Israel possible.

We now define the visible and infrared regions of the spectrum. The visible region extends from 3900 to 7800 Å (390–780 nm or 390–780 mμ or 0.390–0.780 μ). The spectrum goes from violet (shortest wavelength), through blue, green, yellow, orange, and to red (longest wavelength). Chlorophyll absorbs in the blue and red regions and reflects in the green. That is why it looks green. The maximum (peak) absorptions in the blue and red regions for chlorophyll a and b are (Stewart, 1964, p. 51):

- Chlorophyll a
  - 4300 Å (blue)
  - 6600 Å (red)
- Chlorophyll b
  - 4700 Å (blue)
  - 6500 Å (red)

The infrared region goes from 7800 to $4 \times 10^6$ Å (Giese, 1962, p. 164). The near infrared extends from 7800 to $2 \times 10^4$ Å, and the far infrared extends from $2 \times 10^4$ to $4 \times 10^6$ Å.

Figure 3.3 illustrates that water is transparent in visible wavelengths, but absorbs at wavelengths in the infrared region. Note that the abscissa in Figure 3.3 extends to 1400 nm (1 nm = 1 mμ), which is in the near infrared region. The near infrared extends to 2000 nm.

## 3.3.7 Surface Tension

Water has a much higher surface tension than most other liquids because of the high internal cohesive forces between molecules (Kramer,

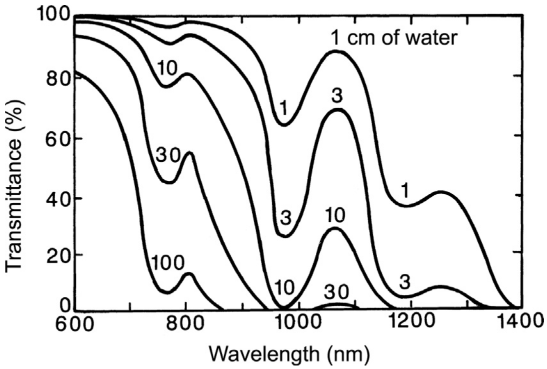

**FIGURE 3.3** Transmission of radiation of various wavelengths through layers of water of different thicknesses. The numbers on the curves refer to the thickness of the layers in centimeters. Transmission is much greater at short than at long wavelengths. *From Kramer (1983). Reprinted by permission of Academic Press.*

1983, p. 8). In Chapter 6 we will discuss surface tension in detail, including Laplace's surface tension theory. The high surface tension of water provides the tensile strength required for the cohesion theory for the ascent of sap (water in the xylem). The cohesion theory is only a theory, but appears to be the best explanation for the rise of water in plants. We shall go into it in detail in Chapter 20 and calculate the tensile strength of water. Surface tension has units of force per unit length or dyne/cm. Table 3.1 gives values of surface tension at different temperatures. Note that the unit given for surface tension in the table is g/s$^2$. This is equivalent to dyne/cm, because, as we saw in Chapter 2,

$$F = ma$$

$$1\ \text{dyne} = 1\ \text{g} \times 1\ \text{cm/s}^2$$

Rearranging, we get

$$g/\text{s}^2 = \text{dyne/cm}.$$

## 3.3.8 Density

Water has a high density and is remarkable in having its maximum density at 4 °C instead of at the freezing point (Kramer, 1983; pp. 8, 9).

## 3.3.9 Expansion Upon Freezing

Water expands on freezing, so that ice has a volume about 9% greater than the liquid water from which it was formed (Figure 3.4). This explains

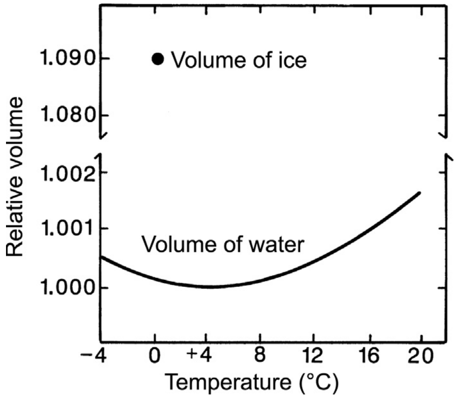

**FIGURE 3.4** Change in volume of water with change in temperature. The minimum volume is at 4 °C, and below that temperature there is a slight increase in volume as more molecules are incorporated into the lattice structure. The volume increases suddenly when water freezes, because all molecules are incorporated into a widely spaced lattice. Above 4 °C, there is an increase in volume caused by increasing thermal agitation of the molecules. *From Kramer (1983). Reprinted by permission of Academic Press.*

why ice floats and pipes and radiators burst when the water in them freezes. If ice sank, bodies of water in the cooler parts of the world would be filled permanently with ice, and aquatic organisms could not survive (Kramer, 1983, p. 9).

### 3.3.10 Ionization

Water is very slightly ionized. Only one molecule in $55.5 \times 10^7$ is dissociated (Kramer, 1983, p. 9).

### 3.3.11 Dielectric Constant

Water has a high dielectric constant. We will not give the equation defining a dielectric, because it requires knowledge of capacitance, which is studied in physics courses. An interested reader can read a physics textbook such as Shortley and Williams (1971, pp. 517–520) to learn more about dielectrics. We will understand a dielectric by using the definition for dielectric in Webster's New World Dictionary of the American Language (1959): "(*dia* = through, across + *electric*: so called because it permits the passage of the lines of force of an electrostatic field, but does not conduct the current); a material, as rubber or glass, that does not conduct electricity; insulator".

Water, therefore, is a good insulator. This might seem contradictory to the fact that we know we shall get electrocuted if we stand in water and put our finger in an electrical outlet. This is because we are standing in tap water, and tap water has salts in it. The electrical conductivity of tap water in Manhattan, Kansas, is 0.54 mmho/cm (=0.54 dS/m where dS is a deci-Siemen) (Kirkham, 1982). So when we say water is a good dielectric, we mean pure water. One should never touch any electrical appliance while taking a bath, including a radio, or work with electrical tools around water.

### 3.3.12 Solvent for Electrolytes

Water is a good solvent for electrolytes, because the attraction of ions to the partially positive and negative charge on water molecules results in each ion being surrounded by a shell of water molecules, which keeps ions of opposite charge separated (Figure 3.5).

### 3.3.13 Solvent for Nonelectrolytes

Water is a good solvent for many nonelectrolytes, because it can form hydrogen bonds with amino and carbonyl groups (Kramer, 1983, p. 9). An amino group has one hydrogen atom in the ammonia molecule replaced by an alkyl or other nonacid radical. A carbonyl is the bivalent radical CO.

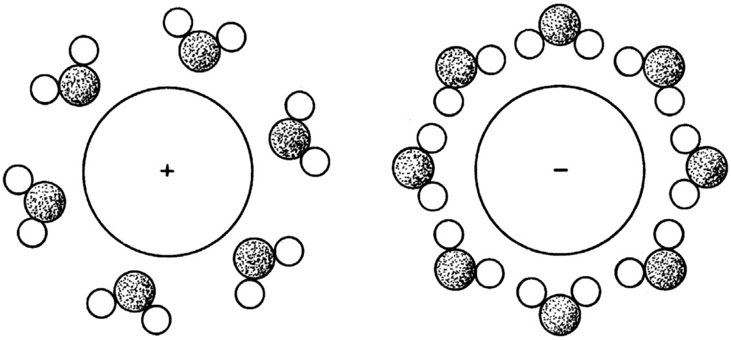

**FIGURE 3.5** Diagram showing approximate arrangement of water molecules in shells oriented around ions. These shells tend to separate ions of opposite charge and enable them to exist in solution. They also disrupt the normal structure of water and slightly increase the volume. *From Kramer (1983). Reprinted by permission of Academic Press.*

### 3.3.14 Adsorption

Water tends to be adsorbed, or bound strongly, to the surfaces of clay micelles, cellulose, protein molecules, and many other substances. This characteristic is of great importance in soil and plant water relations (Kramer, 1983, p. 9). We will see that it is important in the cohesion theory.

### 3.3.15 Viscosity

Water has a high viscosity. The *Handbook of Chemistry and Physics* defines viscosity as follows (Weast, 1964, p. F-62): "All fluids possess a definite resistance to change of form and many solids show a gradual yielding to forces tending to change their form. This property, a sort of internal friction, is called viscosity; it is expressed in dyne seconds per cm$^2$ or poises." The poise is named after Poiseuille, and we will study Poiseuille's law for flow of liquids through capillary tubes in Chapter 15. Table 3.1 gives values for the viscosity of water at different temperatures. The units in the table are g/cm/s. Again, using $F = ma$, we can see that these units are equivalent to dyne seconds per cm$^2$, as follows. We substitute (g cm)/s$^2$ for dyne, and we get

$$(\text{dyne s})/\text{cm}^2 = \left[(\text{g cm})/\text{s}^2\right]\left(\text{s}/\text{cm}^2\right) = \text{g}/\text{cm}/\text{s}.$$

## 3.4 APPENDIX: BIOGRAPHY OF JOHANNES VAN DER WAALS

Johannes Diderik van der Waals (1837–1923), a Dutch physicist, was born in Leyden, The Netherlands, November 23, 1837. He was a self-taught man, who took advantage of the opportunities offered by the University of Leyden. He first attracted notice in 1873 with his treatise "On the Continuity of the Liquid and Gaseous State," the basis for his doctoral degree. He taught physics at various schools, and, in 1877, he was appointed professor of physics at the University of Amsterdam, a post he kept until 1907 (Preece, 1971).

Van der Waals combined the determination of cohesion in the theory of capillarity by Laplace (1749–1827) with the kinetic theory of gases, and this led to the conception of the continuity of the liquid and gaseous states. He arrived at an equation that was the same for all substances by using the values of the volume, temperature, and pressure divided by their critical values (Preece, 1971). His work enabled the liquefaction of gases, which had important practical application during World War I (1914–1918). Although others had studied liquefaction of gases, it was van der Waals who was the first to treat the subject of the continuity of gases and liquids from the standpoint of the mathematical theory of gases (Cajori, 1929, pp. 210–211). Van der Waals was awarded the 1910 Nobel Prize in physics for his research on the equations of state for gases and fluids. He died in Amsterdam on March 9, 1923.

## References

Anderson, J.D., Johnson, T.V., Schubert, G., Asmar, S., Jacobson, R.A., Johnston, D., Lau, E.L., Lewis, G., Moore, W.B., Taylor, A., Thomas, P.C., Weinwurm, G., 2005. Amalthea's density is less than that of water. Science 308, 1291–1293.

Bird, R.J., 1987. Body temperature and the thermodynamics of water. Nature 325, 488–489.

Buchan, G.D., 1996. Ode to $H_2O$. J. Soil Water Conserv. 51, 467–470.

Cajori, F., 1929. A History of Physics. Macmillan, New York.

Calder III, W.A., 1986. Body temperature and the specific heat of water. Nature 324, 418.

Dunitz, J.D., Benner, S.A., 1986. Body temperature and the specific heat of water. Nature 324, 418.

Gerstein, M., Levitt, M., 1998. Molecules of life. Sci. Am. 279 (5), 100–105.

Giese, A.C., 1962. Cell Physiology. W.B. Saunders, Philadelphia.

Haskin, L.A., Wang, A., Jolliff, B.L., McSween, H.Y., Clark, B.C., Des Marais, D.J., McLennan, S.M., Tosca, N.J., Hurowitz, J.A., Farmer, J.D., Yen, A., Squyres, S.W., Arvidson, R.E., Klingelhöfer, G., Schröder, C., de Souza Jr., P.A., Ming, D.W., Gellert, R., Zipfel, J., Brückner, J., Bell III, J.F., Herkenhoff, K., Christensen, P.R., Ruff, S., Blaney, D., Gorevan, S., Cabrol, N.A., Crumpler, L., Grant, J., Soderblom, L., 2005. Water alteration of rocks and soils on Mars at the Spirit rover site in Gusev crater. Nature 436, 66–69.

Haynes, W.M. (Ed.), 2013. Handbook of Chemistry and Physics, ninety-fourth ed. CRC Press, Boca Raton, Florida (pages not numbered sequentially).

Hodgman, C.D. (Ed.), 1959. Handbook of Chemistry and Physics, fortieth ed. Chemical Rubber Publishing, Cleveland, Ohio.

Hotz, R.L., August 3, 2007. In a strange university, we stick to search for familiar life. Wall St. J., 1. Section B.

Isaacs, E.D., Shukla, A., Platzman, P.M., Hamann, D.R., Barbiellini, B., Tulk, C.A., 1999. Covalency of the hydrogen bond in ice: a direct X-ray measurement. Phys. Rev. Lett. 82, 600–603.

Kadler, K., Prockop, D.J., 1987. Protein structure and the specific heat of water. Nature 325, 395.

Kaku, M., November 18, 2009. Water on the moon! Wall St. J., 17. Section A.

Kerr, R.A., 2004. Heavy breathing on Mars? Science 306, 29 (For a picture of sedimentary, water-formed rocks on Mars, see the cover of Science, vol. 306, No. 5702, December 3, 2004, issue, and for a picture of water ice in the north polar region of Mars, see the cover of Science, vol. 307, No. 5715, March 11, 2005, issue.).

Kirkham, D., 1985. Soil, Water, and Hungry Man. Lecture given at the Institute of Water Conservancy and Hydroelectric Power Research, Beijing, China, May, 1985. (Copy available from M.B. Kirkham, Department of Agronomy, Kansas State University, Manhattan, KS 66506.).

Kirkham, D., Powers, W.L., 1972. Advanced Soil Physics. Wiley-Interscience, New York.

Kirkham, M.B., 1982. Water and air conductance in soil with earthworms: an electrical-analogue study. Pedobiologia 23, 367–371.

Kramer, P.J., 1983. Water Relations of Plants. Academic Press, New York.

Leberman, R., Soper, A.K., 1995. Effect of high salt concentration on water structure. Nature 378, 364–366.

London, F., 1930. Zur Theorie und Systematik der Molekularkrafte. Zeitschrift für Physik 63, 245–279.

Luzar, A., Chandler, D., 1996. Hydrogen-bond kinetics in liquid water. Nature 379, 55–57.

Maddox, J., 1985. Recalculating interatomic forces. Nature 314, 315.

McArthur, A.J., Clark, J.A., 1987. Body temperature and heat and water balance. Nature 326, 647–648.

Nobel, P.S., 1974. Introduction to Biophysical Plant Physiology. W.H. Freeman and Company, San Francisco.

Paul, J., 1986. Body temperature and the specific heat of water. Nature 323, 300.

Pauling, L., 1964. College Chemistry, third ed. W.H. Freeman and Company, San Francisco.

Perkowitz, S., 1999. The rarest element. The Sciences 39 (1), 34–38.

Postorino, P., Tromp, R.H., Ricci, M.-A., Soper, A.K., Neilson, G.W., 1993. The interatomic structure of water at supercritical temperatures. Nature 366, 668–670.

Waals, Johannes Diderik van der. In: Preece, W.E. (Ed.), Encycl. Britannica 23, 133.

Rosenberg, N.J., 1974. Microclimate: The Biological Environment. Wiley-Interscience, New York.

Shortley, G., Williams, D., 1971. Elements of Physics, fifth ed. Prentice-Hall, Englewood Cliffs, New Jersey.

Showstack, R., 1999. Scientists discover solar system 44 AU from earth. EOS Trans. Am. Geophys. Union 80, 193–194.

Stevenson, R.D., 1987. Body temperature and the thermodynamics of water. Nature 324, 489.

Stewart, F.C., 1964. Plants at Work. Addison–Wesley, Reading, Massachusetts.

van Wijk, W.R., de Vries, D.A., 1966. The atmosphere and the soil. In: van Wijk, W.R. (Ed.), Physics of Plant Environment, second ed. North-Holland Pub, Amsterdam, pp. 17–61.

Weast, R.C., 1964. Handbook of Chemistry and Physics, forty-fifthth ed. Chemical Rubber Company, Cleveland, Ohio (pages not numbered sequentially).

Webster's New World Dictionary of the American Language, college ed., 1959. World Publishing, Cleveland and New York.

Zubavicus, Y., Grunze, M., 2004. New insights into the structure of water with ultrafast probes. Science 304, 974–976.

CHAPTER

# 4

# Soil—Water Terminology and Applications

Two important expressions used to describe the state of water in the soil are *water content* and *water potential*.

## 4.1 WATER CONTENT

Water content is a measurement of the amount of water in the soil either by weight or volume and is defined as the water lost from the soil upon drying to constant mass at 105°C (Soil Science Society of America, 2008). It is expressed in units of either mass of water per unit mass of dry soil (kg/kg) or in units of volume of water per unit bulk volume of soil ($m^3/m^3$).

## 4.2 WATER POTENTIAL

The second expression utilizes the potential energy status of a small parcel of water (say a milligram) in the soil. The expression applies also to a small parcel of water in a plant. All water in the soil (or plant) is subjected to force fields originating from four main factors: the presence of the solid phase (the matrix); the gravitational field; any dissolved salts; and the action of external gas or water pressure. If the force fields in the soil are compared with a reference point, then they can be expressed on a potential energy basis, and each of the four factors can be assigned a separate potential energy value. The sum of these four potential energy values is called the *water potential* of the soil or the *total water potential* to emphasize that it is comprised of several factors. The water potential is abbreviated using the Greek letter psi, $\Psi$. Subscripts are sometimes added to the letter: $\Psi_W$ stands for water potential and $\Psi_T$ stands for total water potential.

*Principles of Soil and Plant Water Relations*
http://dx.doi.org/10.1016/B978-0-12-420022-7.00004-5

Copyright © 2014 Elsevier Inc. All rights reserved.

The reference point for these potential energies is taken as pure free water at some specified height or elevation. Because water is held in the soil by forces of adsorption, absorption, cohesion, and solution, soil water is usually not capable of doing as much work as pure free water. Hence the soil water potential is normally negative. The old term for soil water potential, no longer used, is the *total soil moisture stress* and it is defined using positive values.

We now describe each component of the water potential.

### 4.2.1 Matric (Capillary) Potential, $\Psi_m$

The *matric potential energy* or the *matric potential* is the portion of the water potential that can be attributed to the attraction of the soil matrix for water. The matric potential used to be called the *capillary potential*, because, over a large part of its range, the matric potential is due to capillary action akin to the rise of water in small, cylindrical capillary tubes (Baver et al., 1972, p. 293). (In Chapter 6, we study in detail the rise of water in soil pores.) However, as the water content decreases in a porous material, water that is held in pores due to capillarity becomes negligibly small, when compared with the water held directly on particle surfaces. The term *matric potential*, therefore, covers phenomena beyond those for which a capillary analogy is appropriate.

The matric potential may be determined with a tensiometer, which measures matric potential of water in situ. (In Chapter 5, we shall describe tensiometers.) The word *tensiometer* refers to the fact that it measures the *soil moisture tension*, a term no longer used in defining the components of the water potential. Other old terms used to describe the matric potential are the *soil moisture suction* or the *matric suction*. As we shall see in Chapter 5, a tensiometer consists of a porous, permeable ceramic cup connected through a water-filled tube to a manometer, vacuum gauge, or other pressure measuring device. Water pressure in the manometer comes into equilibrium with the adjacent soil through flow across the ceramic cup. The height of the liquid column at that time is an index of matric potential. Soil moisture tension has been represented often with a positive sign, in which case it can be considered to be numerically equivalent to, but opposite in sign to, the matric potential.

The units used to measure matric potential, and other potentials, become evident when we consider measurement of matric potential with a tensiometer. The force per unit area, or negative pressure of the water in the porous cup, is the weight per unit cross section of the hanging column. This is the volume of the column divided by the area multiplied by the density of the liquid water and the acceleration due to gravity (Baver et al., 1972, pp. 294–295):

$$P = F/A = mg/A = (V)(\rho_w)(g/A) = (hA\rho_w g)/A = h\rho_w g \qquad (4.1)$$

where $P$ = pressure; $F$ = force; $m$ = mass; $g$ = acceleration due to gravity; $A$ = area; $V$ = volume; $\rho_w$ = density of water; $h$ = height, and the potential (negative pressure) is in units of potential energy or work per unit volume. In the centimeter-gram-second (CGS) system of units, 1020 cm of water would exert a negative pressure of

$$(1020\ \text{cm})\left(1\ \text{g/cm}^3\right)\left(980\ \text{cm/sec}^2\right) = 999,600\ \text{dyne/cm}^2 \qquad (4.2)$$

or $1 \times 10^6$ dyne/cm$^2$ = 1 bar, because, in cgs pressure units, 1 bar = $1 \times 10^6$ dyne/cm$^2$. The SI (Système International) unit for pressure is the Pascal, which is 1 N/m$^2$, and thus 10 bars = 1 MPa or 1 MegaPascal. The unit (dyne/cm$^2$) is the same as potential energy/volume, because if we multiply the top and bottom of the fraction, $F/A$, in Eqn (4.1) by 1 cm (=cm/cm = unity), we get work/volume = potential energy/volume:

$$[(\text{dyne})(\text{cm})]/\left[\left(\text{cm}^2\right)(\text{cm})\right] = \text{potential energy/volume} = \text{erg/cm}^3,$$

because 1 dyne cm = 1 erg.

Units of potential energy per unit volume can be converted to units of potential energy per unit mass by dividing by the density of water, which we shall take to be 1 g/cm$^3$:

$$\left(1 \times 10^6\ \text{dyne/cm}^2\right)/1\ \text{gram/cm}^3 = 1 \times 10^6\ \text{dyne cm/gram}$$
$$= 1 \times 10^6\ \text{erg/gram} = 100\ \text{joule/kg},$$

because 1 J = $1 \times 10^7$ erg. Or, 1 bar can be considered to be the equivalent of 100 J/kg. Note that the units of matric potential are not equal to potential energy units (ergs; joules), but can be given in units of potential energy/vol or potential energy/mass.

Note that in Eqn (4.1), if the acceleration due to gravity, $g$, were not constant, we could not equate pressure to a length unit. However, the acceleration due to gravity can be considered a constant on the earth. We can determine it using Helmert's equation (Weast, 1964, p. F-29):

$$g = 980.616 - 2.5928 \cos 2\varphi + 0.0069 \cos^2 2\varphi - 3.086 \times 10^{-6} H \qquad (4.3)$$

where

$g$ = acceleration due to gravity in cgs units (cm/s$^2$).

$\varphi$ = latitude.

$H$ = elevation (cm).

F.R. Helmert was the director of the Prussian Geodetic Institute. In 1915, Helmert introduced his equation to determine $g$, the acceleration due to gravity (Lambert, 1956).

Helmert's equation comes from the inverse square law of gravity or Newton's law of universal gravitation (Shortley and Williams, 1971, p. 61):

$$F = [G(m_1 m_2)]/R^2 \tag{4.4}$$

where

$F$ = gravitation force.

$m_1$ and $m_2$ are masses of two particles.

$R$ = distance between the two particles.

$G$ = fixed proportionality constant = gravitation constant.

The units of $G = (\mathrm{N\ m^2})/\mathrm{kg}^2$ or $\mathrm{m^3}/(\mathrm{kg\ s^2})$.

Using the first set of units for $G$, $G = 6.67 \times 10^{-11}\ \mathrm{N\ m^2/kg^2}$.

In words, the principle of universal gravitation states that every particle of matter in the universe attracts every other particle with a gravitational force. The magnitude of the gravitational force between two particles is proportional to the product of the masses of the particles and inversely proportional to the square of the distance between them. The gravitational forces of attraction between two particles act along the line joining the two particles (Shortley and Williams, 1971, p. 61).

The following information comes from Don Kirkham (personal communication, February 6, 1992). The law of universal gravitation governs planets and satellites. We can imagine a mass at the center of the earth as the basis for the pull to the earth (the *center of mass*; also called the *center of gravity*; Shortley and Williams, 1971, p. 167). The pull depends upon where on the surface of earth we are, but this pull holds only if earth is static. However, the earth spins and this affects the pull. That is, how close we are to the axis (to the center of the earth) affects the pull. We can imagine ourselves spinning on a saucer or a wheel. We are thrown off differently if we are at the middle or tip of the wheel. If we are standing on the equator, we are thrown off more. The first cosine terms in Helmert's equation (first one to the right of the equal sign in Eqn (4.3)) relates to latitude. At the equator, cos 0 = 1, and when we go up to the North Pole, we are at 90°. The earth spins toward the east, and we have to take this into consideration in Helmert's equation. The cosine term takes into account the Coriolis effect due to the earth's spin. The Coriolis effect is an apparent force, relative to the earth's surface, that causes deflection of moving objects to the right in the Northern Hemisphere and to the left in the Southern Hemisphere due to the earth's rotation. It is named for Gustav Gaspard de Coriolis (1792–1843), a French mathematician who published a quantitative mathematical work on the subject in 1835 (Glickman, 2000). As we get closer to the equator, the Corilois effect gets less. The other cosine term relates to the fact that the earth is not a perfect spheroid, but an ellipsoid. The earth bulges out at the equator. Height, $H$, affects gravity, too, because the further we are away from the center of mass, the less is the pull of gravity. Note we subtract the $H$ term in Helmert's equation. We can calculate $g$ for Manhattan, Kansas, which is 1065 ft (32,461 cm) above sea level and is at latitude 39°12′ or 39.2°. We find that $g$ for Manhattan, Kansas, is 979.99475 cm/s$^2$, which rounds off to 980 cm/s$^2$, the gravitational constant in the CGS system for the earth.

One might say, why bother with $g$? We are bothering with $g$ to show it is a constant, so Eqn (4.1) can be used to equate a pressure to a length. Even though the acceleration due to gravity is essentially a constant, variations in it are important in exploration for minerals. The concentration of many metals will change the period of a pendulum. A pendulum and $g$ are related because the equation giving the frequency of oscillation of a pendulum includes $g$. (See Chapter 8 for definitions of frequency and period.) Therefore, the relation can be used to determine gravitational acceleration by measuring the frequency of a pendulum (Shortley and Williams, 1971, pp. 253–254). This method furnishes one of the most accurate means of measuring $g$.

### 4.2.2 Gravitational Potential, $\Psi_g$ or $\Psi_z$

The *gravitational potential energy* or the *gravitational potential* is the potential energy associated with vertical position. The reference height or datum assigned can vary according to need and is often based on utility. It is generally convenient to keep the reference level sufficiently low so that one does not get negative values. Solutions to problems are prone to error when negative numbers are used. Land surveyors take their datum at a level below the lowest level that they expect to encounter on their survey to ensure that all of their levels will be positive. Soil scientists often take either the soil surface or the groundwater level as the reference level. The reference level usually depends on the direction of water movement: rising or infiltration. If the reference level is below the point in question, work must be done on the water and the gravity potential is positive; if the level is above the point in question, work is done by the water and the gravity potential is negative (Baver et al., 1972, p. 296).

### 4.2.3 Solute Potential, $\Psi_s$

The *solute potential energy* or *solute potential* is the portion of the water potential that can be attributed to the attraction of solutes for water. If pure water and solution are separated by a membrane, pressure will build up on the solution side of the membrane that is equivalent to the energy difference in the water on the two sides of the membrane. This pressure,

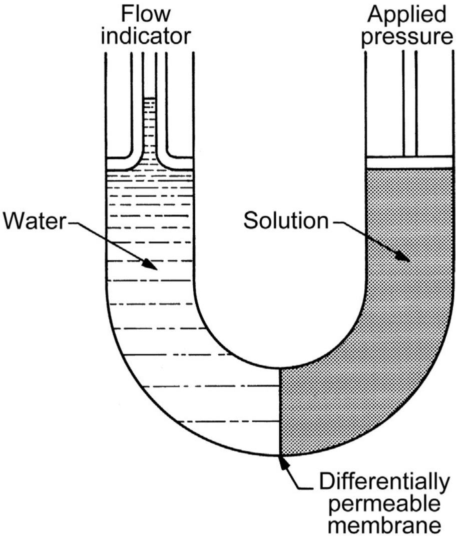

**FIGURE 4.1** Diagram of an osmometer in which a membrane permeable to water but impermeable to a solution separates pure water from the solution. The osmotic pressure of the solution is equal to the pressure that must be applied to prevent movement of water into it. Water movement is observed by a change in the level of water in the capillary tube on the left. *From Kramer (1983). Reprinted by permission of Academic Press.*

which is usually called the *osmotic pressure*, is numerically equivalent, but opposite in sign, to the solute potential. The solute potential in soil is often called the *osmotic potential*, $\Psi_O$, even if no membranes are present. The osmotic potential is usually ignored in determining water movement in the soil, unless the soil is saline. Osmotic potential is important in plants and is discussed in Chapter 17.

An osmometer is used to measure osmotic pressure (Figure 4.1). It consists of a U-tube that contains dissolved substances in solution on one side, which is separated from pure water in the other arm by a semipermeable membrane at the bottom. The osmotic pressure of the solution is equal to the pressure that must be applied to prevent movement of water into it (Kramer, 1983, p. 18). The membrane must have openings that are large enough to permit passage of water molecules but too small for ions of the dissolved substance to pass through (Baver et al., 1972, p. 298).

### 4.2.4 Pressure Potential, $\Psi_P$

The *pressure potential energy*, or *pressure potential*, is the potential energy due to the weight of water at a point under consideration, or to gas pressure that is different from the pressure that exists at a reference position (Baver et al., 1972, p. 297). Sometimes this pressure potential energy is divided into two separate components: the *air pressure potential*, which occurs under unsaturated conditions when the soil has an air phase, and the *hydrostatic pressure potential*, which occurs when the soil is saturated and there is a hydrostatic pressure from an overlying water phase (Jury et al., 1991, p. 51). In saturated soil, the pressure potential is sometimes called the *piezometric potential* (Baver et al., 1972, p. 297), because it can be measured with a *piezometer*. A piezometer is an instrument used to measure pressure. The word comes from the Greek *piezein*, which means "to press", and *meter*, which comes from *metron*, a measure (Webster's New World Dictionary of the American Language, 1959). It is a tube placed in soil with its top end open to the atmosphere. It also may have openings in the wall at the point where the pressure measurement is to be taken. The level of water in the tube, measured from a suitable reference, is the piezometer reading. Piezometers are used to measure groundwater depth. Pressure potentials due to gas may be measured with manometers.

### 4.2.5 Other Potentials Defined

Occasionally, a *tensiometer pressure potential*, which is the potential measured with a tensiometer, is defined (Jury and Horton, 2004, p. 54). The matric potential differs from the potential measured with a tensiometer, because the soil air pressure is maintained at the reference pressure. The reference pressure can be atmospheric pressure. However, the difference between atmospheric pressure and air pressure in the soil is usually ignored, and the potential measured with a tensiometer is considered to be the matric potential. But if one were comparing measurements of matric potential made with a tensiometer on top of a mountain and at sea level, then one would have to consider air pressure differences.

Other potentials may be defined according to need, such as an *overburden potential*, which occurs when the soil is free to move and some part of its weight becomes involved as a force acting upon water at the point in question (Baver et al., 1972, p. 299). Such an overburden potential might occur in soil under a ridge in a ridge-till system. But the pressure exerted by the weight of the soil in the ridge would be small. When a potential that is not zero is neglected, it must be assumed that it is implicitly included in one of those that is explicit in the definition. For example, when overburden potential is neglected, it becomes implicit in the pressure potential or matric potential.

In both soil and plant systems the water potential is usually considered to be the sum of the four potentials described in the preceding sections: matric potential, gravitational potential, solute potential (or osmotic potential), and pressure potential, or

$$\Psi = \Psi_m + \Psi_g + \Psi_s(or\ \ \Psi_o) + \Psi_p \tag{4.5}$$

Water moves in response to differences in water potential. The difference is called the *water potential difference*. The *water potential gradient* is the potential difference per unit distance of flow. Water moves from high potential energy to low potential energy. Under nonsaline, unsaturated conditions, the two most important potentials in the soil are the matric potential and the gravitational potential, and both must be considered in determining the direction of flow of water. Under nonsaline, saturated conditions, the two most important potentials in the soil are the (hydrostatic) pressure potential and the gravitational potential, and the difference in the sum of these two potentials, called the *hydraulic head difference*, governs the soil water flow. In plants, the two most important components of the water potential are the osmotic potential and the pressure potential, also called the turgor potential (see Chapter 17).

## 4.3 HEADS IN A COLUMN OF SOIL

A head is a source of water kept at some height to supply, for example, a mill. Hence, it is a pressure, as in a *head* of steam (Webster's New World Dictionary of the American Language, 1959). Instead of using potential terminology, we can express potential in terms of head (a length). As we saw in Eqn (4.1), the tension, or negative pressure, that develops in a tensiometer is

$$F/A = h\rho_{\mathrm{w}}g,$$

where $F$ = force; $A$ = area; $h$ = height; $\rho_{\mathrm{w}}$ is the density of water; and $g$ is acceleration due to gravity. Because the density of water and acceleration due to gravity are constants, we can relate a pressure or negative pressure, in terms of potential energy per unit volume, to a length. Engineers prefer to work with lengths (heads) rather than potentials because they are easier to measure and keep track of.

So our equation for water potential in soil, Eqn (4.5), $\Psi = \Psi_{\mathrm{m}} + \Psi_{\mathrm{g}} + \Psi_{\mathrm{s}}$ (or $\Psi_{\mathrm{o}}$) + $\Psi_{\mathrm{p}}$, becomes in head terminology the following for a nonsaline soil ($\Psi_{\mathrm{s}}$ or $\Psi_{\mathrm{o}}$ is negligible):

$$h = h_{\mathrm{t}} + h_{\mathrm{g}} + h_{\mathrm{p}} \tag{4.6}$$

where $h$ = total head; $h_{\mathrm{t}}$ = tension head (we call it the tension head instead of the matric head); $h_{\mathrm{g}}$ = gravitational head; and $h_{\mathrm{p}}$ = pressure head.

Under saturated conditions when there is no tension head, the total head is

$$h = h_{\mathrm{p}} + h_{\mathrm{g}}.$$

When the soil is under tension (but the pores can be filled with water, i.e., saturated, yet the water is under tension, which we discuss in Chapter 6), we have

$$h = h_{\mathrm{t}} + h_{\mathrm{g}}.$$

or

$$h = (h_{\mathrm{p}} \text{ or } h_{\mathrm{t}}) + h_{\mathrm{g}}.$$

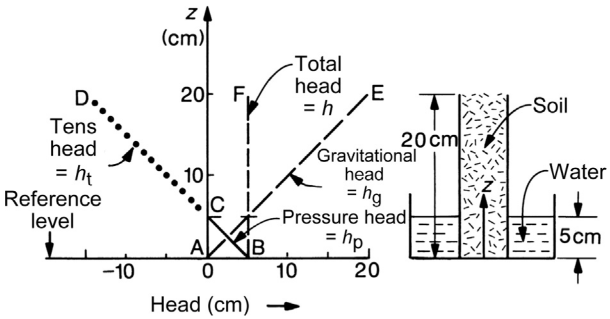

**FIGURE 4.2** Heads in a column of wet soil. *From Kirkham and Powers (1972). This material is used by* permission *of John Wiley & Sons, Inc. and William L. Powers.*

The total head $h$ is usually called the *hydraulic head*. Let us apply head terminology to determine heads in a column of soil. We follow the analysis of Kirkham and Powers (1972, pp. 36–37) and plot the four heads $h$, $h_g$, $h_p$, and $h_t$, in a column of wet soil. (For a biography of W.L. Powers, see the Appendix, Section 5.) In Figure 4.2 we have plotted the various heads against distance $z$ above the base of a soil column standing in 5 cm of water. The water in the column is assumed to be saturated to the top above the 5 cm level by capillarity and is at equilibrium. Evaporation from the top of the soil is prevented. The reference level for heads is the level of the base of the column. The line AE is a graph of height $z$ versus gravitational head $h_g$; the line BC is of $z$ versus pressure head $h_p$; CD is of $z$ versus tension head $h_t$; and BF is of $z$ versus total head $h$. The line BF is vertical because at all heights $z$ in the column the abscissas $h_g$ and $h_t$ (or $h_p$) must add up to the same value $h$, the total head (=5 cm). Otherwise, the water in the column could not be in equilibrium and the water would move. The equilibrium conditions for the column may be written symbolically as

$$h_g + h_p = h = 5\text{ cm}, \quad \text{for } z \text{ between } 0\text{ cm and } 5\text{ cm}$$

and

$$h_g + h_t = h = 5\text{ cm}, \quad \text{for } z \text{ between } 5\text{ cm and } 20\text{ cm}.$$

The line BC in the graph shows that the pressure head decreases linearly from 5 cm of head to 0 cm of head as the height $z$ increases from 0 to 5 cm. From $z = 5$ cm to $z = 20$ cm the pressure becomes negative; that is, tension develops. The tension at level E is 15 cm of water, a negative pressure. If evaporation were permitted at the soil surface, the tension head there would be of greater magnitude than 15 cm and curves CD and BF would change from their shown positions. In Figure 4.2 the tension head $h_t$ is that resulting from water curvature in the pores, which we shall discuss in Chapter 6. "Equivalent" tension heads obtained by indirect methods such as freezing-point depression do not reflect film curvature, and when such equivalent tension heads are plotted on a graph with tensions as measured by a tensiometer, the freezing-point-depression values may be three times as great in magnitude as the tensiometer values, and confusion may result (Kirkham and Powers, 1972, p. 37). The freezing-point method to determine the free energy of water in soil is described by Richards (1965, pp. 137–139).

In Figure 4.2, tension could be determined with a tensiometer for the distance of $z$ between 5 and 20 cm, and pressure could be determined with a piezometer for the distance of $z$ between 0 and 5 cm.

## 4.4 MOVEMENT OF WATER BETWEEN TENSIOMETERS

Because we can equate pressure or negative pressure or tension with height, let us use height to determine the direction of movement of water in soil with two tensiometers. All we need is a ruler. Figure 4.3, as modified from Richards (1941) and reproduced by Kirkham and Powers (1984, p. 240), gives a physical picture of how the tension head $h_t$ and the gravitational head $z$ combine to give the total head $h$. Tensiometers are shown with water manometers inside of the soil. In actuality, the water manometers would be replaced by mercury manometers above the soil. The physical principles are clearer if the water manometers are

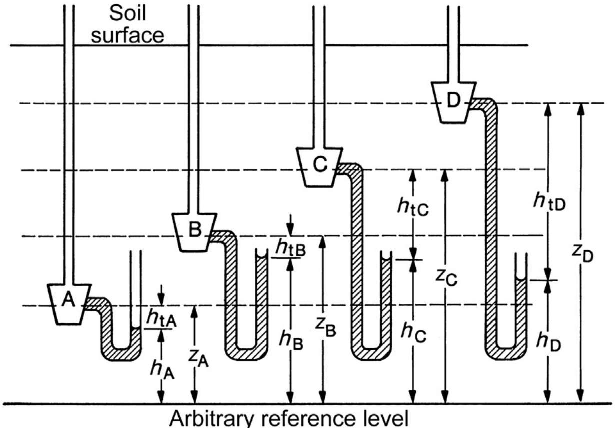

**FIGURE 4.3** Diagram to illustrate water movement between tensiometers. *From Kirkham and Powers (1984), ©1972, John Wiley & Sons, Inc.: New York. This material is used by permission of John Wiley & Sons, Inc. and William L. Powers.*

represented as shown. The reference level for head is taken at a depth $z_D$ below the center of the uppermost tensiometer cup.

In Figure 4.3 we notice that for each location, A, B, C, and D, the total head is given by $h = h_t + z$ (where $h_t$ is negative). For location A and B, $h_{tB}$ has been taken equal to $h_{tA}$. Thus, the soil moisture is of equal dryness at A and B; but this does not mean that the soil moisture will be statically held between A and B. On the contrary, since the total head $h_B$ is seen to be greater than $h_A$, moisture will move from B to A. At locations C and B we see that $h_{tC}$ has been taken to be more negative than $h_{tB}$. Thus, the soil is drier at C than at B, but moisture will not move from the wetter soil at B to the drier soil at C because we have chosen conditions such that the total head $h_B$ is equal to $h_C$. Therefore, moisture neither moves from B to C nor from C to B; the moisture is in equilibrium. Finally, we note that moisture will move upward from C to D because our moisture conditions at points C and D have been chosen such that $h_C$ is greater than $h_D$. However, we notice that because $h_{tD}$ is more negative than $h_{tC}$ (tension is greater for D than C), the soil at D has to be considerably drier than at C to cause the upward movement. In Figure 4.3, if the reference level were at the top of the figure, the values $h_A$, $h_B$, and so on would always be negative; $h_t$, of course, is negative for unsaturated soil regardless of the location of the reference level (Kirkham and Powers, 1984, pp. 241−242).

## 4.5 APPENDIX: BIOGRAPHY OF WILLIAM L. POWERS

William LeRoy Powers is the son of LeRoy Powers, a geneticist and breeder of agronomic and horticultural crops, who worked for the Agricultural Research Service of the United States Department of Agriculture on the campus of Colorado State University in Fort Collins (Cattell, 1961). LeRoy Powers was a famous geneticist and excellent statistician (George L. Liang, personal communication, July 26, 2002), who published a classic paper in plant genetics (Powers, 1963). William Powers received his B.S. degree at Colorado State and joined the Department of Agronomy at Iowa State University in the fall of 1960 to pursue a master's degree and Ph.D. under Don Kirkham. He obtained his M.S. degree in 1962 and the Ph.D in 1966; the title of his Ph.D dissertation was "Solution of Some Theoretical Soil Drainage Problems by Generalized Orthonormal Functions". After he obtained his Ph.D he moved to Kansas State University, where he rose through the academic ranks to professor and became Director of the Evapotranspiration Laboratory and Director of the Kansas Water Resources Research Institute. In 1980, he accepted the position of Director of the Water Resources Center at the University of Nebraska in Lincoln.

He wrote, with Don Kirkham, *Advanced Soil Physics* (Wiley: New York, 1972; reprint edition, 1984). His research included developing formulas for applying organic wastes to soils; water-balance studies; pore-size distribution as an index of atrazine movement; tillage effects on soil water release curves; estimating soil water content from soil strength; 2,4,6-trinitrotoluene (TNT) sorption in soil; spatial series analysis of horizontal soil cores to characterize tracer patterns; physical and chemical characteristics of aging golf greens; and spatial analysis of machine-wheel traffic and its effects on soil physical properties.

He married in 1958, and he and his wife, Marty, a registered nurse, have two daughters, Jenny and Susan. He retired from the University of Nebraska on July 31, 2001, and spends his retirement doing volunteer work, including volunteering at the Veteran's Administration Hospital in Lincoln, Nebraska, and tutoring in the GED (general equivalency degree; it certifies that one has an educational level equivalent to a high school graduate) program at Southeast Community College in Lincoln, Nebraska.

## References

Baver, L.D., Gardner, W.H., Gardner, W.R., 1972. Soil Physics, fourth ed. Wiley, New York.

Cattell, J. (Ed.), 1961. American Men of Science. A Biographical Directory. The Physical and Biological Sciences, 10th ed. Jaques Cattell Press, Tempe, Arizona, p. 3234.

Glickman, T.S. (Ed.), 2000. Glossary of Meteorology, second ed. American Meteorological Society, Boston, Massachusetts.

Jury, W.A., Gardner, W.R., Gardner, W.H., 1991. Soil Physics, fifth ed. Wiley, New York.

Jury, W.A., Horton, R., 2004. Soil Physics, sixth ed. Wiley, Hoboken, New Jersey.

Kirkham, D., Powers, W.L., 1972. Advanced Soil Physics. Wiley, New York.

Kirkham, D., Powers, W.L., 1984. Advanced Soil Physics, Reprint ed. Robert E. Krieger, Malabar, Florida.

Kramer, P.J., 1983. Water Relations of Plants. Academic Press, New York.

Lambert, W.E., 1956. Geodesy. Encyclopaedia Britannica 10, 134.

Powers, L., 1963. The partitioning method of genetic analysis and some aspects of its application to plant breeding. In: Hanson, W.D., Robinson, H.F. (Eds.), Statistical Genetics and Plant Breeding. Pub. No. 982. National Academy of Sciences-National Research Council, Washington, DC, pp. 280–318.

Richards, L.A., 1941. Hydraulics of water in unsaturated soil. Agr. Eng. 22, 325–326.

Richards, L.A., 1965. Physical condition of water in soil. In: Black, C.A., Evans, D.D., White, J.L., Ensminger, L.E., Clark, F.E. (Eds.), Methods of Soil Analysis. Part 1. Physical and Mineralogical Properties, Including Statistics of Measurement and Sampling. American Society of Agronomy, Madison, Wisconsin, pp. 128–152.

Shortley, G., Williams, D., 1971. Elements of Physics, fifth ed. PrenticesHall, Englewood Cliffs, New Jersey.

Soil Science Society of America, 2008. Glossary of Soil Science Terms 2008. Soil Science Society of America, Madison, Wisconsin.

Weast, R.C., 1964. Handbook of Chemistry and Physics, 45th ed. Chemical Rubber Company, Cleveland, Ohio.

Webster's New World Dictionary of the American Language, College ed., 1959. World Publishing, Cleveland.

CHAPTER

# 5

# Tensiometers

As we noted in the Preface and Chapter 1, in this book, we shall study water as it moves through the soil–plant–atmosphere continuum (SPAC) and the ways to measure this water. Now that we have learned the basic physical definitions (Chapter 2), the structure and properties of water (Chapter 3), and the soil–water terminology (Chapter 4), we turn to the main topic of water in the SPAC. We first focus on water in soil. We begin by learning how to measure the status of water in the soil using a tensiometer.

## 5.1 DESCRIPTION OF A TENSIOMETER

A tensiometer is a device for measuring, when the soil is not too dry, the soil matric potential. In old terminology, the matric potential was called the *soil moisture tension* (Chapter 4). Because the instrument measures tension, it was called a *tensiometer*. For a review of the early literature on tensiometers, see Richards (1949). However, the instrument could have been called an "ergmeter" (Don Kirkham, Departments of Physics and Agronomy, Iowa State University, personal communication, February 10, 1994). As we saw in Chapter 4, we can express tension of water in soil in terms of tension head (using units of length) or in terms of potential energy per unit mass (e.g., ergs/gram) or potential energy per unit volume (e.g., joule/m$^3$ or dyne/cm$^2$; remember 1 bar $= 1 \times 10^6$ dyne/cm$^2$).

A tensiometer consists of a porous, permeable ceramic cup connected through a water-filled tube to a manometer, vacuum gauge, pressure transducer, or other pressure measuring device (Soil Science Society of America, 2008). As noted, we use the tensiometer to measure matric potential. A matric potential exists in soil when the soil is unsaturated and the water in the soil is under tension. We use a piezometer to measure water in saturated soil. A piezometer is an instrument used to measure pressure. Some soil physicists call the matric potential the pressure potential or the pressure head. In our work, we shall confine the terms

*Principles of Soil and Plant Water Relations*
http://dx.doi.org/10.1016/B978-0-12-420022-7.00005-7

Copyright © 2014 Elsevier Inc. All rights reserved.

*pressure potential* and *pressure head* to saturated soil (Chapter 4). Tensiometers do not measure osmotic potential because they are not sensitive to the osmotic effects of dissolved salts in the soil solution (Richards, 1965).

Because much soil—water theory and experimentation deals with the matric potential, we need to know how a tensiometer works (Kirkham and Powers, 1972, p. 29). Two key relationships that are necessary before soil physicists can model water in unsaturated soil are (1) the relationship between soil matric potential and soil water content and (2) the relationship between soil hydraulic conductivity and soil matric potential (van Genuchten, 1980).

Let us consider an impractical, but instructive, type of tensiometer in which a tension height $h_t$ is developed by means of the tensiometer porous cup in contact with moist soil (Figure 5.1). The small pores in a tensiometer cup serve to make connections between the soil water held in soil pores and a tension column. The pores of the cup must be smaller than the soil pores in which the tension is to be measured; otherwise, air may enter the cup. If air enters the cup, we have reached the air-entry value for that porous cup. Each porous cup has an air-entry value. Air comes out of solution. If air enters, we have cavitation, which is the formation of partial vacuums in a flowing liquid, as a result of the separation of its parts. Cavitation comes from the Latin word *cavitas*, which means a hollow or a cavity.

In Figure 5.1, we have dug a pit into the soil to accommodate the tensiometer. But it is usually impractical to dig a pit, so in Figure 5.2, a column of water of height $d_1$ extending into the ground is replaced by an

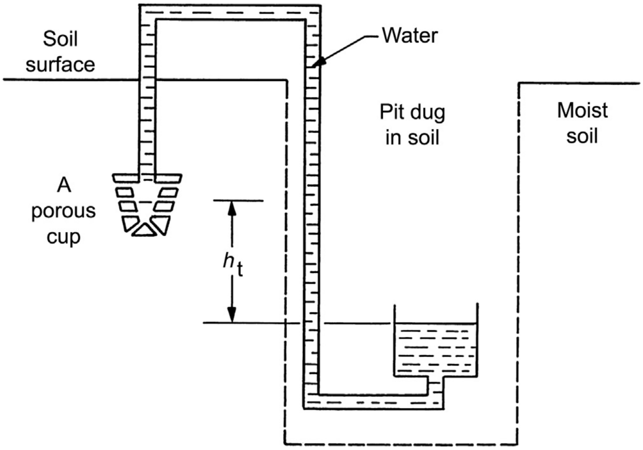

**FIGURE 5.1** A form of tensiometer. *From Kirkham and Powers (1972). This material is used by permission of John Wiley & Sons, Inc. and William L. Powers.*

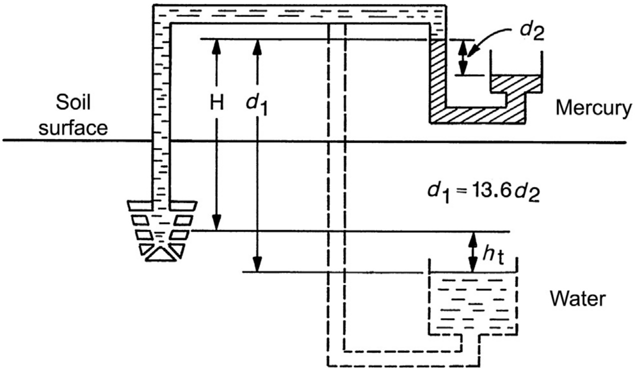

**FIGURE 5.2** Equivalent water and mercury tensiometers. *From Kirkham and Powers (1972). This material is used by permission of John Wiley & Sons, Inc. and William L. Powers.*

equivalent, and much shorter, column of mercury of height $d_2$ above ground. With distances $h_t$, $H$, $d_1$, and $d_2$ as shown in the figure, the tension height $h_t$ is given by $h_t = d_1 - H = 13.6d_2 - H$, where $d_1$ is replaced by $13.6d_2$ because 13.6 g/cm$^3$ is the density of mercury, making 1 cm of mercury column give the same pressure as 13.6 cm of water column. In our equation, we consider that 13.6 is the specific gravity of mercury taken to be numerically equal to its density in gram per cubic centimeter. The units of specific gravity equal unity. Specific gravity is the ratio of the weight or mass of a given volume of a substance to that of an equal volume of another substance (water for liquids and solids; air or hydrogen for gases) used as a standard, and its dimensions are unity.

The pores in the porous cup and the reservoirs in the two figures (Figures 5.1 and 5.2) have been drawn large for instructive purposes. In practice, the reservoirs are made as small as practical to limit water flow to the soil from the cup. In the laboratory, one can use a porous plate apparatus (Figure 5.3) to measure soil moisture tension in soil cores. In Figure 5.3, the height $h_t$ is the tension height.

The tension height $h_t$ of a tensiometer cannot in practice exceed about 3/4 bar or about 750 cm of water column. (In Chapter 4, we showed that 1020 cm water = 1 bar.) This is due to air coming out of solution at the reduced pressure to break the continuity of the water column. The 750 cm value does not mean that water will not have a tension >750 cm in a soil, but that 750 cm of tension is all the tension that a tensiometer can measure (Kirkham and Powers, 1972, p. 30).

Dr L.A. Richards was one of the early developers of the tensiometer (see the Appendix, Section V, for his biography). Before he moved to the U.S. Salinity Laboratory in Riverside, California, he worked at Iowa State University (then called Iowa State College) in Ames, Iowa. In his laboratory in Curtiss Hall, the early tensiometers he used were water-filled

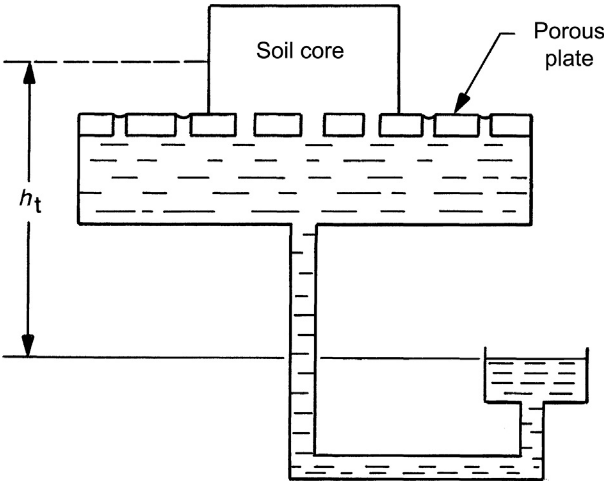

**FIGURE 5.3** Porous plate apparatus. *From Kirkham and Powers (1972). This material is used by permission of John Wiley & Sons, Inc. and William L. Powers.*

tensiometers. To have a long enough water tube, he drilled a hole through the ceiling of one of the floors in Curtiss Hall so the tube could span the length of two floors. When one of his successors, Don Kirkham, moved to Iowa State in 1946, this hole was still in Curtiss Hall. Mercury manometers obviate the need to drill holes through ceilings to take measurements with tensiometers.

For values of $h_t$ >750 cm, pressure apparatus may be used. To see how a pressure apparatus works, we consider Figure 5.4. In this figure, three capillary tubes are shown with the heights of the water rise as $h_{t1}$, $h_{t2}$, and $h_{t3}$. The bottoms of the capillary tubes rest either on a porous ceramic plate or a porous membrane. A bell jar covers the capillary tubes and pressure may be introduced in the jar. The figure is drawn for the case of initially

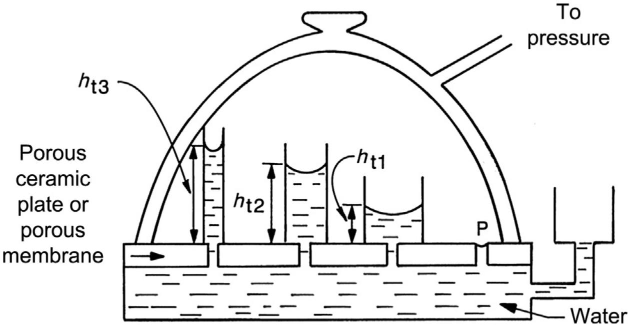

**FIGURE 5.4** Pressure apparatus. *From Kirkham and Powers (1972). This material is used by permission of John Wiley & Sons, Inc. and William L. Powers.*

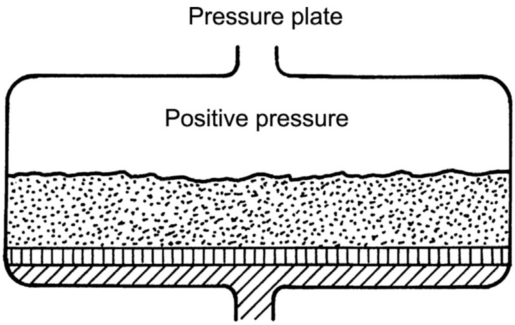

**FIGURE 5.5** Pressure plate. Inside the plate, soil is on a porous membrane. The heavy steel plate allows high pressures to be applied. *From Baver, Gardner, and Gardner (1972). This material is used by permission of John Wiley & Sons, Inc.*

atmospheric pressure. If now a pressure equal to a $h_{t1}$ cm of water column is applied, the column $h_{t1}$ will drain to the top level of the membrane. If $h_{t2}$ cm of pressure is applied, column $h_{t2}$ will drain to the top level of the membrane, and if $h_{t3}$ cm of pressure is applied, all three will drain. If a porous membrane is used, pores in the membrane such as the one at $P$ will not drain unless pressures of about 30 or more bars are applied. At high pressures, a bell jar cannot be used. Instead, pressure equipment made of heavy steel plate, called pressure plate or pressure membrane apparatus, is used (Figure 5.5). It works up to a pressure of 30 or even 100 bars (Kirkham and Powers, 1972, p. 32).

## 5.2 TYPES OF TENSIOMETERS

Tensiometers have three types of read-outs: mercury manometer assemblies, vacuum dial gauges, and pressure transducers. Instruments that have mercury manometers are attached to tubes of varying lengths with porous cups at the base that are inserted into the soil (Figure 5.6). Mercury manometers are no longer available commercially. This is due to the fact that mercury cannot be sent through the mail (Mary C. Knapp, State Climatologist for Kansas, personal communication, September 7, 2011). (Consequently, the mercury thermometers at the official weather station for Manhattan, Kansas, have been replaced by thermometers with a digital display, which is constantly changing.) However, even though mercury manometers have fallen out of favor, one still can build custom-made mercury tensiometers. They then can be employed for special purposes, for example, measuring the matric potential of soil in greenhouse pots. They provide excellent accuracy (Loyd R. Stone, Department of Agronomy, personal communication, June 8, 2013).

Tensiometers now used have read-outs using vacuum dial gauges or pressure transducers. Soilmoisture Equipment Corporation (Santa Barbara, California) provides tensiometers with vacuum dial gauges,

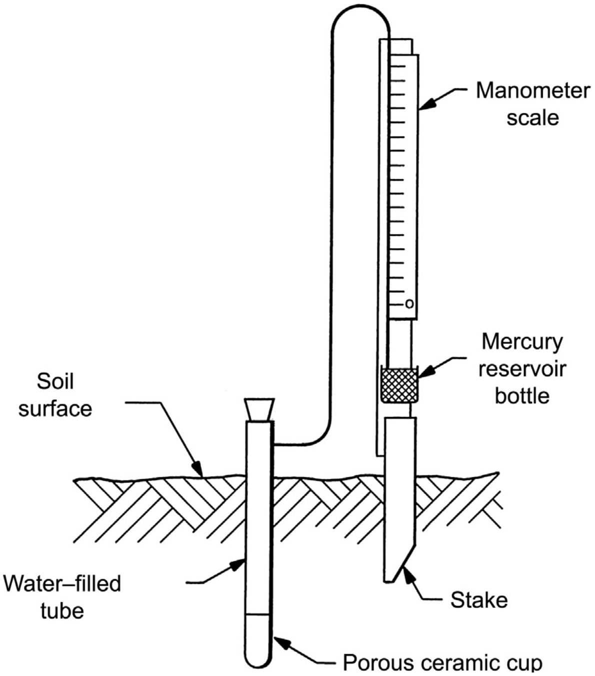

**FIGURE 5.6** A mercury manometer type of tensiometer. *Redrawn from a figure in a Soilmoisture Equipment Corp., Santa Barbara, California, brochure. Reproduced by permission of Soilmoisture Equipment Corp.*

including the "Jet Fill" (Figure 5.7) for fixed installation and the "Quick Draw" probe (Figure 5.8), which is a portable probe designed for rugged field use. Vacuum dial gauge tensiometers can be obtained for different depths from Soilmoisture (6-, 12-, 18-, 24-, 36-, 48-, and 60-in depths or 15, 30, 46, 61, 91, 122, and 152 cm, respectively). Laboratory-built tensiometers can operate at deeper depths. They are termed *advanced tensiometers* and can be used to monitor landfills at depths from 0.15 to 30 m (Hubbell and Sisson, 1998). For greenhouse work with pots, Soilmoisture's Model 2100F with a vacuum dial gauge (ceramic cup: 0.6 cm diameter; 2.4 cm long) can be used because it is a miniature tensiometer (Zhang and Kirkham, 1995).

The Tensimeter™ (Figures 5.9 and 5.10) sold by Soil Measurement Systems (Tucson, Arizona) is a fast, simple, and portable method to read tensiometers with 1 mbar sensitivity using a pressure transducer. This method was originally described by Marthaler et al. (1983), and a diagram of the tensiometer is shown in Figure 5.11. Any ordinary tensiometer can be used. The tubing is closed off with a septum stopper, which forms an airtight seal during and after insertion of a syringe needle through the stopper. The air pressure in the upper end of the tubing is measured by

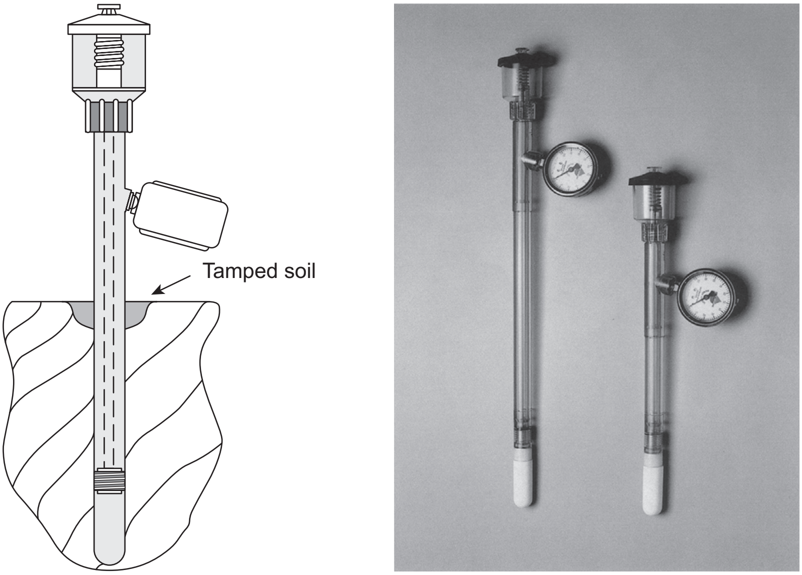

**FIGURE 5.7** The "Jet Fill" tensiometer of Soilmoisture Equipment Corporation. *Courtesy of Soilmoisture Equipment Corp., Santa Barbara, California.*

inserting a syringe needle attached to a pressure transducer through the septum (Figure 5.12). A guide tube keeps the transducer system in a vertical position when placed on the tensiometer and centers the needle in the septum. The inside diameter of the guide tube fits the outside diameter of the stopper and plexiglass tube. The transducer consists of a steel enclosure with a steel transducer membrane separating the enclosure into an upper chamber and a lower chamber. The upper chamber is at atmospheric pressure. Through the syringe needle, the air pressure in the lower chamber equilibrates with the pressure inside the tube, causing a small deflection of the steel membrane. This deflection changes the resistance of silicon semiconductors embedded into the membrane. A shielded four-lead wire connects the silicon element with a resistivity meter. The meter is calibrated to read directly in millibars (mb) (which can be converted to centibars, cb) or centimeters of water. Unlike vacuum gauges, the readings with the Tensimeter™ give a singular reading to the nearest unit (e.g., a value in centibars) (Loyd R. Stone, personal communication, June 8, 2013). (To keep plants under well-watered conditions, Loyd Stone irrigates when a tensiometer at the 50 cm depth reads 50 cb.)

In field use, the tensiometers are inserted into the soil for permanent use during a season. To operate the Tensimeter™, one simply places the transducer over a tensiometer. The needle probe penetrates the septum stopper of the tensiometer. The tension inside the tensiometer is measured

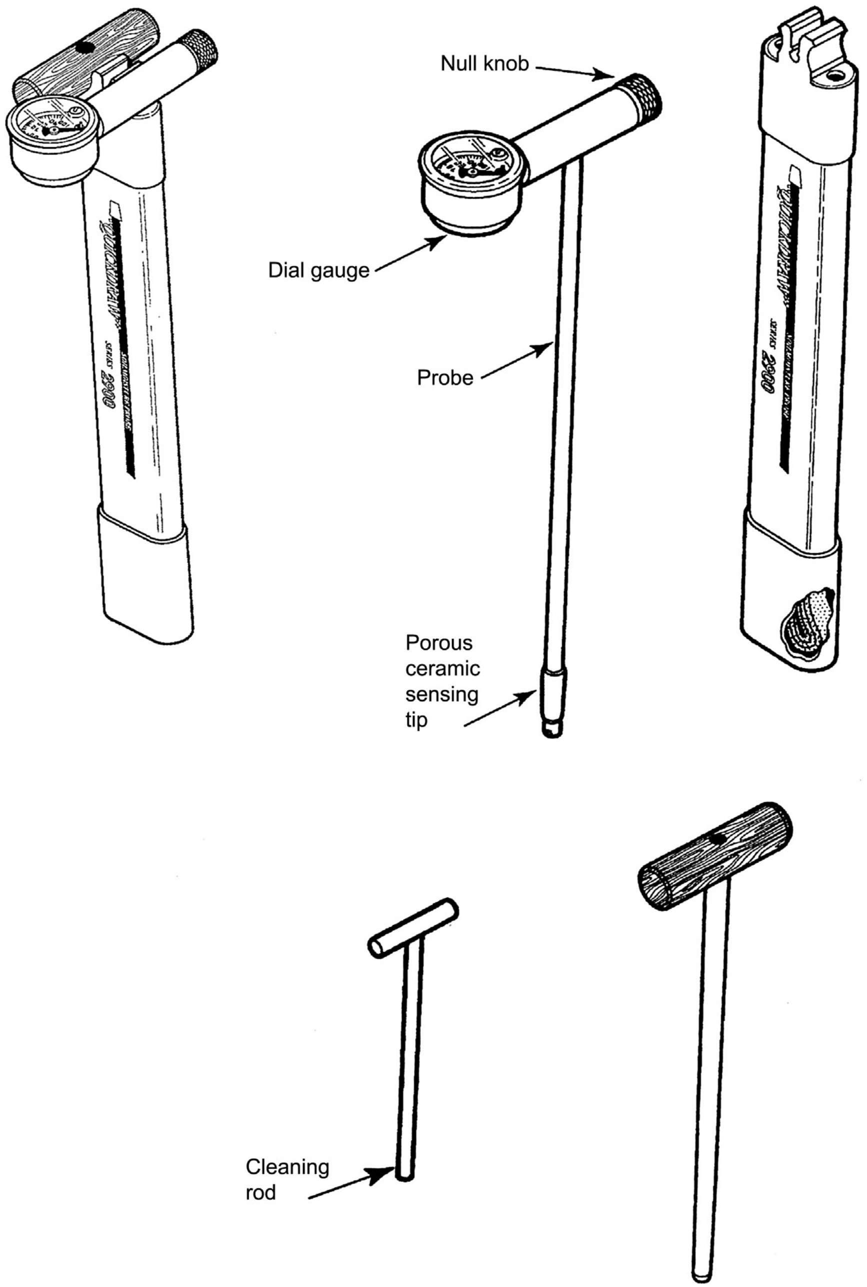
Null knob
Dial gauge
Probe
Porous ceramic sensing tip
Cleaning rod

**FIGURE 5.8** The “Quick Draw” tensiometer of Soilmoisture Equipment Corporation. One side holds a soil corer and the other side holds the tensiometer. *Courtesy of Soilmoisture Equipment Corp., Santa Barbara, California.*

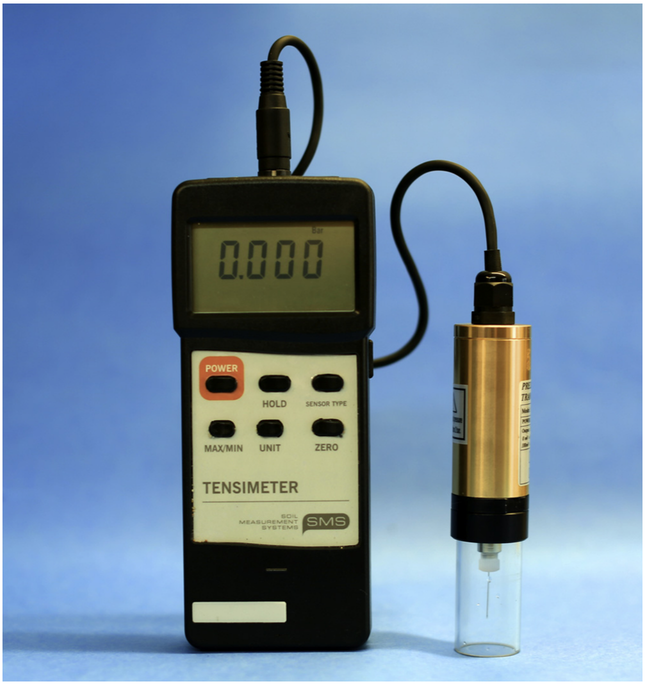

**FIGURE 5.9** Photograph of the Tensimeter™ of Soil Measurements Systems. The needle that punctures the septum stopper, shown diagrammatically in Figure 5.11, is inside the plastic cylinder at the right. The needle is also shown diagrammatically in Figure 5.12. *Courtesy of Soil Measurement Systems, Tucson, Arizona.* (For color version of this figure, the reader is referred to the online version of this book.)

and digitally displayed (in mb or cm). One can get as many as 45 readings per septum (45 needle insertions) before the rubber septum needs to be replaced (Loyd R. Stone, personal communication, June 8, 2013). One can take about 75 readings (read 75 tensiometers) per hour; it takes about 15 s per reading. Readings can be hand-recorded because this is a cheap and accurate method. In a subsurface drip irrigation study of corn (*Zea mays* L.) in the western part of Kansas, dozens of tensiometers were installed for several seasons (Darusman et al., 1997a,b; Lamm et al., 1997), and speed in taking readings was important when measuring numerous tensiometers.

When using the Tensimeter™, one must distinguish between the reading on the read-out and the potential at the point in question in the soil (where the measurement is being taken). These are two different values. Let us assume we have a tensiometer that is 160 cm long. To calibrate such a tensiometer (160 cm long), Loyd Stone puts the ceramic cup in a container of water, so that the ceramic is just covered (Loyd R. Stone, personal communication, July 9, 2013). He puts the tensiometer in a

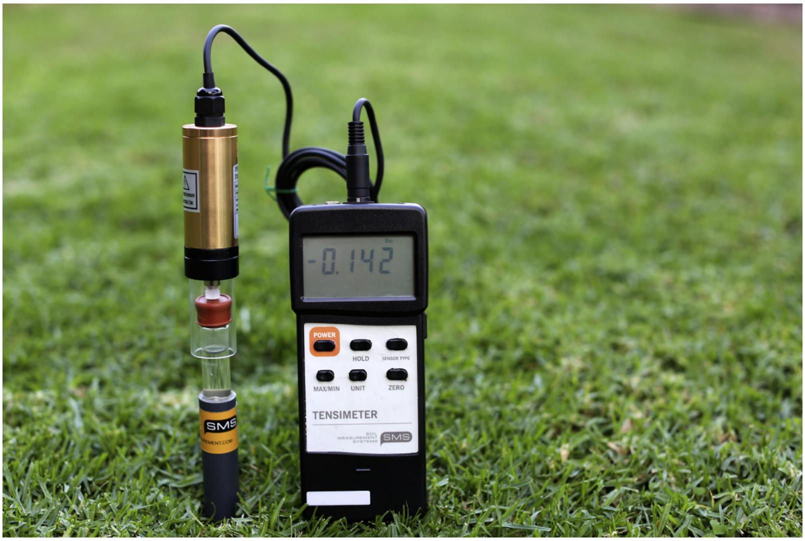

**FIGURE 5.10** Photograph of the Tensimeter™ in field use. *Courtesy of Soil Measurements Systems, Tucson, Arizona.* (For color version of this figure, the reader is referred to the online version of this book.)

completely erect position and lets the ceramic cup wet up for a couple of days. He then reads the read-out on the Tensimeter™. There is no tension, so the read-out should read −160 cm because that is the length of the hanging column of water under tension. Then he places the 160-cm-long tensiometer in the field. If he gets a reading of −180 cm, he knows that there is a matric potential of −20 cm. He must subtract the length of the hanging column of water (−160 cm) to get this value. So the matric potential at the point in question in the soil is −20 cm. If he gets a reading of −140 cm, he knows that he has a submergence (pressure) potential of 20 cm (a positive value) at the point in question in the soil. A matric potential is always negative. He calibrates each tensiometer of a different length, so he knows how much length to subtract from his readings. Marthaler et al. (1983) also explain this procedure with the Tensimeter™. The stem length of the tensiometer must be subtracted from the reading on the Tensimeter™ to get the matric potential (or pressure potential, if there is one). However, with vacuum gauges, the stem length does not need to be subtracted because when one sets them up, one adjusts the gauge to read zero. However, if one did not adjust the vacuum gauge to read zero, its reading reflects the length of the tensiometer. One then could read a submergence potential with the vacuum gauge because the needle would fall and read a lower value, indicating a pressure potential (Loyd R. Stone, personal communication, July 9, 2013). If the needle rises, then one has a matric potential. The reading on a mercury tensiometer also

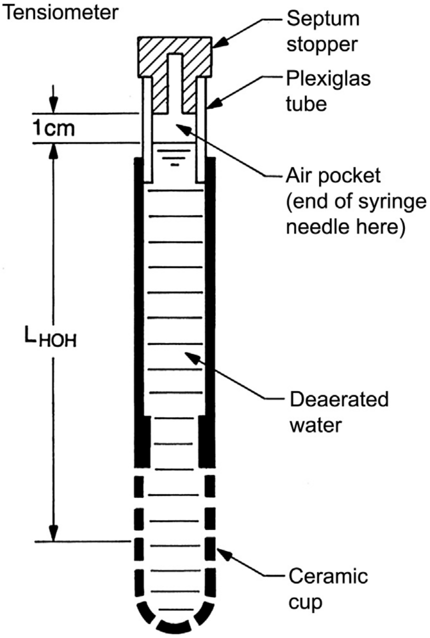

**FIGURE 5.11** Diagram of a tensiometer with septum stopper. The needle of the Tensimeter™, shown in Figure 5.9, punctures the septum stopper. *From Marthaler et al. (1983). Soil Science Society of America: Madison, Wisconsin. Reprinted by permission of the Soil Science Society of America.*

includes the length of the tensiometer. To zero the value on a mercury tensiometer, see Section 5.4 in this chapter. To know the direction of movement of water between two tensiometers, one also must consider the gravitational potential energy and add it to the matric potential, which we did in Chapter 4.

Whether one uses tensiometers with transducers or vacuum gauges depends on cost (Loyd R. Stone, personal communication, June 8, 2013). For example, if one needs just a few measurements and a transducer costs $2000 and a vacuum gauge costs $90, then buying a few vacuum gauges would be the proper procedure. However, if one wants to instrument a field with many tensiometers, then the financially reasonable approach is to buy the transducer.

Electrical resistance sensors are available for estimating soil moisture tension (International Atomic Energy Agency, 2008, p. 123). They consist of a porous body (block) in which a pair of electrodes is embedded. Either the sensor itself is made of $CaSO_4$ (known as gypsum or hydrated plaster of Paris) or there is a pellet of $CaSO_4$ embedded in the sensor body. The sensor may be buried at any desired depth in the soil. The porous sensor exhibits a soil moisture characteristic curve in the same way as does a soil

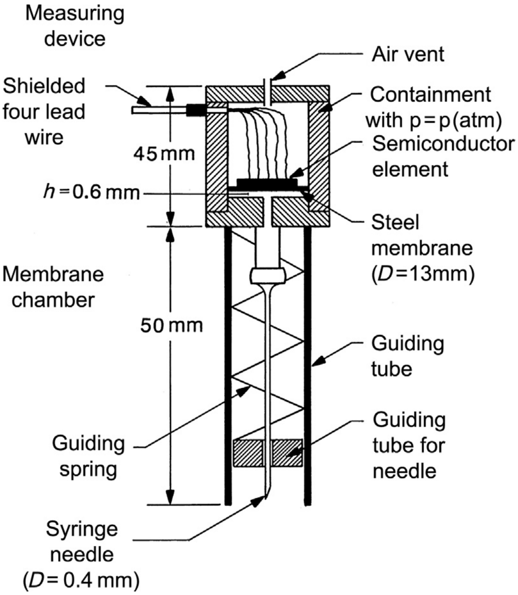
Measuring device
Air vent
Shielded four lead wire
Containment with p=p(atm)
Semiconductor element
45 mm
h=0.6 mm
Steel membrane (D=13mm)
Membrane chamber
50 mm
Guiding tube
Guiding tube for needle
Guiding spring
Syringe needle (D=0.4 mm)

**FIGURE 5.12** Diagram of pressure transducer with attached syringe needle. The needle is shown in the photograph of the Tensimeter™ in Figure 5.9. *From Marthaler et al. (1983). Soil Science Society of America: Madison, Wisconsin. Reprinted by permission of the Soil Science Society of America.*

(see Chapter 6 for a description of a soil moisture characteristic curve). Consequently, as the surrounding soil wets and dries, the sensor also wets and dries. A two-wire lead from the sensor is connected to a meter, which is used to read the sensor resistance. Calcium sulfate is a weakly soluble salt that dissolves in the water in the porous sensor and renders the water conductive. The more water that is in the sensor, the more conductive is the medium between the electrodes. That is, the resistance decreases as the water content increases (International Atomic Energy Agency, 2008). Electrical resistance sensors are widely used to get soil moisture tension. However, for accurate measurements in experimental work, tensiometers should be used rather than electrical resistance sensors. The Tensimeter™ gives a precise, unique reading unlike electrical resistance sensors (Loyd R. Stone, personal communication, June 8, 2013).

## 5.3 TEMPERATURE EFFECTS ON TENSIOMETERS

Temperature affects readings with tensiometers in two ways:

1. Effects of temperature on water in soil.
2. Effects of temperature on the instrument.

Temperature affects the physical properties of water, including density and surface tension (Table 3.1). Therefore, the matric potential (tension) of water in the soil is affected by temperature changes. The major effect of temperature occurs at the soil surface, where temperature changes are greatest. Temperature effects on soil tension account for measurable amounts of water flow (Loyd R. Stone, personal communication, February 1, 1989).

Temperature affects the instrument directly because the mercury is heated (the mercury expands with heating). The metal on the part of the tensiometer that is inserted into the soil can conduct heat from the air to the soil. Plastic instead of metal in the construction of the tensiometer minimizes temperature effects. Tensiometers can be insulated by using shade boxes or temperature effects can be minimized by taking readings early in the morning when the sun is not far up in the sky. Temperature is less of a factor with the Tensimeter™ because it does not have a metal pole (Loyd R. Stone, personal communication, June 8, 2013). Loyd Stone caps his tensiometers that he measures with the Tensimeter™ with a piece of polyvinyl chloride pipe, and this keeps out dew and dust, which plug the needle of the Tensimeter™. It is necessary to keep the needle perfectly clean. However, the soil surface still can heat up and affect readings taken with the Tensimeter™. With the Tensimeter™, Loyd Stone takes his measurements early in the morning to minimize temperature effects.

All tensiometers cannot be used in freezing weather because the water in the tensiometer will freeze and break the tensiometer. But one can bury tensiometers deeply or use methanol—water solutions, which can protect the tensiometers as low as −18 °C (Cassel and Klute, 1986, p. 586). One would need to do a controlled laboratory experiment to determine gradients caused by temperature in the soil and the magnitude of change in soil-water tension with temperature (Loyd R. Stone, personal communication, February 1, 1989). With the dual-probe heat-pulse method (Chapter 9), we can measure soil water content and soil temperature with resolution as fine as measurements 1.5 cm apart (Song et al., 1999). However, tensiometers have not yet been miniaturized enough to measure matric potential at such fine resolution. In the field, one just recognizes that temperature does affect readings with tensiometers and tries to minimize this effect (Loyd R. Stone, personal communication, February 1, 1989), especially in hot, semiarid regions such as Kansas.

## 5.4 APPLICATIONS OF TENSIOMETERS

Tensiometers have five applications (Richards, 1965; Loyd R. Stone, personal communication, June 8, 2013 and July 8, 2013).

1. They are used to determine rooting depth. One can follow readings with time, and the rate of increase in soil tension at any given depth

can be related to the density of the active roots. One can use tensiometers to get water extraction by roots, such as one uses a neutron probes (Frank et al., 2013).

2. They are used for timing of field irrigations. It is time to irrigate when tensiometer readings reach a prescribed value for a soil depth where feeder root concentration is greatest. The duration of irrigation is judged with tensiometers that measure soil tension at a second or greater depth. If tension readings at this second depth are low (high matric potential), an irrigation of short duration is indicated. Conversely, if they are high, irrigation water should be allowed to run until readings are low.
3. They are used to determine timing of greenhouse irrigations for potted plants and greenhouse beds. Under these conditions, only one depth is read.
4. The water table level is determined using tensiometers. If using a mercury manometer, one first zeros the scale of the manometer, which can be carried out by filling the instrument with mercury and water in advance of installation. With the instrument supported in the same orientation that it will have in the field, and with the cup immersed in a container of water, the position that the mercury level attains in the manometer is then marked as the zero setting for the scale. If a reading on this mercury tensiometer in the field is below zero, it is evidence that a water table occurs above the depth of the cup. The negative reading in millibars is equivalent to the distance in centimeters from the water table to the cup depth. Similarly, as described above, one could determine the water table level with a vacuum gauge tensiometer or a Tensimeter™. The depth measured may not necessarily be the depth of the water table (rarely in Kansas), but it could be a perched water table or a flooded condition, which has caused the reading associated with the submergence potential. But the reading will be temporary, and, when water infiltrates (e.g., after a flooding operation is stopped), the reading goes from a submergence potential (positive) to a matric potential (negative).
5. The hydraulic gradient is determined from measurements using two tensiometers. (See Chapter 7 for the definition of the hydraulic gradient.) If one knows the hydraulic gradient, one knows which way water is moving in the soil. The use of two tensiometers at two different depths is the only way to determine the direction of movement of water in the soil (up or down). This knowledge is necessary if one wants to leach out salts or determine the water balance. Two typical depths of installation of tensiometers are at 4.5 and 5.5 feet (1.4 and 1.7 m) because these depths are below the root zone (Darusman et al., 1997a). By reading the tensiometers, one can

determine if the soil is wetting up or draining. This knowledge is critical in water-balance studies because one needs to know the drainage component. In semiarid Kansas, the goal is to minimize drainage to improve irrigation efficiency (Darusman et al., 1997b; Stone et al., 2008).

## 5.5 APPENDIX: BIOGRAPHY OF L.A. RICHARDS

Lorenzo Adolph Richards, known as “L.A.” or “Ren,” was born on April 24, 1904, in Fielding, Utah. At Utah State College, he received his B.S. degree in 1926 and his M.A. in 1927; in 1931, he received the Ph.D. in Physics from Cornell University. He is best known for the “Richards’s equation” (Richards, 1931), which is widely used in numerical simulations (computer models) for water flow in unsaturated soils. He was an assistant at Utah State from 1924 to 1927, an assistant at Cornell from 1927 to 1929, an instructor at Cornell from 1929 to 1935, and a research physicist at Battelle Memorial Institute in Ohio in 1935. He then moved to Iowa State College, where he was an assistant and associate professor of physics and a research assistant and associate professor of soil between 1935 and 1939. He left Iowa State to become senior soil physicist at the U.S. Salinity Laboratory in Riverside, California, where he stayed from 1939 to 1942. He was a National Defense Research Fellow and Group Leader at the California Institute of Technology from 1942 to 1945 (Cattell, 1961). He then returned to the Salinity Laboratory, where he was the chief physicist from 1945 to 1966. He married Zilla Linford of Logan, Utah, in 1930, and they had three children: L. Willard Richards; Paul L. Richards; and Mary Armstead (American Society of Agronomy, 1993). Paul Richards is a professor of Physics at the University of California at Berkeley, specializing in infrared and millimeter wave physics, and he is a member of the National Academy of Sciences and the American Academy of Arts and Sciences.

L.A. Richards received many awards, including honorary Doctor of Science degrees from the Israel Institute of Technology in Haifa in 1952, and later in life, from his alma mater, Utah State University. He was the Fellow of the American Society of Agronomy and won its Stevenson Award in 1949. He was the president of the Soil Science Society of America (1952) and the American Society of Agronomy (1965). In recognition of his military contributions during World War II, he received the U.S. Department of Navy Ordnance Development Award in 1945 and the Presidential Certificate of Merit in 1948. He received the USDA Superior Service Award in 1959 and honorary membership in the International Society of Soil Science in 1968. In 1981, the American Geophysical Union organized a symposium on the impact of the Richards’s (1931) equation, to honor the fiftieth anniversary of his influential publication in *Physics*

(American Society of Agronomy, 1993). He was a long-time member of the American Geophysical Union.

His research interests were in soil physics, retention and flow of water in soil, vacuum tube circuits, rocket ordnance, diagnosis and improvement of saline and alkali soils, the relation of soil water to plant growth, and measurement of aqueous vapor pressure at high humidity (Cattell, 1961). His brother, Sterling Jacob Richards (born 1909; Cattell, 1961), also made contributions in soil physics but was not as famous as his older brother.

L.A. Richards made continuous improvements in the design and operation of the instruments used to provide a quantitative understanding of the energy status of water in the soil. His children helped him build his equipment to provide money to put them through college. They formed a company called Lark (L.A. Richards Kids). Richards (1965, p. 157) cites Lark Instruments in Riverside, California, as a supplier of tensiometers at the time. L.A. Richards initiated and edited the influential 1954 USDA Agricultural Handbook No. 60 entitled, *Diagnosis and Improvement of Saline and Alkali Soils*, a publication still in use today (United States Salinity Laboratory Staff, 1954). He died of Alzheimer's disease on March 12, 1993, in Carmel, California at the age of 88 (American Society of Agronomy, 1993).

## References

American Society of Agronomy., Richards, L.A., 1993. Agronomy News. May 1993, p. 26 (one page only). American Society of Agronomy, Madison, Wisconsin.

Baver, L.D., Gardner, W.H., Gardner, W.R., 1972. Soil Physics, fourth ed. Wiley, New York.

Cassel, D.K., Klute, A., 1986. Water potential: tensiometry. In: Klute, A. (Ed.), Methods of Soil Analysis. Part 1. Physical and Mineralogical Methods, second ed. American Society of Agronomy and Soil Science Society of America, Madison, Wisconsin, pp. 563–596.

Cattell, J. (Ed.), 1961. American Men of Science. A Biographical Directory. The Physical and Biological Sciences, tenth ed. The Jacques Cattell Press: Arizona State University, Tempe, Arizona, p. 3362.

Darusman, Khan, A.H., Stone, L.R., Lamm, F.R., 1997a. Water flux below the root zone vs. drip-line spacing in drip-irrigated corn. Soil Sci. Soc. Am. J. 61, 1755–1760.

Darusman, Khan, A.H., Stone, L.R., Spurgeon, W.E., Lamm, F.R., 1997b. Water flux below the root zone vs. irrigation amount in drip-irrigated corn. Agron. J. 89, 375–379.

Frank, B.J., Schlegel, A.J., Stone, L.R., Kirkham, M.B., 2013. Grain yield and plant characteristics of corn hybrids in the Great Plains. Agron. J. 105, 383–394.

Hubbell, J.M., Sisson, J.B., 1998. Advanced tensiometer for shallow or deep soil water potential measurements. Soil Sci. 163, 271–277.

International Atomic Energy Agency, 2008. Field Estimation of Soil Water Content. Training Course Series 30. Overall coordinator: S. Evett. International Atomic Energy Agency, Vienna.

Kirkham, D., Powers, W.L., 1972. Advanced Soil Physics. Wiley-Interscience, New York.

Lamm, F.R., Stone, L.R., Manges, H.L., O'Brien, D.M., 1997. Optimum lateral spacing for subsurface drip-irrigated corn. Trans. Am. Soc. Agr. Eng. 40, 1021–1027.

Marthaler, H.P., Vogelsanger, W., Richard, F., Wierenga, P.J., 1983. A pressure transducer for field tensiometers. Soil Sci. Soc. Am. J. 47, 624–627.

Richards, L.A., 1931. Capillary conduction of liquids through porous mediums. Physics 1, 318–333.

Richards, L.A., 1949. Methods of measuring soil moisture tension. Soil Sci. 88, 95–112.

Richards, S.J., 1965. Soil suction measurements with tensiometers. In: Black, C.A., Evans, D.D., Ensminger, L.E., White, J.L., Clark, F.E. (Eds.), Methods of Soil Analysis. Part 1. Physical and Mineralogical Properties, Including Statistics of Measurement and Sampling. American Society of Agronomy, Madison, Wisconsin, pp. 153–163.

Soil Science Society of America, 2008. Glossary of Soil Science Terms 2008. Soil Science Society of America, Madison, Wisconsin.

Song, Y., Kirkham, M.B., Ham, J.M., Kluitenberg, G.J., 1999. Measurement resolution of the dual-probe heat-pulse technique. In: van Genuchten, M.T., Leij, F.J., Wu, L. (Eds.), Characterization and Measurement of the Hydraulic Properties of Unsaturated Porous Media. University of California, Riverside, pp. 381–386.

Stone, L.R., Lamm, F.R., Schlegel, A.J., Klocke, N.L., 2008. Storage efficiency of off-season irrigation. Agron. J. 100, 1185–1192.

United States Salinity Laboratory Staff, 1954. Diagnosis and improvement of saline and alkali soils. In: Richards, L.A. (Ed.), Agricultural Handbook No. 60. United States Department of Agriculture, Washington, DC.

van Genuchten, M.T., 1980. A closed-form equation for predicting the hydraulic conductivity of unsaturated soils. Soil Sci. Soc. Am. J. 44, 892–898.

Zhang, J., Kirkham, M.B., 1995. Sap flow in a dicotyledon (sunflower) and a monocotyledon (sorghum) by the heat-balance method. Agron. J. 87, 1106–1114.

CHAPTER

# 6

# Static Water in Soil

We now look at how water interacts with the solid system of the soil. In particular, we shall study surface tension, and then see how it is related to the rise and fall of water in soil pores, which, in turn, explains hysteresis.

## 6.1 SURFACE TENSION

We first recall the definitions of some terms from elementary physics (Kirkham and Powers, 1972, p. 11). An object is under tension if a pull is being exerted on it. In Figure 6.1, the cross-section $A$ of the cylinder is

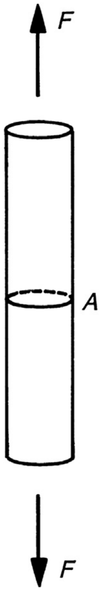

**FIGURE 6.1** Illustration of tension. *From Kirkham and Powers (1972). This material is used by permission of John Wiley & Sons, Inc. and William L. Powers.*

http://dx.doi.org/10.1016/B978-0-12-420022-7.00006-9

Copyright © 2014 Elsevier Inc. All rights reserved.

under tension due to the forces $F$. Tension is a pull or stretching force per unit area. Pressure implies a push and is a compression force per unit area. If we reverse the directions of the arrows in Figure 6.1, the cylinder will be under pressure. In talking about soil water and plant water, we sometimes say that the water is under stress. Stress may be either a pull or a push, tension, or compression. So stress may properly be expressed as a pull or push per unit area.

The term *surface tension* should not be confused with tension (Kirkham and Powers, 1972, pp. 11–12). Surface tension, or more specifically, the surface tension coefficient, an energy per unit area, is equivalently a force per unit length, whereas tension is a force per unit area. We abbreviate the surface tension coefficient using the Greek letter sigma ($\sigma$).

$$\sigma = \text{energy}/\text{area} = (\text{force})(\text{distance})/\text{area} \tag{6.1}$$

or

$$\sigma = \text{force}/\text{length}. \tag{6.2}$$

Surface tension may be compared with the force that develops in a sheet of paper when we pull it on opposite edges. In Figure 6.2, the force $F$ when divided by the length $AB$ gives a surface tension coefficient $\sigma$, which may be denoted by

$$\sigma = F/(2AB), \tag{6.3}$$

where the 2 in the denominator is used because the sheet of paper has an upper and a lower surface even though the paper is thin.

Laplace (1749–1827), a French mathematician and astronomer, explained surface tension. (See the Appendix, Section 6.4, for a biography of Laplace.) A molecule in the body of a fluid (Figure 6.3) is attracted equally from all sides. But a molecule at the surface undergoes a resultant inward pull because there are no molecules outside the liquid causing attraction. Hence, molecules in the surface have a stronger tendency to move to the interior of the liquid than the molecules in the interior have to move to the surface. What results is a tendency for any body of liquid to minimize its surface area. A molecule at the surface of a liquid is acted on

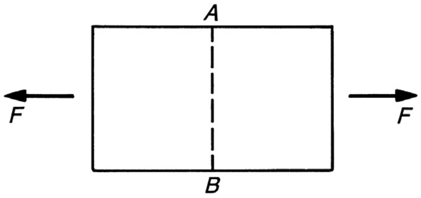

**FIGURE 6.2** Surface tension in a sheet. *From Kirkham and Powers (1972). This material is used by permission of John Wiley & Sons, Inc. and William L. Powers.*

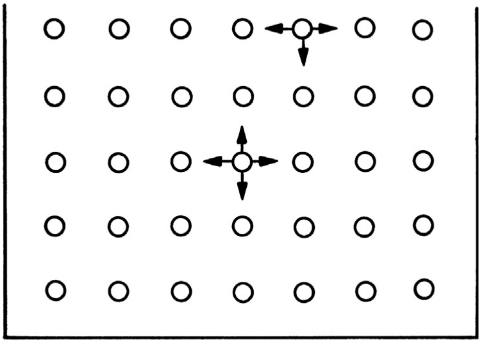

**FIGURE 6.3** Laplace's surface tension theory. *From Kirkham and Powers (1972). This material is used by permission of John Wiley & Sons, Inc. and William L. Powers.*

by a net inward cohesive force that is perpendicular to the surface. So it requires work to move molecules to the surface against this opposing force, and the surface molecules have more energy than interior ones (Schaum, 1961, p. 108).

This tendency to minimize surface area is often opposed by external forces acting on the body of liquid, as gravity acting on a water drop resting on a flat surface, or as adhesive forces between water and other materials. Thus, the actual surface may not be an absolute minimum, but rather a minimum depending on the conditions in which the body of liquid is found (Kirkham and Powers, 1972, pp. 12–13).

The surface tension coefficient has been expressed as a force per unit length. If a wire is pulled horizontally from beneath a liquid, as illustrated in Figure 6.4, the force required to pull it out depends on the length of the wire. Let the symbols in Figure 6.4 be defined as follows:

- $F$ = upward pull required to balance surface tension forces (gravitational forces neglected);
- $L$ = length of wire;
- $\sigma$ = surface tension (units of force per unit length);
- $d$ = distance wire is raised.

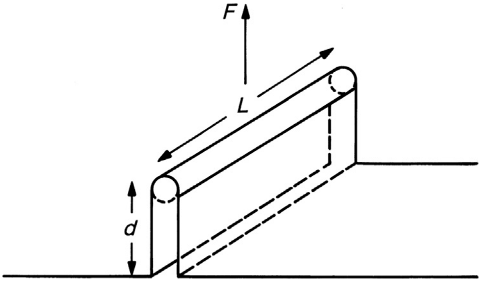

**FIGURE 6.4** Wire being pulled from water with adhering water film. *From Kirkham and Powers (1972). This material is used by permission of John Wiley & Sons, Inc. and William L. Powers.*

Then we have

$$F = 2(\sigma L), \tag{6.4}$$

where the 2 is used because the force to be overcome by surface tension is developed on the two sides of the wire. (Note that the wire is circular, but water adheres to two "sides".) Now the work $W$ required to pull the wire against surface tension forces through the distance $d$ is

$$W = Fd. \tag{6.5}$$

That is, using the relation $F = 2(\sigma L)$, we have

$$W = \sigma(2Ld) \tag{6.6}$$

or

$$\sigma = W/(2Ld) \tag{6.7}$$

or

$$\sigma = W/(\text{increased area of surface}). \tag{6.8}$$

That is, $\sigma$ is the energy stored in the surface per unit increase in its area. So by pulling the wire out of a liquid, we can see that the coefficient of surface tension may be expressed as the energy stored per unit area of increase in the surface.

Surface tension causes the rise or fall of a liquid in a capillary tube. We are going to relate the rise of water in soil to the rise of water in capillary tubes, so we need to understand the rise of water in capillary tubes. The equation for the height of rise in a capillary tube, $h$, is (Schaum, 1961, p. 108)

$$h = (2\sigma \cos \alpha)/(r\rho g), \tag{6.9}$$

where

- $\sigma$ = surface tension of the liquid;
- $r$ = radius of the tube;
- $\rho$ = density of the liquid;
- $\alpha$ = contact angle between the liquid and tube (called the wetting angle in terminology used in soil science);
- $g$ = acceleration due to gravity.

We shall now prove this equation in a simple manner, recognizing that more complicated proofs exist using calculus (Porter, 1971; Sophocleous, 2010).

Let us look at Figure 6.5 (Schaum, 1961, p. 109). Consider the body of liquid inside the tube and above the outside level. The vertical (downward and upward) forces acting on it must balance. The downward force

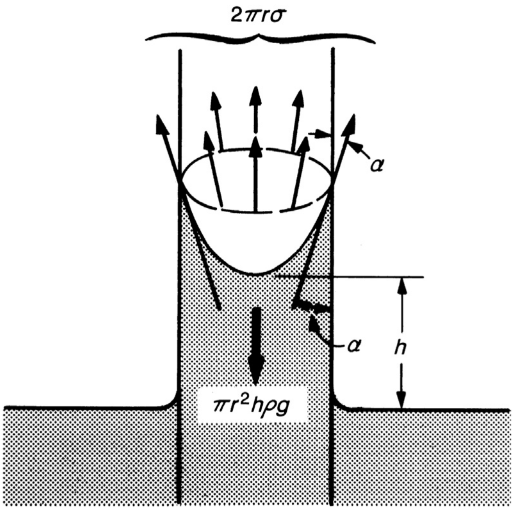

**FIGURE 6.5** Height of rise of a liquid in a capillary tube. *From Schaum (1961). This material is reproduced with permission of The McGraw-Hill Companies.*

is its weight. Remember from Chapter 2 that weight, $w$, is a force and $w = mg$, where $m$ is the mass and $g$ is defined above.

$$\text{weight of liquid inside tube} = \text{volume} \times \text{weight per unit volume}$$

$$= \pi r^2 h \times mg/V = \pi r^2 h \times (m/V)g \tag{6.10}$$

$$= \pi r^2 h\rho g \ \text{ acting downward.} \tag{6.11}$$

The upward force is due to surface tension. Remember that surface tension, $\sigma$, is a force/length and the length of the tube is its circumference, $2\pi r$. The force is the perpendicular force, so to get the normal component, we must multiply $2\pi r$ by cos $\alpha$. So the upward force is $2\pi r\sigma\cos\alpha$, and this is the force due to surface tension. For vertical equilibrium,

$$\text{upward force} = \text{downward force}$$

$$2\pi r\sigma \cos \alpha = \pi r^2 h\rho g \tag{6.12}$$

or

$$h = (2\sigma \cos \alpha)/(rpg). \tag{6.13}$$

The meniscus in the capillary tube can be either convex or concave. (In physics, *meniscus* is defined as the curved upper surface of a column of liquid. It comes from the Greek word *meniskos*, which is a diminutive of *mene*, "the moon.") A convex meniscus is illustrated by mercury on glass and a concave meniscus is illustrated by water on glass (Figure 6.6). Mercury in contact with glass has an angle of contact of 130−140° (Porter,

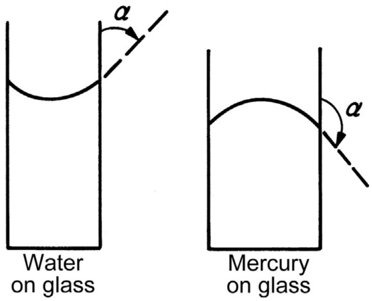

**FIGURE 6.6** Angles of contact. *From Kirkham and Powers (1972). This material is used by permission of John Wiley & Sons, Inc. and William L. Powers.*

1971, p. 447). For water in contact with most soil minerals, the wetting angle, $\alpha$ (also abbreviated $\theta$), is close to zero (Linford, 1930), so in the equation for the height of rise in a capillary tube, we can take $\cos 0 = 1$ or $\cos \alpha = 1$. However, in highly repellent soils, the contact angle is large.

Leon Linford (1930) developed a clever way to measure the wetting angle in soil by using mirrors and the well-known laws of reflection in physics. The angle of incidence is the angle between the incident ray and the normal to the reflecting surface at the point of incidence (Schaum, 1961, p. 214) (Figure 6.7). The angle of reflection is the angle between the reflected ray and the normal to the surface. The laws of reflection are the following: (1) The incident ray, reflected ray, and normal to the reflecting surface lie in the same plane. (2) The angle of incidence equals the angle of reflection. Concave mirrors form real and inverted images of objects located outside of the principal focus; if the object is between the principal focus and the mirror, the image is virtual, erect, and enlarged. Convex

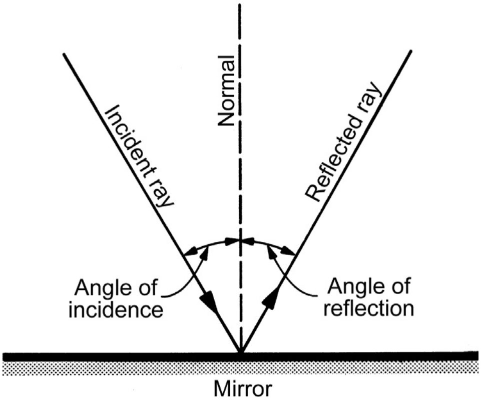

**FIGURE 6.7** The angles of incidence and reflection. *From Schaum (1961). This material is reproduced with permission of The McGraw-Hill Companies.*

mirrors produce only virtual, erect, and smaller images. Linford (1930) beamed light down into soil and said,

> Any point of the [water] meniscus, acting as a cylindrical concave mirror would reflect the light back and upwards at an angle such that it is twice the angle between the tangent to the meniscus at the point in question and the vertical. If the angle of contact is zero, the light reflected from the top of the meniscus would come back horizontally… [B]y photographing the reflected light, the angle of contact was shown to be very small if not zero.

Leon Linford, born July 8, 1904 (Cattell, 1955), was a physicist who worked at Utah State in Logan, Utah, and joined the famous Radiation Laboratory at the Massachusetts Institute of Technology (MIT) in Cambridge, Massachusetts, during the Second World War (Buderi, 1996; Seitz, 1996). After the war, Linford became the Head of the Department of Physics at the University of Utah in Salt Lake City, but died of cancer in 1957 (Cattell, 1961), perhaps from exposure to radioactivity at the Radiation Laboratory.

## 6.2 EXAMPLES OF SURFACE TENSION

The importance of surface tension can be illustrated in five ways.

1. A water beetle or other small aquatic organisms can float on water because of surface tension (Porter, 1971, p. 442; Dickinson, 2003; Hu et al., 2003; Gao and Jiang, 2004). The fact that small insects can float on water shows the close relationship between the way they have evolved and water. (We remember from Chapter 2 that another example of the relationship between animal evolution and properties of water is the fact that water has a minimum specific heat at 35 °C.) One can simulate a water beetle by floating a razor blade on water. The razor blade will float on an unbroken water surface, but it will not float if the surface tension is broken by soap.
2. We can kill mosquitoes by putting oil on water. Because surface tension is broken and the mosquitoes cannot float, they sink and die. Just a little oil will do (Don Kirkham, personal communication, January 30, 1992).
3. Ducks cannot float as easily on a farm pond with oil as on a pond with no oil (Don Kirkham, personal communication, January 30, 1992).
4. Oil is put on ocean waters to calm the waves (Don Kirkham, personal communication, January 30, 1992). For example, this might be done at shipwrecks. Familiar quotations allude to oil calming water. Plutarch (A.D. 46–120) said, "Why does pouring oil on the sea make it clear and calm? Is it for that the winds, slipping the smooth oil, have no force, nor

causeanywaves?"(Bartlett, 1955, p. 49). Pliny the Elder (A.D. 23–79) said, "Everything is soothed by oil, and this is the reason why divers send out small quantities of it from their mouths, because it smooths every part which is rough" (Bartlett, 1955, p. 49). In 1757 on a journey to London, Benjamin Franklin (1706–1790; American statesman, scientist, inventor, and writer) observed that wakes of two ships were remarkably smooth, while others were ruffled by the wind. Seeking an explanation, he asked the captain, who told him that the cooks on those two ships had probably just emptied their greasy water. The captain thought it as a fairly stupid question since the answer was a common knowledge among seamen. Franklin, recollecting what he had read in Pliny, then resolved to carry out himself experiments on the effect of oil on water (Mertens, 2006). Water surfaces in nature are typically contaminated by surfactant films that alter the surface tension (Liu and Duncan, 2003).

**5.** Walnut shells clump together if floated on water. An experiment can be done in which half-shells of walnuts (with the nut meat removed) are used to make little boats floating on water. Put the walnuts in a pan of water—the walls of the pan must be clean (i.e., no soap or grease on the sides of the pan)—and the walnuts pull together by themselves in the small pan. They pull together to keep the surface energy to a minimum. The walnuts will form chains or trains as they clump together. Adding soap to the water would change the wetting angle and the walnuts would not clump together. As noted above, surface tension occurs in any body of liquid and causes the surface area to be minimized.

The walnuts in water simulate soil conditioners, which cause aggregation. There are many types of soil conditioners (Schamp et al., 1975; see their Figure 6.2 for polymers used as soil conditioners). Some of them have charged ions in the molecule (e.g., sodium polyacrylate with $Na^+$ or K-polystyrene-sulfonate with a $K^+$), but many of them have no charged ions in their molecular structure. The popular polyacrylamide (PAM), widely used as a soil conditioner (see the cover of the 1998 November–December issue of the *Soil Science Society of America Journal*, and the accompanying article by Sojka et al., 1998), comes in a nonionic form (Aly and Letey, 1988). For these nonionic polymers, hydrogen bonding may not be as important in binding the polymers to water and soil and helping in aggregation as it would be for ionic polymers. The nonionic soil conditioners probably have an effect like the walnuts; they minimize the surface energy of water in the soil. Marcel De Boodt, who got his Master's Degree at Iowa State University, said (personal communication, 1976) that his career was based on the simple walnut demonstration, which Don Kirkham showed in his soil physics class. Professor De Boodt built a world-famous laboratory focusing on soil conditioners at the University of Ghent, Belgium. The laboratory had projects around the world and utilized soil conditioners to stabilize the sands around landing strips at airports in oil-wealthy desert countries in the Middle East and Africa. Soil conditioners such as sand, clay, peat, and cinders have been used for a long time. The new, commercial chemical soil conditioners were introduced about 1950. The Monsanto Chemical Company supplied one called krilium, a maleic acid of a vinyl acetate polymer (Kirkham and Runkles, 1952). The use of soil conditioners has been limited by their cost. The water-soluble anionic form of PAM is used today as a soil conditioner in agriculture to reduce erosion and manage infiltration in furrow irrigations. In furrow-irrigation trials in Idaho, USA, use of PAM increased yields of corn (*Zea mays* L.) by 4.5% and bean (*Phaseolus vulgaris* L.) by 14.3%, which indicated that the cost of PAM applications may be recoverable (Lentz and Sojka, 2009). Chemical soil conditioners were used to stabilize the slopes of a canal in Ghent, Belgium; plantings along the canal then could be established and the beautification work won a prize (Don Kirkham, personal communication, February 10, 1994). De Boodt (1975) and Wallace and Terry (1998) review soil conditioners.

Many other examples concerning the importance of surface tension could be given, such as the following: two pennies or two thin pieces of glass stick together with water between them; leaf waxes make water roll off leaves; chemicals are put on raincoats to waterproof them so water droplets will run off them; and adjuvants are added to herbicides so they can more readily be absorbed by plant leaves. Drifting small particles that float on water concentrate in either the nodes or antinodes of a standing wave, depending on whether they are hydrophilic or hydrophobic, as a result of a surface tension effect (Falkovich et al., 2005).

## 6.3 RISE AND FALL OF WATER IN SOIL PORES

Water is attracted into soil pores predominantly because of the attraction of water to other surfaces (adhesion) and because of capillarity. Surface tension controls the rise or fall of a liquid in a capillary tube. We have discussed surface tension and the equation to determine the height of rise in capillary tubes. We now discuss the rise and fall of water in soil pores (capillary tubes) and how the rise and fall determine the soil moisture characteristic curve. We follow the analysis of Kirkham (1961, pp. 24–29).

If one keeps track of the moisture withdrawn from an initially saturated soil core as greater tension is successively applied, and then plots on the $x$-axis (abscissa) water content (moisture percent by volume in the soil, not the water sucked out) and on the $y$-axis (ordinate), tension head (positive units) or matric potential (negative units), the curve so obtained will be the so-called *moisture characteristic* or the *soil water characteristic curve* (ABCD in Figure 6.8). The curve also is called the *water retention curve* or the *water release curve* (Soil Science Society of America, 2008). The moisture percentage on such a curve may be based on oven-dry weight, but in drainage work, as in the figure, the soil moisture characteristic is most useful when the moisture is expressed on a volume basis because then the surface centimeters (depth) of irrigation water needed to replenish moisture in the sample is obtained from the characteristic. For example, a moisture percentage of 30% by volume at saturation means that, for a 10 cm dry soil layer, 3 cm of water must be applied to the surface to bring the 10 cm to saturation.

In Figure 6.8, one may think of the tension as being produced by a falling water table. One may verify the following on the figure: initially (point A), the bulk volume of the soil has all of its pore space, that is, 50% of its bulk volume, filled with water. For a 20 cm depth of water table, the moisture percentage at the soil surface is 40%; for a 40 cm depth of water table, 15%; and for a 100 cm depth, 8%. In Figure 6.8, if the water table had fallen to a 40 cm depth and then risen slowly to the soil surface, the moisture percentages would be those corresponding to the dashed line. The failure of the curve to retrace itself in the reverse direction is called *hysteresis*. In Figure 6.8, the soil moisture characteristic ABCD is that of a loam; for finer textured soils, the curves would be higher. If, for Figure 6.8,

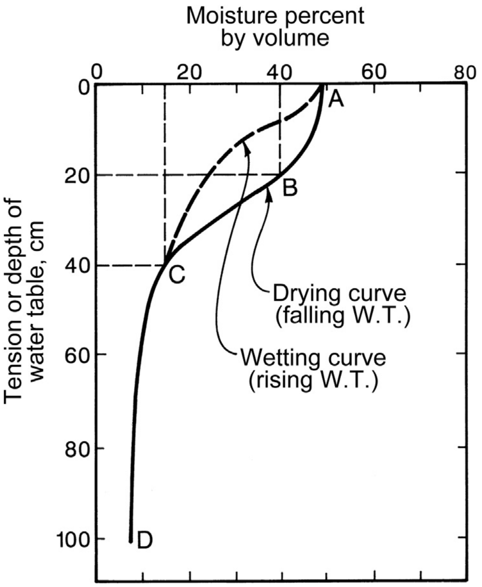

**FIGURE 6.8** A soil moisture characteristic curve for a loam soil. *From Kirkham (1961).*

the water table for the dashed curve had not risen slowly, the moisture percentage for zero depth of the water table would be, because of trapped air, <50%. Even if the water table rises slowly, there is usually a small amount of trapped air, and, when hysteresis loops are determined experimentally, they are not seen to return to the original point.

We pause here to say a few words about hysteresis. It comes from the Greek *hysteresis*, a coming short or deficiency. It is a word used in physics and its definition is "a lag in the effect in a body when the force acting on it is changed; especially, a lag in the change of a magnetization behind the varying magnetizing force" (Webster's New World Dictionary of the American Language, 1959). Because hysteresis relates to a physical system, a hysteretic curve can be repeated (e.g., the curves in Figure 6.8 for a loam soil). Its use to describe a biological system should be approached with caution. For example, curves relating leaf water potential to evapotranspiration have been called *hysteretic* (Sharratt et al., 1983), but such curves are not repeatable and depend on physiological factors such as stomatal closure.

If the soil is saturated to the surface and covered by a thin layer of water, there will be no tension in the soil pores (voids). If the water table falls through the soil surface, tension will develop in the soil pores. If the pores are of the same diameter, they will start to drain and the water level in them will fall the same distance the water table falls. The maximum tension that the falling water table can exert on a soil pore at the soil surface is $\rho_w g h$ dyne/cm$^2$, where $h$ is the depth of the water table below the soil surface. If the diameter of the pore is too large to support this tension, the pore will not be subject to the maximum tension.

However, pores in the soil are not all the same diameter. Figure 6.9 illustrates what happens in a soil pore of variable diameter when the water table falls for six different cases of water table fall. The depth of soil and the length of the pore channel for each case are taken as 15 cm, so that for the heights of capillary rise shown, the diameter of tube nearest the surface is calculated to be 0.075. Thus the scale in the horizontal direction is, as seen in the figure (2/0.075 =), 27-fold that of the vertical direction. In part A of the figure, the soil is shown saturated to the surface. In parts B, C, D, E, and F, the water table is shown at successively greater depths. In parts B and C, a 4 cm height of water column is held. In part D, only sufficient water curvature has developed in the narrow neck to support about 5 cm height of water. In part E, additional curvature has developed in the narrow neck, such that about 8 cm height of water is supported. In part E, the water table is at 13 cm depth, and in part F, it is at 15 cm depth, a drop of 2 cm. In dropping these 2 cm, the ability of the narrow neck to support the needed 2 cm is exceeded and the pore then empties suddenly and discontinuously to about the level of the water table. This example shows that the emptying of individual pores occurs discontinuously. When the water is removed from a large number of pores, as for any soil

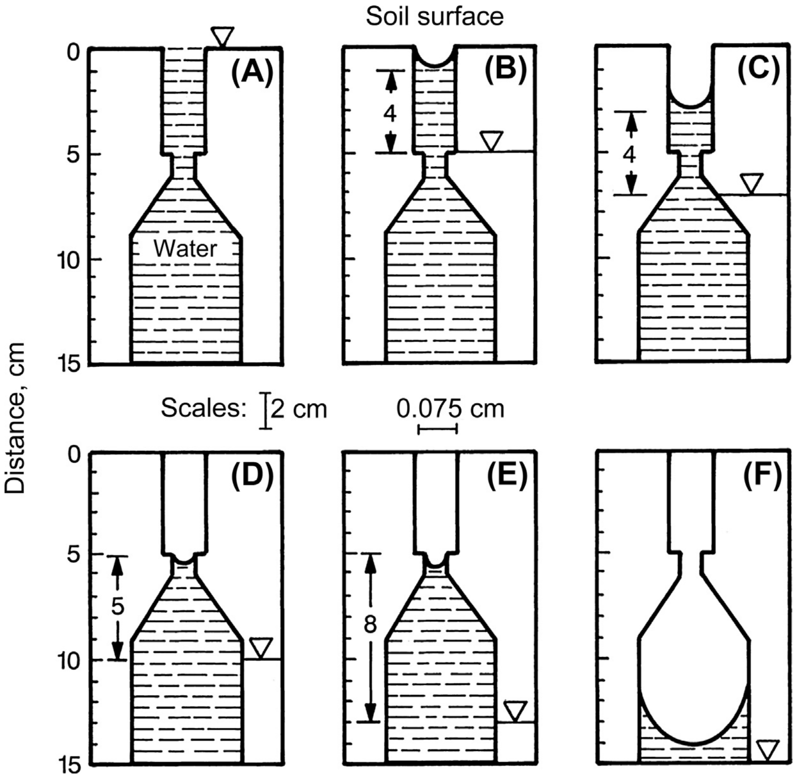

**FIGURE 6.9** The falling water table in a soil pore (channel) of variable diameter. Note the difference in the vertical and horizontal scales. The water table is indicated by the inverted Greek "delta". *From Kirkham (1961).*

sample, a graph of moisture percentage versus tension (or matric potential) does not show the discontinuous nature of the pore-emptying process. The example also shows that soil pores can be filled with water (saturated), yet the water is under tension in the pores.

In Figure 6.10, at the left, three shapes of pores are shown when the water table has fallen from level A to level B. The same three pores are shown at the right when the water table has risen from level C (say) to level B. At the left, the pores are filled up to the height $h_c$, the capillary height of rise. At the right, only one pore is filled up to the height $h_c$; one pore is empty; and one is partially filled. The soil at the left, for the water table falling, has a much higher moisture percentage than the soil at the right, for the water table rising.

Figure 6.10 also gives a physical picture for hysteresis shown in Figure 6.8. A soil that is being wetted up from a rising water table holds less water than a soil that is being dried down. For the falling water table, water is held in tubes of supercapillary size if there is a restriction of

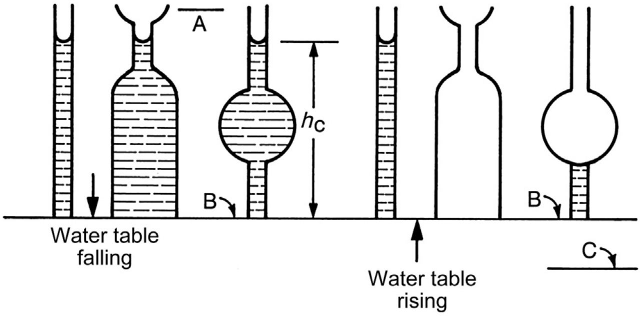

**FIGURE 6.10** Soil pore conditions for a falling and for a rising water table. *From Kirkham (1961).*

capillary size at or below the height of capillary lift. Water can be drawn up above a water table, however, only by a continuous capillary opening without supercapillary enlargements. Hence, more water is held in the *capillary fringe*, which is the thickness of saturated water held by capillarity above the water table, above a sinking water table than above a rising water table. These concepts were explained by Tolman (1937) of Stanford University in his classic book, *Ground Water.*

It is apparent from Figure 6.10 that applications of subirrigation water to raise the water table will not result in the same amount of moisture in the capillary fringe as will applications of surface water. Subirrigation would provide more soil aeration than surface addition of water. This may be desirable in some cases.

## 6.4 APPENDIX: BIOGRAPHY OF MARQUIS DE LAPLACE

Pierre Simon Laplace (1749—1827), the great French mathematician and astronomer, was born at Beaumont-en-Auge in Normandy on March 28, 1749, where his father owned a small estate. At the age of 16, he went to the University of Caen, where his mathematical genius was soon recognized. In 1767, he went to Paris and was appointed professor at the École Militaire. Shortly afterward Laplace discovered that any determinant is equal to the sum of all its minors that can be formed from any selected set of its rows, each minor being multiplied by its algebraic supplement. This theorem has been described as the most important in the subject and has been named after him (Whitrow, 1971).

Laplace next turned his attention to celestial mechanics. In 1773, he took up one of the outstanding problems that until then had resisted all attempts at solution in terms of Newtonian gravitation: the problem of why Jupiter's orbit appeared to be continually shrinking while Saturn's was continually expanding (Whitrow, 1971). In a memoir published in three parts (Academy of Science, 1784–1786), Laplace showed that this phenomenon has a period of 929 years. The phenomenon arises because the mean motions of the two planets are nearly commensurable. The main object of this memoir, however, was to establish the permanence of the solar system for all time. The mutual gravitation interactions of the component bodies of the solar system were so many and varied that Newton had come to the conclusion that divine intervention was required from time to time if the system were to be preserved in anything like its present state. Despite increasing knowledge of planetary perturbations, no advance beyond this position was made until Laplace finally succeeded in showing that, because all planets revolve around the sun in the same direction, the eccentricities and inclinations of their orbits to each other will always remain small, provided they are small at a particular epoch, as in fact they are at present.

Laplace's monumental *Mécanique céleste* appeared in five volumes between 1799 and 1825. It summarized the work of three generations of mathematicians on gravitation. In a supplement to the fourth volume of his treatise on celestial mechanics, Laplace furthered our understanding of capillary phenomena. There he considered free surfaces, including equilibrium shapes of free menisci (Pomeau and Villermaux, 2006). In 1796, he published *Exposition du système du monde*, a semipopular book which is a model of French prose. In a celebrated memoir on the gravitational fields of spheroids, published in 1785, he introduced the potential function and the equation named after him. Laplace is also famous for his *Théorie analytique des probabilités* published in 1812 and his *Essai philosophique* on the same subject published in 1814. The former introduced important new ideas in pure mathematics, in particular, the theory of Laplace transforms (Whitrow, 1971).

In 1799, when Napoleon I became first consul, he appointed Laplace minister of the interior, but dismissed him after 6 weeks for bringing "the spirit of infinitesimals into administration" and elevated him to the senate. Later, Laplace was made a count of the empire, and after the restoration of the Bourbons he was designated a marquis. He died in Paris on March 5, 1827 (Whitrow, 1971).

## References

Aly, Saleh M., Letey, J., 1988. Polymer and water quality effects on flocculation of montmorillonite. Soil Sci. Soc. Am. J. 52, 1453–1458.

Bartlett, John, 1955. Bartlett's Familiar Quotations. Thirteenth and Centennial ed. Little, Brown and Company, Boston.

Buderi, R., 1996. The Weapon that Won the War. Simon Schuster, Little, Brown, New York.

Cattell, J., 1955. In: American Men of Science. A Biographical Directory. vol. 1. Physical Sciences, ninth ed. Science Press, Lancaster, Pennsylvania; and R.K. Bowker, New York, New York, p. 1164.

Cattell, J., 1961. In: American Men of Science. A Biographical Directory. The Physical and Biological Sciences, Tenth ed. Jaques Cattell Press, Tempe, Arizona, p. 2437.

De Boodt, M., 1975. Use of soil conditioners around the world. In: Gardner, W.R., Clapp, C.E., Gardner, W.H., Moldenhauer, W.C., Mortland, M.M., Rich, C.I. (Eds.), Soil Conditioners. SSSA Special Publication No. 7. Soil Science Society of America, Madison, Wisconsin, pp. 1–12.

Dickinson, M., 2003. How to walk on water. Nature 424, 621–622.

Falkovich, G., Weinberg, A., Denissenko, P., Lukaschuk, S., 2005. Floater clustering in a standing wave. Nature 435, 1045 (one page only).

Gao, X., Jiang, L., 2004. Water-repellent legs of water striders. Nature 432, 36 (one page only).

Hu, D.L., Chan, B., Bush, J.W.M., 2003. The hydrodynamics of water strider locomotion. Nature 424, 663–666.

Kirkham, D., 1961. Lectures on Agricultural Drainage. Institute of Land Reclamation, College of Agriculture. Alexandria University, Alexandria, Egypt (Copy in the Iowa State University Library, Ames, Iowa.).

Kirkham, D., Powers, W.L., 1972. Advanced Soil Physics. Wiley-Interscience, New York.

Kirkham, D., Runkles, J., 1952. Evaluation of new soil conditioners. Trans. [Iowa] State Hort. Soc. 37, 41–46.

Lentz, R.D., Sojka, R.E., 2009. Long-term polyacrylamide formulation effects on soil erosion, water infiltration, and yields of furrow-irrigated crops. Agron. J 101, 305–314.

Linford, L.B., 1930. Soil moisture phenomena in a saturated soil. Soil Sci. 29, 227–235.

Liu, X., Duncan, J.H., 2003. The effects of surfactants on spilling breaking waves. Nature 421, 520–523.

Mertens, J., 2006. Oil on troubled waters: Benjamin Franklin and the honor of Dutch seamen. Phys. Today 59 (1), 36–41.

Pomeau, Y., Villermaux, E., 2006. Two hundred years of capillarity research. Phys. Today 59 (3), 39–44. + cover.

Porter, A.W., 1971. Surface tension. Encyclopaedia Britannica 21, 442–450.

Schamp, N., Huylebroeck, J., Sadones, M., 1975. Adhesion and adsorption phenomena in soil conditioning. In: Gardner, W.R., Clapp, C.E., Gardner, W.H., Moldenhauer, W.C., Mortland, M.M., Rich, C.I. (Eds.), Soil Conditioners. SSSA Special Publication No. 7. Soil Science Society of America, Madison, Wisconsin, pp. 13–23.

Schaum, D., 1961. Theory and Problems of College Physics. Schaum Publishing, New York.

Seitz, F., 1996. How Allies Shared Radar Secrets. Book Review of the Weapon that Won the War by Robert Buderi. Simon and Schuster, Little, Brown. Nature 384, 424–425.

Sharratt, B.S., Reicosky, D.C., Idso, S.B., Baker, D.G., 1983. Relationships between leaf water potential, canopy temperature, and evapotranspiration in irrigated and nonirrigated alflafa. Agron. J. 75, 891–894.

Soil Science Society of America, 2008. Glossary of Soil Science Terms 2008. Soil Science Society of America, Madison, Wisconsin.

Sojka, R.E., Lentz, R.D., Westermann, D.T., 1998. Water and erosion management with multiple applications of polyacrylamide in furrow irrigation. Soil Sci. Soc. Am. J. 62, 1672–1680. + cover.

Sophocleous, M.A., 2010. Understanding and explaining surface tension and capillarity: an introduction to fundamental physics for water professionals. Hydrogeol. J. 18, 811–821.

Tolman, C.F., 1937. Ground Water. McGraw-Hill, New York.

Wallace, A., Terry, R.E. (Eds.), 1998. Handbook of Soil Conditioners. Marcel Dekker, New York.

Whitrow, G.J., 1971. Laplace, Pierre Simon. Encyclopaedia Britannica 13, 716–717.

Webster's New World Dictionary of the American Language, college ed., 1959. World Publishing, Cleveland.

# CHAPTER 7

# Water Movement in Saturated Soil

Understanding movement of water in saturated soil is important in drainage and groundwater studies. The French hydraulic engineer, Henry Darcy (1803–1858) experimentally determined the law that governs the flow of water through saturated soil (1856), which is called Darcy's law. (See the Appendix, Section 7.7, for a biography of Darcy.)

## 7.1 DARCY'S LAW

To illustrate Darcy's law, let us consider Figure 7.1, which shows water flowing through a soil column of length $L$ and cross-sectional area, $A$ (Kirkham and Powers, 1972, p. 47). The law can be stated as follows:

$$Q = -KA(h_2 - h_1)/(z_2 - z_1), \tag{7.1}$$

where $Q$ is the quantity of water per second such as in cubic centimeters per second, often called the "flux"; $K$, centimeters per second, is the

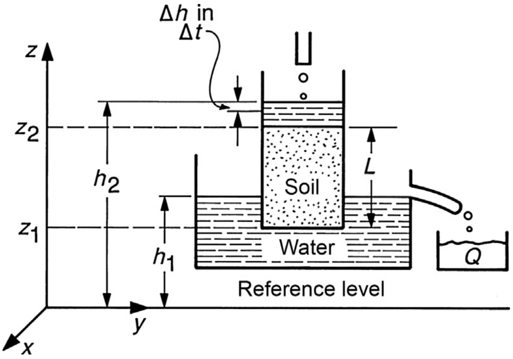

**FIGURE 7.1** Illustration of Darcy's law. *From Kirkham and Powers (1972), p. 47, ©1972. This material is used by permission of John Wiley & Sons, Inc. and William L. Powers.*

http://dx.doi.org/10.1016/B978-0-12-420022-7.00007-0

Copyright © 2014 Elsevier Inc. All rights reserved.

"hydraulic conductivity" (the law defines $K$); heads $h_1$ and $h_2$ and distances $z_1$ and $z_2$ are as shown in Figure 7.1. The reference level here is the $x, y$ plane. The head $h_1$ is the hydraulic head for all points at the bottom of the soil column, that is, at $z = z_1$, and similarly, the head $h_2$ applies to all points at the top of the soil column, $z = z_2$. The length of the column is $z_2 - z_1 = L$. The negative sign in the Darcy equation is used so that a positive value of $Q$ will indicate a flow in the positive $z$ direction. The positive $z$ direction is measured from $z_1$ to $z_2$ (Kirkham and Powers, 1972, pp. 46–47).

In the Darcy law equation, the quantity $(h_2 - h_1)/(z_2 - z_1)$ is called the "hydraulic gradient" $i$; the ratio $Q/A$ is called the "flux per unit cross-section" or "flux density" (cubic centimeters per second) divided by centimeters squared. The ratio $Q/A$ is also called the "Darcy velocity" $v$ or, very often, just the velocity $v$. Therefore, Darcy's law may be written as $v = -Ki$. The "actual velocity" of the water in the soil is much greater than the Darcy velocity. The actual velocity is on the average $v/f$ where $f$ is the "porosity" (Kirkham and Powers, 1972, p. 47). The porosity is the volume of pores in a soil sample divided by the bulk volume of the sample (Soil Science Society of America, 2008). The pores can be filled with air or water. (Because Darcy's law is for saturated soil, the pores are filled with water when it applies). The percent porosity in the soil can be determined from the following equation (Millar et al., 1965, p. 54):

$$\%\ \text{porosity} = [1 - (\text{bulk density}/\text{particle density})] \times 100. \tag{7.2}$$

The Darcy velocity $v$ means more than flux per unit area, $Q/A$. In Figure 7.1, suppose that the supply of water shown dripping into the soil column is abruptly cut off during a short time interval $\Delta t$ during which $h_2$ decreases by $\Delta h$. Let $\Delta q$ be the volume of water flowing downward through the soil in $\Delta t$. Because $Q$ is the flow per second, we may write $\Delta q$ as $\Delta q = Q\Delta t$, and we also have by continuity of flow $\Delta q = A\Delta h$. Therefore, $Q\Delta t = A\Delta h$, and $Q/A = \Delta h/\Delta t$. Physically, $\Delta h/\Delta t$ is a velocity; therefore, so is $v = Q/A$. Thus, the Darcy velocity $v$ represents the rate $\Delta h/\Delta t$ approaches $\mathrm{d}h/\mathrm{d}t$ of fall of surface water in Figure 7.1. If the hydraulic gradient is unity (pressure potential is the same at the top and bottom of the soil column), then $v = -K$. Thus, it is determined that $K$ is numerically equal to the rate of fall of a thin layer of ponded water into the soil, under only the force of the earth's gravitational pull. We also see that $K$ is the velocity under a unit hydraulic gradient (Kirkham and Powers, 1972, p. 48).

Flow in a vertical soil column has been used to derive and illustrate Darcy's law. However, the law and principles developed in the preceding paragraphs apply for the flow of water in any direction in the soil.

For a discussion of the use of Darcy's law in groundwater hydrology, see Anderson (2007).

## 7.2 HYDRAULIC CONDUCTIVITY

The hydraulic conductivity should not be confused with the "intrinsic permeability", sometimes just called the "permeability", of the flow medium. The intrinsic permeability, symbolized by $k$ by *M*. Muskat (1946) in his classic treatise (Muskat was a petroleum engineer in the United States well known for his studies in the 1930s and 1940s of fluid flow through porous media), is equal to $K\eta/\rho g$, where $K$ is the Darcy hydraulic conductivity, $\eta$ is the fluid viscosity, $\rho$ is the fluid density, and $g$ is the acceleration due to gravity. Dimensionally, $k$ is an area ($L^2$). The units of $K$ are meters per day, which is the same as (cubic meters per square meter)/day. That is, $K$ may be interpreted as the cubic meter of water seeping through a square meter of soil per day under a unit hydraulic gradient (Kirkham and Powers, 1972, pp. 48–49).

Hydraulic conductivity in natural field soil is governed by factors such as cracks, root holes, worm holes, and stability of soil crumbs. Texture, that is, the percent of the primary particles of sand, silt, and clay, usually has a minor effect on hydraulic conductivity, except for disturbed soil materials. The hydraulic conductivity of natural soils in place varies from about 30 m/day for a silty clay loam to 0.05 m/day for a clay (Kirkham, 1961a, p. 46; Kirkham, 1961b). The hydraulic conductivity for disturbed soil materials varies from about 600 m/day for gravel to 0.02 m/day for silt and clay. The value of $K$ can be made higher or lower by soil management. Roots of crops after decay increase $K$; compaction of soil by animals or machinery decreases $K$, at least in the surface soil.

Ordinarily one considers $K$ in $v = -Ki$ to be a constant under saturated flow. It is a constant if (1) the physical condition of the soil and of the water does not change in space or time as the water moves through the soil (e.g., the soil is "isotropic", i.e., hydraulic conductivity is the same regardless of the direction of measurement) and if (2) the type of flow is laminar, that is, not turbulent. In laminar flow, two particles of water seeping through the soil will describe paths (streamlines) that never cross each other. In turbulent flow, eddies and whirls develop. The possibility of turbulent flow is considered in soil only if the soil is a coarse sand or gravel, and then only if the hydraulic gradients are large (larger than those found in most problems of interest to agricultural soil scientists).

## 7.3 LAPLACE'S EQUATION

To solve groundwater seepage and drainage problems, it is desirable to have a general differential equation (Kirkham and Powers, 1972, p. 49), and Laplace's equation, which is a familiar equation occurring in nearly all branches of applied mathematics, applies. Laplace's equation is derived from Darcy's law and the *equation of continuity.* (See the appendix of Chapter 6 for a biography of Laplace.) The equation of continuity states mathematically that mass can neither be created nor destroyed. We can state the equation of continuity in words, as follows: For a volume element $x$ times $y$ times $z$, the change in the velocity of water in the $x$ direction plus a change in velocity of water in the $y$ direction plus a change in the velocity of water in the $z$ direction are equal to the total change in water content, $\theta$, per unit time of the volume element under consideration. That is, the inflow of water in the element minus outflow of water is equal to the water accumulated. Let us imagine a rectangular $x$, $y$, $z$ system of coordinates that is established in a homogeneous porous medium of constant hydraulic conductivity, and let $h$ be the hydraulic head referred to an arbitrary reference level for a point $(x, y, z)$ and let time be $t$ and $v_x$, $v_y$, and $v_z$ be the velocity of water flowing in the $x$, $y$, and $z$ directions, respectively; then, with $\theta$ being the volume of water per unit volume of bulk soil, from the equation of continuity,

$$-\left[(\partial v_x/\partial_x) + \left(\partial v_y/\partial_y\right) + (\partial v_z/\partial_z)\right] = \partial\theta/\partial t \tag{7.3}$$

and from Darcy's law, one may, for an incompressible steady-state flow in a porous medium where K is constant, derive the expression (Kirkham and Powers, 1972, p. 52)

$$\left(\partial^2 h/\partial x^2\right) + \left(\partial^2 h/\partial y^2\right) + \left(\partial^2 h/\partial z^2\right) = 0, \tag{7.4}$$

as the expression governing groundwater flow. The equation is abbreviated $\nabla^2 h = 0$.

Charles S. Slichter (1899), a mathematician at the University of Wisconsin, was the first to show in 1899 that Laplace's equation applies to the motion of groundwater (Kirkham and Powers, 1972, p. 52). Many mathematical solutions for groundwater flow using Laplace's equation have been done by Don Kirkham (1908–1998) of Iowa State University.

## 7.4 ELLIPSE EQUATION

In addition to Darcy's equation and Laplace's equation, another important equation for saturated flow is called the Colding equation after the Danish engineer A. Colding, who published it in 1872 (van der Ploeg et al., 1997). It is used to determine drain spacings. The equation is also called the ellipse equation, because it describes an ellipse. Therefore, before we look at the Colding equation, let us study an ellipse.

The locus of a point $P$ that moves in a plane so that the sum of its distances from two fixed points in the plane is constant is called an

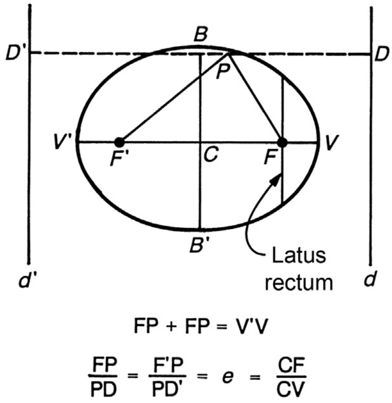

**FIGURE 7.2** The ellipse. It is the locus of a point $P$ that moves in a plane so that the sum of its distances from two fixed points in the plane, $F$ and $F'$, is constant. *From Ayers (1958), p. 322, ©1958. This material is reproduced with permission of The McGraw-Hill Companies.*

"ellipse" (Ayers, 1958, p. 322). The fixed points $F$ and $F'$ are called the "foci", and their midpoint $C$ is called the "center" of the ellipse (Figure 7.2). The line $FF'$ joining the foci intersects the ellipse in the points $V$ and $V'$, called the "vertices". The segment $V'V$ intercepted on the line $FF'$ by the ellipse is called its "major axis"; the segment $B'B$ intercepted on the line through $C$ perpendicular to $F'F$ is called its "minor axis".

A line segment in which the extremities are any two points on the ellipse is called a "chord". A chord that passes through a focus is called a "focal chord"; a focal chord perpendicular to the major axis is called a "latus rectum".

The equation of an ellipse assumes its simplest ("reduced") form when its center is at the origin and its major axis lies along one of the coordinate axes. When the center is at the origin and the major axis lies along the $x$-axis, the equation of the ellipse is (Figure 7.3)

$$\left(x^2/a^2\right) + \left(y^2/b^2\right) = 1. \tag{7.5}$$

Figure 7.3 is an oblate ellipse. "Oblate" comes from the Latin "oblatus", which means "offered" or "thrust forward", and means "being thrust forward at the equator". In geometry, oblate means flattened at the poles.

When the center is at the origin and the major axis lies along the $y$-axis, the equation of the ellipse is (Figure 7.4)

$$\left(x^2/b^2\right) + \left(y^2/a^2\right) = 1. \tag{7.6}$$

Figure 7.4 is a prolate ellipse. "Prolate" comes from the Latin "prolatus", which is the past participle of "proferre", "to bring forward". Prolate means "extended or elongated at the poles".

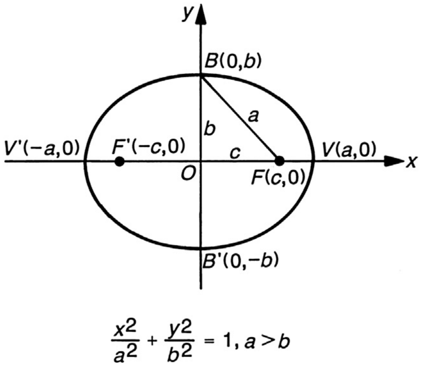
y
B(0,b)
a
b
V'(−a,0)
F'(−c,0)
c
V(a,0)
x
O
F(c,0)
B'(0,−b)
$\frac{x^2}{a^2} + \frac{y^2}{b^2} = 1, a > b$

**FIGURE 7.3** An oblate ellipse. *From Ayers (1958), p. 323, ©1958. This material reproduced with permission of The McGraw-Hill Companies.*

A circle is a special form of an ellipse in which the semimajor and semiminor axes are equal in length. The equation of a circle is

$$x^2 + y^2 = r^2, \tag{7.7}$$

where $r$ is the radius of the circle, and the circle has its center at the origin of the $x$, $y$ coordinate system.

If we are dealing in three dimensions, we have an “ellipsoid”. The locus of the equation

$$x^2/a^2 + y^2/b^2 + z^2/c^2 = 1 \tag{7.8}$$

is called an ellipsoid (Figure 7.5). If at least two of $a$, $b$, $c$ are equal, the locus is called an ellipsoid of revolution, and if $a = b = c$, the locus is a sphere (Ayers, 1958, p. 387).

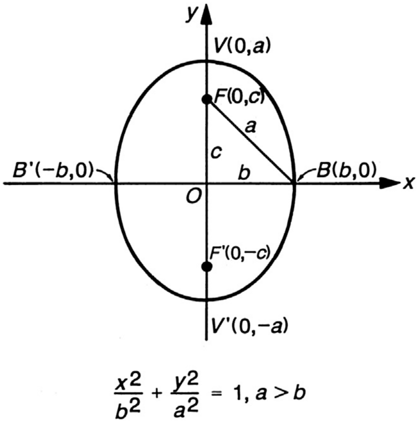
y
V(0,a)
F(0,c)
a
c
B'(−b,0)
b
B(b,0)
x
O
F'(0,−c)
V'(0,−a)
$\frac{x^2}{b^2} + \frac{y^2}{a^2} = 1, a > b$

**FIGURE 7.4** A prolate ellipse. *From Ayers (1958), p. 323, ©1958. This material reproduced with permission of The McGraw-Hill Companies.*

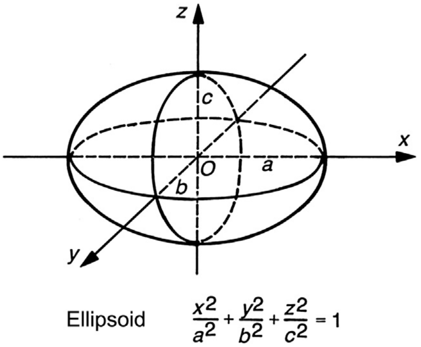
z
c
x
O
a
b
y
Ellipsoid $\frac{x^2}{a^2}+\frac{y^2}{b^2}+\frac{z^2}{c^2}=1$

**FIGURE 7.5** The ellipsoid. *From Ayers (1958), p. 387, ©1958. This material is reproduced with permission of The McGraw-Hill Companies.*

The need for soil drainage is widespread around the world, not only in the wet soils of northern Europe and in the states of the United States that are wet in the spring (e.g., Iowa) but also in irrigated regions. It is generally accepted that the Danish engineer Colding was the first to derive a drain-spacing equation based on modern soil—water flow concepts. For parallel, equally spaced tile (tube) drains resting on an impermeable barrier, and for steady-state flow conditions, Colding (1872) derived the following expression (van der Ploeg et al., 1997, 1999):

$$L^2 = [(4K)/R]b^2, \tag{7.9}$$

where $L$ is the drain distance, $K$ is the soil hydraulic conductivity, $R$ is the constant rate of precipitation, and $b$ is the maximum height of the water table above the drain level, midway between the drains (Figure 7.6). Equation (7.9) describes an ellipse, with the drain distance $L$ being the

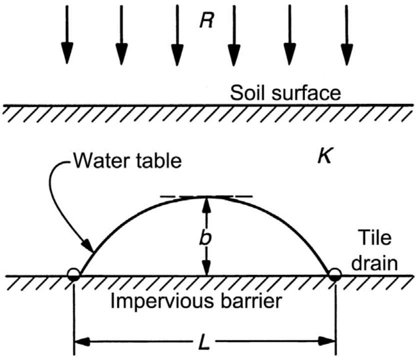

**FIGURE 7.6** Schematic representation of the subsurface drain problem, as considered by Colding. *From van der Ploeg et al. (1999), ©1999, Madison, Wisconsin. Reprinted by permission of the Soil Science Society of America.*

major axis and the maximum water table height *b* above the drain level being the semiminor axis (Kirkham and Powers, 1972, pp. 90, 92).

It is not known if Colding was familiar with the work of Darcy (1856), but apparently he was not, because he does not mention him in his work. Darcy's work on hydraulic conductivity did not receive much attention until the second edition of the book by Dupuit (1863), and even then it took time for people to become familiar with it. Nevertheless, Colding was using Darcy-like theory to derive his equation.

The US Bureau of Reclamation uses the Colding equation, as modified by Hooghoudt (1940) for design purposes (van der Ploeg et al., 1999). Instead of equally spaced tile drains, (Hooghoudt 1937, 1940) considered equally spaced drainage ditches overlying an impervious layer (Figure 7.7). (For a biography of Hooghoudt, see Raats and van der Ploeg, 2005.) In the Imperial Valley in California, the Colding equation, as modified by Aronovici and Donnan (1946) is used (van der Ploeg et al., 1999). Aronovici and Donnan, apparently unaware of the work of Hooghoudt, also developed a modified Colding equation almost identical to the Hooghoudt (1940) equation. It is important to recognize that some of today's most common drainage design practices are based on the Colding (ellipse) equation.

The ellipse is an important geometric form because of its widespread application in soil–water relations and other aspects of nature. Apollonian curves—that is, ellipses, parabolas, and hyperbolas—all have amazing relationships hidden in them (Anvar Kacimov, personal communication, December 9, 1999). (See the Appendix, Section 7.6, for a biography of Apollonius, a Greek geometer.) Johannes Kepler (1571–1639, German astronomer and mathematician) also came to his celestial mechanics formula from the geometric side. (See the appendix of Chapter 30 for a biography of Kepler.) He first selected an ellipse and then applied it to orbits (Goodstein and Goodstein, 1996). To understand the

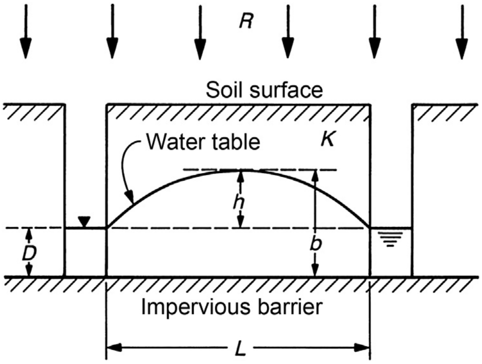

**FIGURE 7.7** Geometric representation of a homogeneous soil, underlain by an impervious barrier, which is drained by parallel, equally spaced ditches, where the ditches reach the impervious barrier, as considered by Hooghoudt. *From van der Ploeg et al. (1999), Madison, Wisconsin. Reprinted by permission of the Soil Science Society of America.*

interception of solar radiation by plant leaves, which we discuss in Chapter 30, we need to study Kepler's laws of planetary motion. He saw that the planets orbit the sun in elliptical paths.

Other examples of Apollonian curves used in soil–water studies include the work by Kacimov (2000), who used the special case of an ellipsoid, the hemisphere, to study three-dimensional groundwater flow to a lake, and the work by Kirkham and Clothier (1994), who used the ellipsoidal equation (Eqn (7.8)) to describe the shape of the wet front as it expands under a surface disc that is infiltrating water into the soil.

## 7.5 LINEAR FLOW LAWS

Darcy's law is a linear flow law. It is linear because the $v$, the Darcy velocity, of $v = -Ki$, varies linearly with the hydraulic gradient $i$ (Kirkham and Powers, 1972, p. 74). Ohm's law is one of the most common linear flow laws and is used in problems concerning the flow of electricity. In Ohm's law, the current transported is linearly related to the difference in the driving potential across the system. We shall return to Ohm's law when we study electrical analogues (Chapter 22). Gauss's law, used in studying electrostatic fields, is another linear flow law (Kirkham, 1961a, p. 104). Poiseuille's law for flow of a liquid through a capillary tube is not a linear flow law, because an exponent >1 occurs in it. Poiseuille found that the volume of fluid moving in unit time along a cylinder is proportional to the fourth power of its radius. We will use Poiseuille's law to study flow of water in the vessel members in the xylem tissue (Chapter 15).

Table 7.1 shows that linear flow laws are similar. For example, Darcy's law is similar to Ohm's law, Fick's law, and Fourier's law. These laws are commonly used in soil physics; Darcy's law is used in studies of water flow, Fick's law in studies of gaseous flow (Kirkham, 1994), and Fourier's law in studies of heat flow. It is important to know the similarities, because, for water flow (Darcy's law) problems for which solutions are desired, there may exist analogous electrical flow (Ohm's law) or heat flow (Fourier's law) problems that have been already solved. These solutions can be used for writing down directly the solution of the desired water flow problem (Kirkham, 1961a, p. 104).

Linear flow phenomena are involved in other studies, as well, as listed by Moon and Spencer (1961):

1. *High-voltage engineering:* Design of high-tension transformer bushings, transmission-line insulators, electrostatic voltmeters, and Van de Graaf generators
2. *Magnetostatics:* Calculations for generators, motors, lifting magnets, solenoids, synchrotrons

**TABLE 7.1** Linear Flow Laws Encountered in Soil—Plant—Water Relationships. No Exponents (Other Than 1) Appear in a Linear Flow Law

**Linear Flow Laws**

| **Law** | **Quantity Transported per sec Across Flow Region** | **Transport Coefficient of Flow Region** | **Difference in Driving Potential Across System** | **Form Factor $F$ for System (e.g., Rectangular Box)**[†] |
|---|---|---|---|---|
| Ohm<br>$I = \frac{\sigma \Delta V A}{L} = \frac{V}{R}$[‡] | $I =$ Amperes or coulombs per sec | $\sigma =$ Specific electrical conductivity (S/cm) | $\Delta V =$ Difference in electrical potential between input and output ($V$) | $F = \frac{A}{L}$ |
| Darcy<br>$Q = \frac{k \Delta h A}{L}$ | $Q = \text{cm}^3/\text{sec}$ | $k =$ Hydraulic conductivity (cm/sec) | $\Delta h =$ Difference in head of water column between input and output (cm) | $F = \frac{A}{L}$ |
| Fick<br>$Q = \frac{D \Delta C A}{L}$ | $Q = \text{g}/\text{sec}$ | $D =$ Diffusion coefficient ($\text{cm}^2/\text{sec}$) | $\Delta C =$ Difference in concentration of gas at input and output ($\text{g}/\text{cm}^3$) | $F = \frac{A}{L}$ |
| Fourier<br>$Q = \frac{K \Delta T A}{L}$ | $Q = \text{cal}/\text{sec}$ | $K =$ Thermal conductivity (cal per sec per $\text{cm}^2$ for a thickness of 1 cm and temperature difference of 1 °C) | $\Delta T =$ Difference in temperature between input and output (°C) | $F = \frac{A}{L}$ |

[†] A = *Cross-sectional area of the system (box) perpendicular to the direction of flow;* L = *length of the system (box) through which the flow occurs. The form factor is for two-dimensional flow problems; it is the same for equal geometries of the flow region.*

[‡] R *in this equation = resistance in ohms, Ω. (1 S = 1/Ω = mho).*

3. *Heat conduction:* Determination of temperature distributions in electric machinery, heating devices, cable ducts, and refrigerators
4. *Fluid flow:* Calculation of flow about airfoils and other obstructions, seepage of fluids through sand
5. *Electrodynamics:* Determination of resistance of irregular-shaped conductors, electrical prospecting
6. *Electrostatics:* Design of vacuum tubes, electron microscopes, and cathode ray oscilloscopes, television tubes
7. Elasticity: Vibration engineering, structural engineering
8. *Diffusion:* Calculation of the heating and cooling of ingots, the annealing of glass, and the diffusion of fluids
9. *Acoustic waves:* Design of loud speakers and microphones
10. *Electromagnetic waves:* Calculation of wave guides and antennas

To the list of Moon and Spencer (1961) can be added an 11th item:

11. *Mass flow of gas under a small pressure gradient*

## 7.6 APPENDIX: BIOGRAPHY OF APOLLONIUS OF PERGA

Apollonius of Perga (Pergaeus), a Greek geometer of the Alexandrian school, was probably born about 25 years later than Archimedes (i.e., ~261 BC). He flourished in the reigns of Ptolemy Euergetes and Ptolemy Philopator (247–205 BC) (Heath and Neugebauer, 1971). His treatise on *Conics* gained him the title of the Great Geometer, and, through this work, his fame has been transmitted to modern times. Most of his other treatises were lost, although their titles and a general indication of their contents were passed on by later writers, especially Pappus. After Apollonius wrote the *Conics* in eight books in a first edition, he brought out a second edition, considerably revised with regard to books I and II.

The degree of originality of the *Conics* can best be judged from Apollonius's own prefaces. He made the fullest use of his predecessors' works, such as Euclid's four books on conics, which is clear from his allusions to Euclid, Conon, and Nicoteles. Books I–IV form an "elementary introduction" (i.e., contain the essential principles) and the rest of the books are specialized investigations. Apollonius introduced the names "parabola", "ellipse", and "hyperbola". Books V–VII are highly original. Apollonius's genius takes its highest form in book V, where he treats normals as minimum and maximum straight lines drawn from given points to the curve (independently of tangent properties), discusses how many normals can be drawn from particular points, finds their feet by construction, and gives propositions determining the center of curvature at any point (Heath and Neugebauer, 1971).

Six other treatises by Apollonius (each in two books) were concerned with cutting off a ratio, cutting off an area, determinate sections, tangencies, inclinations, and plane loci. An Arabic version of the first treatise was found toward the end of the seventeenth century in the Bodleian library by Edward Bernard, who began a translation of it. (The Bodleian library is a famous library at Oxford University in England named after Sir Thomas Bodley, 1545–1613, an English diplomat and man of letters and founder of the library.) Edmund Halley (1656–1742), the English astronomer, finished the translation and published it with a restoration of the second treatise (1706).

Other works by Apollonius referred to by ancient writers include (1) *On the Burning-Mirror*, where the focal properties of the parabola probably were discussed; (2) *On the Cylindrical Helix*; (3) a comparison of the dodecahedron and the icosahedron inscribed in the same sphere; (4) a work which included Apollonius's criticisms and suggestions for the improvement of Euclid's *Elements*; (5) a work in which he showed how to find closer limits for the value of $\pi$ than the $3\frac{1}{7}$ and $3\frac{10}{71}$ of Archimedes; (6) an arithmetic work on a system of expressing large numbers and showing how to multiply such large numbers; and (7) extensions of the theory of irrationals expounded in Euclid.

## 7.7 APPENDIX: BIOGRAPHY OF HENRY DARCY

Henry Philibert Gaspard Darcy (1803–1858) is best known for his scientific work on pipe flow (Howland, 1971). He lived in Dijon, France, for most of his life, where he was inspector general of bridges and highways. His father, a town functionary, died when he was 14 years old (Philip, 1995). His determined mother named him the English "Henry" instead of the French "Henri", and ensured that both Henry and his brother Hugues received the best education possible. Henry won a scholarship to the Dijon Polytechnic and in 1826 graduated brilliantly as a civil engineer. He married Henriette Carey in 1828, but they never had any children (Ik-Jae Kim, Graduate Student, Department of Biological and Agricultural Engineering, Kansas State University, personal communication, September 15, 2004).

Working as an engineer, he devoted his life to providing the town of Dijon with pure water. The waters of cities then, including Dijon, were often inadequate, always in short supply, and dirty. Dijon had at its disposition only wells plus the water of the Ouche, and well waters were not protected from contamination. The town of Dijon was crossed by the ancient bed of a small stream, the Suzon, which was uncovered over almost all its length, with no part paved, and served over a length of 1300 m as the main sewer for wastes of every kind. It was never cleaned, and during hot weather, the town was poisoned by pestilential odors.

To clean up the water, Darcy substituted the method that became standard (Philip, 1995). In 1833, Darcy, on his own initiative, presented his plan to the municipal authorities. The Municipal Council adopted his recommendations, and the General Council of Bridges and Highways (Ponts et Chaussées) approved all parts of the proposed plan. He developed a network of underground conduits with underground reservoirs. On September 6, 1840, without any errors or mishaps, the beneficial waters reached the reservoir of the Porte Guillaume. By 1844, the whole network of underground conduits had been completed (Philip, 1995). Consequently, Dijon possessed from 1840 the benefits that Paris did not discover until 20 years later, and enjoyed an abundance of water. Other towns asked for Darcy's assistance, such as Brussels, which officially asked for his help in 1851 and 1852 and adopted the plan that he provided.

Darcy had given his native town the better part of his life. For this work of 12–15 years, he wished to receive no remuneration. He would not agree even to be reimbursed for his expenses. He accepted only a gold medal that commemorated his work.

In 1848, the revolution overthrew King Louis-Philippe and brought in the radical and short-lived Second Republic. Despite the facts that Darcy was apolitical and that he had given generously of his own money to set up workers' cooperatives, the Second Republic saw him as a dangerous and reactionary collaborator with the ancient regime. Darcy was stripped of his offices and banished from Dijon. In 1852, the Second Republic was succeeded by the Second Empire of Emperor Napoleon III, and Darcy was politically rehabilitated.

In 1854, Darcy was 51, but in poor health. Ever since his days as a young engineer, he had been a prey to nervous troubles and to attacks producing symptoms of meningitis. Time and overwork gradually made these attacks more acute. He suffered a bad period in 1845, while he was directing the works at Blaisy. Later, in Paris, he lost consciousness during a conference, and in 1853, he fell down in the open street. He took leave for several months, but, as he continued to suffer intolerably, he despaired and asked to be released from his responsibilities. Nevertheless, unable to stay inactive, he pursued his hydraulic experiments, and it was during these last years that he was able, thanks to financial help from the Ministry of Public Works, to carry out the work that he wrote up and published in 1856.

In 1857, the Académie des Sciences wished to elect him to the vacancy left by the mathematician Cauchy who had just died. (Baron Augustin Louis Cauchy, 1789–1857, was one of the greatest of modern French mathematicians.) Darcy was elected without discussion, but on January 2, 1858, he succumbed to pleurisy aggravated by angina and died in Paris.

Dijon gave him a public funeral appropriate to his great labors. The whole population went to receive his remains at the railway station, all the functionaries in uniform, armed soldiers lining the streets, the workers of cooperatives founded on his initiative carrying the coffin, and the bishop officiating. Sadly, 135 years after Darcy's death, when the whole town mourned it, nobody in Dijon knew who he was, even though his name appears in many places in Dijon (Philip, 1995).

There is in existence a collection of letters from Darcy to Henri Émile Bazin (1829—1917). Bazin was 26 years younger than Darcy, a hydraulic engineer working in Dijon whose researches on channel and pipe flow are well known. Bazin, acting as Darcy's assistant, was trained to be a careful and assiduous experimenter. He carried on Darcy's original program of tests on open-channel resistance. His studies also extended to wave propagation, to flow over weirs, and to the contraction of the liquid vein coming from an orifice. Bazin was elected to the French Academy of Sciences in 1865. He died on February 7, 1917, at Dijon (Howland, 1971).

## References

Anderson, M.P., 2007. Introducing groundwater physics. Phys. Today 60 (5), 42—47.

Aronovici, V.S., Donnan, W.W., 1946. Soil permeability as a criterion for drainage-design. Trans. Am. Geophys. Union 27, 95—101.

Ayers Jr, F., 1958. Schaum's Outline of Theory and Problems of First Year College Mathematics. Schaum Publishing, New York.

Colding, A., 1872. On the Laws of Water Movement in Soil (In Danish, with a French Summary). Det kgl. Danske Videnskabernes Selskabs Skrifter, 5te Raekke, naturvidenskabelig og mathematisk Afdeling, Copenhagen, 9 B VIII, 563—621.

Darcy, H., 1856. Les Fontaines Publiques de la Ville de Dijon. (The public fountains of the city of Dijon). In: Victor Dalmont (Ed.), Libraire des Corps Impériaux des Ponts et Chaussées et des Mines: Quai des Augustins, 49. Paris (In French).

Dupuit, J., 1863. Theoretical and Practical Studies about the Movement of Water in Open Channels and through Permeable Terrains (In French.), second ed. Dunod, Paris.

Goodstein, D.L., Goodstein, J.R., 1996. Feynman's Lost Lecture: The Motion of Planets Around the Sun. Jonathan Cape, London. Published in the US by Norton.

Heath, T.L., Neugebauer, O.E., 1971. Apollonius. Encyclopaedia Britannica 2, 122—123.

Howland, W.E., 1971. Bazin, Henri Émile (1829—1917). Encyclopaedia Britannica 3, 314.

Hooghoudt, S.B., 1937. Contributions to the Knowledge of Some Physical Soil Properties. No. 6. Determination of the Conductivity of Soils of the Second Kind (In Dutch.) Verslagen van Landbouwkundige Onderzoekingen, no. 43(13) B, Dep. van Economische Zaken, Directie van den Landouw. Algemeene Landsdrukkerij, The Hague, The Netherlands.

Hooghoudt, S.B., 1940. Contributions to the Knowledge of Some Physical Soil Properties. No. 7. General Discussion of the Problem of Drainage and Infiltration by Means of Parallel Drains, Trenches, Ditches and Canals (In Dutch). Verslagen van Landbouwkundige Onderzoekingen, no. 46 (14) B, Dep. van Landbouw en Visscherij, Directie van den Landbouw. Algemeene Landsdrukkerij, The Hague, The Netherlands.

Kacimov, A.R., 2000. Three-dimensional groundwater flow to a lake: an explicit analytical solution. J. Hydrol. 240, 80—89 (See his Figure 1).

Kirkham, D., 1961a. Lectures on Agricultural Drainage. Institute of Land Reclamation. College of Agriculture, Alexandria University, Alexandria, Egypt (Copy in the Iowa State University Library, Ames, Iowa.).

Kirkham, D., 1961b. Soil physical properties. In: Richey, C.B., Jacobson, P., Hall, C.W. (Eds.), Agricultural Engineer's Handbook. McGraw Hill, New York, pp. 793–801.

Kirkham, D., Powers, W.L., 1972. Advanced Soil Physics. Wiley, New York.

Kirkham, M.B., 1994. Streamlines for diffusive flow in vertical and surface tillage: a model study. Soil Sci. Soc. Amer. J. 58, 85–93.

Kirkham, M.B., Clothier, B.E., 1994. Ellipsoidal description of water flow into soil from a surface disc. Trans. Int. Congr. Soil Sci. 2b, 38–39.

Millar, C.E., Turk, L.M., Foth, H.D., 1965. Fundamentals of Soil Science, fourth ed. Wiley, New York.

Moon, P., Spencer, D.E., 1961. Field Theory for Engineers. D. Van Nostrand, Princeton, New Jersey, pp. 2–3.

Muskat, M., 1946. The Flow of Homogeneous Fluids through Porous Media. J.W. Edwards, Ann Arbor, Michigan.

Philip, J.R., 1995. Desperately seeking Darcy in Dijon. Soil Sci. Soc. Am. J. 59, 319–324.

Raats, P.A.C., van der Ploeg, R.R., 2005. Hooghoudt, Symen Barend. In: Hillel, D. (Ed.), Encyclopedia of Soils in the Environment, vol. 2. Elsevier, Amsterdam, pp. 188–195.

Slichter, C.S., 1899. Theoretical investigations of the motion of groundwater. US Geol. Surv. Annu. Rep. 19, 295–384.

Soil Science Society of America, 2008. Glossary of Soil Science Terms 2008. Soil Science Society of America, Madison, Wisconsin.

van der Ploeg, R.R., Marquardt, M., Kirkham, D., 1997. On the history of the ellipse equation for soil drainage. Soil Sci. Soc. Am. J. 61, 1604–1606.

van der Ploeg, R.R., Kirkham, M.B., Marquardt, M., 1999. The Colding equation for soil drainage: its origin, evolution, and use. Soil Sci. Soc. Am. J. 63, 33–39.

# CHAPTER

# 8

# Time Domain Reflectometry

In Chapter 5, we learned how to measure the matric potential energy of water in soil with a tensiometer. Here, we learn how to measure the water content of soil using time domain reflectometry (TDR). This method is the most widely used one, aside from the gravimetric method, to determine soil water content.

TDR makes use of the dielectric constant, $\varepsilon$, of water to determine the volumetric water content of soil. We are going to see how the dielectric constant of a soil sample depends on the amount of water in it. We measure it and then use an empirical relation, which equates the volumetric water content to the dielectric constant.

## 8.1 DEFINITIONS

The dielectric constant of a medium is defined by $\varepsilon$ in the following equation (Weast, 1964, p. F-37):

$$F = \left(QQ'\right)\Big/\left(\varepsilon r^2\right), \tag{8.1}$$

where $F$ is the force of attraction between two charges $Q$ and $Q'$ separated by a distance $r$ in a uniform medium. The dielectric constant of a material is the ratio of the capacitance of a capacitor with the material between the plates to the capacitance with a vacuum between the plates (Shortley and Williams, 1971, p. 519). It is dimensionless. The dielectric constant for a vacuum = 1 exactly. A *capacitor* or *condenser* is a device consisting of two or more conductor plates separated from one another by a dielectric or insulator and used for receiving and storing an electric charge (Websters's New World Dictionary of the American Language, 1959; Schaum, 1961,

http://dx.doi.org/10.1016/B978-0-12-420022-7.00008-2
Copyright © 2014 Elsevier Inc. All rights reserved.

p. 137). The electrical characteristics of a capacitor are determined by its capacitance, which is a measure of the ability of the conductors to store charge when a potential difference is produced between them, whether by a battery, a radio antenna, or any other source of potential difference (Shortley and Williams, 1971, p. 513–514). Capacitance, denoted by $C$, equals $Q/V$, in coulombs per volt of potential difference. This unit, 1 coulomb/volt, is given the name "farad," after Faraday. Coulomb's law gives the force between two charges and is $F = (QQ)'/r^2$, where $Q$ and $Q'$ are the two charges and $r$ is the distance between them in a vacuum (Weast, 1964, p. F-42). Note that the force of attraction existing between two masses (Newton's law of universal gravitation) is inversely related to the square of the distance between the masses.

Before we look at the TDR method, let us first review some basic definitions from physics (Shortley and Williams, 1971, p. 243). A "cycle" is one complete execution of a periodic motion. The "period" of a periodic motion is the "time" $T$ required for the completion of a cycle. The "frequency" of a periodic motion is the number $f$ of cycles completed per unit time (unit = cycles/s).

Thus, it is seen that the period $T$ of a periodic motion is the reciprocal of the frequency $f$, that is, $T = 1/f$ and $f = 1/T$. For example, a pendulum with a period $T = 1/5$ s has a frequency of 5 cycles/s or $f = 5$ /s = 5 Hz.

Frequency is measured in a unit called the hertz (Hz), which corresponds to 1 cycle/s, or 1 Hz = 1 /s. The unit is named after Heinrich Rudolph Hertz (1857–1894), who was a German physicist. (See the Appendix, Section 8.9, for a biography of Hertz.) Hertzian waves are radiowaves or other electromagnetic radiation resulting from the oscillation of electricity in a conductor. Hertz was the first to demonstrate the production and reception of radiowaves.

Mechanical wave motion has a single nonrepeated disturbance, called a "pulse", which is initiated at the source and then travels away from the source through the medium (Shortley and Williams, 1971, p. 415). Another important type of wave motion is the "regular wave train" or "continuous wave". In this type of wave, a regular succession of pulses is initiated at the source and transmitted through the medium. Thus, if a floating block of wood is pushed up and down regularly on a water surface, a regular train of waves will be propagated outward. The simplest type of regular wave train is a sinusoidal wave motion, which is illustrated in Figure 8.1. Part (a) of this figure shows one end of a long stretched string attached to a weight supported by a spring. The weight is arranged so that it can move freely in the vertical "ways" of a frame. If the weight is pulled downward a distance $A$ and then released, the weight will move in the vertical direction with simple harmonic motion

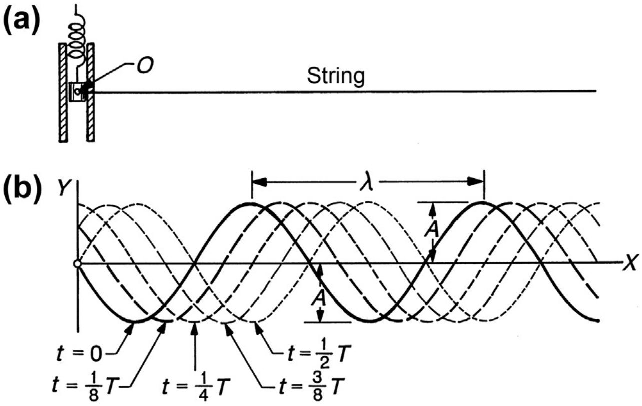

**FIGURE 8.1** Production and propagation of a sinusoidal transverse wave in a long string shown in (a). (b) The motion of the string during one half-cycle of oscillation of $O$, shown in (a), from $Y=0$ to $+A$ and back to 0. *From Shortley and Williams (1971), p. 416. Reprinted by permission of Pearson Education, Inc.: Upper Saddle River, New Jersey.*

of a certain period $T$. Because the end of the string is attached to the weight, the oscillating weight acts as a source of a sinusoidal transverse wave that travels to the right along the string in the manner indicated by the curves of Figure 8.1(b). These curves show successive "snapshots" of the shape of the string during one half-cycle, after the motion has been well established. The distance between adjacent crests or adjacent troughs in such a wave is called the "wavelength"; in the figure, the wavelength is denoted by $\lambda$. Each time the particle $O$ attached to the weight makes a complete oscillation, the wave moves a distance $\lambda$ in the $X$-direction. Hence, the wave speed, $v$, and the wavelength are related by the equation

$$v = \lambda/T, \tag{8.2}$$

where $T$ is the period of oscillation and $\lambda$ is the wavelength. In terms of the frequency $f = 1/T$, this equation can be written as

$$v = f\lambda \tag{8.3}$$

or

$$\lambda = v/f. \tag{8.4}$$

## 8.2 DIELECTRIC CONSTANT, FREQUENCY DOMAIN, AND TIME DOMAIN

We recall the physical properties of water and remember that the dielectric constant varies with temperature (Weast, 1964, p. E-36):

| Temperature | |
|---|---|
| °C | $\varepsilon$ |
| 0 | 88.00 |
| 10 | 84.11 |
| 20 | 80.36 |
| 30 | 76.75 |
| 40 | 73.28 |
| 50 | 69.94 |
| 100 | 55.33 |

One can obtain information about a dielectric in either the frequency domain or the time domain. In the frequency domain, a number of measurements over a wide frequency range are required for the complete characterization of the dielectric, which is time consuming and requires a considerable investment in instrumentation. However, one can obtain the same information over a wide frequency range in only a fraction of a second by making the measurement not in the frequency domain but in the time domain. In TDR, a pulse is used that simultaneously contains all the frequencies of interest (Fellner-Feldegg, 1969). In the frequency range of 1 MHz (megahertz)—1 GHz (gigahertz), the dielectric constant is not strongly frequency dependent (mega $= 10^6$ and giga $= 10^9$). Figure 8.2 shows the wavelength and frequency of commonly used devices, such as radios, televisions, and cellular phones (Clark, 1994).

In passing, we note that the safety of electromagnetic waves, especially those associated with cellular telephones, is still in doubt. A link between brain cancer and electromagnetic fields has been found in some studies (Bishop, 1995). Experiments have shown that radiowaves at about the same power as that emitted by today's cellular phones can breakdown the binding of calcium to the surface of cells. Calcium is essential for virtually all living processes, including enzyme action and cell growth. Data have shown that the breakdown occurs at 145 MHz, the frequency at which ham radios operate, and at 450 MHz, the frequency used by security guards' radiophones. European cellular systems operate at 450 MHz

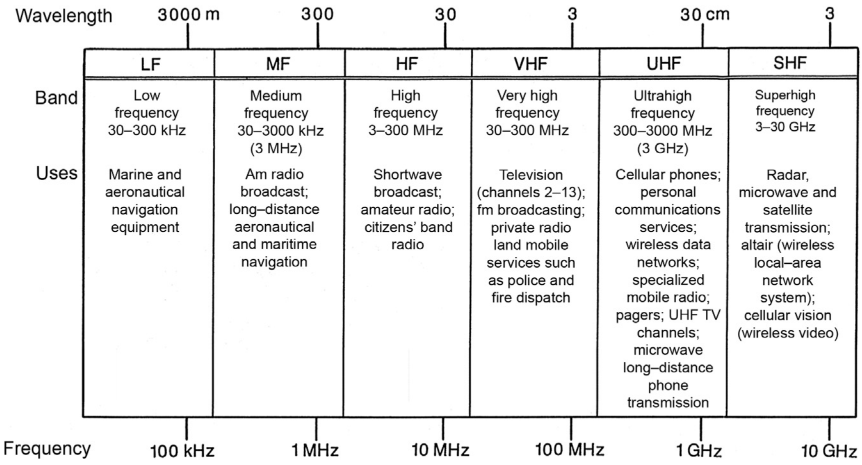
Wavelength
3000 m
300
30
3
30 cm
3
Frequency
100 kHz
1 MHz
10 MHz
100 MHz
1 GHz
10 GHz

| | LF | MF | HF | VHF | UHF | SHF |
|---|---|---|---|---|---|---|
| Band | Low frequency 30–300 kHz | Medium frequency 30–3000 kHz (3 MHz) | High frequency 3–300 MHz | Very high frequency 30–300 MHz | Ultrahigh frequency 300–3000 MHz (3 GHz) | Superhigh frequency 3–30 GHz |
| Uses | Marine and aeronautical navigation equipment | Am radio broadcast; long–distance aeronautical and maritime navigation | Shortwave broadcast; amateur radio; citizens' band radio | Television (channels 2–13); fm broadcasting; private radio land mobile services such as police and fire dispatch | Cellular phones; personal communications services; wireless data networks; specialized mobile radio; pagers; UHF TV channels; microwave long–distance phone transmission | Radar, microwave and satellite transmission; altair (wireless local–area network system); cellular vision (wireless video) |

**FIGURE 8.2** Wavelengths, frequencies, and their uses. *From Clark (1994). Reprinted by permission of Dow Jones & Company, Inc. All rights reserved worldwide.*

(Clark, 1994). Cell phone use appears to increase brain activity (glucose consumption) in regions close to where the phone antenna is held against the head (Park, 2011; Wang, 2011). After studying the results from a large number of available studies, the International Agency for Research on Cancer panel, made of up 31 scientists from 14 countries, concluded that cell phone radiowaves possibly increase the risk of brain cancer (Martin and Hobson, 2011). In May 2011, a World Health Organization panel added cell phones to a list of things that are possibly carcinogenic (Mukherjee, 2011). In 2010, San Francisco became the first city in the USA to pass legislation making cell phone retailers display radiation levels (Dowd, 2010).

## 8.3 THEORY FOR THE USE OF THE DIELECTRIC CONSTANT TO MEASURE SOIL WATER CONTENT

Most of the solid components of soil have dielectric constants in the range of 2–7, and that of air is effectively 1 ($\varepsilon$ of air $= 1.000590$). Thus, a measure of the dielectric constant of soil is a good measure of the water content of the soil.

Here is a brief outline of what we are going to do to use TDR to get the volumetric water content of soil. We are going to measure a travel time, and by knowing the length of the rods (waveguides) in the soil, we are going to get a velocity (velocity = length/time). We are going to relate this velocity to the dielectric constant. Then, we will relate the dielectric constant to volumetric water content.

The TDR technique measures the velocity of propagation of a high-frequency signal (1 MHz−1 GHz). The velocity of propagation is as follows:

$$V = c\Big/\left(K'\right)^{1/2}, \tag{8.5}$$

where

$V$ is the velocity of propagation in the soil;
$c$ is the propagation velocity of light in free space; $c = 3 \times 10^8$ m/s;
$K'$ is the dielectric constant of the soil.

By determining the travel time, $t$, of the pulse traveling in the transmission line or waveguide of length $L$, one can get the velocity as $L/t$.

Equation (8.5) can be rearranged to give the apparent dielectric constant as

$$K_a = [(ct)/L]^2, \tag{8.6}$$

where $K_a$ is the apparent dielectric constant. However, we need to add a "2" to the denominator in Eqn (8.6), because the line length is the distance *traveled*, but commercial cable testers measure the length down and the echo (reflection). Hence, the distance *measured* is twice the line length. So we have

$$K_a = [(ct)/2L]^2. \tag{8.7}$$

The relationship in Eqn (8.5) is approximate, so in Eqns (8.6) and (8.7), we use $K_a$, the apparent dielectric constant, instead of $K'$ (Topp and Davis, 1982).

Commercial TDR cable testers reduce the transfer time to an apparent probe length, $l_a$ (Figure 8.3 from Clothier et al., 1994), so that

$$K_a = [(ct)/2L]^2 = \left(l_a/L\nu_p\right)^2, \tag{8.8}$$

where $\nu_p$ is the relative velocity setting of the instrument (Vogeler et al., 1996; see their Eqn (8.10)). It is relative, so it is unitless ($\nu$ = the Greek letter nu.) The reason the two appears in the first equation of Eqn (8.8) is that the echo must travel down and back along the rods of length $L$, as noted above. On the right-hand side of Eqn (8.8), the travel time is normalized to the length that is found relative to the true length. The length is $2l_a$ over $2L$, so the 2's cancel (B.E. Clothier, personal communication, March 6, 1997). The commercial cable tester made by Tektronix (Model 1502C, Wilsonville, OR) does not display $2l_a$ because it is used as a cable tester to find breaks in a cable. So it knows it is measuring twice the length, and saves the operator the hassle by dividing by two before it puts the trace on the screen (Figure 8.3).

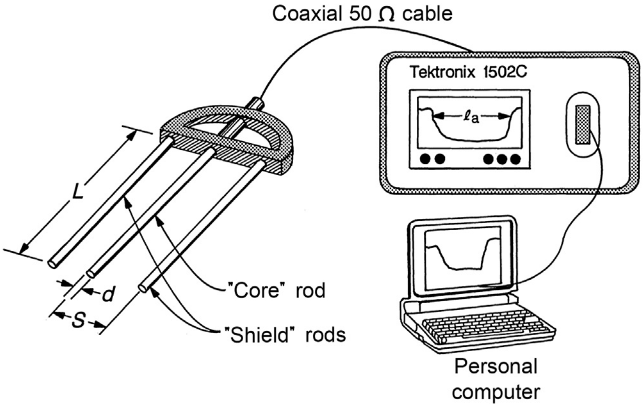

**FIGURE 8.3** Schematic diagram of the time domain reflectometry system with the three-rod probe, the cable tester, and the computer that controls, acquires, and analyzes the data. *From Clothier et al. (1994). Reprinted by permission of Brent E. Clothier.*

Experimental results (Topp et al., 1980) have given the following relation between volumetric water content and the dielectric constant:

$$\theta_v = -0.053 + 0.0292K_a - 5.5 \times 10^{-4}K_a^2 + 4.3 \times 10^{-6}K_a^3. \tag{8.9}$$

Equation (8.9) has been shown to hold for many different types of soils. The relationship between volumetric water content ($\theta$) and the dielectric constant ($K_a$) is essentially independent of soil texture, porosity, and salt content. However, if a soil is high in organic matter, Eqn (8.9) does not hold and a separate calibration equation needs to be determined. Herkelrath et al. (1991), who studied organic soil, found that the equation of Topp et al. (Eqn (8.9)) predicted the values of soil water content that were 30% too low. Topp et al. (1980) also reported a similar shift in their calibration for an organic soil. The soil cores of Herkelrath et al. (1991) had a large fraction of organics: 12.6% carbon.

## 8.4 COAXIAL CABLE AND WAVEGUIDES

Before we go further, let us define a coaxial cable or a coaxial line. A coaxial line is composed of an internal conductor of radius $R_1$ and an external conductor of radius $R_2$ separated by a dielectric (Lorrain and Corson, 1979, p. 172) (Figure 8.4). S.A. Schelkunoff was a developer of the coaxial cable. (See Section 8.10, for a biography of Schelkunoff.) Coaxial lines are widely used for the interconnection of electronic equipment and for long-distance telephony. They can be used with either direct or alternating currents, up to very high frequencies, where the wavelength

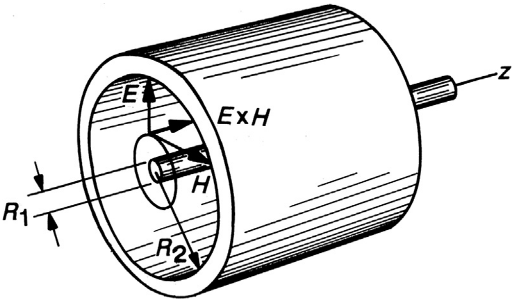

**FIGURE 8.4** Coaxial line. We assume that the wave propagates in the positive direction of the $Z$-axis. $E$ = electric field intensity; $H$ = magnetic field intensity; $R_1$ and $R_2$ = radii of the inner and outer conductors, respectively. *From Lorrain and Corson (1979), p. 488. Used with permission.*

$c/f$ is of the same order of magnitude as the diameter of the line. (Remember $c$ is the speed of light in a vacuum, $2.99792458 \times 10^8$ m/s, and $f$ is the frequency in reciprocal seconds) (Lorrain and Corson, 1979, p. 304). At these frequencies, of the order of $10^{10}$ Hz, the field inside the line becomes much more complicated than that shown in the figure and quite unmanageable (Lorrain and Corson, 1979, p. 304). There is zero electric field outside the line. Because the outer conductor carries the same current as the inner one does (Figure 8.5), there is also zero magnetic field. A structure designed to guide a wave along a prescribed path is called a "waveguide" (Lorrain and Corson, 1979, p. 487). The simplest type is the coaxial line illustrated in Figure 8.4. An electromagnetic wave propagates in the annular region between the two coaxial conductors, and there is zero field outside. The medium of propagation is a dielectric.

If one were using a coaxial cable (as is used in cable testing), one would put the soil sample in the coaxial cable and send a voltage pulse through the cable. When the pulse reached the sample (it would have been traveling through air up to this point), part of the pulse would be reflected (the rest would travel on or we could terminate the cable, so that the pulse would travel no further). The time dependence of the reflection of the pulse from the interface between air and the dielectric medium (soil sample) in the coaxial line is measured. (We measure a "time", which is reduced to an "apparent probe length" by the cable tester.) The reflection from a dielectric sample in a coaxial line is recorded on the oscilloscope of the cable tester. ($Y$-axis = pulse height; $X$-axis = time or apparent probe length.) The time is on the order of nanoseconds (nano = $10^{-9}$).

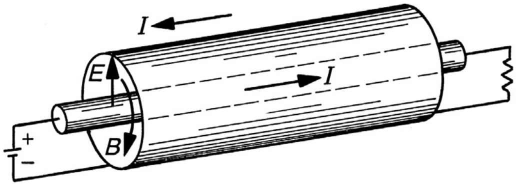

**FIGURE 8.5** Coaxial line. $E$ = electric field intensity; $B$ = magnetic induction; $I$ = electric current. *From Lorrain and Corson (1979), p. 304. Used with permission.*

However, it is impractical to put a soil sample in a coaxial cable to determine soil moisture. Therefore, parallel transmission lines (rods or waveguides) have been developed to determine soil water content by using TDR. The soil between and surrounding the rods serves as the dielectric of the transmission lines (Topp and Davis, 1982). The voltage pulse is propagated down and reflected back from the end of the waveguides in the soil.

## 8.5 MEASUREMENT OF SOIL WATER CONTENT USING TDR

Now let us look at the procedure, when we use TDR (Topp, 1993, pp. 544–549). First, we need the TDR equipment proper (Figure 8.6). This includes the pulser of voltage; a sampling receiver that receives both the pulse and the reflected pulse from the soil; a timing device that synchronizes the timing for pulser, receiver, and data display; and a data display that shows the time and voltage magnitude. (As noted above, commercial cable testers display an apparent length rather than a time.) The TDR cable tester sends square-wave pulses of voltage down the waveguides at a high frequency (in the gigahertz range) and stores on the screen their superpositions so that a single "form" is observed, whereas in fact it is the result of overlaying many forms (B.E. Clothier, personal communication, February 21, 1994).

Second, we need rods (also called probes or waveguides). They can be either two pronged or three pronged. If they are two pronged, we need a balun, which is an impedance matching transformer (Figure 8.7). The

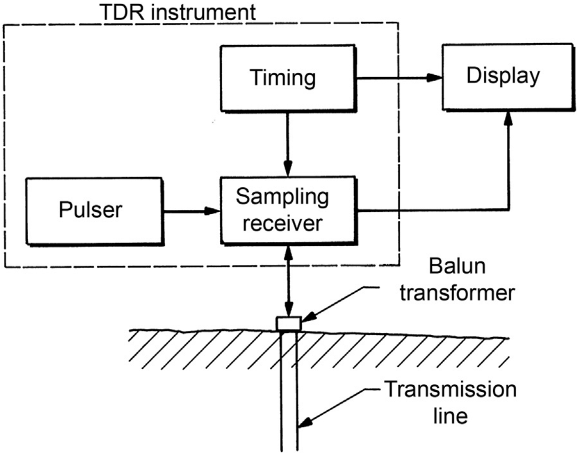

**FIGURE 8.6** A block diagram of a time domain reflectometry instrument and its display units. *From Topp (1993), p. 545, CRC Press.*

coaxial cable in Figure 8.7 is 50 Ω. The coaxial cable is connected to an 185 Ω shielded television cable and a balun to provide a "balanced line" (Herkelrath et al., 1991). "Impedance" is the apparent resistance in an alternating electrical current corresponding to the true resistance in a direct current (Webster's New World Dictionary of the American Language, 1959). If one is using three pronged probes, they simulate the coaxial line and require no impedance matching transformer (Clothier et al., 1994).

Third, we need cables for connecting the TDR instrument and soil probes (Topp, 1993). Cable combinations between the TDR instrument and soil probes are determined by the type of probes used (two pronged, three pronged, or more).

Fourth, we need tools for installation of soil probes. Three procedures can be used for insertion. First, for short probes (in most soils, except the most resistant), we can insert the probes by hand, take a reading, and remove them and move on to the next spot. In this way, we can easily take many readings and quickly get a "feel" of the spatial variability. Second, for longer probes, it is necessary to make "preholes" with a dummy probe.

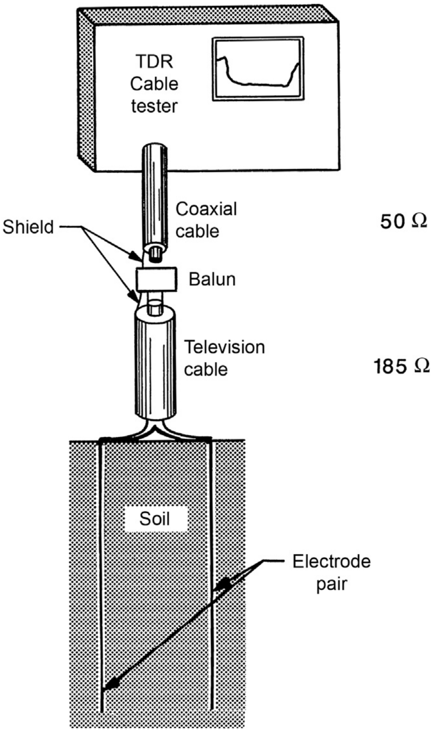

**FIGURE 8.7** The basic TDR circuit for use in determining soil moisture. *From Herkelrath et al. (1991). Reproduced by permission of the American Geophysical Union.*

This could also be done to obtain repeated measurements in space, although once the longer probes are inserted, we tend to leave them in place connected to a multiplexer, or with caps on the coaxial connector if single measurements are to be made. Third, B.E. Clothier and S.R. Green in New Zealand have made "direct-wired" probes that they insert horizontally into a face of a pit that they have dug. The probes are inserted horizontally, the hole backfilled, and the probes remain in place underneath undisturbed soil during the summer. One has to be careful when removing them at the end of the experiment, for it is easy to put a spade right through the connector cable when exhuming them (B.E. Clothier, personal communication, February 23, 1994).

Fifth, if we are automating measurements, we need a multiplexer. Baker and Allmaras (1990) describe a system for automated measurements using a multiplexer. Multiplexers are available commercially from Campbell Scientific Corporation (Logan, UT) (Buckley et al., 2010).

## 8.6 PRACTICAL INFORMATION WHEN USING TDR TO MEASURE SOIL WATER CONTENT

The following are some notes on the use of the TDR technique.

1. Rods normally range in length from 100 mm to 1 m. The shortest depth that I have seen documented in the literature is 50 mm (Mallants et al., 1996). Probes <50 mm do not give good traces (B.E. Clothier and M.B. Kirkham, personal observations, January–April, 1991). Probes >1 m are difficult to insert into the soil without bending them. Sometimes, it is difficult even to insert the probes to this depth (e.g., in the caliche soils of Texas; Todd A. Vagts, personal communication, February 11, 2000). Miller and Buchan (1996) in New Zealand describe the challenges of inserting rods at a depth in a silt loam soil overlying unweathered greywacke gravels and stones with a sand matrix.

   However, the fact that TDR probes measure soil water content only to 1 m does not mean that we do not need to measure deeper than 1 m. Neutron probes can measure to a depth of $\geq$3 m. Even though TDR is replacing the use of neutron probes, because no danger from radioactivity is involved with TDR, we cannot abandon neutron probes. They provide the only method that can be used to get soil water content at great depths. In semiarid regions such as in Kansas, it is important to measure 2–3 m below the surface of the soil, to determine the maximum depth of water depletion by roots. Miller and Buchan (1996) report the widespread use of neutron probes in Australia and South Africa to schedule irrigations.

2. The rods allow flexibility in determining water content. The spacing and geometry can be changed. Probes can be inserted horizontally or vertically. The ability to insert probes horizontally allows calculation of the velocities of both the wet front and solute front in a soil (Duwig et al., 1997).
3. There is some heating involved while using the TDR method, but given the power levels involved, it is minuscule (B.E. Clothier, personal communication, February 22, 1994).
4. The accuracy of the method is ±0.01 $m^3/m^3$ (Topp, 1993). For comparison, Song et al. (1998) found that the dual-probe, heat-pulse technique (described in Chapter 9) monitored soil water content within 0.03 $m^3/m^3$ and changes in soil water content within 0.01 $m^3/m^3$.
5. The magnitude of reflected signals, after the first one for soil water content, can be used to determine the electrical conductivity of the soil (Topp, 1993). The degree to which the signal is "lost" (attenuated) after all the multiple reflections have died away is due to the soil's electrical conductivity, which is, in some large part, due to the salt content of the solution (B.E. Clothier, personal communication, January 20, 1994). Dalton et al. (1984) were the first to show how the attenuation of the TDR trace can be used to calculate the soil bulk electrical conductivity. Since then, numerous papers have been published using TDR to measure electrical conductivity or solute transport as well as water content (Dasberg and Dalton, 1985; Zegelin et al., 1989; Nadler et al., 1991; Lundin and Johnsson, 1994; Ward et al., 1994; Vogeler et al., 1996; Duwig et al., 1997; Persson et al., 2000; Moret-Fernandez et al., 2012). However, TDR measures solutes in the soil only when they are at a low concentration. TDR cannot measure solutes in saline soil. Vogeler et al. (1996) measured up to 4 mmhos/cm (4 dS/m) electrical conductivity using TDR (see their Figure 6). This shows a low level of salts in the soil. Bernstein (1964) gives the following information about crop response to salinity. From 0 to 2 mmhos/cm, salinity effects are mostly negligible; from 2 to 4 mmhos/cm, yields of very sensitive crops may be restricted; from 4 to 8 mmhos/cm, the yields of many crops are restricted; from 8 to 16 mmhos/cm, only tolerant crops yield satisfactorily; and >16 mmhos/cm, only a few very tolerant crops yield satisfactorily. Wraith (2002) gives the principles of using TDR to determine solute transport. Evett (2003) points out that the TDR method has even been extended to measure atmospheric $CO_2$ based on the solution electrical conductivity increase caused by its dissolution in water (Baker et al., 1996).

## 8.7 EXAMPLE OF USING TDR TO DETERMINE ROOT WATER UPTAKE

Many papers have been published that analyze the TDR technique (e.g., Heimovaara and Bouten, 1990) and its use for routine measurements of soil water content (e.g., Grantz et al., 1990), and the literature is growing rapidly. TDR permits observations of the changing pattern of water content in the soil that occurs as a result of root water uptake. Here, we present only one example in which a kiwifruit vine was studied (Clothier and Green, 1994). After an initial irrigation, the soil water content was uniform across the root zone of the kiwifruit vine; also, the water uptake was quite uniform (Figure 8.8, top). Beginning in the tenth week of 1992, just one half of the vine's root zone, the southern half, was wetted by a sprinkler irrigation. Following this differential irrigation of the root zone, the flow of water in the "wet" southern root increased, but the flux in the "dry" northern root was about halved. Thus, the vine quickly switched its pattern of uptake away from the drier parts of its root zone.

Of greater interest, however, was the depthwise pattern of root uptake observed on the wet side. The preference for near-surface water uptake can be seen (Figure 8.8, bottom). The vine continued to extract water in the densely rooted region surrounding its base, but the shift in uptake to the surface roots on the wet southern side was remarkable.

The results show that a greater efficiency in irrigation water might be obtained by applying small amounts of water, more frequently. A small amount of irrigation water would be rapidly used by active, near-surface roots. This would then eliminate drainage of irrigation water into the lower regions of the root zone, where draining water passes by inactive roots and goes to a greater depth. Such observations are made possible by using TDR.

### 8.7.1 Sample Problem

Like Clothier and Green (1994), Clothier and Kirkham (1991) also measured water extraction by roots at different depths in the same kiwifruit orchard (TDR data not published, but data on kiwifruit growth are published in Clothier and Kirkham (1991)). They used TDR equipment supplied by the Soilmoisture Equipment Corporation (Santa Barbara, CA) and waveguides of three different lengths: 20, 40, and 60 cm. Here, are actual data observed on the readout:

20 cm waveguide: 38.0%
40 cm waveguide: 32.3%
60 cm waveguide: 28.0%

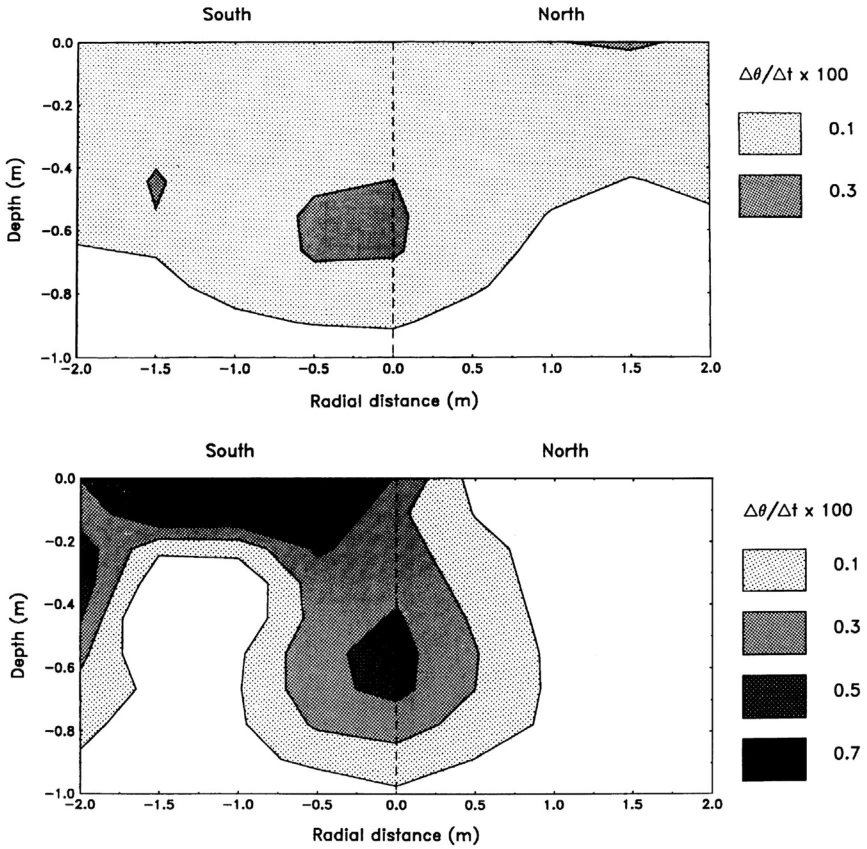

FIGURE 8.8 Measurement by time domain reflectometry of the changing spatial pattern of soil water content in the root zone of a kiwifruit vine growing near Palmerston North, New Zealand. The upper figure depicts the average rate of water content change over the four-week period, February 11–March 9, 1992. The lower figure shows the change that occurred over the two weeks following irrigation of just the south side on March 10. Rate of water extraction $\Delta\theta/\Delta t$ is given in units of cubic meter per cubic meter per second. The vine is located at the center. *From Clothier and Green (1994). Reprinted by permission of Elsevier, Amsterdam.*

Problem: What are the water contents (percent by volume) at the 0–20 cm depth, the 20–40 cm depth, and the 40–60 cm depths? We use $\theta$ to symbolize the volumetric water content and $L$ to symbolize the length of the waveguide.

Answers:

0–20 cm depth: The value observed on the readout is the answer (38.0%).

20–40 cm depth: $\theta_{20-40\text{cm}} = [(L_{40}\theta_{40}) - (L_{20}\theta_{20})]/(L_{40} - L_{20}) =$ $[(40\text{ cm})(0.323) - (20\text{ cm})(0.380)]/(40-20\text{ cm}) = 5.32\text{ cm}/$ $20\text{ cm} = 0.266$ or 26.6%
40–60 cm depth: $\theta_{40-60\text{cm}} = [(L_{60}\theta_{60}) - (L_{40}\theta_{40})]/(L_{60} - L_{40}) =$ $[(60\text{ cm})(0.280) - (40\text{ cm})\ (0.323)]/(60-40\text{ cm}) = 3.88\text{ cm}/$ $20\text{ cm} = 0.194$ or 19.4%.

The answers are as follows:

0–20 cm depth: 38.0%
20–40 cm depth: 26.6%
40–60 cm depth: 19.4%

Note that a waveguide determines the soil moisture over its entire length. To obtain water extraction by roots at specific depths, one must do the above calculations.

## 8.8 COMMERCIALLY AVAILABLE EQUIPMENT

The Soilmoisture Equipment Corporation (Santa Barabara, CA) sells TRASE, which measures soil moisture using TDR. Clarke Topp worked with the Soilmoisture Equipment Corporation to develop the equipment. It comes with two-pronged probes and a balun. The equipment allows one to see the trace of the wave on a screen (see Figure 8.3 for an example of a wave trace). An earlier model sold by the Soilmoisture Equipment Corporation, called Instrument for Reflectometry Analysis of Moisture in Soil (IRAMS), also was developed by Clarke Topp, but the IRAMS did not display the wave trace. As we shall note in Chapter 9, one can also measure soil moisture accurately by using the dual-probe, heat-pulse technique. Many soil moisture sensors are on the market, but, as described in Chapter 9, Section 9.16, their principles of operation are not known. They need to be calibrated with a standard method, such as neutron probes. True TDR (TDR that is calibrated and detects the trace of the electromagnetic signal on an oscilloscope) is a reliable way to measure soil moisture. Buckley et al. (2010) used true TDR in studying the effect of tillage on the hydrology of a claypan soil. They built their own TDR equipment using supplies from Campbell Scientific (Logan, UT). In their experiment, the trace is not seen on an oscilloscope but is detected digitally using the Campbell Scientific equipment. One can save the traces and review them after measurement. Setting up the equipment takes much effort and a knowledge of software. Reproducible results with TDR in different soils are hard to obtain (G.J. Kluitenberg, personal communication, July 17, 2013). Each TDR instrument needs to be calibrated. Results with TDR depend on pH, what is in the soil solution, the type of soil, and the wavelength.

## 8.9 APPENDIX: BIOGRAPHY OF HEINRICH HERTZ

Heinrich Rudolf Hertz (1857–1894), a German physicist, was born on February 22, 1857, at Hamburg. After leaving the gymnasium, he studied civil engineering, but at the age of 20, he came to a turning point in his career (Cajori, 1929, p. 258) and abandoned engineering in favor of physics. He went to Berlin, and worked under Hermann Ludwig Ferdinand von Helmholtz (German physiologist and physicist, 1821–1894), advancing rapidly to become his assistant by 1880. In 1883, he became a private docent (official but unpaid lecturer) at Kiel. There he began the studies of Maxwell's electromagnetic theory (James C. Maxwell, Scottish physicist, 1831–1879), which resulted in the discoveries—between 1885 and 1889, while he was the professor of physics in the Polytechnic in Karlsruhe, Germany (Preece, 1971; cited under Hertz)—that made Hertz's name famous. It was there that he performed his memorable experiments on electromagnetic waves.

In 1888, Hertz found means of detecting the presence of electromagnetic waves arising from a Leyden jar (Cajori, 1929, p. 259). A Leyden jar, named after the Dutch city of Leiden in The Netherlands, where it was invented, is a glass jar coated outside and inside with tin foil and having a metallic rod connecting with the inner lining and passing through the lid (Webster's New World Dictionary of the American Language, 1959). It acts as a condenser for static electricity (Figure 8.9). During the oscillatory discharge of a Leyden jar, electromagnetic waves radiate into space. Such a wave is called "electromagnetic", because it has two components: an electric wave and a magnetic wave. Hertz was able to observe each

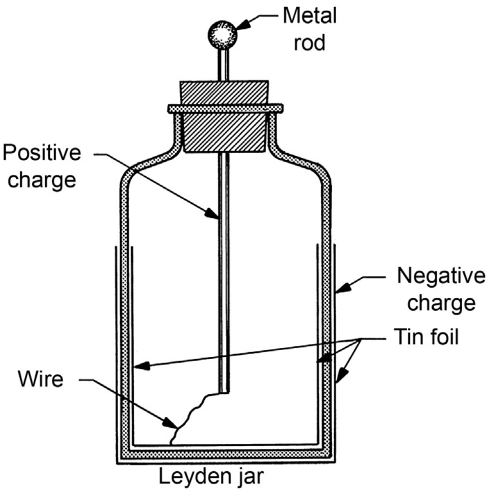

**FIGURE 8.9** Leyden jar. *From Webster's New World Dictionary of the American Language: College Edition (1959). All rights reserved. Rights now owned by Wiley. Reproduced here by permission of Wiley Publishing, Inc., Indianapolis, IN.*

separately, an accomplishment that Maxwell had feared would never be realized (Cajori, 1929, p. 259).

In 1889, Hertz was appointed to succeed Rudolf Julius Emanuel Clausius (German physicist, who made important contributions to molecular physics; 1822–1888) as the professor of physics at the University of Bonn. Thus, at the age of 32, he occupied a position attained much later in life by most men of his time. There he continued his research on the discharge of electricity in rarefied gases, only just missing the discovery of the X-rays described by Wilhelm Konrad Röntgen (German physicist, 1845–1923, who received the Nobel Prize in physics in 1901) a few years later. There Hertz wrote his treatise *Principles of Mechanics*. In 1892, a chronic blood poisoning began to undermine his health, and, after a long illness, he died in the prime of life on January 1, 1894, in Bonn. By his premature death, science lost one of its most promising disciples (Preece, 1971). For a book that describes Hertz's experiments and production of electromagnetic waves, see Buchwald (1994).

## 8.10 APPENDIX: BIOGRAPHY OF SERGEI SCHELKUNOFF

Sergei A. Schelkunoff, inventor and expert on electromagnetism, was born in Samara, Russia. He researched the coaxial cable now widely used for television transmission (Lambert, 1992). He was a student at the University of Moscow when he was caught up in the tumult of World War I and the Bolshevik Revolution. Drafted and trained as a Russian Army officer in 1917, he fought and worked his way across Siberia into Manchuria and on to Japan before landing in Seattle in 1921. He learned English and worked his way through school, earning both bachelor's and master's degrees in mathematics from the State College of Washington, now the University of Washington, and a doctorate from Columbia University in New York City in 1928.

He went to work for Western Electric's laboratories and its successor, Bell Labs, and in his 35 years there, he became assistant director of mathematical research and assistant vice president for university relations. The government granted him 15 patents for radio antennas, resonators, and wavelength guides. In 1935, he and three colleagues reported that the newly developed coaxial cable could transmit television or up to 200 telephone circuits. He specialized in coaxial frequency, impedance, attenuation, coupling, shielding, circuit, and field characteristics. He published four books and dozens of papers in scientific journals, and also taught for five years at Columbia University, where he retired in 1965. The Institute of Radio Engineers awarded him a prize for his contributions to radiowave transmission theory, and the Franklin Institute awarded him a medal for his communication and reconnaissance research. He died of a heart ailment at age 95 on May 2, 1992. He had no immediate survivors. His wife of 51 years, the former Jean Kennedy, died in 1979.

## References

Baker, J.M., Allmaras, R.R., 1990. System for automating and multiplexing soil moisture measurement by time-domain reflectometry. Soil Sci. Soc. Am. J. 54, 1–6.

Baker, J.M., Spaans, E.J.A., Reece, C.F., 1996. Conductimetric measurement of $CO_2$ concentration: theoretical basis and its verification. Agron. J. 88, 675–682.

Bernstein, L., 1964. Salt Tolerance of Plants. Agr Information Bull No. 283. United States Department of Agriculture, Washington, DC.

Bishop, J.E., Wednesday, January 11, 1995. Link between EMF, brain cancer is suggested in major new study. However, no added risk of leukemia is found, unlike previous work. Wall Street Journal, B4.

Buchwald, J.Z., 1994. The Creation of Scientific Effects: Heinrich Hertz and Electric Waves. University of Chicago Press, Chicago, Illinois.

Buckley, M.E., Kluitenberg, G.J., Sweeney, D.W., Kelley, K.W., Stone, L.R., 2010. Effect of tillage on the hydrology of a claypan soil in Kansas. Soil Sci. Soc. Am. J. 74, 2109–2119. http://dx.doi.org/10/2136/sssaj2010.0024.

Cajori, F., 1929. A History of Physics. Macmillan, New York.

Clark, D., Friday, February 11, 1994. Squeeze play. With usable frequencies scarce, companies try to ease the crunch. Wall Street Journal, R16.

Clothier, B.E., Green, S.R., 1994. Rootzone processes and the efficient use of irrigation water. Agr. Water Manage. 25, 1–12.

Clothier, B.E., Kirkham, M.B., 1991. Kiwifruit as Brass Monkeys. WISPAS. A Newsletter about Water in the Soil-Plant-Atmosphere System. No. 49, 3.

Clothier, B., Gaudet, J.-P., Angulo, R., Green, S., 1994. Application of the TDR (time domain reflectometry) method to measure water content and concentration of solutes in soils. In: French Society of Thermal Engineers, One-day Workshop, February 9, 1994, Paris, France, on Methodologies for Porous-Media Measurement. French Society of Thermal Engineers, Paris (In French; English translation by M.B. Kirkham).

Dalton, F.N., Herkelrath, W.N., Rawlins, S.L., Rhoades, J.D., 1984. Time domain reflectometry: simultaneous measurement of soil water content and electrical conductivity with a single probe. Science 224, 989–990.

Dasberg, S., Dalton, F.N., 1985. Time domain reflectometry field measurements of soil water content and electrical conductivity. Soil Sci. Soc. Am. J. 49, 293–297.

Dowd, M., Sunday, June 27, 2010. Are cells the new cigarettes? New York Times, WK11.

Duwig, C., Vogeler, I., Clothier, B.E., Green, S.R., 1997. Nitrate leaching to groundwater under mustard growing on soil from a coral atoll. In: Currie, L.D., Loganathan, P. (Eds.), Nutritional Requirements of Horticultural Crops. Fertilizer and Lime Research Centre, Massey University, Palmerston North, New Zealand, pp. 36–43. Occasional Report No. 10.

Evett, S.R., 2003. Soil water measurement by time domain reflectometry. In: Stewart, B.A., Howell, T.A. (Eds.), Encyclopedia of Water Science. Marcel Dekker, New York, pp. 894–898.

Fellner-Feldegg, H., 1969. The measurement of dielectrics in the time domain. J. Phys. Chem. 73, 616–623.

Grantz, D.A., Perry, M.H., Meinzer, F.C., 1990. Using time-domain reflectometry to measure soil water in Hawaiian sugarcane. Agron. J. 82, 144–146.

Heimovaara, T.J., Bouten, W., 1990. A computer-controlled 36-channel time domain reflectometry system for monitoring soil water contents. Water Resour. Res. 26, 2311–2316.

Herkelrath, W.H., Hamburg, S.P., Murphy, F., 1991. Automatic, real-time monitoring of soil moisture in a remote field area with time domain reflectometry. Water Resour. Res. 27, 857–864.

Lambert, B., May 17, 1992. S.A. Schelkunoff, 95, researcher and developer of coaxial cable. New York Times, 23Y.

Lorrain, P., Corson, D.R., 1979. Electromagnetism. Principles and Applications. W.H. Freeman and Co., San Francisco.

Lundin, L.-C., Johnsson, H., 1994. Ion dynamics of a freezing soil monitored in situ by time domain reflectometry. Water Resour. Res. 30, 3471–3478.

Mallants, D., Vanclooster, M., Toride, N., Vanderborght, J., van Genuchten, M.T., Feyen, J., 1996. Comparison of three methods to calibrate TDR for monitoring solute movement in undisturbed soil. Soil Sci. Soc. Am. J. 60, 747–754.

Martin, T.W., Hobson, K., Wednesday, June 1, 2011. Cellphone cancer warning. Wall Street Journal, A3.

Miller, B., Buchan, G., 1996. TDR vs. neutron probe—how do they compare? WISPAS. A Newsletter about Water in the Soil–Plant–Atmosphere System, vol. 65. The Horticultural and Food Research Institute, Palmerston North, New Zealand, pp. 8–9.

Moret-Fernandez, D., Vicente, J., Latorre, B., Lera, F., Castaneda, C., Lopez, M.V., Herroro, J., 2012. TDR pressure cell for monitoring water content retention and bulk electrical conductivity curves in undisturbed soil samples. Hydrol. Process. 26, 246.

Mukherjee, S., Sunday, July 17, 2011. Patrolling cancer's borderlands. New York Times, 8SR.

Nadler, A., Dasberg, S., Lapid, I., 1991. Time domain reflectometry measurements of water content and electrical conductivity of layered soil columns. Soil Sci. Soc. Am. J. 55, 938–943.

Park, A., March 7, 2011. Mobile threat? Time, 22.

Persson, M., Berndtsson, R., Nasri, S., Albergel, J., Zante, P., Yumegaki, Y., 2000. Solute transport and water content measurements in clay soils using time domain reflectometry. Hydrol. Sci. 45, 833–847.

Hertz, H.R., 1971. In: Preece, W.E. (Ed.), Encyclopaedia Britannica, vol. 11, p. 456.

Schaum, D., 1961. Theory and Problems of College Physics, sixth ed. Schaum Publishing, New York.

Shortley, G., Williams, D., 1971. Elements of Physics, fifth ed. Prentice-Hall, Englewood Cliffs, New Jersey.

Song, Y., Ham, J.M., Kirkham, M.B., Kluitenberg, G.J., 1998. Measuring soil water content under turfgrass using the dual-probe heat-pulse technique. J. Am. Soc. Hort. Sci. 123, 937–941.

Topp, G.C., 1993. Soil water content. In: Carter, M.R. (Ed.), Soil Sampling and Methods of Analysis. Lewis Publishers, Boca Raton, Florida, pp. 541–557.

Topp, G.C., Davis, J.L., 1982. Measurement of soil water content using time domain reflectometry. In: Canadian Hydrology Symposium: 82. Associate Committee on Hydrology National Research Council of Canada, Fredericton, New Brunswick, pp. 269–287.

Topp, G.C., Davis, J.L., Annan, A.P., 1980. Electromagnetic determination of soil water content: measurements in coaxial transmission lines. Water Resour. Res. 16, 574–582.

Vogeler, I., Clothier, B.E., Green, S.R., Scotter, D.R., Tillman, R.W., 1996. Characterizing water and solute movement by time domain reflectometry and disk permeametry. Soil Sci. Soc. Am. J. 60, 5–12.

Wang, S.S., Wednesday, February 23, 2011. Brain reacts to cellphones. Wall Street Journal, A3.

Ward, A.L., Kachanoski, R.G., Elrick, D.E., 1994. Laboratory measurements of solute transport using time domain reflectometry. Soil Sci. Soc. Am. J. 58, 1031–1039.

Weast, R.C., 1964. Handbook of Chemistry and Physics, forty-fifth ed. Chemical Rubber Co., Cleveland, Ohio.

Webster's New World Dictionary of the American Language, College ed., 1959. World Publishing, Cleveland and New York.

Wraith, J.M., 2002. Time domain reflectometry. In: Dane, J.H., Topp, G.C. (Eds.), Methods of Soil Analysis. Part 4. Physical Methods. Soil Science Society of America, Madison, Wisconsin, pp. 1289–1297.

Zegelin, S.J., White, I., Jenkins, D.R., 1989. Improved field probes for soil water content and electrical conductivity measurement using time domain reflectometry. Water Resour. Res. 25, 2367–2376.

CHAPTER

# 9

# Dual Thermal Probes

## 9.1 INTRODUCTION

The hydraulic properties of the surface layer of the soil require a careful study. This is the zone of compacting, cracking, erosion, seed beds, and is often the most dense portion of a root system. The tension infiltrometer is an instrument developed to allow the measurement of surface hydraulic properties (Clothier and White, 1981). We shall discuss it in detail in Chapter 13. With it, preferential flow of water through the macropores and soil cracks in contact with the soil surface is controlled by applying water to the soil at water potentials less than zero. We can obtain the unsaturated hydraulic conductivity, sorptivity, repellency, and mobility of solutes in soil with a tension infiltrometer, but not the soil water content.

To represent the hydraulic character of a soil, the water content needs to be known. It is the most sought-after soil-physical parameter of the four soil-physical factors that affect plant growth. As we saw in the first paragraph of Chapter 1, the other three are soil temperature, aeration, and mechanical impedance (Kirkham, 1973). After soil water, soil temperature is perhaps the most important physical property of soil to affect crop growth (Mohanty et al., 1997). The temperature of the soil surface is of interest to micrometeorologists, because it influences the atmospheric boundary layer (Ham and Senock, 1992). Dual measurements of water and temperature are important for the development of models (Nassar and Horton, 1997a,b; Hiraiwa and Kasubuchi, 2000).

Mohanty et al. (1997) point out the need for improved precision of measurements of water content. Measurement of soil water content can be done by several means, and each method has its advantages and disadvantages. These methods include the gravimetric method, time-domain reflectometry (TDR), which we discussed in Chapter 8, the

http://dx.doi.org/10.1016/B978-0-12-420022-7.00009-4

Copyright © 2014 Elsevier Inc. All rights reserved.

neutron-probe technique, and the dual-probe heat-pulse technique, also called the dual thermal probe technique.

The simplicity and accuracy of the gravimetric method are major advantages (Song et al., 1998). The method also is well suited for measuring the soil water content in the zone of active root water uptake. Unfortunately, the method is time consuming and destructive and cannot be automated. The TDR technique also can provide accurate measurements of soil water content. A significant advantage of TDR over the gravimetric method is that it permits automated, nondestructive measurements. A disadvantage of TDR is that the method requires calibration for soils high in organic matter and other soils in which the standard equation used to determine soil water content (called the "Topp equation") does not work (Topp et al., 1980) (Gerard J. Kluitenberg, Kansas State University, personal communication, July 17, 2013). Other barriers in using the TDR technique are the instrument's cost and its complexity. The neutron-probe technique is well suited for measurements deep in the soil profile, but it is ineffective within about the top 15 cm of the soil surface, the zone of active root water uptake for many plants. However, the neutron probe is still needed for measurements of water uptake at great depths. When monitoring water extraction by roots in semiarid Kansas, we measure to a 3.2 m depth to make sure that we are measuring below the depth of water uptake by roots. Rachidi et al. (1993) found that sunflower (*Helianthus annuus* L.) grown under dry-land conditions depleted water to the 2.7-m depth. No technique other than the neutron-probe method could have measured to such great depths. Although the neutron-probe technique is relatively easy to employ, the method is time consuming, requires calibration, and cannot be automated. The use of a neutron probe also requires special licensing for the handling of radioactive materials. The paper work required for the safe use of the neutron probes deters one from using them (G.J. Kluitenberg, personal communication, July 17, 2013). Improper storage and handling of the radioactive isotopes have caused laboratories to switch from neutron probes to TDR for soil water content measurements.

No traditional method can monitor soil water content near the surface of the soil (<20 mm). Mallants et al. (1996) found that measurements with TDR were valid at an observation depth of 50 mm. The shallowest probe that Clothier and Kirkham (1991) and Clothier et al. (1992) used was 20 mm long. Probes 10 mm long gave aberrant results. In a discussion of wave guide length, Dalton (1992) talks of the maximum probe length, not minimum. He includes an analysis of probes as short as 10 mm, but the analysis is theoretical, not experimental. To quantify the error in propagation time measurement using short transmission lines, Amato and Ritchie (1995) made measurements in air using rod lengths from 10 to 150 mm. The coefficient of variation was greater for times <100 ps for air-dry soil, and it varied from 2.8% to 7.3%. For longer times, corresponding to higher water contents, the coefficient of variation was <3%. Nadler et al. (2002) say that the width of the soil layer affecting the moisture measurement with TDR is close to 30 mm. As far as I know, no one has put TDR wave guides as short at 10 mm in the soil and obtained meaningful soil water contents with them. Thus, I would say that TDR measurements cannot make measurements to the soil surface closer than 20 mm.

The dual-probe heat-pulse technique has been developed to monitor soil thermal properties, that is, heat capacity, thermal conductivity, and thermal diffusivity, which are determined from temperature measurements (Campbell et al., 1991; Bristow et al., 1994b; Bilskie et al., 1998; Bristow, 2002; Kluitenberg, 2002). Campbell et al. (1991) showed that the method can also measure volumetric soil water content ($\theta$), because the soil water content is dependent upon soil thermal properties. Since Campbell et al. (1991) introduced the method, the dual-probe heat-pulse technique has been developed and tested for measuring volumetric water content, $\theta$, and changes in volumetric water content, $\Delta\theta$, in the laboratory and in the field (Bristow et al., 1993, 1994a; Tarara and Ham, 1997; Bristow, 1998; Ham and Knapp, 1998). Dual-probe heat-pulse sensors have been used for routine $\theta$ and $\Delta\theta$ measurement in field experiments (Bremer et al., 1998, 2001; Ham and Knapp, 1998; Bremer and Ham, 1999; Campbell et al., 2002).

Figure 9.1 shows a dual-probe heat-pulse sensor as made by Yan Song and used in the experiment by Song et al. (1998). It consists of two parallel probes each made out of a 1.27-mm-diameter hypodermic needle, which are held apart at a fixed distance (~6 mm) by inserting them through predrilled holes in a polyvinyl chloride (PVC) block (26 × 16 × 6 mm). One needle houses the heater wire, and a voltage is applied to the wire to create a heat pulse. The other needle, which holds a thermocouple

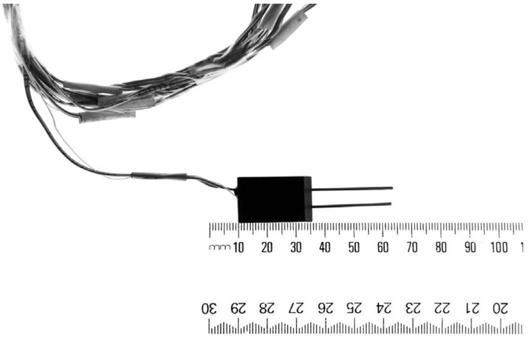

**FIGURE 9.1** A dual-probe heat-pulse sensor. The scale is in millimeters. *Photograph courtesy of Marsha K. Landis, Graphic Designer, Kansas State University, Manhattan, Kansas.*

junction made out of constantan and copper, senses the heat pulse. The length of each sensor, or of the length of the needles protruding from the PVC housing, is 27–29 mm.

A significant advantage of the dual-probe heat-pulse technique is the ability to measure water content close to the surface of the soil (theoretically as close as 6 mm, a value to be discussed later in this chapter) in a nondestructive, automated manner. This should be of great benefit in soil with roots, where often the greatest density of roots is near the surface of the soil. Later in the chapter, we shall turn to the use of the dual-probe heat-pulse technique to monitor the water uptake by roots.

## 9.2 THERMAL PROPERTIES OF SOILS

Because the dual-probe heat-pulse technique measures the thermal properties of the soil, we need to understand them. The amount of heat that will move a given distance through a porous body such as soil depends on how fast the body will conduct the heat (Kirkham and Powers, 1972, p. 463). The rate at which a body conducts heat is called the "thermal conductivity" $K$ and is defined as the number of calories of heat a material will conduct each second across a distance of 1 cm if the temperature difference across this distance is 1 °C. Thermal conductivity has dimensions in metric units of calories per centimeter per second per degrees centigrade. The amount of heat that a volume of soil stores before its temperature rises a certain amount also governs how fast a soil will increase in temperature as heat is applied to it. This quantity is called the "heat capacity". The heat capacity can be based on the mass, when it is called the "gravimetric heat capacity" $c$, or on the volume, when it is called the "volumetric heat capacity" $\rho c$, of the material. The volumetric heat capacity is equal to the gravimetric heat capacity multiplied by the density $\rho$ of the material. The gravimetric heat capacity is defined as the amount of heat required to raise 1 g of material by 1 °C and has units of calories per gram per degrees centigrade. The volumetric heat capacity is defined as the amount of heat required to raise 1 cc of material by 1 °C and has units of calories per cubic centimeter per degrees centigrade. The "specific heat" of a material is the ratio of the heat capacity of the material to that of water and is dimensionless. The "heat content" $q$ in calories of a material can be given as

$$q = \rho c V T, \tag{9.1}$$

where $V$ is the volume of the material and $T$ is the temperature of the material in degrees centigrade.

The time required for a soil to increase in temperature depends on how fast the applied heat is conducted through the soil and its heat capacity.

When heat flow in the soil is studied, a constant $D$ called the "thermal diffusivity" is used and given by

$$D = K/\rho c, \tag{9.2}$$

where $K$ is the thermal conductivity and $\rho c$ is the volumetric heat capacity. The diffusivity has metric units of centimeters squared per second. The water content and the porosity of the soil both have an effect on $K$ and $\rho c$ so that $D$ also changes with changes in water content and porosity (Kirkham and Powers, 1972, p. 463).

There is considerable variety in terminology (Carslaw and Jaeger, 1959, p. 9, first footnote). Some writers regard the definition for gravimetric heat capacity as being the specific heat, as does de Vries (1966). Other writers define the specific heat of a material as the ratio of the heat capacity of the material to that of water, and it is dimensionless. Kirkham and Powers (1972) use the latter definition.

## 9.3 THEORY OF THE DUAL-PROBE HEAT-PULSE METHOD

The theory for obtaining $\theta$ from measurements with dual-probe heat-pulse sensors has been described (Campbell et al., 1991; Bristow et al., 1993, 1994a,b, 1995; Kluitenberg et al., 1993, 1995; Tarara and Ham, 1997; Song et al., 1998). As noted, a dual-probe heat-pulse instrument has a temperature sensor positioned at a fixed distance from a line heat source, which are used to measure the volumetric heat capacity of soil, $\rho c$. We shall follow the analyses of three different references to understand the theory: de Vries (1966); Carslaw and Jaeger (1959); and Campbell et al. (1991).

We first consider the analysis of de Vries (1966). As noted above, two independent thermal properties enter into a quantitative description of the heat transfer by conduction. They are the thermal conductivity, abbreviated as $K$ above and as $\lambda$ by de Vries, who uses units of millicalories per centimeter per second per degrees centigrade, and the heat capacity per unit volume, abbreviated as $C$ by de Vries with units of calories per cubic centimeter per degrees centigrade. Also, as noted above, the volumetric heat capacity, $C$, is equal to $\rho c$, or $C = \rho c$, where $\rho$ is the density of the medium (grams per cubic centimeter) and $c$ is the specific heat (calories per gram per degrees centigrade). In many equations, the quotient of these two quantities appears. It is called the "thermal diffusivity" and is denoted by the symbol $D$ above and as $a$ by de Vries. Thus, using de Vries's symbols, $a = \lambda/C$.

The heat capacity per unit volume of soil can be found by adding the heat capacities of the different soil constituents in 1 cm$^3$. Thus, if $x_{\mathrm{s}}$, $x_{\mathrm{w}}$, and $x_a$ denote the volume fractions of solid material, water (or ice), and air, respectively, one has

$$C = x_s C_s + x_w C_w + x_a C_a. \tag{9.3}$$

The third term on the right-hand side usually can be neglected, because the heat capacity of air is small. The volumetric heat capacity of air at 10 °C is 0.00030 cal/cm$^3$/°C (de Vries, 1966, p. 210) or, at 20 °C, 0.0012 MJ/m$^3$/K (= 0.0012 MJ/m$^3$/°C) (Kluitenberg, 2002, p. 1203). This is small compared to the volumetric heat capacity of water, $C_w$, which at 10 °C is 1.00 cal/cm$^3$/°C (de Vries, 1966, p. 210) (or 4.18 MJ/m$^3$/°C). de Vries (1966, p. 211) reports that the specific heat of most soil minerals varies linearly from $0.16 \pm 0.01$ cal/cm$^3$/°C at −18 °C to $0.19 \pm 0.01$ cal/cm$^3$/°C at 60 °C. One can take a middle value of about 0.17 cal/cm$^3$/°C for the specific heat of mineral soils. Because the specific mass of these minerals is about 2.7 g/cm$^3$, an average value of $C_s$ of about 0.46 cal/cm$^3$/°C or 1.92 MJ/m$^3$/°C holds for a mineral soil at 10 °C.

The specific heat of soil organic matter is about 0.46 cal/g/°C or 1.92 MJ/m$^3$/°C (de Vries, 1966, p. 211). An average value of the specific mass of the organic materials in soil is 1.3 g/cm$^3$, and, therefore, $C_s = 0.60$ cal/cm$^3$/°C or 2.51 MJ/m$^3$/°C is a good average value in the case of organic soils.

If we denote the volume fractions of soil minerals and of organic matter by $x_m$ and $x_o$, respectively, the heat capacity per unit volume equals

$$C = 0.46\, x_m + 0.60\, x_o + x_w \text{ cal/cm}^3/^\circ\text{C} \tag{9.4}$$

or

$$C = 1.92\, x_m + 2.51\, x_o + 4.18\, x_w \text{ MJ/m}^3/^\circ\text{C}, \tag{9.5}$$

where we remind ourselves that

$C$ = volumetric heat capacity of the soil (MJ/m$^3$/°C),
$x_m$ = volume fraction of soil minerals,
$x_o$ = volume fraction of organic matter,
$x_w$ = volume fraction of water.

We also remember

$$C = \rho c, \tag{9.6}$$

where

$C$ = volumetric heat capacity (cal/cm$^3$/°C),
$\rho$ = density (g/cm$^3$),
$c$ = gravimetric heat capacity (cal/g/°C).

So

$$C = \rho c = 1.92\, x_{\mathrm{m}} + 2.51\, x_{\mathrm{o}} + 4.18\, \theta, \tag{9.7}$$

where

$x_{\mathrm{m}}$ = (bulk density)/(particle density),
$x_{\mathrm{o}}$ = organic matter content,
$\theta$ = volumetric water content.

The bulk density of a soil needs to be known. The particle density can be assumed to be 2.65 Mg/m$^3$. $x_{\mathrm{o}}$ can be neglected in soils with low organic matter. We can determine heat capacity and solve for $\theta$.

We next turn to the analysis of Carslaw and Jaeger (1959, p. 258; their Eqn (3)), who present the following equation for a temperature change when heat is applied to a line source:

$$\Delta T = [Q/(4\pi kt)]\left[\exp\left(-r^2/4kt\right)\right], \tag{9.8}$$

where

$\Delta T$ = temperature change (degrees centigrade) (Carslaw and Jaeger use the symbol $v$ for $\Delta T$),
$Q$ = source strength (meter square degrees centigrade) (see later for more discussion of $Q$),
$r$ = distance from the line (meters),
$t$ = time after the instantaneous heat pulse (seconds),
$k$ = thermal diffusivity (meter square per second).

The assumptions in the analysis by Carslaw and Jaeger are as follows: (1) an infinite line; (2) an instantaneous heating; and (3) an infinite, homogeneous medium.

Finally, we turn to the analysis of Campbell et al. (1991). They differentiate the equation of Carslaw and Jaeger with respect to time to find the time of maximum temperature change, $t_{\mathrm{m}}$, at a fixed distance, $r_{\mathrm{m}}$, from the line source. This gives

$$t_{\mathrm{m}} = -r^2 m/(4k). \tag{9.9}$$

We substitute this result for $t_{\mathrm{m}}$ into the equation of Carslaw and Jaeger. We get a maximum temperature rise, $\Delta T_{\mathrm{m}}$ (Campbell et al., 1991; see their Eqn A2),

$$\Delta T_{\mathrm{m}} = Q/\left(e\pi r_{\mathrm{m}}^2\right). \tag{9.10}$$

The source strength, $Q$ (meter square degree centigrade), is defined as

$$Q = q/\rho c, \tag{9.11}$$

where

$\rho c$ = volumetric heat capacity (Joules per cubic meter per degrees centigrade),
$q$ = quantity of heat liberated per unit length of heater (Joules per meter).

So we have (Campbell et al., 1991; see their Eqn A3)

$$\rho c = q/\left(e\pi r_{\mathrm{m}}^2 \Delta T_{\mathrm{m}}\right). \tag{9.12}$$

We see that the volumetric heat capacity is linearly related to the inverse of $\Delta T_{\mathrm{m}}$.

We now combine the above equation from Campbell et al. (1991) with de Vries's equation (Eqn (9.7)), and we get

$$\theta = \left\{\left[q/\left(e\pi r_{\mathrm{m}}^2 \Delta T_{\mathrm{m}}\right)\right] - (1.92\, x_{\mathrm{m}} + 2.51\, x_{\mathrm{o}})\right\}/4.18. \tag{9.13}$$

## 9.4 EXAMPLE CALCULATION

Data collected by Song et al. (1998) on November 13, 1996, from a dual-probe heat-pulse sensor in a column containing a very fine sandy loam were as follows:

Initial temperature (°C) = 20.660
$q$ (J/m) = 693.42
$\Delta T_{\mathrm{m}}$ (°C) = 1.1702
$r_{\mathrm{m}}$ (mm) = 5.83
Bulk density $(\mathrm{Mg/m^3})$ = 1.45
Particle density $(\mathrm{Mg/m^3})$ = 2.65
$x_{\mathrm{m}}$ (b.d./p.d.) = 0.547
$x_{\mathrm{o}}$ = 0.000

$$\rho c = q/\left(e\pi r_{\mathrm{m}}^2 \Delta T_{\mathrm{m}}\right),$$

$$\rho c = 0.0020415\ \mathrm{J/mm^3/^\circ C}\ \text{ or }\ 2.0415\ \mathrm{J/cm^3/^\circ C},$$

$$\theta = \left(\rho c - 1.92\, x_{\mathrm{m}}\ \mathrm{J/cm^3/^\circ C}\right)/\left(4.18\ \mathrm{J/cm^3/^\circ C}\right),$$

$$(1.92\ \mathrm{J/cm^3/°C})(0.547) = 1.05024\ \mathrm{J/cm^3/°C},$$

$$\theta = \left(2.0415\ \mathrm{J/cm^3/°C} - 1.05024\ \mathrm{J/cm^3/°C}\right) \text{ divided by } 4.18\ \mathrm{J/cm^3/°C},$$

$$\theta = 0.237.$$

This is volumetric water content. So, adding the units, we have $0.237\ \mathrm{m^3/m^3}$.

## 9.5 MEANING OF Q

At this point, we need to understand $Q$. A memorandum that I received from Dr Gerald Kluitenberg, Department of Agronomy, Kansas State University, dated December 27, 1997, explains $Q$. I quote directly from the memorandum:

"In your memorandum dated August 28, 1997, you indicated that you were trying to reconcile the units for $Q$ in the Appendix of the Campbell et al. (1991) with the units of $Q$ given in the attached pages of Carslaw and Jaeger (Carslaw and Jaeger, 1959, pp. 1—3). The $Q$ discussed on pages 2—3 of Carslaw and Jaeger is not at all related to the $Q$ in the Appendix of Campbell et al. Note that Campbell et al. refer the reader to page 258 of Carslaw and Jaeger (1959). Bristow et al. 1994a refer the reader to the same place. The units for $Q$ discussed by Campbell et al. and Bristow et al. agree with the units given on page 258 of Carslaw and Jaeger.

"On page 258, Carslaw and Jaeger state that $Q\rho c$ is the heat liberated per unit length of line. Thus, $Q\rho c$, which is the same as $q$, has units of Joules per meter. Dividing $Q\rho c$ (J/m) by $\rho c$ (Joules per cubic meter per degrees centigrade) yields units of $\mathrm{m^2C}$ (meter squared degree centigrade) for $Q$. These are the same units that Campbell et al. (1991) and Bristow et al. (1994a) use for $Q$.

"In your memorandum dated August 29, 1997, you indicated that you are trying to understand the physical meaning of the quantity $Q$. I have struggled with this issue myself. Carslaw and Jaeger consistently call $Q$ the source strength in their chapter on heat sinks and sources (Ch. X) [Chap. X contains p. 258]. $Q$ appears to be simply a mathematical construct that has no physical meaning beyond the physical meaning of $q$ and $\rho c$, whose ratio define $Q$. I have always accepted $Q$ as a mathematical construct that has no particular physical significance of its own, but I've always wondered whether I might be missing something. I delayed my response to you on this issue so that I would have the opportunity to ask this question to Dr. Philip during his KSU visit. This was the first question I asked him during our visit. His response was no different than that of Carslaw and Jaeger. $Q$ is simply a mathematical construct that has no physical significance of its own."

## 9.6 MEASUREMENTS OF DIFFERENCES OF WATER CONTENT, $\Delta\theta$

Tarara and Ham (1997) noted that the real strength of the dual-probe heat-pulse technique is in measuring changes in $\theta$ or $\Delta\theta$, because they are not affected by errors in measurements of soil bulk density and soil organic matter, if these properties do not change between sampling times. From Eqn (9.13), we can obtain Eqn (9.14), which shows that measurements of $\Delta\theta$ between two sampling periods eliminates $x_m$ and $x_o$ (Song et al., 1998; see their Eqn (9.4)):

$$\Delta\theta = \theta_{t2} - \theta_{t1} = \left(1/4.18e\pi r^2\right)\left(q_{t2}/\Delta T_{m,t2} - q_{t1}/\Delta T_{m,t1}\right), \tag{9.14}$$

where the subscripts $t1$ and $t2$ represent two sampling times. Tarara and Ham (1997) found that the dual-probe heat-pulse technique could measure $\Delta\theta$ on a daily basis to within 0.01 $m^3/m^3$ in nonvegetated soil columns. Campbell et al. (1991) reported that the resolution of $\Delta\theta$ with the dual-probe heat-pulse sensor was about 0.005 $m^3/m^3$. These results suggest that the dual-probe heat-pulse sensors may have sufficient resolution to monitor water uptake in a root zone, which we shall discuss at the end of the lecture.

## 9.7 ERRORS

Without roots, Tarara and Ham (1997) found in a laboratory study that the dual-probe heat-pulse method and the gravimetric method agreed to within 0.03 and 0.04 $m^3/m^3$ for a Haynie sandy loam and a Kahola silt loam, respectively, over a range of water contents of 0.10–0.45 $m^3/m^3$. As noted above, they found that the estimates of $\Delta\theta$ for the methods agreed to within 0.01 $m^3/m^3$ for both soils. Campbell et al. (2002) and Noborio et al. (1996) also evaluated the dual-probe heat-pulse method for measuring $\theta$ and $\Delta\theta$. Campbell et al. (2002) inserted dual-probe heat-pulse sensors in undisturbed peat cores obtained from two peat bogs in New Zealand. Dual-probe heat pulse-based $\theta$ estimates were compared with values obtained by the gravimetric method over a water content range of approximately 0.15–0.90 $m^3/m^3$. Regression analysis with $\theta$ estimates obtained by the two methods showed the dual-probe heat-pulse method to be unbiased. The analysis also revealed that excellent precision was achieved with the dual-probe heat-pulse method.

Basinger et al. (2003) evaluated the level of precision that can be achieved with the dual-probe heat-pulse method. Tempe pressure cells fitted with DPHP (dual-probe heat-pulse) sensors were used to conduct desorption experiments in which dual-probe heat pulse-based estimates of $\theta$ and $\Delta\theta$ were compared with values estimated by the gravimetric method.

For water contents corresponding to soil water pressure potentials below $-100$ kPa, comparisons were made by packing the pressure cells with soil wetted to known water contents. The investigation was conducted with seven soil materials representing a wide range of physical properties for mineral soils. Dual-probe heat-pulse sensors slightly overestimated $\theta$ at low water contents, but it was shown that the bias could be removed by using an empirical calibration equation, $\theta = 1.09\theta_{\mathrm{DPHP}} - 0.045$. This relationship appears to be general in as much as it was shown to be applicable for all seven soil materials and for water contents ranging from 0.02 to 0.59 $\mathrm{m}^3/\mathrm{m}^3$. The general calibration equation was also shown to be effective in removing bias in $\Delta\theta$ estimates. Pooled regression analysis (all soil materials) showed that $\theta$ can be measured with a root mean square error (RMSE) of 0.022 $\mathrm{m}^3/\mathrm{m}^3$. Greater precision can be achieved with $\Delta\theta$ measurements (RMSE = 0.012 $\mathrm{m}^3/\mathrm{m}^3$). However, the results indicated a decrease in precision with increasing magnitude of $\Delta\theta$.

## 9.8 ADVANTAGES

One advantage of the dual-probe heat-pulse method is that is requires no calibration (even though a calibration is still needed to determine the apparent probe spacing, which we shall discuss later). Another advantage is that it can be automated to measure $\theta$, volumetric heat capacity, and soil temperature simultaneously and frequently. The technique monitors the thermal properties of rocks and soils and, consequently, can be used to analyze soil water content over a wide range of values, including residual water content. Roots utilize water from bedrock (Zwieniecki and Newton, 1995), so it is important to be able to monitor the water content of rock. Peat soils represent the other end of the scale. They can hold large amounts of water. As noted above, Campbell et al. (2002) in New Zealand showed that dual-probe heat-pulse sensors can be used to measure the wet peat soils endemic to the North Island of that country. They found that the method had a greater sensitivity in peat soils compared with mineral soils and excellent resolution is possible, even at moisture contents as high as 90% by volume.

Because the dual-probe heat-pulse technique samples a small soil volume compared to other methods, the method is well suited for the measurement of water content where fine spatial resolution is required. Some examples are (1) near-surface measurements where other methods fail; (2) measurements near soil heterogeneities such as textural interfaces, rocks, cracks, or holes created by soil organisms or decayed roots; and (3) measurements in the vicinity of live roots. Much research is needed to describe root water uptake as a function of water in the root zone (van Genuchten, 1994), and the dual-probe heat-pulse method now offers an experimental method to obtain data for root models.

## 9.9 CALIBRATION

As noted, an advantage of the dual-probe heat-pulse method is that no calibration is required, because the method is based on a physical model of heat flow in soil. However, calibration is still required to get the distance, $r$, the distance between the two needles. The measured distance cannot be used. Tarara and Ham (1997) tell how this distance can be determined. They suspended probes in three media of known heat capacities. The media were water stabilized with agar, dry glass beads, and glass beads saturated with water. They measured $\rho c$ in each medium. Values of $q$ and $\Delta T_{\mathrm{m}}$, along with measured $r$, were used in Eqn (9.12) to get $\rho c$. Data collected from the water–agar medium were subsequently reanalyzed by inserting the known heat capacity for water into Eqn (9.12) and solving for $r$. This calculated value of probe spacing was denoted by $r'$. This method of calibrating dual probes to a known heat capacity (Campbell et al., 1991) uses calculated probe spacing to account for nonideal heat flow between the heater and the thermocouple junction and extraneous factors in sensor materials or geometry that may affect the accuracy of a dual-probe measurement. All new probes are tested in the water–agar medium and calibrated to the heat capacity of water. The calculated probe spacing ($r'$) for each instrument was then used by Tarara and Ham (1997) for determining $\rho c$ in soil columns and the field.

Tarara and Ham (1997) list mean values of measured $r$ and calculated $r'$ probe spacings for 24 dual probes. Calculated values of $r'$ were in good agreement, regardless of test medium, but were all slightly larger (~0.1 mm) than measured values. Correlation coefficients for the relationship between $r'$ and $r$ were 0.84, 0.81, and 0.74 for water, dry glass beads, and water-saturated glass beads, respectively, which suggests that the variation in probe spacing causes the variability in $\rho c$ measurements among probes immersed in the same medium. These results support the use of the calibration technique described above, in which the input value of probe spacing for each instrument is calculated so that the probe is calibrated to the known heat capacity of water. Calibration to a known heat capacity eliminates the need for precise, accurate, physical measurements of the distance between the heater and the thermocouple junction, and it corrects for the probe's estimate of $\rho c$ for nonideal heat flow. Despite the slight bias between $r'$ and $r$, the results indicate that $r'$ is stable and repeatable, and that the $r'$ measured in one medium can be applied to measurements collected in other media.

The key to successful use of the dual probe is not the magnitude of $r$ or $r'$ per se, but that $r'$ is known and remains fixed. Once the instruments are calibrated in water, the distance between the needle probes must remain constant. Therefore, the probes must be installed in the soil with care (Tarara and Ham, 1997). Because the probe spacing appears as a squared term in Eqn (9.12), any error in measurement of $r$ or $r'$ is squared. Thus, it is important that $r$ remains stable and fixed.

## 9.10 MEASUREMENTS NEAR THE SOIL SURFACE

As stated, a key advantage of the dual-probe heat-pulse technique is its ability to measure soil water content closer to the soil surface than any other instrument now available. But the question arises: How close to the soil surface can one take measurements with the dual-probe heat-pulse method? The soil surface was one form of heterogeneity examined by Philip and Kluitenberg (1999) and Kluitenberg and Philip (1999). They found theoretically that heterogeneity errors are small provided the heterogeneity is no closer to the probes than needle separation. They concluded that the estimates of $C$ may provide a good resolution of soil water content in critical regions such as near soil surfaces, at interfaces between different soils, or behind a wetting front. So, if the needles are 6 mm apart, a typical separation in a dual-probe heat-pulse sensor, one can obtain soil water content as close as 6 mm to the surface, but not closer. The theory has not been checked by measurements. The closest surface measurement that Song et al. (1998, 1999a) took was 15 mm from the soil surface, more than twice as deep the theoretical limit of a near-surface measurement.

Knight et al. (2007) also investigated the measurement volume that a dual-probe heat-pulse sensor is measuring. They found that for a sensor with a probe spacing of 6 mm, the boundary containing 99% of the total spatial sensitivity is closely approximated by an ellipse with an area of 168 $\text{mm}^2$ and a major axis of 15.6 mm in length.

## 9.11 CONVECTION AND ITS EFFECT ON MEASUREMENTS

Kluitenberg and Heitman (2002) studied the effect of convection (movement of water) on soil water content measurements made with the dual-probe heat-pulse method. They noted that the dual-probe heat-pulse method is useful for measuring soil volumetric water near heterogeneities such as the soil surface, but it does not consider convective heat transfer that may result from soil water movement (forced convection). They examined the effect of forced convection on estimates of soil water content using three different dual-probe heat-pulse sensor orientations. Heat transfer theory that explicitly accounts for forced convection was used to test this effect. The three orientations were (1) the heater and temperature probes were parallel in a plane normal to the direction of steady water flow (e.g., the two needles were an equal distance from the soil surface and parallel to the soil surface); (2) the temperature probe was directly downstream from the heater probe (e.g., the temperature probe was deeper in the soil than the heater needle); (3) the temperature probe was upstream from the heater probe (e.g., the temperature probe was closer to the soil surface than the heater probe). They concluded that the effect of forced convection may be large enough to render the dual-probe heat-pulse method useless for orientations where the temperature probe is upstream or downstream from the heater probe (i.e., if the heater and temperature probes are inserted into a soil profile face, so water infiltrating into the soil first hits a heater probe or a temperature probe). However, it does not appear to limit the practical utility of dual-probe heat-pulse sensors when the parallel heater and temperature probes are in a plane normal to the direction of steady water flow (i.e., the heater and temperature probe are side by side and placed horizontally so that each needle is an equal distance from the soil surface). (Note that the two needles cannot be pressed vertically into the soil from the soil surface, as one inserts wave guides on a TDR instrument, because, as noted above, at least 6 mm of soil needs to be above the needles for accurate measurements.)

Dr Kluitenberg (personal communication, March 17, 2003) said that even if the sensors are placed so that water meets the two needles at the same time, errors may still occur during rains or irrigations. For example, he said that if there were a heavy rainfall and the sensors were in a sandy soil, the measurements of soil water content could be off by several per cent.

## 9.12 MEASUREMENT OF ELECTRICAL CONDUCTIVITY

Further development of the dual-probe heat-pulse technique has led to the simultaneous measurement of soil thermal properties, water content, and electrical conductivity using TDR in combination with the dual-probe heat-pulse method (Noborio et al., 1996; Ren et al., 1999). Ren et al. (1999) combined the TDR and dual-probe heat-pulse methods to measure simultaneously soil water content, bulk electrical conductivity, thermal conductivity, heat capacity, and thermal diffusivity. TDR was used to measure soil water content and electrical conductivity, and the dual-probe heat-pulse method was used to determine thermal conductivity, heat capacity, and thermal diffusivity. They called their probe the thermo-TDR probe. Laboratory tests on a silica sand and a clay loam soil showed that the probe determined soil water content accurately, and the measured electrical conductivity values of saturated soil correlated well with values determined by a four-electrode probe. Measurements in agar-immobilized water produced values of thermal conductivity and heat capacity that closely corresponded with standard values of these properties for water, an indication of the sensor's functionality in other media. Bristow et al. (2001) showed that a simple modification of the dual probe with an additional two needles for bulk soil electrical conductivity measurements provides an alternative measure of the soil's electrical conductivity.

## 9.13 DETERMINATION OF SOIL WATER MOVEMENT

Ren et al. (2000) followed up on the work of Ren et al. (1999) and used the same thermo-TDR probe to measure soil water flux density (also called flux density), *J*, in which a heat tracer was used to quantify the magnitude of convective heat transfer resulting from soil water movement. (See Chapter 7, Section 7.1, for the definition of flux density; it is the time rate of transport of a quantity per unit area perpendicular to the direction of flow.) In the method, constant heat input during a small time interval (15 s) is used to emit a heat pulse from a line heat source. Asymmetry in the thermal field near the heat source is quantified by computing the maximum dimensionless temperature difference (MDTD) between upstream and downstream locations. Heat transfer theory was used to relate MDTD to *J*. A thermo-TDR probe was used to obtain measurements of MDTD in water-saturated soil materials of different textures (sand, sandy loam, and clay loam) with imposed water flux densities ranging from $1.16 \times 10^{-5}$ to $6.31 \times 10^{-5}$ $m^3/m^2/s$. A nearly linear relationship between measured MDTD's and fluxes was observed for all soil materials. The experimental results indicated that the proposed method may provide a useful means of measuring *J*. Because the thermo-TDR probe can be used to make TDR-based measurements of volumetric water content, the proposed method also may permit measurement of pore water velocity ($J/\theta$).

The method of Ren et al. (2000) utilized analytical solutions of the heat equation to describe temperature changes that occur upstream and downstream of a line heat source following the emission of a heat pulse. Their solutions contain integrals that must be evaluated using numerical integration techniques. Kluitenberg and Warrick (2001) developed an improved procedure for evaluating the integrals of the analytical solutions by recognizing that they can be reduced to a single function, *W*, known as the well function for leaky aquifers. Thus, numerical integration is not required to implement the heat-pulse method for measuring soil water flux density.

Wang et al. (2002a,b) followed up on the work of Kluitenberg and Warrick (2001). They noted that although their improved method eliminates the need for numerical integration, it still is inconvenient to analyze the relations among variables and to estimate *J*, because the infinite series is complicated. Wang et al. (2002a) analyzed the heat-pulse signal in a new way with the goals of clarifying the relationships between the variables in the heat transfer problem and simplifying the procedure for calculating *J* from heat-pulse measurements. Their new mathematical analysis showed that a simple linear relationship exists between soil water flux and the natural log of the ratio of the temperature increase downstream from the line heat source to the temperature increase upstream from the line heat source. The simplicity of this relationship makes heat-pulse sensors an attractive option for measuring soil water fluxes. In theory, the method is valid for fluxes with magnitudes between $10^{-4}$ and $10^{-7}$ m/s. The range of measurable fluxes is defined by temperature-measurement resolution at the lower end and by the assumptions used in the analysis at the higher end.

The results of Ren et al. (2000) suggested that the method is limited at higher fluxes (larger than about 2.4 m/day), because of a systematic overestimation of MDTD by ≥10% at these higher water velocities (Hopmans et al., 2002). The discrepancy may be the result of ignoring the finite heater geometry in the heat analysis, which assumes infinitely small point sources and sensors with negligible diameter. Although not important for zero-water flow conditions (Kluitenberg et al., 1995), it could be an important consideration when using the dual-probe heat-pulse method for the estimation of water flux. Moreover, the finite physical size of the needles may distort the water flow field between the needles, thereby affecting flow of water and heat between the heat source and sensor. Although the proposed flux density measurement of Ren et al. (2000) requires a priori knowledge of the thermal properties, these can be obtained separately from zero-water flux heat probe measurements, using the method of Bristow et al. (1994a). It is expected that even lower water velocities can be measured for unsaturated soils because of the reduction in the bulk soil heat capacity with decreasing water content.

Hopmans et al. (2002) hypothesized that the difficulties in using the dual-probe heat-pulse method for water flux density measurements are partly caused by the omission of dispersive heat transport in the heat flow equation. Therefore, Hopmans et al. (2002) did a sensitivity analysis to show the influence of thermal dispersion on heat transport and on the estimation of thermal properties and water flow density using parameter estimation by inverse modeling. They showed that inverse modeling provides an accurate estimation of soil water flux density in both unsaturated and saturated soil conditions for a wider range of water velocities than originally thought possible. They suggested that inverse modeling of dual-probe heat-pulse temperature data may allow the simultaneous estimation of soil water retention, when combined with matric potential measurements, and unsaturated hydraulic conductivity through water flux estimation from simple laboratory experiments.

Kluitenberg et al. (2007) described an improved method to determine soil water flux using a three-probe sensor. The center probe heats the soil, and the outer probes measure temperature increases downstream and upstream from the heater. Kamai et al. (2008, 2010) employed large heater needle diameters (4 mm) to increase the capability of the heat-pulse probe technique to estimate low values of water movement in the soil. They were able to measure values near 1 cm/day, which was about 10 times lower than previous values. Knight et al. (2012) present a semianalytical solution that accounts for the finite radius, as well as the finite thermal properties of the probes. For accurate work when using the dual-probe heat-pulse technique, the finite radius and finite heat capacity of the probes should be taken into account.

To eliminate errors associated with needle deflection (note the two needles must be perfectly parallel for the theory to work), Kamai et al. (2009) designed a button heat-pulse probe that does not use needles. Instead, it consists of a ring-shaped 6-mm-radius heating element and a central thermistor, both embedded in the face of a plastic disk (6 mm thick and 16 mm in diameter). The button heat-pulse probe was more robust compared to the conventional heat-pulse probe.

## 9.14 MEASUREMENTS WITH ROOTS IN SOIL

Because no work had been done to determine if the dual-probe heat-pulse technique could be used in soil with roots, Song et al. (1998, 1999a,b) carried out experiments with a fibrous root system (turf grass) and a tap-rooted root system (sunflower) to determine if dual-probe heat-pulse sensors could be used to monitor water content, temperature, and root water uptake in a root zone. In the turf grass experiment, tall fescue (*Festuca arundinacea* Schreb., ‘Kentucky 31’) was chosen because of its dense, uniform root system near the surface of soil. The grass grew in 20-cm diameter containers packed with a Haynie very fine sandy loam (coarse-silty, mixed, calcareous, mesic Mollic Udifluvents). Water content was measured with the dual-probe heat-pulse sensors that were placed horizontally at different depths between 1.5 and 14.4 cm from the surface of the soil columns and at different distances from the axis of the columns. Water content also was monitored gravimetrically from changes in container mass. Measurements started when the soil surface was covered completely by tall fescue. Hence, changes in $\theta$ could be attributed entirely to water being taken up by roots of tall fescue. Daily measurements were taken over multiple six- or seven-day drying cycles. Each drying cycle was preceded by an irrigation, and free drainage had ceased before measurements were initiated. Soil water content dropped from about 0.35 to 0.10 $m^3/m^3$ during each drying cycle. Correlation was excellent between $\theta$ and changes in water content ($\Delta\theta$) determined by the DPHP and gravimetric methods. Comparisons with the gravimetric method showed that the DPHP sensors could measure average container $\theta$ within 0.03 $m^3/m^3$ and $\Delta\theta$ within 0.01 $m^3/m^3$.

In the follow-up of the work with the fibrous root system of turf grass that completely penetrated soil columns, Song et al. (1999b) carried out an experiment to see if the dual-probe heat-pulse sensors could be used with a taprooted plant. A sunflower plant (*Helianthus annuus* L. 'Hysun 354') was grown in a column (0.20 m in diameter and height) with a Haynie very fine sandy loam, the same soil used in the experiments with the turf grass. Eleven dual-probe heat-pulse sensors were in the container. Results from the sensors were compared with those from the gravimetric method. Discrepancies between measurements of soil volumetric water content, $\theta$, and changes in soil volumetric water, $\Delta\theta$, by the DPHP and gravimetric methods were small (within 0.018 and 0.01 $m^3/m^3$, respectively). The sunflower had a small amount of nocturnal transpiration, and roots took up water at a higher rate near the surface of the soil than at greater depths.

At the harvest of the two experiments, roots were extracted and the dual-probe heat-pulse sensors were removed. Both turf grass roots and sunflower roots had grown between the two needles of the dual-probe heat-pulse sensors. Having roots between the needles (rather than soil only) apparently did not affect the readings made with the dual-probe heat-pulse sensors.

Data from the turf grass study (Song et al., 1998) were further analyzed by Song et al. (1999a) to determine the resolution of measurements, including both soil water content and temperature, and to determine root water uptake by monitoring depletion during drying cycles. Moisture depletion at different depths in the soil columns was determined by plotting the soil water content, measured with the dual-probe heat-pulse sensors, at the beginning and end of each of the drying cycles. Water uptake by roots was estimated by averaging depletion during drying cycles and dividing these mean values by root weight.

The columns were usually drier near the surface than at greater depths (Figure 9.2). The dual-probe heat-pulse sensors monitored soil water content as close as 1.5 cm to the surface and to values as low as 0.09 $m^3/m^3$ and as high as 0.44 $m^3/m^3$. Temperatures were usually coolest near the surface of the columns (Figure 9.3), where most roots occurred.

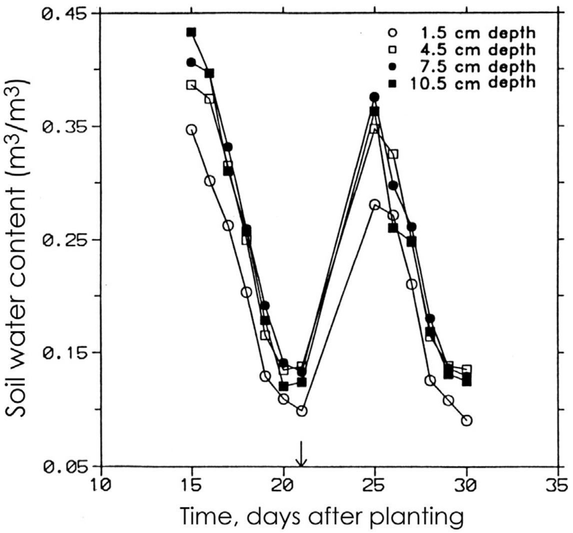

**FIGURE 9.2** Volumetric water content at different depths in a soil column with turf grass determined using dual-probe heat-pulse sensors. The arrow indicates when the column was irrigated. The average coefficient of variation was 10.1%. *From Song et al. (1999a). Reprinted by permission of M. Th. van Genuchten and L. Wu.*

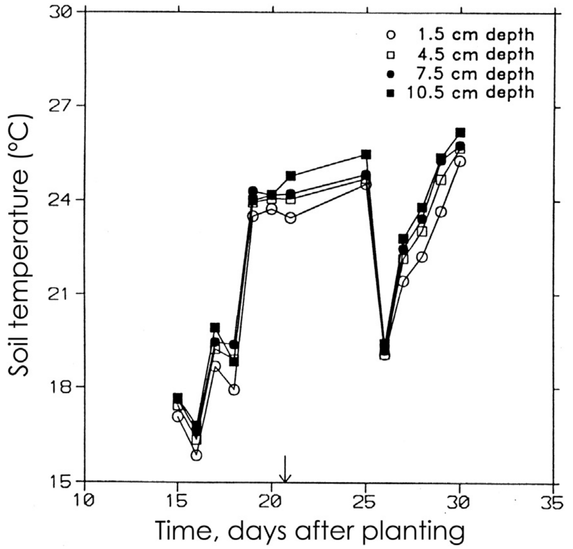

**FIGURE 9.3** Temperature in a soil column with turf grass determined using dual-probe heat-pulse sensors. The arrow indicates when the column was irrigated. The average coefficient of variation was 1.5%. *From Song et al. (1999a). Reprinted by permission of M. Th. van Genuchten and L. Wu.*

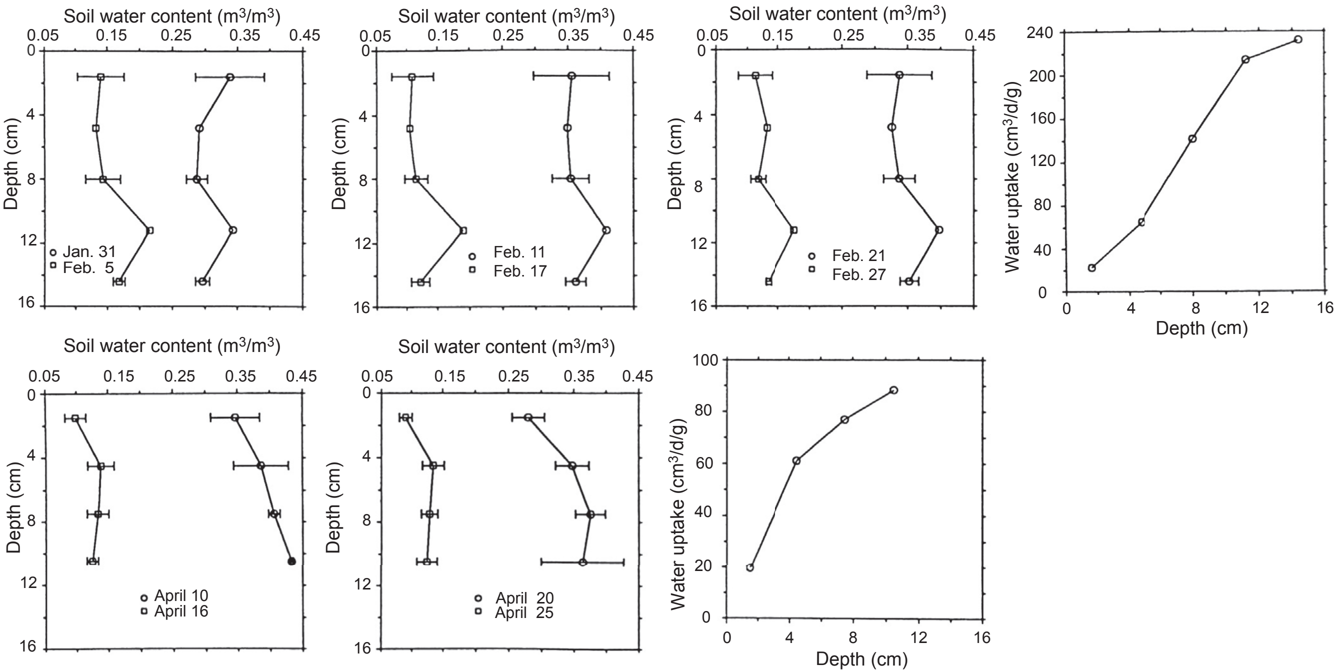

**FIGURE 9.4** Top: three drying cycles during an experiment in which the water content in soil with turf grass was measured using dual-probe heat-pulse sensors. Estimate of root water uptake based on average depletion during the three drying cycles is shown at the right. Bottom: two drying cycles during an experiment in which water content in soil with turf grass was measured using dual-probe heat-pulse sensors. Estimate of root water uptake based on average depletion during the two drying cycles is shown at the right. *From Song et al. (1999a). Reprinted by permission of M. Th. van Genuchten and L. Wu.*

Temperatures were as much as 1 °C cooler near the surface than at greater depths. The smaller range in coefficients of variation for the temperature measurements (1.5%) compared to that for water measurements (10.1%) showed that measurements of soil temperature vary less than those of soil water. Moisture depletion was fairly uniform with depth (Figure 9.4). However, the root distribution was not uniform. Roots were denser near the surface of the soil than close to the bottom of the columns. To maintain a uniform depletion, the roots at the bottom of soil columns apparently were taking up more water than roots near the surface of the columns (Figure 9.4, right-hand side).

From a plant physiological point of view, a main strength of the dual-probe heat-pulse technique, as shown by Song et al. (1999a), is the ability to monitor depletion of water in a root zone on a fine scale (every 2 cm). With the neutron probe, depletion cannot be measured at intervals closer than about 15 cm apart due to the limitations of the method.

## 9.15 HYDRAULIC LIFT

The dual-probe heat-pulse technique was used to see if it could monitor hydraulic lift (Song et al., 2000). Roots are movers of water in the soil. One method of movement is through hydraulic lift, which occurs when plants extract water from a moist subsoil and release it into a dry topsoil. Detection of hydraulic lift has been hampered by the lack of instruments sensitive enough to measure the small amount of water moved. The dual-probe heat-pulse sensors were used to determine if water is released by hydraulic lift. Sunflower was grown in a column (38-cm height; 25-cm diameter; bulk density = 1.45 $\mathrm{Mg/m^3}$) packed with a Haynie very fine sandy loam with its roots divided between a top dry layer and a lower wet layer. Eight DPHP sensors installed in the soil column were used to monitor soil water content. During 24 measurement days, hydraulic lift was evident only when the plant was wilted. This occurred when the lower "wet" layer had been allowed to dry and then it was rewatered. At this time, the roots in the upper dry layer released water, increasing the soil water content in the center of the root mass by 0.019 $\mathrm{m^3/m^3}$ (increase from 0.121 to 0.140 $\mathrm{m^3/m^3}$). The soil water increase was similar to other values reported in the literature and shows that it is small.

## 9.16 COMMERCIALLY AVAILABLE EQUIPMENT

To use the dual-probe heat-pulse technique, as described above in the experiments by Song et al. (1998, 1999a,b, 2000) or Campbell et al. (2002), one needs to know how to build the dual-probe heat-pulse sensors and write the software necessary to take the measures. For people who do not have the time or skill to make the equipment, Decagon Devices (Pullman, Washington) has made an instrument, called the KD2 PRO, which comes with three different sensors. It is marketed to measure the thermal properties of liquids, solids such as rock or concrete, and soils. Thermal properties measured include the specific heat, thermal conductivity, and thermal diffusivity. One sensor, the SH-1, measures specific heat and thermal diffusivity. However, there is no reason that this sensor cannot be used to measure the soil water content using the dual-probe heat-pulse technique (G.J. Kluitenberg, personal communication, July 17, 2013). The SH-1 is 30 mm long, 1.28 mm in diameter, and has a 6-mm spacing between the two probes. It is the only sensor on the market that measures thermal diffusivity and specific heat, and which, hence, can be used to measure soil water content.

The soil water content obtained with the dual-probe heat-pulse technique (i.e., using the SH-1 sensor attached to the KD2 PRO of Decagon Devices) is much more accurate than the water content gotten with soil moisture sensors that are now on the market. Even though the soil moisture sensors are easy to use, require no special training so anyone can deploy them, need only AA batteries (batteries readily available in stores), and are cheap, they are not reliable. One does not know the exact principle of measurement. Some dielectric property of the soil is being measured. They are not capacitance probes, and they are not frequency domain probes, but something in between (G.J. Kluitenberg, personal communication, July 17, 2013). Neutron probes and true TDR (as described in Chapter 8, true TDR is TDR that is calibrated and detects the trace of the electromagnetic signal; some equipment commercially available is not true TDR) are accurate ways to measure soil water content. They are tried pieces of equipment that have stood the test of time and will be around for a long time, unlike soil moisture sensors that may be made by a company that goes out of business. When that happens, the effort that one has put into calibrating soil moisture sensors is useless. One cannot go back and repeat an experiment with equipment that is no longer available (G.J. Kluitenberg, personal communication, July 17, 2013).

The limitations in using neutron probes and TDR were cited in the first section of this chapter. The dual-probe heat-pulse technique allows one to use another method, whose principles are known, to measure soil water content. The equipment can be made in the laboratory, so researchers in the future can use it, even if commercially available equipment is no longer available. However, the dual-probe heat-pulse technique always will remain useful just for researchers, and it will never catch on as a general way to measure soil water content or thermal properties of soils. It is just too hard to use, and it takes a lot of battery power. It is difficult to keep batteries working in the field. But it is the best piece of equipment for accuracy in measuring soil water content (G.J. Kluitenberg, personal communication, July 17, 2013).

## 9.17 SUMMARY

The dual-probe heat-pulse sensors, also called dual thermal probes, offer a method to monitor thermal and hydrological properties of soil near the surface and in the soil and at a fine spatial resolution. It is becoming increasingly clear that multifunctioning sensors are critical for accurate in situ soil-physical measurements because of inherent soil spatial variability (Hopmans et al., 2002). From a plant physiological point of view, the method provides unique opportunities to measure water uptake by plant roots on a small scale. However, the method will not replace other more traditional means of measuring soil water content, such as TDR, which can measure over larger soil volumes, and neutron probes which can monitor soil water at great depths (e.g., 3 m), which is necessary for deep-rooted plants, like sunflower, under dry-land conditions.

## 9.18 APPENDIX: BIOGRAPHY OF JOHN JAEGER

The following biographical material comes from Paterson (1982).

John Conrad Jaeger (1907—1979), coauthor of the classic book *Conduction of Heat in Solids* (Carslaw and Jaeger, 1959), was born in Sydney, Australia on July 30, 1907. Little is known about his father, Carl Jaeger. He was born in Frankfurt-am-Main, Germany, in 1869 or 1870. Carl lived in South Africa and fought in the Boer war on the British side. He married Christine Louisa Sladden, born in England, but who went to Johannesburg, South Africa, for health reasons and where her brother, who managed a gold mine, lived. Carl and Christine Louisa married in Johannesburg on November 7, 1905. They then moved to Sydney where Carl was a cigar manufacturer.

John was an only child. His mother called him Conrad, but everyone else called him John or sometimes Jack. The German pronunciation of his surname was used in his youth, but when he returned from studies at Cambridge in England, he insisted on the English pronunciation. He was a precocious child. He entered Sydney Church of England Grammar School at the young age of 13 and was dux (top pupil) of the school in 1923. In 1924, at the age of 16, he entered Sydney University, where he had a brilliant record. The degree of Bachelor of Science was conferred on him in April 1928. He received a scholarship that allowed him to travel to England at age 21 in 1928 for further mathematical studies at Cambridge

University, where he studied for two years for the mathematical tripos. (At Cambridge University, the tripos is the honors examination for the BA degree.) He completed Part II of the mathematical tripos in 1930, being listed as wrangler (Class I). (At Cambridge University, a wrangler is a person placed in the first class of the mathematical tripos.) After his tripos success, Jaeger stayed on in Cambridge to do research in theoretical physics. In 1931, he was elected to a Research Scholarship at Trinity College. He got an MA in 1934, but he never got a PhD. However, later, in December 1941, he received the DSc degree from the University of Sydney for a thesis entitled "A study of the mathematical theory of heat conduction."

In August 1935, he applied for a post as a lecturer in mathematics at the University of Tasmania. He was attracted to Tasmania, because he had had a three-day sojourn in Hobart while en route to England in 1928 and said, it was "one of the most delightful places in Australia." He started the appointment on February 15, 1936, and taught mathematics. After returning to Australia, Jaeger's links with Carslaw, although never broken during his time at Cambridge, became closer and the famous collaboration began on the mathematical theory of the conduction of heat.

Horatio Scott Carslaw (1870—1954) was a Scot by birth and was educated in Glasgow and Cambridge. He worked in Germany, at Glasgow University, and at Cambridge before being appointed to the Chair of Pure and Applied Mathematics at the University of Sydney in 1903. He held this post until his retirement in 1935. He had married in 1907, but his wife died within a year of his marriage, and he never remarried. His students became his family, and the one to benefit the most from this was John Jaeger. Jaeger visited Carslaw at Carslaw's retirement home, a country property in New South Wales, and they carried on a voluminous correspondence, most of which has been lost. From 1938 to 1941, Carslaw and Jaeger wrote a number of joint papers on the application of the Laplace transformation method, a particular operational method to problems on the conduction of heat. This work represents the beginning of Jaeger's long-continued involvement with the conduction of heat, which he inherited from Carslaw whose publications on the topic date back to 1902. Collaborative efforts tapered off with World War II and with Carslaw's failing health. The task of preparing a new book based on Carslaw's *Introduction to the Mathematical Theory of the Conduction of Heat in Solids* (published by Macmillan in London in 1921) was taken up in 1945, and Jaeger carried the main responsibility. The new *Conduction of Heat in Solids* was published by Oxford University Press in 1946.

At the beginning of World War II, Jaeger was called to the University of Sydney to work on practical projects that involved the production of charcoal and the fracture of sandstone rollers used in newsprint production. The scarcity of liquid fuels during the war years had led to the use of gas producers on motor vehicles, which required supplies of suitable charcoal. When the Australian Newsprint Mills began operations in Tasmania in 1941, trouble was soon experienced with cracking of the grindstones used, which at that time were made of natural sandstone. Jaeger applied the theory of conduction of heat to calculate the temperature profile developed in the grindstone in operation and from this calculated the thermal stresses. Later in the war he worked at the Radiophysics Laboratory in Sydney to engage in researches connected with the generation and propagation of radio waves. Another war-time problem in which Jaeger became involved soon after his transfer to the Radiophysics Laboratory was that of determining the temperature reached in the retina of the eye when looking into the sun. This problem had arisen because eye damage was being suffered by antiaircraft gunners attempting to intercept dive bombers attacking from the direction of the sun.

After the war, Jaeger returned to the University of Tasmania and he published four books between 1946 and 1951, including the first edition of *Conduction of Heat in Solids*. Also in the postwar years, Jaeger worked on several problems, including the nature of the moon's surface. He studied the rate of cooling at the moon's surface during an eclipse and, using values for thermal conductivity of dust without air between the particles, he concluded that over most of the surface of the moon there was a layer of dust of only about 2 mm in thickness. It overlay a granular layer similar to pumice or gravel. His conclusion that the layer of dust was thin became important years later for the landing of space craft on the moon. He also studied the design requirements for electronic computers. His devices for analog computation helped stimulate developments in computers.

In 1951, Jaeger was appointed to a chair at the new Australian National University in Canberra. He was the foundation chair of geophysics, a new area of research in physics at the time. In 1963, Jaeger was appointed Dean of the Research School of Physical Sciences. At the same time, he continued as chair of the Department of Geophysics. He was dean for two years, and then remained chair of the department until 1971. In 1972, he retired from the Australian National University at the age of 65 and returned to Tasmania with his second wife, Martha Elizabeth (Patty) Clarke (born in 1901), whom he had married in Hobart on October 24, 1950. His first marriage had been in England to Sylvia Percival Rees on December 23, 1935. On the same day, they left for Australia. The marriage was not successful, and Jaeger called it "a great mistake". The marriage ended in divorce in 1950. Jaeger's first marriage had no children, and he and Patty were too old to have children when they married. Patty had joined the staff of the University of Tasmania as a typist in 1927. She helped him with his computations and typed his books. It was on her family's property where he carried out research on charcoal during the war.

From 1965, Jaeger began to be troubled by illnesses that were affecting his mobility by 1971. He had three operations between 1971 and 1973 and suffered a heart attack during one of them. In July 1978, Patty, aged 77, had to be taken to the hospital where she died within about two weeks on July 31, 1978. This was a great blow to Jaeger. He lived on in Tasmania and was helped by visits from Patty's nieces. In late 1978, he agreed to move back to Canberra and there died on May 15, 1979, at the age of 71.

He won many awards. In 1954, he became Fellow of the Australian Academy of Science. In 1970, he was elected as Fellow of the Royal Society. He was known as a reticent and shy man. Few people were on intimate terms with him. His interests outside science included a passion for cats. There were always a large number of cats in the Jaeger household. He also had an enthusiasm for old machinery and collected steam engines and agricultural machinery.

The following information comes from a speech that Dr John Philip sent to me on May 1, 1999 (copy of speech available from M.B. Kirkham). Each year the Australian Academy of Sciences gives a Jaeger Medal. Dr Philip received it on April 29, 1999. In his acceptance speech, Dr Philip said, "An occasion such as this is as much about remembering and honouring the dead as encouraging the living. That man up on the screen is John Jaeger. I refer you all to Merv Paterson's biographical memoir of Jaeger, published by both the Royal Society and this Academy in 1982. Merv gives an excellent account of Jaeger the kindly man and pioneering scientist; but I should like to add one thing. It concerns the book 'Conduction of Heat in Solids', nominally by Carslaw and Jaeger. In reality the volume is wholly an expression of John Jaeger's manner of presenting mathematics in the most understanding and useful way possible. I'm afraid the writings of many mathematicians (though, I'm sure, of none here today) seem dedicated rather to showing how smart they are, and the hell with the reader. After Jaeger's death Oxford University Press approached me about a new edition of the book. It was no surprise to learn from them that Carslaw and Jaeger is their mathematical best seller of all time."

## References

Amato, M., Ritchie, J.T., 1995. Small spatial scale soil water content measurement with time-domain reflectometry. Soil Sci. Soc. Am. J. 59, 325–329.

Basinger, J.M., Kluitenberg, G.J., Ham, J.M., Frank, J.M., Barnes, P.L., Kirkham, M.B., 2003. Laboratory evaluation of the dual-probe heat-pulse method for measuring soil water content. Vadose Zone J. 2, 389–399.

Bilskie, J.R., Horton, R., Bristow, K.L., 1998. Test of a dual-probe heat-pulse method for determining thermal properties of porous materials. Soil Sci. 163, 345–355.

Bremer, D.J., Ham, J.M., 1999. Effect of spring burning on the energy balance in a tallgrass prairie. Agric. For. Meteorol. 97, 43–54.

Bremer, D.J., Auen, L.M., Ham, J.M., Owensby, C.E., 2001. Evapotranspiration in a prairie ecosystem: effects of grazing by cattle. Agron. J. 93, 338–348.

Bremer, D.J., Ham, J.M., Owensby, C.E., Knapp, A.K., 1998. Responses of soil respiration to clipping and grazing in a tallgrass prairie. J. Environ. Qual. 27, 1539–1548.

Bristow, K.L., 1998. Measurement of thermal properties and water content of unsaturated sandy soil using dual-probe heat-pulse probes. Agric. For. Meteorol. 89, 75–84.

Bristow, K.L., 2002. Thermal conductivity. In: Dane, J.H., Topp, G.C. (Eds.), Methods of Soil Analysis. Part 4, Soil Science Society of America Book Series No. 5. Soil Science Society of America and American Society of Agronomy, Madison, Wisconsin, pp. 1209–1226.

Bristow, K.L., Campbell, G.S., Calissendorff, K., 1993. Test of a heat-pulse for measuring changes in soil water content. Soil Sci. Soc. Am. J. 57, 930–934.

Bristow, K.L., Kluitenberg, G.J., Horton, R., 1994a. Measurement of soil thermal properties with a dual-probe heat-pulse technique. Soil Sci. Soc. Am. J. 58, 1288–1294.

Bristow, K.L., White, R.D., Kluitenberg, G.J., 1994b. Comparison of single and dual probes for measuring soil thermal properties with transient heat. Aust. J. Soil Res. 59, 447–464.

Bristow, K.L., Bilskie, J.R., Kluitenberg, G.J., Horton, R., 1995. Comparison of techniques for extracting soil thermal properties from dual-probe heat-pulse data. Soil Sci. 160, 1–7.

Bristow, K.L., Kluitenberg, G.J., Goding, C.J., Fitzgerald, T.S., 2001. A small multi-needle probe for measuring soil thermal properties, water content and electrical conductivity. Comput. Electron. Agric. 31, 265–280.

Campbell, G.S., Calissendorff, C., Williams, J.H., 1991. Probe for measuring soil specific heat using a heat-pulse method. Soil Sci. Soc. Am. J. 55, 291–293.

Campbell, D.I., Laybourne, C.E., Blair, I.J., 2002. Measuring peat moisture content using the dual-probe heat pulse technique. Aust. J. Soil Res. 40, 177–190.

Carslaw, H.S., Jaeger, J.C., 1959. Conduction of Heat in Solids, second ed. Clarendon Press of Oxford University Press, Oxford.

Clothier, B.E., White, I., 1981. Measurement of sorptivity and soil water diffusivity in the field. Soil Sci. Soc. Am. J. 45, 241–245.

Clothier, B.E., Kirkham, M.B., 1991. Kiwifruit as brass monkeys. In: WISPAS. A Newsletter about Water in the Soil–Plant–Atmosphere System. No. 49Environmental Physics Section, Department of Scientific and Industrial Research, Palmerston North, New Zealand, p. 4.

Clothier, B.E., Kirkham, M.B., McLean, J.E., 1992. In situ measurement of the effective transport volume for solute moving through soil. Soil Sci. Soc. Am. J. 56, 733–736.

Dalton, F.N., 1992. Development of time-domain reflectometry for measuring soil water content and bulk soil electrical conductivity. In: Topp, G.C., Reynolds, W.D., Green, R.E. (Eds.), Advances in Measurement of Soil Physical Properties: Bringing Theory into Practice. Soil Science Society of America, Madison, Wisconsin, pp. 143–167. SSSA Special Pub. No. 30.

de Vries, D.A., 1966. Thermal properties of soils. In: van Wijk, W.R. (Ed.), Physics of Plant Environment, second ed. North-Holland Pub. Co., Amsterdam, pp. 210–235.

Ham, J.M., Senock, R.S., 1992. On the measurement of soil surface temperature. Soil Sci. Soc. Am. J. 56, 370–377.

Ham, J.M., Knapp, A.K., 1998. Fluxes of $CO_2$, water vapor, and energy from a prairie ecosystem during the seasonal transition from carbon sink to carbon source. Agric. For. Meteorol. 89, 1–14.

Hiraiwa, Y., Kasubuchi, T., 2000. Temperature dependence of thermal conductivity of soil over a wide range of temperature (5–75 °C). Eur. J. Soil Sci. 51, 211–218.

Hopmans, J.W., Šimůnek, J., Bristow, K.L., 2002. Indirect estimation of soil thermal properties and water flux using heat pulse probe measurements: geometry and dispersion effects. Water Resour. Res. 38 (1), 7-1–7-14. http://dx.doi.org/10.1029/2000WR000071.

Kamai, T., Kluitenberg, G.J., Hopmans, J.W., 2009. Design and numerical analysis of a button heat pulse probe for soil water content measurement. Vadose Zone J. 8, 167–173.

Kamai, T., Tuli, A., Kluitenberg, G.J., Hopmans, J.W., 2008. Soil water flux density measurements near 1 cm d$^{-1}$ using an improved heat pulse probe design. Water Resour. Res. 46 (4). http://dx.doi.org/10.1029/2008WR007036. W00D14.

Kamai, T., Tuli, A., Kluitenberg, G.J., Hopmans, J.W., 2010. Correction to "Soil water flux density measurements near 1 cm d$^{-1}$ using an improved heat pulse probe design." Water Resour. Res. 46 (7) http://dx.doi.org/10.1029/2010WR009423. W07901.

Kirkham, D., 1973. Soil physics and soil fertility. Bull. Rech. Agron. Gembloux Fac. Sci. Agron. l'État, (New series) 8 (2), 60–88.

Kirkham, D., Powers, W.L., 1972. Advanced Soil Physics. Wiley, New York.

Kluitenberg, G.J., 2002. Heat capacity and specific heat. In: Dane, J.H., Topp, G.C. (Eds.), Methods of Soil Analysis. Part 4, Soil Science Society of America Book Series No. 5. Soil Science Society of America and American Society of Agronomy, Madison, Wisconsin, pp. 1201–1208.

Kluitenberg, G.J., Philip, J.R., 1999. Dual thermal probes near plane interfaces. Soil Sci. Soc. Am. J. 63, 1585–1591.

Kluitenberg, G.J., Warrick, A.W., 2001. Improved evaluation procedure for heat-pulse soil water flux density method. Soil Sci. Soc. Am. J. 65, 320–323.

Kluitenberg, G.J., Ham, J.M., Bristow, K.L., 1993. Error analysis of the heat pulse method for measuring volumetric heat capacity of soil. Soil Sci. Soc. Am. J. 57, 1444–1451.

Kluitenberg, G.J., Bristow, K.L., Das, B.S., 1995. Error analysis of the heat pulse method for measuring the soil heat capacity, diffusivity, and conductivity. Soil Sci. Soc. Am. J. 59, 719–726.

Kluitenberg, G.J., Heitman, J.L., 2002. Effect of forced convection on soil water content measurement with the dual-probe heat-pulse method. In: Raats, P.A.C., Smiles, D.E., Warrick, A.W. (Eds.), Environmental Mechanics: Water, Mass and Energy Transfer in the Biosphere, Geophysical Monograph Series, vol. 192. American Geophysical Union, Washington, DC, pp. 275–283.

Kluitenberg, G.J., Ochsner, T.E., Horton, R., 2007. Improved analysis of heat pulse signals for soil water flux determination. Soil Sci. Soc. Am. J. 71, 53–55.

Knight, J.H., Jin, W., Kluitenberg, G.J., 2007. Sensitivity of the dual-probe heat-pulse method to spatial variations in heat capacity and water content. Vadose Zone J. 6 (4), 746–758. http://dx.doi.org/10/2136/vzj2006.0170.

Knight, J.H., Kluitenberg, G.J., Kamai, T., Hopmans, J.W., 2012. Semianalytical solution for dual-probe heat-pulse applications that accounts for probe radius and heat capacity. Vadose Zone J. 11 (2). http://dx.doi.org/10/2136/vzj2011.0112.

Mallants, D., Vanclooster, M., Toride, N., Vanderborght, J., van Genuchten, M. Th., Feyen, J., 1996. Comparison of three methods to calibrate TDR for monitoring solute movement in undisturbed soil. Soil Sci. Soc. Am. J. 60, 747–754.

Mohanty, B.P., Bowman, R.S., Hendrickx, J.M.H., van Genuchten, M.Th, 1997. New piecewise continuous hydraulic functions for modeling preferential flow in an intermittent flood-irrigated field. Water Resour. Res. 33, 2049–2063.

Nadler, A., Green, S.R., Vogeler, I., Clothier, B.E., 2002. Horizontal and vertical TDR measurements of soil water content and electrical conductivity. Soil Sci. Soc. Am. J. 66, 735–743.

Nassar, I.N., Horton, R., 1997a. Heat and water transfer in compacted and layered soils. J. Environ. Qual. 26, 81–88.

Nassar, I.N., Horton, R., 1997b. Heat, water, and solute transfer in unsaturated porous media. I. Theory development and transport coefficient evaluation. Transp. Porous Media 27, 17–38.

Noborio, K., McInnes, K.J., Heilman, J.L., 1996. Measurement of soil water content, heat capacity, and thermal conductivity with a single TDR probe. Soil Sci. 161, 22–28.

Paterson, M.S., 1982. Biographical memoirs. John Conrad Jaeger 1907–1979. Hist. Rec. Aust. Sci. 5, 65–88.

Philip, J.R., Kluitenberg, G.J., 1999. Errors of dual thermal probes due to soil heterogeneity across a plane interface. Soil Sci. Soc. Am. J. 63, 1579–1585.

Rachidi, F., Kirkham, M.B., Stone, L.R., Kanemasu, E.T., 1993. Soil water depletion by sunflower and sorghum under rainfed conditions. Agric. Water Manage. 24, 49–62.

Ren, T., Noborio, K., Horton, R., 1999. Measuring soil water content, electrical conductivity, and thermal properties with a thermo-time domain reflectometry probe. Soil Sci. Soc. Am. J. 63, 450–457.

Ren, T., Kluitenberg, G.J., Horton, R., 2000. Determining soil water flux and pore water velocity by a heat pulse technique. Soil Sci. Soc. Am. J. 64, 552–560.

Song, Y., Ham, J.M., Kirkham, M.B., Kluitenberg, G.J., 1998. Measuring soil water content under turfgrass using the dual-probe heat-pulse technique. J. Am. Soc. Hortic. Sci. 123, 937–941.

Song, Y., Kirkham, M.B., Ham, J.M., Kluitenberg, G.J., 1999a. Measurement resolution of the dual-probe heat-pulse technique. In: van Genuchten, M.Th., Leij, F.J. (Eds.), Characterization and Measurement of the Hydraulic Properties of Unsaturated Porous Media. University of California, Riverside, California, pp. 381–386.

Song, Y., Kirkham, M.B., Ham, J.M., Kluitenberg, G.J., 1999b. Dual probe heat pulse technique for measuring soil water content and sunflower water uptake. Soil Tillage Res. 50, 345–348.

Song, Y., Kirkham, M.B., Ham, J.M., Kluitenberg, G.J., 2000. Root-zone hydraulic lift evaluated with the dual-probe heat-pulse technique. Aust. J. Soil Res. 38, 927–935.

Tarara, J.M., Ham, J.M., 1997. Measuring soil water content in the laboratory and field with dual-probe heat-capacity sensors. Agron. J. 89, 535–542.

Topp, G.C., Davis, J.L., Annan, A.P., 1980. Electromagnetic determination of soil water content: measurements in coaxial transmission lines. Water Resour. Res. 16, 574–582.

van Genuchten, M. Th., 1994. New issues and challenges in soil physics research. Trans. 15th Int. Congr. Soil Sci. 1, 5–27.

Wang, Q., Ochsner, T.E., Horton, R., 2002a. Mathematical analysis of heat pulse signals for soil water flux determination. Water Resour. Res. 38 (6), 27-1–27-7. http://dx.doi.org/10.1029/2001WR001089.

Wang, Q., Ochsner, T.E., Horton, R., 2002b. Correction to “Mathematical analysis of heat pulse signals for soil water flux determination” by Wang, Q., Ochsner, T.E., and Horton, R. Water Resour. Res. 38 (12). http://dx.doi.org/10.1029/2002WR001765, 24-1 (one page only).

Zwieniecki, M.A., Newton, M., 1995. Roots growing in rock fissures: their morphological adaptation. Plant Soil 172, 181–187.

CHAPTER

# 10

# Field Capacity, Wilting Point, Available Water, and the Nonlimiting Water Range

The amount of water available for plant uptake has been related to a soil's *water budget*. The three terms associated with the water budget are *field capacity* (FC), *wilting point* (WP), and *available water* (AW).

## 10.1 FIELD CAPACITY

To define FC we consider the following. In many soils, after a rain or irrigation, the water immediately starts draining deeper into the soil. After 1 or 2 days the water content in the soil will reach, with time, for many soils, a nearly constant value for a particular depth in question. This somewhat arbitrary value of water content, expressed as a percentage, is called the field capacity.

It is not known who first used the term field capacity. The term was not used by Briggs and Shantz, who developed the concept of the WP (see next section). Briggs (see Appendix, Section 10.5, for his biography) defined the "moisture equivalent", which was the amount of water held against centrifugation of soil at 3000 × $g$, where $g$ is the acceleration due to gravity (Landa and Nimmo, 2003). The term is no longer accepted (Soil Science Society of America, 1997), but it was a precursor to the idea of FC.

Early researchers recognized that there was a point at which water moved slowly after a rain or irrigation (Taylor and Ashcroft, 1972, p. 299). They wanted to assign a value to this point, and therefore, the concept of FC developed. They recognized it as the amount of water that a well-drained soil holds against gravitational forces and when downward drainage is markedly decreased. They felt it was a true equilibrium and they felt it was the upper limit of AW for plants.

http://dx.doi.org/10.1016/B978-0-12-420022-7.00010-0

Copyright © 2014 Elsevier Inc. All rights reserved.

However, as time progressed, soil scientists realized that FC was an imprecise term. They saw that it was not a unique value, because equilibrium is never reached. Soil water is dynamic; removal of water occurs due to drainage, evaporation, and transpiration and addition of water occurs with dewdrops, rainfall, and irrigation (Taylor and Ashcroft, 1972, p. 300). The movement of water downward does not cease, but continues at a reduced rate for a long time. There is no real value for FC. Therefore, a range of values (soil water contents) are associated with FC (Figure 10.1). Many factors influence FC, as follows (Hillel, 1971, pp. 162–165).

1. *Previous soil water history:* A wetting soil and a drying soil hold different amounts of water. A soil that is saturated and then dries has a higher FC than a soil that is being wetted. This is due to hysteresis (see Chapter 6).
2. *Soil texture and structure:* These change with soil horizon and influence water retention. Clayey soils retain more water, and longer, than sandy soils. The finer the texture is, the higher is the FC, the slower is its attainment, and the less distinct is its value (Hillel, 1971, p. 164).
3. *Type of clay:* The higher the content of montmorillonite is, the greater is the content of water.
4. *Organic matter:* Soil organic matter helps retain water.
5. *Temperature:* The temperature influences the amount of water held, particularly if the soil has been previously wetted. The amount of water retained at FC decreases as the soil temperature increases (Kramer, 1983, p. 71). This results in increased runoff from a watershed as soil warms.

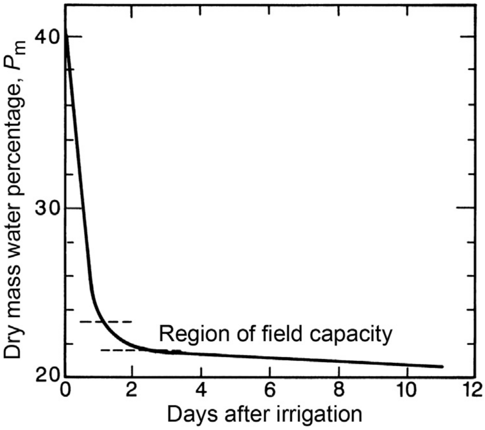

**FIGURE 10.1** Diagram showing field capacity as a range of values of soil water contents. *From Taylor and Ashcroft (1972). Used with permission.*

6. *Water table:* The term "field capacity" is of doubtful value in soils with a water table near the surface. The term applies to free-draining soils.
7. *Depth of wetting:* Usually, the wetter the profile is at the outset, the greater is the depth of wetting during infiltration, the slower is the rate of redistribution, and the greater is the FC.
8. *Presence of impeding layers (e.g., clay, sand, and gravel):* The layers inhibit redistribution and increase the FC. Again, the term "field capacity" is of questionable value for soils having layers of widely differing hydraulic conductivities.
9. *Evapotranspiration:* The rate and pattern of extraction of water by plant roots from soil can affect the gradients and flow directions in the profile and modify redistribution (Hillel, 1971, p. 165).

People have suggested abandoning the concept of FC, because it has caused misleading conclusions. For example, if it is assumed that no drainage occurs, when in fact it is, drainage is included in consumptive use by plants. This leads to consumptive use values that are too large.

Until the 1984 edition of the *Glossary of Soil Science Terms* (Soil Science Society of America, various years), the term "field capacity" was labeled "obsolete". These included the glossaries published in 1971, 1975, 1978, and 1979. More current glossaries (1984, 1987, 1997, 2008) no longer call it obsolete, and the term is widely used in the literature. One is often asked to provide the FC for a soil when publishing a paper. Even though FC is not an exact value, the reason that the term has been brought back into the literature probably relates to the development of computer models. A numerical value like AW (discussed in Section 10.3; it is the difference between FC and permanent WP) is needed to put into computer models to relate water in the soil to plant growth. Along with AW, the non-limiting water range (NLWR) (see Section 10.4) now frequently is used in computer models to relate water in the soil to crop growth or yield. Crop-growth models could be developed when computers became widely available and on the desk of every scientist (late 1980s).

FC is not the upper limit of AW to plants because all water that is not held tightly by soil can be used by plants while it is in contact with roots, even if water is rushing by during rapid drainage. What limits uptake is soil aeration, and, as we shall see (Chapter 12), the air-filled pore space must be at least 10% by volume for most roots to survive (Wesseling and van Wijk, 1957).

Note that FC does not apply to pots in a greenhouse. FC refers only to field conditions. Greenhouse pots do not have underlying soil that pulls water down deep into the soil profile by capillarity. However, one can talk of "pot capacity", which is the amount of water remaining in a pot after irrigation and visible drainage has ceased.

One should always try to measure FC in the field for each soil. The matric potential associated with FC can be as high as −0.0005 MPa in a highly stratified soil or as low as −0.06 MPa in a deep, dryland soil (Baver et al., 1972, p. 382). If one cannot measure FC in the field, it is often estimated to be the soil water content at a soil matric potential of −0.033 MPa or −33 kPA (one-third bar).

## 10.2 WILTING POINT

The WP, also called the *permanent wilting point*, may be defined as the amount of water per unit weight or per unit bulk volume in the soil, expressed in percentage, that is held so tightly by the soil matrix that roots cannot absorb this water and a plant will wilt.

Unlike FC, the term wilting point is associated with known scientists, Briggs and Shantz (1912). They defined the "wilting coefficient" (WP) as "the moisture content of the soil (expressed as a percentage of the dry weight) at the time when the leaves of the plant growing in that soil first undergo a permanent reduction in their moisture content as the result of a deficiency in the soil-moisture supply" (Briggs and Shantz, 1912, p. 9). As with FC, early workers felt that WP was a precise value.

The method of determining permanent WP is as follows (Taylor and Ashcroft, 1972, p. 303). An indicator plant, usually sunflower (*Helianthus annuus*), is put in 500 g of soil in a metal can. The plant grows and is given adequate moisture until the third pair of true leaves is formed. Then the top of the can is sealed with wax. The sunflower grows in a greenhouse or outdoors until it wilts. Then it is transferred to a dark, humid chamber for recovery. If the plant recovers, it is put out again. The procedure is repeated until the plant remains wilted overnight (24 h) in the humid chamber. The soil water content then is at the permanent WP.

For plants that have leaves that do not wilt, like cacti, Briggs and Shantz (1912) developed special procedures to determine the WP. For example, they put a plant with water-storage tissue in a glass container with soil. They glued a knitting needle to one side of the glass. They put the glass with knitting needle in a horizontal position by propping it between two other containers sitting on a table. The needle was free to move up and down a scale. As the cactus used water in the soil, the needle moved in one direction. Then the motion along the scale was gradually reversed, as the cactus shoot itself started to lose water. The WP was the point of reversal of needle movement (Briggs and Shantz, 1912, pp. 47–53).

As with FC, later researchers realized that the WP is not a unique value. It is dynamic, like FC. There are a range of values at which the rate of water supply to a plant is not sufficient to prevent wilting, depending on the soil profile (soil texture, compaction, and stratification); the amounts of water in the soil at different depths, which affect root distribution; the transpiration rate of a plant; and the temperature (Table 10.1). One should use a water bath to determine the WP, to control the temperature. Also, leaves wilt differently. Usually the basal leaves wilt first (Taylor and Ashcroft, 1972, p. 303), so one can refer to the "first permanent wilting point,", at which the basal leaves do not recover, and the "ultimate permanent wilting point,", at which the apical leaves do not recover. The permanent WP depends upon plant osmotic adjustment. Therefore, we recognize that there is a range of values for permanent WP, and it is not a unique value (Figure 10.2).

If one cannot measure the permanent WP, it is usually estimated to be the water content at a soil matric potential of −1.5 MPa or −1500 kPa (−15 bars). However, plants can absorb water from soil at potentials much lower than this; creosote bush (*Larrea divaricata*) can absorb water to −6.0 MPa (Salisbury and Ross, 1978, p. 389). But the amount of water actually held by the soil between −1.5 MPa and −6.0 MPa is small.

The point at which the water content at the soil−root interface reaches the WP is of interest mathematically for root models (Philip, 1957; Gardner, 1960). In the models, the WP is dependent not only on the soil water content at wilting, but also on the diffusivity of the soil, the radius of the root, and the transpiration rate. In his 1957 model of water uptake by plant roots, Philip pointed out that uncritical use of the WP as an invariant index of the lower limit of the availability of soil moisture to plants can be misleading (Philip, 1957; Raats et al., 2002, p. 18).

However, the permanent WP still needs to be determined to calculate AW, which we shall discuss in the next section. As noted above, computer models are now commonplace. A widely used equation in models of soil

**TABLE 10.1** Influence of Temperature on the Soil Water Percentage at Which Sunflowers will Wilt Permanently

| | **Permanent Wilting Percentage for Three Soils** | | |
|---|---|---|---|
| **Temperature (°C)** | **Millville Silt Loam** | **Benjamin Silty Clay Loam** | **Yolo Fine Sandy Loam** |
| 5 | ... | ... | 9.0 ± 0.11 |
| 12.8 | ... | ... | 8.5 ± 0.03 |
| 15 | 8.38 ± 0.13 | 11.63 ± 0.23 | ... |
| 25 | 7.34 ± 0.17 | 10.46 ± 0.26 | ... |
| 35 | 6.66 ± 0.16 | ... | ... |

*From Taylor, S.A., Ashcroft, G.L., 1972. Physical Edaphology: The Physics of Irrigated and Nonirrigated Soils. W.H. Freeman and Company, p. 303. Used with permission.*

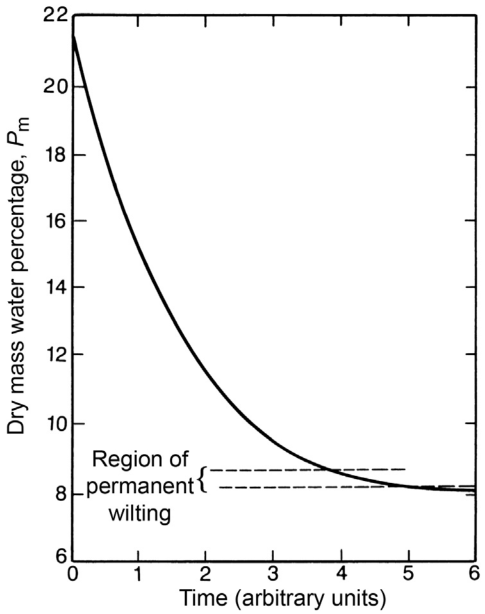

**FIGURE 10.2** Average water percentage in the top foot of soil in which alfalfa is rooted to a depth of 3 m. The permanent wilting percentage is a range of values of soil water contents over which the removal rate is slow. *From Taylor and Ashcroft (1972). Used with permission.*

physicists is the van Genuchten equation (van Genuchten, 1980; see Eqn (21) in his paper). The equation relates soil water content to pressure head (or what we call matric potential in this book). It is used to get hydraulic conductivity in unsaturated soils. It is a key equation, because soils are usually unsaturated. The Darcy equation can be used only in saturated soils (see Chapter 7, Eqn (7.1)). (The title of van Genuchten's paper uses the term "closed form". In an e-mail to me dated March 12, 2004, Dr Brent E. Clothier, Plant and Food Research, Palmerston North, New Zealand, defined the term. He said it is closed form because the parameters used to describe the water characteristic and the conductivity are functionally linked, so that they are closed in the sense that they are related and not just independently fitted parameters. See Chapter 6, for the definition of the soil water characteristic, and Figure 6.8.) In the van Genuchten equation, one must determine the residual water content. The residual water content in the van Genuchten equation is represented by $\theta_r$. The question arises, "What is the relation between the residual water content and the wilting point?"

The residual water content is not defined in the *Glossary of Soil Science Terms 2008* (Soil Science Society of America, 2008) or any previous glossaries. In an e-mail dated January 20, 2006, Dr van Genuchten (formerly of the US Salinity Laboratory, Riverside, California; now in the Department of Mechanical Engineering, Federal University of Rio de Janeiro, Brazil) defines residual water as follows: "The residual water content is the water content where no liquid flow occurs any more, and hence where water moves (or can be removed) only by vapor flow. The wilting point is an excellent approximation of the residual water content of very coarse-textured (sandy) soils. However, the wilting point at pF = 4.2 likely overestimates the residual water content of fine-textured (clay) soils where still lots of bound water may be present that collectively (because of the large surface area) may still yield a reasonable liquid flow rate. Remember that those pressure plate approaches for water content measurements require very long times for equilibrium to develop, and that the water content can still go down significantly for pF much larger than 4 or 5." Bound water is not defined in the *Glossary of Soil Science Terms 2008* (Soil Science Society of America, 2008) or any previous editions. However, when we defined matric potential (Chapter 4, Section II, Part 1), we noted that it was due to both water held directly on particle surfaces as well as water held by capillarity in soil pores. So the definition of bound water could be "water held directly on particle surfaces". The dictionary (Webster's New World Dictionary of the American Language and Publishing, 1959) defines "bound" as meaning "closely connected". When we define mobile water content (Chapter 13, Section IX), we shall see that one reason water is immobilized is due to the fact that is it bound to the surfaces of soil particles. Residual water is considered in detail by Dexter et al. (2012).

Dr van Genuchten uses the term "pF". The *Glossary of Soil Science* lists pF as "obsolete" in the 1971 edition (first one I have), 1975 edition, 1978 edition, and 1979 edition, and it does not appear in the 1984 edition or since then. In the editions where the pF appears, it is defined as "(Obsolete) The logarithm of the soil moisture tension expressed in centimeters height of a column of water".

So for pF = 4.2 (see Dr van Genuchten's value above)
Antilogarithm: 15,849 cm
Divide by 1020 cm/bar:
15.5 bars (close enough to −15 bars or −1.5 MPa for the permanent WP)
1 bar = 0.987 atm; divide by 1033 cm/atm; 15.3 atm.
For pF = 4; antilog = 10,000 cm or 9.8 bars or 0.98 MPa. For pF = 5; antilog = 100,000 cm or 98 bars or 9.8 MPa.

Daniel Hillel has published textbooks on soil physics since 1971 (Hillel, 1971). His most recent ones are Hillel (2004, 2008). However, only his first textbook defines pF. In this book he states (Hillel, 1971, p. 60), "In attempting to express the negative pressure potential of soil water in terms of an equivalent hydraulic head, we must contend with the fact that this head may be as much as −10,000 or even −100,000 cm of water. To avoid the use of such cumbersomely large numbers, Schofield (1935) suggested the use of 'pF' (by analogy with the pH acidity scale) which he defined as the logarithm of the negative pressure (tension, or suction) head in centimeters of water. A pF of 1 is, thus, a tension head of 10 cm $H_2O$, a pF of 3 is a tension head of 1000 cm $H_2O$; and so forth." Note that pF should not be used in the scientific literature, because it is an obsolete term. It does, however, still appear in publications. The matric potential should be expressed in pascals. Heads can be expressed in centimeters, as discussed in Chapter 4, Section III.

## 10.3 AVAILABLE WATER

Plant AW may be defined as the difference between FC and WP. The formula is

$$AW = FC - WP. \tag{10.1}$$

The FC might be measured as 5% of water per unit volume of bulk soil for sand, which we shall label A, and might be measured as 50% per unit volume of bulk soil for heavy clay, which we shall call B. The WP might be 2% water per unit volume for the sand A, and it might be 20% per unit volume for the heavy clay B. Using the numerical values of FC and WP for the sand A and heavy clay B, we find AW as

$$\text{(Sand A) } AW = 5\% - 2\% = 3\%$$

$$\text{(Heavy clay B) } AW = 50\% - 20\% = 30\%.$$

The above two AWs are in percentages referred to a volume of bulk soil. These AWs may be considered to mean that, in 100 cm of the sand A profile, there is 3 cm of equivalent surface water in the plant available form; and in 100 cm of heavy clay B, there is 30 cm of equivalent surface water in plant available form. The clay soil B stores $(30-3) = 27$ cm more of equivalent surface water per meter depth of soil profile than does the sand A. From this example, we see that soil texture can have a large effect on soil water availability.

As noted in the preceding section, the terms field capacity and wilting point should be used with caution. FC should be based on moisture measurements made in the field to a depth of interest, say 100–150 cm, and not on laboratory measurements. Equation (10.1) implies to some agronomists that water can be taken up by plant roots with equal ease, from FC to the WP. This view was promulgated by F.J. Veihmeyer and A.H. Hendrickson at the University of California in Davis, who collaborated for many years starting in the 1920s. For some plants this may be true, because for them the energy of getting water from the soil into the plant will be small compared to the energy required to get the water through the plant and through the stomata on leaves, and then into an

**TABLE 10.2** Yield (metric ton/ha) of Alfalfa, Potatoes, and Sugar Beets at Different Soil Moisture Contents

| | **Moisture Content in Centimeters of Water Per 100 cm of Soil Depth at Time of Irrigation** | | | |
|---|---|---|---|---|
| **Crop** | **30** | **18** | **15** | **5** |
| Alfalfa | 14.3 | 14.3 | 13.4 | 10.3 |
| Potatoes | 33.8 | 35.7 | 32.2 | 7.8 |
| Sugar beets | 43.2 | 42.3 | 40.5 | 28.9 |

*Data obtained from Taylor, 1952.*

evaporated form into the atmosphere. For such plants, one would not worry if the soil were to approach fairly close to the WP before rainfall or irrigation water was supplied. For most crops, however, yields are reduced if the water in the soil approaches the WP before water is supplied. This is illustrated in Table 10.2, where yields of alfalfa, potatoes, and sugar beets are shown when irrigation water was applied at four different moisture levels: 30, 18, 15, and 5% (30, 18, 15, and 5 cm of equivalent surface water per 100 cm of soil profile). The WP of this soil was 3% and FC was about 30%. Yields were reduced before the permanent WP was reached, showing that water is not equally available between FC and WP (Taylor, 1952).

## 10.4 NONLIMITING WATER RANGE

In 1985, John Letey, a soil physicist at the University of California in Riverside, developed a concept called the NLWR, which acknowledges that water may not be equally available to plants between FC and the permanent WP. The interaction between water and other physical factors that affect plant growth must be considered. Bulk density and pore size distribution affect the relationship between water and both aeration and mechanical resistance. The relationship between water and aeration is opposite to that between water and mechanical resistance. Increasing water content decreases aeration, which is undesirable, but decreases mechanical resistance, which is desirable. The NLWR may be affected by aeration and/or mechanical resistance (Figure 10.3). The NLWR becomes narrower as bulk density and aeration limit plant growth. On one end of the scale, oxygen limits root growth and on the other end of the scale, mechanical resistance restricts root growth. The restriction may occur at a water content higher than the value that would be considered limiting to plants on the basis of plant AW.

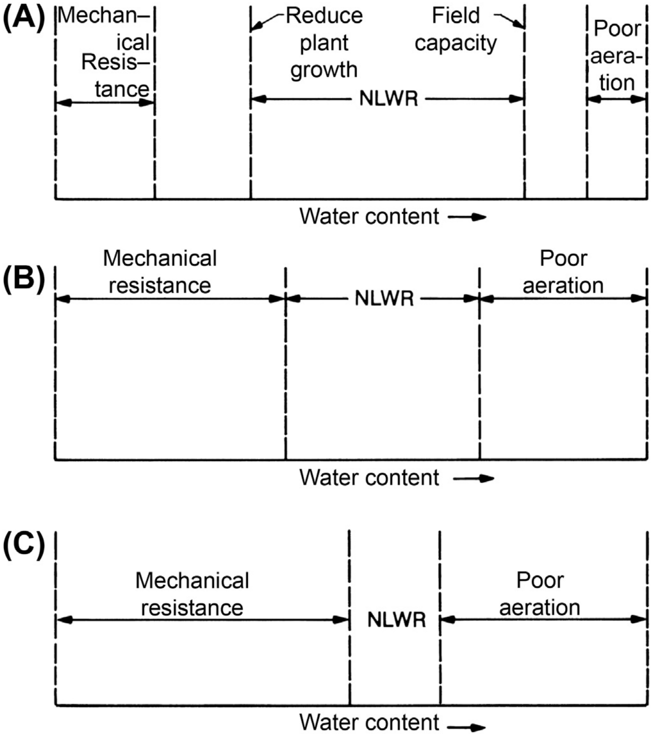
(A)
Mechan-ical Resis-tance
Reduce plant growth
Field capacity
Poor aera-tion
NLWR
Water content
(B)
Mechanical resistance
NLWR
Poor aeration
Water content
(C)
Mechanical resistance
NLWR
Poor aeration
Water content

**FIGURE 10.3** Generalized relationships between soil water content and restricting factors for plant growth in soils with increasing bulk density and decreasing structure in going from case A to C. The nonlimiting water range is abbreviated NLWR. *From Letey (1985). This figure is used by permission of Springer-Verlag and John Letey.*

To determine the NLWR, one must determine the matric potential at which the oxygen diffusion rate (ODR) limits root growth. The oxygen diffusion ratemeter is used to determine this value (see Chapter 12). Then one needs to determine the matric potential at which root growth is inhibited due to too high a resistance. This is done with a penetrometer (see Chapter 11). For example, in a coastal plain soil in South Carolina, researchers found that corn roots stopped growing at a matric potential of −0.08 bar, as determined using the ODR method, and at a matric potential of −0.4 bar due to too high a resistance (Letey, 1985). One needs to use a soil moisture release curve to find the soil water contents associated with these matric potentials. The NLWR is the difference between the two water contents: the larger soil water content minus the lower soil water content.

The *least limiting water range* (LLWR) was introduced by da Silva et al. (1994). They said that the response of plants to variation in water content must be considered using ranges for AW, soil aeration, and mechanical resistance. Inside the range, growth is least limited, and outside of the range, growth is most limited. Consequently, they used the term LLWR rather than NLWR to describe the concept introduced by Letey (1985). Values fall either "in" or "out" of a range (da Silva and Kay, 1996). da Silva et al. (1994) arbitrarily set limits for the growth of plants in response to AW, soil aeration, and mechanical resistance based on data in the literature. The critical values for crop growth that they chose, associated with matric water potential, air-filled porosity (the measure of soil aeration), and soil resistance, were FC at −0.01 MPa (Haise et al., 1955), WP at −1.5 MPa (Richards and Weaver, 1943), air-filled porosity at 10% (Grable and Siemer, 1968), and soil resistance at 2 MPa (Taylor et al., 1966). da Silva and Kay (1996) calculated the air-filled porosity at 10% as $\theta_{sat}-0.10$ where $\theta_{sat}=1$—bulk density/particle density, and $\theta_{sat}$ is the water content in the soil at saturation. (See Chapter 7 and Eqn (7.2) for the calculation of porosity.) As noted above for FC, most roots need at least 10% by volume air space in the soil to survive, and we shall present the scientific data for this conclusion in Chapter 12, Section 1. In determining the LLWR, researchers measure penetration resistance with penetrometers to determine if the soil is within the least limiting range for soil strength. (We discuss penetrometer measurements in Chapter 11.) However, the researchers do not measure the ODR of the soil, as originally proposed by Letey in describing his NLWR (Letey, 1985, p. 284). If values from the literature are used, this eliminates the need for extensive field experiments to determine the water content at which root growth is limited by mechanical strength and oxygen diffusion. However, these values should be measured in each experiment, because the limits for different crops and cultivars will vary. Mohammadi et al. (2010) recommended that oxygen status of the soil should be measured in determining the upper limit of the LLWR, but in the modeling work reported in their paper, they did not measure it. They obtained ODRs from the literature (Stępniewski et al., 2005). Feng et al. (2002) said that the ODR method, which mimics the oxygen supply to the root surface, was the best one to evaluate the aeration status of the soil and other measures like air-filled porosity should not be used.

The LLWR and the NLWR, which is often used synonymously with the LLWR (Verma and Sharma, 2008), have been determined subsequently by many researchers (da Silva and Kay, 1997a,b; Betz et al., 1998; Zou et al., 2000; Groenevelt et al., 2001; Asgarzadeh et al., 2010, 2011). It is used to determine not only the soil physical factors limiting crop growth but also soil quality (Lapen et al., 2004; Verma and Sharma, 2008). The concept of the NLWR or LLWR is useful provided one realizes that it depends on circumstances such as the type of crop, its growth stage, and potential evaporation. The concept of the NLWR is appealing because it can be related to the empirical descriptions of the water uptake term in root models, such as the model of Feddes et al. (1974); see also Feddes and Raats (2004) (P.A.C. Raats, personal communication, January 25, 2006).

The LLWR is becoming popular due to the fact that it can be used not only in root models but also in other models to characterize water availability (Asgarzadeh et al., 2011). In fact, researchers now refer to it as a type of pedotransfer function (Chen et al., 2014). Pedotransfer function is not defined in the *Glossary of Soil Science Terms 2008* (Soil Science Society of America, 2008). Pedotransfer functions have been used to understand hydraulic characteristics of soil since 1989, when Bouma (1989) proposed their use. He suggested that key measures of the soil's characteristics could be used to infer other traits that are more difficult to measure directly. For this process, he defined "pedotransfer functions", which allow existing knowledge to be transferred to deduce something that is unknown or difficult to determine (Clothier et al., 2004). More specifically, pedotransfer functions are regression equations that are used to predict difficult-to-obtain parameters from more easily measured soil properties (Perfect, 2003). They have been widely used to predict input parameters for soil hydrological models from basic soil physical properties such as particle size distribution and bulk density (Pachepsky and Rawls, 2004). Pedotransfer functions were used to estimate reliably FC at −33 kPa and permanent WP at −1500 kPa by knowing soil texture and bulk density (Pollacco, 2008).

## 10.5 BIOGRAPHIES OF BRIGGS AND SHANTZ

Dr Lyman James Briggs (1874−1963), a physicist, was born on May 7, 1874, in Assyria, Michigan, the son of Chauncey L. Briggs and Isabella (McKelvey) Briggs. He got his B.S. degree at Michigan State College in 1893, his M.S. degree at the University of Michigan in 1895, and his Ph.D. at Johns Hopkins in 1901 (Cattell, 1944). He received a Doctor of Science (Sc.D.) degree from Michigan State in 1932; a Doctor of Engineering degree from the South Dakota School of Mines in 1935; a Doctor of Laws (LL.D.) degree from the University of Michigan in 1936; a Sc.D. from George Washington University in 1937; a Sc.D. from Georgetown University in 1939; and a Sc.D. from Columbia University in 1944 (Debus, 1968).

He was in charge of the Physics Laboratory Division (now Bureau of Soils) for the US Department of Agriculture (USDA), 1896−1906. He was physicist in charge of the Biophysical Laboratory, Bureau of Plant Industry, 1906−1912, and from 1912 to 1920, he was in charge of biophysical investigations. He was detailed to the Bureau of Standards by executive order in 1917–1919. He was chief of Division of Mechanics and Sound, Bureau of Standards from 1920 to 1933 and its assistant director of research and testing from 1926 to 1933. He was director of the Bureau of Standards from 1933 to 1945, and was director emeritus from 1945 until his death in 1963. He was a member of the National Advisory Committee for Aeronautics (1933–1945), and was its vice chairman from 1942 to 1945. He was chairman of the subcommittee on aircraft structures, 1937–1945; a member of the aerodynamics subcommittee, 1922–1930; chairman of the Federal Specifications Board, 1932–1940, and of the Federal Fire Council, 1933–1939; president of the National Conference on Weights and Measures, 1935–1945; member of the International Ice Patrol Board, 1933–1945; chairman of the Washington Biophysical Institute Council, 1933–1939; on the board of directors of the American Standards Association, 1933–1945; member of the US National Committee for the International Geophysical Year; on the executive committee of the engineering division of the National Research Council, 1945–1950, and on its Committee of Fundamental Physical Constants; and director of the scientific program for stratospheric balloon flights. He was a trustee of George Washington University from 1945 until his death (Debus, 1968).

He shared the Magellan medal with Paul R. Heyl in 1922, received the Medal of Merit in 1948, and the Gold Medal of the US Department of Commerce for exceptional service. He was an honorary Fellow of the American College of Dentists; a Fellow of the American Association for the Advancement of Science; a Fellow of the American Physical Society (and its vice president in 1937 and president in 1938). He was a member of the National Academy of Sciences; American Society of Mechanical Engineers; Washington Academy of Science (its president in 1917); Philosophical Society of Washington (its president in 1916); American Philosophical Society; American Academy of Arts and Sciences; Institute of Aeronautical Science; Newcomen Society (engineering society); Washington Academy of Medicine (its president, 1945–1946); and an honorary member of the Physical Society of Engineering. He was a member of Tau Beta Pi, Sigma Xi, and Sigma Pi Sigma (Debus, 1968).

His areas of research interest were aerodynamic characteristics of projectiles, bombs, and aerofoils in a high-speed windstream; acceleration of gravity at sea; gyroscopic stabilization; soil analysis; properties of liquids under negative pressures; and defense projects. He collaborated with Paul R. Heyl on the development of an earth inductor compass (Debus, 1968).

Briggs married Katherine E. Cook on December 23, 1896, and they had two children: Mrs Isabel Myers and Albert Cook (deceased) (Debus, 1968). Lyman Briggs died on March 25, 1963. His scientific contributions have been detailed by Landa and Nimmo (2003). A biographical memoir has been cowritten by his grandson, Peter Briggs Myers (Myers and Sengers, 1999).

Dr Homer LeRoy Shantz (1876–1958), a botanist, was born in Kent County, Michigan, on January 24, 1876, the son of Abraham K. Shantz and Mary E. (Ankney) Shantz. He got his B.S. degree at Colorado College, Colorado Springs, in 1901, and his Ph.D. at the University of Nebraska in 1905. In 1926, he received a Sc.D. from Colorado College (Debus, 1968).

He was an instructor of botany and zoology at Colorado College, 1901–1902; of botany at the School of Agriculture in Nebraska, 1903–1904; and in Missouri, 1905–1906. He was professor of botany and bacteriology at the University of Louisiana in 1907. He worked for the Bureau of Plant Industries, USDA, first as an expert in alkali and drought-resistant plant breeding investigations (1908–1909); then as a plant physiologist (1910–1920); and then was in charge of plant geography and plant physiology (1920–1926). He was special lecturer on plant geography in the Graduate School of Geography, Clark University, 1922–1926. Between 1926 and 1928, he was professor of botany and head of the department at Illinois. He was president of the University of Arizona, 1928–1936. He was Chief of the Division of Wildlife Management, US Forest Service, 1936–1944 (Cattell, 1944), and was annuitant collaborator with the USDA from 1945 until his death in 1958. In 1956, he was a professor of botany at the University of Arizona, and in 1956–1957, he was principal investigator for the Arizona African Expedition (Debus, 1968).

He was a Fellow of the American Society of Agronomy and of the Royal Society of Arts. He was a member of the Phytographic Society of Sweden and honorary president of the 7th International Botanical Congress in Stockholm in 1950, and in Paris in 1954. He was a member of the Botanical Society; Washington Association of American Geographers; the American Society of Plant Physiologists (he received its Charles Reid Barnes life membership); Ecological Society; Wildlife Society; the Society pro Fauna et Flora Fennica; International Society for Protection of Nature; the International Institution of African Languages and Cultures; Sigma Xi; and Phi Beta Kappa (Cattell, 1944; Debus, 1968).

He was involved with many special projects. In 1918, he was part of the plant resources “Inquiry” in Africa and Latin America, formed to determine natural plant resources and crop-producing possibilities of large portions of Africa and Latin America for use by the American Commission to Negotiate Peace, 1918–1919. In 1924, he was on the Education Committee of East Africa. In 1931–1934, he was a USDA member of the National Land Use Planning Committee of the US Geological Survey, and was an explorer in the Smithsonian Institution expedition to Africa in 1919–1920. He was a member of the Educational Commission to East Africa under the auspices of the Phelps Stokes Fund and the International Education Board in 1924 (Debus, 1968).

His research interests included the vegetation of the Great Plains and the Great Basin; the indicator value of natural vegetation; the physiology of drought resistance; biological study of the lakes in the Pike's Peak region; North American Branchinecta and their habitats; plant geography of Africa and Latin America; plant geography and plant industry; agriculture of the African natives; wildlife management; and agricultural geography of Africa (Cattell, 1944; Debus, 1968).

He married Lucia Moore Soper on December 25, 1901, and they had two children: Homer LeRoy and Benjamin Soper. He died on June 23, 1958 (Debus, 1968).

### 10.5.1 Importance of Briggs and Shantz

Both Briggs and Shantz are cited in a book listing the most important scientists from antiquity to the present (Debus, 1968). In the seventh edition of *American Men of Science* (Cattell, 1944), they had stars by their names. (A star was prefixed to 1000 biographical entries out of about 34,000 names listed.) The areas of science were broken down into 12 disciplines, and the number of people ranked in each discipline, of the 1000 men ranked, was as follows:

Chemistry, 175
Physics, 150
Zoology, 150
Botany, 100
Geology, 100
Mathematics, 80
Pathology, 60
Astronomy, 50
Psychology, 50
Physiology, 40
Anatomy, 25
Anthropology, 20

In each of the 12 principal sciences, the names were arranged in the order of merit by 10 leading scientists of the discipline, and the position of each scientist then was ranked in his specialty. Briggs was ranked first in physics, and Shantz was ranked third in Botany. (Briggs was ranked even above I.I. Rabi, who was ranked sixth in physics. Rabi won a Nobel Prize in Physics in 1944 for his resonance method, using molecular beams, for recording the magnetic properties of atomic nuclei. Rabi's work laid the basis for nuclear magnetic resonance, now routinely used in medical diagnosis.) The biographies make clear the importance of Briggs and Shantz, who were two of the most important scientists in the United States.

## References

Asgarzadeh, H., Mosaddeghi, M.R., Mahboubi, A.A., Nosrati, A., Dexter, A.R., 2010. Soil water availability for plants as quantified by conventional available water, least limiting water range and integral water capacity. Plant Soil 335, 229–244. http://dx.doi.org/10.1007/s11104-010-0410-6.

Asgarzadeh, H., Mosaddeghi, M.R., Mahboubi, A.A., Nosrati, A., Dexter, A.R., 2011. Integral energy of conventional available water, least limiting water range and integral water capacity for better characterization of water availability and soil physical quality. Geoderma 166, 34–42. http://dx.doi.org/10.1016/j.geoderma.2011.06.009.

Baver, L.D., Gardner, W.H., Gardner, W.R., 1972. Soil Physics, fourth ed. Wiley, New York.

Betz, C.L., Allmaras, R.R., Copeland, S.M., Randall, G.W., 1998. Least limiting water range: traffic and long-term influences in a Webster soil. Soil Sci. Soc. Am. J. 62, 1384–1393.

Bouma, J., 1989. Using soil survey data for quantitative land evalution. Adv. Soil Sci. 9, 177–213.

Briggs, L.J., Shantz, H.L., 1912. The wilting coefficient for different plants and its indirect determination. USDA Bur. Plant Ind. Bull. No. 230. U.S. Dept. Agr: Washington, DC.

Cattell, J. (Ed.), 1944. American Men of Science. A Biographical Directory, seventh ed. Science Press, Lancaster, Pennsylvania.

Chen, G., Weil, R.R., Hill, R.L., 2014. Effects of compaction and cover crops on soil least limiting water range and air permeability. Soil Tillage Res. 136, 61–69.

Clothier, B.E., Green, S.R., Vogeler, I., Robinson, B.H., Mills, T.M., Duwig, C., Roygard, J.K.F., Walter, M., van den Dijssel, C.W., Scotter, D.R., 2004. Contaminants in the soil of the root zone: transport, uptake and remediation. In: Juhasz, A.L., Magesan, G., Naidu, R. (Eds.), Waste Management. Science Publishers, Inc., Enfield, New Hampshire, pp. 3–34.

da Silva, A.P., Kay, B.D., Perfect, E., 1994. Characterization of the least limiting water range of soils. Soil Sci. Soc. Am. J. 58, 1775–1781.

da Silva, A.P., Kay, B.D., 1996. The sensitivity of shoot growth of corn to the least limiting water range of soils. Plant Soil 184, 323–330.

da Silva, A.P., Kay, B.D., 1997a. Estimating the least limiting water range of soils from properties and management. Soil Sci. Soc. Am. J. 61, 877–883.

da Silva, A.P., Kay, B.D., 1997b. Effect of soil water content variation on the least limiting water range. Soil Sci. Soc. Am. J. 61, 884–888.

Debus, A.G. (Ed.), 1968. World Who's Who in Science. From Antiquity to the Present. Marquis-Who's Who, Chicago, Illinois.

Dexter, A.R., Czyż, E.W., Richard, G., 2012. Equilibrium, non-equilibrium and residual water: consequences for soil water retention. Geoderma 177–178, 63–71.

Feddes, R.A., Raats, P.A.C., 2004. Parameterising the soil-water-plant-root system. In: Feddes, R.A., Rooj, G.H. de, Dam, J.C. van (Eds.), Unsaturated Zone Modelling: Progress, Challenges and Applications, Wageningen UR Frontis Series, vol. 6. Wageningen Universiteit en Researchcentrum (Wageningen University and Research Centre), The Netherlands, pp. 95–141.

Feddes, R.A., Bresler, E., Newman, S.P., 1974. Field test of a modified numerical model for water uptake by root systems. Water Resour. Res. 10, 1199–1206.

Feng, G., Wu, L., Letey, J., 2002. Evaluating aeration criteria by simultaneous measurement of oxygen diffusion rate and soil-water regime. Soil Sci. 167, 495–503.

Gardner, W.R., 1960. Dynamic aspects of water availability to plants. Soil Sci. 89, 63–73.

Grable, A.R., Siemer, E.G., 1968. Effects of bulk density, aggregate size, and soil water suction on oxygen diffusion, redox potentials, and elongation of corn roots. Soil Sci. Soc. Am. Proc. 32, 180–186.

Groenevelt, P.H., Grant, C.D., Semetsa, S., 2001. A new procedure to determine soil water availability. Aust. J. Soil Res. 39, 577–598.

Haise, H.R., Haas, H.J., Jensen, L.R., 1955. Soil moisture studies of some great plains soils: II. Field capacity as related to 1/3-atmosphere percentage, and "minimum point" as related to 15- and 26-atmosphere percentages. Soil Sci. Soc. Am. Proc. 19, 20–25.

Hillel, D., 1971. Soil and Water. Physical Principles and Processes. Academic Press, New York.

Hillel, D., 2004. Introduction to Environmental Soil Physics. Elsevier, Amsterdam.

Hillel, D., 2008. Soil in the Environment. Crucible of Terrestrial Life. Elsevier, Amsterdam.

Kramer, P.J., 1983. Water Relations of Plants. Academic Press, New York, 489 pp.

Landa, E.R., Nimmo, J.R., 2003. The life and scientific contributions of Lyman J. Briggs. Soil Sci. Soc. Am. J. 67, 681–693.

Lapen, D.R., Topp, G.C., Gregorich, E.G., Curnoe, W.E., 2004. Least limiting water range indicators of soil quality and corn production, eastern Ontario, Canada. Soil Tillage Res. 78, 151–170.

Letey, J., 1985. Relationship between soil physical properties and crop production. Adv. Soil Sci. 1, 277–294.

Mohammadi, M.S., Asadzadegh, F., Vanclooster, M., 2010. Refining and unifying the upper limits of the least limiting water range using soil and plant properties. Plant Soil 334, 221–234. http://dx.doi.org/10.1007/s11104-010-0377-3.

Myers, P.B., Sengers, J.M.H.L., 1999. Lyman James Briggs 1874–1963. In: Biogr Mem., vol. 77. National Academy Press, Washington, D.C, pp. 3–18.

Pachepsky, Y.A., Rawls, W.J. (Eds.), 2004. Development of Pedotransfer Functions in Soil Hydrology. Elsevier, Amsterdam.

Perfect, E., 2003. A pedotransfer function for predicting solute dispersitivity: model testing and upscaling. In: Pachepsky, Y., Radcliffe, D.E., Selim, H.M. (Eds.), Scaling Methods in Soil Physics. CRC Press, Boca Raton, Florida, pp. 89–96.

Philip, J.R., 1957. The physical principles of soil water movement during the irrigation cycle. In: Proc Congr Int Comm Irrigation Drainage, Third, San Francisco, vol. 8, pp. 125–153.

Pollacco, J.A.P., 2008. A generally applicable pedotransfer function that estimates field capacity and permanent wilting point from soil texture and bulk density. Can J. Soil Sci. 88, 761–774.

Raats, P.A.C., Smiles, D.E., Warrick, A.W., 2002. Contributions to environmental mechanics: introduction. In: Raats, P.A.C., Smiles, D.E., Warrick, A.W. (Eds.), Environmental Mechanics: Water, Mass and Energy Transfer in the Biosphere, Geophys. Monogr, vol. 129. American Geophysical Union, Washington, DC, pp. 1–28.

Richards, L.A., Weaver, L.R., 1943. Fifteen-atmosphere percentage as related to the permanent wilting percentage. Soil Sci. 56, 331–339.

Salisbury, F.B., Ross, C.W., 1978. Plant Physiology, second ed. Wadsworth Pub, Belmont, California.

Schofield, R.K., 1935. The pF of the water in soil. Trans. Intern. Congr Soil Sci. Third 2, 37–48.

Soil Science Society of America, 1971. Glossary of Soil Science Terms. Soil Science Society of America, Madison, Wisconsin.

Soil Science Society of America, 1975. Glossary of Soil Science Terms. Soil Science Society of America, Madison, Wisconsin.

Soil Science Society of America, 1978. Glossary of Soil Science Terms. Soil Science Society of America, Madison, Wisconsin.

Soil Science Society of America, 1979. Glossary of Soil Science Terms. Soil Science Society of America, Madison, Wisconsin.

Soil Science Society of America, 1984. Glossary of Soil Science Terms. Soil Science Society of America, Madison, Wisconsin.

Soil Science Society of America, 1987. Glossary of Soil Science Terms. Soil Science Society of America, Madison, Wisconsin.

Soil Science Society of America, 1997. Glossary of Soil Science Terms. Soil Science Society of America, Madison, Wisconsin.

Soil Science Society of America, 2008. Glossary of Soil Science Terms. Soil Science Society of America, Madison, Wisconsin.

Stępniewski, W., Stępniewska, Z., Bennicelli, P.R., Gliński, J., 2005. Oxygenology in Outline. EU Fifth Framework Program, QLAM-2001—00428. Institute of Agrophysics, Lublin, Poland.

Taylor, H.M., Roberson, G.M., Parker Jr, J.J., 1966. Soil strength-root penetration relations for medium- to coarse-textured soil materials. Soil Sci. 102, 18—22.

Taylor, S.A., 1952. Use of mean soil moisture tension to evaluate the effect of soil moisture on crop yields. Soil Sci. 74, 217—226.

Taylor, S.A., Ashcroft, G.L., 1972. Physical Edaphology: The Physics of Irrigated and Nonirrigated Soils. W.H. Freeman, San Francisco.

van Genuchten, M. Th, 1980. A closed-form equation for predicting the hydraulic conductivity of unsaturated soils. Soil Sci. Soc. Am. J. 44, 892—898.

Verma, S., Sharma, P.K., 2008. Long-term effects of organics, fertilizers and cropping systems on soil physical productivity evaluated using a single value index (NLWR). Soil Tillage Res. 98, 1—10.

Webster's New World Dictionary of the American Language, 1959. College ed. World Publishing, Cleveland and New York.

Wesseling, J., van Wijk, W.R., 1957. Soil physical conditions in relation to drain depth. In: Luthin, J.N. (Ed.), Drainage of Agricultural Lands. American Society of Agronomy, Madison, Wisconsin, pp. 461—504 (See especially Figure 4, p. 468).

Zou, C., Sands, R., Buchan, G., Hudson, I., 2000. Least limiting water range: a potential indicator of physical quality of forest soils. Aust. J. Soil Res. 38, 947—958.

CHAPTER

# 11

# Penetrometers

As we pointed out in Chapter 1, the four soil physical factors that affect plant growth are mechanical impedance, water, aeration, and temperature (Kirkham, 1973). In Chapter 5, we learned how to measure matric potential of water in the soil using tensiometers. In later chapters, we shall study other techniques to measure water in soils and plants, and in the next chapter, we shall see how to measure soil aeration. In this chapter, we learn how to measure mechanical impedance using penetrometer measurements.

We first will define a penetrometer and then look at different kinds of instruments and their uses. We will consider the type of tests that are done with penetrometers and what factors affect the measurements, and then look specifically at the cone penetrometer.

## 11.1 DEFINITION, TYPES OF PENETROMETERS, AND USES

A penetrometer is any device forced into the soil to measure resistance to vertical penetration (Davidson, 1965). The earliest soil penetrometers were fists, thumbs, fingernails, pointed sticks, and metal rods. They are still used for qualitative measurements.

Results of such tests are expressed in terms such as “loose,” “soft,” “stiff,” and “hard”. However, penetrometers are designed to give quantitative measurements of soil penetration resistance for a more precise correlation with properties such as bearing value, safe soil pressure, rolling resistance, trafficability of wheels or crawler tracks on soil, relative density, crop yield, and tilth (Davidson, 1965). *Tilth* is from the Anglo-Saxon word *tilthe* and means a tilling or cultivation of land. Dr Jerry L. Hatfield, a Kansas native and the director of the United States National Soil Tilth Laboratory, located on the campus of Iowa State University in Ames, Iowa, has a nonscientific definition of tilth: “The wellness of the seedbed” (Muhm, 1990). The $11.9 million Tilth Laboratory opened in

*Principles of Soil and Plant Water Relations*
http://dx.doi.org/10.1016/B978-0-12-420022-7.00011-2

Copyright © 2014 Elsevier Inc. All rights reserved.

April, 1989, and has the goal of quantifying the effects of tillage on the soil. Using penetrometers is one method to do this quantification. In 2009, the name of the laboratory was changed to the National Laboratory for Agriculture and the Environment.

## 11.2 TYPES OF TESTS

Two types of tests are done, when making penetration-resistance measurements: a static test or a dynamic test. In a static penetration test, the penetrometer is pushed steadily into the soil. A static penetration test is exemplified by the use of the cone penetrometer, which we discuss in detail in Section 11.4. In a dynamic penetration test, the penetrometer is driven into the soil by a hammer or falling weight. A dynamic penetration test can be done with a spray-tainer or spra-tainer. The apparatus was designed in the 1950s by Professor Champ B. Tanner of the University of Wisconsin in Madison, Wisconsin. For a biography of Tanner, see the Appendix, Section 11.5.

The spra-tainer is shown in Figure 11.1 (Kirkham et al., 1959b). It is a thin-walled can of 12-ounce size (341 g) manufactured to dispense products such as shaving cream and bug spray under pressure. The bottom of the can is removed and the top is left open. The can, which is 8 cm long and 6.9 cm in diameter, is driven into the soil with a special hammer weighing 2.35 kg and dropped from a height of 42.5 cm (Kirkham et al., 1959a). This driving of the cans into the soil is done when

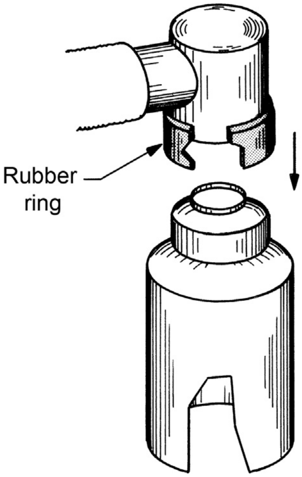

**FIGURE 11.1** The spra-tainer can. *From Kirkham et al. (1959b); Reprinted by permission of Marcel de Boodt for the Landbouwhogeschool en de Opzoekingsstations van de Staat te Gent, Ghent, Belgium.*

the soil is at or near field capacity. The cans are driven entirely into the soil (to a depth of 8 cm). The cans are steel, and, unless they encounter rocks in the soil, they may be used repeatedly. A thin coating of petroleum jelly is wiped on the cans before each use. The special hammer is used, together with a special driving head and driving tube, in order that the driving is done the same way by all operators. The spra-tainer can and the driving head fit in a driving tube, the latter having triangular-shaped legs with spikes in their ends to hold the driving tube vertically on the soil surface. The top of the driving head has, extending upward on its axis, a guide rod. A photograph of the setup is shown by Kirkham et al. (1959b). The number of blows to drive in the cans (acting as penetrometers) is counted, and this number is the quantified measurement. The seamless tube cans are an important feature of the equipment. Because of the thin and sharp walls of the spra-tainer cans, the soil is relatively undisturbed, and, if soil samples are taken after getting the penetration resistance, the samples (8 cm long and 6.9 cm in diameter) may be called undisturbed. After penetrometer measurements are made using the spra-tainers, air permeability measurements may be made on the samples in place in the field (Kirkham et al., 1959a). The method is described by Kirkham et al. (1959b). For the air permeability measurements, air is delivered at a constant small pressure through a vacuum-cleaner-type flexible hose that is attached to the spra-tainer. At the top of Figure 11.1, the end of the air hose which connects to the spra-tainer is shown for the air permeability measurements. Grover (1955) used an equipment similar to Kirkham et al. (1959a) to measure air permeability, and Sweeney et al. (2006) used the method of Grover (1955) plus the cone penetrometer designed by Christensen et al. (1998) to measure air permeability and penetration resistance of soil after wheel-track compaction resulting from commonly used heavy-weight tractors and equipment.

Even though used in past decades, dynamic penetration tests are not often employed in agricultural situations today. Dynamic penetrometers are mostly used for highway pavement evaluations and few include modern, high-resolution automated data acquisitions systems (Lowery and Morrison, 2002).

## 11.3 WHAT PENETROMETER MEASUREMENTS DEPEND UPON

All penetrometer measurements depend upon two factors: the water content of the soil and time. Above freezing, differences in measurements due to temperature are not detectable (Loyd Stone, personal communication, February 4, 1983). Therefore, measurements depend on temperature only if the soil is frozen.

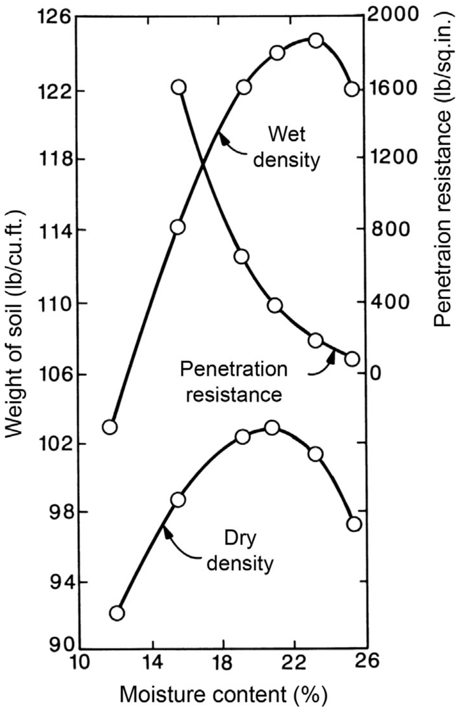

**FIGURE 11.2** Typical curves illustrating the relation of water content of soil to density and penetration resistance. *From Davidson (1965); Reprinted by permission of the American Society of Agronomy.*

Figure 11.2 (Davidson, 1965) shows that as the water content increases, the penetration resistance decreases. As noted above, measurements with the spra-tainers are made when the soil is near field capacity. A measurement made with the cone penetrometer in a cohesive, fine-grained soil is an inverse function of water content (Davidson, 1965). In humid climates, trafficability measurements are made during the wet season. In dry or hard soils, or in soils containing pebbles and stones, any operator will find it difficult to obtain consistent and reliable penetrometer measurements, especially as penetration depth increases. Simultaneous and conjoint measurements of penetration resistance and water content need to be made (Topp et al., 2003).

Measurements depend upon time because of impulse. In physics, impulse is defined as follows (Schaum, 1961, p. 62):

$$\text{Impulse} = \text{force} \times \text{length of time the force acts} = Ft. \tag{11.1}$$

Units of impulse are the N-s in the MKS system, the dyne-s in the CGS system, and the lb-s in the English system.

Impulse and momentum are related. The change of momentum produced by an impulse is equal to the impulse. Thus if an unbalanced force $F$ acting for a time $t$ on a body of mass $m$ changes its velocity from an initial value $v_o$ to a final value $v_t$, then

$$\text{Impulse} = \text{change in momentum},$$

$$Ft = m(v_t - v_o). \tag{11.2}$$

This equation indicates that the unit of impulse in any system is equal to the corresponding unit of momentum. Therefore, 1 N-s = 1 (kg-m)/s and 1 lb-s = 1 (slug-ft)/s (Schaum, 1961, p. 62).

Because of impulse (dependent upon time), a penetrometer, like a cone penetrometer, must be pushed at a steady rate into the soil. It should take about 15 s to go 24 in (4 cm/s) (Davidson, 1965, p. 480). According to Don Kirkham (personal communication, February 20, 1982), penetrometer measurements are a "pain in the neck" for two reasons: their dependence upon time and water content.

## 11.4 CONE PENETROMETER

Now let us look at the cone penetrometer (SoilTest, 1978a), which is a penetrometer that has gained wide acceptance. It was developed by the U.S. Army Corps of Engineers for predicting the carrying capacity of cohesive, fine-grained soils for army vehicles in off-road military operations (Davidson, 1965). The strength of the soil has long been of concern to the military. Frederick I Barbarossa (ca 1123–1190), emperor of the Holy Roman Empire, drowned in Cilicia (now Turkey) on June 10, 1190, while marching his army into Asia Minor (Davis, 1971). He died in quicksand (Don Kirkham, personal communication, undated, who lived in Turkey in 1959 and saw the sight where Barbarossa died). Before D-Day (June 6, 1944; D stands for "Day"), the day of the invasion of western Europe by Allied forces in World War II, General Dwight D. Eisenhower (1890–1969) did not know if the beaches at Normandy in France were rocky and firm enough to hold tanks, or if they would turn out to be soft sand (Smith, 2004).

The applied force required to press the cone penetrometer into a soil is an index of the resistance or impedance of the soil and is called the *cone index* (CI). Cone index readings are taken to depths of 24 in (61 cm) to permit plotting of a cone index curve, which, in addition to its significance in trafficability studies, gives quantitative information on soil compactness or density that can be correlated with other soil physical properties or with crop yields (Davidson, 1965).

The parts of the cone penetrometer made in the United States consist of the handle, proving ring, dial gauge, rod graduated in 6 in (15 cm) or 12 in

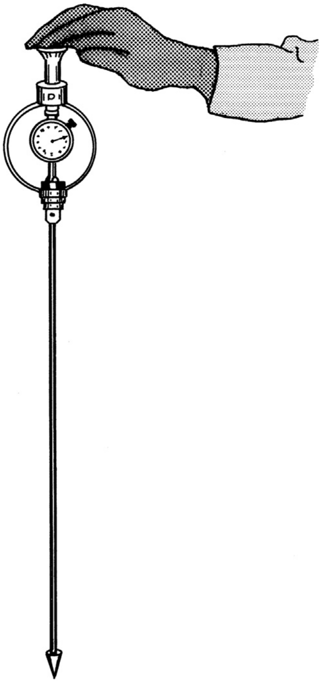

**FIGURE 11.3** The cone penetrometer. *From SoilTest (1978b); Reprinted by permission of ELE International, Loveland, Colorado.*

(30 cm) intervals, and a stainless-steel cone (Figure 11.3) (SoilTest, 1978b). The operator′s handle is mounted at the top of the proving ring. The staff is 19 in long (48.3 cm), making it possible to take readings to that depth. The cone is 1.5 in (3.8 cm) in height and has a 30° apex angle and a base area of 0.5 in squared (3.14 $cm^2$). The diameter of the base of the cone is 0.79 in (2.0 cm). The cone index or force per unit area required to move the cone to a given plane of soil to show the shearing resistance of that soil is indicated on the proving ring dial. The proving ring has 150 pound capacity and the dial indicator reads the cone index in the range of 0–300 pounds per square inch (psi). (See next paragraph for SI units.) In Europe, Eijkelkamp Agrisearch Equipment (Nijverheidsstraat 30, 6987 EM Giesbeek, The Netherlands) sells penetrometers. Hartge et al. (1985) in Germany report results using the Eijkelkamp penetrometer. Gauges in Europe read in kilogram per square centimeter (Don Kirkham, personal communication, February 18, 1982). In Australia, Rimik (1079 Ruthven Street, Toowoomba, Queensland 4350) makes a cone penetrometer that has a cone index read-out in kilopascal (Figure 11.4).

Because the Corps of Engineers′ cone penetrometer is made in the United States, its dial gauge reads out in the English units of pounds per square

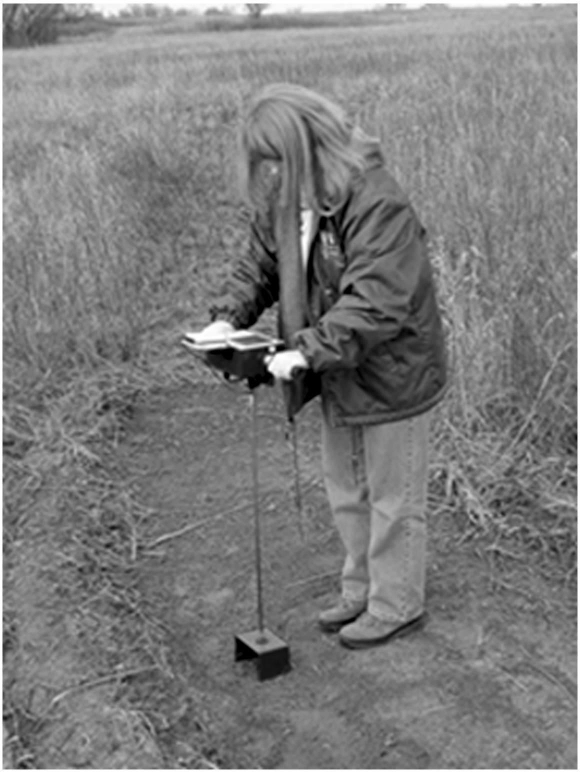

**FIGURE 11.4** Picture of a cone penetrometer in use. The cone penetrometer shown is made by Rimik Pty. Ltd., Toowoomba, Queensland, Australia. *Photograph courtesy of Dr Peggy S. Althoff, Kansas State University, Manhattan, Kansas.*

inch (psi). Therefore, we need to know how to convert the dial readings, in lb/in$^2$, into SI units. Remember $F = ma$ (force = mass times acceleration) and in a gravitational field, $w = mg$ (weight = mass times acceleration due to gravity). So each gram has an earth-pull on it of 980 dynes and each kilogram has an earth-pull on it of 9.8 N. In the CGS system of units, we make the following calculations (remember $1 \times 10^6$ dynes/cm$^2$ = 1 bar).

To convert from the English system to the CGS system,

$$\begin{aligned}1\ \text{psi} &= 1\ \text{lb/in}^2 = [(454 \times 980)\ \text{dynes}]/(2.54\ \text{cm})^2\\ &= 68962.7\ \text{dynes/cm}^2 = 68962.7/10^6\ \text{bar}\\ &= 0.0689627\ \text{bar}\ \text{ or, }\ \text{to 4 significant figures, }\ 0.06896\ \text{bar}.\end{aligned}$$

This agrees with the value that Taylor and Ashcroft (1972, p. 511) give in their extensive list of conversion factors: 1 psi = 0.06895 bar, the slight difference (0.06895 bar vs 0.06896 being due to rounding of values).

We know that 10 bar = 1 MPa. Thus,

$$0.0689627 \text{ bar} = 0.00689627 \text{ MPa} = 6896.27 \text{ Pa}.$$

To convert from the English system to the MKS system,

$$\begin{aligned}1 \text{ psi} &= [(0.454 \times 9.8) \text{ N}]/[(2.54/100) \text{ m}]^2 = 0.68962 \times 10^4 \text{ N/m}^2 \\ &= 6.896 \times 10^3 \text{ N/m}^2 = 6896 \text{ N/m}^2.\end{aligned}$$

Note the conversion units:

$$14.7 \text{ psi} = 1 \text{ atm}; \quad 0.987 \text{ atm} = 1 \text{ bar}.$$

One Pascal = 1 N/m$^2$ and 14.5 lb/in$^2$ = 1 bar; 0.06896 bar per psi × 14.5 psi per bar = 1.0. The value 0.06896 bar per psi checks out.

The cone penetrometer that Loyd R. Stone in the Department of Agronomy at Kansas State University uses was made by the Physics Shop at Kansas State University (personal communication, March 6, 1990). He has penetrometers with different cone tips and base areas. Dr Stone's penetrometers are calibrated by pressing the cone on a balance with known masses in kilograms. The probe scale has no units, just numbers. The readout (number) on the probe is calibrated against kilograms. The value in kilograms is divided by area for that cone tip, and he gets probe readings in units of kg/cm$^2$ (mass per unit area) (Intrawech et al., 1982). Others also use a cone index in units of kg/cm$^2$ (Cruse et al., 1981; Bradford, 1986).

Note that acceleration due to gravity is not included when one gets a reading of mass per unit area (kg/cm$^2$). As noted in Chapter 2, we must express values in SI units, and journals require them for publication. But either kg/cm$^2$ or the units converted to SI units from the English units on the U.S. Army Corps of Engineers' cone penetrometer (force per unit area or MPa) are all right. Engineers around the world (like those in the U.S. Army Corps of Engineers) think in terms of living on earth and talk of weight on earth. For example, they say, "This man weighs 185 lb." They do not say, "This man has a mass of 5.8 slugs." The 185 pounds is the man's force on the surface of a floor. It is a valid reading because the springs on a calibrated bathroom scale will give the man's weight in pounds. If the man were standing on scales on the moon, where surface gravity is 0.17 of the Earth's, he would weigh 31 pounds. So when the astronauts were on the moon, they needed lead weights in their boots to hold them down.

In sum concerning units, we need to recognize that the U.S. Army Corps of Engineers' gauge is reporting a force per unit area or a weight per unit area (remember $w = mg$), and units of kg/cm$^2$ report a mass per unit area. A gravity constant is associated with the Corps of Engineers' gauge, and it is not with a reading given in kg/cm$^2$.

Loyd Stone often uses a penetrometer with a cone angle of 45°. He prefers a wider angle than that on the penetrometer of the Corps of Engineers (45° vs 30°). With the wider angle, the soil does not get so compressed as the cone moves in, especially at lower depths (personal communication, March 6, 1990). To get more accurate readings, he uses a smaller area on the cone and a more sensitive proving ring. If a proving ring needs a 500 pound (227 kg) force to move it, it is no good because a man cannot push 500 pounds. So Dr Stone uses a 0–50 lb proving ring and has a small cone area. The proving ring and the cone area must be matched. Some people like to go to larger cone areas, which are harder to push into the ground, to get better representation of the soil, because a larger area is sampled (Loyd Stone, personal communication, March 6, 1990). Dr Stone's meter has a brake and holds the reading until it is released. The Corp of Engineers' penetrometer does not hold the reading. It is not necessary to core soil first when using a cone penetrometer (Loyd Stone, personal communication, February 17, 1982), but to use a blunt-end penetrometer, it is necessary to core the soil to the depth of interest because the soil becomes compacted.

When reviewing a paper describing a study in which a cone penetrometer has been used, make sure that the authors give (1) the cone angle; (2) the rate of penetration; (3) water content of the soil; and (4) the physical meaning of their units (i.e., whether or not gravity is taken into account in the units).

The correlation between readings made with cone penetrometers is good, if the same model of penetrometer is used at the same location, and even if two different people make the measurements (Loyd Stone, personal communication, February 7, 1983). Differences in readings occur due to fractures in the soil (e.g., holes), which result in much variability between readings. However, there is still some variability due to operators.

In this chapter, only commonly used penetrometers have been noted. Specifically designed ones for laboratory experimentation have been developed. For example, see Whiteley et al. (1981). Perumpral (1987) reviews applications of cone penetrometers in engineering, and Lowery and Morrison (2002) review different types of penetrometers used in soil science.

The need to take penetrometer measurements becomes ever more important as the weight of farm equipment increases (Horn et al., 2007; Zink et al., 2010). Physical soil degradation is occurring due to heavy machinery that farmers are using. In Germany, soil scientists are urging their federal government to limit the weight of the farm machinery. The largest sugar beet (*Beta vulgaris* L.) harvester in Germany weighs, when loaded, about 60 metric tons (60 Mg), just as much as the biggest US battle tank (Rienk van der Ploeg, Professor, University of Hannover, personal communication, February 16, 2004). In Germany, a truck of that weight is not allowed to use the highways, but for arable fields no weight limit exists (van der Ploeg et al., 2006).

Military training commonly results in land degradation but protocols for assessing long-term environmental impacts are lacking. Althoff and Thien (2005) and Althoff et al. (2010) determined the damage done by battle tanks weighing 57.2 Mg (57.2 metric tons) on prairie soil at Fort Riley Military Installation in northeastern Kansas. Soil compaction, as measured by a cone penetrometer, was severe for tank traffic under wet conditions and remained significant to depths of 5 and 10 cm throughout the length of the study (2003–2007). As with heavy pieces of farm equipment (Zink et al., 2010), apparently irreversible soil compaction occurs with battle tanks.

## 11.5 APPENDIX: BIOGRAPHY OF CHAMP TANNER

Champ Bean Tanner, the inventor of the spra-tainer, was born in Idaho Falls, Idaho, on November 16, 1920, the son of Bertrand Myron Tanner and Orea Bean Tanner. After the death of his father in 1924, he was raised by his widowed mother. The family moved to Teton City and then to Rexburg, Idaho, where his mother taught high school until 1930. In 1930, the family (Champ, two brothers, and his mother) moved to Provo, Utah, to continue Orea's education at Brigham Young University. After earning her B.S., Mrs Tanner taught at Provo High until 1938, when she joined the English Department at Brigham Young University.

Tanner graduated from Provo High School in 1938. He received his undergraduate degree from Brigham Young University in 1942 with high honors in chemistry and soil science. After 4 years of service in the U.S. Army (1942–1946), he entered graduate school at the University of Wisconsin in Madison. He earned his Ph.D. in soils in 1950 under the joint direction of Professors E.E. Miller and M.L. Jackson (American Society of Agronomy, 1988). He joined the Department of Soil Science as the first agricultural physicist employed since F.H. King's retirement in 1901. (For a biography of King, see Tanner and Simonson, 1993.) He remained at the University of Wisconsin for 40 years, and served as chair of the department of soil science from 1984 until his retirement in 1988.

In soil physics, he studied water flux in unsaturated soils, the thermal regime in soils, and soil aeration and redox potentials. His ability to develop instrumentation such as the spra-tainer for the dynamic penetration test was recognized by his colleagues (Don Kirkham, personal communication, undated). Tanner was the first to make in situ measurements of oxygen tension in the field. As a pioneer in micrometeorology, he dedicated much of his research to near-ground measurements of heat and water vapor transport from soil, water, and plant surfaces. He was the first to apply approaches of energy balance and the Bowen ratio to agronomic crops, and he devised the instruments for the necessary measurements. He developed the measurement of net radiation absorbance in crop foliar canopies and estimated soil evaporation and plant evaporation as functions of plant density and row spacing (Walsh et al., 1991).

In the area of plant–water relations, Tanner provided fundamental information on the relationship between water availability and plant growth. He created original instruments and techniques for estimating plant physiological responses, including the use of pressure chambers to measure water potential in plant storage organs and in situ water potential measurements of potato tubers and other root crops (Walsh et al., 1991). The paper describing the stomatal meter that he made with graduate students Edward T. Kanemasu and George W. Thurtell (Kanemasu et al., 1969) became a citation classic (Institute for Scientific Information, 1979). His *Soils Bulletin No. 6* (Tanner, 1963) is still regularly referred to.

Tanner directed the research for 25 Ph.D. and 15 M.S. students (American Society of Agronomy, 1990) and worked with several postdoctoral scientists. His students became leaders in agricultural meteorology and soil physics. He took pleasure in their achievements, but little credit, because he believed that the qualities ensuring success, such as integrity, imagination, deep curiosity, and hard work, are native and not taught (American Society of Agronomy, 1988). I worked in Tanner's laboratory when I was a graduate student studying under Wilford R. Gardner at the University of Wisconsin. There Tanner taught me how to weld thermocouples and make thermocouple psychrometers. His attention to detail was well known, and both field and laboratory measurements had to be done exactly right. He started work early in the morning. The going bet was that some day Tanner would arrive so early that he would meet Marvin L. Wesely (Gaffney, 2003), one of his students who worked late into the nights.

Tanner was the first soil scientist to be elected to the National Academy of Sciences (1981). He received the Award for Outstanding Achievement in Biometeorology from the American Meteorological Society in 1980 and the Soil Science Society of America's Soil Science Research award in 1978. He was a Fellow of the American Meteorological Society, the American Society of Agronomy, the Soil Science Society of America, the Crop Science Society of America, and the American Association for the Advancement of Science (American Society of Agronomy, 1988). He was awarded the Emil-Truog named professorship at the University of Wisconsin in 1979. He was a Fulbright lecturer in Australia and Papua New Guinea. He served as editor for the American Meteorological Society, the Soil Science Society of America, the American Society of Agronomy, and the American Society of Plant Physiologists.

A symposium on the subject of biophysical measurements was held at the annual meetings of the American Society of Agronomy in November, 1988, to honor Tanner. Papers from the symposium were published in an issue of *Theoretical and Applied Climatology* (Campbell, 1990).

Tanner married Kay (Catherine May Cox) on September 24, 1941. They had five children: three sons—Bertrand D., Myron S., and Clark B.—and two daughters—Catherine and Terry Lee. Clark—born in 1960, died in 1977 of acute leukemia. Bertrand, like his father, was skilled in instrumentation, and was an executive at Campbell Scientific, Inc., the company best known for its data loggers. Bertrand died of cancer on September 16, 2008 (Meek, 2009). Champ Tanner's accomplishments were all the more remarkable because he got polio in the early 1950s, and, although he recovered, he walked with difficulty. He died of cancer on September 22, 1990, at the age of 69.

## References

Althoff, P.S., Thien, S.J., 2005. Impact of M1A1 main battle tank disturbance on soil quality, invertebrates, and vegetation characteristics. J. Terramechanics 42, 159–176. http://dx.doi.org/10.1016/j.terra.2004.10.014.

Althoff, P.S., Thien, S.J., Todd, T.C., 2010. Primary and residual effects of Abrams tank traffic on prairie soil properties. Soil Sci. Soc. Am. J. 74, 2151–2161. http://dx.doi.org/10.2136/sssaj2009.0091.

American Society of Agronomy, August, 1988. Retirements. C.B. Tanner. Agron. News, 13.

American Society of Agronomy, November, 1990. Deaths. Champ B. Tanner. Agron. News, 27.

Bradford, J.M., 1986. Penetrability. In: Klute, A. (Ed.), Methods of Soil Analysis. Part 1. Physical and Mineralogical Methods, second ed. American Society of Agronomy and Soil Science Society of America, Madison, Wisconsin, pp. 463–478.

Campbell, G.S., 1990. Introduction. Tanner symposium on biophysical measurements and instrumentation. Theor. Appl. Climatol. 42, 201–202.

Christensen, N.B., Sisson, J.B., Sweeney, D.W., Swallow, C.W., 1998. Electronically-controlled, portable, cone penetrometer. Commun. Soil Sci. Plant Anal. 29, 1177–1182.

Cruse, R.M., Cassel, D.K., Stitt, R.E., Averette, F.G., 1981. Effect of particle surface roughness on mechanical impedance of coarse-textured soil materials. Soil Sci. Soc. Am. J. 45, 1210–1214.

Davidson, D.T., 1965. Penetrometer measurements. In: Black, C.A., Evans, D.D., Ensminger, L.E., White, J.L., Clark, F.E. (Eds.), Methods of Soil Analysis. Part 1. Physical and Mineralogical Properties, Including Statistics of Measurement and Sampling. American Society of Agronomy, Madison, Wisconsin, pp. 472–484.

Davis, R.H.C., 1971. Frederick I Barbarossa. Encyclopaedia Britannica 9, 822–823.

Gaffney, J.S., 2003. Marvin Wesely. 1944–2003. Bull. Am. Meteorol. Soc. 84, 812–814.

Grover, B.L., 1955. Simplified air permeameters for soil in place. Soil Sci. Soc. Am. Proc. 19, 414–418.

Hartge, K.H., Bohne, H., Schrey, H.P., Extra, H., 1985. Penetrometer measurements for screening soil physical variability. Soil Till. Res. 5, 343–350.

Horn, R., Hartge, K.H., Bachmann, J., Kirkham, M.B., 2007. Mechanical stresses in soils assessed from bulk-density and penetration-resistance data sets. Soil Sci. Soc. Am. J. 71, 1455–1459. http://dx.doi.org/10/2136/sssaj2006.0044.

Institute for Scientific Information, 1979. This week's citation classic: Kanemasu, E.T., Thurtell, G.W., and Tanner, C.B. Design, calibration, and field use of a stomatal diffusion porometer. Plant Physiol. 44, 881–885, 1969. Current Contents, Agr. Biol. Environ. Sci. 10(41); 10.

Intrawech, A., Stone, L.R., Ellis Jr., R., Whitney, D.A., 1982. Influence of fertilizer nitrogen source on soil physical and chemical properties. Soil Sci. Soc. Am. J. 46, 832–836.

Kanemasu, E.T., Thurtell, G.W., Tanner, C.B., 1969. Design, calibration and field use of a stomatal diffusion porometer. Plant Physiol. 44, 881–885.

Kirkham, D., 1973. Soil physics and soil fertility. Bull. Rech. Agron. Gembloux Fac. Sci. Agron. l'État (New Series) 8 (2), 60–88.

Kirkham, D., De Boodt, M., De Leenheer, L., 1959a. Modulus of rupture determination on cylindrical soil core samples. Overdruk uit Mededelingen van de Landbouwhogeschool en de Opzoekingsstations van de Staat te Gent 24 (1), 369–376.

Kirkham, D., De Boodt, M., De Leenheer, L., 1959b. Air permeability at the field capacity as related to soil structure and yields. Overdruk uit Mededelingen van de Landbouwhogeschool en de Opzoekingsstations van de Staat te Gent 24 (1), 377–391.

Lowery, B., Morrison Jr, J.E., 2002. Soil penetrometers and penetrability. In: Dane, J.H., Topp, G.C. (Eds.), Methods of Soil Analysis. Part 4. Physical Methods. Soil Science Society of America, Madison, Wisconsin, pp. 363–388.

Meek, D., 2009. Bertrand Dee Tanner. Bull. Am. Meteorol. Soc. 90, 250 (one page only).

Muhm, D., February 11, 1990. Ames tilth lab delves into mysteries of soil. Des Moines (Iowa) Regist., 1J–2J.

Perumpral, J.V., 1987. Cone penetrometer applications—a review. Trans. ASAE 30, 939–944.

Schaum, D., 1961. College Physics. Schaum Publishing, New York.

Smith, N. DeWolf, Friday May 28, 2004. The road to D-Day. Wall St. J., W8.

SoilTest, 1978a. Corps of Engineers—Cone Penetrometer. Model CN-973. Operating Instructions. SoilTest, Inc., 2205 Lee Street, Evanston, Illinois (SoilTest is now owned by ELE International, P.O. Box 389, Loveland, Colorado 80539.).

SoilTest, 1978b. Classification and Rapid Testing Equipment (Product Bulletin). SoilTest, Inc., 2205 Lee Street, Evanston, Illinois (SoilTest is now owned by ELE International, P.O. Box 389, Loveland, Colorado 80539.).

Sweeney, D.W., Kirkham, M.B., Sisson, J.B., 2006. Crop and soil response to wheel-track compaction of a claypan soil. Agron. J. 98, 637–643.

Tanner, C.B., 1963. Basic Instrumentation and Measurements for Plant Environment and Micrometeorology. Soils Bull, 6. Univ of Wisconsin Soils Dept, Madison (Univ. Microfilms #OP 62 102).

Tanner, C.B., Simonson, R.W., 1993. Franklin Hiram King—pioneer scientist. Soil Sci. Soc. Am. J. 57, 286–292.

Taylor, S.A., Ashcroft, G.L., 1972. Physical Edaphology: The Physics of Irrigated and Nonirrigated Soils. W.H. Freeman, San Francisco.

Topp, G.C., Lapen, D.R., Edwards, M.J., Young, G.D., 2003. Laboratory calibration, in-field validation and use of a soil penetrometer measuring cone resistance and water content. Vadose Zone J. 2, 633–641.

van der Ploeg, R.R., Ehlers, W., Horn, R., August, 2006. Schwerlast auf dem Acker. Spektrum der Wissenschaft (Deutsche Ausbage des Scientific American), pp. 80–88 (In German only).

Walsh, L.M., Kutzbach, J.E., Miller, E.E., Murdock, J.T., Peterson, A.E., 1991. Champ Bean Tanner (1920–1990). Bull. Am. Meteorol. Soc. 72, 1562–1565.

Whiteley, G.M., Utomo, W.H., Dexter, A.R., 1981. A comparison of penetrometer pressures and the pressures exerted by roots. Plant Soil 61, 351–364.

Zink, A., Fleige, H., Horn, R., 2010. Load risks of subsoil compaction and depths of stress propagation in arable Luvisols. Soil Sci. Soc. Am. J. 74, 1733–1742. http://dx.doi.org/10.2136/sssaj2009.0336.

# CHAPTER

# 12

# Oxygen Diffusion Rate

Air and water comprise a large part of the soil. For an average soil, air and water take up 50% of the space (Figure 12.1). Organic matter and mineral matter take up the other 50%. At optimum moisture content for plant growth, the air and water spaces are about equal, each about 25% of the soil volume (Kirkham and Powers, 1972, p. 1). With so much of the soil volume taken up by air and water, it is obvious that air and water play a major part in soil and plant–water relations.

We have looked at methods to measure the soil-water matric potential (tensiometers and pressure plates; see Chapter 5) and to measure mechanical impedance (penetrometers; see Chapter 11). In this chapter, we look at the most widely used method to monitor aeration status of the soil, the oxygen diffusion rate (ODR) method.

## 12.1 THE OXYGEN DIFFUSION RATE METHOD

Respiration by plant roots depends on soil oxygen. Roots, like animals, do not photosynthesize, and they give off carbon dioxide and take in

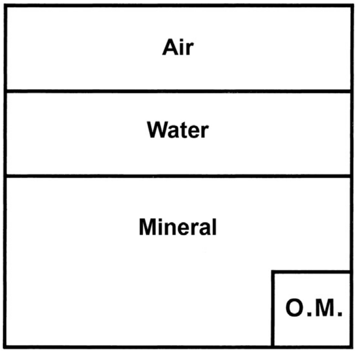

**FIGURE 12.1** Space in a soil. O.M. stands for organic matter. *From Kirkham and Powers (1972). This material is used by permission of John Wiley & Sons, Inc. and William L. Powers.*

*Principles of Soil and Plant Water Relations*
http://dx.doi.org/10.1016/B978-0-12-420022-7.00012-4

Copyright © 2014 Elsevier Inc. All rights reserved.

oxygen during respiration. Diffusion of gases in the soil practically stops when the fraction of air-filled pores is less than 10% (Wesseling and van Wijk, 1957, p. 468) (Figure 12.2). Therefore, roots need at least 10% by volume air space in the soil to survive (Kirkham, 1994).

Evaluation of the aeration conditions at the interface between the root and the soil systems presents the greatest possibility of defining the influence of aeration on plant growth (Phene, 1986). In the process of respiration, plants quickly take up the oxygen surrounding the roots in the rhizosphere, and an increasing oxygen concentration gradient develops between the soil atmosphere and the atmosphere next to the root surrounded by the water film. Movement of oxygen from the atmosphere to a respiring root involves diffusion through the following three phases (Lemon and Erickson, 1952):

1. The gaseous phase of the soil;
2. The gas—liquid phase boundary; and
3. The liquid phase of the water film around the root.

Because the diffusion coefficient of oxygen in water is about $2.4 \times 10^{-5}$ $\text{cm}^2/\text{s}$ and the diffusion coefficient of oxygen in air is about $1.8 \times 10^{-1}$ $\text{cm}^2/\text{s}$, the limiting factor for this transport of oxygen is usually the diffusion rate through the water film rather than through the gas-filled pore space (Phene, 1986). (We can check out how fast one gas diffuses through another by spilling ammonia, for example, in a back corner of a

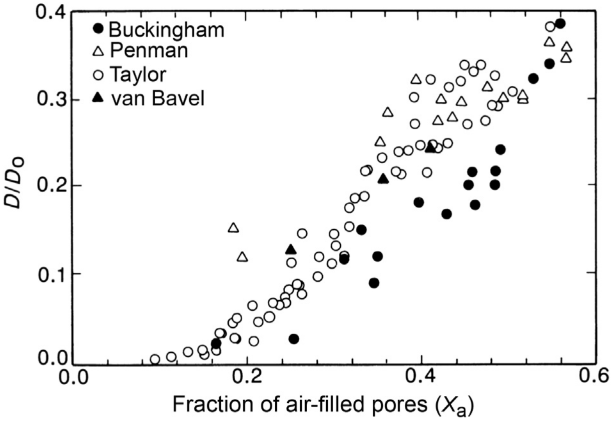

**FIGURE 12.2** Scatter diagram of the relation between the ratio $D/D_o$ and the fraction of air-filled pores $x_a$ calculated from data of Buckingham (1904) (closed circles), Penman (1940) (open triangles), Taylor (1949) (open circles), and van Bavel (1952) (closed triangles). $D_o$ is the coefficient of diffusion of $CO_2$ in still air. $D$ is the coefficient of diffusion of $CO_2$ in the soil. If $x_a$ decreases to 0.1 to 0.2, $D$ appears to become zero. *From Wesseling and van Wijk (1957). Reprinted by permission of the American Society of Agronomy.*

large lecture hall. The speaker would smell the ammonia within a matter of seconds.)

When we are considering oxygen diffusion through air, we need to know the components of air, which are given in Table 12.1 (Weast, 1964, p. F-88). Air contains 20.946% oxygen.

In view of these concepts, a method to measure the ODR through the liquid phase to a reducing surface approximating that of the plant root should be useful for assessment of soil aeration (Phene, 1986). And, indeed, the ODR method is the best index of oxygen availability for plant roots in soil (Gliński and Stępniewski, 1985, p. 189). Direct measurement of the concentration of oxygen in the soil is insufficient to describe plant reactions, as its availability to plants is dependent on other factors (Stępniewski et al., 2005, p. 52), such as the thickness of the liquid layer surrounding the root. The ODR method is advantageous because it simulates a root in the soil. Also, it is easier to measure ODR than the oxygen

**TABLE 12.1** Components of Atmospheric Air (Exclusive of Water Vapor)

| Constituents | Percentage | Parts per Million[1] |
|---|---|---|
| $N_2$ (nitrogen) | 78.084 | |
| $O_2$ (oxygen) | 20.946 | |
| $CO_2$ (carbon dioxide)[2] | 0.033 | |
| Ar (argon)[3] | 0.934 | |
| Ne (neon) | | 18.18 |
| He (helium) | | 5.24 |
| Kr (krypton) | | 1.14 |
| Xe (xenon) | | 0.087 |
| $H_2$ (hydrogen) | | 0.5 |
| $CH_4$ (methane) | | 2 |
| $N_2O$ (nitrous oxide) | | 0.5 |

[1] *1% = 10,000 ppm.*

[2] *The concentration of carbon dioxide is increasing in the atmosphere at a rate of 1–2 ppm/year and has been doing this since the 1980s. This increase is not noted in the 2013–2014* Handbook of Chemistry and Physics *(Haynes, 2013), which lists the components of air as above, except the concentration of oxygen is given as 20.9476% and that of $CO_2$ as 314 ppm or 0.0314%, a value even lower than that in the 1964 handbook (see above; 330 ppm or 0.033%). The concentration of $CO_2$ in the air in 2012 was 392.6 ppm (Hall et al., 2013).*

[3] *Argon, neon, helium, krypton, and xenon are inert gases in Group VIIIA of the periodic table. The sixth element in this group is radon, which is of environmental concern because it is toxic. It is a radioactive gaseous chemical element formed, together with alpha rays, as a first product in the atomic disintegration of radium and used in the treatment of cancer. It is produced naturally in the ground in some regions of the United States and can build up in basements. Homes need to be checked to make sure that they do not have radon.*

*Numbers come from Weast (1964), p. F-88.*

concentration in the soil. Feng et al. (2002) evaluated soil aeration criteria by examining the relationships between ODR and soil—water potential, soil—water content, air-filled porosity, and gas diffusion rate. They concluded that ODR, which mimics the oxygen supply to the root surface, should be used instead of the other measures to evaluate soil aeration status. In the ODR method, developed by Lemon and Erickson (1952), we use a platinum (Pt) microelectrode to simulate the root in an electrolytic solution (the soil water with its dissolved solutes).

## 12.2 ELECTROLYSIS

Because we are dealing with an electrolytic solution, we need to understand electrolysis (Figure 12.3). Electrolysis is defined as the decomposition into ions of a chemical compound in solution by the action of an electric current passing through the solution. In electrolysis, we have the electrolytic solution, an anode, a cathode, and a battery. Electrons flow from the positive terminal, the anode, to the negative terminal, the cathode. The anode is defined as a positive electrode or positive terminal of an electric source. The cathode is defined as the negative pole or electrode of an electrolytic cell. (*Anode* comes from the Greek *anodos*, meaning "a way up", which comes from *ana*, which means "up", and *hodos*, which means "way". *Cathode* comes from the Greek *kathodos*, going down, which comes from *kata-*, which means "down", and *hodos*, which means "way".)

Anions, which are negatively charged, are attracted to the anode, and cations, which are positively charged, are attracted to the cathode. The

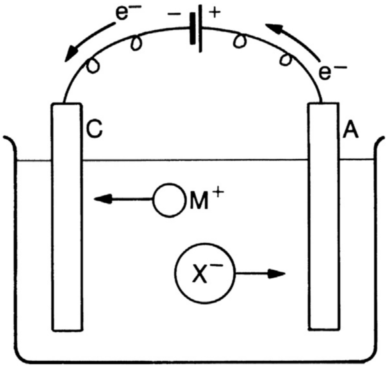

**FIGURE 12.3** Electrolysis. A = anode; C = cathode; battery at top; $X^-$ = anion; $M^+$ = cation. Reduction occurs at cathode. *From Sienko and Plane (1957). This material is reproduced with permission of The McGraw-Hill Companies.*

chemical in a solution, therefore, can be separated into its components (anions going to the anode; cations going to the cathode), if an electrical current passes through the solution. In the ODR method, the root is going to be simulated by a Pt microelectrode, which is the cathode. The root (Pt microelectrode) is a reducing surface. At the cathode, reduction takes place. At the anode, oxidation takes place. Reduction is the gain of electrons, and "to reduce" means to remove $O_2$ from. In oxidation, there is a loss of electrons.

We now need to review the laws of electrolysis. Michael Faraday (1791–1867) (see Appendix for his biography), an English chemist and physicist, who is best known for discovering electromagnetic induction, formulated the laws of electrolysis, which are as follows (Schaum, 1961, p. 169).

## 12.2.1 Faraday's Laws of Electrolysis

1. The mass of a substance liberated or deposited at an electrode is proportional to the quantity of electricity (i.e., to the number of coulombs) that has passed through the electrolyte. The coulomb is named after Charles Augustin de Coulomb (1736–1806), a French physicist. A coulomb is a unit for measuring the quantity of an electric current. It is the amount of electricity provided by a current of one ampere flowing for one second; one ampere = one coulomb per second; in symbols, $I$ (ampere) = $q$ (coulomb)/$t$ (second).
2. The masses of different substances liberated or deposited by the same quantity of electricity are proportional to their equivalent weights. The equivalent weight of an element is its atomic weight divided by its valence. Thus, the equivalent weight of copper is half of its atomic weight for the electrolysis of solutions containing $Cu^{2+}$, because the reaction at the cathode is

$$Cu^{2+} + 2e^- \rightarrow Cu.$$

If a solution of $Cu^+$ were electrolyzed, the equivalent weight of copper would be the same as the atomic weight, because only one electron would be involved in the electrode reaction:

$$Cu^+ + 1e^- \rightarrow Cu.$$

When the equivalent weight of a substance is expressed in grams, it is called the *gram-equivalent weight*.

One *faraday*, or 96,500 coulombs, is the quantity of electricity that will deposit one gram-equivalent weight of any substance. Thus, the mass $m$ in grams of any substance liberated in electrolysis is

$$m = \text{gram} - \text{equivalent weight} \times \text{number of faradays transferred}.$$

## 12.3 MODEL AND PRINCIPLES OF THE ODR METHOD

Let us now consider the model that is assumed in the ODR method (Figure 12.4) (Phene, 1986, p. 1139). As noted, a cylindrical Pt microelectrode simulates the root. Around it are soil particles and the water film, which is right up against the root. The radius of the root (Pt microelectrode) is $a$ and the radius of the root plus the water film is $b$, so the thickness of the water film is the length $(b - a)$.

The governing equations are as follows (Phene, 1986, his Eqn 5):

$$Q/(At) = (D_e c_2)/[a(\ln b - \ln a)] \tag{12.1}$$

where

$Q$ = amount of oxygen flowing to root (g)
$A$ = surface area of electrode ($cm^2$)
$t$ = time (s)
$D_e$ = effective diffusion coefficient of oxygen through the medium surrounding the electrode ($cm^2/s$)
$a$ = radius of root (or of the microelectrode) (cm)
$b$ = radius of root (or of the microelectrode) + water film (cm)
$c_2$ = concentration of oxygen at the liquid–gas interface (radius = $b$) ($g/cm^3$)

We note that there is no $c_1$ in the equation, and this is because $c_1$, the concentration of oxygen at the root surface or at the Pt microelectrode, is considered to be zero, which we shall see later.

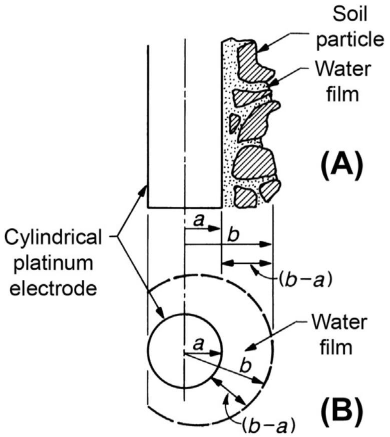

**FIGURE 12.4** The model that is assumed in order to explain microelectrode behavior. (A) Particles and solution separating the electrode from gas-filled pores. (B) Coaxial cylindrical model with water film of mean thickness ($b$–$a$). *From Phene (1986). Reprinted by permission of the American Society of Agronomy.*

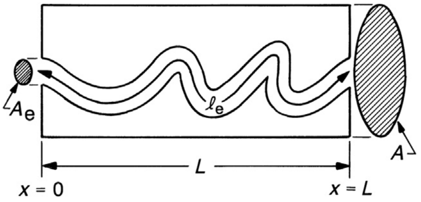

**FIGURE 12.5** Diffusion model relating the actual path length ($l_e$) and area ($A_e$) to the block length ($L$) and cross-section ($A$). *From Troeh et al. (1982). Reprinted by permission of Elsevier, Amsterdam.*

$D_e$ is dependent on the properties of the soil medium surrounding the microelectrode.

$$D_e = D_o\theta(L/L_e)^2 \tag{12.2}$$

where

$D_o$ = the diffusion coefficient of oxygen through pure water
$\theta$ = fraction of the surface area of the microelectrode covered with water as opposed to solid
$L/L_e$ = tortuosity factor of the diffusion path

Troeh et al. (1982) illustrate the effect of tortuosity on diffusion (Figure 12.5). An oxygen molecule must move through the tortuous (twisted) paths of pores in the soil, which is the length $L_e$ (or $l_e$, as shown by Troeh et al., 1982). The length of the way that the crow flies is $L$. The tortuosity factor, therefore, is $L/L_e$ (a ratio and dimensionless).

If the electrical potential of the Pt microelectrode is lowered with respect to a reference electrode (the potential at the reference electrode is known), the oxygen at the microelectrode surface is reduced electrolytically until the oxygen concentration at the surface is zero. The reduction rate and the diffusion rate of oxygen are equal. They must be independent of the voltage. Experimentation shows that the current is independent of the voltage when the applied electrical potential (volts) is between 0.3 and 0.7 V (Figure 12.6). In this range, the current is independent of the voltage and a function only of the diffusion rate of oxygen to the microelectrode surface.

The resulting electrical current is expressed as follows:

$$i = nFAf_{a,t} \tag{12.3}$$

where

$i$ = current (μA)
$n$ = the number of electrons required to reduce one molecule of oxygen ($n = 4$)
$F$ = Faraday constant ($F$ = 96,500 C/mol of oxygen, where C = coulomb)

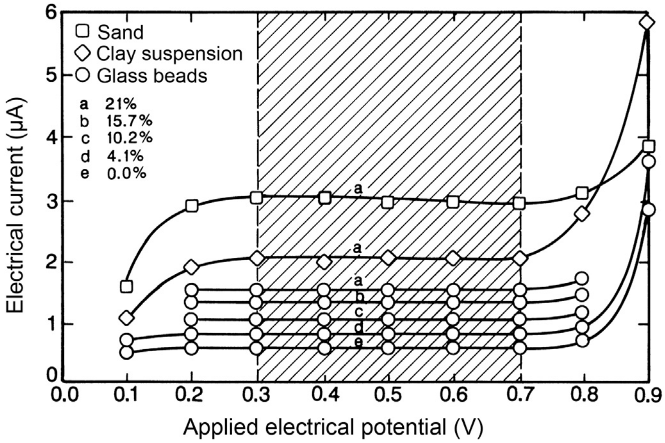

**FIGURE 12.6** Electrical current–voltage relations for water-saturated media: open squares, sand; open diamonds, clay suspension; open circles, glass beads 18 µm median diameter. Letters a–e refer to concentration of $O_2$ in equilibrium with saturating solution. *From Phene (1986). Reprinted by permission of the American Society of Agronomy.*

$A$ = surface area of the microelectrode

$f_{a,t}$ = flux of oxygen at the surface of the microelectrode of radius $a$ at time $t$

The oxygen flux ($f_{a,t}$) is calculated by measuring the steady state current ($i$) after 4 or 5 min, assuming that the rate of oxygen reduction is limited by the rate of oxygen diffusion and equal to it. The transport is strictly a diffusion process.

$$\mathrm{ODR} = f_{a,t} = (i\mathrm{M})/(nFA) = \left[D_o\theta(L/L_e)^2 c_2\right] \Big/ [a(\ln b - \ln a)] \qquad (12.4)$$

where $M$ = molecular weight of oxygen ($M = 32$ g/mol) and is inserted to convert the units from moles to grams.

Substitution of the values for $M$, $n$, and $F$ into Eqn (12.4) gives

$$\mathrm{ODR} = C(i/A)\ \mu\mathrm{g/cm^2/min} \qquad (12.5)$$

where ODR = oxygen diffusion rate ($\mu$g/cm$^2$/min)

$$C = (M60)/(nF) = 0.00497\ \mu\mathrm{g}/\mu\mathrm{A/min}, \qquad (12.6)$$

where A is the SI symbol for ampere (A does not stand for area, as we defined it above).

The 60 is used to convert from seconds to minutes. Remember one coulomb per second is an ampere:

$$(q/t) = I \text{ where } q = \text{coulombs};\ \ t = \text{seconds};\ \text{ and } I = \text{amperes}.$$

Or we can write

$$\begin{aligned}\mathrm{ODR}(\mu\mathrm{g/cm^2/min}) &= (60Mi)/(nFA) = (60 \times 32 \times i)/(4 \times 96,500) \times A \\ &= 0.00497(i/A)\end{aligned} \tag{12.7}$$

where $i$ is the current and $A$ is the surface area of the microelectrode.

Equation (12.5) or (12.7) includes all physical factors that affect the ODR to a single root of constant dimensions similar to that of the Pt microelectrode.

## 12.4 METHOD

For many years (c.1980–2010) in the United States, ODR was determined by using a commercially available soil oxygen diffusion ratemeter available from Jensen Instruments (Tacoma, WA, USA). Jensen Instruments no longer sells the ratemeter as one of its supplies. However, one can construct the equipment based on instructions in the literature (Powers and Kirkham, 1965, pp. 72–73; Farrell et al., 2002). The equipment is easy to make (Witold Stępniewski, personal communication, August 30, 2006, builds the ODR equipment used in his laboratory). The Jensen Instruments Pt microelectrodes have a length of 4.0 mm and a diameter of 0.65 mm. The formula given in Eqn (12.7) then reduces to

$$\mathrm{ODR} = 0.059i(\mu\mathrm{g/cm^2/min}). \tag{12.8}$$

The ODR measurement system consists of the following components (Figure 12.7):

1. The platinum microelectrode (the cathode)
2. The Ag–AgCl half-cell (reference electrode)
3. The anode (Jensen Instruments has a brass anode)
4. The electrical circuit
5. A milliammeter to measure the output current.

Oxidation potentials are available from the literature (for example, see Sienko and Plane, 1957, pp. 600–601), so we know the potential of the reference Ag–AgCl half-cell.

Any spatial arrangement or maximum distance among the three electrodes (cathode, anode, and reference electrode) is permissible, as long as they all contact the same body of soil water. That is, there must be an electrically conductive pathway among electrodes in the soil (Jensen Instruments, 1987). For example, one could not do a split-root experiment, with a root system split between two boxes of soil, and put, say, two electrodes in one soil box and one electrode in the other box. The

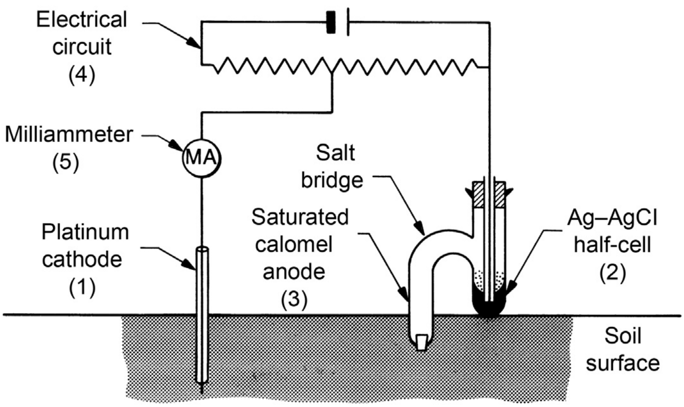

**FIGURE 12.7** Diagram of apparatus used to make in situ soil measurement of $O_2$ diffusion. *From Phene (1986). Reprinted by permission of the American Society of Agronomy.*

electrolytic solution (the soil water with its dissolved ions) must be in common contact with all three electrodes.

Measurements need to be made at the same voltage. A voltage of 0.65 V relative to a Ag—AgCl reference electrode has become a fairly standard voltage for ODR measurements (Jensen Instruments, 1987). The initial current following application of the selected voltage (0.65 V) will be high and will decrease rapidly as oxygen in the immediate vicinity of the microelectrode is depleted. As the current decreases, the rate of decrease will lessen, and the current will tend toward an equilibrium with the rate of oxygen diffusion to the electrodes. After 4 or 5 min, the rate of decrease of the current will be small enough that the current can be observed with sufficient accuracy. The current then is read out on the display. The measurements are simple, and a technician easily can be trained to take the readings. However, they are tedious to take because one needs to wait 4—5 min between each reading.

Let us assume that we measure a current of 7.94 μA with the Jensen Instrument. What is the ODR? Using Eqn (12.8), we find

$$0.059(7.94) = 0.468\ \mu\text{g/cm}^2/\text{min}.$$

We wish to compare this value with others in the literature. We look at values given by Gliński and Stępniewski (1985) in their Figure 20 on page 80 (Figure 12.8). The figure is reproduced by Stępniewski et al. (2005, p. 52). On their ordinate, they give units in μg $O_2/m^2/s$; 50 μg $O_2/m^2/s = 0.3$ μg/cm$^2$/min; 100 μg $O_2/m^2/s = 0.6$ μg/cm$^2$/min; and 150 μg $O_2/m^2/s = 0.9$ μg/cm$^2$/min. So our value of 0.468 μg/cm$^2$/min falls within values they give, and, consequently, seems reasonable. Stępniewski et al. (2005, p. 52) say that ODR values in soils usually vary within the range from 0 to 200 μg/m$^2$/s.

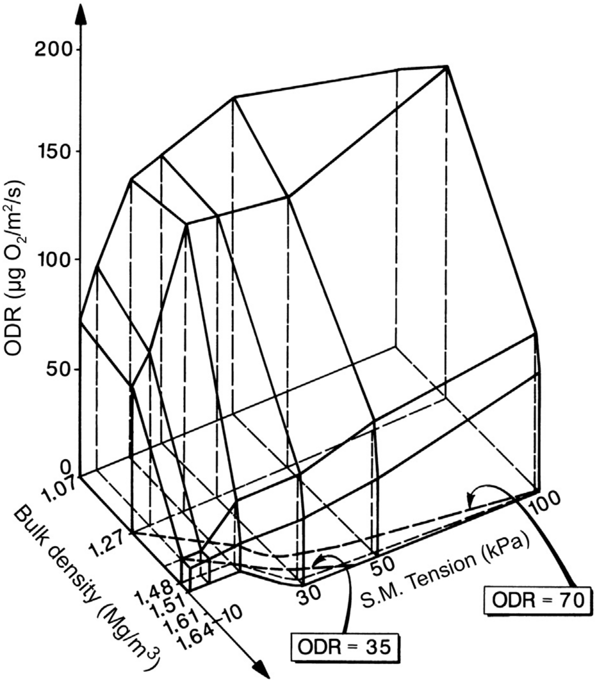

**FIGURE 12.8** Oxygen diffusion rate versus bulk density and soil moisture tension in a loamy textured black earth. *From Gliński and Stępniewski (1985). Reprinted by permission of CRC Press.*

We can also compare our value with those presented by Huang et al. (1998), who studied the effect of temperature and aeration status on creeping bent grass (*Agrostis palustris* Huds.) grown in sand and fritted clay in polyvinyl tubes in a growth chamber. Plants were grown under two temperature regimes (22/15 °C day/night and 35/25 °C day/night) and two soil aeration treatments, a well-aerated one in which the soil oxygen status was maintained at a sufficient level (ODR = 1.5 $\mu g/cm^2/min$) and an overwatered one in which ODR was maintained at a hypoxic level of about 0.2 $\mu g/cm^2/min$ (Figure 12.9). Our ODR value of 0.468 $\mu g/cm^2/min$ again falls within the range of values reported by Huang et al., so we can be reassured that our value is reasonable.

For the factors affecting ODR measurements, see Phene (1986, pp. 1145–1150). Only one factor will be mentioned here: electrode poisoning. This expression is used to indicate anything that can happen to the electrodes other than breakage. Most often, poisoning results from a chemical deposit that changes the characteristics of the Pt surface. Rickman et al. (1968) studied two of the phenomena that cause electrode poisoning: (1) oxide plating at the Pt tip; and (2) the magnitude and nature of the

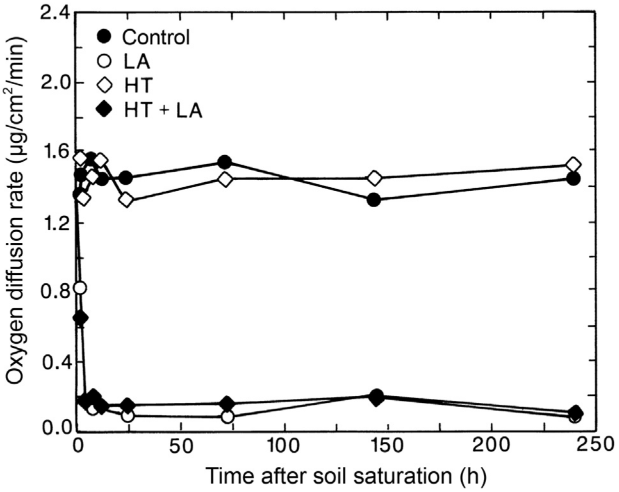

**FIGURE 12.9** Soil aeration status for creeping bent grass expressed as oxygen diffusion rates during the experimental period in the well-aerated and optimum temperature treatment (control), low aeration (LA) treatment, high temperature (HT) treatment, and combination of high temperature and low aeration treatments (HT + LA). *From Huang et al. (1998). Reprinted by permission of the Crop Science Society of America, Madison, Wisconsin.*

poisoning affecting electrodes installed for periods of 4 weeks or more in different soils. They found that salts (principally calcium bicarbonate) and clay particles (principally biotite) were deposited on Pt microelectrodes left in place in a loamy sand for 2 months, and reduced the ODR by an average of 50% when compared to ODRs from periodically reinserted electrodes in the same soil. Devitt et al. (1989) show excellent pictures of electrodes that have been poisoned.

## 12.5 APPENDIX: BIOGRAPHY OF MICHAEL FARADAY

Michael Faraday (1791–1867), who according to Cajori (1929, p. 240–245) was the greatest experimentalist of the nineteenth century in the field of electricity and magnetism, was born on September 22, 1791, at Newington, Surrey, which later became part of the borough of Southwark in south London, but was then in the country. He was the son of a blacksmith. His family was often penniless, sometimes hungry, and his father died before he turned 19 (Morrison, 1991). He, himself, would have said that he was a "natural philosopher" instead of a physicist and chemist (da Costa Andrade, 1971). "My education", he said, "was of the most ordinary description, consisting of little more than the rudiments of reading, writing, and arithmetic at a common day-school. My hours out of school were passed at home and in the streets" (Cajori, 1929).

In 1804, he served as errand boy at a bookstore and bookbindery near his home. The following year, when he was 14 years old, he became an apprentice to the bookbinder. At that time he liked to read scientific books, which happened to pass through his hands. “I made such simple experiments in chemistry,” he said, “as could be defrayed in their expense by a few pence per week, and also constructed an electrical machine” (Cajori, 1929). At the age of 19 years he sometimes in the evening attended lectures given by a Mr Tatum on natural philosophy, his brother paying the admission fee for him. In 1812, he had the good fortune to hear four lectures delivered at the Royal Institution by Sir Humphry Davy, the great English chemist (1778—1829).

About this time, Faraday started to work as a journeyman bookbinder for a Frenchman in London. His new work was uncongenial. “My desire”, he said, “to escape from trade, which I thought vicious and selfish, and to enter into the service of science, which I imagined made its pursuers amiable and liberal, induced me at last to make the bold and simple step of writing to Sir H. Davy, expressing my wishes, and a hope that if an opportunity came in his way he would favor my views; at the same time, I sent the notes I had taken of his lectures” (Cajori, 1929). Davy replied, “I am far from displeased with the proof you have given me of your confidence....” Faraday became Davy’s assistant at the Royal Institution in 1813. In the autumn of that year, Davy and his wife started on a tour abroad, Faraday going with them as amanuensis. Even though Faraday had many menial duties to perform on this trip, he saw much of the active scientific research in Europe, and the trip expanded his view. “His University was Europe; his professors the master whom he served, and those illustrious men to whom the renown of Davy introduced the travellers” (da Costa Andrade, 1971).

After being with Davy in France, Italy, and Switzerland, he returned to the Royal Institution in 1815. Soon after his return he began original researches, and published his first paper in 1816. He also began to lecture before the City Philosophical Society. In a letter he wrote about “the glorious opportunity I enjoy of improving in the knowledge of chemistry and the sciences with Sir H. Davy”. In 1821, in his 30th year, Faraday married and brought his wife to his rooms at the Royal Institution, where they lived together for 46 years. They had no children. In 1824, he was elected member of the Royal Society at a time when Davy was its president, in spite of Davy’s jealous opposition to Faraday’s election (Cajori, 1929). In 1823, Faraday had liquefied chlorine, which aroused the jealousy of Davy, who considered that he had initiated the work and was entitled to the credit (da Costa Andrade, 1971). Nevertheless, Faraday always spoke with respect and admiration for the talents of the man who had done so much to start him in his early scientific career (Cajori, 1929).

In 1825, Faraday made a chemical discovery of the first importance by isolating benzene from a liquid obtained in the production of oil gas (da Costa Andrade, 1971). In that same year Faraday's position at the Royal Institution was improved by his promotion to the post of director of the laboratory. The next year he began to give formal lectures for the members of the Institution on Friday evenings, and those Friday evening discourses have continued ever since (da Costa Andrade, 1971). He also initiated the Christmas lectures for young people, known formally as Christmas Courses of Lectures Adapted to a Juvenile Auditory, of which he himself gave 19 courses. As an inspiring lecturer and deviser of effective lecture experiments Faraday was supreme, and there are many contemporary accounts of the interest and enthusiasm that his discourses aroused.

Faraday's conceptions of electric and magnetic force and their interrelations, expressed in terms of his lines of force, were fundamental. It was from them that James Clerk Maxwell (Scottish physicist, 1831–1879) developed his equations and the concept of electromagnetic waves, which lie at the base of all modern theories of electromagnetic phenomena (da Costa Andrade, 1971).

Cajori (1929, pp. 244–245) says:

> Faraday's first magnetoelectric apparatus, the forerunner of the dynamo, produced such insignificant results that Faraday after lecturing upon it, was asked what on earth was the use of it. A church dignitary had a conception of its dangerous possibilities in the hands of incendiaries, and deplored the discovery. Knowledge antedates understanding.… We live forward, but we understand backwards.…There is an aspect here of our physical research that is often lost sight of, namely, the small proportion of successful discoveries compared with the number of investigators. Certainly the number of unsuccessful attempts, even in the case of those fortunate individuals who make the great discoveries, is very much greater than the number of their successful attempts. Faraday's reputed satisfaction with 1/10 percent return comes to mind.

Faraday was a Sandemanian (Cantor, 1991), a Christian group prevalent in the Pennines (hills in northern England on the Scottish border) that has now died out. Tanford (1991) says: "There is no question about Faraday's faith and that it guided him when addressing moral issues, but Faraday himself never claimed a connection with his scientific work and indeed emphasized the need to separate religious and ordinary beliefs in an 1854 lecture."

It was shortly after his work on electromagnetic induction that Faraday, always in search of unity, showed that the five kinds of electricity then distinguished—frictional, galvanic, voltaic, magnetic (induced current), and thermal—were fundamentally the same. In this same period of his researches (c.1831–1844), he arrived at the basic laws of electrolysis that bear his name, and introduced the terms that are universally used: anode, cathode, anion, cation, and electrode.

In 1858, he retired to live near Hampton Court, Surrey, but retained a lively interest in science. His health gradually waned, and there he died on August 25, 1867. Faraday was possibly the greatest experimental genius the world has known (da Costa Andrade, 1971). He was incessantly prompted by the belief that certain fundamental relations were waiting to be found. He was not dismayed by dozens of fruitless experiments, and he persisted until basic discoveries were established. To all his other gifts he added the ability to describe his ideas in clear and simple language. Five books about Faraday were published in 1991 and 1992, and have been reviewed by Hunt (1992).

## References

Buckingham, E., 1904. Contributions to our knowledge of the aeration of soils. USDA Bur. Soils Bull. 25, 52.

Cajori, F., 1929. A History of Physics. Macmillan, New York.

Cantor, G., 1991. Michael Faraday: Sandemanian and Scientist. A Study of Science and Religion in the Nineteenth Century. St. Martin's, New York.

da Costa Andrade, E.N., 1971. Faraday, Michael. In: Encyclopaedia Britannica, vol. 9, 66–67.

Devitt, D.A., Stolzy, L.H., Miller, W.W., Campana, J.E., Sternberg, P., 1989. Influence of salinity, leaching fraction, and soil type on oxygen diffusion rate measurements and electrode "poisoning". Soil Sci. 148, 327–335.

Farrell, R.E., De Jong, E., Elliott, J.A., 2002. Gas sampling and analysis. In: Dane, J.H., Topp, G.C. (Eds.), Methods of Soil Analysis. Part 4. Physical Methods. Soil Science Society of America, Madison, Wisconsin, pp. 1076–1111.

Feng, T., Wu, L., Letey, J., 2002. Evaluating aeration criteria by simultaneous measurement of oxygen diffusion rate and soil-water regime. Soil Sci. 167, 495–503.

Gliński, J., Stępniewski, W., 1985. Soil Aeration and Its Role for Plants. CRC Press, Boca Raton, Florida.

Hall, B.D., Dlugokencky, E.J., Montzka, S.A., Dutton, G., Mühle, J., Elkins, J.W., 2013. Long-lived greenhouse gases. In: Blunden, J., Arndt, D.S. (Eds.), State of the Climate in 2012. Bull. Am. Meteorol. Soc. 94 (8), S31–S33.

Haynes, W.M. (Ed.), 2013. CRC Handbook of Chemistry and Physics, ninty fourth ed. CRC Press, Boca Raton, Florida.

Huang, B., Liu, X., Fry, J.D., 1998. Shoot physiological responses to two bent grass cultivars to high temperature and poor soil aeration. Crop Sci. 38, 1219–1224.

Hunt, B.J., 1992. Faraday at home and abroad. Nature 256, 1059–1060.

Jensen Instruments, 1987. Operating Instructions. Soil Oxygen Diffusion Ratemeter, Model D. 10 pp. Received 15 Sept. 1987 from Jensen Instruments, 2021 South Seventh Street, Tacoma, Washington 98405-3014.

Kirkham, D., Powers, W.L., 1972. Advanced Soil Physics. Wiley, New York.

Kirkham, M.B., 1994. Streamlines for diffusive flow in vertical and surface tillage: a model study. Soil Sci. Soc. Am. J. 58, 85–93.

Lemon, E.R., Erickson, A.E., 1952. The measurement of oxygen diffusion in the soil with a platinum microelectrode. Soil Sci. Soc. Am. Proc. 16, 160–163.

Morrison, P., 1991. Nothing is too wonderful to be true. Book Reviews Sci. Am. 265 (4), 129–133.

Penman, H.L., 1940. Gas and vapor movement in the soil. Int. J. Agr. Sci. 30, 437–462.

Phene, C.J., 1986. Oxygen electrode measurement. In: Klute, A. (Ed.), Methods of Soil Analysis. Part 1. Physical and Mineralogical Methods, second ed. American Society of Agronomy, Soil Science Society of America, Madison, Wisconsin, pp. 1137–1159.

Powers, W.L., Kirkham, D., 1965. Soil Physics Laboratory Manual (Unpublished laboratory manual). Iowa State University, 76 pp. (Available from Kirkham, M.B. Department of Agronomy, Kansas State University, Manhattan, Kansas).

Rickman, R.W., Letey, J., Aubertin, G.M., Stolzy, L.H., 1968. Platinum microelectrode poisoning factors. Soil Sci. Soc. Am. Proc. 32, 204−208.

Schaum, D., 1961. Theory and Problems of College Physics, sixth ed. Schaum Publishing, New York.

Sienko, M.J., Plane, R.A., 1957. Chemistry. McGraw-Hill, New York.

Stępniewski, W., Stepniewska, Z., Bennicelli, P.R., Gliński, J., 2005. Oxygenology in Outline. EU 5th Framework Program, QLAM-2001−00428. Institute of Agrophysics, Lublin, Poland.

Tanford, C., 1991. Religious resonances. Book Review of Michael Faraday: Sandemanian and Scientist. By Geoffrey Cantor. Macmillan, New York. 359 pp Nature 351, 705.

Taylor, S.A., 1949. Oxygen diffusion in porous media as a measure of soil aeration. Soil Sci. Soc. Am. Proc. 14, 55−61.

Troeh, F.R., Jabro, J.D., Kirkham, D., 1982. Gaseous diffusion equations for porous materials. Geoderma 27, 239−253.

van Bavel, C.H.M., 1952. Gaseous diffusion and porosity in porous media. Soil Sci. 73, 91−96.

Weast, R.C., 1964. Handbook of Chemistry and Physics. Chemical Rubber Co, Cleveland, Ohio.

Wesseling, J., van Wijk, W.R., 1957. Soil physical conditions in relation to drain depth. In: Luthin, J.N. (Ed.), Drainage of Agricultural Lands. American Society of Agronomy, Madison, Wisconsin, pp. 461−504.

C H A P T E R

# 13

# Infiltration

In previous chapters we have introduced fundamental concepts about water in soil, including static water in soil and water movement in saturated soil. In this chapter we consider infiltration, the tension infiltrometer, and four soil characters (unsaturated hydraulic conductivity, sorptivity, repellency, and mobility) that we can measure with the tension infiltrometer.

## 13.1 DEFINITION OF INFILTRATION

*Infiltration rate* may be defined as the meters per unit time of water entering into the soil regardless of the types or values of forces or gradients. The term *hydraulic conductivity*, which has been defined as the meters per day of water seeping into the soil under the pull of gravity or under a unit hydraulic gradient, should not be confused with infiltration rate. Infiltration rate need not refer to saturated conditions. If two raindrops of total volume $2\ \mathrm{mm}^3 = 0.000002\ \mathrm{m}^3$ fall per day on a square meter of soil and are absorbed into the soil, the infiltration rate is 0.000002 m/day.

Water entry into soil is caused by matric and gravitational forces. Therefore, this entry may occur in the lateral and upward directions as well as the downward one (Baver et al., 1972, p. 365). Infiltration normally refers to the downward movement. The matric force usually predominates over the gravitational force during the early stages of water entry into soil, so that observations made during the early stages of infiltration are valid when considering the absence of gravity.

If water infiltrates into a dry soil, a definite *wetting front*, also called a *wet front*, can be observed. This is the boundary between the wetted upper part of the soil and the dry lower part of the soil. If water is infiltrating into soil contained in a clear plastic column, one can observe the progress of the wet front and mark wet fronts as they change with time (Figure 13.1). At present, it is impossible to measure the matric potential exactly at the

http://dx.doi.org/10.1016/B978-0-12-420022-7.00013-6

Copyright © 2014 Elsevier Inc. All rights reserved.

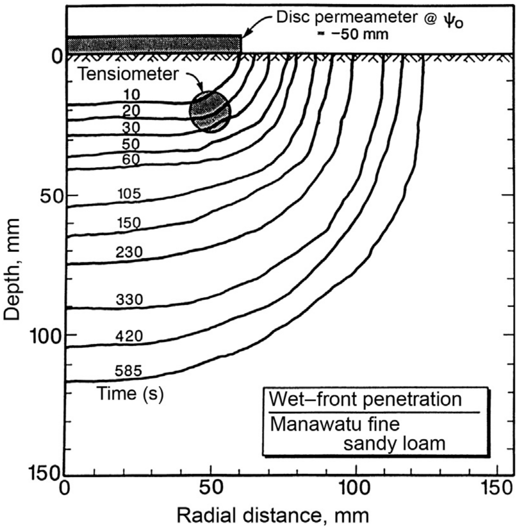

**FIGURE 13.1** Wet fronts for a sandy loam soil. *From Kirkham, M.B., Clothier, B.E., ©1994a. Ellipsoidal description of water flow into soil from a surface disc. Trans. Int. Congr. Soil Sci. 2b, 38–39. Reprinted by permission of The International Society of Soil Science.*

wet front, because it progresses too rapidly into the soil. However, one can measure the amount of water infiltrated and the depth and shape of the wet front, and come to important conclusions about the entry of water into the soil. Infiltration is extremely important, because it determines not only the amount of water that will enter a soil, but also the entrainment of the "passenger" chemicals (nutrients and pollutants) dissolved in it.

## 13.2 FOUR MODELS OF ONE-DIMENSIONAL INFILTRATION

Four models for infiltration into the soil have been developed. They all deal with one-dimensional, downward infiltration into the soil (Baver et al., 1972; pp. 366–371).

### 13.2.1 Lewis Equation

From work initiated in 1926, Mortimer Reed Lewis, an irrigation engineer at Oregon State College, used the following equation for infiltration:

$$I = \gamma t^a \tag{13.1}$$

where $I$ is the cumulative infiltration between time zero and $t$, and $\gamma$ and $a$ are constants. The *cumulative infiltration* is the total volume of water infiltrated per unit area of soil surface during a specified time period (Soil

Science Society of America, 2008). It has units such as length (e.g., centimeters). Note that infiltration rate has units of length per unit time (e.g., centimeters per second). Equation (13.1) has been erroneously attributed to A.N. Kostiakov, and often appears in the literature as the "Kostiakov" equation (Swartzendruber, 1993). The parameters in Eqn (13.1) are evaluated by fitting the model to experimental data. By definition, the infiltration rate $i = \mathrm{d}I/\mathrm{d}t$. Thus, the infiltration rate for the Lewis equation is given by

$$i = a\gamma t^{a-1}. \tag{13.2}$$

The Lewis equation has no physical basis. Exponential relations are simple and useful and can cover a wide range of values. They are often the first ones thought of by scientists when trying to describe a process (Don Kirkham, personal communication, undated).

### 13.2.2 Horton Equation

In the 1930s, Robert E. Horton, a pioneer in the study of infiltration in the field, developed the following equation:

$$i = i_\mathrm{f} + (i_\mathrm{o} - i_\mathrm{f})\exp(-\beta t) \tag{13.3}$$

where $i_\mathrm{o}$ is the initial infiltration rate at $t = 0$, $i_\mathrm{f}$ is the final constant infiltration rate that is achieved at large times, and $\beta$ is a soil parameter that describes the rate of decrease of infiltration.

Horton felt that the reduction in infiltration rate with time was largely controlled by factors operating at the soil surface. These included swelling of soil colloids and the closing of small cracks, which progressively sealed the soil surface. He also recognized that a bare soil surface was compacted by raindrops, but crop cover mitigated their effect. Horton's field data showed that the infiltration rate eventually approached a constant value, which was often somewhat smaller than the saturated permeability of the soil. The latter observation was thought to be due to air entrapment.

### 13.2.3 Green and Ampt Equation

The preceding models are empirical. W. Heber Green and G.A. Ampt in Australia published in 1911 an infiltration equation that was based on a simple physical model of the soil. It has the advantage that the parameters in the equation can be related to physical properties of the soil. Physically, Green and Ampt assumed that the soil was saturated behind the wetting front and that one could define some "effective" matric potential at the wetting front. During infiltration, if the soil surface is held at a constant matric potential or head $h_\mathrm{o}$ with associated water content $\theta_\mathrm{o}$ (e.g., by ponding water over it), water enters the soil behind a sharply defined wet front that moves downward with time (Figure 13.2(A)) (Jury et al., 1991, pp. 131–134). Green and Ampt replaced this process with one that has a discontinuous change in water content at the wetting front (Figure 13.2(B)). In addition, they made the following assumptions: (1) The soil in the wetted region has constant properties ($K_o$, $\theta_o$, $D_o$, $h_o$, where $K_o$ and $D_o$ are the hydraulic conductivity and soil water diffusivity in the Green–Ampt model, respectively) and (2) the matric potential (head) at the moving front is constant and equal to $h_F$. *Soil water diffusivity* is the unsaturated hydraulic conductivity times the rate of change of soil matric potential with water content. It has units of square millimeters per second. In the 1930s, Ernest Childs in England pointed out that, under unsaturated conditions, water moves according to diffusion equations. It is beyond the scope of this book to discuss the theory of water flow in unsaturated soils, in which partial differential equations are used. However, for a brief, general description, see Kirkham (1994), and for a description that requires calculus, see Jury and Horton (2004, p. 105).

The Green–Ampt model can be used to calculate the infiltration rate into a horizontal soil column initially at a uniform water content $\theta_i$ such that $\theta_o > \theta_i$ and an associated matric potential or head $h_o$ maintained at the entry surface for all times >0. Using the assumptions of the model and Darcy's law, the following equation can be derived:

$$i = (\mathrm{d}I/\mathrm{d}t) = \Delta\theta(D_o/2t)^{1/2} \tag{13.4}$$

where $i =$ infiltration rate; $I =$ infiltration; $t =$ time; $\Delta\theta = \theta_o - \theta_i > 0$, $D_o = K_o\Delta h/\Delta\theta$ is the soil water diffusivity of the wet soil region $0 < x < L$, the depth of the wetting front, and $\Delta h = h_o - h_F > 0$, and $K_o$ is the constant hydraulic conductivity of the wet region, and $h_F$ is the matric potential or head of the moving front. Note in this model that the infiltration rate into the soil is proportional to $t^{-1/2}$. A similar expression is obtained for infiltration into a vertical soil column at short times after infiltration begins.

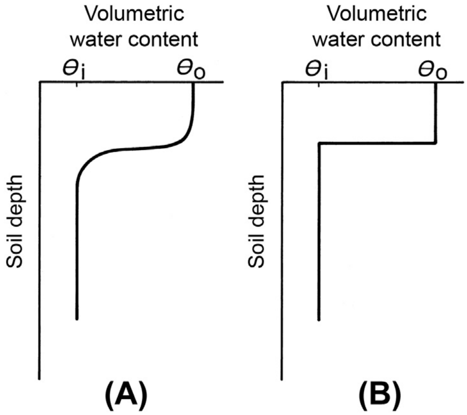

**FIGURE 13.2** Water content profiles during infiltration. (A) A profile that actually occurs during infiltration. (B) A profile corresponding to the Green–Ampt infiltration model. *From Jury, W.A., Gardner, W.R., Gardner, W.H., ©1991. Soil Physics, fifth ed. John Wiley & Sons, New York, p. 132. This material is used by permission of John Wiley & Sons, Inc.*

The model has been used as a conceptual aid in visualizing a complex process. Indirect evaluation of $h_F$ has permitted the model to be used in practical applications.

### 13.2.4 Philip Infiltration Model

J.R. Philip in 1957 suggested an approximate algebraic equation (based on sound physical reasoning) for vertical infiltration under ponded conditions. (See the Appendix, Section 13.11, for a biography of Philip.) The equation, which is simple yet physically well founded, is as follows:

$$I = St^{1/2} + At \tag{13.5}$$

where $I$ is the cumulative infiltration (millimeters), $S$ is the sorptivity (millimeters hour$^{-1/2}$), and $A$ is an empirical constant (millimeters per hour). The first term on the right-hand side of Eqn (13.5) gives the gravity-free absorption into a ponded soil due to capillarity and adsorption. The second term represents the infiltration due to the downward force of gravity. $S$ and $A$ may be found empirically by fitting Eqn (13.5) to infiltration data. Alternatively, these parameters may be derived from the hydraulic properties of the soil. This is not possible for other empirical infiltration equations. For horizontal (gravity-free) infiltration, cumulative infiltration $I$ is given by

$$I = St^{1/2} \tag{13.6}$$

## 13.3 TWO- AND THREE-DIMENSIONAL INFILTRATION

The previous discussion dealt with one-dimensional infiltration in which water is assumed to flow vertically (or more rarely horizontally) into the soil. Multidimensional infiltration theory is an area of soil physics research dominated by the works of J.R. Philip, who published on the topic in a major paper in 1969. Sequels to his work have been carried out by Raats (1971) in the Netherlands and Wooding (1968) in New Zealand.

According to Jury et al. (1991, p. 143), Wooding (1968) derived an approximate expression for the steady rate of infiltration from a circular pond of radius $r_o$, overlying a soil in which the hydraulic conductivity-matric potential function was assumed to be

$$K(h) = K_o \exp(\alpha h) \tag{13.7}$$

where $K_o$ and $\alpha$ are constants representing the soil properties and $h$ is the matric potential (head). Wooding (1968) says that the parameter $\alpha$ is defined as the logarithmic derivative of the hydraulic conductivity with respect to capillary potential (what we now call matric potential). Since

$K = K_o$ when $h = 0$, $K_o$ represents the saturated hydraulic conductivity of a soil. Using this expression and a simplified form of the three-dimensional water flow equation, Wooding derived the following equation for the steady infiltration flux rate:

$$i_f = K_o[1 + (4/\pi\alpha r_o)]. \tag{13.8}$$

(Note that in the equation on p. 143 of Jury et al. (1991), there is a mistake. The last symbol, $r_o$ is squared in Jury et al. This is incorrect. Wooding's equation is written correctly in Eqn (13.8) above. Wooding's equation is written correctly, but using different symbols, in Jury and Horton (2004, p. 136).) It is notable that, contrary to one-dimensional flow, the final infiltration rate in Wooding's equation (Eqn (13.8)) exceeds $K_o$. This occurs because water may enter and move laterally as well as vertically.

Multidimensional infiltration models have utilized difficult mathematics. However, practical advances in infiltration can be made with simple models. For example, a simple, ellipsoidal description of the pattern of wetting to approximate the depth to the wetting front underneath a disc permeameter, set at $\Psi_o$ and supplying water to soil initially at water content $\theta_n$, will be described in Section 13.10 of this chapter.

## 13.4 REDISTRIBUTION

The term *redistribution* refers to the continued movement of water through a soil profile after irrigation or rainfall has stopped at the soil surface. Redistribution occurs after infiltration and is complex, because the lower part of the profile ahead of the wet front will increase its water content and the upper part of the profile near the surface will decrease its water content, after infiltration ceases. Thus, hysteresis can have an effect on the overall shape of the water content profile. See Jury et al. (1991, p. 144–151) or Jury and Horton (2004, p. 147–155) for a discussion of redistribution and figures illustrating it.

## 13.5 TENSION INFILTROMETER OR DISC PERMEAMETER

Recognition of the importance of macropores and preferential flow has led to the development of instruments that can be used in the field to control preferential water flow through macropores and soil cracks. Let us first define macropores and see their size in relation to other soil pores. Pores in the soil can be classified into five categories (Clothier, 2008): macropores, with diameters ranging from 75 to >5000 μm; mesopores with diameters ranging from 30 to 75 μm; micropores with diameters ranging from 5 to 30 μm; ultramicropores with diameters ranging from 0.5 to 5 μm; and cryptopores with diameters <0.1 μm. Xylem vessels, by comparison, range in diameter from 8 to 500 μm, with 40 μm a reasonable value to use in calculations (Nobel, 1983, p. 493).

The first practical instrument to control macropore flow was developed in 1981 by Brent E. Clothier of New Zealand and Ian White of Australia (Clothier and White, 1981). This simple instrument was known as the sorptivity tube (Figure 13.3), then as the tension infiltrometer, and later still it evolved into the disc permeameter (Figure 13.4), as described by Perroux and White (1988). Originally, the term "disc permeameter" was used when three-dimensional infiltration was being considered, and the term "tension infiltrometer" was used when one-dimensional infiltration was being considered, but today the terms are used interchangeably. One must state if one is considering one-dimensional or three-dimensional flow when using the instruments. With these instruments, the amount of macropore flow measured is controlled by applying water to soil at water potentials $\Psi_o$, less than 0. The maximum diameter of vertical pores, connected to the soil surface, through which

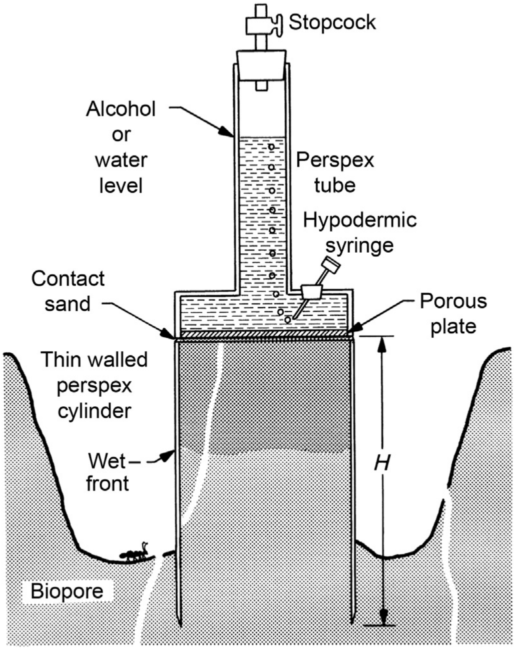

**FIGURE 13.3** The sorptivity tube. An ant hole of greater than 0.75 mm in diameter is shown, which has no effect on the infiltration process. $H = 9.5$ cm. The original sorptivity tube was made out of glass. Alcohol can be put in the glass supply tower to determine if a soil is repellent. *From Clothier, B.E., White, I., ©1988, Soil Science Society of America. Reprinted by permission of the Soil Science Society of America.*

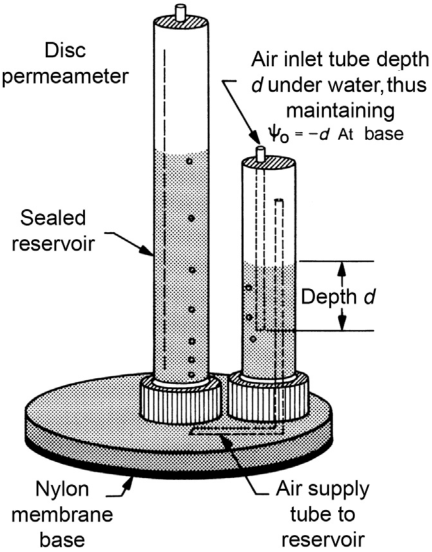
Disc permeameter
Air inlet tube depth d under water, thus maintaining Ψo = −d At base
Sealed reservoir
Depth d
Nylon membrane base
Air supply tube to reservoir

**FIGURE 13.4** The disc permeameter. *From a talk given by Brent E. Clothier at the International Soil Science Congress, Acapulco, Mexico, July, 1994. The paper from the Congress is published as Clothier et al., 1994; but the figure is not published in the paper. Reprinted by permission of Brent E. Clothier.*

water can enter is given by the capillary rise equation (also given in Chapter 6 as Eqn 6.9):

$$h_c = (2\sigma \cos \alpha)/(r\rho g), \tag{13.9}$$

where $\sigma$ = surface tension (surface tension coefficient) of the liquid (units of grams per square second or dynes per centimeter); $\alpha$ = contact angle between the liquid and tube; $r$ = radius of tube (centimeter); $\rho$ = density of liquid (grams per cubic centimeter); and $g$ = acceleration due to gravity (centimeters per square second).

This maximum diameter is proportional to the matric potential, $(-\Psi_o)^{-1}$. The more negative the $\Psi_o$, the smaller the maximum diameter of a pore that can participate in flow from the soil surface. These two instruments (tension infiltrometer and disc permeameter) are being used to supply water to soil in situ at readily selectable zero or negative pressures. A "ready reckoner" of the relationship between the negative pressure $\Psi$, where $\Psi$ is in terms of energy per unit weight (in centimeters of $H_2O$ head), and the capillary diameter $d$ in millimeters is $-3/d$ (Clothier, 2008). For example, a 4-cm head will fill pores up to 0.75 mm.

In Figure 13.4 we see that a disc permeameter consists of two towers: one that is open to the air and one that is sealed off from the air. The one that is sealed off from the air supplies water to the soil under tension. The amount of tension is determined by the depth, *d*, that the air-inlet tube is below the water surface. The two towers are connected by an air-supply tube to the reservoir at the bottom. But note that the bubble tower (with air-inlet tube) is not connected to the reservoir. Hence, one needs only to replenish the reservoir with a tracer solution such as KBr, when determining mobility (see Section 13.9). The nylon membrane base determines the tension that can be held, and it is similar to the porous cup on a tensiometer. The amount of tension that a tensiometer can hold is determined by the size of the pores in the ceramic cup. The smaller the pores, the more tension that can be held. The nylon membrane used in the type of disc permeameter shown in Figure 13.4 is Nybolt Nylon Monofil Mesh, Reference PA40/23, 40 μm opening and 23% free surface, purchased from Ure Pacific, Auckland, New Zealand (Kirkham and Clothier, 2000).

The maximum tension that a tension infiltrometer can hold is about −150 mm, but on a good day it can hold −200 mm (B.E. Clothier, personal communication, October 18, 1996). Although this might not seem like much compared to 1 bar (−1020 cm water), when we consider the height of water being held (15−20 cm), this is a significant amount of water.

Remember that we are infiltrating water into soil under tension, but the pores are filled with water. The water in the pores is under tension. Whether the water under the tension infiltrometer is part of the vadose zone depends on the definition of the term. The *Glossary of Soil Science Terms* (Soil Science Society of America, 2008) defines *vadose zone* as "The aerated region of soil above the permanent water table". Sometimes it is defined as the "unsaturated" zone. The *Glossary*'s definition would not include the water under a tension infiltrometer. The water under a tension infiltrometer is similar to water in the falling-water-table situation, when the water table has fallen below the soil surface, and the capillary tubes (soil pores) hold water under tension (see Figure 6.9). When the water table is at the soil surface, the water is not under tension. Under these conditions, or saturated conditions with no tension, Darcy's law applies.

When using the tension infiltrometer, vegetation is scraped away from the soil and a thin layer of contact sand is put between the tension infiltrometer and the soil surface, as shown in Figure 13.3. When set up this way, tension-disc infiltrometry is a practical means for hydraulic characterization of soil close to saturation (Angulo-Jaramillo et al., 1997). The tension infiltrometer is used to determine the unsaturated hydraulic conductivity and sorptivity; the repellency of soils; and the mobility of chemicals through the soil, which we shall discuss in Sections 13.7−13.9, respectively.

The tension infiltrometer is sold in the United States by Soil Measurements Systems (SMS), Tucson, Arizona, with a system patented by Iowa State University (Ankeny et al., 1989). SMS pays a royalty to Iowa State University for sale of the equipment. SMS makes two models, one with an 8-cm-diameter base plate and one with a 20-cm base plate. The reason the equipment could be patented was because Ankeny et al. (1989) added an adjustment to the bubble tower to provide variable tension. The Clothier and White (1981) and Perroux and White (1988) models (Figures 13.3 and 13.4; not patented) have only one air-inlet tube and provide only one tension, but a tension that can be adjusted by moving the air-inlet tube up and down in the water reservoir. The Ankeny et al. (1989) model has three air-inlet tubes. Two are clamped off while the third tension is used.

## 13.6 MINIDISK INFILTROMETER

The minidisk infiltrometer is made by Decagon Devices (Pullman, WA, USA). The original minidisk infiltrometer, first sold in 1997, consists of a plastic tube, 22.5 cm long and 3.1 cm in outside diameter, marked with milliliter gradation (0–100 ml), a rubber stopper placed in the top, and a styrofoam-looking base that holds the tension. One-half centimeter above the base is an air-inlet tube. It infiltrates water at a set suction (tension) of 2.0 cm and has a radius of 1.59 cm. Decagon Devices developed two more minidisk infiltrometers at set suctions of 0.5 and 6.0 cm (each with a radius of 1.59 cm). The minidisk infiltrometer is especially suited for greenhouse work with pots, even though it can also be used in the field. The hydraulic conductivity of soil can be measured with it using the method of Zhang (1997).

What the base is made out of is proprietary information, but it corresponds to the nylon membrane at the bottom of the tension infiltrometer. The base of the minidisk infiltrometer can get clogged when working on organic soils, such as occurred in the experiments of Kirkham and Clothier (2000), but the disk can be modified by puncturing the bottom with small needle holes and replacing the tension it held with the nylon used in the tension infiltrometer designed by Clothier and White (1981). Kirkham and Clothier (2000) did this modification to maintain functionality of the minidisk infiltrometer. The original base was not removed because it was necessary to have a base to place on the soil during infiltration.

The tension of 2 cm is established by the length of the plastic tube inserted near the bottom of the infiltrometer. There are two forces that balance out to establish the 2 cm. First, there is a gravitational head that must be offset. This is the height of the air entry point from the base of the minidisk. This head is offset by the capillarity of the thin plastic tube, plus the hydraulic resistance of the length of the tube. Personnel at Decagon Devices have worked out this length, so that the tension is 2 cm (B.E. Clothier, personal communication, March 28, 2001).

Some people have misunderstood the minidisk infiltrometer and think that water in it is under pressure. Water is not under pressure, but has to be under tension; if it were under pressure, the water would jump out of the tube. To get water into the infiltrometer before a run, one places the minidisk infiltrometer in a large bucket of water and plugs the top with the rubber stopper. The water stays in the minidisk infiltrometer until it is placed on soil, when it is then sucked out of the tube.

The minidisk infiltrometer has the advantage of being portable. It can be carried to any soil on the globe in a purse or carry-on suitcase, where it can be used to determine the hydraulic conductivity of the soil. No checking of baggage is needed, as for the larger versions of the tension infiltrometer.

## 13.7 MEASUREMENT OF UNSATURATED HYDRAULIC CONDUCTIVITY AND SORPTIVITY WITH THE TENSION INFILTROMETER

Even though the minidisk infiltrometer can be used to get hydraulic conductivity, the tension infiltrometer (Figure 13.4) is more widely used. Two methods can be used to get unsaturated hydraulic conductivity with the tension infiltrometer: the method of Smettem and Clothier (1989) and the method of Ankeny et al. (1991). In the Smettem and Clothier method, two tension infiltrometers with different radii are used to get both unsaturated hydraulic conductivity and sorptivity. In their method, two equations with two unknowns (unsaturated hydraulic conductivity and sorptivity) are solved simultaneously. The Ankeny et al. (1991) method requires the use of the equation developed by Gardner (1958) to get the relationship between the hydraulic conductivity and water content. In both methods, three-dimensional infiltration is assumed and the Wooding equation is used. For the Wooding equation to be used, infiltration must be at steady state. Thus, before either method is used, one must make sure that the water is infiltrating into the soil at steady state (i.e., the infiltration rate, millimeters per second, is a constant value). Let us first look at sorptivity, because we will be determining it along with hydraulic conductivity when we consider the method of Smettem and Clothier (1989).

The concept of sorptivity comes from the theoretical work that Philip (1969) did on infiltration. The sorptivity of a soil is a measure of the ability of the soil to attract water by capillary action. When considering sorptivity, think of the soil as a sponge. Each soil (sponge) has its ability to absorb water. The units of sorptivity are length divided by square root of time (e.g., millimeters second$^{-1/2}$). Infiltration into a soil is affected by gravity and capillarity. Equation (13.5) gives Philip's equation for vertical infiltration and Eqn (13.6) gives Philip's equation for gravity-free infiltration. In both equations, infiltration goes as the square root of time and from Eqn (13.6) we can see that the units of sorptivity are length divided by the square root of time.

Here is the theoretical development of Smettem and Clothier (1989) based on theory developed by Philip (1969):

$$S_\mathrm{o}^2 = [(\theta_\mathrm{o} - \theta_\mathrm{n})/b] \int_{\theta_\mathrm{n}}^{\theta_\mathrm{o}} D\mathrm{d}\theta, \tag{13.10}$$

where

$S_\mathrm{o}$ = sorptivity
$\theta_\mathrm{n}$ = initial soil water content
$\theta_\mathrm{o}$ = water content to which the soil surface is wetted
$D$ = diffusivity
$D = k \cdot (\partial\varphi/\partial\theta)$
$k$ = hydraulic conductivity under unsaturated conditions

$b$ is a parameter and is a function of the slope of the diffusivity function; $½ < b < \pi/4$; $b$ can be approximated as 0.55.

Combining Wooding's (1968) equation (Eqn (13.8)) and Philip's theory (1969), Smettem and Clothier (1989) obtained the following equation:

$$q_\infty / \left(\pi r^2\right) = K_\mathrm{o} + \left(2.2 S_\mathrm{o}^2\right) / (\pi r \Delta\theta), \tag{13.11}$$

where $q_\infty$ = flow at long times (steady conditions); this is the same as $i_\mathrm{f}$ in Eqn 11.8.

$$\Delta\theta = \theta(\Psi_\mathrm{o}) - \theta(\Psi_\mathrm{n}). \tag{13.12}$$

$\Psi_\mathrm{o}$ is the supply potential (i.e., the tension with which the water is applied to the soil). Smettem and Clothier (1989) used a supply potential of −35 mm when they did their experiment. $\Psi_\mathrm{n}$ is the potential of the soil before the tension infiltrometer is put on top of it. For practical purposes, $\Delta\theta = \theta_\mathrm{o} - \theta_\mathrm{n}$.

The theoretical development is difficult, but the resulting equation is simple to use for the experimentor. Two tension infiltrometers with different radii are taken to the field where one wants to determine unsaturated hydraulic conductivity and sorptivity. The antecedent volumetric water content is determined ($\theta_\mathrm{n}$) and the tension infiltrometers are set close by. After steady infiltration has been reached for each, one records the value. One then takes the tension infiltrometers off the soil and gets the volumetric water content of soil right under the tension infiltrometers. This is $\theta_\mathrm{o}$. One then determines $\Delta\theta$ and solves Eqn (13.11) for $K_\mathrm{o}$ and $S_\mathrm{o}$ by simultaneous solution using data from the discs with two different radii. We have the known parameters, $\Delta\theta$, $r$, and $q_\infty$, and we have the two unknowns, $S_o$ and $K_o$.

The method of Smettem and Clothier (1989) is simple and results in two values ($K_o$ and $S_o$). However, many people cannot obtain or afford two tension infiltrometers with different radii; hence the method of Ankeny et al. (1991) provides a means of obtaining unsaturated hydraulic conductivity with just one tension infiltrometer.

The determination of unsaturated hydraulic conductivity using the method of Ankeny et al. (1991) is not straightforward or obvious from reading the paper. On November 7, 1995, Dr Brent E. Clothier visited Kansas State University and demonstrated to students how to determine unsaturated hydraulic conductivity with this method. We now go through the procedure, step by step, as he explained it.

We need to know the hydraulic conductivity as a function of head, $h$. We use the following equation (rewritten from Eqn 11.7 where $K_s$ is used instead of $K_o$ used by Jury et al. (1991)):

$$K(h) = K_s \exp(\alpha h), \tag{13.13}$$

where $K_s$ and $\alpha$ are constants. In Eqn (13.13), $K_s$ represents gravity and $\alpha$ represents capillarity; $\alpha$ also is a slope (the slope of the hydraulic conductivity versus head). We can relate $K$ in Eqn (13.13) to the $K$ in a form of Darcy's law, as follows:

$$J_w = K(\partial\Psi)/(\Psi z), \tag{13.14}$$

where $J_w$ is the soil water flux.

The soil that Clothier used in his demonstration was a Haynie sandy loam. It has 65% sand, 24% silt, and 11% clay.

In the Ankeny et al. (1991) method, we use two heads. In this experiment, the two heads will be as follows:

$$h_1 = -10 \text{ cm}$$

$$h_2 = -2 \text{ cm}$$

We will have two unknowns and two equations and will solve the equations to get the unsaturated hydraulic conductivity. We need to run the tension infiltrometer two times; therefore, we shall put it two times on the soil. Water flows into the soil by gravity and capillarity.

In his analysis, Clothier used the following form of Wooding's (1968) equation:

$$Q = \pi r^2 K_o + (4rK_o)/\alpha, \tag{13.15}$$

where $Q$ (cubic meters per second) is the flow through a disc, which is proportional to the surface area of the disc times the hydraulic conductivity plus capillarity (movement of water that goes off the perimeter).

The first term on the right-hand side of Eqn (13.15) represents the gravity component, and the second term on the right-hand side of Eqn (13.15) represents the capillary component. We can measure $Q$, how fast the water in the sealed reservoir drops in the tension infiltrometer.

From Eqn (13.15), we write

$$q = K_o[1 + 4/\pi\alpha r]. \tag{13.16}$$

We shall apply this equation at one head and then at another head.

$$K = K_1 \exp(\alpha h_1) = K_2 \exp(\alpha h_2) \tag{13.17}$$

$$K_1/K_2 = \exp[\alpha(h_1 - h_2)] \tag{13.18}$$

$$\alpha = [\ln(K_1/K_2)]/(h_1 - h_2) = [\ln(q_1/q_2)]/(h_1 - h_2). \tag{13.19}$$

We are taking the functional form, $K = K_s \exp(\alpha h)$. We have a fixed radius and $\alpha$ is constant.

$$(K_1/K_2) = q_1/q_2. \tag{13.20}$$

So we shall measure two $q$'s ($q_1$ and $q_2$).

If we have a clay soil, capillarity dominates and $\alpha$ (slope of the hydraulic conductivity versus head) is small. If we have a sandy soil, $\alpha$ is large. For our first head, $h_1 = -10$ cm (the air tube is 10 cm under water). We apply the tension infiltrometer to the soil. We wait until steady state flow.

We need to know the ratio, $R$, of the areas of the reservoir to the disc (the area that touches the soil) for the tension infiltrometer. The nylon base of the tension infiltrometer had a diameter of 6.57 cm. The reservoir had a diameter of 3.37 cm.

$$(3.37/6.57)^2 = R = 0.263. \tag{13.21}$$

We time the drop in the sealed reservoir and get the steady state rate. We multiply this rate by 0.263 to get $q_1$. We find the following:

$$q_1 = 0.115 \text{ cm/s}. \tag{13.22}$$

We have done the −10 cm head.

Now we set the tension infiltrometer at the −2 cm head. We find the following:

$$q_2 = 0.175 \text{ cm/s}. \tag{13.23}$$

From Eqn (13.19), we have

$$\alpha = [(\ln(q_1/q_2)]/(h_1 - h_2)$$

$$\alpha = [\ln(0.115/0.175)]/[-10 \text{ cm} - (-2 \text{ cm})] = 0.05/\text{cm} \tag{13.24}$$

$$K = \exp(0.05h). \tag{13.25}$$

We use Eqn (13.16), Wooding's equation, to calculate $K_o$:

$$q = 0.175 \text{ cm/s}$$

$$\alpha = 0.05/\text{cm}$$

$$r = 6.57 \text{ cm}/2 = 3.285 \text{ cm}.$$

We solve for $K_o$:

$$K_o = 0.02 \text{ cm/s} \tag{13.26}$$

at 0.175 cm/s ($q_2$ for $-2$ cm head).

$$K = 0.02 \exp(0.05h) \tag{13.27}$$

Equation 13.27 is for $K(h)$ for $h > 2$ cm.

## 13.8 MEASUREMENT OF REPELLENCY WITH THE TENSION INFILTROMETER

Although some sands and peats are observed to become water repellent when dry, most soils show no obvious reluctance to wet, so it is assumed that they absorb water and ethanol freely (Scotter et al., 1989). Given the same effective contact angle, sorptivity of a liquid into a porous material should be proportional to $(\sigma/\mu)^{½}$ where $\sigma$ and $\mu$ are the surface tension and viscosity of the liquid, respectively (Philip, 1969; see his Eqn 45 on p. 238). Thus, dry soil should imbibe water about twice as fast as alcohol. Organic coatings on peds or particles in some soils can induce some water repellence, but do not affect their ability to absorb alcohol. So in water-repellent dry soil the sorptivity of alcohol will be greater than water. Scotter et al. (1989) checked this observation out in the field, where they took a sorptivity tube (Figure 13.3) to measure the sorptivity of ethanol and water by a fine sandy loam, a common agricultural soil in the region of Palmerston North, New Zealand. They did as much as they could to reduce the likelihood of water repellence. They removed the top 50 mm of soil because organic coatings are most likely to be at the surface. They did the experiments in November in the first drying cycle following an unusually wet winter, when the initial water content of the soil was 0.24 $\text{m}^3/\text{m}^3$. The soil appeared to absorb water normally, proportional to the square root of time and with a uniform wet front. But to their surprise the ethanol was absorbed an order of magnitude faster than the water, indicating significant water repellence.

On the same day of the first experiment, Scotter et al. (1989) took some of the soil back to the laboratory, sieved it, packed it into a tube and again measured the sorptivity of the two liquids. This time the water went in faster than the ethanol, presumably due to the abrasion during sieving.

Other experiments showed that after a few days sieved soil again became water repellent, apparently due to a reorientation of the organic coatings on the soil particles or aggregates.

Further work on repellent soils of New Zealand (Clothier et al., 2000) confirmed the earlier work (Scotter et al., 1989). Clothier et al. (2000) showed that a Ramiha silt loam, another agricultural soil in the region of Palmerston North, was ephemerally hydrophobic. Temporal changes in the measured infiltration rate changed as the repellency broke down. Clothier et al. (2000) cautioned that repellency might not be evident in a soil if infiltration is not observed over a long period. It may take time for the repellency to break down before the infiltration rate climbs to a rate characteristic of the nonrepellent soil.

Peat soils are notoriously repellent. They are common in The Netherlands and much research has been done in that country to study repellency (Ritsema, 1998; Dekker, 1998). When the polders in The Netherlands were drained, the peat soils were allowed to get too dry. They never could be wetted up because of their extreme repellency. So the engineers learned that the peat soils had to be kept wet, if farmers were going to be able to plant seeds and make the soils arable (Don Kirkham, personal communication, undated). In Turkey highly organic soils have been seen to catch on fire (Don Kirkham, personal communication, undated). Forest soils are also repellent because they are organic (Kirkham and Clothier, 2000). John Letey at the University of California at Riverside, in the heart of orange-grove country before population expansion, is well known for his studies of the repellency of soils (Letey et al., 1975). Organic drippings from citrus groves make orchard soils repellent. Soils with organic materials, such as no-till soils with residues, often do not wet readily (Woche et al., 2005). For a further discussion of water repellency and methods to determine it, see Bachmann et al. (2003).

One cannot use alcohol in the commercially available tension infiltrometers from Soil Measurement Systems (Tucson, AZ, USA) and Decagon Devices, because the towers are made of plastic and the alcohol would corrode the plastic. One needs a tension infiltrometer made out of glass, as was the original sorptivity tube (Figure 13.3) to carry out experiments in which one infiltrates alcohol into the soil to determine repellency.

## 13.9 MEASUREMENT OF MOBILITY WITH THE TENSION INFILTROMETER

Many water flow processes of interest such as groundwater recharge are concerned only with area-averaged water input. Therefore, preferential flow of water through structural voids does not necessarily invalidate equations that assume homogeneous flow, like Darcy's law. However, preferential flow is of critical importance in solute transport, because it enhances chemical mobility and can increase pollution hazards. Many times we need to monitor chemical mobility along with hydraulic properties. We now shall see how we can determine mobility of chemicals.

Water and nutrients not taken up by roots move to depth and eventually to groundwater with deleterious consequences. With the tension infiltrometer (disc permeameter), we can measure hydraulic properties of soil that control infiltration and retention. In particular, we can distinguish mobile and immobile water with it.

The soil water content, $\theta$, is made up of the mobile-water content, $\theta_m$, and the immobile-water content, $\theta_{im}$. Figure 13.5 shows a mobile-water soil, and Figure 13.6 shows a mobile–immobile water soil. Water is immobilized due to several factors: it can be in an occluded pore, it can be bound water, it can be in a dead-end pore, or it can be in the soil's microporosity and unable to move. $\theta_m$ is active in chemical transport,

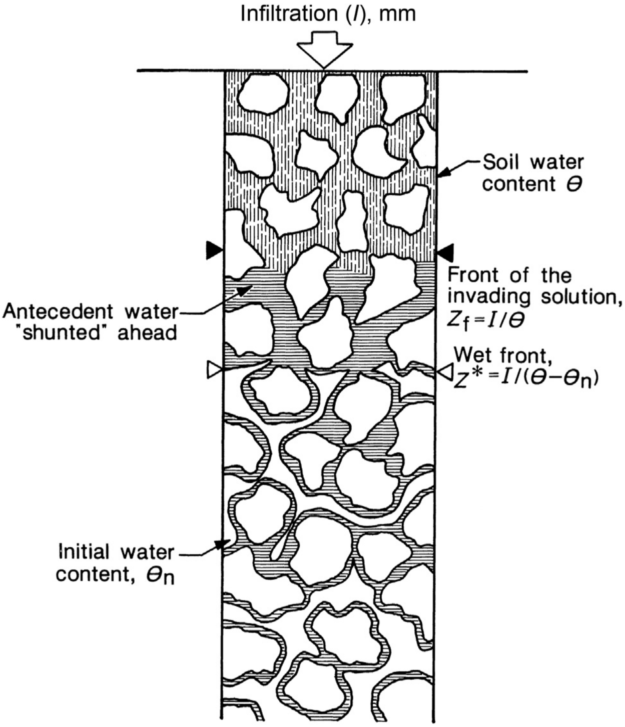
Infiltration (I), mm
Soil water content Θ
Front of the invading solution, $Z_f = I/\Theta$
Wet front, $Z^* = I/(\Theta - \Theta_n)$
Antecedent water "shunted" ahead
Initial water content, $\Theta_n$

**FIGURE 13.5** A "mobile-water" soil. *Redrawn from a slide by Brent E. Clothier. Reprinted by permission of Brent E. Clothier.*

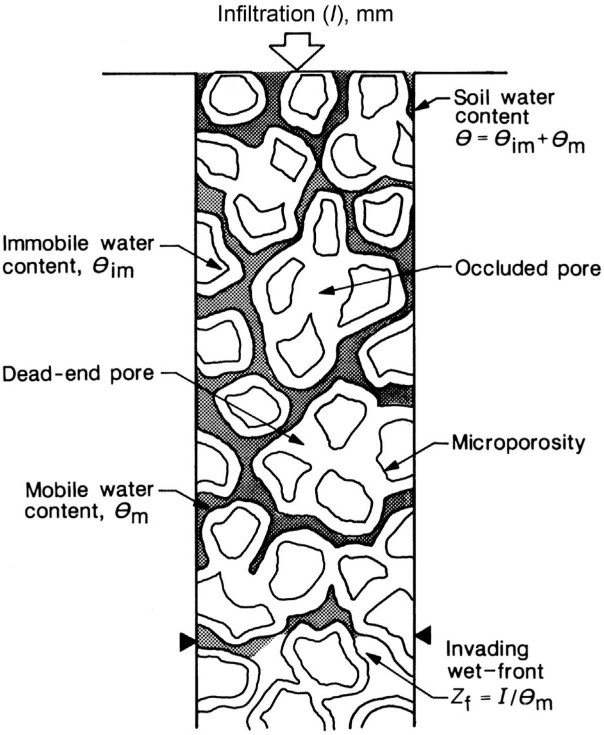
Infiltration (I), mm
Soil water content $\theta = \theta_{im} + \theta_m$
Immobile water content, $\theta_{im}$
Occluded pore
Dead-end pore
Microporosity
Mobile water content, $\theta_m$
Invading wet–front
$Z_f = I/\theta_m$

**FIGURE 13.6** A "mobile–immobile" water soil. *Redrawn from a slide by Brent E. Clothier. Reprinted by permission of Brent E. Clothier.*

while $\theta_{im}$ is not. If we know $\theta_m$, we can develop management strategies to minimize leaching losses of chemicals.

The method of using the disc permeameter to get $\theta_m$ and $\theta_{im}$ relies on using it to supply a tracer solution to soil (Clothier et al., 1992). The tracer is not originally in the soil. If a tracer is added to a disc permeameter at a concentration $c_m$, then from the observed solution concentration $c^*$ in soil samples extracted from underneath the disc, $\theta_m$ can be calculated from the dilution by the water of the immobile phase that must have remained in place during the passage past it of the invading solution of tracer. So we have

$$c^*\theta = c_m\theta_m + c_{im}\theta_{im}. \tag{13.28}$$

But if $c_{im} = 0$ (there was no tracer in the soil to begin with), then the last term on the right-hand side of Eqn (13.28) drops out and we have:

$$\theta_m = \theta(c^*/c_m). \tag{13.29}$$

In other words, the fraction, $\theta_m/\theta$, is directly proportional to the relative concentration of solute found in the soil, $c^*$, to that applied, $c_m$:

$$c^*/c_m = \theta_m/\theta. \tag{13.30}$$

In the experiments of Clothier et al. (1992), the tracer was bromide. (Chloride could not be used, because of the proximity of the Pacific Ocean and salt in the air that lands on the soil.) They applied water to the soil with a tension infiltrometer with $h_o = \Psi_o = -20$ mm. (See Figure 13.4.) The air-inlet tube was 20 mm under the surface of the water in the tower on the right-hand side of the figure. The soil was near saturation.

In the first experiment, pure water was used to first wet the soil. Then a tracer at concentration 0.1 mol/L KBr or 0.1 M KBr was drawn into this already wet soil predominantly by gravity. The original water content of the soil, a Manawatu fine sandy loam, was 0.414 $m^3/m^3$. Three runs were done. Bromide in the soil was determined after each run. The method is shown in Figure 13.7. The ratio $c^*/c_m$ was determined for the three runs, and they were 0.46, 0.48, and 0.50, with an average of 0.49. Therefore,

$$\theta_m/0.414 = 0.49\ m^3/m^3 \tag{13.31}$$

$$\theta_m = 0.203\ m^3/m^3 \tag{13.32}$$

so only half of the soil water was mobile (0.414 $m^3/m^3$ vs 0.203 $m^3/m^3$).

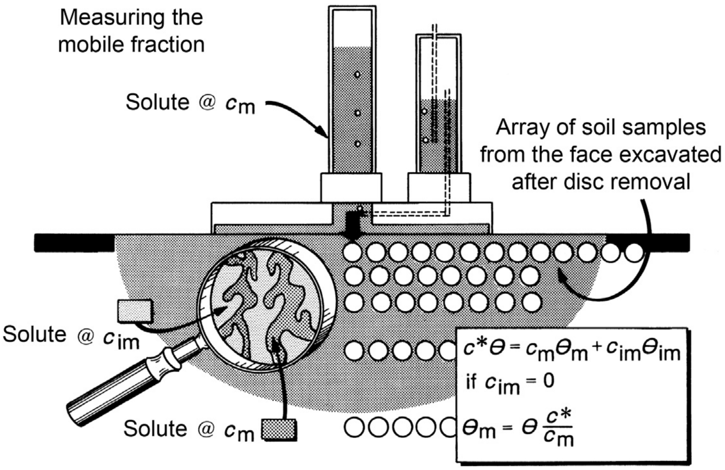
Measuring the mobile fraction
Solute @ $c_m$
Array of soil samples from the face excavated after disc removal
Solute @ $c_{im}$
$c^*\theta = c_m\theta_m + c_{im}\theta_{im}$
if $c_{im} = 0$
$\theta_m = \theta \frac{c^*}{c_m}$
Solute @ $c_m$

**FIGURE 13.7** Measuring the mobile fraction. *From Clothier, B.E., Green, S.R., Magesan, G.N., ©1994. Soil and plant factors that determine efficient use of irrigation water and act to minimise leaching losses. Trans. Int. Congr. Soil Sci. 2a; 41–47. Reprinted by permission of The International Society of Soil Science.*

We can determine the depth of penetration of the solute using the following equation:

$$Z_s^* = I/\theta_m \tag{13.33}$$

where

$Z_s^*$ = depth of the solute front (the asterisk, *, after the s for solute indicates that we are dealing with a tracer)
$I$ = cumulative infiltration
$\theta_m$ = mobile-water content.

For the three runs, average $I$ was 15.7 mm. So $Z_s^* = 15.7\ \text{mm}/(0.203\ \text{m}^3/\text{m}^3) = 77.3\ \text{mm}$.

If all the water were mobile, then $\theta_m = \theta$.

$$15.7\ \text{mm}/\left(0.414\ \text{m}^3/\text{m}^3\right) = 37.9\ \text{mm}.$$

The observed front of the bromide, determined experimentally at the end of the experiment, showed that it was at about 77 mm, not at about 38 mm. So the experimental data backed up the calculation. Because not all the water was mobile, the tracer penetrated to deeper depths than it would have, had $\theta_m = \theta$.

The longitudinal mobility (the depth of penetration) is inversely related to $\theta_m$. This is sometimes hard for people to understand when they are using the method initially, because they think that the more mobile the water the deeper will be the penetration of a solute. This is not so. The larger the mobile volume fraction, (i.e., $\theta_m$) the less longitudinally mobile is the solute (the smaller $Z_s^*$). In other words, the solution carrying the dissolved solute travels through a larger volume fraction of the soil's wetted pore space, such that for a given amount of water infiltrated, $I$, the less the penetration into the soil. As $\theta_m$ becomes a smaller fraction of the wetted $\theta$ (total water content), the volume fraction of the soil's wetted pore space that transports the invading solution becomes smaller. Hence, for an equivalent amount of $I$, the greater is the depth, due to the fact that $Z_s^*$ is inversely related to $\theta_m$.

In another experiment (Clothier et al., 1992), the tracer was put on a dry soil. The tension infiltrometer was still set at −20 mm, but there was no prewetting. The tracer solution was now drawn into the soil more by capillarity than by gravity. The mobile fraction measured right under the disc rose to $\theta_m = 0.291\ \text{m}^3/\text{m}^3$. (Remember that the previous value, when a wet soil was used, $\theta_m = 0.203\ \text{m}^3/\text{m}^3$.) This rise is attributed to the direct, capillary-induced movement of the invading solute into more of the soil's microporosity. The solute invasion depth was less (shallower) than half of the former case (prewetted, $\Psi_o = -20$ mm). The prewetting had destroyed the capillary attractiveness of the micropores. The "dry-soil" effect keeps fertilizers near the soil surface. One can think of bromide as a tracer for nitrate. Thus effluent and other nutrient-laden fertilizer waters should be applied to dry soil. This applied chemical can be drawn by capillarity into more of the soil's microporosity, close to the soil surface (where roots are) and not escape to depth and groundwater. Once in the soil's microporosity, the applied nutrients are rendered less likely to be leached by subsequent rainfall.

## 13.10 ELLIPSOIDAL DESCRIPTION OF WATER FLOW INTO SOIL FROM A SURFACE DISC

The disc permeameter is being widely used to characterize the hydraulic properties of the surface of the soil. It is important to describe the multidimensional flow of water away from the circular source. Little work has been done to analyze precisely the flow of water away from a circular source of water applied at a constant negative potential, $\Psi_o$. The Wooding equation (1968; his Eqn 64) does describe the steady rate of three-dimensional infiltration from a circular pond. His equation applies to profiles at infinite time and does not give information about the shape of wet fronts of transient wetting. Kirkham and Clothier (1994a,b) used a unique approach to analyze the flow pattern, because they assumed that the three-dimensional wetting fronts under the circular source were ellipsoidal.

They described mathematically the three-dimensional flow of water away from a disc source placed upon the soil's surface at constant negative potential, $\Psi_o$ less than 0, when the water is being applied to the soil at a steady rate, $q$ in cubic millimeters per second. The wet fronts analyzed are shown in Figure 13.1. The wet fronts resulted from water being infiltrated from a quarter-disc permeameter set in the corner of a plastic box with soil. The setup is shown as Figure 1 in Kirkham and Clothier (1994b). It allowed markings of the wet fronts as they penetrated the soil under the quarter-disc permeameter set at −50 mm supply potential ($\Psi_o$). The reason for using this suction was to allow the soil to be unsaturated but not too far away from saturation, such that the flow would be unrealistically slow.

The mathematical development is given by Kirkham and Clothier (1994a,b). Assuming the volume wetted in each wetted area (delineated in Figure 13.1) is an ellipsoid, the following equation can be used for the volume of water, $V(t)$, that infiltrated from the disc:

$$V(t) = (2/3\pi)(\theta_m - \theta_n)R^2(t)Z(t), \tag{13.34}$$

where the extent of radial wetting at the surface is $R$ at any time $t$, and vertically under the disc is $Z$. The initial volumetric water content of the soil is $\theta_n$ and the disc wets the soil surface to water content $\theta_o$, a function of

$\Psi_o$. A weighted-average water content can be ascribed to the wetted field, designated $\theta_m$.

It can be seen from the wet fronts (Figure 13.1) that the ellipsoid describing the spatial pattern of wetting goes from being an oblate (egg on its side; see Figure 7.3) at early times, through to being spheroidal by about the end of the experiment. It would eventually become prolate (egg on its end; see Figure 7.4), with further extension being limited to the vertical.

As noted above, profiles predicted from Wooding's (1968) equation hold only at infinite time, and thus, they cannot give any information about transient wet fronts. Where the ellipsoidal idea has merit over Wooding's equation is in the practical operation of the disc permeameter. The ellipsoidal equation can give answers to the following questions: How deep is the wet front at any time? By what means can it be reckoned simply? Also, we can answer other questions relating to the modus operandi of the disc permeameter. How much of the soil's volume has been wetted during a disc experiment? What volume of soil has been sampled, and, hence, to what depth of soil do the Wooding $K$ and $S$ values apply?

The disc permeameter might be practically applied to different tillage situations. If the soil will not suck in water, as determined by the disc permeameter, then we need to till the soil. If there is a crust on the soil surface or the soil surface is repellent, water cannot infiltrate. Water runs off and moves preferentially through the macropores instead of through the soil matrix. Tillage of the soil is critical so that rainwater will not sit on the surface and evaporate (Figure 13.8). We want water to go into the soil,

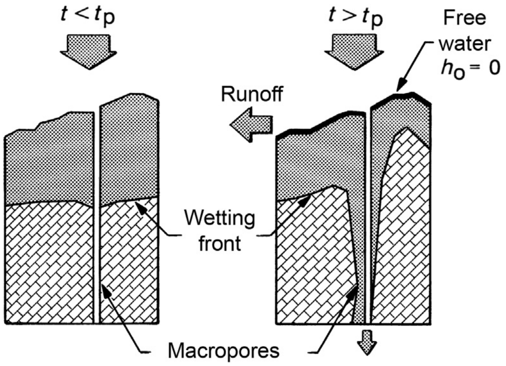

**FIGURE 13.8** Infiltration of an applied flux of water into soil. Left: Nonponding infiltration when the flux through the surface is less than the saturated hydraulic conductivity, $K_s$, or ponding infiltration when the flux through the surface is greater than $K_s$ prior to the time of ponding $t_p$. Right: Pattern of infiltration after incipient ponding, $t > t_p$, when the possibility of runoff exists, as does the entry of free water into macropores. *From Clothier, B.E., Infiltration. In: Soil and Environmental Analysis. Physical Methods, second ed., Marcel Dekker, Inc., New York, ©2001. This material is reprinted with permission of Marcel Dekker, Inc.*

where it will be used by plants. The disc permeameter also can be practically applied to different irrigation systems, including drip and furrow irrigation. Perhaps one could put the disc permeameter, set at a constant negative potential, on a dry soil and see how far water is sucked out to the side and calculate the volume wetted, based on the ellipsoidal equation. The distance could be measured with a ruler. Then one could place irrigation sources at distances from each other based on the measurements.

The ellipsoidal equation has another advantage. It is simple to use and people with essentially no mathematical training can apply it. A small hand-held calculator could be programmed easily to make the calculations.

## 13.11 APPENDIX: BIOGRAPHY OF JOHN PHILIP

John Robert Philip, soil physicist, was born on January 13, 1927, in Ballarat in rural Victoria, Australia (Burges et al., 1999). He acquired a love of learning from his schoolteacher mother, and won a scholarship to the prestigious Scotch College for boys in Melbourne, where his mathematical ability was recognized and developed. He also was encouraged to write poetry, and this remained a lifelong passion, his poems appearing in many literary publications. He graduated from Scotch College at age 13 years, and he spent another 2 years at school before being deemed old enough (at 16 years) to study civil engineering at the University of Melbourne. Bored by the undemanding engineering courses, which he described as merely “learning which handbook to look up”, he spent much of his time reading and writing poetry. He earned his Bachelor’s of Civil Engineering degree at age 19 years, the youngest ever engineering graduate.

He was offered a research assistantship by the University of Melbourne and was sent to the Council for Industrial and Scientific Research (renamed CSIRO in 1949) station at Griffith to work on problems of furrow irrigation. His fellowship ended after a year and he left to work as an engineer in Queensland. In 1951, he was asked to join the CSIRO Division of Plant Industry at Deniliquin, in New South Wales. Otto Frankel became Philip’s boss. Frankel, a distinguished plant geneticist, was charged with revitalizing the division. He consulted with John Jaeger (see the Appendix of Chapter 9 for a biography of Jaeger) and Pat Moran, two famous mathematicians at the Australian National University, who reported positively on Philip’s proposed research plans in agricultural physics. Frankel gave Philip freedom to proceed (Burges et al., 1999), and Philip praised Frankel for allowing the environment in which he could thrive (personal communication, December 9, 1997). Philip’s papers at Deniliquin dealt with the analysis of environmental water and heat flow, which earned him a D.Sc. in physics from the University of Melbourne. Modern theory is based on his analysis (American Society of Agronomy, 1999).

In 1964, he moved from Deniliquin to Canberra to head the Agricultural Physics section of the Division of Plant Industry (headed by Frankel) (Burges et al., 1999). A bequest to CSIRO provided the funds to build a laboratory to house the team of researchers Philip assembled to work on fluid mechanics of porous media, micrometeorology, plant physical ecology, and soil physics. Philip helped to design the building, called the F.C. Pye Laboratory, built in 1966. The productivity of the team was aided by the architecture of the Pye Lab, which encouraged collaboration; it was open and such that one easily encountered colleagues in the sunny walkways. In 1970, the Division of Environmental Mechanics was created, and Philip was the chief until his retirement in 1992 (American Society of Agronomy, 1999).

Philip was a strong defender of scientific autonomy. In 1975, he chaired the Science Task Force of the Royal Commission on Australian Government Administration. The report he drafted for this task force argued for governmental science characterized by freedom of action and outlined the environment necessary for effective and creative scientific research (American Society of Agronomy, 1999; Burges et al., 1999). In the article he prepared for the seventy-fifth anniversary issue of *Soil Science* (Philip, 1991), he criticized the lack of freedom that scientists now have.

Philip was the preeminent mathematician who solved difficult unsaturated flow problems. The solutions led to practical benefits, including how to handle infiltrating irrigation water. His work was the basis for numerous theoretical advances in infiltration and soil–plant–water relationships and his vertical infiltration model is used worldwide. He also dominated multidimensional infiltration theory. He published more than 300 papers. While he is best known for his work in soil and porous media physics, fluid mechanics, and hydrology, his papers in the plant physiology literature are classic. He published on osmotic and turgor properties of plant cells. He pioneered the concept of the *s*oil, plant, atmosphere as a thermodynamic *c*ontinuum (SPAC) for water transfer. Everyone now talks about the SPAC, most of the time without acknowledging that Philip was the person who first used the term. (See Chapter 22 for more information about the SPAC.)

Philip received numerous honors, including honorary doctor's degrees from the University of Melbourne, the Agricultural University of Athens, and the University of Guelph in Canada. He was a Fellow of the Australian Academy of Sciences and, in 1974, became a Fellow of the Royal Society of London, the highest scientific honor in the Commonwealth. In 1991, he was elected corresponding member of the All Union (now Russian) Academy of Sciences. In 1995, he received the International

Hydrology prize awarded jointly by UNESCO, the World Meteorological Association, and the International Association for Hydrological Science. He also received much recognition in the United States. He was named Fellow of the Soil Science Society and honorary member of the American Water Resources Association and was the first non-American to receive the Robert E. Horton Medal, the highest award for hydrology from the American Geophysical Union (American Society of Agronomy, 1999). In 1995, he was elected as a foreign associate by the National Academy of Engineering in Washington, D.C., for his pioneering research contributions to soil-water hydrology.

Philip and his wife, Francis, had two sons and a daughter. Philip was struck by a car as he stepped off a bus and was killed on June 26, 1999, in Amsterdam, The Netherlands, where he was visiting the Centre for Mathematics and Information Science (American Society of Agronomy, 1999). The driver was sentenced to 1 month in jail and suspension of his driver's license for a year. A volume honoring Philip was published by the American Geophysical Union (Raats et al., 2002), and a tribute plus complete bibliography appeared in the *Australian Journal of Soil Research* (Smiles, 2001).

## References

American Society of Agronomy, December 27, 1999. Deaths. John Robert Philip. Crop Science-Soil Science-Agronomy News.

Angulo-Jaramillo, R., Moreno, F., Clothier, B.E., Thony, J.L., Vachaud, G., Fernandez-Boy, E., Cayuela, J.A., 1997. Seasonal variation of hydraulic properties of soils measured using a tension disk infiltrometer. Soil Sci. Soc. Am. J. 61, 27–32.

Ankeny, M.D., Kaspar, T.C., Horton Jr., R., 1989. Automated Tension Infiltrometer. United States Patent No. 4,884,436. Date of Patent: Dec. 5, 1989. Filed: Oct. 20, 1988. Assignee. Iowa State University Research Foundation, Inc., Ames, Iowa.

Ankeny, M.D., Ahmed, M., Kaspar, T.C., Horton, R., 1991. Simple field method for determining unsaturated hydraulic conductivity. Soil Sci. Soc. Am. J. 55, 467–470.

Bachmann, J., Woche, S.K., Goebel, M.-O., Kirkham, M.B., Horton, R., 2003. Extended methodology for determining wetting properties of porous media. Water Resour. Res. 39 (12), 11-1–11-14. http://dx.doi.org/10/1029/2003WR002143. Section SBH (Subsurface Hydrology).

Baver, L.D., Gardner, W.H., Gardner, W.R., 1972. Soil Physics, fourth ed. Wiley, New York.

Burges, S.J., Ford, P.W., White, I., 1999. John Robert Philip (1927–1999). EOS Trans., Am. Geophys. Union 80, 574–577.

Clothier, B.E., 2001. Infiltration. In: Smith, K.A., Mullins, C.E. (Eds.), Soil and Environmental Analysis. Physical Methods, second ed. Marcel Dekker, New York, pp. 239–280.

Clothier, B.E., 2008. Soil pores. In: Chesworth, W. (Ed.), Encyclopedia of Soil Science. Springer, Dordrecht, The Netherlands, pp. 693–699.

Clothier, B.E., White, I., 1981. Measurement of sorptivity and soil water diffusivity in the field. Soil Sci. Soc. Am. J. 45, 241–245.

Clothier, B.E., Green, S.R., Magesan, G.N., 1994. Soil and plant factors that determine efficient use of irrigation water and act to minimise leaching losses. Trans. Int. Congr. Soil Sci. 2a, 41–47.

Clothier, B.E., Kirkham, M.B., McLean, J.E., 1992. In situ measurement of the effective transport volume for solute moving through soil. Soil Sci. Soc. Am. J. 56, 733–736.

Clothier, B.E., Vogeler, I., Magesan, G.N., 2000. The breakdown of water repellency and solute transport through a hydrophobic soil. J. Hydrol. 231–232 (double volume issue), 255–264.

Dekker, L.W., 1998. Moisture Variability Resulting from Water Repellency in Dutch Soils (Doctoral thesis). Wageningen Agricultural University, The Netherlands.

Gardner, W.R., 1958. Some steady-state solutions of the unsaturated moisture flow equation with applications to evaporation from a water table. Soil Sci. 85, 228–232.

Jury, W.A., Horton, R., 2004. Soil Physics, sixth ed. Wiley, Hoboken, New Jersey.

Jury, W.A., Gardner, W.R., Gardner, W.H., 1991. Soil Physics, fifth ed. Wiley, New York.

Kirkham, M.B., 1994. Soil-water relationships. In: Arntzen, C.J., Ritter, E.M. (Eds.), Encyclopedia of Agricultural Science, vol. 4. Academic Press, San Diego, pp. 151–168.

Kirkham, M.B., Clothier, B.E., 1994a. Ellipsoidal description of water flow into soil from a surface disc. Trans. Int. Congr. Soil Sci. 2b, 38–39.

Kirkham, M.B., Clothier, B.E., 1994b. Wetted soil volume under a circular source. In: Jensen, H.E., Schjønning, P., Mikkelsen, S.A., Madsen, K.B. (Eds.), Proceedings of the 13th International Conference, International Soil Tillage Research Organization. The Royal Veterinary and Agricultural University and the Danish Institute of Plant and Soil Science, Lyngby and Copenhagen, Denmark, pp. 573–578.

Kirkham, M.B., Clothier, B.E., 2000. Infiltration into a New Zealand native forest soil. In: Rosenzweig, C. (Ed.), A Spectrum of Achievements in Agronomy. American Society of Agronomy, Crop Science Society of America, and Soil Science Society of America, Madison, Wisconsin, pp. 13–26. ASA Special Pub. No. 62.

Letey, J., Osborn, J.F., Valoras, N., 1975. Soil Water Repellency and the Use of Nonionic Surfactants. Technical Completion Report. Office of Water Research and Technology, U.S. Department of the Interior; Office of Water Research and Technology; and Water Resources Center, University of California, Davis. Contrib. No. 154. Department of Soil Science and Agricultural Engineering: University of California, Riverside.

Nobel, P.S., 1983. Biophysical Plant Physiology and Ecology. W.H. Freeman, San Francisco.

Perroux, K.M., White, I., 1988. Designs for disc permeameters. Soil Sci. Soc. Am. J. 52, 1205–1215.

Philip, J.R., 1969. Theory of infiltration. Adv. Hydrosci. 5, 215–296.

Philip, J.R., 1991. Soils, natural science, and models. Soil Sci. 151, 91–98.

Raats, P.A.C., 1971. Steady infiltration from point sources, cavities, and basins. Soil Sci. Soc. Am. Proc. 35, 689–694.

Raats, P.A.C., Smiles, D., Warrick, A.W. (Eds.), 2002. Environmental Mechanics. Water, Mass and Energy Transfer in the Biosphere. The Philip Volume. American Geophysical Union, Washington, DC. Geophysical Monograph 129.

Ritsema, C.J., 1998. Flow and Transport in Water Repellent Sandy Soils (Doctoral thesis). Wageningen Agricultural University, The Netherlands.

Scotter, D., Tillman, R., Wallis, M., Clothier, B., 1989. Alcophilic Soils. WISPAS. A Newsletter about Water in the Soil-Plant Atmosphere System. Plant Physiology Division, Department of Scientific and Industrial Research, Palmerston North, New Zealand. No. 43, p. 3.

Smettem, K.R.J., Clothier, B.E., 1989. Measuring unsaturated sorptivity and hydraulic conductivity using multiple disc permeameters. J. Soil Sci. 40, 563–568.

Smiles, D. (Coordinating Ed.), 2001. The environmental mechanic. Aust. J. Soil Res. 39, 649–681.

Soil Science Society of America, 2008. Glossary of Soil Science Terms 2008. Soil Science Society of America, Madison, Wisconsin.

Swartzendruber, D., 1993. Revised attribution of the power form infiltration equation. Water Resour. Res. 29, 2455–2456.

Woche, S.K., Goebel, M.-O., Kirkham, M.B., Horton, R., van der Ploeg, R.R., Bachmann, J., 2005. Contact angle of soils as affected by depth, texture, and land management. Eur. J. Soil Sci. 56, 239–251.

Wooding, R.A., 1968. Steady infiltration from a shallow circular pond. Water Resour. Res. 4, 1259–1273 (See Eq. 64 for Wooding's equation.).

Zhang, R., 1997. Determination of soil sorptivity and hydraulic conductivity from the disk infiltrometer. Soil Sci. Soc. Am. J. 61, 1024–1030.

# CHAPTER 14

# Pore Volume

Soil not only permits entry of water and nutrients and their storage there but also allows wasteful passage past roots. We have seen how with the tension infiltrometer we can measure mobility of solutes (see Section 13.9, Chapter 13). An older method to analyze movement of solutes through the soil is based on measuring pore volumes. This method does not divide the soil water into mobile, $\theta_{\mathrm{m}}$, and immobile, $\theta_{\mathrm{im}}$, regions, but considers the water in the soil to be the sum of both, the total volumetric water content, $\theta$. By measuring pore volume, we consider the physical process of the movement of solutes in fluids (Kirkham and Powers, 1972, p. 380). It gives us information concerning what takes place in a porous medium as one fluid displaces another.

## 14.1 DEFINITIONS

The *Glossary of Soil Science Terms* (Soil Science Society of America, 2008) defines *pore volume* as "pore space". And then the definition of *pore space* is given as follows: "The portion of soil bulk volume occupied by soil pores." This is a valid definition of pore volume. We see the pore volume defined this way in Figure 12.1. Pores are filled with air or water. However, pore volume has another, special meaning in soil physical work. It is important to understand this meaning because pore volumes are widely determined when one is studying the movement of solutes (e.g., dissolved fertilizers or pollutants) through a soil. The term has been misapplied, so it is important to know how to calculate pore volumes.

First let us review definitions. From Darcy's law, we remember that the quantity of flow $Q$ (cm$^3$/h) is the volume of fluid passing through a porous medium in an hour. We also recall that the *Darcy velocity*, which we here shall abbreviate $v_{\mathrm{d}}$ in (cm/h), is the quantity of flow per cross-sectional area $A$ of the flow medium; that is, $v_{\mathrm{d}}$ is $Q/A$. The Darcy velocity is sometimes called the *flux* (Kirkham and Powers, 1972, p. 400).

*Principles of Soil and Plant Water Relations*
http://dx.doi.org/10.1016/B978-0-12-420022-7.00014-8

Copyright © 2014 Elsevier Inc. All rights reserved.

The *Glossary of Soil Science Terms* (Soil Science Society of America, 2008) defines *flux* as follows: "The time rate of transport of a quantity (e.g., mass or volume of fluid, electromagnetic energy, number of particles, or energy) across a given area. See also *flux density*." The *Glossary* defines *flux density* as follows: "The time rate of transport of a quantity (e.g., mass or volume of fluid, electromagnetic energy, number of particles, or energy) per unit area perpendicular to the direction of flow." Flux and flux density often are used interchangeably.

If we were passing water through a vertical soil column by placing a constant head of water on the soil surface, $v_d$ would be the downward velocity of the surface of the water above the soil surface. The *average pore velocity*, $v$, is the velocity in (cm/h) per unit cross-sectional area (cm$^2$) in the pore space. In terms of the Darcy velocity, the average pore velocity is given by

$$v = v_d/\alpha \tag{14.1}$$

where $v_d$ is the Darcy velocity and $\alpha$ is the water-filled porosity of the flow medium (not to be confused with the $\alpha$ in Wooding's equation—e.g., see Eqn (13.8)). Because $\alpha$ is always $<1$, the average pore velocity will always be greater than the Darcy velocity (flux). This is logical because we would expect an element of water in the soil to move faster than the surface of the water standing over the soil (Kirkham and Powers, 1972, p. 400).

We also want to remember that the *actual velocity* of the water is on the average $v/f$, where $f$ is the porosity. (See Eqn (7.2) for the equation to calculate porosity.) The actual velocity of the water in the soil is much greater than the Darcy velocity. The actual velocity, for Darcy's law (saturated, no tension conditions), refers to water in soil that has all the pores completely filled with water. So there is no air-filled porosity. The average pore velocity can refer to completely saturated conditions when it is the actual velocity. But in most situations, we are dealing with unsaturated soil, so both air and water are in the pores, and $\alpha$ refers just to the water-filled porosity.

We are making a special point here to distinguish among the Darcy velocity, the actual velocity, and the average pore velocity because the literature often is not clear as to which velocity is being used in mathematical models. Readers should make sure that they know which velocity is being used (Kirkham and Powers, 1972, pp. 400–401).

## 14.2 ILLUSTRATION OF BREAKTHROUGH CURVES AND PORE VOLUMES

To analyze concentration changes of solute in the effluent from a soil column, we present the data in a standard form called a *breakthrough curve*.

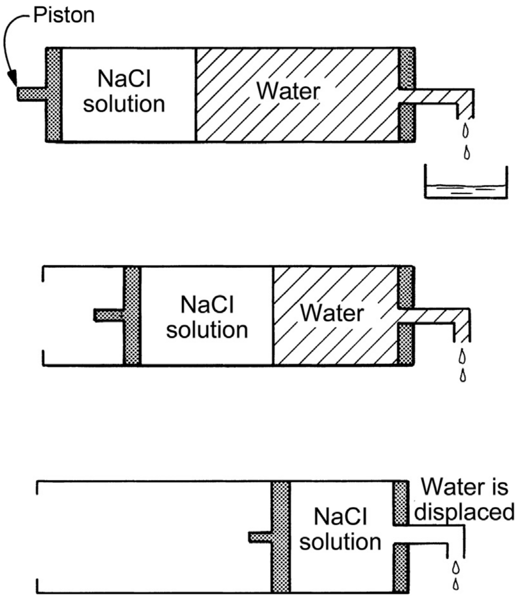
Piston
NaCl solution
Water
NaCl solution
Water
NaCl solution
Water is displaced

**FIGURE 14.1** Schematic drawing of piston flow in a tube. *From Advanced Soil Physics by Kirkham, D., Powers, W.L., p. 382, ©1972, John Wiley & Sons, Inc.: New York. This material is used by permission of John Wiley & Sons, Inc. and William L. Powers.*

A breakthrough curve is a plot of the ratio $C/C_0$ versus the number of pore volumes of effluent collected. Here $C$ is the concentration of the solute found in the effluent (or leachate; we are not referring to wastewater effluent here, but the liquid that comes out of the bottom of a column of soil when it is leached). $C_0$ is the initial concentration of the solute in the displacing fluid, and the pore volume $V_0$ is the volume of the porous medium occupied by fluid (Kirkham and Powers, 1972, p. 381).

Figures 14.1–14.4 illustrate the different kinds of flow of a solute in solution through a medium. Figure 14.1 shows the piston flow for an NaCl

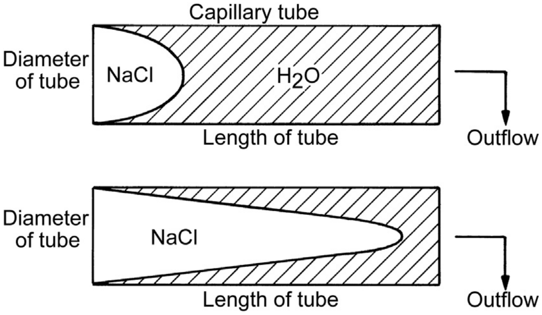
Capillary tube
Diameter of tube
NaCl
H2O
Length of tube
Outflow
Diameter of tube
NaCl
Length of tube
Outflow

**FIGURE 14.2** Schematic drawing of actual flow in a tube. *From Advanced Soil Physics by Kirkham, D., Powers, W.L., p. 383, ©1972, John Wiley & Sons, Inc.: New York. This material is used by permission of John Wiley & Sons, Inc. and William L. Powers.*

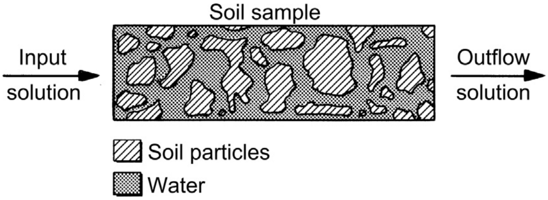

**FIGURE 14.3** Schematic drawing of flow in a saturated soil. *From Advanced Soil Physics by Kirkham, D., Powers, W.L., p. 384, ©1972, John Wiley & Sons, Inc.: New York. This material is used by permission of John Wiley & Sons, Inc. and William L. Powers.*

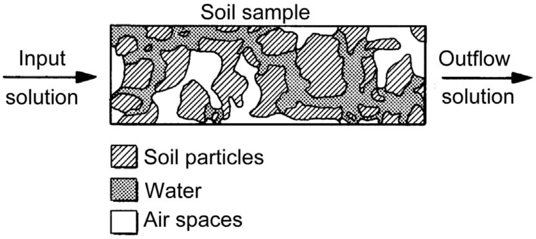

**FIGURE 14.4** Schematic drawing of flow in an unsaturated soil. *From Advanced Soil Physics by Kirkham, D., Powers, W.L., p. 384, ©1972, John Wiley & Sons, Inc.: New York. This material is used by permission of John Wiley & Sons, Inc. and William L. Powers.*

solution replacing water. Piston flow, in fact, is not a mixing process at all, but is a 100% displacement process as illustrated in the figure. Figure 14.2 shows the actual flow in a tube where an NaCl solution is invading water. Figure 14.3 shows the flow in saturated soil, and Figure 14.4 shows the flow in unsaturated soil (Kirkham and Powers, 1972, pp. 382–384). (The columns are all oriented horizontally because Kirkham and Powers are looking at transmission of water as it moves horizontally—i.e., gravity free, desk-top experiments.) The breakthrough curves for each of these four types of flow are shown in Figures 14.5–14.8. Figures 14.9 and 14.10 show the breakthrough curves for chloride in an Oakley sand and an Aiken clay loam, respectively, and Figure 14.11 shows the breakthrough

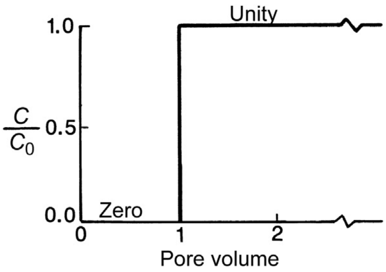

**FIGURE 14.5** Breakthrough curve for piston flow. *From Advanced Soil Physics by Kirkham, D., Powers, W.L., p. 385, ©1972, John Wiley & Sons, Inc.: New York. This material is used by permission of John Wiley & Sons, Inc. and William L. Powers.*

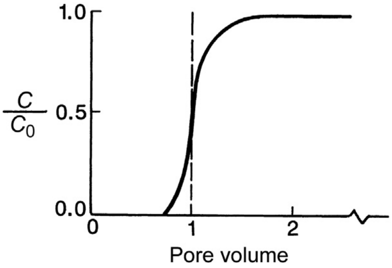

**FIGURE 14.6** Breakthrough curve for flow in a tube. *From Advanced Soil Physics by Kirkham, D., Powers, W.L., p. 385, ©1972, John Wiley & Sons, Inc.: New York. This material is used by permission of John Wiley & Sons, Inc. and William L. Powers.*

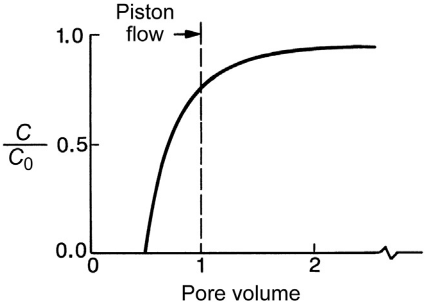

**FIGURE 14.7** Breakthrough curve for wide range in pore velocities as in a saturated soil. *From Advanced Soil Physics by Kirkham, D., Powers, W.L., p. 386, ©1972, John Wiley & Sons, Inc.: New York. This material is used by permission of John Wiley & Sons, Inc. and William L. Powers.*

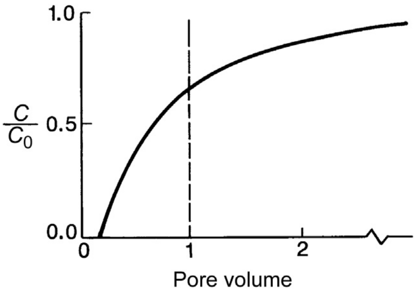

**FIGURE 14.8** Breakthrough curve characteristic of an unsaturated soil. *From Advanced Soil Physics by Kirkham, D., Powers, W.L., p. 386, ©1972, John Wiley & Sons, Inc.: New York. This material is used by permission of John Wiley & Sons, Inc. and William L. Powers.*

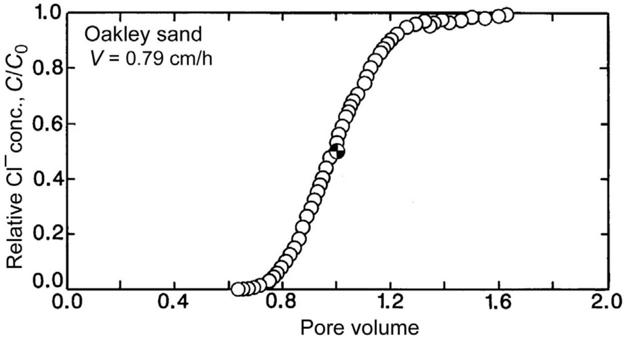

**FIGURE 14.9** Chloride breakthrough curve for Oakley sand. The bicolored circle shows where 0.5 pore volume would occur. *From Advanced Soil Physics by Kirkham, D., Powers, W.L., p. 387, ©1972, John Wiley & Sons, Inc.: New York. This material is used by permission of John Wiley & Sons, Inc. and William L. Powers.*

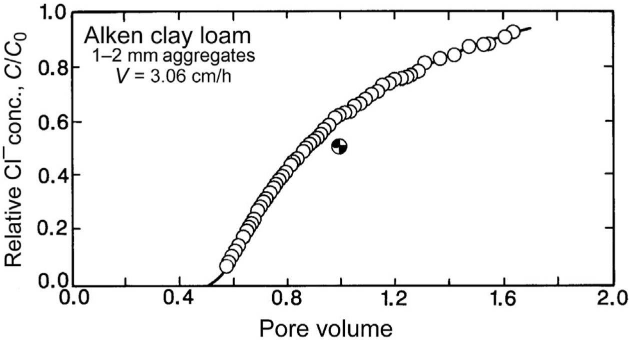

**FIGURE 14.10** Chloride breakthrough curve for Aiken clay loam. The bicolored circle shows where 0.5 pore volume would occur. *From Advanced Soil Physics by Kirkham, D., Powers, W.L., p. 387, ©1972, John Wiley & Sons, Inc.: New York. This material is used by permission of John Wiley & Sons, Inc. and William L. Powers.*

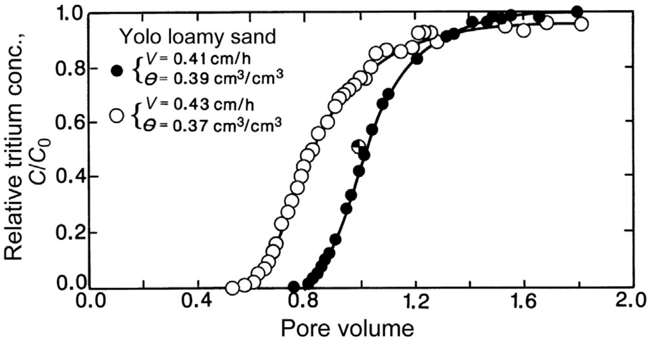

**FIGURE 14.11** Tritium breakthrough curve for Yolo loamy sand at two different water contents. The bicolored circle shows where 0.5 pore volume would occur. *From Advanced Soil Physics by Kirkham, D., Powers, W.L., p. 388, ©1972, John Wiley & Sons, Inc.: New York. This material is used by permission of John Wiley & Sons, Inc. and William L. Powers.*

curve for tritium in a Yolo loamy sand (Kirkham and Powers, 1972, pp. 385–388).

## 14.3 MATHEMATICAL ANALYSIS OF PORE VOLUME

A pore volume $V_o$ is the volume of the porous medium in question occupied by fluid and may be defined by (Kirkham and Powers, 1972, p. 401)

$$V_o = \alpha V \tag{14.2}$$

where $V$ is the bulk volume of the porous medium and $\alpha$ is the water-filled porosity, and we note that the right-hand side of Eqn (14.2) yields one pore volume. The number of pore volumes $p$ of fluid passed through a medium in time $t$ is equal to the volume $Qt$ of fluid moved through the medium divided by its pore volume, that is,

$$p = Qt/V_o \tag{14.3}$$

which, on dividing the numerator and denominator by $A$, yields

$$p = [(Qt)/A]/[(\alpha V/A)] \tag{14.4}$$

In Eqn (14.4), we can substitute $LA$ for $V$, where $L$ is the length of the soil column, and we have $v_d = Q/A$. We can thus write

$$p = v_d t/\alpha L \tag{14.5}$$

Knowing the equation for average pore velocity, we can substitute $v$ for $v_d/\alpha$, and we can write Eqn (14.5) as

$$p = vt/L \tag{14.6}$$

Kirkham and Powers (1972, p. 401 and following) then use Eqn (14.6) to express $C/C_o$ in terms of pore volumes $p$. However, the derivation involves calculus (the use of an error function), so we will not derive the equation. The advanced mathematical reader is referred to this derivation. For those without knowledge of calculus, a method is needed to calculate pore volumes.

## 14.4 CALCULATION OF A PORE VOLUME

To learn how to calculate pore volumes, let us use an example from the experiment by Vogeler et al. (2001). They studied phytoremediation of soil contaminated with copper using poplar. The lysimeter with the poplar is shown on the cover of the book edited by Iskandar and Kirkham (2001). A solution of copper in the form of $Cu(NO_3)_2$ was added to the surface of the soil (Manawatu fine sandy loam) in the lysimeter. Then, every day, the lysimeter was irrigated and drainage water was collected. After running the experiment for 1 week, Vogeler et al. (2001) wanted to know how many pore volumes had passed through the lysimeter. One pore volume was calculated as follows. The shape of the lysimeter was that of a large cylinder, 1.30 m long with a diameter of 0.85 m. The volume of the lysimeter was

$$\text{volume} = \pi r^2 h$$

$$\text{volume} = \pi(0.85/2)^2 1.30 = 0.737\ \text{m}^3.$$

Let $\theta_s$ = saturated water content = 0.40 $\text{m}^3/\text{m}^3$. This value was known from previous measurements.

$$\text{One pore volume} = \text{volume} \times \theta_s = 0.737\ \text{m}^3 \times 0.40\ \text{m}^3/\text{m}^3 = 0.295\ \text{m}^3.$$

$$0.295\ \text{m}^3 \times \left(1 \times 10^6\ \text{cm}^3\right)/\left(1\ \text{m}^3\right) = 295{,}000\ \text{cm}^3 = 295\ \text{liters}.$$

After 7 days of drainage, 70 L had been collected. Thus, (70 L)/(295 L) = 0.24 or about 1/4 pore volume.

To get one pore volume, Vogeler et al. (2001) needed to collect drainage water for 1 month. The experiment was run for 2 months to get two pore volumes.

Another example of calculating pore volumes is given by Singh and Kanwar (1991). They did a column study and calculated the value of one pore volume for each column by multiplying total porosity by the total volume of the soil column. Soil porosity for each column was estimated by using bulk density and particle density (Eqn 7.2). Note that in either case (the experiment by Vogeler et al. (2001) or the experiment by Singh and Kanwar (1991)), the whole pore volume is used to calculate pore volume. Vogeler et al. (2001) used the saturated water content (all pores filled with water); Singh and Kanwar used the total porosity.

In the theoretical development of pore volume (Section 14.3), the water-filled porosity, $\alpha$, is used to calculate a pore volume. In practice, we do not know which pores have air and which pores have water, and hence, which pores are carrying the solute. So in our calculations in this section (above), the water-filled porosity becomes the porosity or the saturated water content. However, we note that the level of saturation affects the shape of the breakthrough curve. We see this by comparing Figure 14.7, the breakthrough curve for a saturated soil, with Figure 14.8, the breakthrough curve for an unsaturated soil. As one pore volume is attained, the slope in Figure 14.7 is steeper than in Figure 14.8.

## 14.5 PORE VOLUMES BASED ON LENGTH UNITS

Jury et al. (1991, pp. 224–225) and Jury and Horton (2004, pp. 230–232) calculate pore volumes by multiplying the length of a column by the water content. They give the formula

$$d_{\mathrm{wb}} = J_{\mathrm{w}} t_{\mathrm{b}} = J_{\mathrm{w}} L/V = L\theta, \tag{14.7}$$

where $d_{\mathrm{wb}}$ is the drainage water (cm) evolved at the breakthrough time $d_{\mathrm{wb}} = J_{\mathrm{w}} t_{\mathrm{b}}$, $J_{\mathrm{w}}$ is the soil water flux (cm/s), $t_{\mathrm{b}}$ is the breakthrough time (s), $L$ is the length of the soil column (cm), and $V$ is the solute velocity (cm/s) (Figures 14.12 and 14.13). (We will assume this velocity as the average pore velocity that Kirkham and Powers define; the definition is given in a preceding section.) Jury et al. (1991, p. 225) and Jury and Horton (2004, p. 232) say that the value $L\theta$ is the volume of water per unit area held in the wetted soil pores of the column during transport. For this reason, $d_{\mathrm{wb}} = L\theta$ is called a pore volume, and it requires approximately one pore

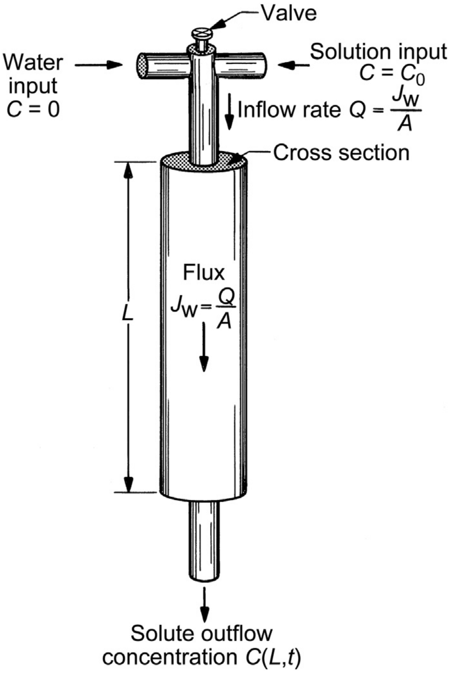

**FIGURE 14.12** Schematic diagram of a soil column outflow experiment, where solute is added at $t = 0$. *From Jury, W.A., Gardner, W.R., Gardner, W.H., Soil Physics, fifth ed., p. 224, ©1991, John Wiley & Sons: New York. This material is used by permission of John Wiley & Sons, Inc.*

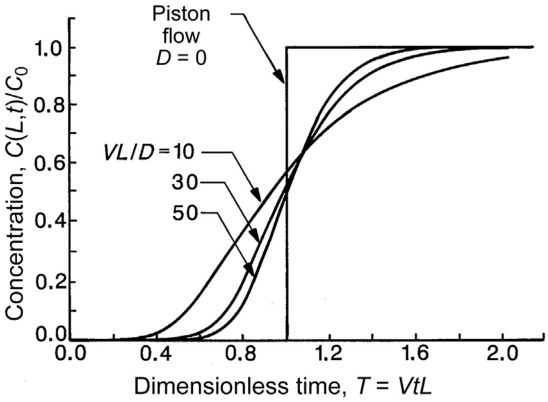

**FIGURE 14.13** Outflow concentration versus time for a step change in solute input at $t=0$. $D=$ dispersion coefficient and it has units of length$^2$/time. If $D=0$, there is no dispersion. Curves correspond to different values of $D$ ($V=2$ cm/day, $L=30$ cm). *From Jury, W.A., Gardner, W.R., Gardner, W.H., Soil Physics, fifth ed., p. 224, ©1991, John Wiley & Sons: New York. This material is used by permission of John Wiley & Sons, Inc.*

volume of water to move a mobile solute through a soil column (Jury et al., 1991, p. 225; Jury and Horton, 2004, p. 232).

Why do Jury et al. (1991) and Jury and Horton (2004) use a length instead of a volume in getting a pore volume? A pore volume is a calculation of the equivalent amount of transmitted water in depth units (where the area has been taken out, as with evapotranspiration, where we use the units of millimeter). So in the case of Kirkham and Powers (1972), they deal with soil in which the water is being transmitted through the water-filled porosity. The calculation is turning the water that is being transmitted (i.e., a $\theta$) into a volume, by multiplying by the soil's volume. But if one is dealing with areas, one can divide through by an area, as we do when we turn a (volumetric) water content (m$^3$/m$^3$) into a depth of storage water (mm) (B.E. Clothier, personal communication, February 25, 1999).

## 14.6 MISCIBLE DISPLACEMENT

Pore volumes are analyzed in miscible displacement studies. Miscible displacement is the process that occurs when one fluid mixes with and displaces another fluid. Leaching of salts from a soil is an example because the added water mixes with and displaces the soil solution. A pioneer in the application of miscible displacement techniques to soil science is D.R. Nielsen. (For a biography of Nielsen, see the Appendix, Section 14.8.) In a key paper, Nielsen et al. (1965) showed that chloride movement in soil depends upon the method of water application. They found that intermittently ponding the soil with 2 in (5 cm) increments of water was more efficient in leaching applied chloride from the soil surface than continuous ponding or leaching with 6 in (15 cm) increments. This finding has important applications in salinity management.

For a mathematical discussion of miscible displacement, the interested reader is referred to Kirkham and Powers (1972, see their Chapter 8).

## 14.7 RELATION BETWEEN MOBILE WATER CONTENT AND PORE VOLUME

As noted in the first paragraph of this chapter, calculation of pore volumes does not tell us about the mobility of a solute, as we determined in Section 13.9, Chapter 13. The question arises, "How does one relate mobile water content to pore volumes?" Or, in other words, "How does the ratio of $c^*/c_m$, needed to determine mobility, relate to $C/C_o$ on the ordinate in breakthrough curves?" The answer to this question is tricky. If we know that the soil wets to $\theta_o$ (the soil water content under a tension infiltrometer), then we can calculate the nonpreferential pore volume using this $\theta_o$. But if our solute comes through earlier (i.e., a smaller pore volume), then not all the pore volume could have been active. So we could define an active pore volume, which we could directly relate to a mobile (volume) fraction, $\theta_m$ (B.E. Clothier, personal communication, February 25, 1999).

## 14.8 APPENDIX: BIOGRAPHY OF DONALD NIELSEN

Donald Rodney Nielsen, soil and water science educator, was born in Phoenix, Arizona, on October 10, 1931. He got his B.S. degree in agricultural chemistry and soils at the University of Arizona in 1953; his M.S. degree in soil microbiology at the University of Arizona in 1954; and his Ph.D. in soil physics at Iowa State University in 1958. His career has been spent at the University of California, Davis, where he started as an assistant professor in 1958, moved to associate professor in 1963, and then to professor in 1968. He became Professor Emeritus in 1994. He was the director of the Kearney Foundation of Soil Science from 1970 to 1975; associate dean, 1970–1980; director of the Food Protection and Toxicology Center, 1974–1975; chairman of the Department of Land, Air, and Water Resources, 1975–1977; executive associate dean of the College of Agricultural and Environmental Sciences, 1986–1989; and chairman of the Department of Agronomy and Range Science, 1989–1991 (Marquis Who's Who, 1994). In his administrative duties, he emphasized the important links between agriculture and environmental science.

Nielsen has been a pioneer in three areas of soil-science research: linking theory to field measurements of water movement, miscible displacement (Nielsen and Biggar, 1962), and geostatistics. One of his first papers with colleagues on geostatistics (Nielsen et al., 1973) became a citation classic (Institute for Scientific Information, 1983). He is the coauthor of a book on soil hydrology (Kutílek and Nielsen, 1994) and a book on spatial and temporal statistics (Nielsen and Wendroth, 2003). He has edited several books, including a major compendium on nitrogen (Nielsen and MacDonald, 1978).

Nielsen has had an outstanding career not only in research and administration but also in teaching and serving as editor on important journals. Nielsen was an associate editor of *Water Resources Research* from when it was established in 1965 until 1986, and he was its editor-in-chief from 1986 to 1989. He has taught 15 different courses dealing with soil physics, water science, and irrigation. He has guided 17 students through to the M.S. degree and 20 students through to the Ph.D., and they are leaders in the field now. Seventy-five scientists from around the world have spent leaves with him.

He has taught workshops at numerous locations around the world, including the International Atomic Energy Agency in Vienna, Austria, and the famous International Center for Theoretical Physics, established by the Nobel Prize-winning Pakistani physicist, Abdus Salam, in Trieste, Italy.

Nielsen has won many awards. He is the Fellow of the American Society of Agronomy, the Soil Science Society of America, and the American Geophysical Union. He has been the president of the Soil Science Society of America, the American Society of Agronomy, and the Hydrology Section of the American Geophysical Union. He was on the National Research Council's Board on Agriculture. He received an honorary doctor of science degree from Ghent State University in Belgium and received the M. King Hubbert Award of the National Ground Water Association. He was made an honorary member of the European Geophysical Society and an honorary member of the Romanian Academy of Sciences. In 2001, he received the Horton Medal from the American Geophysical Union for outstanding contributions to the geophysical aspects of hydrology.

Nielsen maintains an active professional program and dedicates his time in educating soil physicists and hydrologists by daily answering their questions via e-mail. He collaborates with Miroslav Kutílek in writing about soils and climate (Kutílek and Nielsen, 2010, 2013). He married Joanne Joyce Locke on September 26, 1953. They have three daughters and two sons.

# References

Institute for Scientific Information, 1983. This Week's Citation Classic: Nielsen, D.R., Biggar, J.W., and Erh, K.T. Spatial variability of field-measured soil-water properties. Hilgardia 42, 215–259, 1973. Curr. Cont. Agr. Biol. Environ. Sci. 14 (1), 16.

Iskandar, I.K., Kirkham, M.B. (Eds.), 2001. Trace Elements in Soil. Bioavailability, Flux, and Transfer. Lewis Publishers, Boca Raton, Florida.

Jury, W.A., Horton, R., 2004. Soil Physics, sixth ed. Wiley, Hoboken, New Jersey.

Jury, W.A., Gardner, W.R., Gardner, W.H., 1991. Soil Physics, fifth ed. Wiley, New York.

Kirkham, D., Powers, W.L., 1972. Advanced Soil Physics. Wiley-Interscience, New York.

Kutílek, M., Nielsen, D.R., 1994. Soil Hydrology. Catena Verlag, Cremlingen-Destedt, Germany.

Kutílek, M., Nielsen, D.R., 2010. Facts about Global Warming. Catena Verlag, Reiskirchen, Germany.

Kutílek, M., Nielsen, D.R., 2013. Soils, climate, and human adaptability: review of history in the Holocene. In: Brevik, E.C., Burgess, L.C. (Eds.), Soils and Human Health. CRC Press, Taylor & Francis Group, Boca Raton, Florida, pp. 323–343.

Marquis Who's Who, 1994. Who's Who in America, 48th ed. Marquis Who's Who, New Providence, New Jersey. p. 2541.

Nielsen, D.R., Biggar, J.W., 1962. Miscible displacement. III. Theoretical considerations. Soil Sci. Soc. Am. Proc. 26, 216–221.

Nielsen, D.R., MacDonald, J.G. (Eds.), 1978. Nitrogen in the Environment. Two Volumes. vol. 1. *Nitrogen Behavior in Field Soil*. 526 pp. vol. 2. *Soil-Plant-Nitrogen Relationships*. 538 pp. Academic Press, New York.

Nielsen, D.R., Wendroth, O., 2003. Spatial and Temporal Statistics. Catena Verlag, Reiskirchen, Germany.

Nielsen, D.R., Miller, R.J., Biggar, J.W., 1965. Chloride displacement in Panoche clay loam in relation to water movement and distribution. Water Resour. Res. 1, 63–73.

Nielsen, D.R., Biggar, J.W., Erh, K.T., 1973. Spatial variability of field-measured soil-water properties. Hilgardia 42, 215–259.

Singh, P., Kanwar, R.S., 1991. Preferential solute transport through macropores in large undisturbed saturated soil columns. J. Environ. Qual. 20, 295–300.

Soil Science Society of America, 2008. Glossary of Soil Science Terms 2008. Soil Science Society of America, Madison, Wisconsin.

Vogeler, I., Green, S.R., Clothier, B.E., Kirkham, M.B., Robinson, B.H., 2001. Contaminant transport in the root zone. In: Iskandar, I.K., Kirkham, M.B. (Eds.), Trace Elements in Soil. Bioavailability, Flux, and Transfer. Lewis, Boca Raton, Florida, pp. 175–197.

## C H A P T E R

## 15

# Root Anatomy and Poiseuille's Law for Water Flow in Roots

We now turn to water movement in plant roots. We shall apply Poiseuille's law for the flow through the xylem. But first let us review root anatomy and the cell types that make up the xylem.

## 15.1 ROOT ANATOMY

### 15.1.1 The Four Regions of an Elongating Root

Elongating roots usually possess four regions: the root cap, the meristematic region, the region of cell elongation, and the region of differentiation and maturation (Figure 15.1). But these regions are not always clearly delimited (Kramer, 1983, p. 122). The root cap is composed of loosely arranged cells and is usually well defined. Because it has no direct connection with the vascular system, it probably has little role in absorption. It is the site of perception of the gravitation stimulus. Higher plants sense their orientation with respect to gravity in the columella cells of the root cap (Silady et al., 2004). The columella is the central part of a root cap in which the cells are arranged in longitudinal files (Esau, 1977, p. 505). [In this chapter and in subsequent chapters where we talk of stem anatomy (Chapter 17), leaf anatomy (Chapter 23), and stomatal anatomy (Chapter 24), we shall rely on the books by Esau (1965, 1977) for descriptions and figures. Even though other books since her death in 1997 have been published on plant anatomy (Bowes, 2000; Simpson, 2006; MacAdam, 2009), her books remain the standard and should be consulted for information on plant anatomy. They are illustrated with line drawings that represent anatomical parts with accuracy. Recent plant anatomy books mainly use photographs to illustrate plant parts. One cannot point out in a photograph what can be depicted in a drawing. Botanical illustration is a lost art. Draftsmen are no longer are available to make

http://dx.doi.org/10.1016/B978-0-12-420022-7.00015-X

Copyright © 2014 Elsevier Inc. All rights reserved.

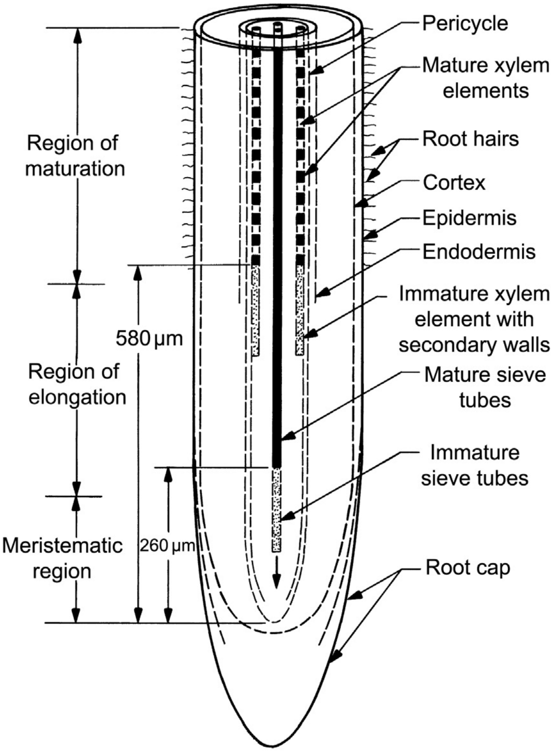
Pericycle
Mature xylem elements
Root hairs
Cortex
Epidermis
Endodermis
Immature xylem element with secondary walls
Mature sieve tubes
Immature sieve tubes
Root cap
Region of maturation
580 μm
Region of elongation
Meristematic region
260 μm

**FIGURE 15.1** Diagram of a tobacco root tip showing relative order of maturation of various tissue. The distance from the tip at which the various tissues differentiate and mature depends on the kind of root and the rate of growth. *From Kramer, 1983, p. 123. Reprinted by permission of Academic Press.*

drawings for textbooks. The diagrams in early textbooks are masterpieces (Hayden, 1986; Desmond, 1989; Lack, 2001). See Appendix, Section 15.8 for a biography of Esau.]

Plant roots need gravity to grow into soil. In space, roots grow in any direction, including upward. It is felt that statoliths (amyloplasts, which contain starch, a product of photosynthesis) are gravisensors, and they are capable of responding swiftly when the organ that houses them (e.g., a root) is displaced relative to the gravity vector (Barlow, 1995). The response is rapid (Esau, 1977, p. 226), taking place in <2 min (Kimbrough et al., 2004). See Esau, 1977 (p. 227, her Figure 14.11) for diagrams illustrating the response to gravity of statoliths in root caps oriented vertically and horizontally. How the statoliths maintain straight growth downward remains an unsolved puzzle. Information suggests they contact the cell membrane (plasma membrane), which contains gravity receptors. Hormones are then produced that cause the root to grown down and the shoot to grow up (Kirkham, 2008).

The meristematic region typically consists of numerous small, compactly arranged, thin-walled cells almost completely filled with cytoplasm. Relatively little water or salt is absorbed through this region, largely because of the high resistance to movement through the cytoplasm and the lack of a conducting system (Kramer, 1983, p. 122).

Usually there is a zone of rapid cell elongation and expansion, a few tenths of a millimeter behind the root apex. It is difficult to indicate a definite zone of differentiation because various types of cells and tissues are differentiated at different distances behind the root apex (Kramer, 1983, p. 122). Typically, sieve tubes of the phloem differentiate before the xylem elements (Esau, 1965, p. 498). As the newly enlarged, thin-walled cells at the base of the zone of enlargement cease to elongate, they become differentiated into the epidermis, cortex, and stele, which constitute the primary structures of roots.

### 15.1.2 Root Hairs

Root hairs appear when the epidermis differentiates. The epidermis has specialized cells that are root hair cells. Much attention has been given to root hairs because of their presumed importance as absorbing surfaces. The epidermis is usually composed of relatively thin-walled, elongated cells that form a compact layer covering the exterior of young roots. Sometimes a second compact layer, the hypodermis, lies beneath the epidermis. In some plants, including citrus and conifers, root hairs can arise not only from the epidermis, but also from the layer of cells beneath the epidermis, or even from deeper in the cortex (Kramer, 1983, p. 125).

### 15.1.3 Dicotyledonous Roots

The arrangement of the principal tissues in a dicotyledonous root is shown in Figure 15.2. The conductive tissues form a solid mass in the center, instead of being dispersed in bundles around the periphery of the pith, as in stems of most herbaceous, dicotyledonous plants (Kramer, 1983, p. 124) (We will study stem anatomy in Chapter 17.). The primary xylem in the roots of dicots usually consists of two to several strands extending radially outward from the center, with the primary phloem located between them. The outermost layer of the stele is the pericycle. The stele comprises pericycle, the vascular system, and the associated

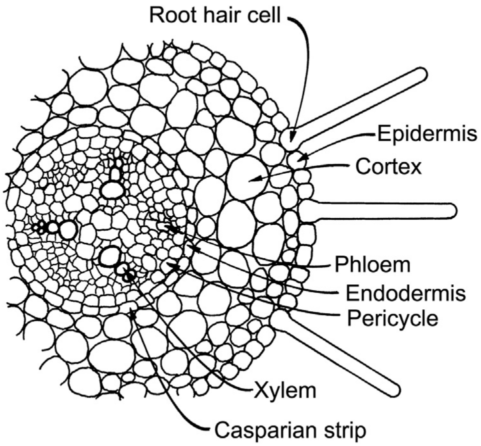

**FIGURE 15.2** A dicotyledonous root (a squash root). Note the central stele of vascular tissue. *From Kramer, 1983, p. 12. Reprinted by permission of Academic Press.*

ground tissue (Esau, 1977, p. 527). The cells of the pericycle retain their ability to divide, and they give rise not only to branch roots but also to the cork cambium, if secondary growth occurs. The endodermis usually consists of a single layer of cells and forms the inner layer of the cortex. The endodermis has the casparian strip, which is a band-like wall formation within primary walls that contains suberin and lignin. It occurs on the radial and transverse walls in the endodermis (Esau, 1977, p. 504).

### 15.1.4 Monocotyledonous Root

In monocotyledonous plants, a variable number of xylem vessels are arranged in a circle around a pith (Figure 15.3). However, in some monocotyledonous roots such as wheat (Figure 15.4), a single vessel occupies the center and is separated by nontracheary elements from other vessels (Esau, 1965, p. 496). The large central xylem vessel is part of the metaxylem. The metaxylem is part of the primary xylem that differentiates after the protoxylem and before the secondary xylem, if any secondary xylem is formed in a given species. Protoxylem is the first-formed element of the xylem in a plant organ. It is the first part of the primary xylem. The protoxylem gets crushed as the metaxylem develops. Although most monocotyledons lack secondary growth from a vascular cambium, they can undergo a type of "secondary growth" by an intense and protracted thickening growth. Large trees can result, such as palm trees (Esau, 1965, p. 400), which are monocotyledons.

### 15.1.5 Movement of Water and Solutes across the Root

The structure of the root is of particular interest with regard to the movement of water and the dissolved salts in it from the absorbing cells to

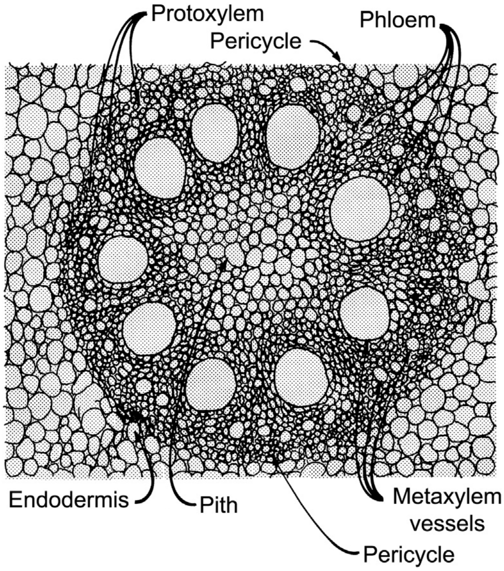
Protoxylem
Pericycle
Phloem
Endodermis
Pith
Metaxylem vessels
Pericycle

**FIGURE 15.3** A monocotyledonous root (a corn root). Note the central pith. *From Esau, 1965, p. 713. This material is used by permission of John Wiley & Sons, Inc.*

the conducting tissues, and their release from the living cells of the vascular cylinder into the nonliving tracheary elements. Figure 15.5 illustrates the pathway of the soil solution in the wheat root (Esau, 1965, pp. 516—517). The arrows indicate the direction of movement in certain selected cells. The living cells among these are stippled. The most notable features of this pathway are: (1) the presence of abundant intercellular spaces in the cortex, (2) the lack of such spaces in the vascular cylinder,

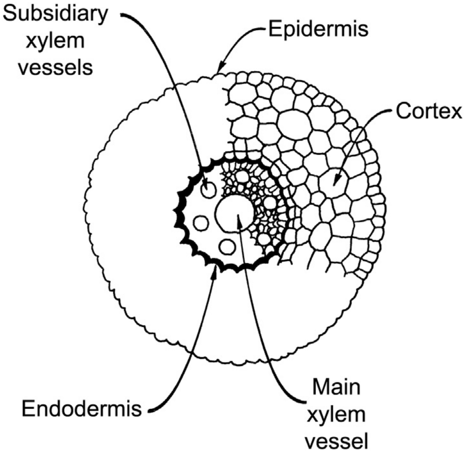
Subsidiary xylem vessels
Epidermis
Cortex
Endodermis
Main xylem vessel

**FIGURE 15.4** A monocotyledonous root (a wheat root). Note the central large xylem vessel, part of the metaxylem. *From Richards, R.A., Passioura, J.B., p. 250, 1981a. Crop Science Society of America. Madison, Wisconsin. Reprinted by permission of the Crop Science Society of America.*

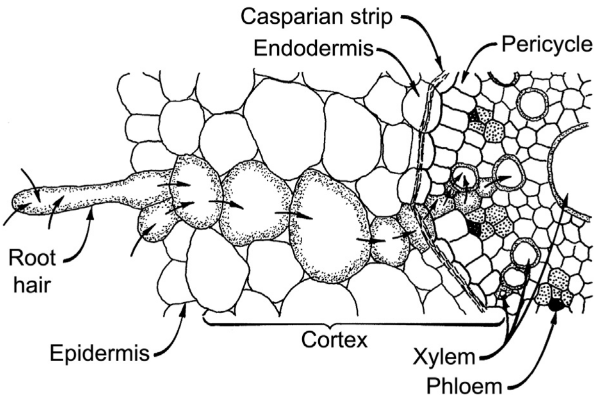

**FIGURE 15.5** Part of a transection of a wheat root, illustrating the kinds of cells that may be traversed by water and salts absorbed from the soil before they reach the tracheary elements of the xylem. Arrows indicate the direction of movement through a selected series of cells. Among these, the living cells are partly stippled. The casparian strip in the endodermis is shown as though exposed in surface views of end walls. *From Esau, 1965, p. 517. This material is used by permission of John Wiley & Sons, Inc.*

and (3) the presence of a specialized endodermis between the two systems. The endodermis between the two distinct systems (cortex and vascular cylinder) acts as a barrier that facilitates the development of hydrostatic pressure in the vascular cylinder by preventing a leakage of solutes from the vascular cylinder into the cortex.

## 15.1.6 Endodermis

Let us consider the endodermis and its casparian strip in more detail. A prominent feature of the primary structure of most roots is the endodermis, the inner layer of cells of the cortex which separates it from the stele. The endodermis is not part of the stele. The stele comprises the vascular system (xylem and phloem) and the associated ground tissue (pericycle; interfascicular regions, and pith, if it occurs). Early in the development of the endodermis, suberin (a fatty substance) is deposited in bands on the radial walls and transverse walls in the longitudinal direction, forming the casparian strip (Figure 15.6). It renders them relatively impermeable to water and presents a barrier to inward movement of water and solutes in the apoplast (Kramer, 1983, p. 128). The apoplast is the supposedly dead part of the plant tissue, including the cell walls. The symplast or symplasm is the continuum of communicating cytoplasm, which is created by the intercellular connections. Plasmodesmata are fine, cytoplasmic threads that pass from a protoplast through a cell wall directly into the protoplast of a second cell (Nobel, 1974, p. 37).

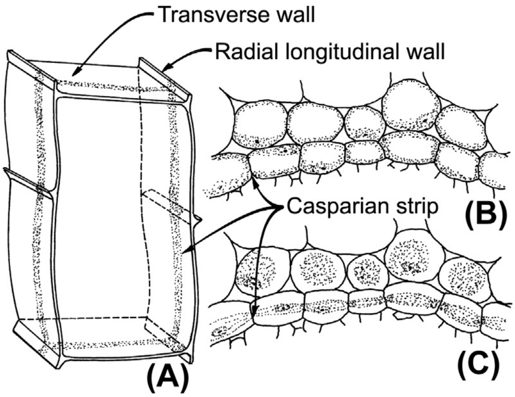

**FIGURE 15.6** Endodermal cells. (A) Entire cell showing location of casparian strip. (B and C) Effect of treatment with alcohol on cells of endodermis and of parenchyma. (B) Cells before treatment and (C) after treatment. (B, C) The casparian strip is seen only in the sectional views. *From Esau, 1965, p. 489, 1965. This material is used by permission of John Wiley & Sons, Inc.*

The endodermis characterized by casparian strips is almost universally present in roots (Esau, 1965, p. 489). It is made up of both suberin and lignin (Esau, 1977, p. 504). The strip is formed during the early ontogeny of the cell and is a part of the primary wall. It varies in width and is often much narrower than the wall in which it occurs. The incrustation of the cell wall by the material constituting the casparian strip presumably blocks the submicroscopic capillaries in the wall and hinders the movement of substances through the walls (Esau, 1965, p. 517). Moreover, the cytoplasm of the endodermal cells is relatively firmly attached to the casparian strip, so that it does not readily separate from the strip when the tissue is subjected to the effects of plasmolytic or other agents normally causing a contraction of protoplasts (Figure 15.6). Thus the casparian strip appears to form a barrier at which the soil solution is forced to pass through the selectively permeable cytoplasm (the symplasm) rather than through the cell wall (apoplast) (Grebe, 2011). When the casparian strip is broken down, which may occur when herbicides or chelating agents are added to the soil, free passage of ions into the stele occurs (Nowack et al., 2006). When the root cells are so damaged and there is uncontrolled inflow of soil solution into the stele, the plant dies (Brett H. Robinson, Soil and Physical Sciences, Lincoln University, Christchurch, New Zealand, personal communication, June 17, 2012). For an assessment of the endodermis using molecular data from *Arabidopsis*, see Petricka et al. (2012) and Geldner (2013).

## 15.1.7 Cell Types in Xylem Tissue

Xylem is a tissue that is composed of four cell types (Table 15.1): tracheids and vessel members, which make up the tracheary elements, fibers, and parenchyma cells (Esau, 1977, p. 103). The tracheary elements

**TABLE 15.1** The Four Cell Types in Xylem Tissue: Tracheids, Vessel Members, Fibers, and Parenchyma Cells

| Cell Types | Principal Function |
|---|---|
| • Axial system | |
| ✓ Tracheary elements | |
| • Tracheids | Conduction of water |
| • Vessel members | |
| ✓ Fibers | |
| • Fiber-tracheids | Support; sometimes storage |
| • Libriform fibers | |
| ✓ Parenchyma cells | Storage and translocation of ergastic substances |
| • Ray system | |
| ✓ Parenchyma cells (Tracheids in some conifers) | |

*From Esau, 1977, p. 106, ©1977. This material is used by permission of John Wiley & Sons, Inc.*

are the most highly specialized cells of the xylem and are concerned with the conduction of water and substances in water. They are nonliving cells at maturity. They have lignified walls with secondary thickenings and a variety of pits.

The two kinds of tracheary cells, the tracheids and the vessel members, differ from each other in that the tracheid is an imperforate cell, whereas the vessel member has perforations, one or more at each end and sometimes also on a side wall (Esau, 1977, p. 106). The longitudinal series of vessel members interconnected through their perforations are called *xylem vessels* or simply, *vessels*. The perforated part of a wall of a vessel member is called the *perforation plate*. A plate may be simple, with only one perforation, or multiperforate, with more than one perforation.

The fibers are long cells with secondary, commonly lignified, walls (Esau, 1977, p. 108). The walls vary in thickness but are usually thicker than the walls of tracheids in the same wood (wood is secondary xylem, which we discuss in the next paragraph). Two principal types of xylem fibers are recognized—the fiber-tracheids and the libriform fibers. If both occur in the same wood, the libriform fiber is longer and has thicker walls than the fiber-tracheid. Fibers give support to the xylem.

Parenchyma cells of the primary xylem occur in interfascicular regions and are considered to be part of the ground tissue (Esau, 1977, pp. 112–113). In the root, the primary xylem forms a core with parenchyma (as in some monocotyledonous roots) or a core without parenchyma (as in dicotyledonous roots). In secondary xylem, the parenchyma cells make up the axial and ray parenchyma. These parenchyma cells store starch, oils, and many other ergastic substances. Ergastic substances are products of protoplasts such as starch grains, fat globules, crystals, and fluids. They occur in the cytoplasm, organelles, vacuoles, and cell walls (Esau, 1977, p. 509). Rays are important in plants that undergo secondary growth (e.g., trees). We shall consider them when we discuss the anatomy of stems (Chapter 17). Rays extend radially in the secondary xylem (called the *wood*) and the secondary phloem (the *bark*) (Esau, 1977, p. 531, 503), and they are shown in the wood in Figure 17.3, which illustrates secondary vascular tissue. Ray parenchyma cells function as a radial route for nutrient distribution in woody plants. Wood rays are known to play an important role in tree development and may allow some trees to live more than 1000 years (Larisch et al., 2012).

We can list the characteristics of tracheids, vessel members, fibers, and parenchyma cells as follows:

Tracheids

- More primitive (in angiosperms, gymnosperms, and lower vascular plants)
- Tapered ends
- Long cells
- Thin cells
- Lignified secondary cell walls
- No protoplasts at maturity (dead)

Vessel members

- Present only in angiosperms (more evolved than tracheids)
- Short cells
- Broad cells
- Flat ends
- Perforated end walls with perforation plates
- Lignified secondary cell walls
- No protoplasts at maturity (dead)
- Several together form a continuous tube, which is called a xylem vessel
- A xylem vessel is a low-resistance circuit
- Width varies from 10 to 800 μm; an average diameter is about 40 μm
- Length of a xylem vessel varies from few hundred microns (μm) to a few millimeters. Long and wide xylem vessels occur in tropical plants such as vines (e.g., kiwifruit) and rattans (climbing palms). Fisher et al (2002) of the Fairchild Tropical Garden in Miami, Florida, found a vessel in a rattan that was 3 m long and 532 μm in diameter.

Fibers
- For structural support
- Long cells
- Thin cells
- Heavily lignified cell walls
- No protoplasts at maturity (dead)

Parenchyma cells
- For storage
- For lateral movement of water and solutes into and out of conducting cells (the ray system in secondary xylem) (Table 15.1).

## 15.2 POISEUILLE'S LAW

Poiseuille, a French physiologist, discovered the law on velocity of flow of a liquid through a capillary tube (For a biography of Poiseuille, see the Appendix, Section 15.6.). He found that the volume of fluid moving in unit time along a cylinder is proportional to the fourth power of its radius and that the movement depends on the drop in pressure. Poiseuille's law applies to cylindrical, capillary tubes. Even though the soil can be considered to consist of cylindrical tubes, Poiseuille's law is usually not applied to water movement in soil. Darcy's law is used. As noted in Table 7.1, Darcy's law is a linear-flow law (Poiseuille's law is not), and Darcy's law applies to an area-averaged section of the soil. Darcy's law does not consider water movement at the small scale of a capillary tube.

Poiseuille's law states (Weast, 1964, p. F-62):

$$v = \left(\pi p r^4\right)/(8X\eta), \tag{15.1}$$

where

$v =$ volume (cm$^3$) escaping per second
$p =$ difference of pressure at the ends of the tube (dyn/cm$^2$)
$r =$ radius of the tube (cm)
$X =$ length of tube (cm)
$\eta =$ coefficient of viscosity (poise or dyn-s/cm$^2$).

The volume will be given in cm$^3$/s if $X$ and $r$ are in cm, $p$ in dyn/cm$^2$, and $\eta$ in poises or dyn-s/cm$^2$.

We take a moment here to consider viscosity (Weast, 1964, p. F-62). All fluids possess a definite resistance to change of form and many solids show a gradual yielding of forces tending to change their form. This property, a sort of internal friction, is called *viscosity*. It is expressed in dyn-s/cm$^2$ or poises. The unit is named after Poiseuille. Remember that poise also can be expressed as g/cm/s if we replace dyne by (g cm)/s$^2$ using Newton's law, $F = ma$.

We present the Poiseuille equation in the form that Nobel (1974, p. 392; 1983, p. 494; 1991, p. 508; 1999, p. 375; 2005, p. 448; 2009, p. 471) gives

$$v = -\left(\pi r^4/8\eta\right)(\partial P/\partial X), \tag{15.2}$$

where

$v$ = rate of volume movement (e.g., in units of $\text{cm}^3/\text{s}$)
$r$ = radius of the capillary tube (cm)
$\eta$ = viscosity of the solution (poise)
$-(\partial P/\partial X)$ = the negative gradient of the hydrostatic pressure.

Hydrostatics (construed as singular) is the branch of physics having to do with the pressure and equilibrium of water and other liquids. Statics is the branch of mechanics dealing with bodies, masses, or forces at rest or in equilibrium. Henceforth, instead of saying "hydrostatic pressure", we simply will say "pressure". Because positive flow occurs in the direction of decreasing pressure [$(\partial P/\partial X)$ is $<0$], the minus sign is necessary in Eqn (15.2).

In Eqn (15.2), we use partial derivatives. When a quantity is a function of more than one independent variable, it is necessary to use partial derivatives when discussing differentials or derivatives. For example, if $u = f(x,y)$, the partial derivative of $u$ with respect to $x$, $(\partial u/\partial x)_y$, is the rate with which $u$ changes with a change in $x$ at a constant value of $y$. A subscript is used on the partial derivative when it is important to emphasize which variable is held constant (Daniels and Alberty, 1966, p. 740). See Appendix 6 of Nobel, 1974, (pp. 435–450) for a discussion of calculus, including partial derivatives. Note that $v$ depends both on $P$ and $X$.

In Poiseuille's law, we are concerned with the volume flowing per unit time and area, often represented by $J_v$, and called *flux*. For flow in a cylinder of radius $r$, and hence area $\pi r^2$, $J_v$ is

$$v/\pi r^2 = J_v = -\left(r^2/8\eta\right)(\partial P/\partial X), \tag{15.3}$$

where $J_v$ has units of length/time. This is the form of Poiseuille's law that we shall use in our calculations (Section 15.4).

## 15.3 ASSUMPTIONS OF POISEUILLE'S LAW

Before we use Poiseuille's law, we need to consider the assumptions used in deriving it. These assumptions are important to know so we can apply the law correctly.

Poiseuille's law assumes two things. First, it assumes that the fluid in the cylinder moves in layers or laminas, each layer gliding over the adjacent one. In laminar flow, two particles of water moving will describe paths (streamlines) that will never cross each other (Kirkham, 1961, p. 47). Such laminar movement occurs only if flow is slow enough to meet a criterion deduced by Reynolds in 1883 (Nobel, 1974, p. 392) called the Reynolds number, Re, which is the dimensionless quantity:

$$\mathrm{Re} = (\rho J_{\mathrm{V}} r)/\eta. \tag{15.4}$$

The symbols in Eqn (15.4) are the same as those defined above and $\rho$ is the solution density (Reynolds did not call the number "the Reynolds number"; his students started to refer to it as "the Reynolds's number". It is usually called the Reynolds number and the possessive form is not used. For a biography of Reynolds, see the Appendix, Section 15.7.). Re must be <2000 to have laminar flow. Otherwise, a transition to turbulent flow occurs and Eqn (15.3) is no longer valid. In turbulent flow, whirls and eddies develop. An eddy is a current of water or air running contrary to the main current, especially, a small whirlpool. For an article on turbulence, see Moin and Kim (1997). Turbulence is still one of the great unsolved problems of classical physics (Nelkin, 1992). The number 2000 is not exact and other numbers in this range are cited in the literature as the Reynolds number at which turbulence takes over.

Second, Poiseuille's law assumes that the fluid in Poiseuille (laminar) flow is actually stationary at the wall of the cylinder. The velocity of solution flow increases in a parabolic manner to a maximum value in the center of the tube. Thus the flux in Eqn (15.3) is actually the mean flow averaged over the entire cross-section of cylinder of radius *r*.

Poiseuille's law requires advanced mathematics for its proof. For a proof, see Childs, 1969 (pp. 194–196). For a discussion of Poiseuille velocity distribution in a circular tube, see Bird et al., 1960 (pp. 123–130).

## 15.4 CALCULATIONS OF FLOW BASED ON POISEUILLE'S LAW

Following the analysis of Nobel (1974, pp. 391–395; 1983, pp. 493–498; 1991, pp. 508–513; 1999, pp. 375–378; 2005, pp. 448–453; 2009, pp. 471–476), we now shall use Poiseuille's law to estimate the pressure gradient in different parts of the pathway that water takes when it goes from outside the root and through the apoplast to the endodermis, where it is forced into the living part of the plant (symplasm) because of the casparian strip. The region of a plant made up of cell walls and the hollow xylem vessels is part of the apoplast. Water and the solutes that it contains can move fairly readily in the apoplast. But they must cross a membrane to enter the symplast, the living part of the cells (Nobel, 1974, p. 395). The role of the apoplast in water transport is not fully understood and is an area of active investigation (Steudle and Frensch, 1996; Schreiber et al., 1999).

Nobel first calculates the pressure gradient that occurs in the xylem vessels of diffuse-porous wood. Before we continue with his analysis, we review wood anatomy. There are two types of wood (secondary xylem): diffuse-porous wood and ring-porous wood (Esau, 1965, 1977). In diffuse-porous wood, the xylem members have more or less equal diameters in the spring and summer wood. Esau, 1977 (p. 508) defines diffuse-porous wood as secondary xylem, in which the pores (vessels) are distributed fairly uniformly throughout a growth layer or change in size gradually from early to late wood. Examples of diffuse-porous wood are *Acer* (maple), *Betula* (birch), and *Liriodendron* (tulip tree). In ring-porous wood, the vessel members are large in diameter in the spring wood and are small in diameter in the summer wood. Esau, 1977 (p. 524) defines ring-porous wood as secondary xylem in which the pores (vessels) of the early wood are distinctly larger than those of the late wood and form a well-defined zone or ring in a cross-section of wood. Examples of ring-porous wood are *Castanea* (chestnut), *Fraxinus* (ash), *Robinia* (locust), and some *Quercus* (oak).

We note that Nobel's analysis is for wood, which can occur in woody stems or woody roots. His calculations for Poiseuille-law flow, therefore, are not confined to roots.

Nobel assumes, based on experimental data, that the velocity of sap ascent in the xylem of a transpiring tree with diffuse-porous wood is 0.1 cm/s. This is the value for $J_V$. For a tree with ring-porous wood, he assumes $J_V$ is 10 times faster (1.0 cm/s). He assumes that the radius of the vessel member in the diffuse-porous wood is 20 μm and the radius of the vessel member in the ring-porous wood is 100 μm. Nobel also assumes that the xylem sap is a dilute aqueous solution, so the volume flow (flux) ($J_V$) is essentially the same as the volume of water flow, and the viscosity of the solution is the same as that for water.

We now use Eqn (15.3) to solve for the pressure gradient in a tree with diffuse-porous wood:

$$J_V = -\left(r^2/8\eta\right)(\partial P/\partial X)$$

$$0.1\ \text{cm/s} = -\left(20 \times 10^{-4}\right)^2/8\left(0.010\ \text{dyn-s/cm}^2\right)(\partial P/\partial X)$$

or

$$(\partial P/\partial X) = -2 \times 10^3\ \text{dyn-s/cm}^3.$$

We know that $1\ \text{bar} = 1 \times 10^6\ \text{dyn-s/cm}^2$. Therefore, $-2 \times 10^3\ \text{dyn-s/cm}^3 = -2 \times 10^{-3}\ \text{bar/cm}$ or $-0.2$ bar/m. Remember this number. We will come back to it.

We digress to calculate Reynolds number for water movement in diffuse-porous and ring-porous wood. We use a density for the sap in the xylem of $1\ \text{g/cm}^3$ (same as water at 20 °C). We now change the units of density to dyn-s$^2$/cm$^4$. Remember $F = ma$; 1 dyn = 1 g × 1 cm/s$^2$; so 1 g = dyn-s$^2$/cm. Substituting into the formula for density, $\rho$, we get units for density of dyn-s$^2$/cm$^4$. We find the Reynolds number, Re, for diffuse-porous wood with a radius of 20 μm for the vessel members and a velocity of sap flow of 0.1 cm/s to be

$$\mathrm{Re} = (\rho J_\mathrm{v} r)/\eta$$

$$\mathrm{Re} = \left[\left(1\ \text{dyn-s}^2/\text{cm}^4\right)(0.1\ \text{cm/s})\left(2 \times 10^{-3}\ \text{cm}\right)\right]/0.010\ \text{dyn-s/cm}^2$$
$$= 0.02\ (\text{unitless}).$$

For a ring-porous tree with a radius of 100 μm for the vessel members and a velocity of sap flow of 1 cm/s, Re is

$$\left[\left(1\ \text{dyn-s}^2/\text{cm}^4\right)(1\ \text{cm/s})(0.01\ \text{cm})\right]/0.010\ \text{dyn-s/cm}^2 = 1\ (\text{unitless}).$$

The value of Re = 1 for the ring-porous tree is still far less than the value of 2000, where turbulence generally starts. Therefore, we can be assured that Poiseuille's law applies even to plants with large-diameter vessel members.

Let us get back to the main problem of determining the pressure gradient in different parts of the pathway that water takes as it crosses a root. We have calculated the pressure gradient that occurs in the xylem vessels. Now let us calculate the pressure drop in the cell walls, again following Nobel's (1974, 1983, 1991, 2005, 2009) analysis.

The interfibrillar spaces in a cell wall have diameters of about 10 nm. Let us assume that the average radius of these interstices is 5 nm. We are forgetting tortuosity and we are assuming that the cell walls are tubes where Poiseuille's law applies. Let us assume the same $J_\mathrm{v}$ that we used previously ($J_\mathrm{v} = 0.1$ cm/s). The pressure gradient in the cell walls is

$$J_\mathrm{v} = -\left(r^2/8\eta\right)(\partial P/\partial X)$$

$$0.1\ \text{cm/s} = -\left(5 \times 10^{-7}\right)^2/8\left(0.010\ \text{dyn-s/cm}^2\right)(\partial P/\partial X)$$

or

$$(\partial P/\partial X) = -3.2 \times 10^{10}\ \text{dyn-s/cm}^3 = -3.2 \times 10^6\ \text{bars/m}.$$

A $(\partial P/\partial X)$ of only −0.2 bar/m is needed for the same $J_\mathrm{v}$ in the vessel member having a radius of 20 μm. Thus, the $(\partial P/\partial X)$ for Poiseuille flow through the small interstices of a cell wall is over $10^7$ times greater than for the same flux through the lumen of the vessel member. Because of the tremendous pressure gradients required to force water through the small interstices available for solution conduction in the cell wall, a solution cannot flow rapidly enough up a tree in the cell walls, as has been suggested, to account for the observed rates of water movement (Nobel, 1974, p. 394).

Now let us calculate the pressure gradient for the cell membrane. The Poiseuille law no longer applies because we have no capillary tubes. We use the following equation for flux, $J_v$, through the plasmalemma (Nobel, 1974, p. 395 and p. 144):

$$J_v = L_p(\Delta P - \sigma \Delta \pi), \tag{15.5}$$

where

$L_p$ = hydraulic conductivity coefficient of the cell membrane
$\Delta P$ = difference in pressure across the membrane
$\sigma$ = reflection coefficient. This is a unitless number and varies between 0 and 1. If $\sigma = 1$, all solutes are reflected from the membrane and no solute gets across it. If $\sigma = 0$, all solutes can cross the membrane.
$\Delta\pi$ = osmotic pressure difference across the membrane.

We are considering a dilute solution. The xylem sap is very dilute and we can consider it to be like water. So we shall consider that $\Delta\pi = 0$ and the last term in Eqn (15.5) drops out.

So we have $J_v = L_p\,(\Delta P)$. Let us assume we are still studying plants with a $J_v$ of 0.1 cm/s. A reasonable value to assume for $L_p$ is $1 \times 10^{-5}$ cm/s-bar (Nobel, 1974, p. 395). So,

$$\Delta P = (0.1 \text{ cm/s})/1 \times 10^{-5} \text{ cm/s-bar} = 10{,}000 \text{ bar} = 1 \times 10^{4} \text{ bar}.$$

Now let us consider a vessel member before the plasmalemma has broken down (This is probably an unrealistic situation because in the mature vessel member, the cell membrane is broken down. But we continue with the analysis of Nobel, 1974 (p. 395), and compare flux through the vessel member, cell wall, and cell membrane.). Let us assume that the lumen in our vessel member is 1000 μm long and has a diameter of 20 μm and that the cell wall is 5 μm thick all the way around the cell. As water moves from below and up through this rectangular cell, it passes through the cell wall (5 μm), then the cell membrane, then goes into the lumen that is 1000 μm long, and then passes another membrane and finally another cell wall (5 μm). With these distances, we now can compare the pressure drop across the membrane, cell wall, and lumen. For the membrane, it is $-2 \times 10^{4}$ bar. This value includes both ends of the cell (the water traverses the membrane two times—going into the cell and coming out of the cell).

Now let us consider the cell walls. Again, the water moves through one cell wall at the proximal end of the cell and another cell wall through the distal end. Taking the value for $(\partial P/\partial X)$, $-3.2 \times 10^{6}$ bars/m, and multiplying it by $10 \times 10^{-6}$ m (each end of the cell has a cell wall that is 5 μm thick for a total cell wall thickness that the water must traverse of 10 μm), we get

$$-3.2 \times 10^6\ \text{bar/m} \times 10 \times 10^{-6}\ \text{m} = -30\ \text{bars (rounding off)}.$$

For the lumen, we found $(\partial P/\partial X) = -0.2$ bar/m. If we multiply this by the length of the lumen, 1000 μm or $1 \times 10^{-3}$ m, we get $-0.2$ bar/m $\times$ $1 \times 10^{-3}$ m $= -2 \times 10^{-4}$ bar.

Comparison gives the following:

Membranes: $-2 \times 10^4$ bar
Cell walls: $-30$ bar
Lumen: $-2 \times 10^{-4}$ bar

The main barriers to water transport are the cell membranes. The interstices of the cell walls provide a much easier pathway for solution flow, while a hollow xylem vessel presents the least obstacle. The evolution of xylem, in particular, the vessel members in the angiosperms, provides a plant with a tube well suited for moving water over long distances.

## 15.5 AGRONOMIC APPLICATIONS OF POISEUILLE'S LAW

One of the first important agronomic uses of Poiseuille's law was in a pioneering paper by Passioura (1972) in Australia where wheat plants face *terminal drought*, as they do in other semiarid areas. This is a term that is used when plants are grown in dry land. If they are not irrigated, the crops often use up water stored in the soil by the time they reach flowering, and then no water is available for flowering, grain fill, and the remainder of the life cycle. So the drought at the end part of the life cycle is called "terminal".

Passioura (1972) suggested that when wheat is growing predominantly on stored water, it is an advantage for the plants to have root systems of high hydraulic resistance, so that they will conserve water during early growth and thus have more water available while filling their grain. The xylem of the seminal roots in wheat is dominated by one large metaxylem element (vessel member), the diameter of which (about 50 μm in diameter on average) probably determines the amount of water flowing through the wheat plant, and, thus, indirectly, its hydraulic resistance (Note: Poiseuille's law says nothing about resistance—only the flux in a capillary tube as it is related to the pressure drop.). Passioura (1972) suggested that the resistance to flow in the wheat root could be increased in one of the two ways: (1) by decreasing the size of the central metaxylem element, or (2) by reducing the number of seminal roots.

Passioura (1972) chose to reduce the number of seminal roots. He forced wheat plants to grow on one seminal root. The number of seminal roots that different cultivars (varieties) of wheat produce is under genetic control. Percival (1921) reported that the wheat plant may produce up to eight seminal roots. (Note: The words *cultivar* and *variety* are used interchangeably. A "cultivar" is a "cultivated variety", i.e., a native variety cultivated for specific characteristics.)

Passioura (1972) grew wheat in two columns of soil in a greenhouse. The wheat plants in one column had only one seminal root because he cut off all the others. The wheat plants in the other column had their natural number of seminal roots (three seminal roots). He irrigated at the beginning of the experiment when the plants were young and then let the plants reach terminal drought. He applied Poiseuille's law to the central large metaxylem element for both treatments. His measurements and calculations showed the following:

| | **$J_v$ (Measured) (mm/s)** | **$\partial P/\partial X$ (Pressure Gradient) (Calculated) (bar/mm)** |
|---|---|---|
| 1 seminal root | 800 | $\lvert 0.1 \rvert$ |
| 3 seminal roots | 250 | $\lvert 0.03 \rvert$ |

The single-rooted plants had double the available water at anthesis and produced double the grain yield. The plants with the one seminal root had a large pressure gradient. [Note, for comparison, Nobel, 1974 (p. 393) found for a diffuse-porous tree with a $J_v$ of 0.1 cm/s the pressure drop was $-0.2$ bar/m or $-0.0002$ bar/mm.] However, the plant with one root could not sustain the large pressure drop and closed its stomata. Passioura (1972) concluded that it might be possible to conserve water by growing wheat plants with a single seminal root, and it may be possible to breed high root resistance into existing cultivars by breeding for smaller vessels. Passioura's (1972) classic paper showed that Poiseuille's law can be used to calculate the pressure drop in crops and that this value can be used to breed for drought-resistant varieties.

This idea was carried forward when Richards and Passioura (1981a,b) screened the world's wheat collection for the two factors that control resistance to water movement in the wheat root: number of axes (number of seminal roots) and central metaxylem vessel diameter. They screened about 1000 accessions in the collection, and they found that the number of axes varied between 3 and 5 and the central metaxylem vessel diameter varied between 35 and 75 μm. Because there was greater variability in the vessel diameter than in the number of axes, they said that the diameter was more important in determining resistance than the number of axes. One should breed for diameter, not for number of axes.

The wheat breeding program, as suggested by Passioura (breeding for small central metaxylem element), has been applied in Australia (Richards and Passioura, 1989). In field trials over 5 years in dry environments, narrow xylem vessel selections yielded between 3% and 11% more than unselected controls. However, many factors other than metaxylem vessel diameter and number of seminal roots determine the amount of water lost by a wheat plant. For example, even if the seminal roots are cut (or the wheat is bred for a small number of them), or if a small central metaxylem element diameter in the axes is bred for, the wheat plant develops adventitious roots. The large number of adventitious roots swamps the change in number of seminal axes or metaxylem vessel diameter. Nevertheless, the application of Poiseuille's law to a breeding program is important. Perhaps only a small amount of water can be saved through this breeding method. However, if applied over a large land area (dry land wheat is planted on huge acreages), then a large amount of water could be saved.

Meyer and Alston (1978) saw that the diameter of root vessels of wheat increased with depth. On average, a plant with metaxylem vessels that change in diameter from 30 μm at the soil surface to 45 μm at 1 m depth carries five times the water at 1 m depth as at the surface (Note: One metaxylem vessel would not be 1 m long.). This adaptation (wheat vessel diameter at depth is wider) might be valuable evolutionarily. If the soil surface is dry (as it often is under dry land conditions), then the vessel at depth, where more water might be, can have a higher flow rate and allow survival. But, at any one level in soil, we would like the diameter of the metaxylem vessels of a drought-resistant variety to be smaller in diameter than the metaxylem vessels of a drought-sensitive variety. This would allow water conservation in the drought-resistant variety.

Meyer et al. (1978) grew wheat that depended for moisture on subsoil water extracted below 45 cm. The plants had one, three, or five seminal roots. The size of the metaxylem vessel in the seminal axes affected water uptake. Using Poiseuille's law, they calculated that the flow rate at a subcrown potential of $-15$ bars would be increased by 30% in a plant with three axes without changing the root length, if the radius of each metaxylem vessel were increased by 3 μm.

Meyer and Ritchie (1980) also applied Poiseuille's law to sorghum. They suggested that cultivars with small vessels might have higher resistances and, therefore, be better adapted to dry conditions because they use less water.

The main limitations in the use of the Poiseuille equation to calculate pressure drop in the xylem (and indirectly resistance to water movement) are the inability to measure xylem vessel radii sufficiently accurately, lack of knowledge about effects of growth conditions on longitudinal variations in vessel radii, lack of knowledge about numbers of vessels that carry water from one layer to another in field crops, and inability to account for water exchange along the vessel length (Klepper and Taylor, 1979, p. 61). The most serious of these limitations is that associated with vessel radii, especially in view of the fact that vessel radii enter the Poiseuille equation as $r^4$. However, with improved scanning electron microscopes (e.g., Cooper and Cass, 2001), vessel member characteristics are being described with better resolution than in the past. Most investigators measure vessel diameter at one depth within the profile (Klepper and Taylor, 1979). To understand the hydraulics of the xylem vessels, their diameters at different depths in the root zone need to be known.

## 15.6 APPENDIX: BIOGRAPHY OF J.L.M. POISEUILLE

Jean Leonard Marie Poiseuille was a French physiologist born in Paris, France, on April 22, 1799. He got his M.D. in 1828 and practiced medicine in Paris. He received the Gold Medal of the French Academy of Sciences. He was the author of "Sur la force du coeur aortique" (1828) (*On the force of the aorta of the heart*) (The aorta is the main artery of the body; it carries blood from the left ventricle of the heart to all organs except the lungs.). Poiseuille also wrote "Le Mouvement des liquides dans des tubes de petits diamètres" (1844) (*The movement of liquids in tubes of small diameters*). In 1828, he was the first to use the mercury manometer for measurement of blood pressure, and this is still the most accurate method to measure blood pressure. In 1843, he discovered the law on velocity of flow of a liquid through a capillary tube, and in 1846, he studied the flow of viscous liquids. He invented the hemodynamometer for measuring blood pressure inside arteries and also invented the viscosimeter. He died in Paris on December 26, 1869 (Debus, 1968).

## 15.7 APPENDIX: BIOGRAPHY OF OSBORNE REYNOLDS

Osborne Reynolds (1842—1912), an English engineer and physicist, is best known for his work in the fields of hydraulics and hydrodynamics. He was born in Belfast (seaport and capital of Northern Ireland) on August 23, 1842. Gaining early workshop experience and graduating at Queens' College, Cambridge, England, in 1867, he became in 1868 the first professor of engineering at Owens College, Manchester, England. He was elected a fellow of the Royal Society in 1877 and a Royal medalist in 1888. He retired in 1905 and died at Watchet, Somerset, England on February 21, 1912 (Priestley, 1971).

Reynolds's studies of condensation and the transfer of heat between solids and fluids brought radical revision in boiler and condenser design, and his work on turbine pumps laid the foundation for their rapid development. A fundamentalist among engineers, he formulated the theory of lubrication (1886), and, in his classical paper on the law of resistance in parallel channels (1883), he investigated the transition from smooth, or laminar, to turbulent flow. He later (1889) developed the mathematical framework that became standard in turbulence work. His name is perpetuated in the "Reynolds stress," or drag exerted between adjacent layers of fluid due to turbulent motion, and in the "Reynolds number," which provides a criterion for correct modeling in many fluid flow experiments. He developed corresponding criteria for wave and tidal motions in rivers and estuaries. Among his other work was the explanation of the radiometer and an early absolute determination of the mechanical equivalent of heat. Reynolds's *Scientific Papers* were published in three volumes (1900–1903) (Priestley, 1971).

## 15.8 APPENDIX: BIOGRAPHY OF KATHERINE ESAU

Katherine Esau (1898–1997), author of classic textbooks on plant anatomy and considered the greatest plant anatomist of the twentieth century, was born on April 3, 1898 in Yekaterinoslav, now called Dnepropetrovsk, in the Ukraine (Evert, 1992). Her family was Mennonite, descendants of German Mennonites invited to Russia by Katherine the Great to promote agriculture on the steppes of the Ukraine. After finishing high school, she enrolled at the Golitsin Women's Agricultural College in Moscow. In 1918, after 1 year of study, she, her parents, and brother fled the Bolshevik Revolution in Russia (Evert, 1997; Thorsch and Evert, 1997). At the time of their departure from Yekaterinoslav, Dr Esau's father, a mechanical engineer by profession, was the mayor of the city (Evert, 1992). They went to Germany where she enrolled in the Berlin Landwirtschafliche Hochschule (Agricultural College of Berlin). In 1922, she completed her college education in Germany majoring in plant breeding (Mitchell et al., 1968). There she knew Professor Erwin Baur (1875–1933), a famous experimental geneticist who founded the Institut für Vererbungsforschung (Institute for Investigation of Heredity) (Encyclopaedia Britannica, 1971) and who was known for his work on chimeras (Jones, 1971). The Esaus left Germany for the United States in 1922. They settled in Reedley, California, a Mennonite community. In 1923, she took a job with Sloan Seed Company in Oxnard, California, but the company went bankrupt 1 year after she started work there (Thorsch and Evert, 1997). She then worked at Spreckels Sugar Company in Salinas, California, and bred strains of sugar beets for resistance to the virus causing curly-top disease (Evert, 1997). She stayed at Spreckels until 1928 when she left to begin graduate studies at the University of California, where she studied the effect of curly-top virus on sugar beet. She completed her graduate work in December 1931, and the formal granting of the Ph.D. degree occurred on the campus of Berkeley in 1932 (Evert, 1992). Immediately after graduation she joined the staff at Davis to become, by 1949, Professor of Botany and Botanist of the Experiment Station (Mitchell et al., 1968). She studied the effect of disease on the anatomy of plants, an area called *pathological anatomy* (Evert, 1992). Her work on curly-top virus in tobacco showed the dependence of this virus on the phloem tissue for initiating infection and spreading it throughout the plant (Thorsch and Evert, 1997). During World War II, she became involved with a project to develop more productive rubber-yielding strains of guayule. After the war, she turned her attention to Pierce's disease in grapevine and studied the importance of the phloem in its infection (Evert, 1992).

In the 1950s, she began collaborating with Vernon I. Cheadle (1910–1995), who in 1952 had moved from Rhode Island State College to join the Botany Department at the University of California at Davis as Chair. They shared an interest in vascular tissues, especially the phloem (Evert, 1995). They studied the comparative structure of phloem in dicotyledons.

In 1963, 2 years before she was to retire, she moved to Santa Barbara, California, to continue her collaboration with Vernon Cheadle, who had been appointed in 1962 as Chancellor of the University of California at Santa Barbara (Evert, 1997). She had been introduced to electron microscopy at Davis in 1960, and her move to the University of California at Santa Barbara led to the development of electron microscopy in the biology department there (Evert, 1992). She applied this new tool to her anatomical research (Thorsch and Evert, 1997). She studied phloem and viruses including the tobacco mosaic virus and the beet western yellows disease that causes yellowing of sugar beet leaves (Evert, 1992). She reached the Emeritus status on June 30, 1965, but remained actively engaged in research into her late 80s and was working on a third revision of *Anatomy of Seed Plants* in her 90s. She was the oldest person to hold a National Science Foundation grant (Theodore M. Barkley, Professor of Biology, Kansas State University, personal communication, c.1985).

She is best known for her two classic textbooks: *Plant Anatomy* (first edition, 1953; second edition, 1965) and *Anatomy of Seed Plants* (first edition, 1960; second edition, 1977). In these books, she provided a standard terminology that is used in plant anatomy today (Thorsch and Evert, 1997). Each edition of *Anatomy of Seed Plants* has a glossary. Her two textbooks have been published in several languages including Russian (Evert, 1997). She had 15 Ph.D. graduate students, who got their degrees with her between 1950 and 1981 (Thorsch and Evert, 1997). One of her students was Ray F. Evert. He got his Ph.D. with her in 1958 and spent his career at the University of Wisconsin. He became the leading plant anatomist in the USA after her. He said as a graduate student he was the recipient of Katherine Esau's "wisdom, knowledge, and insight" (Evert, 2002). When Ray Evert first met Dr Esau, she was riding a bicycle, which she did regularly to and from the Botany Department at the University of Davis. She set new standards for excellence. She told Dr Evert, "Ray, one can never be too careful" (Evert, 1997).

At many universities, including Kansas State University, plant anatomy is no longer taught. Teaching emphasizes molecular biology instead of taxonomy or anatomy. Therefore, Katherine Esau's textbooks are all more important, because students now must teach themselves plant anatomy, which they can do by reading her books.

Dr Esau received many awards for her accomplishments. She was elected to the American Academy of Arts and Sciences, the American Philosophical Society, the National Academy of Sciences, and the Swedish Royal Academy of Science (Evert, 1997). She was the President of the Botanical Society of America in 1951 (Mitchell et al., 1968). She received a Certificate of Merit on the Golden Jubilee Anniversary of the Botanical Society of America in 1956. The Certificate reads "Katherine Esau, plant anatomist and histologist, for her numerous contributions on tissue development of vascular plants and in particular for her outstanding studies on the structure, development, and evolution of phloem" (Evert, 1997). She received honorary degrees from Mills College, Oakland, California (1962), and the University of California (1966). In 1989, she was awarded the President's National Merit of Science. The citation accompanying the medal reads "In recognition of her distinguished service to the American community of plant biologists, and for excellence of her pioneering research, both basic and applied, on plant structure and development, which has spanned more than six decades; for her superlative performance as an educator, in the classroom and through her books; for the encouragement and inspiration she has given to a legion of young, aspiring plant biologists; and for providing a special role model for women in science".

## References

Barlow, P.W., 1995. Gravity perception in plants: a multiplicity of systems derived by evolution? Plant Cell Environ. 18, 951–962.

Bird, R.B., Stewart, W.E., Lightfoot, E.N., 1960. Transport Phenomena. Wiley, New York.

Bowes, B.G., 2000. A Color Atlas of Plant Structure. Iowa State University Press, Ames, Iowa.

Childs, E.C., 1969. An Introduction to the Physical Basis of Soil Water Phenomena. Wiley-Interscience, John Wiley and Sons, London.

Cooper, R.L., Cass, D.D., 2001. Comparative evaluation of vessel elements in *Salix* spp. (Salicaceae) endemic to the Athabasca sand dunes of northern Saskatchewan, Canada. Am. J. Bot. 88, 583–587.

Daniels, F., Alberty, R.A., 1966. Physical Chemistry, third ed. Wiley, New York.

Debus, A.G. (Ed.), 1968. Poiseuille, Jean Leonard Marie. In World Who's Who in Science. A Biographical Dictionary of "Notable" Scientists from Antiquity to the Present, first ed. A.N. Marquis Company, Marquis-Who's Who, Chicago, Illinois, p. 1357.

Desmond, R., 1989. Pens and petals. Nature 342, 306 (one page only).

Encyclopaedia Britannica, 1971. Baur, Erwin. Encyclopaedia Britannica 3, 298.

Esau, K., 1965. Plant Anatomy, second ed. Wiley, New York.

Esau, K., 1977. Anatomy of Seed Plants, second ed. Wiley, New York.

Evert, R.F., 1992. Commentary: the contributions of Katherine Esau. Int. J. Plant Sci. 153 (3), v–ix.

Evert, R.F., 1995. Vernon Irvin Cheadle 1910–1995. Plant Sci. Bull. 41 (3), 48–49.

Evert, R.F., 1997. Katherine Esau 1898–1997. Plant Sci. Bull. 43 (3), 64–65.

Evert, R.F., 2002. Reflections. Plant Sci. Bull. 48 (2), 42–44.

Fisher, J.B., Tan, H.T.W., Toh, L.P.L., 2002. Xylem of rattans: vessel dimensions in climbing palms. Am. J. Bot. 89, 196–202.

Geldner, N., 2013. The endodermis. Annu. Rev. Plant Biol. 64, 531–558.

Grebe, M., 2011. Unveiling the Casparian strip. Nature 473, 294–295.

Hayden, R., 1986. Mrs Delany. Her Life and Her Flowers. A Colonnade Book, Reprint ed. British Museum Publications, London.

Jones, W.N., 1971. Chimera. Encyclopaedia Britannica 5, 550–551.

Kimbrough, J.M., Salina-Mondragon, R., Boss, W.F., Brown, C.S., Sederoff, H.W., 2004. The fast and transient transcriptional network of gravity and mechanical stimulation in the *Arabidopsis* root apex. Plant Physiol. 136, 2790–2805.

Kirkham, D., 1961. Lectures on Agricultural Drainage. Institute of Land Reclamation, College of Agriculture, Alexandria University, Alexandria, Egypt (Copy in the Iowa State University Library, Ames, Iowa.).

Kirkham, M.B., 2008. Horizontal root growth: water uptake and stomatal resistance under microgravity. Vadose Zone J. 7, 1125–1131. http://dx.doi.org/10.2136/vzj2007.0097.

Klepper, B., Taylor, H.M., 1979. Limitations to current models describing water uptake by plant root systems. In: Harley, J.L., Scott Russell, R. (Eds.), The Soil-root Interface. Academic Press, London, pp. 51–65.

Kramer, P.J., 1983. Water Relations of Plants. Academic Press, New York.

Lack, H.W., 2001. Floral tributes. Nature 411, 137 (one page only).

Larisch, C., Dittrich, M., Wildhagen, H., Lautner, S., Fromm, J., Polle, A., Hedrich, R., Rennenberg, H., Müller, T., Ache, P., 2012. Poplar wood rays are involved in seasonal remodeling of tree physiology. Plant Physiol. 160, 1515–1529.

MacAdam, J.W., 2009. Structure and Function of Plants. Wiley-Blackwell, Ames, Iowa.

Meyer, W.S., Alston, A.M., 1978. Wheat responses to seminal root geometry and subsoil water. Agron. J. 70, 981–986.

Meyer, W.S., Ritchie, J.T., 1980. Resistance to water flow in the sorghum plant. Plant Physiol. 65, 33–39.

Meyer, W.S., Greacen, E.L., Alston, A.M., 1978. Resistance to water flow in the seminal roots of wheat. J. Exp. Bot. 29, 1451–1461.

Mitchell, J.E., Evert, R.F., Kelman, A., Sequeira, L., Williams, P.H., Walker Lecture Committee, 1968. John Charles Walker Lectures. Announcement of Three Lectures Given by Dr Katherine Esau, April 29, April 30, and May 2, 1968. Department of Plant Pathology, University of Wisconsin, Madison.

Moin, P., Kim, J., 1997. Tackling turbulence with supercomputers. Sci. Am. 276, 62–68 (+ cover).

Nelkin, M., 1992. In what sense is turbulence an unsolved problem? Science 255, 566–570.

Nobel, P.S., 1974. Introduction to Biophysical Plant Physiology. W.H. Freeman, San Francisco.

Nobel, P.S., 1983. Biophysical Plant Physiology and Ecology. W.H. Freeman, San Francisco.

Nobel, P.S., 1991. Physicochemical and Environmental Plant Physiology. Academic Press, San Diego.

Nobel, P.S., 1999. Physicochemical and Environmental Plant Physiology, second ed. Academic Press, San Diego.

Nobel, P.S., 2005. Physicochemical and Environmental Plant Physiology, third ed. Elsevier, Amsterdam.

Nobel, P.S., 2009. Physicochemical and Environmental Plant Physiology, fourth ed. Elsevier, Amsterdam.

Nowack, B., Schulin, R., Robinson, B.H., 2006. Critical assessment of chelant-enhanced metal phytoextraction. Environ. Sci. Technol. 40, 5225–5232.

Passioura, J.B., 1972. The effect of root geometry on the yield of wheat. Aust. J. Agric. Res. 23, 745–752.

Percival, J., 1921. The Wheat Plant. E.P. Dutton, New York.

Petricka, J.J., Winter, C.M., Benfey, P.N., 2012. Control of *Arabidopsis* root development. Annu. Rev. Plant Biol. 63, 563–590.

Priestley, C.H.B., 1971. Reynolds. Encyclopaedia Britannica 19, 252.

Richards, R.A., Passioura, J.B., 1981a. Seminal root morphology and water use of wheat. I. Environmental effects. Crop Sci. 21, 249–252.

Richards, R.A., Passioura, J.B., 1981b. Seminal root morphology and water use of wheat. II. Genetic variation. Crop Sci. 21, 253–255.

Richards, R.A., Passioura, J.B., 1989. A breeding program to reduce the diameter of the major xylem vessel in the seminal roots of wheat and its effect on grain yield in rain-fed environments. Aust. J. Agr. Res. 40, 943–950.

Schreiber, L., Hartmann, K., Skrabs, M., Zeier, J., 1999. Apoplastic barriers in roots: chemical composition of endodermal and hypodermal cell walls. J. Exp. Bot. 50, 1267–1280.

Silady, R.A., Kato, T., Lukowitz, W., Sieber, P., Tasaka, M., Somerville, C.R., 2004. The *gravitropism defective* 2 mutants of Arabidopsis are deficient in a protein implicated in endocytosis in *Caenorhabditis elegans*. Plant Physiol. 136, 3095–3103.

Simpson, M.G., 2006. Plant Systematics. Elsevier, Amsterdam.

Steudle, E., Frensch, J., 1996. Water transport in plants: role of the apoplast. Plant Soil 187, 67–79.

Thorsch, J.A., Evert, R.F., 1997. Katherine Esau's contributions to botany. Am. J. Bot. 84, 1621–1623.

Weast, R.C., 1964. Handbook of Chemistry and Physics, forty fifth ed. Chemical Rubber Co., Cleveland, Ohio.

CHAPTER

# 16

# Gardner's Equation for Water Movement to Plant Roots

W.R. Gardner was one of the first people to model analytically water movement to plant roots. His solution is widely cited today and known by any plant or soil scientist modeling water movement to plant roots. Therefore, it is important for us to understand this basic work. (For a biography of Gardner, see the Appendix, Section 16.10.)

## 16.1 DESCRIPTION OF THE EQUATION

In his paper, Gardner (1960) solved the flow equation to determine water movement to a plant root. His solution was the first (Green et al., 2006) and followed up on the outline of the problem by Philip (1957). The flow equation for a single root in an infinite, two-dimensional medium is

$$\partial\theta/\partial t = (1/r)(\partial/\partial r)[rD(\partial\theta/\partial r)] \tag{16.1}$$

where $\theta$ is the water content of the soil on a volumetric basis, $D$ is the diffusivity, $t$ is the time, and $r$ is the radial distance from the axis of the root. The solution to Eqn (16.1), subject to boundary conditions that Gardner (1960) defines, is given by Carslaw and Jaeger (1959) (Gardner cites a 1947 reprint of the first edition of Carslaw and Jaeger published in 1946):

$$\tau - \tau_0 = (q/4\pi k)\left[\ln\left(4Dt/a^2\right) - \gamma\right], \tag{16.2}$$

where $\gamma = 0.57722\ldots$ is Euler's constant, $a$ is the radius of the root, $k$ is the unsaturated hydraulic conductivity of the soil, $q$ is the rate of water uptake by the root, $D$ is the diffusivity of the soil, $\tau$ is the soil suction, and $\tau_0$ is the suction in the soil for initial conditions. We are interested in the difference in suction required at the boundary between the plant root and the (bulk) soil to maintain a constant rate of water movement to the plant.

http://dx.doi.org/10.1016/B978-0-12-420022-7.00016-1

Copyright © 2014 Elsevier Inc. All rights reserved.

(We will refer to the soil at some distance from the root as the "bulk" soil.) The solution to Eqn (16.2) assumes a constant $k$ and $D$. Because root diameters are small, it is possible to consider the root as a line source, or in this case, sink, of strength $q$ per unit length for which the solution of Eqn (16.1) also is given by Carslaw and Jaeger (1959):

$$\tau - \tau_0 = (q/4\pi k)\left[\ln\left(4Dt/r^2\right) - \gamma\right]. \tag{16.3}$$

When $r = a$, Eqns (16.2) and (16.3) are the same.

Gardner pointed out that study of Eqn (16.3) shows that a large part of the water being taken up by the roots comes from some distance from the roots. It is instructive to compare Eqn (16.2) with the steady-state solution for flow in a hollow cylinder:

$$\tau - \tau_0 = (q/4\pi k)\left[\ln\left(b^2/a^2\right)\right], \tag{16.4}$$

where $\tau_0$ is now the suction at the outer radius of the cylinder $r = b$ and $\tau$ is the suction at the inner radius $r = a$. If we take $b = 2(Dt)^{½}$, Eqn (16.4) becomes identical with Eqn (16.2) except for the constant term $\gamma$. $\gamma$ is relatively small compared with the logarithmic term, so that the distribution of suction in the transient case is not very different from that in the steady-state case, with all the water coming from a distance $b = 2(Dt)^{½}$. The maximum radius $b$ is limited by the density of roots and can be taken as one-half the average distance between neighboring roots.

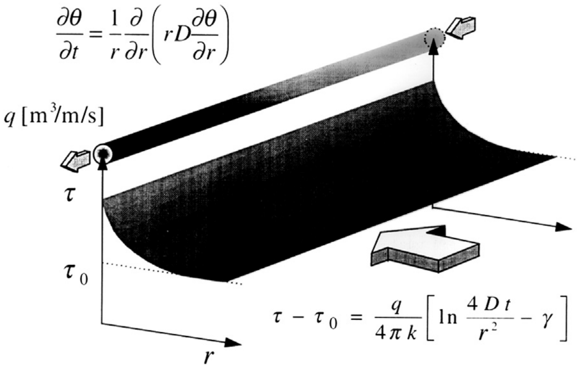
$\frac{\partial\theta}{\partial t} = \frac{1}{r}\frac{\partial}{\partial r}\left(rD\frac{\partial\theta}{\partial r}\right)$
$q$ [m$^3$/m/s]
$\tau$
$\tau_0$
$r$
$\tau - \tau_0 = \frac{q}{4\pi k}\left[\ln\frac{4Dt}{r^2} - \gamma\right]$

**FIGURE 16.1** For the gravity-free, linearized form of the Richards equation with a radial coordinate (equation at top of figure), Gardner (1960) solved for the field of suction surrounding a root of sink strength $q$, in terms of the suction $\tau$, distance $r$, and time $t$, given the soil's hydraulic characteristics (the unsaturated hydraulic conductivity $k$ and diffusivity $D$). $\gamma$ is Euler's constant. *From Clothier and Green (1997). This material is used by permission of Lippincott Williams & Wilkins, A Wolters Kluwer Company: Hagerstown, Maryland; and Brent E. Clothier.*

Using the modern terminology of matric potential instead of the old terminology of soil suction, Eqn (16.4) becomes (Baver et al., 1972, p. 404):

$$\Psi_b - \Psi_a = (q/4\pi k)\left[\ln\left(b^2/a^2\right)\right], \tag{16.5}$$

where $\Psi_b$ (bars or MPa) is the matric potential midway between roots and is that which could be measured by any finite-sized measuring device, $\Psi_a$ (bars or MPa) is the matric potential at the plant root—soil boundary, $q$ is the volume of water taken up per unit length of root per unit time (cm$^3$/cm/s or mL/cm/day), and $k$ is the unsaturated hydraulic conductivity of the soil (cm$^2$/s-bar). Gardner (1960) neglects any contact resistance at the soil—root interface. Figure 16.1 from Clothier and Green (1997) provides a picture of Gardner's model.

## 16.2 ASSUMPTIONS

Gardner (1960) made several assumptions in deriving Eqn (16.4) (or Eqn (16.5)), as follows:

1. The roots are infinitely long cylinders and a distance $2b$ apart.
2. The roots have a uniform radius $= a$.
3. There is uniform water absorption along the root. (Kramer (1969, p. 179) reports that, as expected, the highest rate of water entry into roots is found in root hairs and unsuberized roots and the lowest rate of water entry into roots occurs in suberized woody roots. However, even suberized roots do have a low rate of water entry. They are not completely impermeable to water.)
4. Water moves in a radial direction only (gravity-free movement).
5. There is a uniform value for the initial soil water content, $\theta_0$, and it corresponds to an initial matric potential in the bulk soil, $\Psi_0$ for $\Psi_b$.

## 16.3 VALUES FOR THE RATE OF WATER UPTAKE

What might values of $q$ be? The uptake of water by a young root 1 mm in diameter is usually 0.1—0.5 mL/day/cm of root length (e.g., see Nobel, 1974, p. 389). If we take an intermediate value of 0.3 mL/day/cm of root, this corresponds to:

$$q = \left(0.3\ \text{cm}^3/\text{day}\right)(1\ \text{day}/86,400\ \text{s}) = 3.5 \times 10^{-6}\ \text{cm}^3/\text{s/cm of root.}$$

As an aside, we can compare this $q$ to values of flux ($J_v$) reported by Nobel (1974, p. 393) for transpiration rates of diffuse-porous and ring-porous wood. This $q$ of $3.5 \times 10^{-6}$ cm$^3$/s occurs over a root surface area

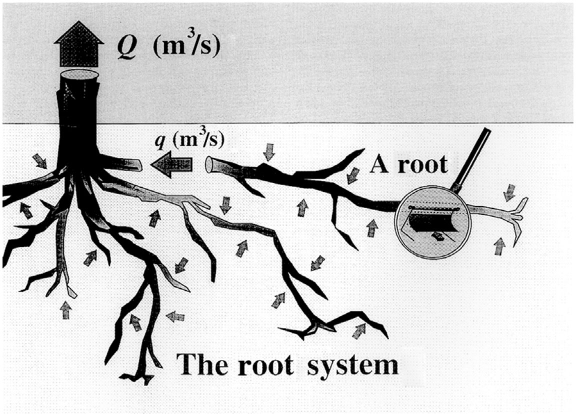

**FIGURE 16.2** Gardner's (1960) model of uptake describes the local field of flow in the soil that is required to supply active root segments with an internal flux of sap flow $q$ (magnifying glass). The anastomosis of these spatially distributed fluxes in the roots forms the plant's total transpiration $Q$. *From Clothier and Green (1997). This material is used by permission of Lippincott Williams & Wilkins, A Wolters Kluwer Company: Hagerstown, Maryland; and Brent E. Clothier.*

of $2\pi rl$, which is the surface area of a cylinder with radius $r$ and length $l$. So, we have

$$(2\pi)(0.05\ \text{cm})(1\ \text{cm}) = 0.31\ \text{cm}^2.$$

Thus $J_v$ or flux at the root surface is

$$\left(3.5 \times 10^{-6}\ \text{cm}^3/\text{s}\right)/\left(0.31\ \text{cm}^2\right) = 1.1 \times 10^{-5}\ \text{cm/s}.$$

Nobel assumed a $J_v$ for diffuse-porous wood of 0.1 cm/s and for ring-porous wood of 1 cm/s. The $J_v$ for the root is four orders of magnitude less than that for the diffuse-porous tree and five orders of magnitude less than that for the ring-porous tree. We note that the $q$ (or $J_v$) being considered by Gardner is that to a root, which is much less than the total flux that accumulates in the shoot from numerous roots penetrating the soil and funneling all the water into one stem (Figure 16.2). Water absorption by plant roots occurs at a slower rate than movement of water through the open vertical tubes of the xylem vessels in the stems of plants.

## 16.4 EXAMPLES

Let us follow an example given by Nobel (1974, p. 389). Let us assume that at $b = 1.05$ cm, $\Psi_b = -2$ bars, which we can measure with a device such as a thermocouple psychrometer. (Note: We could not measure

2 bars tension with a tensiometer because it is beyond the tensiometer range.) Let us assume that $k = 1 \times 10^{-6}\ \mathrm{cm^2/s\ bar}$, which might apply to a loam of moderately low water content.

Using Eqn (16.5):

$$-2\ \text{bars} - (\Psi_a) = \left\{3.5 \times 10^{-6}\ \mathrm{cm^3/cm\ s}/(4\pi)\left(1 \times 10^{-6}\ \mathrm{cm^2/s\ bar}\right)\right\}$$
$$\times \left\{\ln\left[(1.05\ \mathrm{cm})^2/(0.05\ \mathrm{cm})^2\right]\right\}$$

Solving, we get $\Psi_a = -3.7$ bars or about $-4$ bars. Thus, the matric potential drops about 2 bars across a distance of 1.05 cm in the soil next to the root.

We can consider an osmotic (solute) component in the soil that is constant throughout the soil. As we saw in Chapter 4 (Eqn (4.3)), the equation for total water potential, $\Psi$, is

$$\Psi = \Psi_m + \Psi_s + \Psi_g + \Psi_p,$$

where $\Psi_m$ is the matric potential, $\Psi_s$ is the osmotic (solute) potential, $\Psi_g$ is the gravitational potential, and $\Psi_p$ is the pressure potential. But the last two terms on the right-hand side drop out because water is moving laterally in the soil (gravity stays the same) and we are dealing with unsaturated conditions, so $\Psi_p = 0$. The $\Psi_s$ is additive to the $\Psi_m$. Let us assume $\Psi_s = -1$ bar.

For $\Psi_a$, we have:

$$\Psi_m + \Psi_s = -4\ \text{bars} + (-1\ \text{bar}) = -5\ \text{bars}.$$

For $\Psi_b$, we have:

$$\Psi_m + \Psi_s = -2\ \text{bars} + (-1\ \text{bar}) = -3\ \text{bars}.$$

The difference in matric potential between the root–soil boundary and the bulk soil at 1.05 cm away from the root remains the same (2 bars) as in the nonsaline case.

## 16.5 EFFECT OF WET AND DRY SOIL

Gardner (1960) applied his equation to different situations. Figure 16.3 shows the matric potential at the root ($\Psi_a$) as a function of the distance from the root, when the matric potential in the bulk soil ($\Psi_b$) is $-5$ or $-15$ bars and the rate of uptake is 0.1 mL/cm/day. At $-5$ bars matric potential, the gradient is very small, except right at the root, so that the matric potential is virtually uniform throughout the soil. When $\Psi_b = -15$ bars, a large gradient is required for the same $q$, because of the lower hydraulic conductivity.

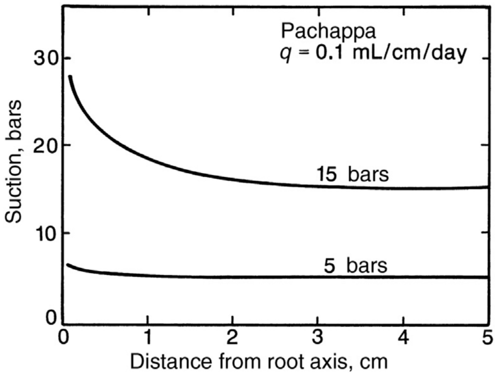

**FIGURE 16.3** A solution to Gardner's equation. It shows the suction at the plant root as a function of the distance from the root when the suction in the bulk soil is 5 or 15 bars. In current terminology, suction (positive value) is now called matric potential (negative value). *From Gardner (1960). This material is used by permission of Lippincott Williams & Wilkins, A Wolters Kluwer Company: Hagerstown, Maryland; and Wilford R. Gardner.*

## 16.6 EFFECT OF ROOT RADIUS

Figure 16.4 shows the effect of root radius. On the ordinate is the relative value of $\Delta\tau$ (difference in matric potential between the bulk soil and soil—root boundary). The scale on the ordinate is arbitrary because the actual matric potential would depend on the initial matric potential, $q$, and $k$. The figure shows that root radius is not extremely important. A tenfold increase in root radius can bring about only approximately a twofold decrease in the difference in matric potential between the bulk soil and soil—root boundary.

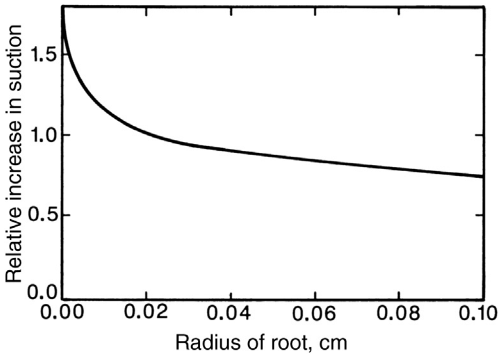

**FIGURE 16.4** A solution to Gardner's equation. It shows the relative increase in suction at the plant root as a function of the root radius. *From Gardner (1960). This material is used by permission of Lippincott Williams & Wilkins, A Wolters Kluwer Company: Hagerstown, Maryland; and Wilford R. Gardner.*

## 16.7 COMPARISON OF MATRIC POTENTIAL AT ROOT AND IN SOIL FOR DIFFERENT RATES OF WATER UPTAKE

Figure 16.5 shows suction at the plant root plotted as a function of the suction in the bulk soil for a Pachappa sandy loam for three different rates of water uptake. Except for unusual circumstances, the lowest rate indicated (0.05 $cm^2$/day) is probably more nearly that which occurs in nature and may, in fact, be high for a fully developed root system. The value of $q = 0.1$ $cm^2$/day is consistent with data of Ogata et al. (1960) for alfalfa. The figure shows that the suction at the root does not exceed the bulk soil suction appreciably until the suction difference is a few bars. When the bulk soil suction is as high as 15 bars, the suction at the root must be 30 or 40 bars to maintain a given value of $q$. The figure shows that, over a short distance, there is little difference in the suction between the root and bulk soil. But as the soil becomes dry, the difference becomes large in order to maintain a constant $q$. (Figure 16.5 from the original 1960 paper has been reproduced by Baver et al., 1972, p. 405.)

The main point of Figure 16.5 is that over short distances there is little difference in suction between the root and soil in the vicinity of the root until the soil becomes very dry. Even then, the flux tends to decrease markedly due to plant wilting. Gardner's analysis shows that in many cases one can probably assume that the roots are at very nearly the same potential as the surrounding soil (Baver et al., 1972, p. 404).

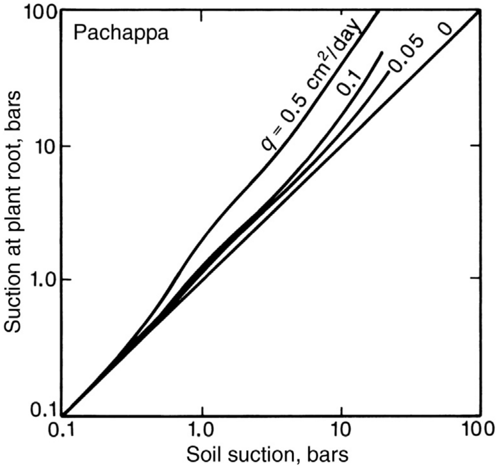

**FIGURE 16.5** Suction at the root—soil boundary as a function of the bulk soil suction for different rates of water uptake $q$. *From Gardner (1960). This material is used by permission of Lippincott Williams & Wilkins, A Wolters Kluwer Company: Hagerstown, Maryland; and Wilford R. Gardner.*

## 16.8 EFFECT OF ROOT DISTRIBUTION ON WILTING

The rate of uptake of water per unit length of root is proportional to the total transpiration rate, and inversely proportional to the length of the root system (Gardner, 1960, p. 68). Assuming a given rate of transpiration, the more extensive the root system the lower is the rate of uptake per unit length of root. The uptake rate $q$ thus depends on the transpiration rate and the extent of the root system. To study the effect of transpiration rate and extent of root system on the wilting of a plant, Gardner (1960) assumed that wilting occurs when the suction in the plant root is above some value, say 20 bars. In Figure 16.6 the average soil suction that results in a suction of 20 bars in the plant root is plotted as a function of $q$. This is, then, a plot of the soil suction at the wilting point as a function of $q$. For low rates of uptake, the wilting suction of the soil is very nearly the suction in the plant. For high values of $q$, large differences between the two are possible (Gardner, 1960).

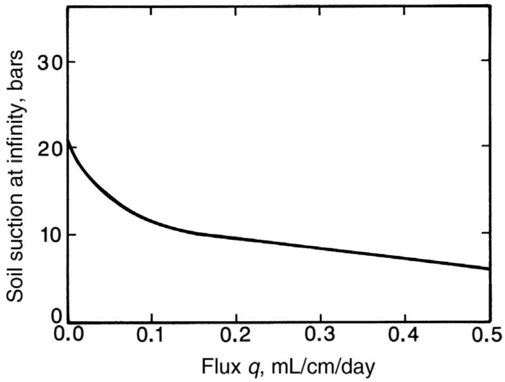

**FIGURE 16.6** The soil suction at a distance from the root, when suction at the plant root is 20 bars, plotted as a function of water uptake rate. *From Gardner (1960). This material is used by permission of Lippincott Williams & Wilkins, A Wolters Kluwer Company: Hagerstown, Maryland; and Wilford R. Gardner.*

## 16.9 FINAL COMMENT

Gardner said, when his 1960 paper became a citation classic (Institute for Scientific Information, 1985), "I believe this paper has been so frequently cited because the approach is essentially the same that all computer models of plant water uptake now follow". Clothier and Green (1997) and Green et al. (2006) discuss the incorporation of Gardner's theoretical ideas into the many simulation models of root zone function that have followed.

## 16.10 APPENDIX: BIOGRAPHY OF WILDFORD GARDNER

Wilford Robert Gardner, a physicist and educator, was born on October 19, 1925, in Logan, Utah, the son of Robert and Nellie (Barker) Gardner. After serving in the U.S. Army during World War II (1943–1946) (Marquis Who's Who, 2003), he got his B.S. degree from Utah State University in 1949 and his M.S. degree from Iowa State University in 1951 under the direction of Don Kirkham. They did the pioneering work on the neutron probe, which is now widely used to monitor soil water content (Gardner and Kirkham, 1952). Gardner got his Ph.D. degree at Iowa State University in 1953 under the guidance of Gordon C. Danielson. Gardner's uncle, Willard Gardner, brother to his father Robert, was the famous soil physicist at Utah State College (as it was known then). Willard Gardner is considered to be the "Father of Soil Physics in America." Gardner's cousin, Walter H. Gardner, the son of Willard, spent his career as a soil physicist at Washington State University in Pullman.

After obtaining his Ph.D., Wilford joined the U.S. Salinity Laboratory in Riverside, California. There, Gardner did seminal work deriving equations for flow of water under unsaturated conditions (Gardner, 1958; Gardner and Mayhugh, 1958), which are used worldwide by mathematical soil physicists today. This theoretical work has resulted in a soil being named after him, the "Gardner soil" (Kirkham and Powers, 1972, p. 275; Kacimov, 2007; Youngs and Kacimov, 2007). At the U.S. Salinity Laboratory he also wrote his important paper on water movement to a plant root (Gardner, 1960).

In 1966, Gardner moved to the University of Wisconsin, where he was a professor in the Soil Science Department. His students there included M.B. Kirkham, Frank N. Dalton, David B. Lesczynski (who died of a heart attack on August 4, 2001, at the age of 55 years), William A. Jury, William N. Herkelrath, John H. Knight, Don F. Yule, and K. John McAneney. In 1980, he moved from the University of Wisconsin to become head of the Department of Soil and Water Science at the University of Arizona, Tucson. In 1987, he accepted the position of dean of the College of Natural Resources at the University of California, Berkeley. In addition to being dean, he was associate director of the California Agricultural Experiment Station and professor of soil physics in the Departments of Plant & Soil Biology and Forestry & Resource Management. He was one of the few scientists who was both an outstanding researcher and an able administrator. In 1994, he became dean emeritus, and from 1995 until his death on May 20, 2011, from Parkinson's disease (Kirkham, 2011), he was adjunct professor at Utah State University.

Gardner received many recognitions. In 1959, he was National Science Foundation (NSF) Senior Fellow and in 1971−1972, he was a Fulbright Fellow. In 1972, he was recipient of an Honorary Faculty Award at the University of Ghent, Belgium. In 1983, he was elected to the National Academy of Sciences. He received the Centennial Alumnus Award at Utah State University in 1986. He was Fellow of the American Association for the Advancement of Science, the American Society of Agronomy, and the Soil Science Society of America. He was President of the Soil Science Society of America in 1990 and received its Research Award in 1962. He was an Honorary Member of the International Union of Soil Science (Marquis Who's Who, 2003). In 2002, he received an honorary doctor's degree from The Ohio State University.

He was a strong believer in basic research. At the annual William H. Pierre Lecture, which he gave at Iowa State University on April 1, 1986, he ended his talk with the admonition that basic research should be supported, even if it does not accomplish immediate practical results for specific, desired goals.

Gardner married Marjorie Louise Cole, the granddaughter of Willard Gardner, on June 9, 1949. They had three children, Patricia (died in 2008), Robert, and Caroline. He wrote his memoirs in two volumes, both self published: *My War* (304 pages; undated but distributed in 2009) and *Memoirs of a 'A Fair to Middlin' Physicist* (454 pages; 2009).

## References

Baver, L.D., Gardner, W.H., Gardner, W.R., 1972. Soil Physics, fourth ed. Wiley, New York.

Carslaw, H.S., Jaeger, J.C., 1959. Conduction of Heat in Solids, second ed. Clarendon Press, Oxford (First ed., 1946).

Clothier, B.E., Green, S.R., 1997. Roots: the big movers of water and chemical in soil. Soil Sci. 162, 534−543.

Gardner, W.R., 1958. Some steady-state solutions of the unsaturated moisture flow equation with application to evaporation from a water table. Soil Sci. 84, 228−232.

Gardner, W.R., 1960. Dynamic aspects of water availability to plants. Soil Sci. 89, 63−73.

Gardner, W.R., Kirkham, D., 1952. Determination of soil moisture by neutron scattering. Soil Sci. 73, 391−401.

Gardner, W.R., Mayhugh, M.S., 1958. Solutions and tests of the diffusion equation for the movement of water in soil. Soil Sci. Soc. Am. Proc. 22, 197−201.

Green, S.R., Kirkham, M.B., Clothier, B.E., 2006. Root uptake and transpiration: from measurements and models to sustainable irrigation. Agr. Water Manage. 86, 165−176. http://dx.doi.org/10.1016/j.agwat.2006.06.008.

Institute for Scientific Information, Gardner, W.R., 1985. Dynamic aspects of water availability to plants. Soil Sci. 89, 63−73. This Week's Citation Classic. Current Contents, Agr. Biol. Environ Sci. 16(35); 20.

Kacimov, A., 2007. Dipole-generated unsaturated flow in Gardner soils. Vadose Zone J. 6, 168−174. http://dx.doi.org/10.2136/vzj2005.0141.

Kirkham, D., Powers, W.L., 1972. Advanced Soil Physics. Wiley, New York.

Kirkham, M.B., 2011. Vale−Wilford R. Gardner (October 19, 1925−May 20, 2011). Eulogy. In: A Newsletter about Water in the Soil−Plant−Atmosphere System, vol. 109. WISPAS, 10.

Kramer, P.J., 1969. Plant and Soil Water Relationships: A Modern Synthesis. McGraw-Hill Book Co., New York.

Marquis Who's Who, 2003. Who's Who in America, fifty seventh ed. Marquis Who's Who, New Providence, New Jersey.

Nobel, P.S., 1974. Introduction to Biophysical Plant Physiology. W.H. Freeman, San Francisco.

Ogata, G., Richards, L.A., Gardner, W.R., 1960. Transpiration of alfalfa determined from soil water content changes. Soil Sci. 89, 179–182.

Philip, J.R., 1957. The physical principles of soil water movement during the irrigation cycle. In: Proceedings of the Congress of the International Commission on Irrigation and Drainage, Third, Algiers. R. 7, Question 8, 8.125–8.154.

Youngs, E.G., Kacimov, A.R., 2007. Critical tunnel cavities for water exclusion in "Green and Ampt" and "Gardner" soils. Water Resour. Res. 43 (5). http://dx.doi.org/10.1029/2006WR004907. W05501.

## CHAPTER

## 17

# Stem Anatomy and Pressure—Volume Curves

In this chapter we consider pressure—volume curves, which are used to determine osmotic potential and turgor potential. They are constructed from data obtained from the volume of sap exuded from the cut end of a stem protruding from a pressure chamber. Therefore, we need to understand stem anatomy before we turn to pressure—volume curves.

## 17.1 STEM ANATOMY

### 17.1.1 General Structure

The close association of the stem with the leaves makes the aerial part of the plant axis structurally more complex than the root (Esau, 1977, p. 257). The term *shoot*, which refers to the stem and leaves as one system, serves to express this association. The stem, like the root, consists of three tissue systems: the dermal (epidermis), the fundamental or ground (pith and cortex), and the fascicular or vascular. The variations in the primary structure in stems of different species are based chiefly on differences in the relative distribution of the fundamental and vascular tissues (Esau, 1977, p. 257).

### 17.1.2 Dicotyledonous Stem

In dicotyledons, the vascular system of the internode commonly appears as a hollow cylinder delimiting an outer and an inner region of ground tissue, the cortex and the pith, respectively. Figure 17.1 shows bird's foot trefoil, which has a typical dicotyledonous stem. The subdivisions of the vascular system, the vascular bundles, are separated from each other by more or less wide panels of ground parenchyma—the interfascicular parenchyma—that interconnects the pith and the cortex.

http://dx.doi.org/10.1016/B978-0-12-420022-7.00017-3

Copyright © 2014 Elsevier Inc. All rights reserved.

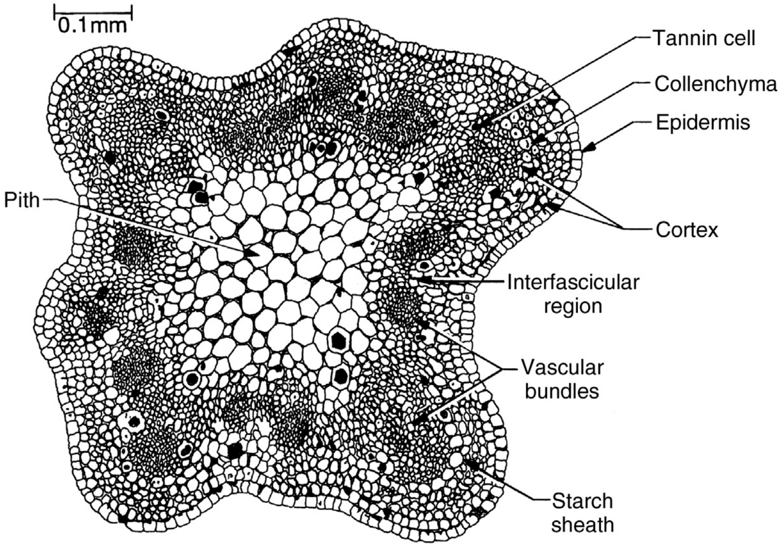

**FIGURE 17.1** Cross section of an herbaceous dicotyledon stem, *Lotus corniculatus* or bird's foot trefoil (Leguminosae family or legume family), in primary state of growth. The phloem is on the outside of each vascular bundle, and the xylem is on the inside. *From Esau (1977). This material is used by permission of John Wiley & Sons, Inc.*

This tissue is called interfascicular because it occurs between the bundles or fascicles (Esau, 1977, pp. 257–258).

### 17.1.3 Monocotyledonous Stem

Stems of most monocotyledons have a complex arrangement of vascular tissues. The bundles may occur in more than one ring or may appear scattered throughout the cross section. The stems (culms) of the Poaceae (grass family), seen in cross section, have widely spaced vascular bundles not restricted to one circle (Esau, 1977, p. 313). The bundles are either in two circles (*Avena*, oat; *Hordeum*, barley; *Secale*, rye; *Triticum*, wheat; *Oryza*, rice) or scattered throughout the section (*Bambusa*, bamboo; *Saccharum*, sugarcane; *Sorghum*, sorghum; *Zea*, corn). Figure 17.2 shows a cross section of a corn stem. The delimitation of the ground tissue into cortex and pith is less precise or does not exist when the vascular bundles do not form a ring in cross sections of internodes.

Monocotyledons other than Poaceae also have vascular bundles scattered or in rings near the periphery, as seen in stem transections. In *Tradescantia* (spiderwort) (Commelinaceae; spiderwort family), the central cylinder has scattered bundles. Compaction of vascular tissue characteristic of hydrophytes is common in aquatic monocotyledons. In *Potamogeton* (pondweed) (Potamogetonaceae; pondweed family), for example, a wide

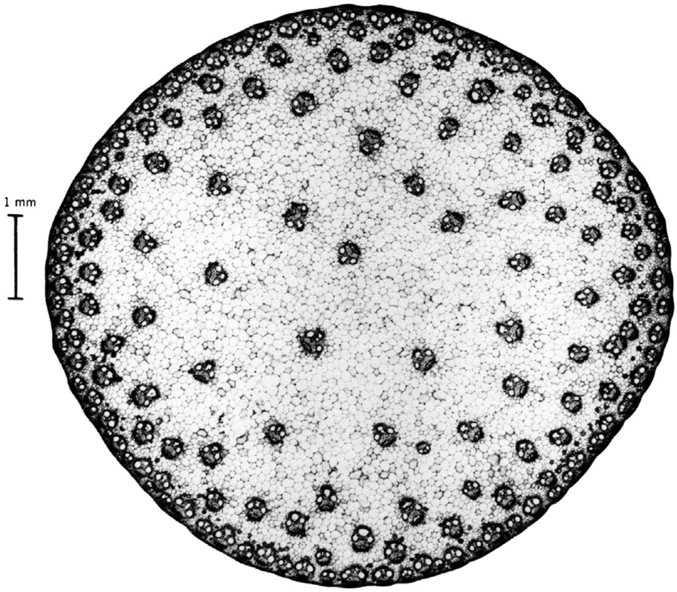

**FIGURE 17.2** Cross section of a monocotyledonous stem, *Zea mays* or corn (Poaceae family or grass family). Note vascular bundles are distributed throughout the section, but are more numerous near the periphery. In each vascular bundle, the xylem is oriented toward the center of the stem and three large vessels ("monkey faces"), part of the metaxylem, are visible in each bundle. The phloem in each vascular bundle is oriented toward the outside of the stem. *From Esau (1977). This material is used by permission of John Wiley & Sons, Inc.*

cortex consisting of aerenchyma encloses a compact vascular cylinder delimited by a small-celled endodermis. Variable amounts of pith tissue occur in different species of the genus (Esau, 1977, p. 314).

In general, we can say that dicotyledonous stems usually have a pith at the center of the stem surrounded by vascular bundles. Monocotyledonous stems often have scattered vascular bundles in a ground tissue, and no pith and cortex are delineated.

### 17.1.4 Stomata, Cortex, Pith, and Vascular Bundles in Primary Xylem

Stomata can be present on stems, but constitute a less prominent epidermal component in the stem than in the leaf (Esau, 1977, p. 259). The stem epidermis commonly consists of one layer of cells and has a cuticle and cutinized walls. It is a living tissue capable of mitotic activity, an important characteristic in view of the stresses to which the tissue is subjected during the primary and secondary increase in thickness of the stem. The epidermal cells respond to these stresses by enlargement and divisions (Esau, 1977, p. 259).

The cortex of stems contains parenchyma, usually with chloroplasts. Intercellular spaces are prominent, but sometimes are largely restricted to the median part of the cortex. In many aquatic angiosperms, the cortex develops as an aerenchyma with a system of large intercellular spaces (Esau, 1977, p. 259). The peripheral part of the cortex frequently contains collenchyma (Figure 17.1). *Collenchyma* is a supporting tissue composed of more or less elongated living cells with unevenly thickened, nonlignified primary walls. It is in regions of primary growth in stems and leaves. In some plants, notably grasses, sclerenchyma rather than collenchyma develops as the primary supporting tissue in the outer region of the stem. *Sclerenchyma* is a tissue composed of sclerenchyma cells. A sclerenchyma cell is a cell variable in form and size and having more or less thick, often lignified, secondary walls. It is a supporting cell and may or may not be devoid of a protoplast at maturity.

As noted when we studied root anatomy (Chapter 15), the innermost layer of the cortex (endodermis) of roots of vascular plants has the casparian strip. Stems commonly lack a morphologically differentiated endodermis. In young stems, the innermost layer or layers may contain abundant starch and thus be recognized as a starch sheath (Figure 17.1). Some dicotyledons, however, do develop casparian strips in the innermost cortical layer of the stem, and many lower vascular plants have a clearly differentiated stem endodermis (Esau, 1977, p. 259).

The pith of stems is commonly composed of parenchyma, which may contain chloroplasts. In many stems, the central part of the pith is destroyed during growth. Frequently, this destruction occurs only in the internodes, whereas the nodes retain their pith. The pith has prominent intercellular spaces, at least in the central part. The peripheral part may be distinct from the inner part in having compactly arranged small cells and greater longevity (Esau, 1977, p. 261).

The discrete individual strands of the primary vascular system of seed plants are commonly referred to as vascular bundles. The phloem and xylem show variations in their relative position in vascular bundles. The prevalent arrangement is *collateral*, in which the phloem occurs on one side (*abaxial*, or directed away from the axis) of the xylem (Figures 17.1 and 17.2). That is, the phloem is closest to the outside of the stem, even in monocots with scattered vascular bundles (Figure 17.2). The xylem in the corn plant shown in Figure 17.2 makes "monkey faces" (two eyes and one large mouth) and is directed toward the center of the stem (away from the epidermis). In some dicotyledons (e.g., Cucurbitaceae, the squash family, and Solanaceae, the nightshade family, which includes potato), one part of the phloem occurs on the outer side and another on the inner side of the xylem. This arrangement is called *bicollateral*, and the two parts of the phloem are referred to as the *external* (abaxial) and the *internal* (adaxial) phloem (Esau, 1977, p. 261). *Adaxial* means directed toward the axis.

### 17.1.5 Structure of Secondary Xylem

In Chapter 15, Section 15.4, we considered secondary xylem when making calculations of Poiseuille law flow through wood. Here we look at the structure of secondary xylem. A study of a block of wood reveals the presence of two distinct systems of cells (Figure 17.3) (Esau, 1977, p. 101): the *axial* (longitudinal or vertical) and the *radial* (transverse or horizontal) or *ray* system. The axial system contains files of cells with their long axes oriented vertically in the stem or the root, that is, parallel to the main, or longitudinal, axis of these organs. The radial system is composed of files of cells oriented horizontally with regard to the axis of the stem or root.

Each of the two systems has its characteristic appearance in the three kinds of sections employed in the study of wood (Esau, 1977, p. 102). In the *transverse* section, that is, the section cut at right angles to the main axis of stem or root, the cells of the axial system are cut transversely and reveal their smallest dimensions. The rays, in contrast, are exposed in their longitudinal extent in a cross section. When stems or roots are cut lengthwise, two kinds of longitudinal sections are obtained: the *radial* (parallel to a radius) and the *tangential* (perpendicular to a radius) (Figure 17.3).

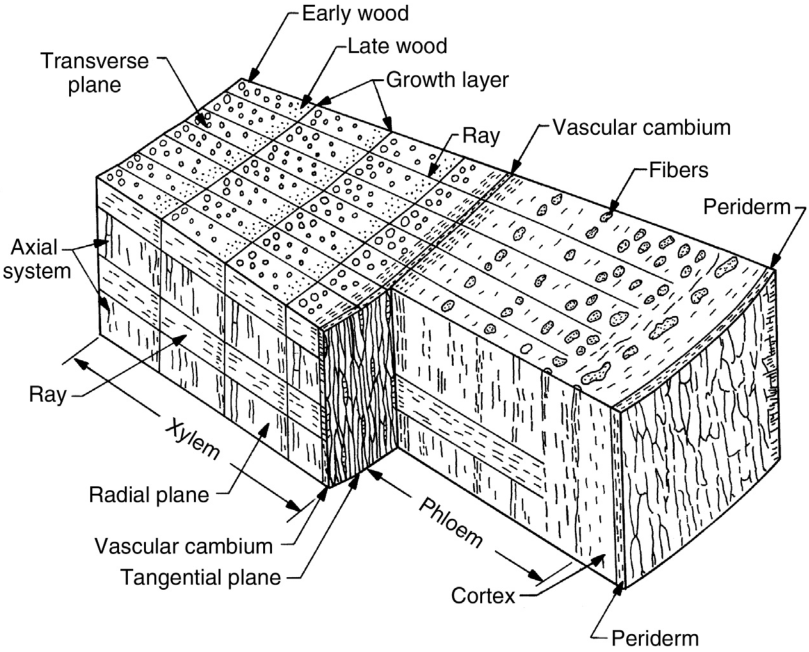
Early wood
Late wood
Transverse plane
Growth layer
Ray
Vascular cambium
Fibers
Periderm
Axial system
Ray
Xylem
Radial plane
Vascular cambium
Tangential plane
Phloem
Cortex
Periderm

**FIGURE 17.3** Block diagram illustrating the basic features of secondary vascular tissue. *From Esau (1977). This material is used by permission of John Wiley & Sons, Inc.*

With little or no magnification, the wood shows the layering resulting from the presence of more or less sharp boundaries between successive growth layers (Figure 17.3). Each growth layer may be a product of one season's growth, but various environmental conditions may induce the formation of more than one growth layer in one season (Esau, 1977, p. 103). When conspicuous layering is present, each growth layer is divisible into early and late wood. The early wood is less dense than the late wood, because wider cells with thinner walls predominate in the early wood and narrower cells with thicker walls occur in the late wood.

Although woody stems are usually not used to make pressure–volume curves, we are interested in the structure of wood when we consider the rise of sap in plants. Its structure is a key part of the cohesion theory (see Chapter 20), which explains how water can ascend to the top of tall trees.

## 17.2 MEASUREMENT OF THE COMPONENTS OF THE WATER POTENTIAL

Differences in total water potential, osmotic potential, pressure potential, matric potential, and gravitational potential can develop in the water of part of a plant, for example, a leaf. (We say "potential," when we recognize that we mean "potential energy". "Potential" is shorter than "potential energy" and saves spaces in printing.) As we saw in Chapter 4 (Eqn 4.3), when we were focusing on soil water, these five potentials for water at a particular point in a plant or soil are related by the equation:

$$\Psi = \Psi_s + \Psi_p + \Psi_m + \Psi_g \qquad (17.1)$$

in which the total water potential $\Psi$ for a particular unit mass of water (say a milligram) at a particular point is composed of four components, that is the potentials due to solutes, $\Psi_s$, pressure, $\Psi_p$, matrix, $\Psi_m$, and gravity, $\Psi_g$. The term $\Psi_m$ is associated with capillary or adsorption forces, which in a plant are forces such as those at the cell walls. Equation (17.1) can be compared, term by term, with the classical equation of plant physiology (Meyer et al., 1960, p. 56):

$$\mathrm{DPD} = \mathrm{OP} - \mathrm{TP}, \qquad (17.2)$$

where

DPD = diffusion pressure deficit
OP = osmotic pressure
TP = turgor pressure

and terms corresponding to $\Psi_m$, the matric potential, and $\Psi_g$, the gravitational potential, are neglected. If $\Psi_m$ and $\Psi_g$ are ignored, the

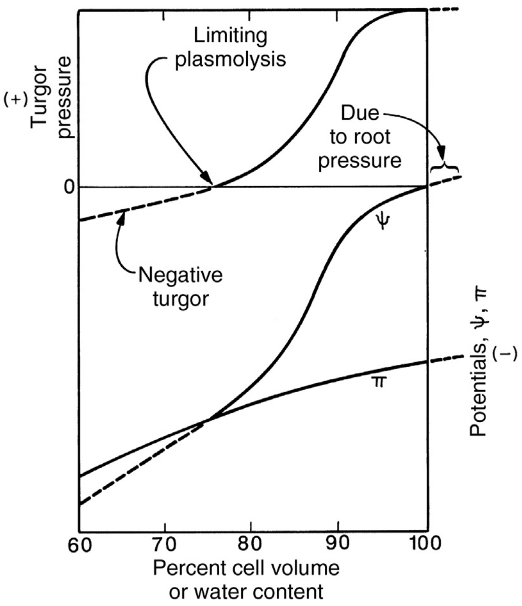

**FIGURE 17.4** A type of Höfler diagram; relationship between cell volume or water content and total water potential or its components for a single cell. *From Barrs (1968). Reprinted by permission of Academic Press.*

relation of $\Psi$, $\Psi_s$, and $\Psi_p$ to water content or cell volume may be described by means of a Höfler-type diagram (Höfler, 1920). In a Höfler-type diagram, the three potentials—water potential, osmotic potential, and turgor potential—are shown together. Figures 17.4 and 17.5 show two types of Höfler diagrams. A quantitative estimate of $\Psi$ is possible if the sum of $\Psi_s$ and $\Psi_p$ is known (Barrs, 1968, p. 236). In this chapter, we wish to discuss methods to measure $\Psi_s$ and $\Psi_p$.

## 17.3 OSMOTIC POTENTIAL ($\Psi_S$)

Two methods are commonly used to determine osmotic potential of plant leaves. In the first method, leaves are frozen, which breaks cell membranes and releases the solutes in the cell. Alternatively, the tissue can be crushed instead of frozen to break the cell membranes, but one has to devise a crushing device. With freezing, one is assured of breaking all the membranes after a tissue has been in a freezer overnight or in dry ice for a few minutes. Some people freeze the tissue and then squeeze out sap from the frozen tissue. With this method it is certain that the sap contains the solute component of the total water potential. The concentration of the

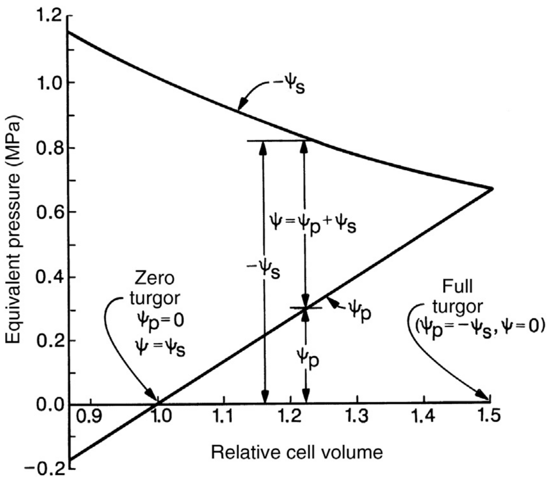

**FIGURE 17.5** A type of Höfler diagram; relationship between pressure potential ($\Psi_p$), solute potential ($\Psi_s$), and the resultant water potential ($\Psi$) in an idealized (elastic) plant cell. *From Baker (1984). Reprinted by permission of Pearson Education Limited, Essex, United Kingdom, and Dennis A. Baker.*

solutes in the sap from crushed tissue or from the frozen and crushed tissue then can be measured with a thermocouple psychrometer or an osmometer (see this chapter, Section 17.8, for a discussion of the osmometer).

Tissue can be handled in two ways in the frozen tissue method. First, a piece of tissue can be put into a thermocouple psychrometer. Water potential, $\Psi$, is determined. The chamber with the tissue is removed from the thermocouple, corked, and frozen. After freezing of the tissue, the chamber with the tissue is reattached to the thermocouple, and osmotic potential of the same tissue for which water potential was determined (same geometry, same cells), is measured. Second, water potential can be analyzed on a sample of a plant by using one instrument (e.g., a pressure chamber). The osmotic potential then is determined on another sample of the plant by freezing the sample, exuding sap from it, putting the sap on a piece of filter paper, and measuring its osmotic potential with a thermocouple psychrometer or an osmometer (Clarke and Simpson, 1978). This second way has the disadvantage that, because water potential and osmotic potential are not determined on the same piece of tissue, osmotic potential readings can be higher than water potential readings (Singh et al., 1983). This is not possible and is due to experimental error or ignoring potentials other than the solute potential and turgor potential that contribute to the total water potential. Osmotic potential is lower or equal to the water potential, unless matric or gravitational potentials are significant.

## 17.4 THEORY OF SCHOLANDER PRESSURE–VOLUME CURVES

The second method for determination of osmotic potential employs a pressure chamber to create a pressure–volume curve. We need to know the background of pressure–volume curves to understand them. The method now used is based on concepts developed by Scholander and colleagues (Scholander et al., 1964, 1965). We first need to define the term *hydrostatic pressure*, which Scholander et al. (1964, 1965) use. It is generally accepted that water is under tension (negative pressure) in the vessels in the xylem tissue. Scholander et al. (1964, 1965) refer to this pressure as "hydrostatic pressure". The *Handbook of Chemistry and Physics* (Weast, 1964, p. F-45) defines hydrostatic pressure as follows:

Hydrostatic pressure at a distance $h$ from the surface of a liquid of density $d$, is

$$P = hdg. \tag{17.3}$$

The total force on an area $A$ due to hydrostatic pressure is

$$F = PA = Ahdg, \tag{17.4}$$

where

$F$ = force (dynes)
$P$ = hydrostatic pressure (dynes/cm$^2$)
$h$ = distance (cm)
$d$ = density (g/cm$^3$)
$g$ = acceleration due to gravity (cm/s$^2$).

We sometimes denote $d$ by the Greek letter rho, $\rho$. Nobel (1974, p. 38; 1983, p. 41) and Barrs (1968, p. 336) equate the hydrostatic pressure with turgor pressure. There is, however, no turgor pressure in mature xylem vessels, because cell membranes have disintegrated.

Scholander et al. (1964) show a leaf cell with vessel, as it exists outside and inside a pressure chamber, in a fresh state (Figure 17.6) and in a wilted state (Figure 17.7). They assume that negative hydrostatic pressure exists in a vessel connected to a living cell (Figures 17.6 and 17.7(A)). They further assume that ambient air cannot enter the system because of surface tension. Water is extruded from the cut end of the stem when pressure is applied by using the pressure chamber (Figures 17.6 and 17.7(B)). They assume that the membrane surrounding the cell (Figures 17.6 and 17.7) is semipermeable and that no solutes come out of the cell when pressure is applied. Therefore, they assume that the extruded liquid is plain water and that the rise in intracellular solute concentration (which occurs as water is pushed out of the cell) is proportional to the rise in the equilibrium pressure.

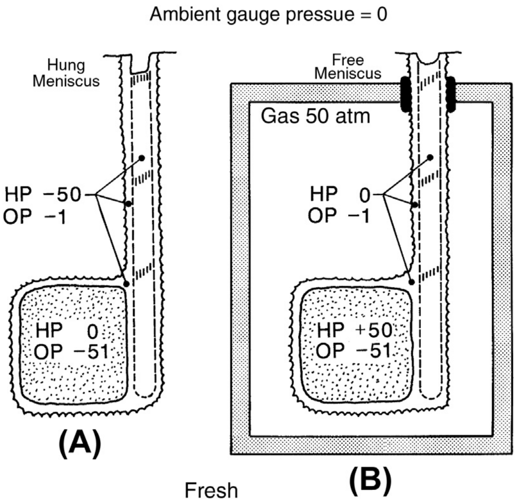
Ambient gauge pressue = 0
Hung Meniscus
HP −50
OP −1
HP 0
OP −51
(A)
Free Meniscus
Gas 50 atm
HP 0
OP −1
HP +50
OP −51
Fresh
(B)

**FIGURE 17.6** (A): Leaf cell with vessel. Air cannot enter the system because of surface tension (indicated as concave menisci). HP = hydrostatic pressure, OP = osmotic potential. (B): Balancing pressure on the same system, produced by compressed nitrogen. Notice the free meniscus at the cut end of the vessel. *From Scholander et al. (1964). Reprinted by permission of Harold T. Hammel.*

We now need to define *equilibrium pressure.* When the vessels (capillary tubes) are cut in a stem to put a leafy shoot in a pressure chamber, the water recedes from the cut (Figures 17.6 and 17.7(A)). The reason for the recession is because atmospheric pressure is higher on the outside of the cut end than on the inside. If the same difference in pressure were reestablished, the meniscus would move back exactly to the cut. The cut shoot, therefore, is placed in a pressure chamber, leaving the vessels (capillaries) protruding. Gas pressure (usually nitrogen gas) is applied,

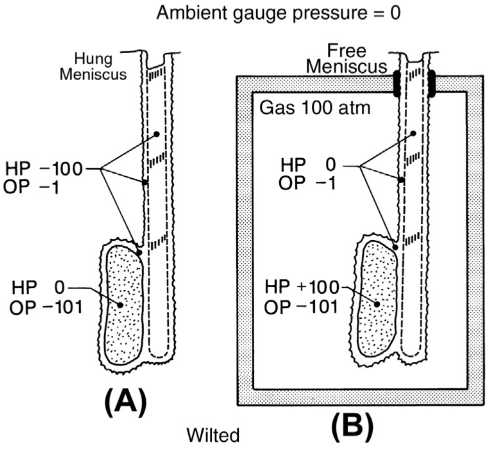
Ambient gauge pressure = 0
Hung Meniscus
HP −100
OP −1
HP 0
OP −101
(A)
Free Meniscus
Gas 100 atm
HP 0
OP −1
HP +100
OP −101
Wilted
(B)

**FIGURE 17.7** Same system as in Figure 17.6, but wilted, with about half of the intracellular water extruded. *From Scholander et al. (1964). Reprinted by permission of Harold T. Hammel.*

and when the meniscus is back at the cut, we have the equilibrium pressure (Scholander et al., 1965, p. 340).

Using these assumptions, Scholander et al. (1965) provide the following analysis: If external gas pressure is applied in excess of the balancing pressure, pure water runs out, and at zero turgor the molal concentration in the cell should, therefore, be proportional to the sap pressure, according to the following equation:

$$S/(I - V) = KP \tag{17.5}$$

or

$$I - V = K_1 P^{-1} \tag{17.6}$$

where $S$ stands for the intracellular solutes, $I$ the cell volume, $V$ the water that has run out, and $P$ the equilibrium pressure. They do not define $K$ or $K_1$. But they must be constants, and $K_1$ must equal $S/K$. If the inverse of pressure ($1/P$) is plotted against liquid removed ($V$), Scholander and colleagues say that a straight line results whenever the concentration is proportional to the pressure, and the intercept on the abscissa gives the volume of water that is being concentrated—that is, the intracellular water ($I$). The studies by Scholander et al. (1964, 1965) have been cited many times, as has a subsequent paper by Tyree and Hammel (1972).

We can refer to physical chemistry textbooks for the foundation of pressure–volume curves (see, for example, Moore, 1962, p. 135; Daniels and Alberty, 1966, p. 170). Let us follow the analysis of Daniels and Alberty (1966, pp. 170–172). When a solution is separated from the solvent by a semipermeable membrane, which is permeable by solvent but not by solute, the solvent flows through the membrane into the solution, where the chemical potential of the solvent is lower. This process is known as osmosis. This flow of solvent through the membrane can be prevented by applying a sufficiently high pressure to the solution. The osmotic pressure $\pi$ is the pressure difference across the membrane required to prevent spontaneous flow in either direction across the membrane. Figure 4.1 shows a diagram of an osmometer, which can be used to measure osmotic pressure.

The phenomenon of osmotic pressure was described by Abbé Nollet in 1748. Pfeffer, a botanist, made the first direct measurements of it in 1877. (For a biography of Pfeffer, see the Appendix, Section 17.9.) Van’t Hoff analyzed Pfeffer’s data on the osmotic pressure of sugar solutions and found empirically that an equation analogous to the ideal gas law gave approximately the behavior of a dilute solution, namely (Daniels and Alberty, 1966, p. 170)

$$\pi \overline{V} = RT \tag{17.7}$$

where $\overline{V}$ is the volume of solution containing a mole of solute and $R$ is the ideal gas constant and $T$ is the absolute temperature. The origin of the pressure is different from that for a gas, however, and the equation of the form of the ideal gas equation is applicable only in the limit of low concentrations. See Figure 17.8 for the ideal gas law.

Daniels and Alberty (1966) then proceed to derive the van't Hoff law using calculus, which we shall not do. (For a biography of van't Hoff, see the Appendix, Section 17.10.) The van't Hoff law, which J.H. van't Hoff developed in 1885 (Moore, 1962, p. 135; see Hammel and Scholander, 1976; for references by van't Hoff) and which applies only to dilute solutions, is as follows (Daniels and Alberty, 1966, p. 171):

$$\pi = (cRT)/M \tag{17.8}$$

where $c$ is the concentration of solute in grams per unit volume and $M$ is the molecular weight of the solute. This is the approximate equation that van't Hoff found empirically. Moore (1962, p. 135) writes the van't Hoff law as follows:

$$\pi = cRT \tag{17.9}$$

where $c = n/V$ and $n =$ number of moles (g/M) and $V$ is volume. We can write Eqn (17.9) as follows:

$$\pi = (nRT)/V. \tag{17.10}$$

Equation (17.10) is similar in form to Eqn (17.6), developed by Scholander et al. (1965). That is, we have pressure inversely related to

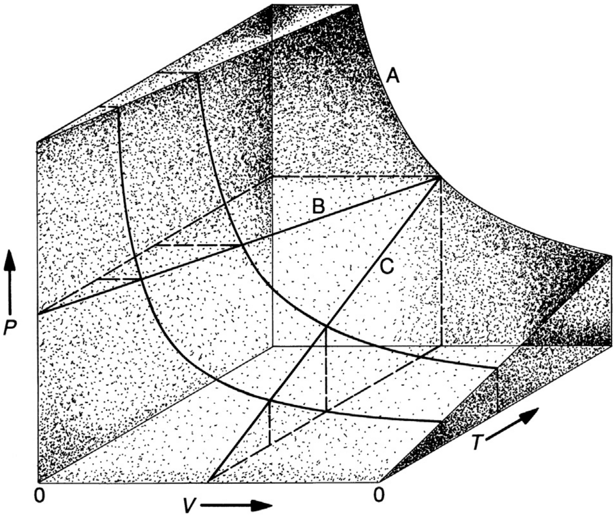

FIGURE 17.8 Pressure–volume–absolute temperature relation for an ideal gas. *From Daniels and Alberty (1966, p. 8). This material is used by permission of John Wiley & Sons, Inc.*

volume, if we are considering a dilute solution. However, we must note that Scholander et al. (1964, 1965) plot $1/P$ versus volume exuded (not volume left in the plant), and $1/P$ in their curves is inversely related to $V$. Note in Eqn (17.10) and in Figure 17.8 that $P$ (or $\pi$), not $1/P$, is inversely related to $V$. Also, at constant temperature, $P$ versus $V$ is a rectangular hyperbola (Daniels and Alberty, 1966, p. 9) and the curve never touches the $y$ or $x$ axis, as it does in the curves developed by Scholander and colleagues (e.g., see Figure 17.9 from Hammel and Scholander (1976); note the right-hand side ordinate is $1/P$).

Gardner and Rawlins (1965), who discussed the paper by Scholander et al. (1965), said that their procedure measured the difference in free energy per unit volume between water in the plant and the same water outside of the plant. The pressure chamber operates on the same principle as the pressure-membrane apparatus used to measure the potential energy of water in soils (see Chapter 5, Figure 5.5). Gardner and Rawlins said:

> When air pressure is applied to the sample chamber, the free energy of the water is raised. If this pressure increase is carried out isothermally, the free energy of the water would be raised by approximately $V\Delta P$, where $V$ is the volume of water in the sample and $\Delta P$ is the pressure increase necessary to establish equilibrium between water in the system and that outside. It is common practice to express this energy difference in terms of energy per unit volume (the water potential), which, of course, is dimensionally the same as pressure. In the experiment of Scholander et al., the plant itself provides the membrane which is permeable to water but not to air.

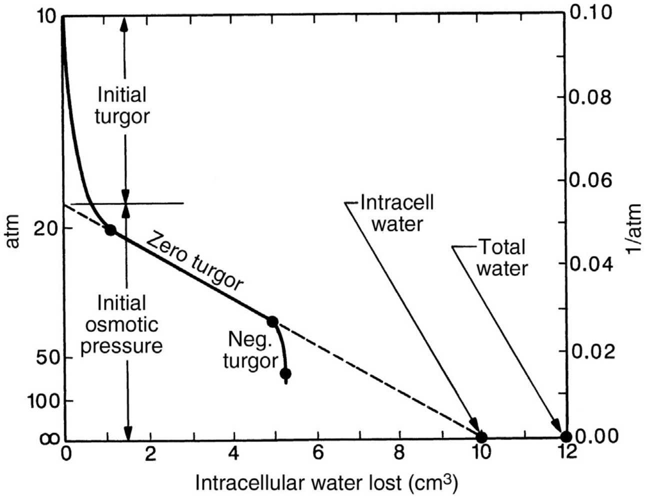

**FIGURE 17.9** Schematic presentation of a pressure–volume curve. *From Hammel and Scholander (1976, Figure 24, p. 36). Reprinted by permission of Springer-Verlag and Harold T. Hammel.*

## 17.5 HOW TO ANALYZE A PRESSURE–VOLUME CURVE

Now let us return to the actual measurement of osmotic potential using a pressure–volume curve. Pressure is applied incrementally to a plant sample. After each increase in pressure, the volume of exudate from the cut end of the plant (e.g., stem, petiole) is collected and measured, and a curve of the reciprocal of pressure versus cumulative volume exuded is plotted (Figures 17.10 and 17.11). From this pressure–volume curve, the osmotic potential at full turgor and the osmotic potential at zero turgor are indirectly determined by reading values on the ordinate (Figure 17.10). Sometimes, instead of plotting pressure versus volume exuded, pressure versus water content (or relative water content) of the plant is plotted. In this case, the plot is called a water-release curve instead of a pressure–volume curve, and is similar to water–release curves developed for soils, in which pressure

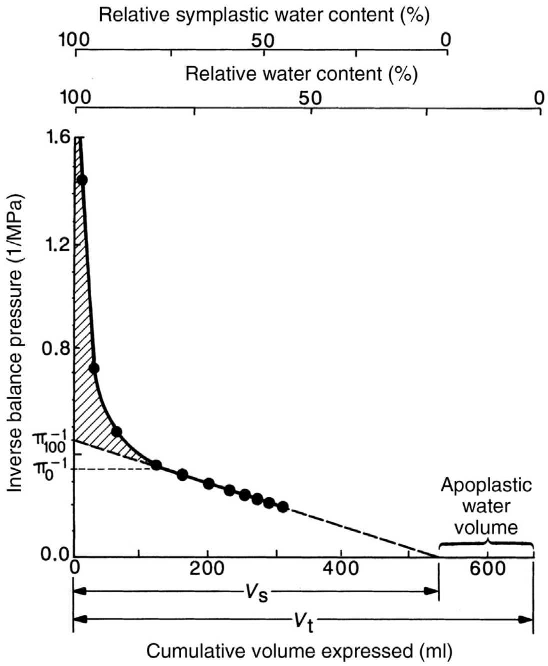

**FIGURE 17.10** A pressure–volume curve, i.e., the relationship between the inverse of the balance pressure and the cumulative volume of cell sap expressed, for wheat leaves. $V_s$ is the volume of symplast water and $V_t$ is the total volume of water in the leaf. $\pi_{100}^{-1}$ and $\pi_0^{-1}$ are the inverse of the osmotic potentials at full and zero turgor, respectively. The hatching indicates the inverse of the turgor pressure. *From Turner (1981, Figure 7, p. 355). With kind permission of Kluwer Academic Publishers and Neil C. Turner.*

(or potential) is plotted versus soil water content. Turner (1981) (Figure 17.10) illustrates how to determine osmotic potential from either a pressure–volume curve or a water–release curve.

Figure 17.11 can be used to learn how one gets $\Psi$, $\Psi_s$, and $\Psi_p$ from the $1/P$ values obtained with the pressure chamber. The top part of Figure 17.11 has the data and the bottom part has the converted data. There are 11 data points that line up in the top and bottom part of the figure. The first 6 data points, starting in the upper left in the top part of the figure, are in the region of turgor potential. This is the region of turgor, because the relationship between $1/P$ and volume of sap exuded is curvilinear. (As we shall calculate, Point 6 is right at the break between the region of turgor and no turgor.) Points 7, 8, 9, 10, and 11 are in the region of zero turgor potential where a straight line relation exists between $1/P$ and volume of sap expressed (compare the straight line in Figure 17.11, top, with the straight line for zero turgor in Figure 17.9). First we determine $P$ (from $1/P$) and get the curve for $\Psi_w$ (this is the total water potential or $\Psi$ in Eqn (17.1)). The six values (in the region of turgor) are about −0.71, −1.11, −1.43, −1.82, −2.00,

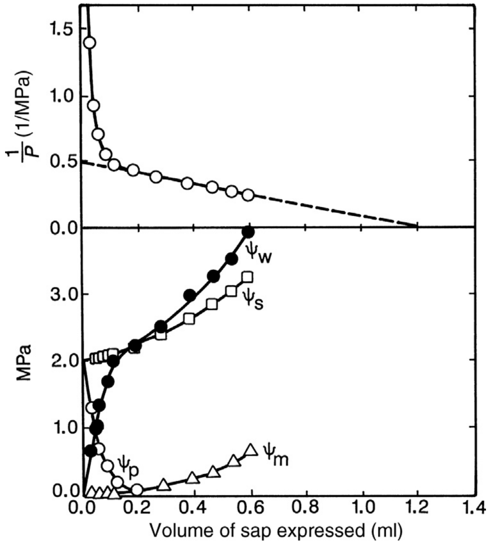

**FIGURE 17.11** The upper graph is a pressure–volume curve for *Ilex opaca* (American holly). The ordinate is the reciprocal of the pressure, and the abscissa is the volume of water expressed, in milliliters. The dashed line is the calculated extension of the linear part of the curve. It intersects the ordinate at 0.51, equal to an osmotic potential of −1.96 MPa, and the abscissa at 1.23 ml. The data in the lower graph were obtained by analysis of the pressure–volume curve. Curves are shown for turgor ($\Psi_p$), osmotic ($\Psi_s$), and matric ($\Psi_m$) potentials, and total water potential ($\Psi_w$). The turgor potential is positive, and all other potentials are negative. The abscissa of the lower graph represents water volume in milliliters, and the ordinate is given in megaPascals. *From Kramer (1983, p. 53). Reprinted by permission of Academic Press.*

and −2.13 MPa. The water potential, $\Psi_w$, is negative, so we need to add negative signs in front of these values. Then we determine $1/\Psi_s$ by measuring down from the data point in the top part of the figure to the dashed line and then reading the value on the ordinate. We then take the reciprocal of $1/\Psi_s$ to get $\Psi_s$. The six values for $\Psi_s$ in the region of turgor in Figure 17.11 are about −1.98, −2.00, −2.02, −2.04, −2.08, and −2.13 MPa. We add negative signs because they are the solute potential. Subtracting $\Psi_s$ from $\Psi_w$, we get the six values for turgor potential, $\Psi_p$, which are 1.27, 0.89, 0.59, 0.22, 0.08, and 0.00 MPa (positive values). The last value is zero, showing that Point 6 is in the region of zero turgor.

In addition to water potential, osmotic potential, and turgor potential, the pressure—volume curves can be used to find the modulus of elasticity (Melkonian et al., 1982; Sinclair and Venables, 1983). (In Chapter 23 we will determine modulus of elasticity of leaves, but not using pressure—volume curves.) Pressure—volume or water-release curves also can be obtained with dew point hygrometers instead of pressure chambers (Richter, 1978; Wilson et al., 1979).

The osmotic potential of the sap exuded during a pressure-chamber measurement can be determined by placing the sap on filter paper and measuring its osmotic potential with a thermocouple psychrometer or an osmometer (Meyer and Ritchie, 1980). The sap in the dead cells that conduct water (vessel members or tracheids) has a much higher osmotic potential (less negative, i.e., it is very dilute) than that in the sap of living cells (Scholander et al., 1964; Ike et al., 1978).

There is disagreement as to which method (frozen tissue; or pressure—volume curve, or water-release curve) provides the more reliable results. Brown and Tanner (1983) used alfalfa (*Medicago sativa* L.) to compare the two methods for determining osmotic potential. Osmotic potential of sap expressed from thawed tissue was 0.21—0.89 MPa lower than the osmotic potential obtained from water-release curves. They felt that the difference was due primarily to the production of solutes in thawed tissue by enzymatic hydrolysis and suggested that the water-release curve method was a better way to measure osmotic potential than the frozen tissue method. In contrast, Rakhi et al. (1978) said that, because the pressure chamber dehydrated the tissues that they studied (*Carex physodes* M. Bieb. (sedge) and *Populus tremula* L. (European aspen)), the values for osmotic potential determined by freezing the tissue were more reliable than the ones derived from water-release curves. Walker et al. (1983) investigated wheat (*Triticum aestivum* L.) and found that the osmotic potential, as measured by the pressure—volume method, compared favorably with the osmotic potential, as measured on frozen tissue with psychrometers. Experiments with other plants are needed to find out if these two methods for determining osmotic potential give similar results.

## 17.6 TURGOR POTENTIAL ($\Psi_P$)

Turgor potential normally is determined in one of two ways. First, turgor potential can be calculated, if the water potential and osmotic potential are measured with thermocouple psychrometers. The turgor potential is the difference between osmotic potential and water potential, assuming that matric potential (Barrs, 1968, p. 337) and gravitational potential are negligible. (Kirkham (1983) discusses situations in which gravity can be important.) Second, turgor potential can be estimated by using pressure—volume curves (Turner, 1981, Figure 17.10; Melkonian et al., 1982; Sinclair and Venables, 1983). Both of these methods require excised samples.

For many years, people have tried to measure turgor potential (pressure) directly by using probes (Barrs, 1968, p. 336). The practical difficulties, however, have been enormous, because of the small size of most plant cells. Most of the work, until recent years, was done with large-celled algae (e.g., *Nitella*, *Chara*). Now a pressure probe has been developed to measure turgor potential of higher plants directly. According to Wei et al. (2001), the contemporary cell pressure probe was designed in Germany by Steudle and Zimmermann (1971). In the United States, Nonami and Boyer (1984) were probably the first to publish on the pressure probe, and they reported the turgor potential of a higher plant, soybean (*Glycine max* L. Merr.). Boyer (1995) has described in detail the pressure probe. The equipment is expensive, complex, requires extensive training to learn how to use it, and takes precise control. The smallest vibration (such as an air movement or vibration of the floor) can cause pressure probe measurements to fail. A vibration damping table is advised.

Tomos and Leigh (1999) review how the pressure probe has evolved from an instrument for measuring cell turgor into a device for sampling the contents of individual higher plant cells in situ in the living plant. In addition, the probe is being used to measure root pressure, xylem tension (negative pressure), hydraulic conductivity, the reflection coefficient of solutes, elasticity, solute concentrations, and enzyme activities at the resolution of single cells. Tomos and Leigh (1999) also review the controversy surrounding the interpretation of measurements of xylem tension obtained with the pressure probe. It is critical to know what these tensions (negative pressures) are, if we are to confirm or refute the cohesion theory for the rise of sap in plants (see Chapter 20). Tensions in the xylem measured with the pressure probe under transpiring conditions in both small plants and tall trees have been less negative than those obtained with the pressure chamber, and in many cases are positive, which would refute the cohesion theory, because it assumes negative pressures (tensions) in the xylem. Wei et al. (2001) state that controversy over the cohesion theory resulting from measurements made with the pressure probe is due to improper probing technique. They point out that handling and methodology of the probe are critical to its success.

Despite the questions surrounding the pressure probe, its cost, and the difficulty in learning how to use it, the instrument gives us a basic understanding about water and solute relations at the cellular level. Using the probe, Thomas et al. (2006) measured cell turgor in grape (*Vitis vinifera* L.) before and after veraison. Veraison is a term used in viticulture. It comes from the French word *véraison* and refers to fruits, especially grapes, when they begin to change color at maturity. They found that cell turgor in berries at predawn was 0.02 MPa preveraison and was reduced by an order of magnitude to 0.02 MPa postveraison. The fact that a measurable cell turgor of about 0.02 MPa was exhibited in postveraison berries indicated that cell membranes remained intact after veraison, contrary to current hypotheses that veraison is associated with a loss of membrane function and cellular compartmentation in the grape berry. Bouchabké et al. (2006) used the pressure probe to measure cell turgor in the elongating zone of maize (*Zea mays* L.) leaves and showed that leaf elongation rate was positively correlated with turgor.

Calbo et al. (2010) described a portable instrument, called a wiltmeter, to estimate turgor pressure by measuring the flatness of a leaf. They compared their wiltmeter measurements with those made with a pressure probe. The wiltmeter produced leaf pressure estimates that were close to the leaf cell turgor pressure as measured by the pressure probe. They suggested that the wiltmeter would be a practical field substitute for the pressure probe and could be used to determine leaf freshness before harvest or to schedule irrigations.

## 17.7 MEASUREMENT OF PLANT WATER CONTENT AND RELATIVE WATER CONTENT

Höfler-type curves plot plant potentials versus water content (Figure 17.4) and pressure–volume curves plot the inverse balance pressure versus relative water content (Figure 17.10). Therefore, we need to know how to measure both plant water content and relative water content.

Plant water status is usually described by two basic parameters: the content of water in the plant or the energy status of the water in the plant, expressed as the (total) water potential, $\Psi$ (Barrs, 1968, p. 236). We have studied the water potential and its components in this chapter, in

Sections 17.2 through 17.6. Here we determine how to measure plant water content and relative water content.

Old techniques to measure plant water content expressed the water content on the following bases: dry weight, fresh weight, or leaf area. These are not acceptable because they are not stable. They change diurnally and seasonally, and the leaf area is reduced with drought.

Soil water content is expressed on a dry weight basis as:

$$\text{soil water content } (\%) = [(\text{wet weight} - \text{dry weight})/\text{dry weight}] \times 100. \tag{17.11}$$

The soil water content is almost always less than 100% when expressed on a dry weight basis. Exceptions are highly organic soils, such as those that occur on forest floors. For example, the 0–5, 5–10, and 10–15 cm layers of forest soil from the Craigieburn Range in the South Island of New Zealand had water contents of 382.3%, 134.4%, and 89.1%, respectively (Kirkham and Clothier, 2000).

If we do express plant water content on a weight basis, then we choose the fresh weight basis:

$$\text{plant water content } (\%) = [(\text{fresh weight} - \text{dry weight})/\text{fresh weight}] \times 100. \tag{17.12}$$

If we put the water content on a dry weight basis, the water content always would be greater than 100%, because of the high water content of plants.

Plant water content changes with age and condition of the plant. Therefore, some standard must be used in determining water content. The water content at full turgor has been used as a standard since the work of Stocker (1928, 1929) in Germany. He determined plant water content using the following equation:

$$\begin{aligned}\text{WD } (\%) &= \text{WSD } (\%)\\ &= [(\text{turgid weight} - \text{fresh weight})/(\text{turgid weight} - \text{dry weight})] \times 100\end{aligned} \tag{17.13}$$

where WD is the water deficit and WSD is the water saturation deficit; the two terms are equivalent. He determined the turgid weight by cutting off a whole leaf, or, when working with conifers, a small branch, and standing it in a little water in a closed container for 48 h (Barrs, 1968, p. 243). The fresh weight is the weight at time of sampling. The dry weight is the weight after oven drying.

The method that Stocker developed was a reliable one to determine plant water content. However, some scientists ignored its importance and used the following equation (Barrs, 1968, p. 243):

$$\text{"WD"} = [(\text{turgid weight} - \text{fresh weight})/\text{dry weight}] \times 100. \tag{17.14}$$

This equation neglects the importance of using the fully turgid weight as the basis for water content. Note that turgid weight does not appear in the denominator of Eqn (17.14).

The following equation was used to avoid getting dry weight:

$$\text{RSD} = \text{DSH} = [(\text{turgid weight} - \text{fresh weight})/\text{turgid weight}] \times 100, \tag{17.15}$$

where RSD = relative saturation deficit and DSH is the *déficit de saturation hydrique* (the French term for water saturation deficit). The DSH was confused in English with the WSD. However, the RSD or DSH method is not reliable. Dry weight needs to be determined. These many methods (WD, "WD", WSD, RSD, DSH) resulted in chaos in the literature and no standard technique existed.

In 1950, Weatherley (1950) standardized the technique. He used punched disks instead of standing whole leaves in water. He floated the disks for 24 h (sometimes 48 h) in closed Petri dishes that were exposed to diffuse daylight and a constant temperature. He then calculated relative turgidity, RT, as follows:

$$\text{RT} = [(\text{fresh weight} - \text{dry weight})/(\text{turgid weight} - \text{dry weight})] \times 100. \tag{17.16}$$

The relative turgidity is related to the water saturation deficit (or water deficit), as follows:

$$100 - \text{RT} = \text{WSD}. \tag{17.17}$$

Later Barrs and Weatherley (1962) revised Weatherley's (1950) method. They noted that there are two phases for water uptake: Phase I, which is in response to the initial water deficit and during which rapid uptake of water occurs, and Phase II in which a continued slow uptake of water continues due to growth of the tissue, even though it is excised (Figure 17.12). The aim of the Barrs and Weatherley (1962) method to determine relative turgidity was to measure only Phase I. One needs to determine for each species when rapid uptake of water ceases (end of Phase I) and then float disks for this length of time. If an initial experiment to determine this time is not done, leaves can be floated for 3–6 h, which is the normal time for Phase I for most plants. Four hours is the time most often chosen.

The Barrs and Weatherley (1962) technique is the standard method to measure relative turgidity, which is now called relative water content

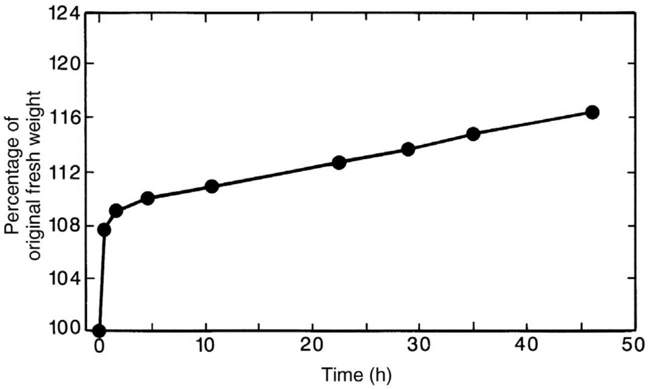

**FIGURE 17.12** Change over time in fresh weight of floating leaf disks. The leaves are from the castor-oil plant (*Ricinus communis* L.). Note the two phases in water uptake: a first phase in which water is taken up rapidly (0–5 h) and a second phase in which water is taken up slowly (5–46 h). *From Barrs and Weatherley (1962). Permission to reprint granted by CSIRO Publishing, Collingwood, Victoria, Australia, the original publisher of the information.*

(RWC). The old term *relative turgidity* has been abandoned because early workers confused relative turgidity with turgor pressure (turgor potential) (Barrs, 1968, pp. 244–245). For example, Box and Lemon (1958) referred to "turgor pressure" instead of "relative turgidity" in discussing Weatherley's (1950) results with cotton. The turgor potential is an energy-based measurement. Relative turgidity (or relative water content) is a measure of plant water content.

The Barrs and Weatherley (1962) RWC technique consists of doing the following:

1. A punch is used to punch disks out of a leaf. The punch must be sharp to minimize cut-edge effects. When plant tissue is cut, cells are damaged, causing infiltration of water. This creates excessive uptake of water and gives spuriously low RWCs. These errors are hard to quantify and appear not always to be present (Barrs, 1968, p. 247). A sharp punch, along with a good-sized leaf disk, avoids the cut-edge effect. Small disks are more prone to higher RWCs than are larger disks, and disks should not be smaller than 8 mm in diameter. A Number 8 cork borer, which has a diameter of 14 mm, is a good size to use.
2. The same diameter disks must be used in an experiment; 12 disks are recommended (Barrs, 1968, p. 251).
3. Mature or nearly mature leaves should be used rather than rapidly growing or senescent leaves. If mature leaves are used (e.g., third, fourth, or fifth leaf from the top of a plant), a time of 3–4 h for

floating should be sufficient and will coincide with Phase I (Barrs, 1968, p. 246).

4. Leaf disks must be placed in a closed Petri dish to maintain a constant humidity.
5. A constant temperature must be used. A thermometer should be placed on the laboratory bench to record the temperature. Results will differ depending on the temperature used (Figure 17.13). Barrs and Weatherley (1962, p. 415) used 20 °C in a constant temperature room.
6. The leaf disks must be exposed to diffuse light, such as that on a laboratory bench out of direct sunlight, to minimize growth and heating due to the sun.
7. After floating, the leaf disks are removed using tweezers from the Petri plate, blotted dry on a paper towel, and then put in a drying oven at 85 °C (Barrs, 1968, p. 239).
8. All weights should be weighed on an analytical balance to the fourth decimal point and then rounded off to the third decimal point.
9. For conifer needles and grass leaves, which are not wide enough for punched disks, razors mounted on a block are used to cut constant-length segments. A length of 15–25 mm is normally used (Barrs, 1968, p. 250). Grass leaves can be floated, but conifer leaves should be placed upright in a beaker of water, because needles can become waterlogged and sink.

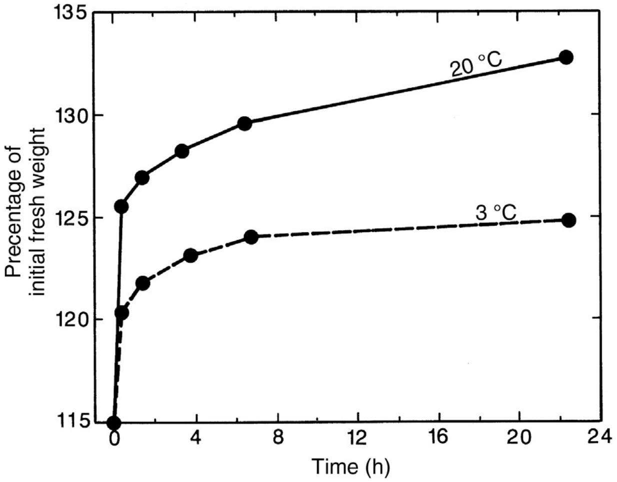

**FIGURE 17.13** Effects of floating on water at 20 and 3 °C on changes of fresh weight of leaf disks from the castor-oil plant (*Ricinus communis* L.). *From Barrs and Weatherley (1962). Permission to reprint granted by CSIRO Publishing, Collingwood, Victoria, Australia, the original publisher of the information.*

The advantages of the Barrs and Weatherley method (1962) are:

1. It standardizes sampling.
2. It is sparing of tissue.
3. It allows some leaves to be sampled more than once.
4. It can be done in a shorter time (3–6 h) than previous methods (24–48 h).
5. Even though the measurements are tedious, the relative water content method is simple and requires only an analytical balance, Petri dishes, paper towels, a thermometer, tweezers, and a drying oven. No special skills other than carefulness and patience are needed to take the measurements.

Relative water content measurements are important for several reasons. First, they are used to construct pressure–volume curves (Figure 17.10). Second, relative water content can be used as a guide to irrigation. Ehrler and Nakayama (1984) in Arizona found that relative water content measurements were a good guide to schedule irrigations of guayule (a small shrub of northern Mexico and the southwestern part of the United States cultivated for the rubber obtained from its sap). Third, the measurements show variation of water status in different portions of a leaf, if the leaf is large enough for such sampling. Slavík (1963) measured water saturation deficit (see Eqn (17.17)) across a tobacco leaf and found that the WSD was least at the base of the leaf and most at the center edge and tip of the leaf. The high WSD at the tip of the leaf was associated with a low transpiration rate. The transpiration rate was highest at the base of the leaf.

Diaz-Perez et al. (1995) state that the relative water content method is a good measure of water status and is easier to measure than water potential. The value of relative water content measurements versus water-potential measurements has been debated (Kramer, 1988; Passioura, 1988; Schulze et al., 1988). Each has its place in measurement of plant water status. However, only by measuring plant water potential can we determine the direction of movement of water in the plant. Water moves according to a potential-energy gradient (from high to low potential energy). The same holds true for water in the soil. It is important to know soil water content, but only measurements of soil water potential (or the total head) tell us the direction of movement of water (e.g., see Figure 4.3).

In sum, by using the Barrs and Weatherley (1962) technique, the problems associated with measurements of plant water content (i.e., dry weight increases with time, continued increase in water content after attainment of full turgidity, and injection of water into the intercellular spaces at the cut edge) can be minimized. The method provides a standard technique that can be replicated by workers at any location. When it is used, the paper by Barrs and Weatherley (1962) always should be cited.

## 17.8 OSMOMETER

We have mentioned that osmotic potential can be determined with an osmometer. The osmometer measures osmolality, not osmotic pressure, so we must learn how we can relate osmolality to osmotic pressure (or its negative value, osmotic potential).

Osmolality expresses the total concentration of dissolved particles in a solution without regard for the particle size, density, configuration, or electrical charge (Wescor, 1989). All these items listed are *particle characters*. A *colligative property* depends on the number of solute and solvent particles present in a solution, not their character. Osmotic pressure is a colligative property, not a cardinal property, which we shall now discuss.

Consider a solvent and a solute (a solution). There are three cardinal properties of a solvent (e.g., water): freezing point, which is lowered by solutes; boiling point, which is raised by solutes; and vapor pressure, which is lowered by solutes. Measurement of solution concentration or osmolality can be made indirectly by comparing a colligative property of the solution (solute + solvent) with a corresponding cardinal property of the pure solvent (e.g., water).

The first instruments to measure osmolality were based on freezing point depression. The Wescor osmometer (5500 Series; Logan, Utah; Figure 17.14) measures osmolality through measurement of vapor pressure by using thermocouple hygrometery (same principle that we shall see for measuring water potential with thermocouple psychrometers in Chapter 18). The dew point depression is determined using the Peltier effect. The relationship between vapor pressure depression and dew point temperature depression is given by (Wescor, 1989) as:

$$\Delta T = \Delta e / S, \tag{17.18}$$

where $\Delta T$ is the dew point temperature depression in °C, $\Delta e$ is the difference between saturated and chamber vapor pressure, and $S$ is the slope

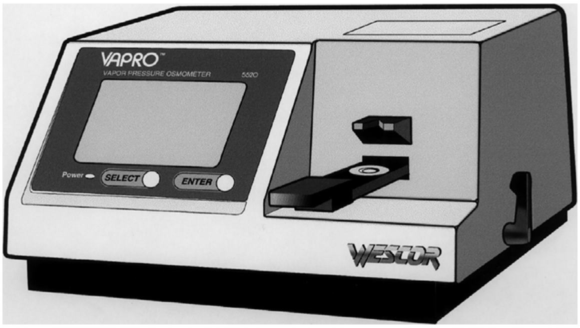

**FIGURE 17.14** The vapor pressure osmometer made by Wescor, Inc., Logan, Utah. *From a Wescor, Inc., Logan, Utah, brochure. Reprinted by permission of Wescor, Inc., Logan, Utah.*

of the vapor pressure—temperature function at ambient temperature (37 °C in the osmometer). (The osmometer probably operates at 37 °C, because it is used in medical clinics and the human body is normally at this temperature.) The Clausius—Clapeyron equation gives $S$ as a function of temperature ($T$ in °K), saturation vapor pressure ($e_0$), and the latent heat of vaporization ($\lambda$), as follows (Wescor, 1989)

$$S = (e_0\lambda)/\left(RT^2\right), \tag{17.19}$$

where $R$ is the universal gas constant. (For a biography of Clausius, see the Appendix, Section 17.11.)

Figure 17.15 shows the relation between vapor pressure and $1/T$ from a physical chemistry textbook (Daniels and Alberty, 1966, p. 127). Note the slopes for the different compounds are essentially linear.

The vapor pressure depression is a linear function of osmolality. A calibration line is obtained with two solutions that come with the equipment: 290 and 1000 mmol. The salt in the calibrating solutions is not given because it does not matter, but the calibrating solutions are probably NaCl solutions.

The Wescor instrument gives us osmolality, but we would like to relate these values to osmotic pressure. Let us determine a relationship between osmolality and osmotic pressure. We know the van't Hoff law from Eqn (17.8), $\pi = (cRT)/M$, or from Eqn (17.10), $\pi = (nRT)/V$.

**Example**: What is the osmotic pressure, $\pi$, for 2 mol of NaCl ($58.5 \times 2 = 117.0$ g)?

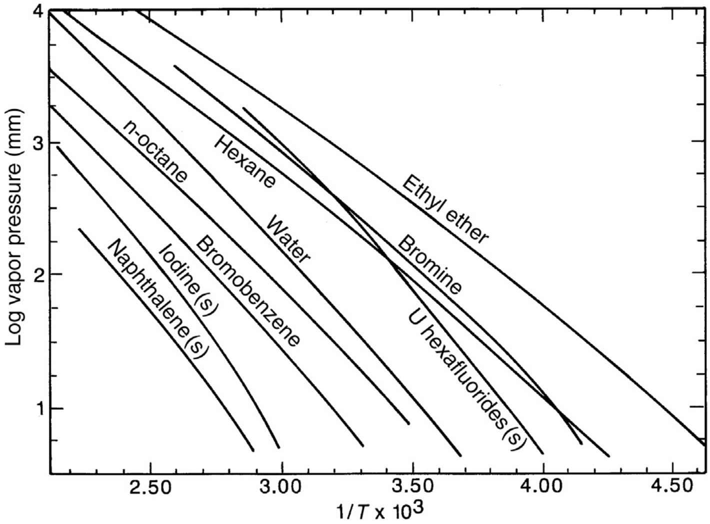

FIGURE 17.15 Log of vapor pressure versus $1/T$ for various vaporization processes. $T$ = temperature in degrees Kelvin. *From Daniels and Alberty (1966, p. 127). This material is used by permission of John Wiley & Sons, Inc.*

If we have NaCl, we have 2 ions from one molecule of salt.

$$\pi = (nRT)/V = (\text{grams/volume})\ RT/M$$

$$\pi = (117.0/1\ \text{l})(0.0821\ \text{l} - \text{atm/mol/deg})(310\ \text{K})/58.5 = 50.84\ \text{atm}.$$

$$50.84\ \text{atm} \times 2\ \text{ions} = 101.68\ \text{atm} = 103.02\ \text{bars}.$$

The table published by Lang (1967) and reproduced by Barrs (1968, p. 288) gives 101.60 bars at 35 °C. The value of 103.02 bars we calculated is close to the value given by Lang (1967).

If we want to convert osmolality to osmotic potential, and we do not know the number of ions (as we do with an NaCl or KCl solution), we use the following equation (Taiz and Zieger, 2002, p. 40):

$$\Psi_s = -C_s RT, \tag{17.20}$$

where

$C_s$ = osmolality (in mol/kg or mol/l).

So if we measure with the osmometer 2 mmol/1 kg = 0.002 molal

$$\Psi_s = -0.002\ RT =$$
$$(-\ 0.002\ \text{mol/l})$$
$$(0.0821\ \text{l atm/mol/deg})(310\ \text{K}) = -0.05\ \text{atm}.$$

Note that (0.0821 l-atm/mol/deg) (310 K) = a constant = 25.45 or (0.0832 l-bar/mol/deg) (310 K) = a constant = 25.8.

To summarize the method to use the osmometer:

1. With the osmometer, $\Delta T$ is measured to get $\Delta e$, and we know

$$\Delta T = \Delta e/S,$$

where we get $S$ from the Clausius–Clapeyron equation.

2. Then $\Delta e$ is related to osmolality (linear function). Vapor pressure depression is a linear function of osmolality.
3. We make a calibration line with two solutions. Wescor provides 290 and 1000 mmol/kg for the calibrating solutions.
4. We report the reading as osmolality (mmol/kg) or as osmotic pressure using

$$\Psi_s = -C_s RT.$$

## 17.9 APPENDIX: BIOGRAPHY OF WILHELM PFEFFER

Wilhelm Friedrich Philipp Pfeffer (1845–1920) was a German physiological botanist. He was born in Grebenstein, where his father owned a chemist's shop (pharmacy) (Frommhold, 1996), on March 9, 1845 (McIlrath, 1971). There he learned fundamental knowledge and manual skills for his later profession. After earning a degree in botany and chemistry from Göttingen University in 1865, he spent the next several years studying botany and pharmacy at Marburg University. He continued his botanical studies at Berlin (1869–1870) and Würtzburg University (1870–1871). In 1871 he returned to lecture at Marburg, and in 1873 he was appointed lecturer at Bonn University. In 1877 he became a professor at Basel University and later at the universities of Tübingen (1878) and Leipzig (1887). In Leipzig, Pfeffer began his scientific research which lasted more than three decades (Frommhold, 1996). There he was director of the Botanical Institute and the Botanical Gardens. In 1884, Pfeffer married Henrika Volk (Frommhold, 1996), and in May of 1885 his son Otto was born.

His laboratories in the Botanical Institute in Leipzig were modern for the time. He had microscopes and a room with a constant temperature (the precursor of the growth chamber). He positioned measuring instruments so they were free from vibration. He installed a dark room and made devices by which alteration of light and dark conditions could be done automatically. He improved equipment such as the clinostat and the auxanometer. Pfeffer's institute attracted students and visiting scientists from around the world. One of his famous students was Carl Correns, who studied mutants in the Botanical Gardens. Pfeffer knew Wilhelm Ostwald, who also went to Leipzig in 1887.

Pfeffer made significant contributions in the following areas of plant physiology: respiration, photosynthesis, protein metabolism, and tropic and nastic movements. In 1881 he published the first part of his *Handbuch der Pflanzenphysiologie* (English translation by A.J. Ewart, *Physiology of Plants*, three volumes, 1906), which was an important text for many years.

During his life Pfeffer received numerous awards. His seventieth birthday (March 9, 1915) and his golden doctor's jubilee (February 10, 1915) were both celebrated on the same day in the first year of the First World War (1914–1918). The hardest blow in Pfeffer's life hit shortly before the end of the war. A few weeks before the armistice, he was informed that his son Otto was missing, and in the middle of 1919 he learned that Otto had been killed in France. He also suffered physically, because he, like many other Germans at the end of the war, did not have enough to eat. He destroyed all his scientific manuscripts because he felt that he could not complete his work. His research publications ended in 1916. However, he kept teaching, and in 1919–1920, his lectures often had to be offered twice, as the rooms were overcrowded with returned soldiers (Frommhold, 1996).

His last year of life was difficult. In addition to the loss of his son, he also faced the loss of his official residence upon enforced retirement in

1920 (Frommhold, 1996). On the day of his last physiology lecture on January 31, 1920, he died without having been seriously ill.

## 17.10 APPENDIX: BIOGRAPHY OF JACOBUS VAN'T HOFF

Jacobus Hendricus van't Hoff (1852–1911) was a Dutch physical chemist, who received the first Nobel Prize in chemistry (1901) for his work on chemical dynamics and osmotic pressure in solutions (Preece, 1971a). He was born in Rotterdam on August 30, 1852, and studied at the Polytechnic at Delft and at the University of Leiden. He then studied under Friedrich A. Kekulé von Stradonitz (1829–1896; German chemist) at Bonn, Charles A. Wurtz at Paris in the École de Médecine, and G.J. Mulder at Utrecht, where he obtained his doctorate in 1874. He was a lecturer in physics at the veterinary school in Utrecht (1876); professor of chemistry, mineralogy, and geology in Amsterdam University (1878); and professor at the Prussian Academy of Sciences in Berlin (1896), accepting an honorary professorship in the university so that he might lecture if he wished. He was elected a foreign member of the Royal Society in 1897 and awarded its Davy medal in 1893. He died in Berlin on March 1, 1911.

van't Hoff's earliest important contribution was made in 1874. Starting with the results of the work of Johannes Wiclicenus (1835–1902; German chemist, who studied isomers), he showed that the four valencies of the carbon atom were probably directed in space toward the four corners of a regular tetrahedron. In this way optical activity, shown to be always associated with an asymmetric carbon atom, could be explained. An identical idea was put forward two months later (November 1874), independently, by Joseph Achille Le Bel (1847–1930; French chemist). van't Hoff and le Bel had been fellow students under Wurtz but had never exchanged a word about the carbon tetrahedron. The concept was attacked by Hermann Kolbe (1818–1884; German chemist), but its value was soon universally realized, and it laid the foundation stone of the science of stereochemistry (Preece, 1971a).

In 1877 van't Hoff published *Ansichten über die organischen Chemie*, which contains the beginnings of his studies in chemical thermodynamics. In *Études de dynamique chimique* (1884) he developed the principles of chemical kinetics, described a new method of determining the order of a reaction, and applied thermodynamics to chemical equilibriums. In 1886 he published the results of his study of dilute solutions and showed the analogy existing between them and gases, because they both obey equations of the type $pv = RT$. During the next nine years he developed this work in connection with the theory of electrolytic dissociation enunciated by Svante August Arrhenius (1859–1927; Swedish chemist).

With Wilhelm Ostwald (1853–1932; German chemist who won the 1909 Nobel Prize in chemistry), he started the important *Zeitshrift für physikalische Chemie* in 1887, the first volume of which contained the famous paper by Arrhenius on electrolytic dissociation, along with the fundamental paper by van't Hoff (Preece, 1971a).

## 17.11 APPENDIX: BIOGRAPHY OF RUDOLF CLAUSIUS

Rudolf Julius Emanuel Clausius (1822–1888) was a German physicist who made important contributions to molecular physics (Preece, 1971b). He was born in Köslin in Pomerania. In 1848 he got his degree at Halle, and in 1850 he was appointed professor of physics in the royal artillery and engineering school at Berlin and *Privatdocent* in the university. In 1855 he became an ordinary professor at the Zürich Polytechnic and professor at the University of Zürich. Clausius moved to Würzburg in Germany in 1867 as professor of physics, and two years later he was appointed to the same chair at Bonn, a position that he held until his death.

The work of Clausius, who was a mathematical rather than an experimental physicist, was concerned with many of the most abstruse problems of molecular physics. He made thermodynamics a science; he enunciated the second law, in a paper contributed to the Berlin Academy in 1850, in the well-known form, "Heat cannot of itself pass from a colder to a hotter body". He applied his results to an exhaustive development of the theory of the steam engine.

The kinetic theory of gases owes much to his researches. He raised it to the level of a theory, and he carried out many numerical determinations in connection with it, such as determining the mean free path of a molecule. Clausius also made an important advance in the theory of electrolysis, suggesting that molecules in electrolytes are continually interchanging atoms. This view found little favor until 1887, when it was taken up by S.A. Arrhenius, who made it the basis of the theory of electrolytic dissociation.

## References

Baker, D.A., 1984. Water relations. In: Wilkins, M.B. (Ed.), Advanced Plant Physiology. Pitman, London, pp. 297–318.

Barrs, H.D., 1968. Determination of water deficits in plant tissues. In: Kozlowski, T.T. (Ed.), Water Deficits and Plant Growth, Development, Control, and Measurement, vol. 1. Academic Press, New York, pp. 235–368.

Barrs, H.D., Weatherley, P.E., 1962. A re-examination of the relative turgidity technique for estimating water deficits in leaves. Aust. J. Biol. Sci. 15, 413–428.

Bouchabké, O., Tardieu, F., Simonneau, T., 2006. Leaf growth and turgor in growing cells of maize (*Zea mays* L.) respond to evaporative demand under moderate irrigation but not in water-saturated soil. Plant Cell Environ. 29, 1138–1148.

Box, J.E., Lemon, E.R., 1958. Preliminary field investigations of electrical resistance–moisture stress relations in cotton and grain sorghum plants. Soil Sci. Soc. Am. Proc. 22, 193–196.

Boyer, J.S., 1995. Measuring the Water Status of Plants and Soils. Academic Press, San Diego.

Brown, P.W., Tanner, C.B., 1983. Alfalfa osmotic potential: a comparison of the water-release curve and frozen-tissue methods. Agron. J. 75, 91–93.

Calbo, A.G., Ferreira, M.D., Pessoa, J.D.C., 2010. A leaf lamina compression method for estimating turgor pressure. HortScience 45, 418–423.

Clarke, J.M., Simpson, G.M., 1978. Leaf osmotic potential as an indicator of crop water deficit and irrigation need in rapeseed (*Brassica napus* L.). Agr. Water Manage. 1, 351–356.

Daniels, F., Alberty, R.A., 1966. Physical Chemistry, third ed. John Wiley and Sons, New York.

Diaz-Perez, J.C., Shackel, K.A., Sutter, E.G., 1995. Relative water content and water potential of tissue-cultured apple shoots under water deficits. J. Exp. Bot. 46, 111–118.

Ehrler, W.L., Nakayama, F.S., 1984. Water stress status in guayule as measured by relative leaf water content. Crop Sci. 24, 61–66.

Esau, K., 1977. Anatomy of Seed Plants, second ed. Wiley, New York.

Frommhold, I., 1996. The 150th Birthday of Wilhelm Pfeffer. JSPP Newsletter, August issue, pp. 10–15. Japanese Society of Plant Physiologists, Kyoto, Japan.

Gardner, W.R., Rawlins, S.L., 1965. Sap pressure in plants. Science 149, 920.

Hammel, H.T., Scholander, P.F., 1976. Osmosis and Tensile Solvent. Springer-Verlag, Berlin.

Höfler, K., 1920. Ein Schema für die osmotische Leistung der Pflanzenzelle [A scheme for the osmotic capacity of plant cells] Berichte der Deutschen Botanischen Gesellschaft (Report Ger. Bot. Society) 38, 288–298.

Ike, I.F., Thurtell, G.W., Stevenson, K.R., 1978. Evaluation of the pressure chamber technique for measurement of leaf water potential in cassava (*Manihot* species). Can. J. Bot. 56, 1638–1641.

Kirkham, M.B., 1983. Physical model of water in a split-root system. Plant Soil 75, 153–168.

Kirkham, M.B., Clothier, B.E., 2000. Infiltration into a New Zealand native forest soil. In: Rosenzweig, C. (Ed.), A Spectrum of Achievements in Agronomy. American Society of Agronomy, Crop Science Society of America, and Soil Science Society of America, Madison, Wisconsin. ASA Special Pub. No. 62.

Kramer, P.J., 1983. Water Relations of Plants. Academic Press, New York.

Kramer, P.J., 1988. Changing concepts regarding plant water status. Plant Cell Environ. 11, 565–568.

Lang, A.R.G., 1967. Osmotic coefficients and water potentials of sodium chloride solutions from 0 to 40 °C. Aust. J. Chem. 20, 2017–2023.

McIlrath, W.J., 1971. Pfeffer, Wilhelm (Friedrich Philipp). Encyclopaedia Britannica 17, 791.

Melkonian, J.J., Wolfe, J., Steponkus, P.L., 1982. Determination of the volumetric modulus of elasticity of wheat leaves by pressure–volume relations and the effect of drought conditioning. Crop Sci. 22, 116–123.

Meyer, B.S., Anderson, D.B., Böhning, R.H., 1960. Introduction to Plant Physiology. D. Van Nostrand, Princeton, New Jersey.

Meyer, W.S., Ritchie, J.T., 1980. Resistance to water flow in the sorghum plant. Plant Physiol. 65, 33–39.

Moore, W.J., 1962. Physical Chemistry, third ed. Prentice-Hall, Englewood Cliffs, New Jersey.

Nobel, P.S., 1974. Introduction to Biophysical Plant Physiology. W.H. Freeman, San Franciso, California.

Nobel, P.S., 1983. Biophysical Plant Physiology and Ecology. W.H. Freeman, San Francisco, California.

Nonami, H., Boyer, J.S., 1984. Regulation of growth of soybean at low water potentials. Plant Physiol. 75 (Suppl.), 174.

Passioura, J.B., 1988. Response to Dr P.J. Kramer's article, "Changing concepts regarding plant water relations," Volume 11, Number 7, pp. 565–568. Plant Cell Environ. 11, 569–571.

Preece, W.E. (General Ed.), 1971a. Van't Hoff, Jacobus Hendricus. Encyclopaedia Britannica, vol. 22; p. 887.

Preece, W.E. (General Ed.), 1971b. Clausius, Rudolf Julius Emanuel. Encyclopaedia Britannica, vol. 5; p. 888.

Rakhi, M.O., Zavadskaya, I.G., Bobrovskaya, N.I., 1978. Errors in determining components of the leaf water potential with the aid of a pressure chamber. Soviet Plant Physiol. 25 (4, Part 2), 689–696.

Richter, H., 1978. Water relations of single drying leaves: evaluation with a dewpoint hygrometer. J. Exp. Bot. 29, 277–280.

Scholander, P.F., Hammel, H.T., Hemmingsen, E.A., Bradstreet, E.D., 1964. Hydrostatic pressure and osmotic potential in leaves of mangroves and some other plants. Proc. Natl. Acad. Sci. U.S.A. 52, 119–125.

Scholander, P.F., Hammel, H.T., Bradstreet, E.D., Hemmingsen, E.A., 1965. Sap pressure in vascular plants. Science 148, 339–346.

Schulze, E.-D., Steudle, E., Gollan, T., Schurr, U., 1988. Response to Dr P.J. Kramer's article, "Changing concepts regarding plant water relations," Volume 11, Number 7, pp. 565–568. Plant Cell Environ. 11, 573–576.

Sinclair, R., Venables, W.N., 1983. An alternative method for analysing pressure–volume curves produced with the pressure chamber. Plant Cell Environ. 6, 211–217.

Singh, P., Kanemasu, E.T., Singh, P., 1983. Yield and water relations of pearl millet genotypes under irrigated and nonirrigated conditions. Agron. J. 75, 886–890.

Slavík, B., 1963. The distribution of transpiration rate, water saturation deficit, stomata number and size, photosynthetic and respiration rate in the area of the tobacco leaf blade. Biol. Plant 5, 143–153.

Steudle, E., Zimmermann, U., 1971. Hydraulische Leitfähigkeit von Volonia utricularis. Z. Naturforsch 26, 1302–1311.

Stocker, O., 1928. Das Wasserhaushalt ägyptischer Wüsten-und Salzpflanzen. In: Botanische Abhandlungen, vol. 13.

Stocker, O., 1929. Das Wasserdefizit von Gefässpflanzen in verschiedenen Klimazonen. Planta 7, 382–387.

Taiz, L., Zeiger, E., 2002. Plant Physiology, third ed. Sinauer Associates, Sunderland, Massachusetts.

Thomas, T.R., Matthews, M.A., Shackel, K.A., 2006. Direct *in situ* measurement of cell turgor in grape (*Vitis vinifera* L.) berries during development and in response to plant water deficits. Plant Cell Environ. 29, 993–1001.

Tomos, A.D., Leigh, R.A., 1999. The pressure probe: a versatile tool in plant cell physiology. Annu. Rev. Plant Physiol. Plant Mol. Biol. 50, 447–472.

Turner, N.C., 1981. Techniques and experimental approaches for the measurement of plant water status. Plant Soil 58, 339–366.

Tyree, M.T., Hammel, H.T., 1972. The measurement of the turgor pressure and the water relations of plants by the pressure-bomb technique. J. Exp. Bot. 23, 267–282.

Walker, S., Oosterhuis, D.M., Savage, M.J., 1983. Field use of screen-caged thermocouple psychrometers in sample chambers. Crop Sci. 23, 627–632.

Weast, R.C. (Ed.), 1964. Handbook of Chemistry and Physics, forty-fifth ed. Chemical Rubber Co, Cleveland, Ohio.

Weatherley, P.E., 1950. Studies in the water relations of the cotton plant. I. The field measurement of water deficits in leaves. New Phytol. 49, 81–97.

Wei, C., Steudle, E., Tyree, M.T., Lintilhac, P.M., 2001. The essentials of direct xylem pressure measurement. Plant Cell Environ. 24, 549–555.

Wescor, Inc, 1989. Instruction/Service Manual M2448–4 for the 5500 Vapor Pressure Osmometer. Wescor, Inc., Logan, Utah. Pages not numbered sequentially. (See Section 8, p. 8–1 to 8-4, for the theory of operation.).

Wilson, J.R., Fisher, M.J., Schulze, E.-D., Dolby, G.R., Ludlow, M.M., 1979. Comparison between pressure–volume and dewpoint-hygrometer techniques for determining the water relations characteristics of grass and legume leaves. Oecologia 41, 77–88.

CHAPTER

# 18

# Thermocouple Psychrometers

Thermocouple hygrometers are generally accepted as the standard for measurement of plant-water potential (Oosterhuis et al., 1983; Savage et al., 1983a). They measure vapor pressure in a small chamber by using either a psychrometric (wet bulb/dry bulb) or dewpoint technique. Because both are used, the more general term thermocouple hygrometer is sometimes used rather than thermocouple psychrometer (Campbell and Campbell, 1974). However, most people call the instruments thermocouple psychrometers.

We use thermocouple psychrometers to determine water potential by measuring relative humidity. But we actually are measuring a temperature depression (either the wet-bulb or the dewpoint temperature depression). To relate the temperature depression to relative humidity, we use the psychrometric equation. Let us look at these points now in detail.

## 18.1 RELATION BETWEEN WATER POTENTIAL AND RELATIVE HUMIDITY

The use of thermocouple psychrometers to measure water potential is based on a sound physical–chemical foundation. A definite, quantitative relation exists between water potential of a sample and the relative vapor pressure above it (Barrs, 1968, p. 281; Rawlins, 1972; Savage and Cass, 1984), as follows:

$$\Psi = \left[(RT)/V_{\mathrm{w}}^{\mathrm{o}}\right]\ln\left(e/e^{\mathrm{o}}\right), \tag{18.1}$$

where $\Psi =$ water potential, $R =$ ideal gas constant, $T =$ absolute temperature (K), $V_{\mathrm{w}}^{\mathrm{o}} =$ molar volume of pure water, $e =$ partial pressure of water vapor in air, $e^{\mathrm{o}} =$ saturated vapor pressure, and $e/e^{\mathrm{o}} =$ relative humidity. Equation (18.1) is called the Kelvin equation (Rawlins, 1972).

Except for $T$, which is always in K, units vary according to values used. If $\Psi$ is expressed in bars, then $R = 83.2\ \mathrm{cm}^3$ bar/mole degree, $V_{\mathrm{w}}^{\mathrm{o}} = 18.048\ \mathrm{cm}^3/\mathrm{mol}$ at 20 °C, $e$ and $e^{\mathrm{o}} =$ bars (or millibars). Other values

http://dx.doi.org/10.1016/B978-0-12-420022-7.00018-5

Copyright © 2014 Elsevier Inc. All rights reserved.

of $R$ are: 0.0821 l atm/mole degree; 0.0832 l bar/mole degree; and 82.1 $\text{cm}^3$ atm/mole degree. We remember that K = °C + 273.16. Absolute zero is at −273.16 (or −459.69 °F) and it is the temperature at which a gas would show no pressure if the general law for gases would hold for all temperatures (Weast, 1964, p. F-29). Absolute zero is the hypothetical point at which a substance would have no molecular motion and no heat (Webster's New World Dictionary of the American Language, 1959). The Kelvin scale of temperature measured is in degrees centigrade from absolute zero and is named after William Thomson, Baron Kelvin. (For a biography of William Thomson, see the Appendix, Section 18.11.) In 1967 the 13th General Conference on Weights and Measures adopted the unit *kelvin* (K) as its standard for temperature, making it one of the seven base units of Le Système International d'Unités (SI system; see Chapter 2, Section 2.2). The definition of the 1967 thermometric unit replaced degrees Celsius and degrees absolute in scientific work (Patterson, 1988). The kelvin now is defined as the fraction 1/273.16 of the thermodynamic temperature of the triple point of water (Haynes, 2013, pp. 1−22). (The *triple point* is defined as the point in *pressure*, *temperature* space where the solid, liquid, and gas phases of a substance are in thermodynamic equilibrium. The corresponding temperature and pressure are called the triple point temperature and the triple point pressure (Haynes, 2013, pp. 2−67). For water, the triple-point temperature is 0.01 °C and the triple-point pressure is 611.657 Pa (Haynes, 2013, pp. 6−9)).

A measurement of relative vapor pressure, or of some related property, gives the water potential of the sample directly, provided that the sample and the space in the chamber have first come to equilibrium. Suitable electrical transducers are thermocouple psychrometers (Barrs, 1968, p. 281) or, using the more general term, thermocouple hygrometers. A hygrometer is an instrument for measuring humidity or the moisture in the air. A psychrometer is a type of hygrometer in which the humidity is measured with wet and dry bulb thermometers. The initial combining form of the word is *psychro-*, which comes from the Greek word *psychros*, meaning "cold" (Webster's New World Dictionary of the American Language, 1959).

## 18.2 THERMOELECTRIC EFFECTS

Before discussing thermocouple psychrometers used in plant-water measurements, let us review the thermoelectric effects on which they are based. Figure 18.1 shows an electric circuit of two metals formed into two junctions. If a temperature difference exists between the two junctions, an electric current will flow between them (Barrs, 1968, p. 287). This is the Seebeck effect, named after Johann Seebeck in Berlin, who

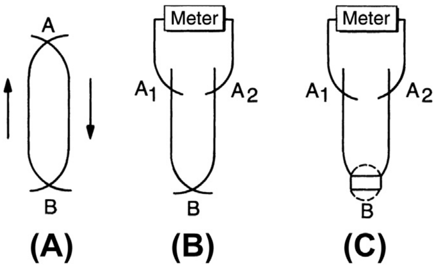

**FIGURE 18.1** Thermoelectric effects used in thermocouple psychrometry. (A) The Seebeck effect; current flows due to a temperature difference between junctions A and B; (B) Measurement of temperature difference between A and B. B may initially be cooled by the Peltier effect (Spanner psychrometer); (C) Maintenance of permanently wet junction at B (Richards-and-Ogata psychrometer). *From Barrs (1968). Reprinted by permission of Academic Press.*

discovered it in 1821 (Shortley and Williams, 1971, p. 578). Holding the two junctions at different temperatures causes a current when no other source of electromotive force (emf) is present. The Seebeck effect is used in solid-state physics to generate currents (Ong, 2008; Uchida et al., 2008).

If both junctions are initially at the same temperature, then, by passing an electric current through them, one junction will cool and the other will heat (Barrs, 1968, p. 287). This is the Peltier effect, named after Jean Charles Athanase Peltier in Paris, who described the phenomenon about 1834 (Shortley and Williams, 1971, p. 577). (For a biography of Peltier, see the Appendix, Section 18.9) The rates of heat generation and absorption are proportional to the current. When the current is reversed, the roles of the two junctions are reversed. Although the Peltier current tends to heat the reference junction, while the free junction is cooled, the rise in temperature is negligible due to the rapid outflow of heat along the massive copper wires attached to junctions $A_1$ and $A_2$ (Figure 18.1) or the junctions at the top of the thermocouple psychrometer (Figure 18.2, right).

The Peltier effect can give only a small degree of cooling, but it is of interest biologically. For example, if the osmotic pressure of a solution is 10 atm, depression of the dewpoint temperature is about 0.124 °C at 25 °C, which corresponds to a relative humidity of 99.3%. For a dewpoint depression of 1 °C, osmotic pressure would be 80 atm (94.3% relative humidity) (Spanner, 1951).

## 18.3 JOULE HEATING

The temperature changes associated with the Peltier effect appear in addition to increases in temperature resulting from the normal joule heating, which we now review. (For a biography of Joule, see the

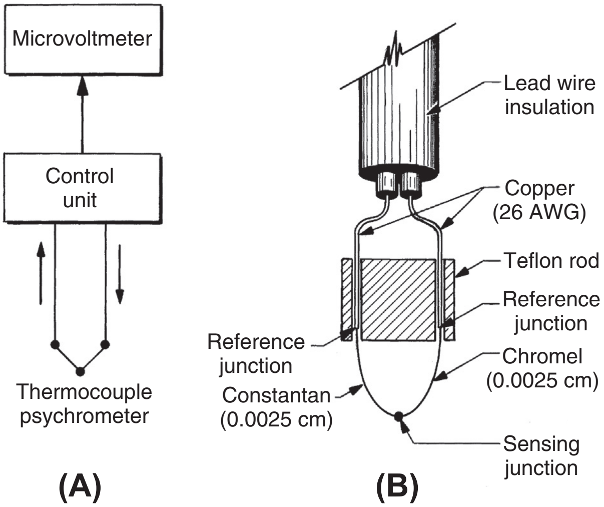
Microvoltmeter
Control unit
Thermocouple psychrometer
(A)
Lead wire insulation
Copper (26 AWG)
Teflon rod
Reference junction
Chromel (0.0025 cm)
Reference junction
Constantan (0.0025 cm)
Sensing junction
(B)

**FIGURE 18.2** A Peltier thermocouple psychrometer system used to measure water potential consisting of (A) a microvoltmeter, control unit, and the thermocouple psychrometer; (B) a single-junction Peltier thermocouple psychrometer illustrated in detail. *From van Haveren and Brown, 1972. Reprinted by permission of the Utah Agricultural Experiment Station.*

Appendix, Section 13.10.) The work $W$ in joules done in transferring in a circuit a charge of $q$ coulombs between two terminals having a potential difference $V$ volts is

$$W = qV = It(V) = IVt, \tag{18.2}$$

[Remember from Chapter 12, Section 12.2 on electrolysis, that $I$ (amperes) $= q$ (coulombs)$/t$ (s).] Because $V = IR$, where $R$ is resistance, $IVt = I(IR)t = I^2Rt$. Thus the electrical energy in joules converted into heat in a conductor of resistance $R$ ohms carrying a current $I$ amperes is

$$W = I^2Rt, \tag{18.3}$$

which is called Joule's law of heating (Schaum, 1961, p. 153). Because 1 Joule = 0.239 calories, the heat $H$ in calories developed in the conductor is

$$H = 0.239I^2Rt. \tag{18.4}$$

By use of low-resistance pieces of metal, it is possible, in spite of Joule heating, to get one of the junctions to cool below room temperature (Shortley and Williams, 1971, p. 578). The maximum degree of cooling due to the Peltier effect is limited by Joule heating.

The value of a thermocouple, when used as a thermometer (measurement of temperature difference between two junctions), depends on the fact that the net emf developed is directly related to the temperature difference between the junctions. For small temperature differences, it is approximately proportional to the temperature difference (Shortley and Williams, 1971, p. 578).

The thermoelectric effect is not an unmixed blessing. In any electrical apparatus in which the circuits contain different metals or even different grades of the same metal, temperature differences arising from any cause will set up small “thermal emfs” and “thermal currents”, as they are called. Even when a piece of equipment is constructed of a single grade of metal, small thermal emfs exist if there are temperature differences between different portions of the equipment. These emfs appear as a result of a phenomenon known as the Thomson effect. If a copper rod is heated at one end and cooled at the other, a difference of potential is observed between the ends. This Thomson difference of potential arises from a temperature dependence of the density of free electrons in the metal (Shortley and Williams, 1971, p. 579).

## 18.4 THERMOELECTRIC POWER

The thermoelectric power of thermocouples varies. One of the most commonly used thermocouples in plant-water measurements is constantan–chromel, because it is commercially available. Its thermoelectric power is 60 μV/°C. Bismuth–bismuth + 5% tin is preferred by some workers, because its thermoelectric power (126 μV/°C) is twice as high as that of constantan–chromel (Barrs, 1968, p. 289). A further point in favor of the bismuth–bismuth + 5% tin thermocouple is that the maximum Peltier cooling possible is 4.9 °C as against 1.5 °C for constantan–chromel. There is a maximum Peltier cooling (dewpoint temperature). If the temperature depression is greater than the dewpoint-temperature depression, it is not possible to condense dew on the wet junction. With most biological systems, this is not a limitation, because such low potentials usually are not encountered. For example, if one uses constantan-chromel, the lower useful limit is about −65 bars (Barrs, 1968, p. 291), which is below the potentials measured in most plants.

## 18.5 RELATIONSHIP BETWEEN VAPOR PRESSURE AND TEMPERATURE

As stated earlier, we obtain water potential by observations of vapor pressure. The changes in temperature measured are actually minute. The relation between vapor pressure and temperature is as follows:

$$e = e^{o}_{W} - \gamma(T_A - T_W), \tag{18.5}$$

where $e$ = partial pressure of water vapor in air; $e_W^o$ = saturated vapor pressure at the wet-bulb temperature; $T_A$ = dry-bulb temperature (air temperature); $T_W$ = wet-bulb temperature; $\gamma$ = psychrometric constant, taken to be 0.658/°C at 20 °C and 1000 mb pressure (Monteith, 1973, p. 221). ($\gamma$ is 0.655 at 15 °C; 0.662 at 25 °C; 0.665 at 30 °C; 0.668 at 35 °C; and 0.671 at 40 °C—all at 1000 mb.) The interested reader can study Monteith (1973, pp. 171–173) or Monteith and Unsworth (2013, pp. 221–224) for an explanation of the psychrometric constant and the basis for Eqn (18.5).

The Smithsonian Meteorological Tables (List, 1951) give exact values of saturation vapor pressure over water in metric and English units. In the metric units, values for saturation vapor pressure over water in millibars are given for temperatures ranging from −50.0 to 120.0 °C, in tenths of degree increments (List, 1951; pp. 351–353, Table 94). Rigorous expressions for the dependence of saturation vapor pressure on temperature are obtained by integrating the Clausius–Clapeyron equation (Monteith and Unsworth, 1990, p. 8; 2013, p. 11). Many authors have proposed simpler equations for estimating the saturation vapor pressure of water at different temperatures. Perhaps the most useful form is the Tetens (1930) formula (Ham, 2005). Values of saturation vapor pressure from the Tetens formula are within 1 Pa of the exact values from −5 to 35 °C (Monteith and Unsworth, 1990, p. 10; 2013, p. 13). The Tetens formula, as given by Murray (1967; see his Eqn 6), is

$$e_s = 6.1078 \exp[a(T - 273.16)/(T - b)] \tag{18.6}$$

where $a = 17.2693882$ and $b = 35.86$.

Buck (1981) also gives a form of the Tetens formula, and most microclimatologists now use the Buck formula (Jay M. Ham, Department of Agronomy, Kansas State University, personal communication, December 30, 2003). Ham (2005) compares the coefficients in the Murray (1967) and Buck (1981) formulas.

To avoid the necessity of knowing coefficients, we can use Eqn (18.5) and Table 94 from List (1951) to determine the partial pressure of water vapor in air ($e$), as well as relative humidity (RH), and vapor pressure deficit (VPD). van Haveren and Brown (1972, pp. 266–277) also give tables of saturated vapor pressure over water both in mb and mm Hg. Or one can get values from Monteith (1973, pp. 222–223) or Monteith and Unsworth (1990, p. 269, 2008, p. 397, and 2013, p. 377). Monteith (1973) gives values in mb, and Monteith and Unsworth (1990, 2008, and 2013) give values in kPa, for saturation vapor pressure at temperatures ranging from −5 to 45 °C. Our method is simple. All we need is Eqn (18.5) and Table 94 to determine $e$, RH, and VPD.

### 18.5.1 Sample Problem

Assume that the dry-bulb temperature is 27.2 °C and the wet-bulb temperature is 23.9 °C. Find $e$, RH, VPD, and dewpoint temperature ($T_{\text{dewpoint}}$). Let $\gamma = 0.66/°\text{C}$.

*Solution*: From Table 94 in List (1951), we find at 27.2 °C, $e^{\text{o}} = 36.070$ mb ($e^{\text{o}}$ = saturated vapor pressure at the dry-bulb temperature); at 23.9 °C, $e^{\text{o}}_{\text{w}} =$ 29.652 mb ($e^{\text{o}}_{\text{w}}$ = saturated vapor pressure at wet-bulb temperature).

Putting the known values in Eqn (18.5), we get:

$$e = 29.652 - [(0.66/°\text{C})\ (27.2\ °\text{C} - 23.9\ °\text{C})] = 27.474\ \text{mb}.$$

$$\text{RH} = e/e^{\text{o}} = 27.474\ \text{mb}/36.070\ \text{mb} = 0.76\%\ \text{or}\ 76\%.$$

$$\text{VPD} = e^{\text{o}} - e = 36.070\ \text{mb} - 27.474\ \text{mb} = 8.596\ \text{mb}.$$

$$T_{\text{dewpoint}} = 22.6\ °\text{C}.$$

(Read Table 94 backwards for dewpoint temperature; temperature for saturated vapor pressure of 27.474 mb = 22.6 °C.)

## 18.6 CALIBRATION

Each thermocouple psychrometer is calibrated to yield an answer in units such as bars, megapascals, or atmospheres. Calibration solutions are often NaCl because water potentials of sodium-chloride solutions at different molalities have been published by Lang (1967) and have been reproduced (e.g., see Barrs, 1968, p. 288; Brown and van Haveren, 1972, pp. 304–305). A table of water potentials of potassium-chloride solutions also has been published (Rawlins and Campbell, 1986). Care must be taken that the filter paper soaked with the salt solution is exposed in the same way as subsequent samples to minimize effects of changed geometry (Barrs, 1968, p. 294).

The calibrating solution is put on filter paper in the thermocouple psychrometer chamber and the sample is equilibrated. Solutions take less time for equilibration than do plant samples; a solution may take an hour or less for equilibration, depending upon the concentration. After equilibration, a cooling current (e.g., 3 mA for 15 s) is passed through the thermocouple psychrometer. A microvoltmeter is used to measure the microvolt output of the different salt solutions. Salt solutions varying from 0.05 molal NaCl (−2.3 bars at 25 °C) to 1 molal NaCl (−46.4 bars at 25 °C) cover the range of interest when measuring plant-water potential. Most plants are severely wilted well above −46.4 bars. After calibration, the plant tissue is put in the chamber, using the same geometry for the sample as was used for the filter paper. The tissue is equilibrated. This usually takes 2–3 h. A cooling current again is passed through the thermocouple psychrometer, and the microvolt output is recorded. From the calibration curve, the water potential of the tissue is determined.

## 18.7 IMPORTANCE OF ISOTHERMAL CONDITIONS WHEN MAKING MEASUREMENTS

The measurements of plant-water potential made with thermocouples must be done under isothermal conditions. Rawlins and Dalton (1967) (summarized by Savage and Cass (1984)) point out four ways in which temperature affects the measurements:

1. Through the relationship between water potential and relative humidity (Eqn (18.1));
2. Through the temperature dependence of the relationship between wet-bulb depression and vapor pressure (Eqn (18.5));
3. Through differences in temperature between the sensing junction of the thermocouple and the sample (arising, for example, from respiration by the tissue);
4. Through changes of temperature within the cavity formed by the thermocouple psychrometer and sample, which will alter the relative humidity of the air in the cavity, if water vapor cannot be exchanged with the surrounding system.

In the first two cases (temperature dependence of water potential on relative humidity and temperature dependence of wet-bulb depression on relative humidity), the errors are relatively small, and are about 0.3%/°C and 2%/°C, respectively (Rawlins and Dalton, 1967). These errors can be reduced by following suitable calibration procedures (Savage and Cass, 1984). Heat-of-respiration effects are corrected by reading the psychrometer with its free junction first dry and then wet (Barrs, 1968, pp. 302–303 and 311–312). By using thermocouple walls with adequate conductivity, temperature effects due to number 4 above can be minimized and will not be significant (Rawlins and Dalton, 1967). If one cannot take readings at a constant temperature, Comstock (2000) tells how to convert readings made under variable temperature conditions to equivalent readings expected if measured at 25 °C.

There are several other sources of error, in addition to those caused by temperature. They include resistance to diffusion of water vapor into or out of a leaf, adsorption of water on the walls of the container, effects of excision of leaves from plants, and surface contamination. Errors resulting from low tissue permeability are probably negligible, unless leaves are heavily cutinized (Barrs, 1968, p. 311). Adsorption errors can be minimized by using Teflon for the sample container.

Cut-edge effects can be decreased by using samples with a small cut-edge-to-volume ratio (Barrs, 1968, p. 307—308; Nelsen et al., 1978). Extraneous dust and soil can be easily washed off. But water potential apparently cannot be measured reliably in salt-extruding species such as cotton (Barrs, 1968, p. 309).

## 18.8 TYPES OF THERMOCOUPLE PSYCHROMETERS

Four types of instruments with thermocouples are in use to measure water potential of plants:

1. Isopiestic thermocouple psychrometer (Boyer, 1972a,b) (Figure 3) in which solutions of varying concentrations are put manually on the wet junction of the thermocouple psychrometer. Boyer (1972a) uses sucrose solutions (p. 53, legend to his Figure 18.3). The isopiestic solution is the solution that has the same vapor pressure

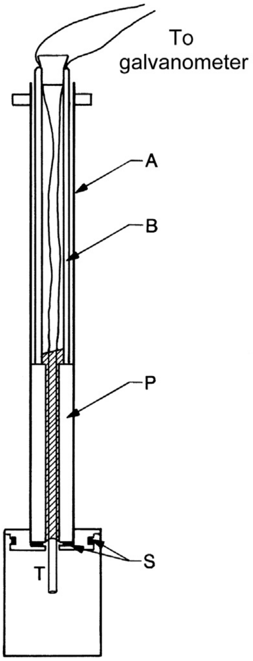

**FIGURE 18.3** Thermocouple for making isopiestic determinations. The psychrometer chamber and barrel are made of brass and are submerged in a constant-temperature water bath. Key to symbols: barrel, A; Plexiglas tube, B; plunger heat sink, P; diagrammatic representation of O-ring seal (coated with stopcock grease) for chamber and seal of stopcock grease for plunger, S; thermocouple with ring junction, T. *From Boyer (1972). Reprinted by permission of the Utah Agricultural Experiment Station.*

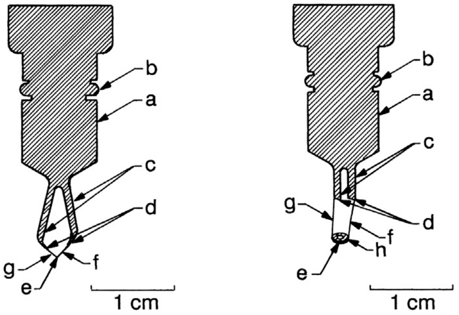

**FIGURE 18.4** *Left*, Silhouette of Spanner-type thermocouple psychrometer; *Right*, silhouette of Richards-and-Ogata-type thermocouple psychrometer. Symbols: a, brass mount; b, O-ring seal; c, twin core, PVC-covered copper flex, bared in this region; d, reference junction; e, free junction; f, chromel-P 0.001 in (0.0254 mm) diameter; g, constantan 0.001 inch (0.0254 mm) diameter; h, silver cylinder. *From* Barrs (1968). *Reprinted by permission of Academic Press.*

as that of the tissue and produces no thermocouple output (the "null point").

2. The Peltier thermocouple psychrometer (Figure 18.4, left) in which the wet junction is cooled, using the Peltier effect, to the dewpoint temperature. The junction then quickly rises to the wet-bulb temperature. This thermocouple psychrometer is also called the Spanner thermocouple psychrometer, named after Spanner (1951), who described the instrument. The degree of cooling is a function of the water potential of the tissue.
3. The thermocouple psychrometer in which a drop of water is put manually on the wet junction (Figure 18.4, right; Figure 18.1, right), instead of having a cooling current form the drop of water, as is done with the Peltier thermocouple psychrometer. This instrument is known as the Richards-and-Ogata thermocouple psychrometer or just the Richards thermocouple psychrometer, named after Richards and Ogata (1958), who developed the psychrometer. As with the Spanner thermocouple psychrometer, the degree of cooling is a function of the water potential of the tissue.

   The Richards-and-Ogata thermocouple psychrometer is similar to the isopiestic one in that both require a liquid to be placed on the wet junction. The liquid is sucrose in Boyer's isopiestic method and water in the Richards-and-Ogata thermocouple psychrometer.
4. The dewpoint hygrometer (Neumann and Thurtell, 1972) (Figure 18.5) in which the wet junction is cooled to the dewpoint and stays at the dewpoint for the measurement. This method uses the Peltier effect to cool the wet junction, but differs from the Peltier thermocouple psychrometer in that it detects the dewpoint

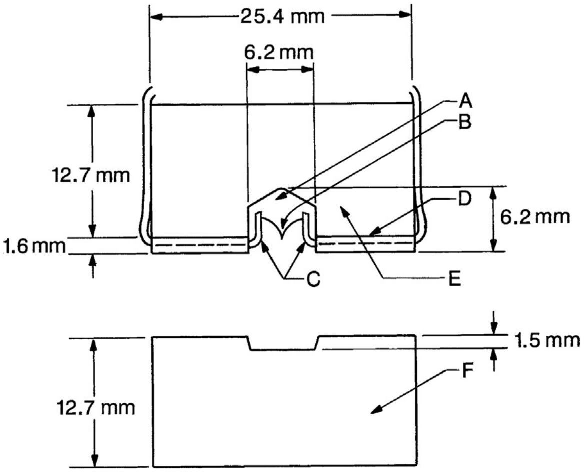

**FIGURE 18.5** Cross-section view of leaf hygrometer. A, cavity; B, thermocouple; C, posts supporting thermocouple; D, faceplate; E, cavity containing section; F, base plate. *From Neumann and Thurtell, 1972. Reprinted by permission of the Utah Agricultural Experiment Station.*

depression rather than the wet-bulb depression (Neumann and Thurtell, 1972). Neumann and Thurtell (1972) reported that a dewpoint measurement is preferable to a wet-bulb measurement in determination of water potential, because with a dewpoint measurement, no net water exchange occurs at the wet junction, allowing the measurement to be made without disturbing the vapor equilibrium within the chamber.

The dewpoint technique is similar to the isopiestic procedure (Boyer, 1972a,b). Both methods adjust the vapor pressure of the droplet on the wet junction until it is in equilibrium with the vapor within the chamber. In the isopiestic technique, the vapor pressure of the droplet is adjusted by changing the osmotic potential. With the dewpoint hygrometer, the vapor pressure is regulated by controlling the temperature of the droplet (Neumann and Thurtell, 1972).

Dewpoint hygrometers were designed to minimize the need for temperature control (Neumann and Thurtell, 1972; Campbell and Campbell, 1974). Internal temperature gradients between the sample and the thermocouple, however, must be small (Neumann and Thurtell, 1972; Shackel, 1984). Savage et al. (1981a, 1983a) reported that dewpoint hygrometers were less sensitive to temperature than thermocouple psychrometers, but the accuracy of dewpoint hygrometers was dependent upon the correct setting of the dewpoint cooling coefficient. Measurements made with thermocouple psychrometers (isopiestic, Spanner, Richards-and-Ogata) require careful temperature control (Rauscher and Smith, 1978; Bristow and de Jager, 1980; Slack and Riggle, 1980; Bruckler, 1984).

In situ hygrometers, which measure the water potential of intact plants, have been extensively studied (Savage et al., 1979, 1981a,b, 1982, 1983a; McBurney and Costigan, 1982; Savage and Cass, 1984). They can be used either in the psychrometric or dewpoint mode. Several designs have been described (Neumann and Thurtell, 1972; Michel, 1977, 1979; Brown and McDonough, 1977), including one that is commercially available (Campbell and Campbell, 1974) (Figures 18.6 and 18.7) and one that measures water potential of the soil (McAneney et al., 1979). The advantage of an in situ measurement is that tissue does not need to be excised to determine water potential, which avoids errors due to cutting (Campbell and Campbell, 1974; Baughn and Tanner, 1976b; Nelsen et al., 1978; Savage et al., 1984a).

Measurements obtained with in situ hygrometers have been compared to those obtained with other methods. Baughn and Tanner (1976a) found that readings of water potential of plants in a greenhouse, made with a pressure chamber, did not agree with those made with an in situ hygrometer. The pressure chamber gave a lower (drier) water potential than the hygrometer in the high potential range and a higher potential than the hygrometer in the dry potential range. Under field conditions, however,

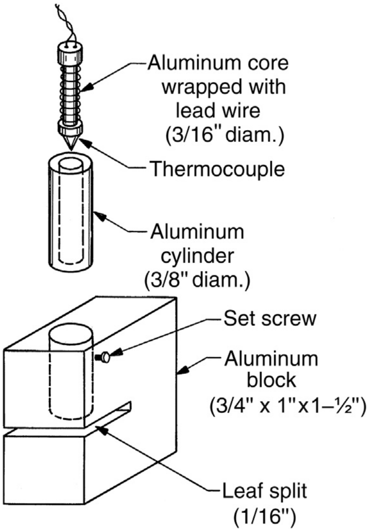
Aluminum core wrapped with lead wire (3/16" diam.)
Thermocouple
Aluminum cylinder (3/8" diam.)
Set screw
Aluminum block (3/4" x 1"x1–½")
Leaf split (1/16")

**FIGURE 18.6** Expanded view of in situ leaf hygrometer. *From Campbell, G.S., Campbell, M.D., 1974. American Society of Agronomy, Madison, Wisconsin. Reprinted by permission of the American Society of Agronomy.*

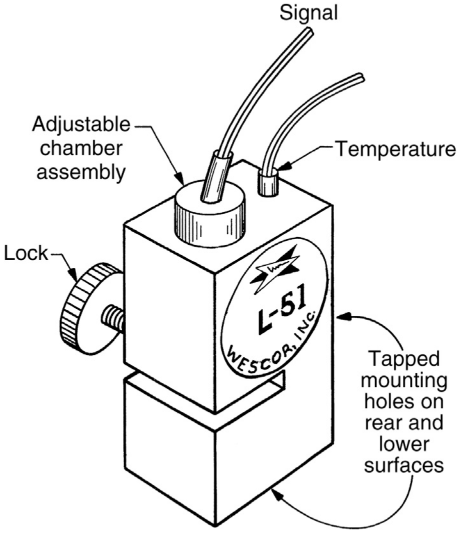
Signal
Adjustable chamber assembly
Temperature
Lock
L-51
WESCOR, INC.
Tapped mounting holes on rear and lower surfaces

**FIGURE 18.7** A commercially available in situ hygrometer. *From a figure in a brochure from Wescor, Inc., Logan, Utah. Reprinted by permission of Wescor, Inc., Logan, Utah.*

water potentials measured with a hygrometer were about 0.2 MPa (2 bars) greater (less negative) than those measured with a pressure chamber (Brown and Tanner, 1981). Brown and Tanner (1981) felt that the higher potential obtained with the hygrometer was caused by its covering the leaf and decreasing transpiration. In contrast, Savage et al. (1983b) found that the water potential of field-grown plants, obtained with an in situ hygrometer, agreed well with that measured by using a pressure chamber.

In all these experiments (Baughn and Tanner, 1976a; Brown and Tanner, 1981; Savage et al., 1983b), the cuticle of the leaf was abraded to obtain rapid vapor equilibrium between the leaf and the hygrometer. Savage et al. (1984b) showed that the water potential was dependent upon the amount of abrasion. Coarse abrasion resulted in deep cavities in the epidermis and large variability in readings of water potential. Turner et al. (1984) said that in situ hygrometers should not be used on plants with thick cuticles because, even after abrasion, the instruments gave inaccurate values of water potential.

Oosterhuis et al. (1983) compared measurements of water potential obtained by using three instruments: an in situ hygrometer, a pressure chamber, and screen-caged psychrometers, described by Brown and Bartos (1982) (Figure 18.8). They found that measurements made with the in situ hygrometer gave reliable, nondestructive measurements of water potential, if precautions were followed. These included thermal insulation of the aluminum housing, careful positioning of the hygrometer to

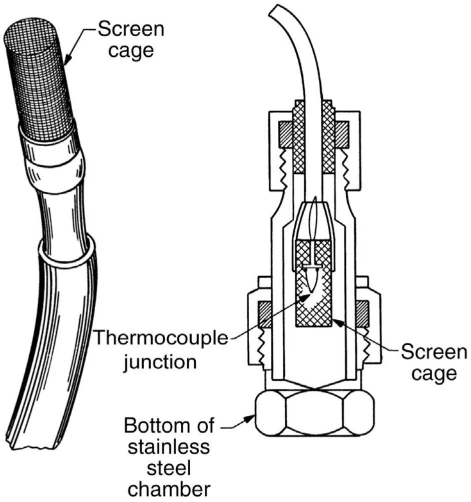

**FIGURE 18.8** Screen cage psychrometer. *From a figure in a brochure from J.R.D. Merrill Specialty Equipment, Logan, Utah.*

the leaf to minimize shading, and allowing adequate time for vapor equilibrium.

The Spanner and dewpoint methods are more popular than the isopiestic and Richards-and-Ogata methods. The isopiestic technique takes more time than the other three techniques. It is not readily adaptable to automatic measurements (Boyer, 1972a). The solutions must be put quickly on the wet junction to minimize evaporation, which changes their potentials. The chamber holding the thermocouple is perturbed each time a new solution is introduced into it. With the Spanner, Richards-and-Ogata, and dewpoint methods, the chamber remains closed after the sample is placed in it. Instruments commercially available utilize the Spanner or dewpoint methods (Figures 18.9 and 18.10). Boyer's laboratory used the isopiestic procedure (Matthews et al., 1984). The laboratory of Robert E. Sharp of the University of Missouri also has used the isopiestic procedure (personal communication, December 3, 1994).

All four techniques require precise electrical measurements and expensive equipment: for example, voltmeters that can read in the microvolt range. Measurements of water potential using thermocouple psychrometers were not possible until about the early 1960s, when microvoltmeters came on the market. Microvoltmeters are not necessary to determine plant-water potential, and it can be measured, using liquid-phase or vapor-phase techniques, with simple equipment (Barrs, 1968, pp. 263–285). Zyalalov (1977) described a method to measure water potential that used only salt solutions, capillary tubes, a weighing bottle with a greased ring to hold the capillary tubes, and a ruler. Learning how to take proper measurements with thermocouple psychrometers requires much

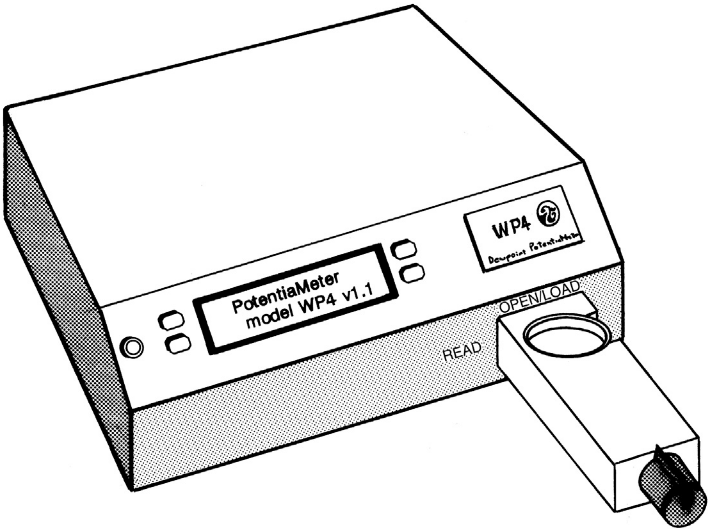
PotentiaMeter
model WP4 v1.1
WP4
Dewpoint PotentiaMeter
OPEN/LOAD
READ

**FIGURE 18.9** A dewpoint hygrometer. *From a figure in a brochure from Decagon, Pullman, Washington. Reprinted by permission of Decagon Devices, Inc., Pullman, Washington.*

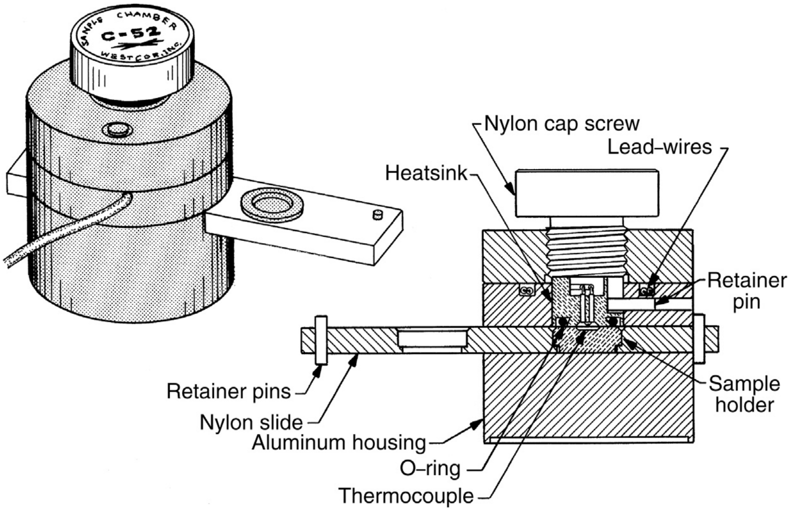
SAMPLE CHAMBER
C-52
WESCOR, INC.
Nylon cap screw
Lead–wires
Heatsink
Retainer pin
Sample holder
Retainer pins
Nylon slide
Aluminum housing
O–ring
Thermocouple

**FIGURE 18.10** An instrument that operates either as a hygrometer or psychrometer. It measures water potential of small samples in the laboratory or in the field without requiring a constant temperature bath. The large aluminum casing insulates the sample from temperature changes. A thermocouple in an internal chamber functions either as a psychrometer (wet-bulb depression method) or a hygrometer (dew-point depression method), depending on the type of readout equipment employed. *From a figure in a brochure from Wescor, Inc., Logan, Utah. Reprinted by permission of Wescor, Inc., Logan, Utah.*

training (several months) and skill. Many precautions are required for accurate measurements (Brown and Oosterhuis, 1992). Most people do not have the time or dedication to learn how to use thermocouple psychrometers, which is why the pressure chamber is the most popular method to measure water potential (see Chapter 19).

## 18.9 APPENDIX: BIOGRAPHY OF J.C.A. PELTIER

Jean Charles Athanase Peltier (1785–1845), French physicist, was born at Ham (Somme), France, on February 22, 1785. He was originally a clockmaker, but retired at about the age of 30 to devote himself to experimental and scientific observations. He is best known for his discovery (1834) that an electric current produces, according to direction, either heat or cold at the junction of two dissimilar metals in a circuit. This is called the Peltier effect. Peltier is also remembered for introducing the concept of electrostatic induction. His papers, which are numerous, are devoted in great part to atmospheric electricity, waterspouts, the polarization of skylight, the temperature of water in the spheroidal state, and the boiling point at great elevations. There are also a few papers devoted to points of natural history. He died in Paris on October 27, 1845 (McKie, 1971b).

## 18.10 APPENDIX: BIOGRAPHY OF JAMES PRESCOTT JOULE

James Prescott Joule (1818–1889) was an English physicist who established the principle of the interconvertibility of the various forms of energy (i.e., the first law of thermodynamics), and whose name was given to an energy unit, the "joule" (McKie, 1971a). He was born at Salford, Lancashire, on Christmas Eve, 1818, into a famous brewing family and spent some of his early years working for the firm (Hughes, 1989). Eventually his scientific interests predominated. The requirements of brewing technology and the accountancy needed to run a business helped to mold his scientific attitudes. A spinal weakness at birth turned him into a hunchback, and this shy and unassertive man was always sensitive about his public appearances (Hughes, 1989). Science at the time of Joule was changing from being the affair of the gentleman devotee to being the occupation of the full-time professional, ensconced in the university laboratory. Joule was in the first category. Almost all of his research was carried out in his laboratory at home and at his own expense. His reticence often meant that his discoveries were attributed to more verbose and flamboyant researchers. Joule's main interest lay in exact measurement and his special genius showed itself at its best in the invention of methods for obtaining greater accuracy in quantitative experiments. He was systematic and hardworking (Hughes, 1989).

Joule found that the heat generated by the flow of electricity was proportional to the electrical resistance multiplied by the square of the current. His experimental skills firmly established the law of conservation of energy. We take this law for granted now, but in Joule's time the complete conversion of heat into work or work into heat was not conceivable (Hughes, 1989).

Except for some instruction from John Dalton (1766–1844; English chemist and physicist and originator of the atomic theory), Joule was self-taught in science. He early realized the importance of accurate measurement. In a long series of experiments, he studied the quantitative relation between electrical, mechanical, and chemical effects, and was thus led to his great discovery. Joule announced in 1843 his determination of the amount of work required to produce a unit of heat. This is called the mechanical equivalent of heat. He used several methods to show this. The best-known method produced heat from friction in water by means of paddles rotating under the action of a falling weight. His paddle-wheel experiment, which showed that any fluid could be heated merely by agitating it, is famous. Because of this simple fact, the water that has dropped 49 m over Niagara Falls is 0.11 °C higher in temperature than the water at the top of the falls (Hughes, 1989). In 1853, with W. Thomson (later Lord Kelvin; see next section), he researched the work done in compressing gases and the thermal changes gases undergo when forced under pressure through small apertures. Joule's *Scientific Papers* were collected and published in two volumes by the Physical Society of London (1885–1887). Joule died at Sale, Cheshire, on October 11, 1889 (McKie, 1971a).

## 18.11 APPENDIX: BIOGRAPHY OF WILLIAM THOMSON, BARON KELVIN

Baron William Thomson Kelvin (1824–1907) was a British physicist, who discovered the second law of thermodynamics and was an inventor of telegraphic and scientific instruments. He was born in Belfast, Ireland, on June 26, 1824. He was first educated by his father, but at the age of 11 he entered the University of Glasgow, Scotland, where his father was professor of mathematics. Leaving Glasgow without taking a degree, in 1841 he entered Peterhouse, Cambridge, and in 1845 took his degree as second wrangler. Wranglers were mathematically brilliant boys who competed to get the top prize in mathematics at Cambridge University.

At that time (1845) there were few facilities for the study of experimental science in Great Britain. On his father's advice (Gooding, 1990), Thomson traveled to Paris to learn experimental methods in the laboratory of Henri Victor Regnault (1810–1878; French chemist and physicist noted for his work on the properties of gases), who was then engaged in his classical researches on the thermal properties of steam. In 1846 Thomson accepted the chair of natural philosophy at the University of Glasgow, which he filled for 53 years (Preece, 1971). Within four years of his appointment as professor at the age of 22, Thomson established the century's most successful applied physics laboratory, remembered for its compasses and precision instruments. It also was known for another innovation: using laboratory instruction to teach experimental practice and habits of accuracy and precision (Gooding, 1990). This was Britain's first teaching laboratory. It harnessed the skills of a large corps of students to produce intellectual capital, which Thomson invested in new ventures (Gooding, 1990).

In 1847 Thomson first met James Prescott Joule, whose views of the nature of heat strongly influenced Thomson's mind. In 1848 Thomson recognized −273 °C as absolute zero and proposed a new scale of temperature, which is independent of the properties of any particular thermometric substance. In 1851 Thomson presented to the Royal Society of Edinburgh a paper on the dynamical theory of heat. It was in this paper that the principle of the dissipation of energy, briefly summarized in the second law of thermodynamics, was first stated.

Although his contributions to thermodynamics may properly be regarded as his most important scientific work, it is in the field of electricity, especially in its application to submarine telegraphy, that Lord Kelvin is best known (Preece, 1971). The compass went through a process of complete reconstruction in his hands, a process that enabled both the permanent and the temporary magnetism of the ship to be readily compensated, while the weight of the 10-inch (25-cm) card (the dial of a compass) was reduced to one-seventeenth of that of the standard card previously in use (Preece, 1971). Thomson also invented his sounding apparatus, whereby soundings can be taken in shallows and in deep water. Thomson's tide gauge, tidal harmonic analyzer, and tide predictor are famous. He developed tables to simplify the method for determining the position of a ship at sea. The firm of Kelvin and White, in which he was a partner, was formed to manufacture his inventions (Preece, 1971).

In 1866 Thomson was knighted for helping to engineer that year the first successful trans-Atlantic cable (Gooding, 1990). He was raised to the peerage in 1892 with the title of Baron Kelvin of Largs. Thomson took the name Kelvin from the river that flows past the University of Glasgow. In 1890 he became president of the Royal Society and in 1902 received the Order of Merit. In 1904 he was elected chancellor of the University of Glasgow. Thomson published more than 300 original papers bearing upon nearly every branch of physical science. Thomson's extraordinary productivity shows how effectively his father taught him to expend his energy in highly efficient ways (Gooding, 1990), typical of the Scottish attitude of never wasting anything, even time. He wrote, "When you can measure what you are speaking about… you know something about it, and when you cannot measure it… your knowledge is of a meager and unsatisfactory kind…" (Gooding, 1990). Kelvin died on December 17, 1907, at his residence, Netherhall, near Largs, Scotland, and was buried in Westminster Abbey (Preece, 1971).

## References

Barrs, H.D., 1968. Determination of water deficits in plant tissues. In: Kozlowski, T.T. (Ed.), Water Deficits and Plant Growth, Development, Control, and Measurement, vol. 1. Academic Press, New York, pp. 235−368.

Baughn, J.W., Tanner, C.B., 1976a. Leaf water potential: comparison of pressure chamber and *in situ* hygrometer on five herbaceous species. Crop Sci. 16, 181−184.

Baughn, J.W., Tanner, C.B., 1976b. Excision effects on leaf water potential of five herbaceous species. Crop Sci. 16, 184−190.

Boyer, J.S., 1972a. Use of isopiestic technique in thermocouple psychrometry. I. Theory. In: Brown, R.W., van Haveren, B.P. (Eds.), Psychrometry in Water Relations Research. Utah Agricultural Experiment Station, Logan, Utah, pp. 51−55.

Boyer, J.S., 1972b. Use of isopiestic technique in thermocouple psychrometry. II. Construction. In: Brown, R.W., van Haveren, B.P. (Eds.), Psychrometry in Water Relations Research. Utah Agricultural Experiment Station, Logan, Utah, pp. 98−102.

Bristow, K.L., de Jager, J.M., 1980. Leaf water potential measurements using a strip chart recorder with the leaf psychrometer. Agric. Meteorol. 22, 149−152.

Brown, P.W., Tanner, C.B., 1981. Alfalfa water potential measurement: a comparison of the pressure chamber and leaf dewpoint hygrometer. Crop Sci. 21, 240−244.

Brown, R.W., van Haveren, B.P. (Eds.), 1972. Psychrometry in Water Relations Research. Utah Agr Exp Sta, Logan, Utah.

Brown, R.W., McDonough, W.T., 1977. Thermocouple psychrometer for *in situ* leaf water potential determinations. Plant Soil 48, 5−10.

Brown, R.W., Bartos, D.L., 1982. A Calibration Model for Screen-Caged Peltier Thermocouple Psychrometers. United States Department of Agriculture, Forest Service Research Paper INT-293. Intermountain Forest and Range Experiment Station, Ogden, Utah.

Brown, R.W., Oosterhuis, D.M., 1992. Measuring plant and soil water potentials with thermocouple psychrometers: some concerns. Agron. J. 84, 78−86.

Bruckler, L., 1984. Utilisation des micropsychrometres pour la mesure du potential hydrique du sol en laboratoire et *in situ*. Agronomie 4, 171−182 (In French, English sum.).

Buck, A.L., 1981. New equation for computing vapor pressure and enhancement factor. J. Appl. Meteorol. 20, 1527−1532.

Campbell, G.S., Campbell, M.D., 1974. Evaluation of a thermocouple hygrometer for measuring leaf water potential *in situ*. Agron. J. 66, 24−27.

Comstock, J.P., 2000. Correction of thermocouple psychrometer readings for the interaction of temperature and actual water potential. Crop Sci. 40, 709−712.

Gooding, D., 1990. First lord of British science. Book review of "Energy and Empire: A Biographical Study of Lord Kelvin" by Crosbie, S., Norton Wise, M. Cambridge University Press, 1989, 866 pp. Nature 344, 900.

Ham, J.M., 2005. Useful equations and tables in micrometeorology. In: Hatfield, J.L., Baker, J.M. (Eds.), Micrometeorology in Agricultural Systems. American Society of

Agronomy, Soil Science Society of America, Crop Science Society of America, Madison, Wisconsin, pp. 533–560.

Haynes, W.M. (Ed.), 2013. Handbook of Chemistry and Physics, ninety-fourth ed. CRC Press, Boca Raton, Florida.

Hughes, D.W., 1989. The northern light. Book review of "James Joule: A Biography" by Donald, S.L. Cardwell. Manchester University Press, 1989, 333 pp. Nature 340, 686.

Lang, A.R.G., 1967. Osmotic coefficients and water potentials of sodium chloride solutions from 0 to 40°C. Aust. J. Chem. 20, 2017–2023.

List, R.J., 1951. Hygrometric and Psychrometric Tables. Smithsonian Misc. Collections. Smithsonian Meteorological Tables, sixth rev ed., vol. 114. Smithsonian Institution, Washington, DC.

Matthews, M.A., van Volkenburgh, E., Boyer, J.S., 1984. Acclimation of leaf growth to low water potentials in sunflower. Plant Cell Environ. 7, 199–206.

McAneney, K.J., Tanner, C.B., Gardner, W.R., 1979. An *in situ* dewpoint hygrometer for soil water potential measurement. Soil Sci. Soc. Am. J. 43, 641–645.

McBurney, T., Costigan, P.A., 1982. Measurement of stem water potential of young plants using a hygrometer attached to the stem. J. Exp. Bot. 33, 426–431.

McKie, D., 1971a. Joule, James Prescott. Encyclopaedia Britannica 13, 93.

McKie, D., 1971b. Peltier, Jean Charles Athanase. Encyclopaedia Britannica 17, 542.

Michel, B.E., 1977. A miniature stem thermocouple hygrometer. Plant Physiol. 60, 645–647.

Michel, B.E., 1979. Correction of thermal gradient errors in stem thermocouple hygrometers. Plant Physiol. 63, 221–224.

Monteith, J.L., 1973. Principles of Environmental Physics. American Elsevier, New York.

Monteith, J.L., Unsworth, M.H., 1990. Principles of Environmental Physics, second ed. Edward Arnold, London.

Monteith, J.L., Unsworth, M.H., 2008. Principles of Environmental Physics, third ed. Elsevier, Amsterdam.

Monteith, J.L., Unsworth, M.H., 2013. Principles of Environmental Physics, fourth ed. Elsevier, Amsterdam.

Murray, F.W., 1967. On the computation of saturation vapor pressure. J. Appl. Meteorol. 6, 203–204.

Nelsen, C.E., Safir, G.R., Hanson, A.D., 1978. Water potential in excised leaf tissue. Comparison of a commercial dewpoint hygrometer and a thermocouple psychrometer on soybean, wheat, and barley. Plant Physiol. 61, 131–133.

Neumann, H.H., Thurtell, G.W., 1972. A Peltier cooled thermocouple dewpoint hygrometer for *in situ* measurement of water potentials. In: Brown, R.W., van Haveren, B.P. (Eds.), Psychrometry in Water Relations Research. Utah Agricultural Experiment Station, Logan, Utah, pp. 103–112.

Ong, N.P., 2008. Recipe for spin currents. Nature 455, 741–742.

Oosterhuis, D.M., Savage, M.J., Walker, S., 1983. Field use of *in situ* leaf psychrometers for monitoring water potential of a soybean crop. Field Crops Res. 7, 237–248.

Patterson, E.C., 1988. Eponyms. Temperature – why kelvin? Am. Sci. 76, 103.

Preece, W.E. (General Ed.), 1971. Kelvin, William Thomson. Encyclopaedia Britannica 13, 275.

Rauscher, H.M., Smith, D.W., 1978. A comparison of two water potential predictors for use in plant and soil thermocouple psychrometry. Plant Soil 49, 679–683.

Rawlins, S.L., 1972. Theory of thermocouple psychrometers for measuring plant and soil water potential. In: Brown, R.W., van Haveren, B.P. (Eds.), Psychrometry in Water Relations Research. Utah Agricultural Experiment Station, Logan, Utah, pp. 43–50.

Rawlins, S.L., Campbell, G.S., 1986. Water potential: thermocouple psychrometry. In: Klute, A. (Ed.), Methods of Soil Analysis. Part 1. Physical and Mineralogical Methods, second ed. American Society of Agronomy, Soil Science of America, Madison, Wisconsin, pp. 597–618.

Rawlins, S.L., Dalton, F.N., 1967. Psychrometric measurement of soil water potential without precise temperature control. Soil Sci. Soc. Am. Proc. 31, 297–301.

Richards, L.A., Ogata, G., 1958. Thermocouple for vapor pressure measurements in biological and soil systems at high humidity. Science 128, 1089–1090.

Savage, M.J., Cass, A., 1984. Measurement of water potential using *in situ* thermocouple hygrometers. Adv. Agron. 37, 73–126.

Savage, M.J., de Jager, J.M., Cass, A., 1979. Calibration of thermocouple hygrometers using the psychrometric technique. Agrochemophysica 11, 51–56.

Savage, M.J., Cass, A., de Jager, J.M., 1981a. Calibration of thermocouple hygrometers. Irrigation Sci. 2, 113–125.

Savage, M.J., Cass, A., de Jager, J.M., 1981b. Measurement of water potential using thermocouple hygrometers. S. Afr. J. Sci. 77, 24–27.

Savage, M.J., Cass, A., de Jager, J.M., 1982. An accurate temperature correction model for thermocouple hygrometers. Plant Physiol. 69, 526–530.

Savage, M.J., Cass, A., de Jager, J.M., 1983a. Statistical assessment of some errors in thermocouple hygrometric water potential measurement. Agric. Meteorol. 30, 83–97.

Savage, M.J., Wiebe, H.H., Cass, A., 1983b. *In situ* field measurement of leaf water potential using thermocouple psychrometers. Plant Physiol. 73, 609–613.

Savage, M.J., Cass, A., Wiebe, H.H., 1984a. Effect of excision on leaf water potential. J. Exp. Bot. 35, 204–208.

Savage, M.J., Wiebe, H.H., Cass, A., 1984b. Effect of cuticular abrasion on thermocouple psychrometric *in situ* measurement of leaf water potential. J. Exp. Bot. 35, 36–42.

Schaum, D., 1961. Theory and Problems of College Physics, sixth ed. Schaum, New York.

Shackel, K.A., 1984. Theoretical and experimental errors for *in situ* measurements of plant water potential. Plant Physiol. 75, 766–722.

Shortley, G., Williams, D., 1971. Elements of Physics, fifth ed. Prentice-Hall, Englewood Cliffs, New Jersey.

Slack, D.C., Riggle, F.R., 1980. Effects of Joule heating on thermocouple psychrometer water potential determinations. Trans. Am. Soc. Agr. Eng. 23, 877–833.

Spanner, D.C., 1951. The Peltier effect and its use in the measurement of suction pressure. J. Exp. Bot. 11, 145–168.

Tetens, O., 1930. Über einige meteorologische Begriffe. Z. Geophys. 6, 297–309.

Turner, N.C., Spurway, R.A., Schulze, E.-D., 1984. Comparison of water potentials measured by *in situ* psychrometry and pressure chamber in morphologically different species. Plant Physiol. 74, 316–319.

Uchida, K., Takahashi, S., Harii, K., Ieda, J., Koshibae, W., Ando, K., Maekawa, S., Saitoh, E., 2008. Observation of the spin Seebeck effect. Nature 455, 778–781.

van Haveren, B.P., Brown, R.W., 1972. The properties and behavior of water in the soil-plant-atmosphere continuum. In: Brown, R.W., van Haveren, B.P. (Eds.), Psychrometry in Water Relations Research. Utah Agricultural Experiment Station, Logan, Utah, pp. 1–27.

Weast, R.C. (Ed.), 1964. Handbook of Chemistry and Physics, forty-fifth edition. Chemical Rubber Co, Cleveland, Ohio.

Webster's New World Dictionary of the American Language, 1959. College Ed., World Publishing, Cleveland and New York.

Zyalalov, A.A., 1977. Indices of the state of water and determination of depression of the water chemical potential. Soviet Plant Physiol. 24 (Part 2, No. 6), 1004–1007.

CHAPTER

# 19

# Pressure Chambers

The pressure chamber described by Scholander and colleagues (1964, 1965) is the most popular method used to measure water potential of plants. (For a biography of Scholander, see the Appendix, Section 19.5.) The method consists of increasing the pressure around a leafy shoot until sap from the xylem appears at the cut end of the shoot, which extends outside of the chamber and is exposed to atmospheric pressure (Figures 19.1 and 19.2). The pressure necessary to retain this condition represents the negative pressure existing in the intact stem. It is felt that the amount of pressure necessary to force water out of the leaf cells into the xylem is a function of the water potential of the leaf cells (Boyer, 1967).

## 19.1 COMPARISON OF MEASUREMENTS MADE WITH THE PRESSURE CHAMBER AND THE THERMOCOUPLE PSYCHROMETER

For accurate measurements, one should compare measurements made with a thermocouple psychrometer with those made with a pressure

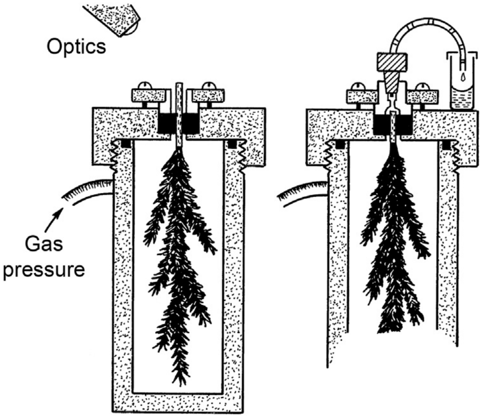

**FIGURE 19.1** Pressure chamber for measurement of sap pressure in the xylem of a twig. Left: direct observation; right: stepwise sap extrusion and pressure measurement to obtain a pressure–volume curve. *Reprinted with permission from Scholander et al. (1965), American Association for the Advancement of Science.*

http://dx.doi.org/10.1016/B978-0-12-420022-7.00019-7

Copyright © 2014 Elsevier Inc. All rights reserved.

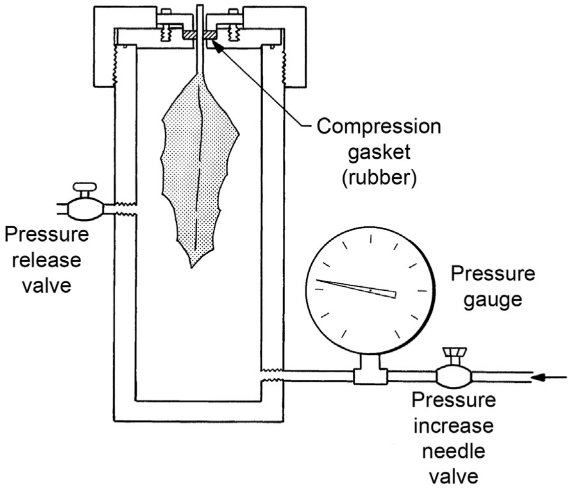

**FIGURE 19.2** Diagrammatic cross-section through a pressure chamber for measurement of leaf water potential by pressure equilibration. *From Kramer (1983). Reprinted by permission of Academic Press.*

chamber before assuming that the pressure chamber is giving valid measurements of water potential. Because the thermocouple-psychrometer method is based on sound physics using the Kelvin equation (Rawlins, 1972), measurements made with thermocouple psychrometers are the standard ones. But relatively few comparisons exist in the literature. Most people take for granted that the pressure chamber is giving an accurate measurement of water potential and most people use the pressure chamber when measuring plant water potential. It has the advantages of relative simplicity and provision of pressure–volume curves to estimate osmotic potential and turgor potential (see Chapter 17).

Boyer (1967) was one of the first to compare measurements made with thermocouple psychrometers with those made with a pressure chamber. (For a biography of Boyer, see the Appendix, Section 19.6.) He estimated leaf water potentials from the sum of the balancing pressure measured with a pressure chamber and the osmotic potential of the xylem sap in leafy shoots or leaves of yew (*Taxus cuspidata* Sieb. & Zucc.), rhododendron (*Rhododendron roseum* Rehd.), and sunflower (*Helianthus annuus* L.). Measurements made with the pressure chamber were within ±2 bar of the psychrometric measurements with sunflower and yew (Figures 19.3 and 19.4). In rhododendron, water potentials measured with the pressure chamber plus xylem sap were 2.5 bar less negative to 4 bar more negative than the psychrometric measurements (Figure 19.5). As we shall see when we discuss the ascent of sap in plants (Chapter 20), xylem sap is very dilute. Boyer (1967) found xylem sap in yew, rhododendron, and

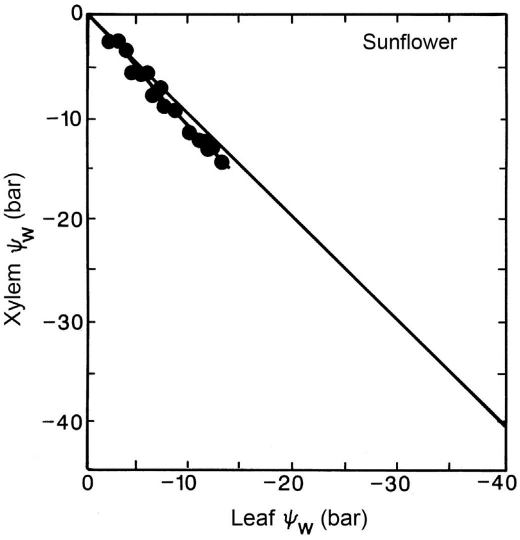

**FIGURE 19.3** Xylem and leaf water potentials in sunflower. The equipotential values are represented by the diagonal line. Each point represents a single determination. *From Boyer (1967), American Society of Plant Physiologists. Reprinted by permission of the American Society of Plant Biologists, Rockville, Maryland.*

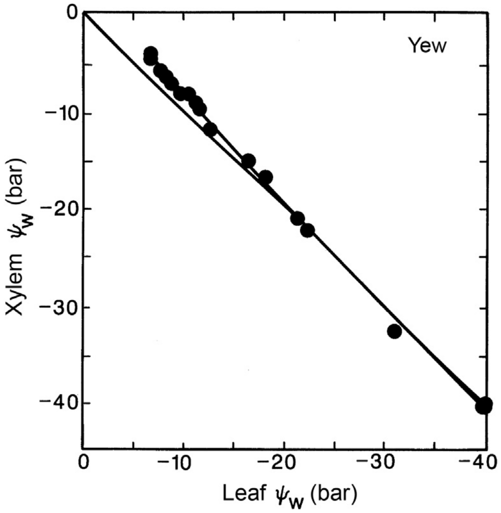

**FIGURE 19.4** Xylem and leaf water potentials in yew. The equipotential values are represented by the diagonal line. Each point represents a single determination. *From Boyer (1967), American Society of Plant Physiologists. Reprinted by permission of the American Society of Plant Biologists, Rockville, Maryland.*

sunflower to have a solute potential of about −0.5 bar (Figure 19.6). Only when plants got very stressed (e.g., when the rhododendron leaves were at −30 bar) was the xylem sap about −2.0 bar. So the solute potential of the sap was usually within the error of comparison (±2 bar). When making measurements with pressure chambers, the osmotic potential of the xylem sap is ignored, and it is assumed that the balancing pressure is the water potential of the leaves.

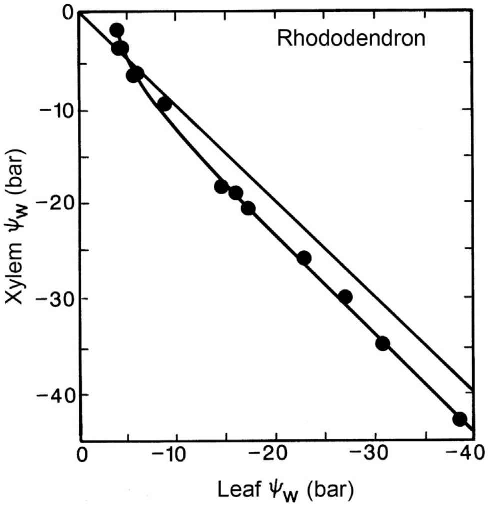

**FIGURE 19.5** Xylem and leaf water potentials in rhododendron. The equipotential values are represented by the diagonal line. Each point represents a single determination. *From Boyer (1967), American Society of Plant Physiologists. Reprinted by permission of the American Society of Plant Biologists, Rockville, Maryland.*

Gandar and Tanner (1975) compared potato (*Solanum tuberosum* L.) leaf and tuber water potentials measured with both a pressure chamber and thermocouple psychrometers. They used soil psychrometers to measure the tuber water potential. They bored holes in the tuber and put the soil psychrometer in the hole. For leaves drier than −3 bar, the pressure chamber gave estimates of water potential that were 0–3 bar drier than potentials measured using thermocouple psychrometers. Pressure chamber readings ranged ±2.5 bar from the psychrometric value for leaves wetter than −3 bar. The psychrometric measurement usually was drier than that obtained using the pressure chamber when leaves were sampled in the evening. With tubers, water potential measurements using the in situ soil psychrometers and the pressure chamber agreed to within 1 bar, except in tubers drier than −7 bar, in which there were discrepancies of ±2.5 bar. However, if the interval between psychrometer insertion and water potential measurement was longer than 24 h, serious errors arose in the psychrometer measurements, apparently from suberization of tissues surrounding the psychrometers that prevented vapor equilibrium.

## 19.2 ADVANTAGES AND DISADVANTAGES OF THE PRESSURE CHAMBER

The Scholander pressure chamber is commercially available (Figures 19.7–19.9), and it is widely used (Cochard et al., 2001) because of its many advantages. They include simplicity, comparative speed of measurement,

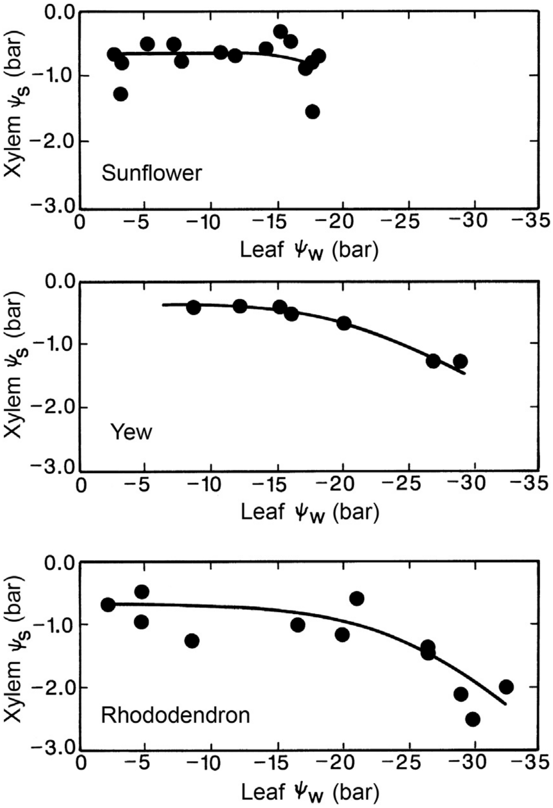

**FIGURE 19.6** Xylem osmotic potentials (xylem $\Psi_s$) measured at various leaf water potentials in sunflower, yew, and rhododendron. Each point represents a single determination. *From Boyer (1967), American Society of Plant Physiologists. Reprinted by permission of the American Society of Plant Biologists, Rockville, Maryland.*

and fair portability (Oosterhuis et al., 1983). Even though thermocouple psychrometers appear to provide more accurate measurements than pressure chambers (Millar, 1982) and are based on sound theory, they are not used widely, because they require patience and experience before meaningful data can be obtained. In addition, precise temperature control is needed.

However, care also is necessary to gather accurate readings with a pressure chamber. Samples must be protected against transpiration following excision. They must be measured immediately. In field experiments, the pressure chamber has to be protected against wind, so the exuded sap does not evaporate before a measurement can be recorded. When conditions are windy, the pressure chamber can be put in the open hatchback of a van. An operator can stand outside the van on the ground

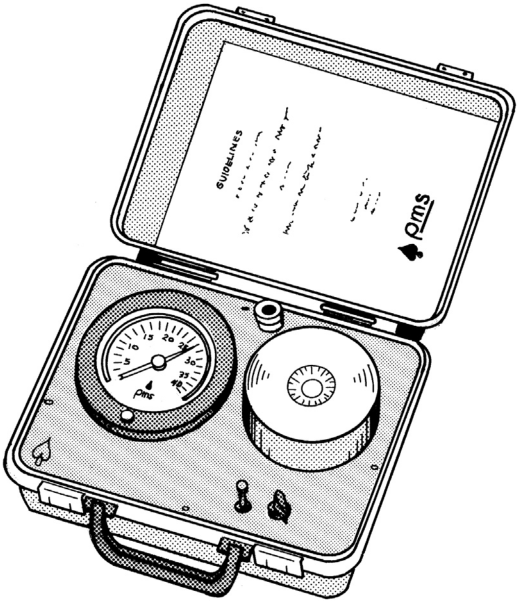
GUIDELINES
pms
5
10
15
20
25
30
35
40
pms

**FIGURE 19.7** A commercially available pressure chamber. The pressure chamber is designed for either laboratory or field use. A safety valve on the lug cover ensures that pressure can be applied to the chamber only when the cover is properly and completely secured. The gas tank is an accessory and is not shown. *From a PMS Instrument Company, Corvallis, Oregon, brochure. Reprinted by permission of PMS Instrument Company.*

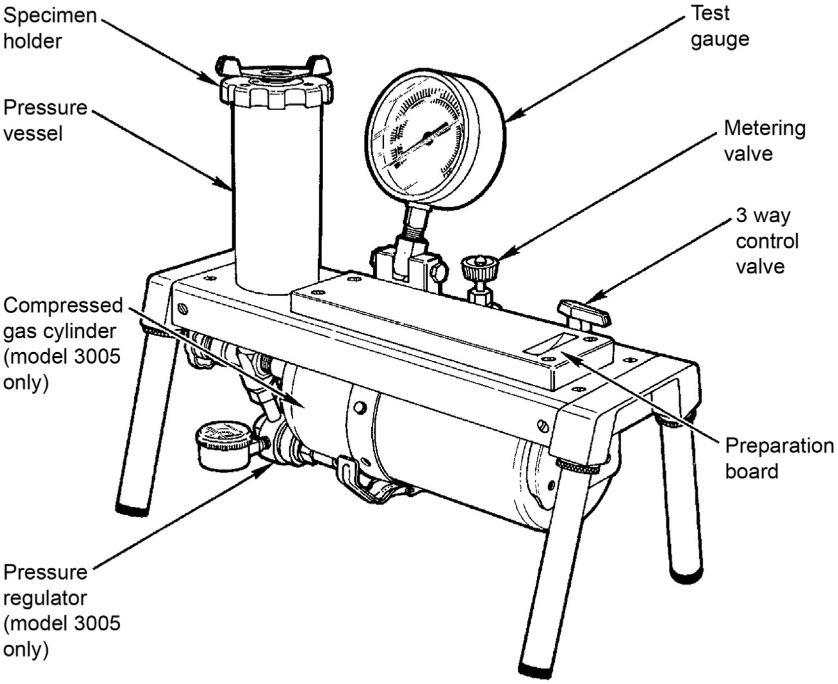
Specimen holder
Test gauge
Pressure vessel
Metering valve
3 way control valve
Compressed gas cylinder (model 3005 only)
Preparation board
Pressure regulator (model 3005 only)

**FIGURE 19.8** A commercially available pressure chamber, the Plant Water Status Console. A canister of gas is attached to the bottom of the hardwood base, making the unit self-contained. *Courtesy of Soilmoisture Equipment Corp., Santa Barbara, California.*

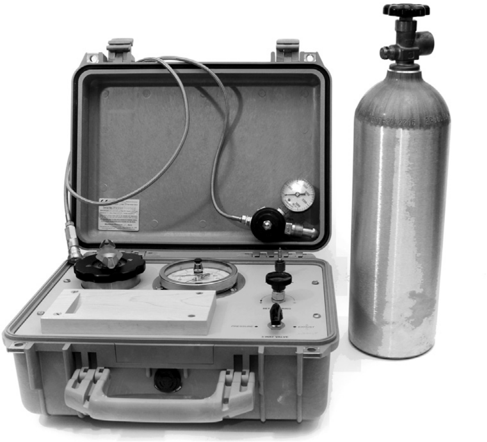

**FIGURE 19.9** A commercially available, portable pressure chamber made by Soilmoisture Equipment Corp., Santa Barbara, California. *Photograph courtesy of Marsha K. Landis, Graphic Designer, Kansas State University, Manhattan, Kansas.*

and use a magnifying glass to see the endpoint. The plant sample itself is out of the wind. If a large field is being sampled, "runners" carry the sample from the field to the pressure chamber, so a reading can be made within a matter of seconds after the stem has been cut. Sometimes samples are protected against water loss by putting them in a container with wet cheesecloth and then taking them to the pressure chamber. But the wet cheesecloth could provide water to the sample and result in an erroneous measurement.

Low pressurization rates must be used to avoid false endpoints (Tyree et al., 1978; Wenkert et al., 1978; Karlic and Richter, 1979; McCown and Wall, 1979; Turner and Long, 1980; Brown and Tanner, 1981; Leach et al., 1982). Brown and Tanner (1981) suggest that the pressurization rate should be 0.006 MPa/s (0.06 bar/s).

If the proper technique is used, measurements made with pressure chambers can agree with those made with thermocouple hygrometers (Faiz, 1983; Walker et al., 1983). Values for the flow of water through stems, obtained by applying pressure to plants in a pressure chamber, also agree with those obtained by applying vacuums to plants with vacuum pumps (Dryden and van Alfen, 1983).

The Scholander pressure chamber is not well suited to measurements of small plants such as grasses because a petiole must extend through the seal of the pressure chamber. Plants with tender tissues (e.g., new tillers on grasses) are easily damaged by the seal and cannot be used. "Telescoping" of inner leaves of grass tillers at high pressure is another problem. The inner leaves are pushed out of the seal by the high pressures in the chamber. Leaves of a substantial size must be sampled, and, if they exist in an experiment, the sampling results in rapid denudation of leaves. This is a problem in studies with limited plant material.

Large stems, like those of mature sunflower plants, cannot be measured, because commercially available pressure chambers do not have rubber grommets, which make the seal, wide enough to accommodate the large stems. There is an interest in exuding sap from plants such as sunflower in phytoremediation studies to determine if the pollutant has been taken up by the plant. If the stem is too big for the pressure chamber, the sap cannot be exuded.

Pressure chambers are heavy and cumbersome, not only because they require a heavy tank of high-pressure gas, but also because the equipment itself is heavy. The gas supply limits the number of measurements that can be made in the field. The use of high-pressure gas can be dangerous for two reasons: (1) If not noncombustible, it is a fire hazard; (2) Plants can blow out of the chamber and hit a person in the eye. The commercially available pressure chambers (Figures 19.7–19.9) use nitrogen ($N_2$) gas, which is noncombustible. One must always wear glasses or safety glasses when using a pressure chamber, in case the sample blows out of the chamber and hits the eye.

Even though a measurement with a pressure chamber is faster than with a thermocouple psychrometer, it still takes about 5 min per sample. Pressure chambers and the constant supply of gas are expensive. Relatively unskilled workers can take measurements with a pressure chamber, but some training is required for reliable readings.

## 19.3 HYDRAULIC PRESS

The hydraulic press operates on the same principle as the pressure chamber, yet overcomes some of the pressure chamber’s limitations (Campbell and Brewster, 1975). The press consists of a commercial 1.5 ton (1360 kg) hydraulic automobile jack modified to apply pressure through a thin rubber membrane covered with nylon (a lady’s stocking) to a leaf sample, which is observed through a 1.27 cm thick Plexiglas plate (Campbell and Brewster, 1975; Jones and Carabaly, 1980). The instrument applies pressure to a leaf and squeezes the leaf between the membrane and a Plexiglas plate. When the applied pressure equals the water potential, cell walls and intercellular spaces become saturated. The leaf color changes (becomes darker) at this pressure, so that the pressure then can be read on a dial gauge attached to the jack. The hydraulic press can be used not only with leaves but also stems, twigs, needles, and soil.

The hydraulic press used to be available commercially, but it no longer can be bought. However, it represents a type of instrument that is useful in soil–plant–water relations. It has several advantages. A variety of soils and plants can be measured, including tender leaves and tillers. It weighs only 5 kg. It is rugged and never breaks down. Only the nylon stocking needs to be replaced occasionally. No high-pressure gas is required. Measurements are fast (about 20 s per sample), and inexperienced workers also can use it.

The main disadvantage of the hydraulic press appears to be that it does not have a sound theoretical basis (Shayo-Ngowi and Campbell, 1980). It is also difficult to get precise readings. But, because of its advantages, the instrument deserves study by theoreticians and plant physiologists. What, for example, is the effect of pressure on leaf cells? Why can a leaf in the hydraulic press turn completely black under pressure and then immediately spring back to its normal green color and apparent turgidity once the pressure is released?

## 19.4 PUMP-UP PRESSURE CHAMBER

Around the year 2000, Plant Moisture Stress (PMS) Instrument Company in Corvallis, Oregon, introduced a new type of pressure chamber (Figure 19.10). It is different from the conventional gas chamber in that it does not require a source of compressed gas such as nitrogen, which can be dangerous to use, as noted in Section 19.2. The pressure required to take water-potential readings is created by pumping the instrument as one would a bicycle pump. The relatively small chamber allows the user to achieve about 0.5 bar (7.25 psi) pressure per stroke (Figure 19.11). The instrument is limited to 20 bar and is designed primarily for irrigation scheduling and monitoring, particularly for managing deficit irrigation. A picture of the instrument in use is shown by Goldhamer and Fereres (2001).

## 19.5 APPENDIX: BIOGRAPHY OF PER SCHOLANDER

Per Fredrik Scholander a physiologist, was born in Örebro, Sweden, on November 29, 1905, and he married in 1951 (American Men of Science, 1961). He got his M.D. degree in Oslo in 1932 and his PhD in botany in 1934. He was an instructor of anatomy in Oslo between 1932 and 1934 and was a research fellow in comparative physiology between 1932 and 1939. He moved to the United States and became a naturalized citizen. He was a research associate in respiratory physiology at Swarthmore College in Swarthmore, Pennsylvania, from 1939 to 1943. He was a Rockefeller fellow from 1939 to 1941 and a research biologist from 1946 to 1949. He was a major for the U.S. Army Air Force Research from 1943 to 1946, and during this time was chief physiologist test officer, Air Force Base, Eglin Field near Valparaiso, Florida (1943–1945), and an aviation physiologist at the aeromedical laboratory of Wright Field, Dayton, Ohio (1945–1946).

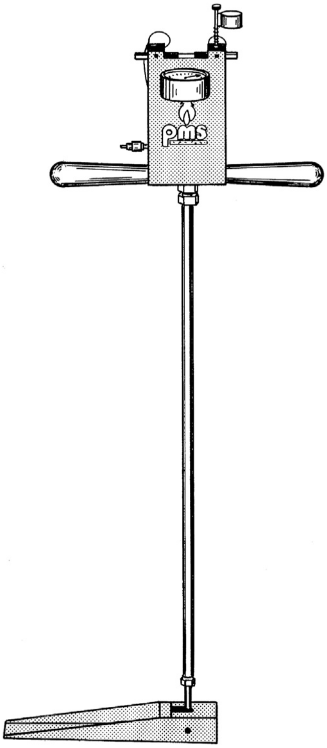

**FIGURE 19.10** Overall view of the pump-up pressure chamber, an alternative type of pressure chamber that does not use compressed gas. *From a PMS Instrument Company, Corvallis, Oregon, brochure. Reprinted by permission of PMS Instrument Company.*

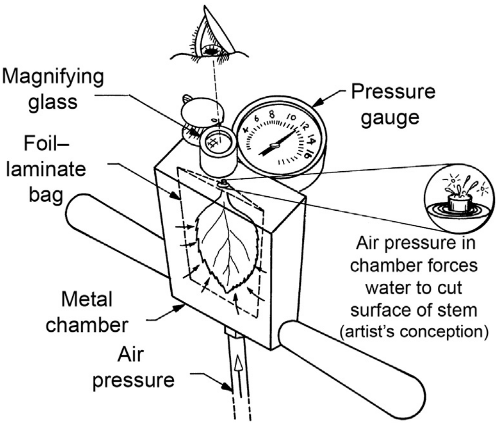
Magnifying glass
Pressure gauge
4
6
8
10
12
14
16
Foil–laminate bag
Air pressure in chamber forces water to cut surface of stem
(artist's conception)
Metal chamber
Air pressure

**FIGURE 19.11** A close-up of the top part of the pump-up pressure chamber. *From a PMS Instrument Company, Corvallis, Oregon, brochure. Reprinted by permission of PMS Instrument Company.*

From 1949 to 1951, he was a special research fellow in biochemistry at Harvard Medical School. He was a physiologist at the Oceanographic Institute in Woods Hole, Massachusetts, between 1952 and 1955. In 1955, he returned to Oslo, where he was a professor of physiology and director of the institute of zoophysiology until 1958. During this time (1955–1958) he also was an associate at the Oceanographic Institute in Woods Hole. In 1958, he became a professor of physiology at the Scripps Institute of Oceanography in La Jolla, California, where he spent the rest of his career.

His honors included being an investigator in the Arctic Research Laboratory of the Office of Naval Research in Alaska and Panama from 1947 to 1949. He was a member of the polar research committee of the National Academy of Sciences and participated in arctic and tropical expeditions. He received the Legion of Merit in 1946. He was a member of the National Academy of Sciences, American Association for the Advancement of Science, Physiology Society, Society of Zoologists, Society of Plant Physiologists, Society of General Physiology, American Academy, Arctic Institute of North America, Norwegian Academy of Science, Norwegian Physiology Society, and Botanical Association of Norway. His major research areas were arctic botany, respiration of diving, cold adaptation, microtechniques, gas secretion, water and gas transport in plants, and gas in glaciers (American Men of Science, 1961).

According to the *Newsletter of the American Society of Plant Physiologists* (vol. 7, No. 5, p. 4, October, 1980), Per Scholander died June 13, 1980, at the age of 74.

## 19.6 APPENDIX: BIOGRAPHY OF JOHN BOYER

John Strickland Boyer, a biochemist and biophysicist, was born May 1, 1937, in Cranford, New Jersey (Marquis Who's Who, 2000). He married Jean R. Matsunami and they have two children. In 1961 he got his master's degree at the University of Wisconsin under the direction of Gerald C. Gerloff, a mineral nutritionist, and in 1964 he obtained his PhD in botany at Duke University under the direction of Paul J. Kramer. The last book by Kramer was written jointly with Boyer (Kramer and Boyer, 1995). (Paul Kramer was born May 8, 1904, and died May 24, 1995.)

Boyer was visiting assistant professor of botany at Duke University from 1964 to 1965, and an assistant physiologist at the Connecticut Agricultural Experiment Station during 1965–1966. In 1966 he moved to the University of Illinois at Urbana and rose from assistant professor to professor of botany and agronomy. In 1978, he joined the U.S. Department of Agriculture (USDA) as a plant physiologist on the University of Illinois campus. Between 1984 and 1987 he was a professor at Texas A&M University. In 1987 he became the du Pont Professor of Marine Biochemistry and Biophysics at the University of Delaware. He retired from the faculty on June 30, 2005, and is now E.I. du Pont Professor of Biochemistry and Biophysics Emeritus at the University of Delaware (Chell, 2013).

He has won many recognitions. He is a member of the visitor committee, Carnegie Institute of Washington, Stanford University, and Harvard University. In 1983, he received the German Humboldt Senior Scientist award. He is a fellow of the Climate Laboratory (New Zealand), American Society of Agronomy, Crop Science Society of America, Australian National University, and the Japanese Society for the Promotion of Science. In 1990, he was elected member of the U.S. National Academy of Sciences. In 2005, he was elected a corresponding member of the Australian Academy of Science. He is a member of the American Society of Plant Physiologists (now called the American Society of Plant Biologists) and was president of the society in 1981—1982. He won the society's Shull award in 1977 (Marquis Who's Who, 2000).

## References

American Men of Science, 1961. A Biographical Directory. The Physical and Biological Sciences, tenth ed. Jaques Cattell Press, Tempe, Arizona, p. 3598.

Boyer, J.S., 1967. Leaf water potentials measured with a pressure chamber. Plant Physiol. 42, 133—137.

Brown, P.W., Tanner, C.B., 1981. Alfalfa water potential measurement: a comparison of the pressure chamber and leaf dew-point hygrometer. Crop Sci. 21, 240—244.

Campbell, G.S., Brewster, S.F., 1975. Leaf water potential, matric potential and soil water content measured with a simple hydraulic press. In: Paper Presented at the Western Regional Research Project W-67: "Quantification of Water-Soil Plant Relations for Efficient Water Use." Honolulu, Hawaii, January, 1975, p. 11 (Paper available from Dr. Gaylon S. Campbell, Decagon Devices, Inc., 950 NE Nelson Court, Pullman, WA 99163).

Chell, K., 2013. Policy Update. John Boyer Speaks at ASPB-Cosponsored Drought Briefing on Capitol Hill. American Society of Plant Biologists, Rockville, MD. ASPS News 40 (2), 11—12.

Cochard, H., Forestier, S., Améglio, T., 2001. A new validation of the Scholander pressure chamber technique based on stem diameter. J. Exp. Bot. 52, 1361—1365.

Dryden, P., van Alfen, N.K., 1983. Use of the pressure bomb for hydraulic conductance studies. J. Exp. Bot. 34, 523—528.

Faiz, S.M.A., 1983. Use of pressure bomb in the determination of soil water potential. Plant Soil 73, 257—264.

Gandar, P.W., Tanner, C.B., 1975. Comparison of methods for measuring leaf and tuber water potentials in potatoes. Am. Potato J. 52, 387—397.

Goldhamer, D.A., Fereres, E., 2001. Simplified tree water status measurements can aid almond irrigation. Calif. Agric. 55 (3), 32—37.

Jones, C.A., Carabaly, A., 1980. Estimation of leaf water potential in tropical grasses with the Campbell-Brewster hydraulic press. Trop. Agric. 57, 305—307.

Karlic, H., Richter, H., 1979. Storage of detached leaves and twigs without changes in water potential. New Phytol. 83, 379—384.

Kramer, P.J., 1983. Water Relations of Plants. Academic Press, New York.

Kramer, P.J., Boyer, J.S., 1995. Water Relations of Plants and Soils. Academic Press, San Diego.

Leach, J.E., Woodhead, T., Day, W., 1982. Bias in pressure chamber measurements of leaf water potential. Agric. Meteorol. 27, 257—263.

Marquis Who's Who, 2000. Who's Who in America, fifty-fourth ed. Marquis Who's Who, New Providence, New Jersey.

McCown, R.L., Wall, B.H., 1979. Improvement of pressure chamber measurements of two legumes by constriction of stems. Plant Soil 51, 447–451.

Millar, B.D., 1982. Accuracy and usefulness of psychrometer and pressure chamber for evaluating water potentials of *Pinus radiata* needles. Aust. J. Plant Physiol. 9, 499–507.

Oosterhuis, D.M., Savage, M.J., Walker, S., 1983. Field use of in situ leaf psychrometers for monitoring water potential of a soybean crop. Field Crops Res. 7, 237–248.

Rawlins, S.L., 1972. Theory of thermocouple psychrometers for measuring plant and soil water potential. In: Brown, R.W., van Haveren, B.P. (Eds.), Psychrometry in Water Relations Research. Utah Agricultural Experiment Station, Utah State University, Logan, pp. 43–50.

Scholander, P.F., Hammel, H.T., Hemmingsen, E.A., Bradstreet, E.D., 1964. Hydrostatic pressure and osmotic potential in leaves of mangroves and some other plants. Proc. Nat. Acad. Sci. 52, 119–125.

Scholander, P.R., Hammel, H.T., Bradstreet, E.D., Hemmingsen, E.A., 1965. Sap pressure in vascular plants. Science 148, 339–346.

Shay-Ngowi, A., Campbell, G.S., 1980. Measurement of matric potential in plant tissue with a hydraulic press. Agron. J. 72, 567–568.

Turner, N.C., Long, M.J., 1980. Errors arising from rapid water loss in the measurement of leaf water potential by the pressure chamber technique. Aust. J. Plant Physiol. 7, 527–537.

Tyree, M.T., MacGregor, M.E., Petrov, A., Upenieks, M.I., 1978. A comparison of systematic errors between the Richards and Hammel methods of measuring tissue–water relation parameters. Can. J. Bot. 56, 2153–2161.

Walker, S., Oosterhuis, D.M., Savage, M.J., 1983. Field use of screen-caged thermocouple psychrometers in sample chambers. Crop Sci. 23, 627–632.

Wenkert, W., Lemon, E.R., Sinclair, T.R., 1978. Changes in water potential during pressure bomb measurement. Agron. J. 70, 353–355.

## CHAPTER

## 20

# The Ascent of Water in Plants

The problem of the rise of water in tall plants is as old as the science of plant physiology. In this chapter, we consider the cohesion theory, which is the best formulation to explain how water can get to the top of tall trees and vines.

## 20.1 THE PROBLEM

Let us consider why it is hard for water to get to the top of trees. A suction pump can lift water only to the barometric height, which is the height that is supported by atmospheric pressure (1.0 atm) or 1033 cm (10.33 m; 33.89 ft) (Salisbury and Ross, 1978; p. 49). If a hose or pipe is sealed at one end and filled with water, and then placed in an upright position with the open end down and in water, atmospheric pressure will support the water column to 10.33 m, theoretically. At this height, the pressure equals the vapor pressure of water at its temperature. Above this height of 1033 cm, water turns to vapor. When the pressure is reduced in a column of water so that vapor forms or air bubbles appear (the air coming out of solution), the column is said to cavitate (Salisbury and Ross, 1978; p. 49). My father, Don Kirkham, and his students tried to see how far they could climb the outside back stairs of the Agronomy Building at the Iowa State University with a hose, closed end in hand and with the hose's bottom in a water bucket on the ground. The column of water in the hose collapsed before they climbed 10.33 m. This was probably because of impurities on the hose wall. Engineers cannot pull water up out of waterlogged mines more than about 9 m (Surridge, 2008).

## 20.2 HOW WATER GETS TO THE TOP OF TALL BUILDINGS AND ANIMALS

How does water get to the top of tall trees? The tallest tree in the world was thought to be a *Sequoia* (an evergreen tree) in California, and its height

http://dx.doi.org/10.1016/B978-0-12-420022-7.00020-3

Copyright © 2014 Elsevier Inc. All rights reserved.

was estimated to be 111.6 m (366.1 ft) (Salisbury and Ross, 1978; p. 49). In 2000, a tree 367.5 ft tall was discovered (National Geographic, 2000). Then, in the summer of 2006, the world's tallest tree to date, a coastal redwood, was discovered (Preston, 2006, 2008; Economist, 2007). It is 379.1 ft tall (115.5 m). Redwoods can reach 150 ft in $<100$ years (Bourne, 2009; unpaged fold-out between p. 38 and p. 39).

Let us first consider how water gets to the top of skyscrapers. Modern buildings in cities use electrical pumping systems to get water to high floors. But before electrical pumps were available, wooden tanks that hold water were used, and still are used, to raise water. People who live in a tall building and are not getting a good strong shower are probably too close to the holding tank (Weber, 1989). In those buildings in which the plumbing requires the help of gravity to create sufficient water pressure, a tank needs to be elevated at least 25 ft (762 cm) above a building's highest standpipe. One gets 1 lb/in$^2$ (0.06896 bars) of pressure for every 2.3 (70 cm) ft in height. In New York City, the skyline is dotted with $>10{,}000$ of these tanks, and they vary in size from 5000 to 50,000 gallons (19,000 to 190,000 L) and run from 12 to 20 ft (3.658–6.096 m) high. They have been in use since 1890. Tanks last for 60 years (Weber, 1989). To make a wooden tank, lumber is cut from yellow cedar from British Columbia or from California redwood. The people who replace the wooden tanks are highly trained and have a difficult and dangerous job getting the planks to great heights (National Public Radio, 2002).

Physicists who question how water can get to the top of trees point out that animals have pumps (hearts) that plants do not have. So let us consider how fluids get to the top of a giraffe, probably the tallest animal. An upright giraffe ought to suffer massive edema in its feet; moreover, when it lowers its head to drink, the blood should rush down into it and be unable to flow up again (Pedley, 1987). But pressure measurements in the giraffe reveal why neither of these things happens.

A countergravitational gradient of venous pressure ($P_v$) exists in the giraffe's neck. Measurements of the gravitational (or hydrostatic) gradient of pressure with height, in an upright animal 3.5 m tall, show that blood pressure in an artery in the head is as much as 110 mm Hg ($\sim$1.5 m $H_2O$ or about 15 kPa) lower than the level of the heart, which is about 200 mm Hg above atmospheric pressure, double the human value. This high arterial pressure near the giraffe's heart provides normal blood pressure and perfusion to the brain (Hargens et al., 1987).

Two features of the peripheral circulation that inhibit edema in a standing giraffe are (1) a high resistance to flow in the thick-walled arterioles, which keeps venous pressure, and hence capillary pressure, well below arterial pressure [an arteriole is a small branch of an artery leading into capillaries (Hickman, 1961; p. 511)]; and (2) very tight skin in the lower legs (an "antigravity suit"), which allows tissue pressure to be much higher than in humans (in humans, tissue pressure is about 0).

Even so, there is a net filtration pressure of >80 mm Hg, and quietly standing giraffes will be susceptible to some edema. In the ambulant giraffe, however, the "muscle pump" comes into play, as in humans, squeezing blood up out of the lower veins as the skeletal muscles contract, and sucking it in again through the capillaries as they relax, backflow in the veins being prevented by valves. These pressures move fluid upward against gravity. The giraffe's jaw muscles (chewing actions) do the same to pump blood up the neck. (A vein is about twice the cross-section of its corresponding artery. Veins, especially in the lower parts of the body, are provided with valves to prevent the backflow of blood (Hickman, 1961; p. 629).) Dinosaurs were even taller than giraffes, and they may have had several hearts to raise fluids to their heads (Dr Octave Levenspiel, Sigma Xi Lecture, "A Chemical Engineer Visits Dinosaurland", Kansas State University, April 8, 2002).

## 20.3 COHESION THEORY

In plants, no standing tanks, pumps (hearts), or valves have been observed. If one looks through books on plant anatomy, one sees no such structures (Esau, 1965, 1977). So, again we ask, "How does water get to the top of tall trees?"

At present, the *cohesion theory*, or sap-tension theory, is the theory generally accepted as the one that explains most satisfactorily the way that water ascends in plants. (The dictionary defines *sap* as "the juices of a plant, especially the watery solution which circulates through the vascular tissue" (Webster's Collegiate Dictionary, 1939).) Here we will use interchangeably the terms "sap" and "water in the tracheary cells of the xylem tissue". We recognize that the fluid in the tracheary cells is not pure water, but a dilute aqueous solution (Nobel, 1974; p. 393). Even in mangroves, which grow in salt water, the sap in the xylem tissue is very nearly salt free and changes the melting point of water <0.1 °C (Hammel and Scholander, 1976; p. 32). A 0.1 °C depression of the freezing point of water would be brought about by a 0.027 molal solution of NaCl at 25 °C, which is about $-1$ bar (Lang, 1967). The <0.1 °C depression in the freezing point, as observed by Hammel and Scholander (1976), would mean that the sap has an osmotic potential of $>-1.0$ bar Scholander et al. (1965) show that the osmotic potential ($\Psi_\pi$) in the sap in mangrove is $-0.3$ atm (Figure 20.1).

Let us review xylem tissue (Chapter 15, Section 15.1, Part G). The xylem tissue is made up of four types of cells (Table 15.1): vessel members (also called xylem elements), the conducting cells that occur only in

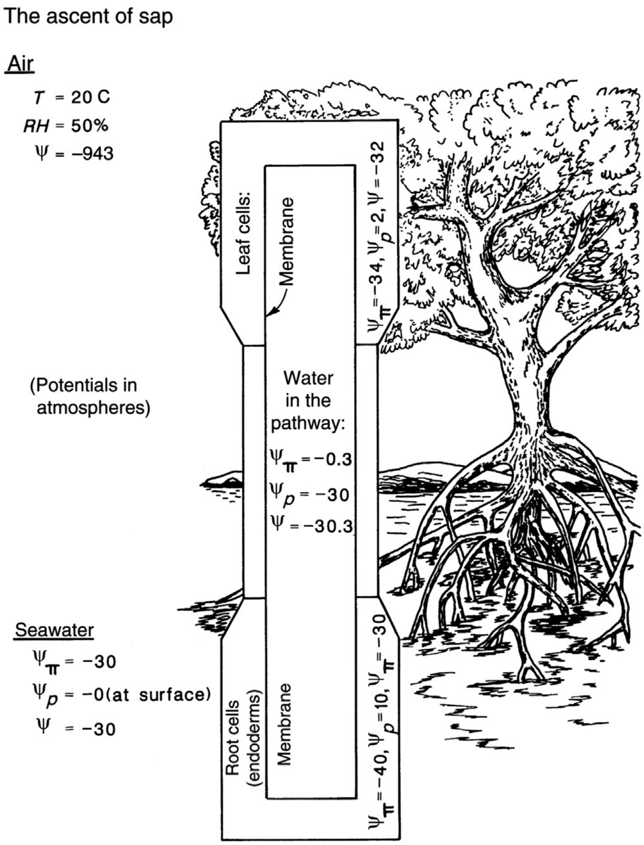
The ascent of sap
Air
$T$ = 20 C
$RH$ = 50%
$\Psi$ = −943
(Potentials in atmospheres)
Seawater
$\Psi_\pi$ = −30
$\Psi_p$ = −0(at surface)
$\Psi$ = −30
Leaf cells:
Membrane
$\Psi_\pi = -34, \Psi_p = 2, \Psi = -32$
Water in the pathway:
$\Psi_\pi = -0.3$
$\Psi_p = -30$
$\Psi = -30.3$
Root cells (endoderms)
Membrane
$\Psi_\pi = -40, \Psi_p = 10, \Psi_\pi = -30$

**FIGURE 20.1** Water relations of a mangrove growing with its roots immersed in seawater. The diagram indicates the essential parts of the mangrove tree from the standpoint of water relations, particularly the membranes of the endodermis and of the leaf cells. It is important to note that if leaf membranes should suddenly cease to be differentially permeable, salt and subsequently water would move from leaf cells into the pathway due to the high tension of water there, and thus, the leaf cells would collapse. *Data from Scholander et al. (1965). From Salisbury and Ross (1978), p. 61. Reprinted with permission of Brooks/Cole, a division of Thomson Learning: www.thomsonrights.com. Fax 800 730-2215.*

angiosperms (the flowering plants), the most highly evolved plants; tracheids, the conducting cells that occur in angiosperms and gymnosperms (e.g., the conifers); fibers, which give structural support; and parenchyma cells, which store carbohydrates and assist in lateral movement of water and solutes into and out of the conducting cells. At maturity, vessel members, tracheids, and fibers are dead. Only the parenchyma cells are living. Also, at maturity, the end walls of vessel members disintegrate, and, consequently, a long tube, called a xylem vessel, is formed (Esau, 1977; pp. 101–124).

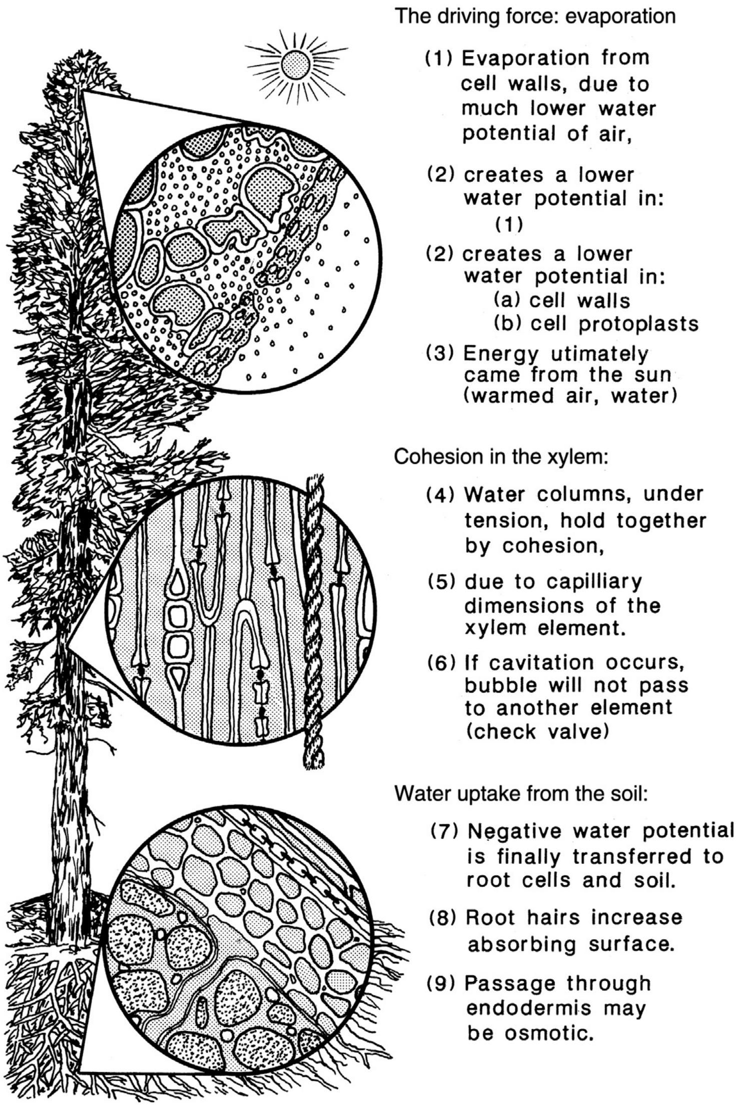

The driving force: evaporation

(1) Evaporation from cell walls, due to much lower water potential of air,

(2) creates a lower water potential in:
(1)

(2) creates a lower water potential in:
(a) cell walls
(b) cell protoplasts

(3) Energy utimately came from the sun (warmed air, water)

Cohesion in the xylem:

(4) Water columns, under tension, hold together by cohesion,

(5) due to capilliary dimensions of the xylem element.

(6) If cavitation occurs, bubble will not pass to another element (check valve)

Water uptake from the soil:

(7) Negative water potential is finally transferred to root cells and soil.

(8) Root hairs increase absorbing surface.

(9) Passage through endodermis may be osmotic.

**FIGURE 20.2** The cohesion theory of the ascent of sap summarized. *From Salisbury and Ross (1978), p. 58. Reprinted with permission of Brooks/Cole, a division of Thomson Learning: www.thomsonrights.com. Fax 800 730-2215.*

The cohesion theory of the ascent of sap was foreshadowed by Stephen Hales (1677–1761; English clergyman, physiologist, chemist, and inventor, famous for his pioneering studies in animal and plant physiology), Julius von Sachs (1832–1897; German botanist and outstanding plant physiologist), and Eduard Strasburger (1844—1912; German botanist and one of first to realize the importance of the nucleus and chromosomes in heredity). They all concluded that transpiration produces the pull causing the ascent of sap (Kramer, 1983; p. 282). The first successful attempt to measure cohesion in water experimentally seems to have been made by Berthelot in 1850 (Greenidge, 1957). He obtained values to 50 atm by a method similar to that used later by Dixon and Joly (1895). Boehm (1893) demonstrated that transpiring branches could raise mercury above barometric pressure, but the demonstration by Askenasy (1895) and Dixon and Joly (1895), showing that water has considerable tensile strength, was necessary to make the cohesion theory acceptable (Kramer, 1983; p. 282).

The cohesion theory, as first set forth by Dixon and Joly (1895) and Dixon (1895, 1897, 1914), assumes that diffusion of water from the noncollapsible xylem elements in contact with the leaf cells creates a state of tension within the water columns in the xylem vessels. This tension is possible because of the cohesion of water molecules and their adhesion to the hydrophilic walls of the xylem elements. Briggs (1917, p. 108) points out the importance of adhesion. He said, “We may consider the outer surfaces of these cells to be saturated with water, which retreats into the wall tissue in such a way as to form a great number of capillary surfaces of high curvature, this curvature in fact being such as would be necessary to support a capillary column of the observed height”. Tension in the water columns is assumed to lift water from the roots to the leaves, in addition to reducing the potential energy of the water in the root xylem tissue until water diffuses from the soil into the root during absorption of the water. The cohesion theory assumes continuity of water columns, laterally and vertically, in the conducting elements of the xylem tissue. These water columns are ultimately placed under tensile strain. But widespread rupture is believed not to occur in the water columns under tensile strain owing to the purported cohesive properties of water when entrapped in small capillaries. Figure 20.2 from Salisbury and Ross (1978, p. 58) outlines the cohesion theory. (For a biography of Dixon, see the Appendix, Section 20.9, and for that of Joly, see the Appendix, Section 20.10.)

## 20.4 LIMITATIONS OF THE COHESION THEORY

Even though most plant physiologists feel that the cohesion theory is probably the correct explanation for the rise of water in plants, the theory has limitations. The main difficulty is that it postulates a system of potentially great instability and vulnerability, although it is clear that the water-conducting system in plants must be both stable and invulnerable. Objections to the theory include three major points (Kramer, 1983, p. 283; Salisbury and Ross, 1978, pp. 58–60):

1. The tensile strength of water is inadequate under the great tensions necessary to pull water to the top of plants, especially tall plants.
2. There is insufficient evidence for the existence of continuous water columns (i.e., water columns under tension are not stable and they cavitate, or form cavities, hollows, or bubbles).
3. It seems impossible to have tensive channels in the presence of free air bubbles, which can occur when trees in cold climates freeze and then thaw.

Let us consider each point. First, is the tensile strength of water adequate to pull water to the top of plants? Tensile strength is defined as the "resistance to lengthwise stress, measured by the greatest load in weight per unit area pulling in the direction of length that a given substance can bear without tearing apart" (Webster's New World Dictionary of the American Language, 1959).

Nobel (1970, pp. 35–36, p. 40; 1974, pp. 46–47, pp. 52–53) calculates the tensile strength of water. Let us do the calculations that Nobel does. We must consider the structure of ice (Nobel, 1974; p. 46). Ice is a coordinated crystalline structure in which essentially all the water molecules are joined by hydrogen bonds (Figure 3.2). When heat is added so that the ice melts, some of these intermolecular hydrogen bonds are broken. The heat of fusion of ice at 0 °C is 80 cal/g or 1.44 kcal/mol (Remember: 18 g/mol for water; 80 cal/g × 18 g/mol = 1400 cal/mol = 1.44 kcal/mol) The total rupture of the intermolecular hydrogen bonds involving each of its hydrogens would require 9.6 kcal/mol of water. The 9.6 kcal/mol is a given value. Nobel (1974, p. 46) gives references for the value. He cites work by Eisenberg and Kauzmann (1969; e.g., see p. 145, p. 269) and Pauling (1964; e.g., see p. 456) for references on the hydrogen bond energy. Nobel (1974, p. 46) points out that the actual magnitude of the hydrogen bond energy assigned to ice depends somewhat on the particular operational definition used in the measurement of the various bonding energies. Therefore, the quoted values vary somewhat.

The heat of fusion thus indicates that (100) (1.44)/(9.6), or at most 15%, of the hydrogen bonds are broken when ice melts. Some energy is needed to overcome van der Waal's attractions, so that <15% of the hydrogen bonds are actually broken upon melting (Nobel, 1974; p. 46).

Conversely, >85% of the hydrogen bonds remain intact for liquid water at 0 °C. Because 1.00 cal is needed to heat 1 g of water 1 °C (1.00 cal/g)(25)(18 g/mol)(0.001 kcal/cal), or 0.45 kcal/mol is required to heat water from 0 to 25 °C. If all this energy were used to break hydrogen bonds, >80% of the bonds would still remain intact at 25 °C. (Note: 0.45/9.6 = 0.047, which is <5%; so 85−<5% = >80%.) The extensive amount of intermolecular hydrogen bonds present in the liquid state contributes to the unique and biologically important properties of water, including its high tensile strength, which is of interest to us now.

If 80% of the hydrogen bonds are intact in water at 25 °C (Nobel, 1974; p. 52), then the energy will be (0.80)(9.6) or 7.7 kcal/mol, which is (7.7 kcal/mol)/(18 g/mol) or 0.43 kcal/g of water. For a density of 1.00 g/cm$^3$, and replacing kilocalories by $4.184 \times 10^{10}$ erg, we calculate that the energy of the hydrogen bonds is $1.8 \times 10^{10}$ erg/cm$^3$. (Remember: $1\ \text{J} = 10^7$ erg; 1 cal = 4.184 J; therefore, 1 cal = $4.184 \times 10^7$ erg; 1 kcal = $4.184 \times 10^{10}$ erg.) The tension that is applied to a water column acts against this attractive energy of the hydrogen bonds.

When the fracture is just about to occur at each hydrogen bond, the maximum possible tensile strength is developed. Thus, the maximum tensile strength would represent an input of $1.8 \times 10^{10}$ erg/cm$^3$. Since an erg = dyne-cm and a bar = $10^6$ dyn/cm$^2$, the maximum tensile strength of water corresponds to 18,000 bars.

Nobel's (1974) theoretical considerations, therefore, show that the calculated value for the tensile strength of water is large (18,000 bars) and would permit the rise of water in plants even under great tensions. Tensions in higher (more evolved) plants probably never exceed 100 atm. Lower plants such as fungi apparently can grow in soil with a tension (or absolute value of matric potential) of |400| bars (Harris, 1981; p. 26). What values of the tension of water have been measured experimentally? Dixon and Joly (1895) estimated that water entrapped in glass tubes of a small diameter could withstand tensions >200 atm without fracture. Ursprung (1929) calculated that tensions on the order of 300 atm were reached in annulus cells of discharging fern sporangia. Briggs (1950) employed a centrifugal method to obtain values of about 220 atm for the tensile strength of water. (See Figure 20.3 for Briggs's method of measuring the cohesive properties of water using a bent centrifuge tube, called a Z-tube. His biography is given in Chapter 10, Section 20.5.) Centrifugal methods are now being used with xylem tissue segments (e.g., 28 cm long) to determine xylem vulnerability to embolism (Cochard et al., 2005, 2010).

In contrast to the foregoing rather large values, a number of other investigators have demonstrated that water may have a relatively low tensile strength. Loomis et al. (1960) suggested that Ursprung's values of the tensile strength of water were open to question because of a confusion of adsorption forces with cohesion. Scholander et al. (1955), through centrifugation in glass tubes, observed tensive values from 10 to 20 atm without producing cavitation of water. When the experiments were repeated using plant material, they observed much lower values (1–3 atm). Also, they were unable to fit hydrostatic pressures in transpiring grape vines into a pattern that followed the cohesion theory. Measured pressure did not indicate cohesion tension at any time, and they concluded that tensile sap

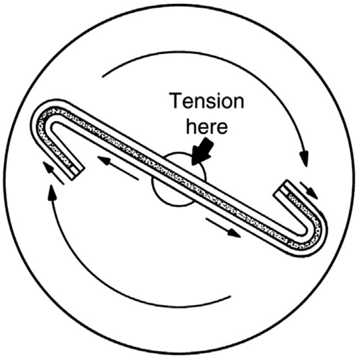

**FIGURE 20.3** Method of measuring the cohesive properties of water using a centrifuged Z-tube. Small arrows indicate the direction of centrifugal force and principle of balancing due to the Z-tube. These tubes are centrifuged causing tension on the water at the center of the tube. The tension present when the water column breaks can be calculated. *From Salisbury and Ross (1978), p. 59. Reprinted with permission of Brooks/Cole, a division of Thomson Learning: www.thomsonrights.com. Fax 800 730–2215.*

columns, if any exist in the vessels of grapevine, are few. Measurements taken on Douglas fir (*Pseudotsuga menziesii*) trees, however, did follow the pattern that one would expect if water were rising in the plants according to the cohesion theory (Scholander et al., 1965) (Figure 20.4). That is, the hydrostatic pressure at the top of the trees was more negative than at the

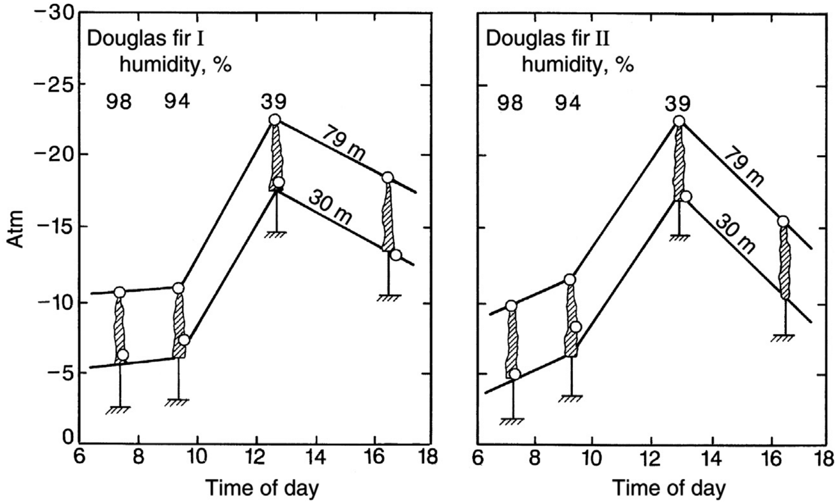

**FIGURE 20.4** Differences in hydrostatic pressure in the upper and lower parts of crowns of Douglas fir trees at various times of the day as measured on excised twigs in a pressure chamber. *Reprinted with permission from Scholander et al. (1965), American Association for the Advancement of Science.*

bottom of the trees. Greenidge (1957) discusses different techniques used to measure the tensile strength of water that yield values ranging from 0.05 to 10 atm. Smith (1994) reviewed experimental measurements, which showed that the likely range of negative pressures that can be sustained in the xylem tissue is between −0.1 and −0.6 MPa.

It appears that, experimentally, water can withstand negative pressures (tensions) only up to about 300 bars without breaking (Nobel, 1974; p. 52). The observed tensile strength depends on the wall material, the diameter of the xylem vessel, and any solutes present in the water. Local imperfections in the semicrystalline structure of water, such as those caused by $H^+$ and $OH^-$, which are always present, even in pure water, reduce the observed tensile strength from the maximum value predicted based on hydrogen bond strengths. Nevertheless, the measured tensile strength for water provided by the intermolecular hydrogen bonds (up to 300 bars) is nearly 10% of that for copper or aluminum, and is sufficiently high to meet the demands encountered for water movement in plants (Nobel, 1974; p. 53). The tensile strength of copper is 4140–4830 bars; for aluminum, it is 2070–2760 bars (Weast, 1964; p. F-15).

Let us now consider the second problem with the cohesion theory. Are water columns in the xylem tissue stable under tension? Much has been written about the instability of water columns under tension and the ease with which they break by cavitation in glass capillary tubing (Kramer, 1969; p. 275). It has been suggested that if they break as easily in the xylem of trees, they would soon become inoperative because of shocks such as those caused by swaying in the wind.

Considerations of nucleation prompted Silver (1942) to infer that the tensile strength of water is negligible. There is evidence of widespread fracture of stretched water columns and a high percentage of gas-filled, nonfunctional elements under field conditions (Preston, 1938; Greenidge, 1957; Scholander, 1958). However, it seems probable that the nature of the walls of the dead xylem tissue, which is filled with imbibed water, makes the water columns in the stems of plants more stable than those in glass tubes. If cavitation caused by air entry should occur in the conducting tubes of the xylem tissue, the matric potential component attributed to the hydrophilic nature of the surfaces involved could be expected to maintain surface films of water capable of transporting water up the stem (Gardner, 1965). The cell walls in the conducting cells of the xylem tissue are probably charged and exhibit double-layer characteristics. Thus, even if a column breaks, there is a thin layer of adsorbed water, with a concave curvature, which ensures that entrapped air eventually will be dissolved (W.R. Gardner, personal communication, February 29, 2000).

Greenidge (1955, 1957) did experiments in which a dye was injected into the xylem of trees after severing all vessels of the stem by two or more opposing saw cuts. The dye not only moved readily to the top of such trees but it also completely stained the wood immediately below and above the saw cuts, indicating capillary movement under low tension and showing no evidence of rupture of stressed water columns. In other experiments, the dye moved to the top of tree trunks from which all leafy branches had been removed and all vessels severed at one or more points.

It is true that the water columns in large xylem vessels often break and that smaller vessels remain water filled. If vessels become filled with air (gas bubbles), the bubbles usually cannot spread beyond the vessel members or tracheids in which they developed (Kramer, 1983; p. 284). We will come back to this point in the next section when we see how bubbles cannot spread. Thus, the entire conducting system is not suddenly blocked by expanding bubbles. Utsumi et al. (2003) found that even though some tracheids in the sapwood of conifers had no water, some tracheids retained water. Water transport occurred mainly in earlywood tracheids, whereas latewood tracheids played no role or only a minor role in water transport. In a study of moisture relations in tall lianas, Scholander et al. (1957) found that allowing vessels of a cut vine to become plugged with air caused a lowered hydrostatic pressure in the plant, but did not reduce the rate of water uptake, indicating that water movement was shifted to the numerous tracheids of the stem. Again they found no direct evidence of cohesion tension. The work by Scholander (1958) and Scholander et al. (1957) indicated that there is a large "safety factor" (Kramer, 1983; p. 284) in the xylem. Although partial blockage increases the resistance to flow of water, the volume of flow is not necessarily reduced. The ability to hear the water columns break is supporting evidence that the columns are under tension, and, when they cavitate, the sound can be picked up acoustically. Milburn and Johnson (1966) developed an acoustic detector, and subsequent experimenters have monitored cavitation using the technique (e.g., see Tyree et al., 1986; Jackson and Grace, 1996). The method has been used to monitor water stress in crop plants and to tell when to irrigate (Senft, 1986).

Let us now consider the third problem. Microscopic observations have shown that an air blockage occurs when some trees in cold climates are frozen (Johnson, 1977). Inability to restore the water columns in the spring may well be the factor that excludes certain trees and especially vines with large vessels from these regions (Salisbury and Ross, 1978; p. 60) (Figure 20.5). But how do trees grow in such regions?

Imagine a northern tree thawing in the spring. As the ice melts, the tracheids become filled with liquid containing the many bubbles of air that had been forced out by freezing. As melting continues and transpiration begins, tension begins to develop in the xylem tissue. Because of the small dimensions of the tracheids involved, the pressure difference across the curved air—water interface bounding the bubbles would be considerable, resulting in a much higher pressure in an air bubble than would

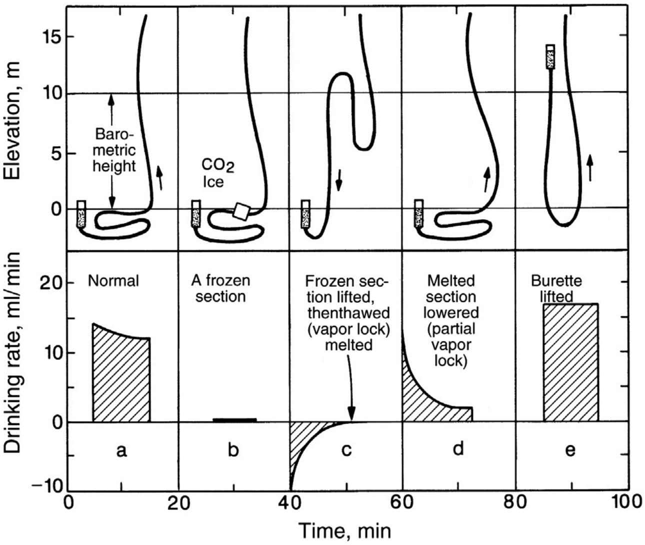

**FIGURE 20.5** Scholander's experiments with tropical rattan vines (*Calamus* sp.). (a) The vine is cut off under water and a burette is attached, allowing measurement of the rate of water uptake. If the burette is stoppered, water continues to be taken up until a vacuum is created in the burette, and the water boils. (b) To freeze the water in the vine, the burette first had to be taken off so that air entered all the xylem elements, vapor-locking the system. Then, after freezing, the vapor-locked portion (~2 m) was cut off under water and the burette was attached again. There was still no water uptake, indicating that freezing had indeed blocked the system. (c) If the vapor-locked portion was hoisted above the barometric height and allowed to thaw, some water ran out, but there was no uptake, indicating that the system was now vapor locked. (d) If the vapor-locked portion was lowered to the ground, there was a rapid initial uptake as vapor condensed to water, breaking the vapor lock, but then the uptake was slower than it was originally because some air had been excluded from freezing. (e) When the burette was elevated 11 m, the rate of water uptake returned to the original level, indicating that the vapor lock had now been completely eliminated. *Data from Scholander et al. (1961). Reprinted with permission from Scholander et al. (1961), American Association for the Advancement of Science.*

exist in the water. Any bubbles that form should dissolve fairly readily, restoring the integrity of the water column (Gardner, 1965). Studies of wood in the spring indicate that about 10% of the tracheids are filled with vapor, but the remaining 90% appear ample to handle sap movement (Salisbury and Ross, 1978, p. 60; Kramer, 1983) (Figure 20.6). Gymnosperms with their tracheids are especially well adapted to cold climates. Trees, and especially vines with large, long vessels, are practically absent from cold climates, but are abundant in the tropics.

Dividing cambial cells in the spring also produce new water-filled conducting cells in the xylem tissue. In some ring-porous trees (trees with large vessel members) virtually all the water moves in these newly

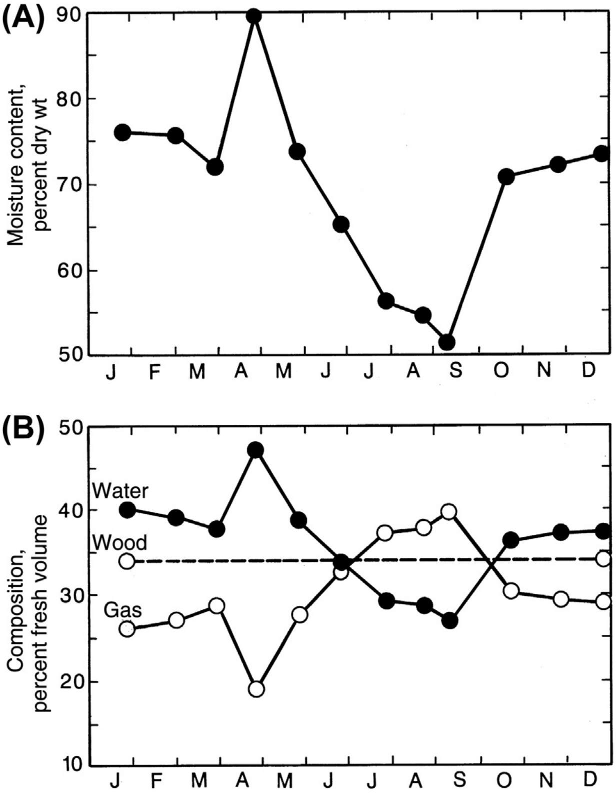

**FIGURE 20.6** (A) Seasonal changes in the water content of yellow birch trunks calculated from disks cut from the base, middle, and top of the trunks. (B) Seasonal changes in the gas and water content of yellow birch tree trunks calculated as the percentage of the total volume. *From Kramer (1983), p. 285. Reprinted by permission of Academic Press.*

formed tubes (Salisbury and Ross, 1978; p. 60). Root pressure may also help in filling vessel members and tracheids in the spring after freezing. *Root pressure* is a positive pressure that develops in the xylem resulting in guttation or exudation from stumps of detopped plants (Kramer, 1983; p. 198). Root pressure appears to be an osmotic process in which root systems function as osmometers because of the accumulation of solutes in the xylem sap. Two factors are necessary for root pressures to exist: a differentially permeable membrane, which in most cases occurs in the endodermis in roots, and a source of solutes, which are in the xylem sap (Kramer, 1983; p. 223). Root pressures of 5 or 6 bars have been recorded (Salisbury and Ross, 1978; p. 50). These pressures are not sufficient to get water to the top of tall trees. Root pressures are not seen in conifer trees, including the *Sequoia* and the Douglas fir trees, under any conditions

(Salisbury and Ross, 1978; p. 50). Douglas fir trees reach over 200 ft (61 m) (Bailey, 1974; p. 117). Therefore, root pressure cannot be invoked for the force that moves water to the top of tall trees, even though it may be important for water transport in short plants such as rice (*Oryza sativa*), as pointed out by Singh et al. (2009).

## 20.5 ALTERNATIVE THEORIES TO THE COHESION THEORY

For many decades, the cohesion theory was accepted and essentially no experiments related to it were performed between about 1960 and mid-1990s. With the advent of the pressure probe (Chapter 17, Section 17.6), measurements made with it contradicted the cohesion theory (Zimmermann et al., 1994, 1995). They showed that the necessary high tensions in the xylem were not present and that the gradient of tension with height was not present. Canny (1995), therefore, put forward a theory, called the *compensating-pressure theory*, to account for the rise of water in plants. He noted that the xylem has ray cells throughout it. These are living parenchyma cells. He said that compensating pressure is provided by the tissue pressure of xylem ray cells pressing onto the closed fluid spaces of the tracheary elements and squeezing them. The driving force is provided, as in the cohesion theory, by evaporation and the tensions generated in curved menisci in the wet cell walls of the leaf. The force is transmitted, as in the cohesion theory, by tension in the water in the tracheary elements. But this tension is maintained by compression from tissue pressure around the tracheary elements. The gravitational gradient of tension up a tall tree is compensated by increasing tissue pressure of the xylem parenchyma with height, and the need for a tension gradient to sustain the standing columns disappears. Canny's theory apparently considers that solutes in the parenchyma cells of the tissue around the tracheids and vessel members cause an imbibing of water and create a pressure on the tracheary elements. This pressure on the tracheary elements keeps the water in them from cavitation. Canny's theory was challenged by Comstock (1999), who pointed out that extreme reinforcement would be needed to sustain tissue pressures postulated by Canny's model and they are unlikely to exist. If the water potential gradient were such that the parenchyma cells have a lower water potential than the tracheary cells, water would move from the tracheary cells to the parenchyma, which does not happen. Canny's model postulates a pump-and-valve system. Flow characteristics are set by an active water pump in the roots and a one-way, regulating valve in the leaves, but a viable mechanism has not been identified (Comstock, 1999).

The pressure probe has been reevaluated (Steudle, 2001). The earlier measurements with the probe, which did not support the cohesion theory, were likely due to experimental artifacts and limitations of the probe. Tensions as high as 10 MPa are claimed to exist in the xylem, and pressure probes cannot measure such high values (Steudle, 2001). Old and more recent evidence provides strong support for the cohesion theory (Wei et al., 1999; Steudle, 2001).

Nevertheless, the cohesion theory is still challenged. Zimmermann et al. (2004) said that the rise of water in tall trees cannot depend on negative pressure gradients of several megaPascals through continuous water columns from the roots to the foliage because water under such negative pressure is unstable. They postulated other forces that are involved in water ascent and suggested that water can be lifted by a series of "watergates" such as those that exist on ships in staircase locks. However, Esau (1965, 1977) does not show watergates in her books on plant anatomy. The article by Zimmermann et al. (2004) was challenged by many scientists involved in the study of long-distance water transport in plants (Angeles et al., 2004). Angeles et al. (2004) list 23 articles that support the cohesion theory.

Even though a pump-and-valve system as postulated by Canny (1995) and watergates as postulated by Zimmermann et al. (2004) have not been identified anatomically, the pit membrane in cell walls of tracheids and vessel members does have a structure that operates like a valve to shut off water moving from one part of the xylem to another (Figure 20.7, Esau, 1965; p. 40). A *pit* is a recess or cavity in the cell wall where the primary wall is not covered by a secondary wall. A pit is usually a member of a pit pair. A *pit pair* is two complementary pits of two adjacent cells. Essential components of a pit pair are two pit cavities and the pit membrane. A *pit cavity* is the entire space within a pit from pit membrane to the cell lumen. The *pit membrane* is the part of the intercellular layer and primary cell wall that limits a pit cavity externally (Esau, 1977; p. 520). A *bordered pit* is a pit in which the secondary wall overarches the pit membrane (Esau, 1977; p. 504). The *torus* is the central thickened part of the pit membrane in a bordered pit consisting mainly of middle lamella and two primary walls (Esau, 1977; p. 529).

The closest structure in a plant that looks like a valve is the pit membrane, which, as noted in the previous paragraph, is part of the intercellular layer and primary cell wall that limits a pit cavity in a cell wall. But pit membranes do not act in the same ways as valves do in veins. The pit membrane, as shown in Figure 20.7, is a middle lamella (not a living membrane), which is a layer of intercellular material, chiefly pectic substances, cementing together the primary walls of contiguous cells (Esau, 1977; p. 516). The torus in the center of the pit can move to one side to plug the pit, behaving like an inanimate valve.

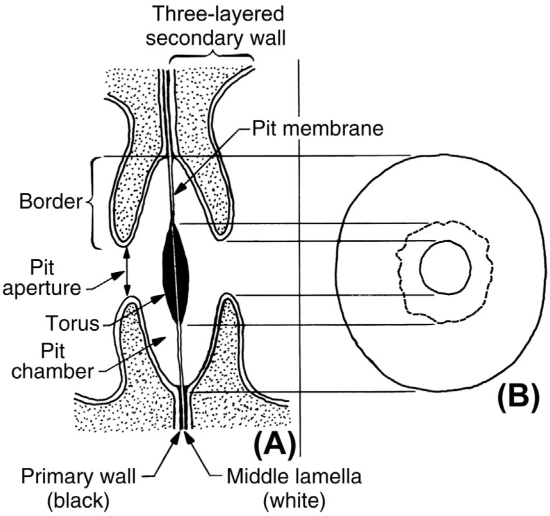

**FIGURE 20.7** Bordered pit pair of *Pinus* in sectional (A) and face (B) views. The pit membrane consists of two primary walls and the intercellular lamella, but is thinner than the same triple structure in the unpitted part of the wall. The torus is formed by the thickening of the primary wall. In (B), the outline of the torus is uneven. *From Esau (1965), p. 40. This material is used by permission of John Wiley & Sons, Inc.*

Water under tension, when it is transported to substantial heights against the force of gravity, is susceptible to spontaneous phase changes from liquid to vapor (cavitation), which results in embolism that can severely limit water transport. To counteract this potentially lethal problem (Holbrook and Zwieniecki, 2008), plants employ a highly compartmentalized transport system of xylem conduits (a *conduit* is a pipe or channel) that allows failure in the integrity of a water column to be isolated from functioning conduits. The conduits are separated by the pit membranes that permit the movement of water from one conduit to the next but limit the movement of gas (Choat et al., 2006). The pit membranes have very small holes (typically 5–20 nm in diameter) that allow the passage of water (van Doorn et al., 2011). These pits prevent air in already damaged conduits from entering functional ones and "air seeding" (Wheeler et al., 2005; Cochard et al., 2009). Air seeding through the pit membranes is the principal mechanism of spread of drought-induced embolisms (Brodersen et al., 2013). Cavitation apparently occurs when the torus slips from its sealing position against the aperture, allowing air to enter the functional conduit (Pittermann et al., 2006). The adhesion of the torus to the pit border may be a main determinant of cavitation resistance (Delzon et al., 2010). Older vessels are more vulnerable to cavitation than are younger vessels. Melcher et al. (2003) found that in sugar maple (*Acer saccharum*) bordered pit membranes of vessels located in current year xylem withstood greater applied gas pressure (3.8 MPa) compared to bordered pit membranes in vessels located in older annual rings (2.0 MPa). Pit membranes also limit the movement of pathogens. Bacteria are able to passively move long distances from stem to leaf, when pit membranes are broken (Thorne et al., 2006). Plants can refill cavitated vessels by hydraulically isolating the damaged tissue, pumping ions from the surrounding cells, and fostering water entry through bordered pits (Bloom and Holbrook, 2001). The twining habit (Silk and Holbrook, 2005) also might allow water to move to heights. When the vine is wrapped horizontally around its support, water is under less tension than when the vine is oriented vertically. Water could puddle in the horizontal locations forming a new "ground level", which might help push the water up the vine by capillarity.

## 20.6 NEW TECHNIQUES TO CONFIRM THE COHESION THEORY

Experiments to study tensive values of water in plants have been done with plants that have been punched with manometers (Scholander et al., 1955), cut (Scholander et al., 1957), sawed (Greenidge, 1955), punctured with a pressure probe (Tomos and Leigh, 1999), frozen (Cochard et al., 2000), or otherwise disturbed. If it were possible to study plants under natural conditions, when they were intact, one might come to a better understanding as to what tension water is under in plants, and if tensions are built up, if they are sufficient to account for the rise of water.

Equipment has been developed that can be used to nondestructively measure the characteristics of water transport in the soil–plant–atmosphere continuum, such as nuclear magnetic resonance imaging (Scheenen et al., 2000) or sap flow gauges (Green and Clothier, 1988). The difficulty is in getting the equipment to the top of giant trees. Tall platforms have been constructed to access the top of forest canopies (12 m high) (Ellsworth, 1999). (See the cover of *Plant*, *Cell Environment*, March, 2006, issue for a photograph of a platform and an accompanying article (Ryan et al., 2006) that discusses hydraulic limitation to growth of tall trees.) For example, sap flow gauges could be put at the top of a tall tree to see if the flux was upward, as predicted by the cohesion theory, or downwards. Reverse flow occurs in plants if the water potential gradients allow it (Kirkham, 1983; Emerman, 1996; Song et al., 2000; Huang, 1999). Maybe Scholander's measurements were correct (1955, 1957) and the tension does not increase with height. (It has been said that Scholander got his measurements of tension in the top of tall vines and trees by shooting branches down with a gun and then putting them in his pressure chamber.) It may be that tall trees and vines absorb water from the air during rainfall and that water does not need to rise from the roots. Researchers have found that giant redwood trees can absorb water through their branches hundreds of meters above the ground (Royal Society of New Zealand, 2002). Measurements of the direction of sap flow in the tops of intact tall plants are needed.

Even though the water in the xylem is frozen, the cryoscanning electron microscope (SEM) technique has been used to validate the Scholander assumption, that is, that the vessels cut open should fill with air as the water is drained away by continued transpiration (Tyree et al., 2003). In the method, petioles are frozen in liquid nitrogen soon after the petiole is cut. The petioles are then cut at different distances from the original cut surface while frozen and examined in a cryo-SEM facility, where one can distinguish vessels filled with air from those filled with ice.

A synthetic tree that duplicates the tensions observed in tall trees has been developed (Surridge, 2008; Wheeler and Stroock, 2008). Water flows in the tree at pressures of around −10 atm (−10.1 bars). To create their tree, Wheeler and Stroock (2008) used a hydrogel, which mimics the mesophyll of leaves by holding water in molecular-scale pores. Even though the tree is only 5 cm long and the flow is a little over 2 μg of water per second, the synthetic tree can provide a test device for theories of how water rises in tall trees.

## 20.7 CONTROVERSY ABOUT THE COHESION THEORY

In spite of difficulties in demonstrating, in some experiments, appreciable values of tension in water columns of plants, most plant physiologists continue to assume that high tension values are readily obtainable and that the cohesion theory is correct (Kramer, 1983; Baker, 1984). Feelings get vehement when scientists are either defending or refuting the cohesion theory, and this has been the case for decades. When a physicist published a book questioning the validity of the cohesion theory (Bose, 1923), plant physiologists who reviewed the book used strong language to show that he was wrong. For example, MacDougal and Overton (1927) said, “Every page of Bose’s book on the ascent of sap … is utterly lacking in scientific significance. Such books appearing on the lists of scientific publications constitute a menace and danger to sound science”. Other reviewers were critical of Bose’s work (Anonymous, 1929; Shull, 1923). The Bose questioning the cohesion theory was Sir Jagadis Chunder Bose, who was the teacher of Satyendra Nath Bose (Ghosh, 1992). S.N. Bose was the Bose of the Bose–Einstein condensation, a purely quantum phenomenon whereby a macroscopic number of identical atoms occupy the same single-particle state (Wyatt, 1998). (In physics, bosons compromise one of two classes of elementary particles and they are named after Satyendra Nath Bose. Examples of bosons include fundamental particles such as the Higgs boson. The Nobel Prize in Physics in 2013 was awarded to Peter Higgs and François Englert, who developed theory that predicted the Higgs boson.) The heated debates about the cohesion theory continue today. In their book on the ascent of sap in trees, Tyree and Zimmermann (2002, p. 49) say, "At the time of writing, there has been more controversy over the cohesion theory than at any other time, excluding the initial controversy when it was originally proposed". Charged words were used in the review of Zimmermann et al. (2004) (note the first author is Ulrich Zimmermann, not Martin Zimmermann, the coauthor with Tyree of the 2002 book on the ascent of sap), who said that "many plant physiologists still view the Cohesion Theory as the absolute and universal truth because [of] clever wording from the proponents". Zimmermann et al. (2004) continued by saying that "the arguments of the proponents of the Cohesion Theory are completely misleading". Angeles et al. (2004), who believe that the fundamentals of the cohesion theory remain valid, responded to the review by Zimmermann et al. (2004), and the exchange between them was moderated by Woodward (2004), who said that debate is encouraged. Brown (2013) reviews the argument between Zimmermann et al. (2004) and Angeles et al. (2004) as well as other literature dealing with the theory of the rise of sap in trees. He points out (Brown, 2013; p. 351), the "complexity" of the problem. The ongoing controversy about the cohesion theory shows that more experiments are needed to accept its assumptions fully.

## 20.8 POTENTIALS IN THE SOIL—PLANT—ATMOSPHERE CONTINUUM

No matter how water gets to the top of tall trees, the gradient in water potential from the soil to the top of the tree is calculated to be large. Nobel (1974, p. 402; 1983, p. 507; 1991, p. 521; 1999, p. 384; 2005, p. 460; 2009, p. 484) shows representative values for the water potential, $\Psi$, and its components ($\Psi_m$, matric potential; $\Psi_s$, solute potential; $\Psi_g$, gravitational potential; $\Psi_p$, turgor potential) in the soil—plant—atmosphere continuum. Let us choose three values of the water potential and its components that he gives: one for the soil, one for the plant, and one for the atmosphere just over the plant (the reference level is at the soil surface):

Soil: 0.1 m below the ground and 10 mm from the root:
$\Psi$, −0.3 Mpa.
$\Psi_m$, −0.2 Mpa.
$\Psi_s$, −0.1 Mpa.
$\Psi_g$, 0.0 MPa.

Vacuole of leaf mesophyll cell at 10 m:
$\Psi$, −0.8 Mpa.
$\Psi_p$, 0.2 Mpa.
$\Psi_s$, −1.1 Mpa.
$\Psi_g$, 0.1 MPa.
Air just across the boundary layer of the leaf at 50% relative humidity:
$\Psi$, −95.1 Mpa.
$\Psi_p$, 0.0 Mpa.
$\Psi_s$, 0.0 Mpa.
$\Psi_g$, 0.1 MPa.
Potential of the air at 50% RH (relative humidity): −95.2 MPa.

Therefore, we see that the water potential changes from −0.3 MPa in the soil to −95.1 MPa in the air just outside the leaf—a change of 94.8 MPa.

The representative values will, in actuality, be affected by three factors. First, the water potential goes through a diurnal cycle (Nobel, 1974; pp. 406–408; 1983, pp. 516–518; 1991, pp. 532–533; 1999, pp. 393–394; 2005, pp. 471–473; 2009, pp. 495–497) (Figure 20.8). The water potential is typically at its highest value just before dawn, when the plant has had a chance to rehydrate during the night, and it is usually the lowest right after midday. Because the water potential is always changing throughout a day, it is important to measure it at the same time each day during an experiment, unless one wishes to document the diurnal changes. Figure 20.8 is for a general situation. The format of Figure 20.8 was

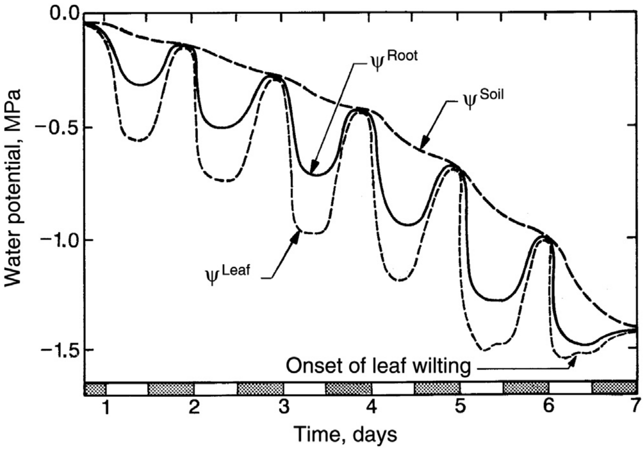

**FIGURE 20.8** Schematic representation of daily changes in the water potentials in the soil, root, and leaf of a plant in an initially wet soil that dries out over a one-week period. $\Psi^{soil}$ is the water potential in the bulk soil, $\Psi^{root}$ is that in the root xylem, and $\Psi^{leaf}$ is the value in a leaf mesophyll cell. *From Nobel (1983), p. 517. Used with permission.*

originally drawn by Gardner and Nieman (1964), who presented actual data for a pepper (Figure 20.9).

Second, marked changes in the hydrostatic pressure in the xylem can cause plants to have measurable diurnal fluctuations in their diameters (Nobel, 1974; p. 404). When the transpiration rate is high, the large tension within the xylem vessel members is transmitted to the water in the cell walls of the xylem vessels, then to water in adjacent cells, and eventually all the way across the stem. The decrease in the hydrostatic pressure in a trunk can, therefore, cause a whole tree to contract during the day. At night, the hydrostatic pressure in the xylem may become positive, and the tree diameter then increases, generally by about 1%. Such changes in tree diameter, and therefore volume, represent the net release of water during the day and storage at night.

Strain gauges are used to monitor the change in stem diameter. In an experiment done at the Iowa State University, strain gauges were cemented to poplar trees (Iowa State University, 1984). When light intensity increased at sunrise, the stem contracted in response to increased evaporation. The stem reached its smallest size around 3:00 pm. As evaporative demand dropped in the evening, the stem expanded. Two hours after sunset, the stem was back to the size of the previous night plus the growth of the day. As the tree dried out, the stem contracted, and eventually it did not recover at night and the stem did not expand. The measurements with strain gauges can be used to determine when to irrigate; however, they cannot be used on small stems, like those of soybean plants, because they do not stay attached.

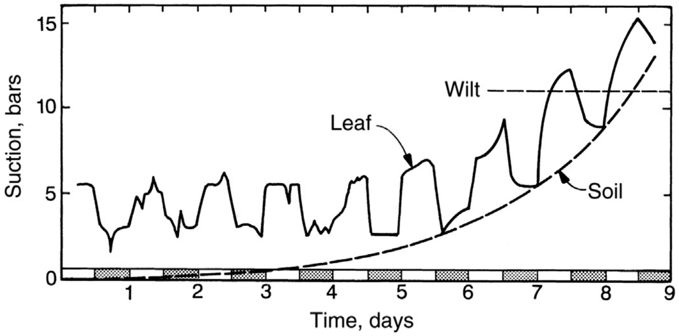

**FIGURE 20.9** Diurnal fluctuation of the suction (diffusion pressure deficit) of a pepper leaf (solid line) and average soil suction in root zone (dashed line). Solid bars along the abscissa indicate 12 h dark periods. The horizontal dashed line indicates leaf suction at which wilting symptoms appear. The plant was grown in a 3-gallon (11.4-L) jar containing clay loam soil. *Reprinted with permission from Gardner and Nieman (1964), American Association for the Advancement of Science.*

Third, the water potential in the vacuole of the leaf will depend on osmotic adjustment. Osmotic adjustment is the lowering of the osmotic potential of a plant when the osmotic potential of the root medium decreases (Bernstein, 1961, 1963). At the cell level, osmotic adjustment is defined as the net accumulation of solutes in a cell in response to a fall in the water potential of the cell's environment. As a consequence of this net accumulation, the osmotic potential of the cell is lowered, which, in turn, attracts water into the cell and tends to maintain turgor potential (Blum et al., 1996). Osmotic adjustment is under genetic control (Zhang et al., 1999). Therefore, the representative value for osmotic potential given by Nobel (1974, 1983, 1991, 1999, 2005, 2009) (−1.1 MPa) can be changed by osmotic adjustment. Under arid conditions or in halophytes, the osmotic potential could fall to as low as −5.0 MPa.

## 20.9 APPENDIX: BIOGRAPHY OF HENRY DIXON

Henry Horatio Dixon (1869−1953), Irish botanist, was born in Dublin, Ireland, in 1869, the son of George and Rebecca (Yeates) Dixon. He got his Sc.D. at Trinity College, Dublin, and also was educated at the University of Bonn in Germany (Marquis Who's Who, 1968). He married Dorothea Mary Franks in 1907, and they had three sons. Between 1892 and 1904, he rose from assistant to professor of botany at Dublin University and was university professor of botany from 1904 to 1950. He was professor of plant biology at Trinity College, Dublin, from 1922; director of the botanical gardens at Trinity College from 1906 to 1951; and its keeper of the herbarium from 1910 to 1951. He was a trustee of the Imperial Library of Ireland. He became a commander of the Irish Lights from 1924. He was a visiting professor at the University of California in 1927. He was honorary chairman of the 6th International Botanical Congress held in Amsterdam, The Netherlands, in 1935; and he was honorary president of the International Botanical Congress held in Stockholm, Sweden, in 1950.

He was recipient of the Boyle Medal in 1917. In 1908, he became a fellow of the Royal Society and was its Croonian lecturer. He was a member of the International Institute of Agriculture and was its chairman for the Committee on Biochemistry in 1927. He was a member of the Royal Dublin Society and was its president from 1945 to 1949. He was a corresponding member of the American Society of Plant Physiologists. He was a member of the British Association for the Advancement of Science and was the president of its Botanical Section in 1922. He was author of several books, including *Transpiration and the Ascent of Sap in Plants* (1914), *Practical Plant Biology* (1922), and *The Transpiration Stream* (1924). He is best known for his research on plant transpiration. He died December 20, 1953 (Marquis Who's Who, 1968).

## 20.10 APPENDIX: BIOGRAPHY OF JOHN JOLY

John Joly (1857–1933), a British physicist and geologist, was born in 1857 (Calef, 1971). He was the son of J.P. and Julia (de Lusi) Joly. He was educated at Trinity College, Dublin, Ireland, where he got a B.A., M.A., and D.Sc. (Marquis Who's Who, 1968). He got an LL.D. at the University of Michigan; an Sc.D. (honorary) at Cambridge University, England; and an Sc.D. at the National University of Ireland. At Trinity College, he was a demonstrator in civil engineering from 1882 to 1891, a demonstrator of experimental physics in 1893, and from 1897 a professor of geology and mineralogy. He was Warden, Alexandra College for Higher Education of Women.

He was senior commander of the Irish Lights and was science adviser to Dr Steevens' Hospital, Dublin. He was a member of the British educational mission to the United States in 1918. He became a fellow of the Royal Society in 1892 and he got its Royal Medal in 1910. He was a fellow of the Geological Society and got its Murchison Medal in 1923. He was a member and president of the Royal Dublin Society and got its Boyle Medal in 1911. He was a member of the British Association and was president of the Geological Section in 1908. He was an honorary member of the Academy of Science of Russia.

He was the author of several books, including *On the Specific Heats of Gases at Constant Volume*, *On a Method of Photography in Natural Colours* (1896), *Radio-activity and Geology*, *The Local Application of Radium in Therapeutics* (1914), *The Birth-Time of the World and Other Scientific Essays* (1915), *Synchronous Signalling in Navigation*, *Reminiscences and Anticipations* (1920), *Radioactivity and the Surface History of the Earth* (1924), and *The Surface History of the Earth* (1925; 2nd ed., 1930). He was editor (with others) of the *Philosophical Magazine* from 1901. He devised the diffusion phytometer, meldometer, and steam calorimeter. (The meldometer, described in an article by Joly in *Nature* in 1885, was an apparatus that was an adjunct to the mineralogical microscope, and it allowed the approximate determination of the melting point of minerals.) He developed a uniform radiation method for use in cancer treatment and was a color-photography pioneer (Marquis Who's Who, 1968).

Joly's work on crust formation of the earth is his best known, in which he presented a theory on continental origins based on the process of convection (Calef, 1971). He proposed that heat was generated in the interior of the earth by decay of radioactive elements. Because the heat could not escape sufficiently rapidly by other means, it started convection currents that carried hot material toward the surface where it cooled and sank, thus setting up a convective cell circulation. He suggested that the earth's crust was dragged sidewise at the top of the cell, which caused buckling and folding and thus mountain making, and the crust collapsed above the sinking portion of the convection cell. The greatest difficulty with this theory was a lack of observational data indicating any convection currents or cells (Calef, 1971). Joly died December 8, 1933.

## References

Angeles, G., Bond, B., Boyer, J.S., Brodribb, T., Brooks, J.R., Burns, M.J., Cavender-Bares, J., Clearwater, M., Cochard, H., Comstock, J., Davis, S.D., Domec, J.-C., Donovan, L., Ewers, F., Gartner, B., Hacke, U., Hinckley, T., Holbrook, N.M., Jones, H.G., Kavanagh, K., Law, B., López-Portillo, J., Lovisolo, C., Martin, T., Martínez-Vilalta, J., Mayr, S., Meinzer, F.C., Melcher, P., Mencuccini, M., Mulkey, S., Nardini, A., Neufeld, H.S., Passioura, J., Pockman, W.T., Pratt, R.B., Rambal, S., Richter, H., Sack, L., Salleo, S., Schubert, A., Schulte, P., Sparks, J.P., Sperry, J., Teskey, R., Tyree, M., 2004. The cohesion-tension theory. New Phytol. 163, 451–452.

Anonymous, 1929. News and views. Nature 124, 103.

Askenasy, E., 1895. Ueber [sic] das Saftsteigen. Botanisches Centralblatt 62, 237–238.

Bailey, L.H., 1974. Manual of Cultivated Plants, 14th printing. Macmillan Pub. Co., New York.

Baker, D.A., 1984. Water relations. In: Wilkins, M.B. (Ed.), Advanced Plant Physiology. Pitman, London, pp. 297–318.

Bernstein, L., 1961. Osmotic adjustment of plants to saline media. I. Steady state. Am. J. Bot. 48, 909–918.

Bernstein, L., 1963. Osmotic adjustment of plants to saline media. II. Dynamic phase. Am. J. Bot. 50, 360–370.

Bloom, A.J., Holbrook, N.M., 2001. United Kingdoms. Plant Physiol. 126, 952–955.

Blum, A., Munns, R., Passioura, J.B., Turner, N.C., 1996. Genetically engineered plants resistant to soil drying and salt stress: how to interpret osmotic relations? Plant Physiol. 110, 1051.

Boehm, J., 1893. Capillarität und Saftsteigen. Berichte der Deutschen Botanischen Gesellshaft 11, 203–212.

Bose, J.C., 1923. The Physiology of the Ascent of Sap. Longmans, Green: London.

Bourne Jr, J.K., 2009. Redwoods. The super trees. Natl. Geogr. 216 (4), 28–49, 58–59 (October issue).

Briggs, L.J., 1917. Biophysics. The living plant as a physical system. J. Wash. Acad. Sci. 7 (4), 89–111.

Briggs, L.J., 1950. Limiting negative pressure of water. J. Appl. Phys. 21, 721–722.

Brodersen, C.R., McElrone, A.J., Choat, B., Lee, E.F., Shackel, K.A., Matthews, M.A., 2013. In vivo visualizations of drought-induced embolism spread in *Vitis vinifera*. Plant Physiol. 161, 1820–1829.

Brown, H.R., 2013. The theory of the rise of sap in trees: some historical and conceptual remarks. Phys. Perspect. 15, 320–358. http://dx.doi.org/10.1007/s00016-013-0117-1.

Calef, W.C., 1971. Continent. Encyclopaedia Britannica 6, 417–419.

Canny, M.J., 1995. A new theory for the ascent of sap—Cohesion supported by tissue pressure. Ann. Bot. 75, 343–357.

Choat, B., Brodie, T.W., Cobb, A.R., Zwieniecki, M.A., Holbrook, N.M., 2006. Direct measurements of intervessel pit membrane hydraulic resistance in two angiosperm tree species. Am. J. Bot. 93, 993–1000.

Cochard, H., Bodet, C., Améglio, T., Cruiziat, P., 2000. Cryo-scanning electron microscopy observations of vessel content during transpiration in walnut petioles. Facts or artifacts? Plant Physiol. 124, 1191–1202.

Cochard, H., Damour, G., Bodet, C., Tharwat, I., Poirier, M., Améglio, T., 2005. Evaluation of a new centrifuge technique for rapid generation of xylem vulnerability curves. Physiol. Plant 124, 410–418.

Cochard, H., Hölttä, T., Herbette, S., Delzon, S., Mencuccini, M., 2009. New insights into the mechanisms of water-stress-induced cavitation in conifers. Plant Physiol. 151, 949–954.

Cochard, H., Herbette, S., Barigah, T., Badel, E., Ennajeh, M., Vilagrosa, A., 2010. Does sample length influence the shape of xylem embolism vulnerability curves? a test with the Cavitron spinning technique. Plant Cell Environ. 33, 1543–1552.

Comstock, J.P., 1999. Why Canny's theory doesn't hold water. Am. J. Bot. 86, 1077–1081.

Delzon, S., Douthe, C., Sala, A., Cochard, H., 2010. Mechanism of water-stress induced cavitation in conifers: bordered pit structure and function support the hypothesis of seal capillary-seeding. Plant Cell Environ. 33, 2101–2111.

Dixon, H.H., 1895. On the ascent of sap. Philos. Trans. R. Soc. London B186, 563–576.

Dixon, H.H., 1897. The tensile strength of cell-walls. Ann. Bot. 11, 585–588.

Dixon, H.H., 1914. Transpiration and the Ascent of Sap in Plants. Macmillan and Co, London.

Dixon, H.H., Joly, J., 1895. The path of the transpiration-current. Ann. Bot. 9, 403–420.

Economist, 2007. Ancient giants. Book review of the wild trees: a story of passion and daring. By Richard Preston. Allen Lane, London, 294 pp The Economist 383 (8524), 95–96. April 14, 2007, issue.

Eisenberg, D., Kauzmann, W., 1969. The Structure and Properties of Water. Oxford University Press, Oxford.

Ellsworth, D.S., 1999. $CO_2$ enrichment in a maturing pine forest: are $CO_2$ exchange and water status in the canopy affected? Plant Cell Environ. 22, 461–472.

Emerman, S.H., 1996. Towards a theory of hydraulic lift in trees and shrubs. In: Morel-Seytoux, H.J. (Ed.), Proceedings of the 16th Annual American Geophysical Union Hydrology Days. April 15–18, 1996. Colorado State University, Fort Collins, pp. 147–157. Hydrology Days Publications: Atherton, California.

Esau, K., 1965. Plant Anatomy, second ed. Wiley, New York.

Esau, K., 1977. Anatomy of Seed Plants, second ed. Wiley, New York.

Gardner, W.R., 1965. Dynamic aspects of soil-water availability to plants. Annu. Rev. Plant Physiol. 16, 323–342.

Gardner, W.R., Nieman, R.H., 1964. Lower limit of water availability to plants. Science 143, 1460–1462.

Ghosh, A., 1992. Vignette: looking toward Calcutta. Nature 257, 1775.

Green, S.R., Clothier, B.E., 1988. Water use of kiwifruit vines and apple trees by the heat-pulse technique. J. Exp. Bot. 39, 115–123.

Greenidge, K.N.H., 1955. Studies in physiology of forest trees. III. The effect of drastic interruption of conducting tissues in moisture movement. Am. J. Bot. 42, 582–587.

Greenidge, K.N.H., 1957. Ascent of sap. Annu. Rev. Plant Physiol. 8, 237–256.

Hammel, H.T., Scholander, P.F., 1976. Osmosis and Tensile Solvent. Springer-Verlag, Berlin.

Hargens, A.R., Millard, R.W., Pettersson, K., Johansen, K., 1987. Gravitational haemodynamics and oedema prevention in the giraffe. Nature 329, 59–60.

Harris, R.F., 1981. Effect of water potential on microbial growth and activity. In: Parr, J.F., Gardner, W.R., Elliott, L.F. (Eds.), Water Potential Relations in Soil Microbiology. Soil Science Society of America, Madison, Wisconsin, pp. 23–95. SSSA Special Pub. No. 9.

Hickman, C.P., 1961. Integrated Principles of Zoology, second ed. The C.V. Mosby, St. Louis.

Holbrook, N.M., Zwieniecki, M.A., 2008. Transporting water to the tops of trees. Phys. Today 61 (1), 76–77.

Huang, B., 1999. Water relations and root activities of *Buchloe dactyloides* and *Zoysia japonica* in response to localized soil drying. Plant Soil 208, 179—186.

Iowa State University, 1984. And you thought watching trees was boring. The Iowa Stater 10 (7), 8.

Jackson, G.E., Grace, J., 1996. Field measurements of xylem cavitation: are acoustic emissions useful? J. Exp. Bot. 47, 1643—1650.

Johnson, R.P.C., 1977. Can cell walls bending round xylem vessels control water flow? Planta 136, 187—194.

Kirkham, M.B., 1983. Physical model of water in a split-root system. Plant Soil 75, 153—168.

Kramer, P.J., 1969. Plant and Soil Water Relationships: A Modern Synthesis. McGraw-Hill, New York.

Kramer, P.J., 1983. Water Relations of Plants. Academic Press, New York.

Lang, A.R.G., 1967. Osmotic coefficients and water potentials of sodium chloride solutions from 0 to 40°C. Aust. J Chem. 20, 2017—2023.

Loomis, W.E., Santamaria, R., Gage, R.W., 1960. Cohesion of water in plants. Plant Physiol. 35, 300—306.

MacDougal, D.T., Overton, J.B., 1927. Sap flow and pressure in trees. Science 65, 189—190.

Marquis Who's Who, 1968. World Who's Who in Science: From Antiquity to the Present, first ed. Marquis-Who's Who, Chicago.

Melcher, P.J., Zwieniecki, M.A., Holbrook, N.M., 2003. Vulnerability of xylem vessels to cavitation in sugar maple. Scaling from individual vessels to whole branches. Plant Physiol. 131, 1775—1780.

Milburn, J.A., Johnson, R.P.C., 1966. The conduction of sap. II. Detection of vibrations produced by sap cavitation in *Ricinus* xylem. Planta 69, 43—52.

National Geographic, 2000. A giant among trees. 197 (4), (unpaged), April issue.

National Public Radio, 2002. The water tower man. In: All Things Considered. Transcript of February 13, 2002. National Public Radio, Washington, DC, pp. 7—11 (Transcript produced by Burrelle's Information Services, Box 7, Livingston, New Jersey 07039.).

Nobel, P.S., 1970. Plant Cell Physiology. W.H. Freeman, San Francisco.

Nobel, P.S., 1974. Introduction to Biophysical Plant Physiology. W.H. Freeman, San Francisco.

Nobel, P.S., 1983. Biophysical Plant Physiology and Ecology. W.H. Freeman, San Francisco.

Nobel, P.S., 1991. Physicochemical and Environmental Plant Physiology. Academic Press, San Diego.

Nobel, P.S., 1999. Physicochemical and Environmental Plant Physiology, second ed. Academic Press, San Diego.

Nobel, P.S., 2005. Physicochemical and Environmental Plant Physiology, third ed. Elsevier, Amsterdam.

Nobel, P.S., 2009. Physicochemical and Environmental Plant Physiology, fourth ed. Elsevier, Amsterdam.

Pauling, L., 1964. College Chemistry, third ed. W.H. Freeman, San Francisco.

Pedley, T.J., 1987. Haemodynamics. How giraffes prevent oedema. Nature 329, 13—14.

Pittermann, J., Sperry, J.S., Hacke, U.G., Wheeler, J.K., Sikkema, E.H., 2006. Inter-tracheid pitting and the hydraulic efficiency of conifer wood: the role of tracheid allometry and cavitation protection. Am. J. Bot. 93, 1265—1273.

Preston, R., October 9, 2006. Tall for its age. The New Yorker, 32—36.

Preston, R., 2008. The Wild Trees. Random House Trade Paperback Edition. Random House, New York.

Preston, R.D., 1938. The contents of the vessels of *Fraxinus americana* L., with respect to the ascent of sap. Ann. Bot. (New Series) 2, 1—21.

Royal Society of New Zealand, Tuesday, September 3, 2002. RSNZ-dailynews. Royal Society of New Zealand, Wellington.

Ryan, M.G., Phillips, N., Bond, B.J., 2006. The hydraulic limitation hypothesis revisited. Plant Cell Environ. 29, 367–381.

Salisbury, F.B., Ross, C.W., 1978. Plant Physiology, second ed. Wadsworth, Belmont, California.

Scheenen, T.W.J., van Dusschoten, D., de Jager, P.A., Van As, H., 2000. Quantification of water transport in plants with NMR imaging. J. Exp. Bot. 51, 1751–1759.

Scholander, P.F., 1958. The rise of sap in lianas. In: Thimann, K.V. (Ed.), The Physiology of Forest Trees. A Symposium Held at the Harvard Forest, April, 1957. Ronald Press, New York, pp. 3–17.

Scholander, P.F., Love, W.E., Kanwisher, J.W., 1955. The rise of sap in tall grapevines. Plant Physiol. 30, 93–104.

Scholander, P.F., Ruud, B., Leivestad, H., 1957. The rise of sap in a tropical liana. Plant Physiol. 32, 1–6.

Scholander, P.F., Hemmingsen, E., Garey, W., 1961. Cohesive lift of sap in rattan vine. Science 134, 1835–1838.

Scholander, P.F., Hammel, H.T., Bradstreet, E.D., Hemmingsen, E.A., 1965. Sap pressure in vascular plants. Science 148, 339–346.

Senft, D., 1986. Microphones monitor plants' water needs. Agric. Res. 34 (3), 13.

Shull, C.A., 1923. Book reviews. Physiology of ascent of sap. Bot. Gaz. 76, 316–317.

Silk, W.K., Holbrook, N.M., 2005. The importance of frictional interactions in maintaining the stability of the twining habit. Am. J. Bot. 92, 1820–1826.

Silver, R.S., 1942. Tensile strength of water and liquid structure theory. Nature 150, 605.

Singh, S., Singh, T.N., Chauhan, J.S., 2009. Water transport in crop plants with special reference to rice: key to crop production under global water crisis. J. Crop Improv. 23, 194–212.

Smith, A.M., 1994. Xylem transport and the negative pressures sustainable by water. Ann. Bot. 74, 647–651.

Song, Y., Kirkham, M.B., Ham, J.M., Kluitenberg, G.J., 2000. Root-zone hydraulic lift evaluated with the dual-probe heat-pulse technique. Aust. J. Soil Res. 38, 927–935.

Steudle, E., 2001. The cohesion-tension mechanism and the acquisition of water by plant roots. Annu. Rev. Plant Physiol. Mol. Biol. 52, 847–875.

Surridge, C., 2008. Negative success in tiny tree. Nature 455, 181 (one page only).

Thorne, E.T., Young, B.M., Young, G.M., Stevenson, J.F., Labavitch, J.M., Matthews, M.A., Rost, T.L., 2006. The structure of xylem vessels in grapevine (Vitaceae) and a possible passive mechanism for the systemic spread of bacterial disease. Am. J. Bot. 93, 497–504.

Tomos, A.D., Leigh, R.A., 1999. The pressure probe: a versatile tool in plant cell physiology. Annu. Rev. Plant Physiol. Plant Mol. Biol. 50, 447–472.

Tyree, M.T., Zimmermann, H.M., 2002. Xylem Structure and the Ascent of Sap, second ed. Springer, Heidelberg.

Tyree, M.T., Cochard, H., Cruiziat, P., 2003. The water-filled versus air-filled status of vessels cut open in air: the 'Scholander assumption' revisited. Plant Cell Environ. 26, 613–621.

Tyree, M.T., Fiscus, E.L., Wullschleger, S.D., Dixon, M.A., 1986. Detection of xylem cavitation in corn under field conditions. Plant Physiol. 82, 597–599.

Ursprung, A., 1929. The osmotic quantities of the plant cell. Proc. Int. Congr. Plant Sci. 2, 1081–1094.

Utsumi, Y., Sano, Y., Funada, R., Ohtani, J., Fujikawa, S., 2003. Seasonal and perennial changes in the distribution of water in the sapwood of conifers in a sub-frigid zone. Plant Physiol. 131, 1826–1833.

van Doorn, W.G., Hiemstra, T., Fanourakis, D., 2011. Hydrogel regulation of xylem water flow: an alternative hypothesis. Plant Physiol. 157, 1642–1649.

Weast, R.C. (Ed.), 1964. Handbook of Chemistry and Physics. Chemical Rubber Co, Cleveland, Ohio.

Weber, B., September 3, 1989. Keeping up the pressure. New York Times Magazine, 62.

Webster's Collegiate Dictionary, fifth ed., 1939. G. & C. Merriam Co, Springfield, Massachusetts.

Webster's New World Dictionary of the American Language, college ed., 1959. World Publishing, Cleveland, Ohio.

Wei, C., Tyree, M.T., Steudle, E., 1999. Direct measurement of xylem pressure in leaves of intact maize plants. A test of the cohesion-tension theory taking hydraulic architecture into consideration. Plant Physiol. 121, 1191−1205.

Wheeler, J.K., Sperry, J.S., Hacke, U.G., Hoang, N., 2005. Inter-vessel pitting and cavitation in woody Rosaceae and other vesselled plants: a basis for a safety versus efficiency trade-off in xylem transport. Plant Cell Environ. 28, 800−812.

Wheeler, T.D., Stroock, A.D., 2008. The transpiration of water at negative pressures in a synthetic tree. Nature 455, 208−212.

Woodward, I., 2004. Tansley reviews. New Phytol. 163, 453 (one page only).

Wyatt, A.F.G., 1998. Evidence for a Bose−Einstein condensate in liquid $^4$He from quantum evaporation. Nature 391, 56−59.

Zhang, Jingxian, Hguyen, H.T., Blum, A., 1999. Genetic analysis of osmotic adjustment in crop plants. J. Exp. Bot. 50, 291−302.

Zimmermann, U., Meinzer, F.C., Benkert, R., Zhu, J.J., Schneider, H., Goldstein, G., Kuchenbrod, E., Haase, A., 1994. Xylem water transport: is the available evidence consistent with the cohesion theory? Plant Cell Environ. 17, 1169−1181.

Zimmermann, U., Meinzer, F., Bentrup, F.-W., 1995. How does water ascend in tall tress and other vascular plants? Ann. Bot. 76, 545−551.

Zimmermann, U., Schneider, H., Wegner, L.H., Haase, A., 2004. Water ascent in tall trees: does evolution of land plants rely on a highly metastable state? New Phytol. 162, 575−615.

CHAPTER

# 21

# Sap Flow

We defined sap in the previous chapter (Chapter 20). Sap is the water in the tracheary cells of the xylem tissue. Measurement of the flow of sap through stems of plants to obtain accurate water-use data has long been a challenge for agronomists (Bloodworth et al., 1956). Two methods have been developed to measure sap flow (also called stem flow, even though the stem is not flowing): the heat-pulse method, an older method that has been in use since the time of Huber (1932) in Germany and the heat-balance method, a newer method that can be traced to Vieweg and Ziegler (1960) (Baker and van Bavel, 1987). The heat-pulse method is invasive and is often used on woody plants, such as orchard trees, and the heat-balance method is noninvasive and usually used on herbaceous plants. Herbaceous means "having the nature of a herb" and a herb is "any seed plant whose stem withers away to the ground after each season's growth, as distinguished from a tree or shrub whose woody stem lives from year to year" (Webster's New World Dictionary of the American Language, 1959). In this chapter, we consider these two methods. The heat-pulse and heat-balance methods, as well as other invasive and noninvasive methodologies to get water flow, have been reviewed by Escalona and Ribas-Carbó (2010).

## 21.1 HEAT-PULSE METHOD

With the heat-pulse method, flow is obtained from the time required for a heat input (the pulse) to travel from its source to a sensor up or down the stem. Measurements are in units of length per time (a velocity). This technique has been used on a variety of plants by researchers since Huber's (1932) pioneering work. The method is illustrated in Figure 21.1 on use in the stem of a kiwifruit vine (*Actinidia chinensis* Planch) (Clothier and Green, 1986). The method is used to schedule irrigations of water for kiwifruit grown in New Zealand. The widely spaced vines (5 × 5 m plant spacing) are grown on a trellis and often develop a full-cover leaf canopy.

http://dx.doi.org/10.1016/B978-0-12-420022-7.00021-5

Copyright © 2014 Elsevier Inc. All rights reserved.

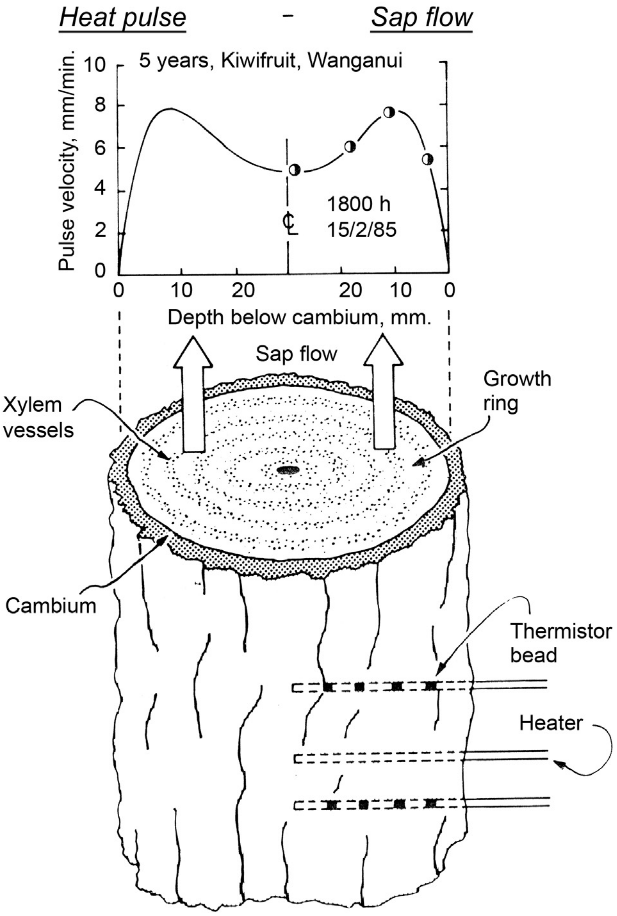
Heat pulse - Sap flow
5 years, Kiwifruit, Wanganui
Pulse velocity, mm/min.
10
8
6
4
2
0
1800 h
15/2/85
℄
0
10
20
20
10
0
Depth below cambium, mm.
Sap flow
Xylem vessels
Growth ring
Cambium
Thermistor bead
Heater

**FIGURE 21.1** Heat-pulse method used to measure sap flow in a kiwifruit stem in Wanganui, New Zealand. Measurements are being taken at four different distances away from the cambium. In the graph in the upper part of the figure, the symbol that looks like the letter C with the letter L through it is the abbreviation used by engineers for "center line". *From Clothier and Green (1986). Reprinted by permission of the American Geophysical Union; John Wiley & Sons, Inc.; and Brent E. Clothier.*

The trellises are arranged in orchards surrounded by tall belts of shelter trees. The kiwifruit plant is unusual in that the water being lost by each individual vine through its massive leaf area (~100 $m^2$) must all travel up a 2 m length of a narrow vine (~50–100 mm diameter). The kiwifruit plant achieves this with a very high velocity of sap flow through the huge xylem vessels in its stem (up to 0.5 mm diameter and 200 mm length). These are arranged in an annular pattern of growth rings.

Heat is used as a tracer to infer the rate of vine water use. A brief pulse of heat (1–2 s) (Green et al., 2003) is supplied to the vine with a heater probe inserted radially into the stem. Thermistors (temperature sensors) placed asymmetrically on either side of the heater (one upstream and one downstream of the heater) measure the propagation of the heat wave (Figure 21.1). [A *thermistor thermometer* is a device for estimating the temperature based on a known relationship of its electrical resistance to temperature (Glickman, 2000, p. 770).] Equidirectional conduction of heat through the woody matrix and convection upward of heat in the moving sap lead to a characteristic pattern of temperature rise at both locations. The time delay for an equal temperature rise at both temperature sensors is recorded. The heat-pulse velocity can be related to the rate of sap movement and so, ultimately, to instantaneous plant water use. The radial pattern of heat flow through the vine can be obtained from paired thermistors placed through the stem.

The most widely used heat-pulse method is the *compensation* heat-pulse method (Edwards et al., 1996). It was originally conceived by Huber and Schmidt (1937). Because time is the primary measurement, the compensation method is robust and suited to field measurement. The time measured is the time required for a temperature difference between sensors to return to zero following a heat-pulse input (Edwards et al., 1996). In the USA, Bloodworth et al. (1955, 1956) were early users of this method and pointed out that Rein (1929) first used the method for studying the rate of flow in blood vessels.

In the method, the temperature rise following the release of a pulse of heat is measured at distances Xu upstream and Xd downstream from the heater (Green and Clothier, 1988). Heat-pulse velocity, $V$ (in units of length/time), is calculated from

$$V = [(\mathrm{Xu} + \mathrm{Xd})/2t], \tag{21.1}$$

where $t$ is the time delay for the temperatures at points Xu and Xd to become equal. If the sap and woody matrix are considered to form a homogeneous medium, then sap flux density, $J$ (in units such as cubic meter per squared meter per second or meters per second), can be calculated from

$$J = P(0.33 + M) \cdot V, \tag{21.2}$$

where $P$ is the wood density (oven dry weight of wood/green volume, in units such as kilogram per cubic meter) and $M$ is the moisture content [(wet weight − oven dry weight)/(oven dry weight)] of the sapwood. (We define sapwood in the next paragraph.) The units in the numerator and denominator for $M$ cancel, so $M$ can be considered to be a pure number, which then can be added to 0.33 in Eqn (21.2). The kilogram in the numerator of $P$ can be changed to cubic meter assuming that the density of water is 1 g/cm$^3$, which then gives units of $J$ in length/time, such as meter per second.

Sap velocity varies with depth into the stem. To calculate volumetric flow rates, sap flux density is measured at different distances away from the cambium, such as shown in Figure 21.1, where it is measured at four different distances. [Remember the *vascular cambium* is a meristem (a tissue that divides to make new cells), which produces phloem on the outside and xylem (wood) on the inside. See Figure 17.3 for the location of the vascular cambium. It is present in stems that undergo secondary growth.] A second-order least squares regression equation is fitted to the sap flux density measurements. The resulting flux profile is then integrated over the sapwood cross-section to calculate the volume flux $Q$ (in units such as cubic decimeter per day) (Green and Clothier, 1988, 1995)

$$Q = 2\pi \int_{H}^{R} rJ(r)\mathrm{d}r, \tag{21.3}$$

where $J(r)$ is the sap flux at radial depth $r$ in a stem of cambium radius $R$ and heartwood radius $H$. Esau (1977, pp. 511–512) defines the *heartwood* as the inner layers of secondary xylem that have ceased to function in conduction. It is generally darker colored than the functioning sapwood. Esau (1977, p. 524) defines the *sapwood* as the outer part of the wood that contains living cells and in which conduction of water takes place. It is generally lighter colored than the heartwood (Esau, 1977, pp. 511–512 and 524).

Equation 21.2 underestimates sap flow. This is a result of blockage of the flow by the probes placed in the sapwood. A correction to Eqn (21.2) needs to be calculated that depends on the wound width. The theoretically derived correction factor is then used to correct the heat-pulse measurements for probe-induced effects of wounding. Without such a correction, the heat-pulse measurements of sap flow are typically low by a factor of ≥50% (Green and Clothier, 1988; Green et al., 2003).

The accuracy of the heat-pulse measurements has been checked by comparing them with independent measurements of sap flow. A kiwifruit vine (*Actinidia deliciosa*) and an apple tree (*Malus sylvestris* × Red Delicious) each were cut off at the ground level and the ends placed in a container of water. The drop in water level was measured, while simultaneous heat-pulse measurements were made. The heat-pulse measurements showed a good agreement with the physical measurement of the quantity of water imbibed from the container (Green and Clothier, 1988). Figure 21.2 shows the heat-pulse method in use on an apple tree in the field. Note in Figures 21.1 and 21.2 the asymmetrical placement of the

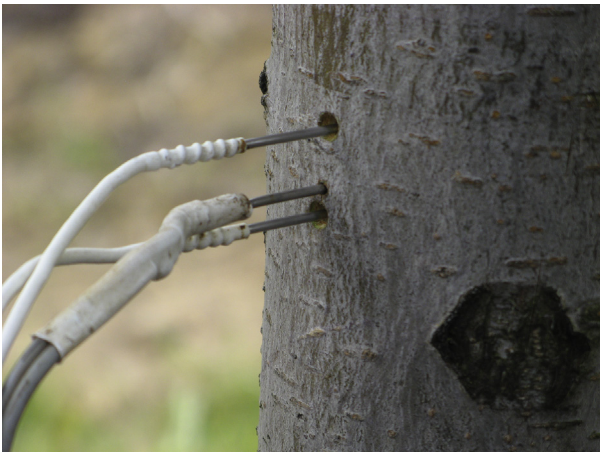

**FIGURE 21.2** The heat-pulse method in use on an apple tree. *Photograph courtesy of Steven R. Green, The New Zealand Institute for Plant and Food Research, Ltd., Palmerston North, New Zealand.* (For color version of this figure, the reader is referred to the online version of this book.)

thermistors on either side of the heater. In Figure 21.2, the heater is the middle probe.

An alternative method to the compensation heat-pulse method was developed by Cohen et al. (1981) and is called the *T-max* heat-pulse method (Green et al., 2003). It relies on measuring the time for the maximum temperature rise to be recorded by a single sensor located a distance downstream from a line heater. The theory for the method is reviewed by Green et al. (2003), who also give correction factors for both the compensation and T-max heat-pulse methods. The correction factors were confirmed by comparing heat-pulse measurements in the trunk of a willow (*Salix alba* L.) and a poplar (*Populus deltoides* W. Bartram ex. Marsh), against the actual rates of transpiration determined from measured weight loss of the trees growing in large lysimeters. On a daily basis, both heat-pulse measurements were found to be within 5–10% of the actual transpiration. The compensation method accurately measured flows close to 2 cm/h. The T-max method had difficulty in resolving any flows slower than about 10 cm/h.

The heat-pulse technique has several advantages. It can be used to measure sap flow in tree stems with minimal disruption to the sap stream. The measurements are reliable and accurate, use relatively simple and inexpensive instrumentation, provide a good time resolution of sap flow, and are well suited to automatic data collection and storage (Green et al., 2003). Sequential or simultaneous measurements on numerous trees are possible. This permits the estimation of transpiration losses from whole stands of trees. Other advantages of the method are the following: (1) one can get flow at different depths into the stem; probes can be inserted into the stem from 0.5 to 4 in (13–102 mm); (2) one can measure sap flow in thick stems (trees); (3) measurements are fast; and (4) roots can be measured, if they are woody. Clothier and Green (1992) and Green and Clothier (1995) were the first to obtain measurements of sap flow in roots (Figure 21.3). They used the heat-pulse technique to monitor sap flow in the stem and several large roots of kiwifruit vines to see how the flow of water in roots responded with local changes in soil water availability. They found that inactive roots in dry soil were able to recover their activity quickly when irrigated. In 2013, a miniature sap-flow sensor using

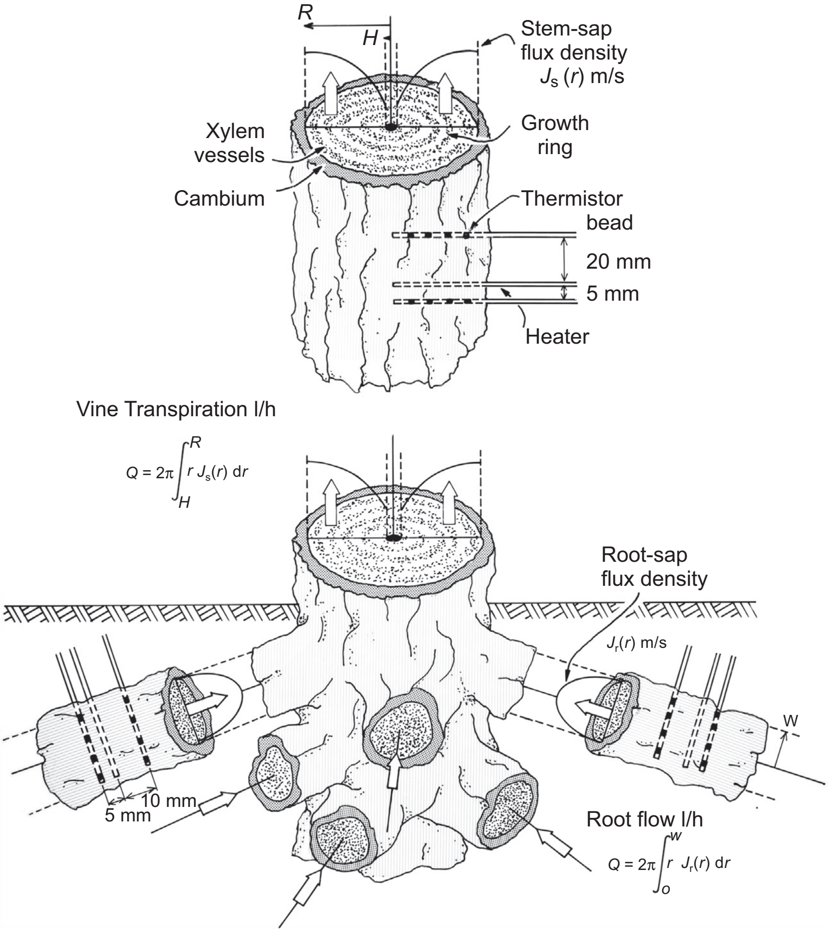
R
H
Stem-sap flux density $J_s(r)$ m/s
Xylem vessels
Growth ring
Cambium
Thermistor bead
20 mm
5 mm
Heater
Vine Transpiration l/h
$Q = 2\pi \int_H^R r\,J_s(r)\,dr$
Root-sap flux density
$J_r(r)$ m/s
W
10 mm
5 mm
Root flow l/h
$Q = 2\pi \int_o^W r\,J_r(r)\,dr$

**FIGURE 21.3** A schematic diagram of the arrangement of the heat-pulse sensors in the stem and two probed roots of a kiwifruit vine. For abbreviations, see the text. *From Clothier and Green (1992). Reprinted by permission of Brent E. Clothier.*

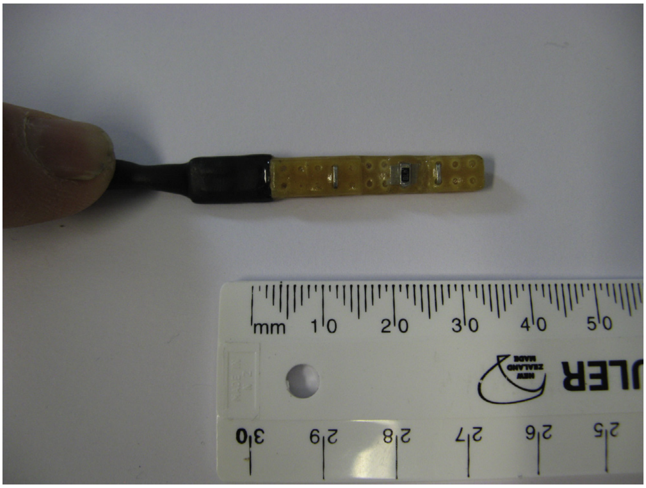

**FIGURE 21.4** Miniature sap-flow sensor that uses the heat-pulse method. *Photograph courtesy of Steven R. Green, The New Zealand Institute for Plant and Food Research, Ltd., Palmerston North, New Zealand.* (For color version of this figure, the reader is referred to the online version of this book.)

the heat-pulse method became available from Tranzflo NZ, Ltd, Palmerston North, New Zealand (Figure 21.4).

The disadvantages of the heat-pulse technique are that (1) it is an invasive technique and a small amount of xylem tissue is damaged by the probes; and (2) one needs to adjust readings for the area of the probes. Also, there has been confusion about the terminology used in the heat-pulse method, and different units are used (e.g., cm $h^{-1}$, $cm^3$ $s^{-1}$ $cm^{-2}$; $10^{-3}$ kg $m^{-1}s^{-1}$) (Edwards et al., 1996). Reports on the heat-balance method, which we now turn to, have been more consistent, because of the simplicity of the underlying theory (Edwards et al., 1996).

## 21.2 HEAT-BALANCE METHOD

The heat-balance method is ideal for thin-stemmed, barkless species such as herbaceous plants. In the heat-balance method, flow is obtained by balancing heat fluxes into and out of the stem. The units of the heat-balance method are mass per unit time. Note that the units of the heat-pulse method (usually expressed as length/time) and heat-balance method (mass/time) are fundamentally different and cannot be compared directly.

There are two approaches for the heat-balance method. In one approach, used for trees, heat input to a segment of the trunk (stem) is automatically and continuously adjusted to maintain a constant temperature difference between the heated segment and unheated trunk (stem) below. As sap flow changes (transpiration changes), the required heat input must also change in order to provide the basis for stem-flow measurements (Baker and van Bavel, 1987).

Another approach is used for herbaceous plants, and it is the constant-heating method. This method was developed by Sakuratani (1981, 1984) in Japan. In this approach, the heat input from an external annular (round) heater is kept constant and fluxes of heat out of the system are calculated from measured temperature gradients, enabling direct calculation of the mass flow rate of water in the stem. Stem-flow gauges, called Dynagages, made by Dynamax (Houston, Texas), are based on this method. They won the Agricultural Engineering Society's 1989 award for outstanding innovations in product technology (Ploskonka, 1990). The President of Dynamax is Michael van Bavel, the son of C.H.M. van Bavel, who helped to design the stem-flow gauges. (For a biography of C.H.M. van Bavel, see the Appendix, Section 21.3.) In this section, we shall focus on theory of these gauges, and we follow the analysis of Baker and van Bavel (1987).

Figure 21.5 shows the physical situation. A flexible heater, 10 mm in length, is wrapped around a segment of a stem, and it provides a small, steady, known amount of heat. Foam insulation, with a thermal conductivity much lower than that of the plant tissue, encloses the

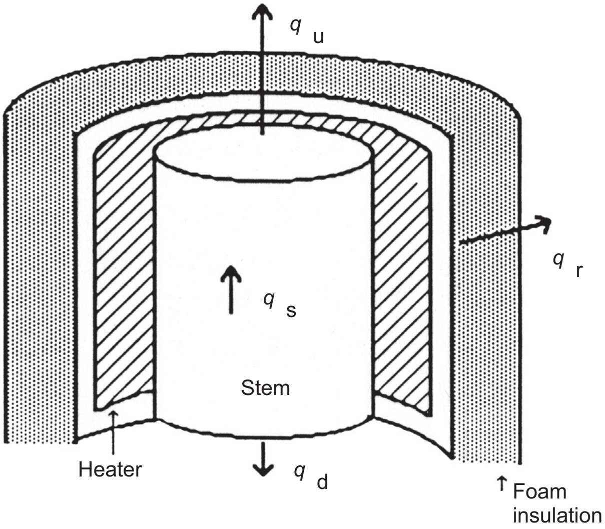

**FIGURE 21.5** Heat balance of the heated stem segment using the heat-balance method. It is a schematic diagram, not drawn to scale. The length of the heater is 10 mm. The thickness of the insulation is 12 mm and its length is 50 mm. Symbols refer to Eqns (21.4–21.6); $q_s$ is the rate of heat transport by the sap stream, given by $F$ in Eqn (21.8). *From Baker and van Bavel (1987). This material is used by permission of Wiley-Blackwell and John M. Baker.*

heated segment and extends for several centimeters both above and below the heated segment. Heat then moves by conduction upward, downward, or in the radial direction, and from these heat fluxes, the rate of heat transported on a mass basis by the sap stream can be calculated.

Now, let us look at each of these heat flows.

## 21.2.1 Heat Up

The conductive heat upward ($q_u$, in units of watts) can be calculated with Fourier's law for a one-dimensional heat flow. (Fourier's law is a linear flow law, and we presented it in Chapter 7 in Table 7.1.)

$$q_u = k_{st} A(\mathrm{d}T/\mathrm{d}X), \tag{21.4}$$

where

$k_{st}$ = the thermal conductivity of the stem tissue (W/m/K) (remember a watt is a joule per second and a watt is a unit of power; power = work/time),

$A$ = the cross-sectional area of the stem (m$^2$),

$\mathrm{d}T/\mathrm{d}X$ = temperature gradient (K/m),

$\mathrm{d}T/\mathrm{d}X$ is obtained from the output of two differentially wired thermojunctions (thermocouples) which are 3 mm apart and in direct contact with the stem, the lower of the two being immediately above the heater. We assume (due to insulation) that the gradient of temperature is uniform over the cross-section.

## 21.2.2 Heat Down

Another pair of thermojunctions is located below the heater and allows the determination of the conductive flux downward, $q_d$, in units of watts:

$$q_d = k_{st} A(\mathrm{d}T/\mathrm{d}X), \tag{21.5}$$

where $k_{st}$, $A$, and $\mathrm{d}T/\mathrm{d}X$ have been defined for Eqn (21.4).

In the equations for upward and downward flux, the value of $A$ must be known from an actual measurement, and the value of $k_{st}$ (thermal conductivity of stem) is taken to be 0.54 W/(m K), a value that is the average of measured values for herbaceous species, and is slightly less than that of water. From Table 3.1, we see that water at 20 °C has a thermal conductivity of 0.00144 cal/cm/s/°C. We can convert 0.54 W/m/K to units of calories per centimeter per second per degree as follows knowing from Chapter 2 that 1 cal = 4.184 J and 1 W = 1 J/s, so 1 W = 0.239 cal/s (Schaum, 1961, p. 153):

[0.54 W/(m K)] (0.239 cal/s/W) (1 m/100 cm) = 0.0012906 cal/cm/s/K.

We note that this is a correct conversion, even though Table 3.1 has degrees centigrade for thermal conductivity and we are using degrees Kelvin in the analysis of the theory for the heat-balance method. Lide (1994) gives the conversion on pp. 1–38. He says that, to convert watts per meter per Kelvin to calories per centimeter per second per degrees centigrade, we multiply by 0.00239006. This is what we have done in the above conversion.

This value, 0.0012906 cal/cm/s/k for the thermal conductivity of the stem, is not much different from 0.00144 cal/cm/s/K. So we can accept the assumption that the thermal conductivity for herbaceous species is slightly less than that of water.

### 21.2.3 Radial Flow

The radial outward flow of heat is calculated from the voltage output of a thermopile composed of eight thermojunctions (thermocouples) in series located on either side of a 2-mm cork sheath between the heater and the foam insulation. A *thermopile* is an instrument consisting of a series of thermocouples, used for measuring minute changes in temperature or for generating thermoelectric current (Webster's New World Dictionary of the American Language, 1959). The flux is approximated by Eqn (21.6), the integrated form of the equation for radial heat flow ($q_r$, in units of watts) in a cylinder of infinite length (Carlslaw and Jaeger, 1959).

$$q_r = 2\pi k_{co} L(T_i - T_o)/\ln(r_i/r_o), \tag{21.6}$$

where

$k_{co}$ = the thermal conductivity of cork (W/m/K),
$L$ = length of the heated segment (m),
$T_i$ = temperature at the inner surface of the cork sheath (K),
$T_o$ = temperature at the outer surface of the cork sheath (K),
$r_i$ = the radius of the inner surface of the cork sheath (m),
$r_o$ = radius of the outer surface of the cork sheath (m).

All parameters in Eqn (21.6) ($\pi$, $k_{co}$, $L$, $T_i$, $T_o$, $r_i$, $r_o$) are constant and can be combined giving us Eqn (21.7), below. The conversion factor relates the thermopile output ($E$) to the temperature difference ($T_i - T_o$), and one gets a simple sheath "conductance", $K_{sh}$, with the units of watts per voltage output ($W/V_o$, the subscript signifies voltage output from the thermopile), so that Eqn (21.6) may be rewritten:

$$q_r = K_{sh}E, \tag{21.7}$$

where

$K_{sh}$ = sheath conductance ($W/V_o$),
$E$ = voltage output from thermopile ($V_o$).

Subtraction of the three fluxes (up, down, and radially) from the known heat input gives the heat transported by the sap stream. To calculate the mass flow rate (grams per second) of water from the sap heat transport, it is necessary to know the temperature difference between the water entering and leaving the heated portion of the stem. To obtain this value, the upper thermojunction nearest the heater is differentially wired to the lower junction nearest the heater. Again, the assumption of radial thermal homogeneity is made. The temperature difference, multiplied by the heat capacity of water (not that of the stem), is divided into the sap heat transport, yielding the mass flow rate of the sap itself.

$$F = \left(P - q_u - q_d - q_r\right) / \left[C_p\left(T_{out} - T_{in}\right)\right], \tag{21.8}$$

where

$F$ = sap-flow rate (g/s),

$P$ = power input to the heater (W),

$C_p$ = heat capacity of the xylem sap (J/g/K),

$T_{out}$ = temperature of the junction above the heater (K),

$T_{in}$ = temperature of the junction below the heater (K), and $q_u$, $q_d$, and $q_r$ are as defined above, all in units of watts.

Figure 21.5 shows $F$ as $q_s$, the rate of heat transport by the sap stream with units of grams per second. The value $K_{sh}$, required in Eqn (21.7) ($q_r = K_{sh}E$), is calculated from Eqn (21.8) by setting $F = 0$ and making measurements on a stem that has been excised and sealed with vaseline to ensure that the sap-flow rate is zero. This is a zero-set procedure, not to be confused with a calibration. If $F = 0$, we can solve for $q_r$ and then put $q_r$ in Eqn (21.7) and solve for $K_{sh}$.

In the method, we are assuming that the heat capacity of the xylem sap is the heat capacity of water. We also are assuming that the thermal conductivity of the stem is the same for all herbaceous plants. We are assuming that most heat is transported by the xylem. Also, we are assuming the whole cross-section is heated uniformly across the stem. The method is absolute, not transient, and it needs no calibration.

The heat-balance method has the advantages of providing direct, accurate, fast, and noninvasive measurements of sap flow in stems of plants. No calibration is required. Like the heat-pulse method, not only can the sap-flow rate of individual plants be determined, but also the transpiration rate of an entire field can be determined with the heat-balance method. Ham et al. (1990) used heat-balance gauges to determine near-instantaneous measurements of transpiration of cotton (*Gossypium hirsutum* L.) in Lubbock, Texas. Transpiration on a unit land area basis was calculated by normalizing stem-flow measurements by leaf area or plant density. However, the heat-balance method does have the disadvantage of overestimating high flow rates. To correct this problem, one can use larger heaters (20 mm instead of 10 mm). The method also requires a minimum diameter of a stem, but sensors have been miniaturized so that stems 2 mm in diameter can be measured. The method cannot be used on roots, as can the heat-pulse method.

The heat-balance method also cannot measure low flow rates. The gauge has a good accuracy when sap-flow rates are ≥20 g/h (Zhang and Kirkham, 1995). Sap flow in both dicotyledonous (dicots) and monocotyledonous (monocots) plants can be measured with the heat-balance method, even though they differ in stem anatomy. Dicots usually have the xylem tissue oriented in a cylinder (in cross-section) around a central pith of the stem, while monocots have vascular bundles that are scattered across a stem. (See Chapter 17, Section 17.1, for the difference in stem anatomy between dicots and monocots.) The conducting cylinder of dicots, therefore, is close to the heat of the gauge. Zhang and Kirkham (1995) found that the heat-balance method could be used on monocots and dicots. The limiting factor was the sap-flow rate. The monocot in their study [*Sorghum bicolor* (L.) Moench] had a low sap-flow rate even under well watered conditions (<18.9 g/h). The well watered sunflower (*Helianthus annuus* L.), a dicot under the same conditions, had a sap-flow rate of 64.7 g/h. However, this sap-flow rate was less than sap-flow rates for woody plants under field conditions, which are often >100 g/h. Zhang and Kirkham (1995) concluded that sap-flow rate is more important than stem anatomy in determining the accuracy of the heat-balance gauge.

## 21.3 APPENDIX: BIOGRAPHY OF C.H.M. VAN BAVEL

Cornelius H.M. van Bavel, a pioneer in the study of the soil–plant–atmosphere continuum using experimental and simulation methods, was born on September 15, 1921, in Ginneken, a small town just south of Breda, The Netherlands. In September 1938, he entered Wageningen Agricultural College (now University), where he obtained an engineering degree (Ir.) in horticulture in October 1945 (Brown, 1988; van Bavel, 2008), following a turbulent and stressful five years of Nazi occupation (van Bavel, 2000a). During World War II, he distributed underground papers and met with other individual opponents of the German occupiers. He helped to prepare false identity papers and provide money or food for individuals in hiding, who had escaped from concentration camps. They got around by train or bicycle. The work was risky, and there was a continuous battle in the air, and he very nearly lost his life a couple of times (C.H.M. van Bavel, personal communication, May 8, 2011). Wageningen Agricultural College was closed in 1943 by the German authorities (van Bavel, 2008), and the students were ordered to report for work in Germany. That was even more dangerous, but he, with many others, ignored this command and he was able to survive. Some of his professors also were active in the resistance movement and had to leave their homes and go into hiding (van Bavel, 2008).

Supported by a generous grant from The Netherlands-America Foundation, he was able to come to the USA and entered Iowa State College (now University) in January 1946, and received his master's degree in soil physics under the direction of Don Kirkham in December 1946. On May 27, 1947, he married, in The Netherlands, Margaret Lips, whom he became engaged to while in the war-torn Netherlands. She is an artist specializing in jewelry work (van Bavel, 2008). He was an agronomic consultant in La Paz, Bolivia, in 1947, and he reentered Iowa State College in February 1948, and obtained a Ph.D. degree in soil physics under Don Kirkham in December 1949. For his Ph.D. research, he investigated the stability of soil aggregates and means for increasing aggregation. He has a patent, dated May 28, 1957, and entitled "Soil stabilizer and soil treated thereby" (USA Patent No. 2,793,960) resulting from this research. At Iowa State, he also worked with Kirkham on developing an electrical analog of the auger-hole method for measuring soil permeability. He also explored the possibilities of numerical simulation for solving problems, an area that he became more interested in, when electronic computers became available about 15 years after he left Iowa State (van Bavel, 2000a).

After receiving his Ph.D., van Bavel was an Associate Professor of Agronomy at North Carolina State University in Raleigh. There he studied the energy balance of a transpiring plant surface and how its water use could be derived from meteorological data. Howard Penman in England had collected data on the water use by turf, from which he formulated the famous Penman equation in 1948. (See the Appendix of Chapter 28 for a biography of Penman.) A visit by Penman to Raleigh in 1951 was the prelude for a number of measurements in the North Carolina environment of evapotranspiration that van Bavel made (van Bavel, 2008). Van Bavel was instrumental in undertaking analysis of regional drought incidence in the Southeastern states (American Society of Agronomy, 1964). In Raleigh, he studied the limits to plant growth when oxygen and water were insufficiently available to the root system. He also investigated the practical implementation of the neutron scattering method for measuring soil moisture as well as a similar method to measure soil density with gamma radiation (van Bavel, 2008).

In September 1958, he moved to the new US Water Conservation Laboratory in Tempe, Arizona, where he was Chief Physicist. There, he instigated an intensive study of evapotranspiration and related soil and climatic processes (American Society of Agronomy, 1964). He invented, along with two colleagues, the first leaf resistance meter, called a porometer. The paper describing the porometer (van Bavel et al., 1965) is a citation classic (Institute for Scientific Information, 1983). It became the basis for a commercial model made by Li-Cor, Inc., Lincoln, Nebraska, which is no longer manufactured by Li-Cor. However, the porometer is marketed by Delta-T Devices in England. It uses the transient method of measurement and the use of porous plates for its calibration. (See Chapter 24 for a description of porometers.) Also at Tempe, he developed with Ray Jackson a desert survival kit (Jackson and van Bavel, 1965). (See the Appendix of Chapter 26 for a biography of Jackson.) The kit, called a solar survival still, was awarded a US patent.

Missing the opportunity to work with students, he decided to move in 1967 to Texas A&M University in College Station, where he was Professor in the Department of Soil and Crop Sciences. There he was influenced by the publications of C.T. de Wit and his students in Wageningen and started to focus on computer-assisted numerical modeling. He also codirected a University-wide program involving cogeneration of energy, desalination of irrigation water, and food production (Council for Agricultural Science and Technology, 1986). At Texas A&M, he coinvented a fluid roof solar greenhouse and developed design principles of controlled environmental facilities and of commercial greenhouses (American Society of Agronomy, 1987). While in Texas, he and his family were active citizens, not only in local environmental politics but also in trying to practice what they preached. They traveled by bicycles, used a compact car, and installed a solar water heating system in their home (van Bavel, 2008).

In 1983, van Bavel accidentally discovered an obscure description of a method done in Japan for attaching a sap-flow meter to the stem of a plant and using it to monitor the rate of transpiration. This was the basis for the work that he and his student, John Baker, did with sap-flow gauges (Baker and van Bavel, 1987). They were responsible for the design and first tests of a robust, constant heat stem-flow gauge that was suitable for field work. From this work, it was a logical step to develop it commercially, which was done in 1986 by Dynamax, Inc., a company started by his son, Michael van Bavel. Everyone now in the plant–water relation field is familiar with the method and hundreds of gauges are in use over the entire world (van Bavel, 2008).

Van Bavel worked on temporary duty at the University of California in Riverside in 1963, the Center for Ecophysiological Studies in Montpellier, France, in 1973 (American Society of Agronomy, 1987), the University of Reading in England, and the Hokuriku Agricultural Experiment Station in Joetsu, Japan (van Bavel, 2008).

His accomplishments were recognized in 1958 when he was awarded the United States Department of Agriculture Superior Service Award (American Society of Agronomy, 1964). He is Fellow of the American Society of Agronomy (1963) and Soil Science Society of America (SSSA)

(1963). He received the SSSA Soil Science Award (1985) (American Society of Agronomy, 1987) and the Faculty Distinguished Achievement Award in research in 1986 from Texas A&M University (Fette, 1986).

Van Bavel retired on January 31, 1987, after 19 years of service at Texas A&M University (American Society of Agronomy, 1987). In retirement, he and his wife have traveled widely around the world. He also has translated three books written in Dutch by Hugo de Vries (1848–1935) during three long journeys to the USA in 1904, 1906, and 1912 (van Bavel, 2000b). De Vries was a famous Dutch botanist known for his studies on mutation (Benton, 1971). The three travel books contain detailed impressions obtained by a European plant scientist (de Vries) of the emerging institutes of higher learning in the US, the agricultural experiment stations, the land grant colleges, and the programs of the US Department of Agriculture.

He and Margaret, who have five sons, three daughters, and 11 grandchildren, reside in Kerrville, Texas, where two of their sons live.

## References

American Society of Agronomy, van Bavel, C.H.M., 1964. Fellows of the american society of agronomy elected in 1963. Agron. J. 56, 98–99.

American Society of Agronomy, van Bavel, C.H.M., June 1987. Retirements. Agron. News, 9. American Society of Agronomy: Madison, Wisconsin.

Baker, J.M., van Bavel, C.H.M., 1987. Measurement of mass flow of water in the stems of herbaceous plants. Plant Cell Environ. 10, 777–782.

Benton, W., 1971. De Vries, Hugo. Encyclopaedia Britannica 7, 344.

Bloodworth, M.E., Page, J.B., Cowley, W.R., 1955. A thermoelectric method for determining the rate of water movement in plants. Soil Sci. Soc. Am. Proc. 19, 411–414.

Bloodworth, M.E., Page, J.B., Cowley, W.R., 1956. Some applications of the thermoelectric method for measuring water flow rates in plants. Agron. J. 48, 222–228.

Brown, K.W., 1988. C.H.M. van Bavel—soil physicist and environmental agronomist. J. Agron. Educ. 17, 139–140.

Carslaw, H.S., Jaeger, J.C., 1959. Conduction of Heat in Solids, pp. 188–213. Clarendon Press, Oxford.

Clothier, B., Green, S., 1986. Heat pulse—sapflow. Eos Trans. Am. Geophys. Union 67 (15) cover and p. 187.

Clothier, B., Green, S., 1992. Heat Pulse Down-under…the Soil. In: WISPAS. A Newsletter about Water in the Soil–Plant–Atmosphere System, vol. 53, 3.

Cohen, Y., Fuchs, M., Green, G.C., 1981. Improvement of the heat pulse method for determining sap flow in trees. Plant Cell Environ. 4, 391–397.

Council for Agricultural Science and Technology, 1986. van Bavel in the vanguard. Sci. Food Agr. 4 (2), 27.

Edwards, W.R.N., Becker, P., Čermák, J., 1996. A unified nomenclature for sap flow measurements. Tree Physiol. 17, 65–67.

Esau, E., 1977. Anatomy of Seed Plants, Second ed. Wiley, New York.

Escalona, J.M., Ribas-Carbó, M., 2010. Methodologies for the measurement of water flow in grapevines. In: Delrot, S., Medrano, H., Or, E., Bavaresco, L., Grando, S. (Eds.), Methodologies and Results in Grapevine Research. Springer, Dordrecht, pp. 57–69.

Fette, B., 1986. Faculty/staff honored for dedication and talent. Tex. Aggie 67 (4), 26–27.

Glickman, T.S. (Ed.), 2000. Glossary of meteorology. American Meteorological Society, Boston.

Green, S.R., Clothier, B.E., 1988. Water use of kiwifruit vines and apple trees by the heat-pulse technique. J. Exp. Bot. 39, 115–123.

Green, S.R., Clothier, B.E., 1995. Root water uptake by kiwifruit vines following partial wetting of the root zone. Plant Soil 173, 317–328.

Green, S., Clothier, B., Jardine, B., 2003. Theory and practical application of heat pulse to measure sap flow. Agron. J. 95, 1371–1379.

Ham, J.M., Heilman, J.L., Lascano, R.J., 1990. Determination of soil water evaporation and transpiration from energy balance and stem flow measurements. Agr. For. Meteorol. 52, 287–301.

Huber, B., 1932. Beobachtung und Messung pflanzlicher Saftströme. Berichte der Deutschen Botanische Gesellschaft 50, 89–109.

Huber, B., Schmidt, E., 1937. Eine Kompensationsmethode zur thermoelektrischen Messung langsamer Saftströme. Berichte der Deutschen Botanische Gesellschaft 55, 514–529.

Institute for Scientific Information, Van Bavel, C.H.M., Nakayama, F.S., Ehrler, W.L., 1983. Measuring transpiration resistance of leaves. Plant Physiol. 40, 535–540. This Week's Citation Classic. Current Contents, Agr. Biol. Environ. Sci. 14(27); 24.

Jackson, R.D., van Bavel, C.H.M., 1965. Solar distillation of water from soil and plant materials: simple desert survival technique. Science 149, 1377–1379.

Lide, D.R. (Ed.), 1994. CRC Handbook of Chemistry and Physics, 75th ed. CRC Press, Boca Raton, Florida.

Sap-flow gauge. Advertisement. In: Ploskonka, C.A. (Ed.), Agr. Eng. 71 (2), 21 (one page only).

Rein, H., 1929. Die Thermo-Stromuhr, II. Mitteilung. Arbeitsbedingungen und Arbeitsmöglichkeiten im Tierversuch. Zeitschrift für Biologie 89, 195–201.

Sakuratani, T., 1981. A heat balance method for measuring water flux in the stem of intact plants. J. Agr. Meteorol. 37, 9–17.

Sakuratani, T., 1984. Improvement of the probe for measuring water flow rate in intact plants with the stem heat balance method. J. Agr. Meteorol. 40, 273–277.

Schaum, D., 1961. Theory and Problems of College Physics, Sixth ed. Schaum Publishing, New York.

van Bavel, C.H.M., November 2, 2000a. Statement for Book of Letters—Kirkham Conference 2000. Iowa State University, Ames. Available from M.B. Kirkham, Dept. Agronomy, Kansas State Univ., Manhattan, KS 66506.

van Bavel, C., 2000b. Hugo de Vries. Travels of a Dutch Botanist in America 1904–1912. Pecan Valley Press, Center Point, Texas, 58 pp.

van Bavel, C., 2008. An Account of My Life and Work 1921–2008. Self published. 30 pp.

van Bavel, C.H.M., Nakayama, F.S., Ehrler, W.L., 1965. Measuring transpiration resistance of leaves. Plant Physiol. 40, 535–540.

Vieweg, G.H., Ziegler, H., 1960. Thermoelektrische Registrierung der Geschwindigkeit des Transpirationsstromes I. Berichte der Deutschen Botanischen Gesellschaft 73, 221–226.

Webster's New World Dictionary of the American Language, College ed., 1959. World Publishing, Cleveland and New York.

Zhang, J., Kirkham, M.B., 1995. Sap flow in a dicotyledon (sunflower) and a monocotyledon (sorghum) by the heat-balance method. Agron. J. 87, 1106–1114.

CHAPTER

# 22

# Electrical Analogs for Water Movement through the Soil—Plant—Atmosphere Continuum

In the Preface, we noted that this book follows water as it moves through the soil—plant—atmosphere continuum (SPAC). John R. Philip pioneered the concept of the SPAC for water transfer. (See the Appendix of Chapter 13 for a biography of Philip.) He defined the SPAC as follows (Philip, 1966, p. 246): "Because water is generally free to move across the plant—soil, soil—atmosphere, and plant—atmosphere interfaces it is necessary and desirable to view the water transfer system in the three domains of soil, plant, and atmosphere as a whole. Under some circumstances, and for some purposes, we can, of course, isolate certain parts of the total system and study only certain modes of water transfer; but a general appreciation of the plant water relations of the whole plant in nature must involve the soil—plant—atmosphere continuum (SPAC)". In an earlier paper, Philip (1957) discusses the SPAC and diagrams it (Figure 22.1), but he does not use the abbreviation SPAC.

Philip (1966, p. 257) credits Gradmann (1928) for providing the initial steps toward the formulation of the SPAC. Gradmann recognized the existence of systematic gradients of potential in the plant and atmosphere, with continuity of potential at the interface. Gradmann's Figure 1 (1928, p. 3; reproduced here as Figure 22.2) represents the "Schema des Saugkraftabfalles" ("Diagram of the Decrease in Suction Force"), and it has three lines: AB, BC, and CD. Line CD shows the fall in suction force between the air and the surface of the plant; line BC shows the fall from the outside surface of the plant to the plant; and line AB shows the fall from the plant to the soil. The total drop goes from 1000 atm (in the air) to 0 atm (in the soil). Gradmann's insight was neglected by other workers for nearly

http://dx.doi.org/10.1016/B978-0-12-420022-7.00022-7

Copyright © 2014 Elsevier Inc. All rights reserved.

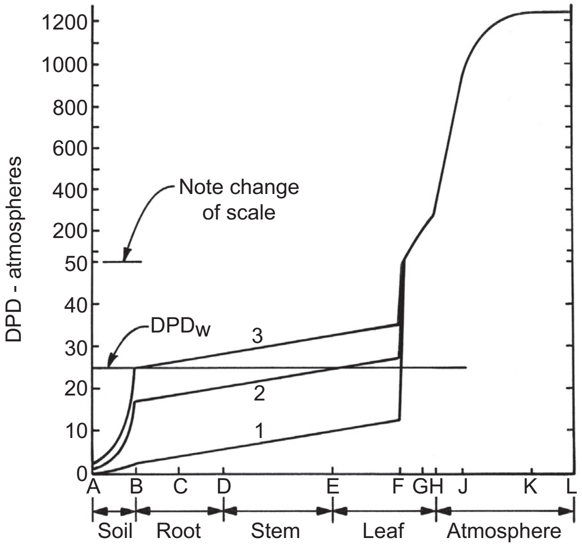

**FIGURE 22.1** The soil-plant-atmosphere continuum, showing energy profiles, (1) during normal transpiration; (2) during temporary wilting; (3), at permanent wilting. DPD = diffusion pressure deficit. Points on the transpiration path: A. Soil (a definite distance from plant root); B. Surface of root hairs and of absorbing epidermal cells; C. Cortex; D. Endodermis; DE. Vessels and tracheids in the xylem; E. Leaf veins; F. Mesophyll cells; FG. Intercellular space and substomatal cavity; GH. Stomatal pore; HJ. Laminar sublayer; JK. Turbulent boundary layer; KL. Free atmosphere. *Redrawn from Philip (1957). From Kirkham (2002, Figure 1, p. 328). Reproduced by permission of the American Geophysical Union, CSIRO Publishing, and John Wiley and Sons.*

20 years, when van den Honert (1948) drew attention to it in the English literature (Kirkham, 2002). Later, in this chapter, we shall return to van den Honert's analysis.

Electrical analogs have long been used to study the movement of water in soil. The analogy between the flow of electricity through conducting media and the flow of water through porous media (i.e., soil) was pointed out by Slichter (1899), a mathematician at the University of Wisconsin. The analogy was later expanded to include the movement of water through the entire SPAC. We now consider why the analogy works and its application.

## 22.1 THE ANALOGY

The analogy can be seen when we compare Ohm's law with Darcy's law. Ohm's law states (Kirkham and Powers, 1972, p. 183) that

$$I = -\sigma A(V_2 - V_1)/L = V/R, \tag{22.1}$$

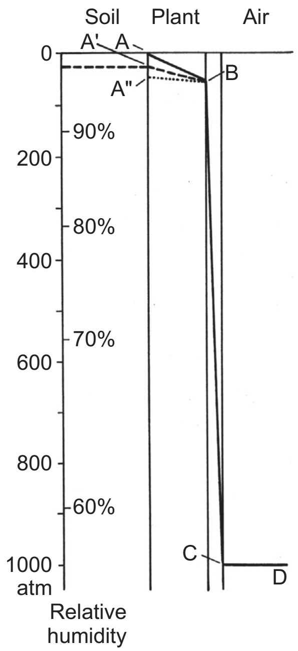

**FIGURE 22.2** Diagram of the decrease in suction force. *Redrawn from Gradmann, 1928; translated into English; original German words at the top were Boden, Pflanze, Luft, and the "relative humidity" at the bottom was abbreviation R.F. by Gradmann. From Kirkham (2002, Figure 2, p. 328). Reproduced by permission of the American Geophysical Union, CSIRO Publishing, and John Wiley and Sons.*

where

$I$ = quantity of electricity flowing per unit time (coulombs of electricity per unit time) (coulombs per second or amperes),
$\sigma$ = specific electrical conductivity or electrical conductivity (Siemens per centimeter),
$L$ = length of the element through which current flows (centimeters),
$A$ = cross-sectional area of the element (square centimeter),
$V_2$ and $V_1$ = voltages (volts),
$(V_2 - V_1)/L$ = potential gradient,
$R$ = resistance (ohms).

For water flow in porous media (Darcy's law), we can write (Kirkham and Powers, 1972, p. 183)

$$Q = -KA(\phi_2 - \phi_1)/L, \tag{22.2}$$

where

$Q$ = cubic centimeter of water flowing per unit time (cubic centimeter per second),
$K$ = hydraulic conductivity (centimeter per second),
$L$ = length (centimeter),
$A$ = cross-sectional area (square centimeter),
$\varphi_2$ and $\varphi_1$ = hydraulic heads (centimeter),
$(\varphi_2 - \varphi_1)/L$ = hydraulic gradient.

We immediately see the close analogy between Ohm's law (Eqn (22.1)) and Darcy's law (Eqn (22.2)). (For a biography of Ohm, see the Appendix, Section 22.8.)

## 22.2 MEASUREMENT OF RESISTANCE WITH THE WHEATSTONE BRIDGE

To measure $R$ (resistance in ohms; the Greek letter capital omega, Ω, is used to symbolize resistance in ohms), we use a Wheatstone bridge, which is an instrument for measuring the value of an unknown resistance by comparing it with a standard. This method, devised in 1833 by S. Hunter Christie, was brought to public attention by the English physicist, Sir Charles Wheatstone (1802–1875) and has remained associated with his name (Hausmann and Slack, 1948, p. 388). (For a biography of Wheatstone, see the Appendix, Section 22.9.) The Wheatstone bridge is the most convenient, and at the same time accurate, way of measuring resistances of widely different values (Ingersoll et al., 1953). It works on the principle of a divided circuit, which is illustrated in Figure 22.3. The current from the battery divides between the two branches abc and adc. Because the potential drop is the same along the two branches, corresponding

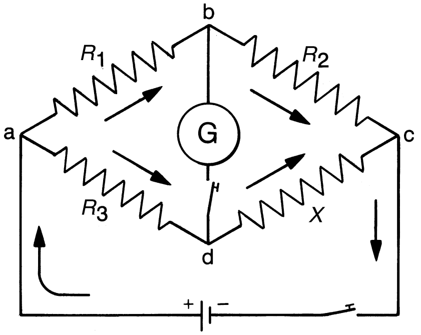

**FIGURE 22.3** Wheatstone bridge circuit. *From Ingersoll et al. (1953, p. 134). This material is reproduced with permission of The McGraw-Hill Companies.*

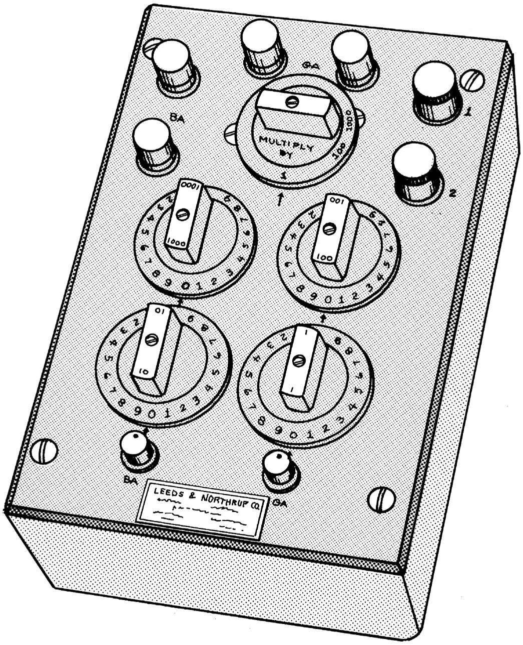

**FIGURE 22.4** A Wheatstone bridge. *From a brochure of Leeds and Northrup Co., North Wales, Pennsylvania. Courtesy of Honeywell International, Inc.*

intermediate points b and d may be found that are at the same potential. Under these circumstances, no current will flow through the galvanometer, G, connected between b and d. The bridge is then said to be balanced, and

$$R_1/R_2 = R_3/X. \tag{22.3}$$

Thus, any one of the four resistances may be obtained in terms of the three others.

A Wheatstone bridge often looks like a black box with knobs on the top (Figure 22.4), but there are also "slide-wire" Wheatstone bridges. In the slide-wire form of the bridge, one of the branches (e.g., abc in Figure 22.3), consists of a wire of uniform cross-section. The point *b* is located by a sliding contact. The unknown resistance *X* is placed in one arm of the other branch, the remaining arm containing the known resistance $R_3$ usually in the form of a resistance box. Because only the ratio of the resistances $R_1$ and $R_2$ is required, this ratio may be replaced by the ratio of the lengths of the two arms of the slide wire (Ingersoll et al., 1953, p. 135).

## 22.3 LAW OF RESISTANCE

We know *R*, by measuring it with the Wheatstone bridge, but now, we need to know conductivity. To determine conductivity, we use the law of resistance. The law of resistance is true by experimentation, and states that

$$R = \rho L/A, \tag{22.4}$$

where

$R$ = resistance (ohms),
$L$ = length (centimeter),
$A$ = area (square centimeter),
$\rho$ = resistivity (ohms centimeter).

Figure 22.5 illustrates how we can apply the law of resistance. If we have a cube of material that is 1 cm on a side for a total cross-sectional area of 1 $\text{cm}^2$ and a length of 1 cm through which the electricity flows, and we have a 1-V potential difference in our circuit and we have 1 ampere of electricity flowing ($I$) (1 ampere = 1 coulom b/s or 1 A = 1 C/s), we have 1 Ω of resistance, because by Ohm's law $R$ (ohms) = $V$ (volts)/ $I$ (amperes). We know $R$, $L$, $A$, and we can determine resistivity from the law of resistance. From resistivity, we determine conductivity, as follows:

$$\sigma = \text{conductivity} = 1/\text{resistivity} = 1/\rho.$$

The units of conductivity = 1/(ohms centimeter) or mhos per centimeter. (These are not SI units; we will change these to SI units in the next section.)

Resistivity ($\rho$) varies with materials. The resistivity of materials can be found in an early edition of the *Handbook of Chemistry and Physics* (Hodgman, 1959, p. 2598). The resistivity of rocks and soils is high. For example, the resistivity of granite varies between $10^7$ to $10^9$ Ω-cm, and the resistivity of sand varies between $10^5$ to $10^6$ Ω-cm. (The temperature at which the resistivity of rocks and soils was determined is not stated in the handbook.) The resistivity of metals is small (Hodgman, 1959,

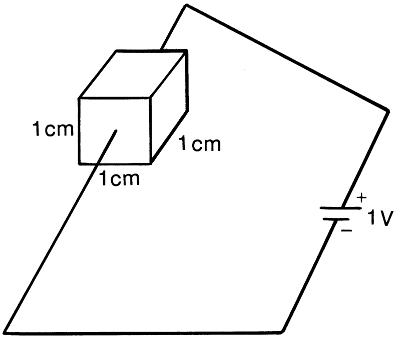

**FIGURE 22.5** Illustration showing how to use the law of resistance to get resistivity. *From a sketch by Don Kirkham.*

pp. 2587–2593). For example, the resistivity of aluminum at 20 °C is $2.828 \times 10^{-6}$ Ω-cm. The resistivity of copper at 20 °C is $1.77 \times 10^{-6}$ Ω-cm. The resistivity of gold at 20 °C is $2.44 \times 10^{-6}$ Ω-cm. The resistivity of silver at 18 °C is $1.629 \times 10^{-6}$ Ω-cm.

## 22.4 UNITS OF ELECTRICAL CONDUCTIVITY

Electrical conductivity is used to measure the salinity of a soil. Old units of electrical conductivity were mmhos per centimeter; the United States Department of Agriculture (USDA) Handbook No. 60 (1954), edited by L.A. Richards, is still in use for standard measurements of saline soils, uses the old unit of mmhos per centimeter. We need to know how to convert mmhos per centimeter into SI units. The SI unit for conductance is the Siemens. (For biographies of members of the Siemens family, see the Appendix, Section 22.10.) Conductance is $1/R$, and its non-SI unit is the mho, which is ohm spelled backward.

$$1 \text{ Siemen} = 1/R = 1/1 \text{ ohm} = 1 \text{ mho.}$$

The SI unit for electrical conductivity is the decisiemen per meter.

$$1 \text{ decisiemen/m} = 1 \text{ dS/m} = 1 \text{ mmho/cm.}$$

**Example:** Assume that we have saltwater in a container that is 24 cm long and 5 cm wide. The saltwater stands to a height of 9 mm in the container. We measure a resistance of 400 Ω with a Wheatstone bridge. What is the conductance? What is the electrical conductivity? (Hint: From the law of resistance, get resistivity and take its reciprocal.)

Conductance = 1/400 Ω =0.0025 mhos.

Area = $0.9 \times 5$ cm = 4.5 cm$^2$.

$400\ \Omega = (\rho\ 24\ \text{cm})/4.5\ \text{cm}^2$.

$\rho = 75$ Ω-cm. This is the resistivity.

1/75 Ω-cm = 0.013 mho/cm = 13 mmho/cm = 13 dS/m. This is the electrical conductivity.

## 22.5 EXAMPLE OF AN ELECTRICAL ANALOG APPLIED TO SOIL WITH WORMHOLES

The same container cited in the preceding example (24 cm long and 5 cm wide) was used to determine, in an electrical-analog study, the water and air conductance in soil with earthworms (Kirkham, 1982). The objective was to quantify the relationship between conductance and wormholes of different sizes oriented in the horizontal and vertical directions, which simulated wormholes oriented horizontally to the soil

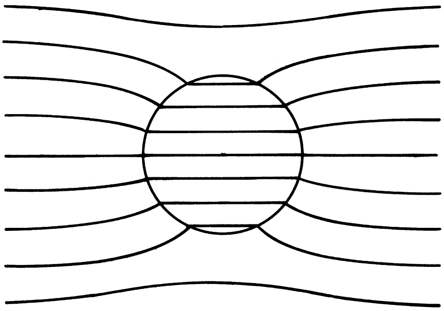

**FIGURE 22.6** Electrical analog of oxygen-flow concentration or nutrient-flow concentration (flow lines are close together) in an isolated vertical wormhole with flow perpendicular to the hole axis. The figure is for a conductivity in the "wormhole" equal to five times that in the soil. *From Smythe (1950, p. 68). This material is reproduced with permission of The McGraw-Hill Companies.*

surface or perpendicularly to the soil surface. Copper pipes of different diameters, placed horizontally and vertically in the center of the electrolyte (tap water) in the container, simulated the wormholes. The results showed that wormholes, when their diameter and/or length is increased, cause an increase in soil conductance. Large increases (e.g., 100%) in conductance did not occur for holes in the vertical direction (and flow perpendicular to the holes) until a hole had a diameter that was >70% of the length of the unit volume. Similarly, large increases in conductance did not occur in the horizontal direction unless the wormhole length was an appreciable amount of the soil length associated with the hole.

The experiment simulated the concentration of oxygen in the moving air, or nutrients in the moving soil water, in the wormholes (Figure 22.6). The increased concentration of oxygen in air, or nutrients in water, may be one reason why roots concentrate in wormholes. The increased concentration of oxygen or nutrients in the hole will occur even when the wormholes are not directly connected to the soil surface, as was the case in this experiment (Kirkham, 1982). The experiment showed that electrical-analog studies can provide information that is not easily measured in the field.

## 22.6 VAN DEN HONERT'S EQUATION

The analogy for water movement through the entire SPAC and the flow of electricity has been discussed in the literature for decades. According to van den Honert (1948), "It was Gradmann's (1928) idea to apply an analogue of Ohm's law to this water transport as a whole". However, if one looks at the Gradmann paper, one sees no place where Ohm is mentioned. So Gradmann must have suggested a linear flow law, such as

Ohm's law, without mentioning Ohm specifically. We remember that Ohm's law is one of the linear flow laws that is so important in transport (Table 7.1). Kramer (1983, p. 190) cites Huber (1924) as the originator of the idea, and also lists Gradmann (1928) as one who developed it. Despite the uncertainty about who originated the idea that water flow through the soil–plant–atmosphere system is similar to the flow of electricity, the paper published by van den Honert (1948) (in English) is the most cited paper on the topic.

Let us first look at the more simple form of Ohm's law in Eqn (22.1), $V = IR$. A current $I$ of electricity exists in a conductor whenever electric charge $q$ is being transferred from one point to another in that conductor. If charge is transferred at a uniform rate of 1 C per second, then the constant current existing in the conductor is 1 A (Schaum, 1961, pp. 146–147). The potential difference $V$ between two points in a conductor is measured by the work $W$ required to transfer unit charge from one point to the other. The volt is the potential difference between two points in a conductor when 1 J of work is required to transfer 1 C of charge from one point to the other. The resistance $R$ of a conductor is the property that depends on its dimensions, material, and temperature, and that determines the current produced in it by a given potential difference. The *ohm* is the resistance of a conductor in which there is a current of 1 A when the potential difference between its ends is 1 V. Ohm's law states that the value of the steady electrical current $I$ in a metallic conductor at a constant temperature is equal to the potential difference $V$ between the ends of the conductor divided by the resistance $R$ of the conductor (Figure 22.7), or

$$I \text{ (current)} = V \text{ (potential difference)}/R \text{ (resistance)}, \tag{22.5}$$

$$I \text{ (amperes)} = V \text{ (volts)}/R \text{ (ohms)}.$$

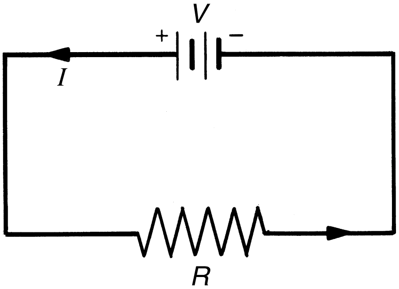

**FIGURE 22.7** Diagram illustrating Ohm's law. *Adapted from Schaum (1961, p. 149). This material is reproduced with permission of The McGraw-Hill Companies.*

Ohm's law may be applied to any part of a circuit or to the entire circuit. Thus, the potential difference, or voltage drop, across any part of a conductor is equal to the current $I$ in the conductor multiplied by the resistance $R$ of that part, or $V = IR$. When Ohm's law is applied to the SPAC, the following analogies are made:

$V$ is the potential difference between any two parts in the system. The potential in each part of the system is the (total) water potential ($\Psi_w$), which is measured, for example, with a thermocouple hygrometer or pressure chamber and is usually expressed using the unit of megapascals.

$I$ is the flow of water (transpiration rate). This is what Nobel (e.g., 1974, p. 142) calls $J_v$ or volume flow measured in units such as meters per second.

$R$ is the resistance. Its units depend upon how $V$ (or $\Psi_w$) and $I$ have been defined.

van den Honert (1948) uses the Ohm's law analogy to develop an equation similar to the following, which Baker (1984, p. 310) modified using modern terminology ($\Psi$ in place of the old terminology of diffusion pressure deficit, which van den Honert used):

$$\begin{aligned} J_v &= (\Delta\Psi)/r = (\Psi_{\text{soil}} - \Psi_{\text{root}})/r_1 = (\Psi_{\text{root}} - \Psi_{\text{stem}})/r_2 \\ &= (\Psi_{\text{stem}} - \Psi_{\text{leaf}})/r_3 = (\Psi_{\text{leaf}} - \Psi_{\text{air}})/r_4 \\ &= (\Psi_{\text{soil}} - \Psi_{\text{air}})/(r_1 + r_2 + r_3 + r_4), \end{aligned} \tag{22.6}$$

where $J_v$ is the steady rate of water flow, $\Psi$ is the water potential at different parts in the system (the subscript designates the location), and $r_1$, $r_2$, $r_3$, and $r_4$ are the resistances between the soil and root, the root and stem, the stem and leaf, and the leaf and air, respectively. This equation has been reproduced in many textbooks (e.g., see Kramer, 1983, p. 190).

## 22.7 PROOF OF VAN DEN HONERT'S EQUATION

It is not obvious why the string of equations in Eqn (22.6) should equal each other. In fact, some have questioned the "equal" signs in Eqn (22.6) and suggested that they should be "plus" signs. So we shall now prove Baker's (van den Honert's) equation (Eqn (22.6)), or we shall prove that

$$J_v = (\Psi_{\text{soil}} - \Psi_{\text{air}})/(r_1 + r_2 + r_3 + r_4).$$

We divide up the string of equations into individual equations.

$$J_v = (\Psi_{\text{soil}} - \Psi_{\text{root}})/r_1, \tag{22.7}$$

$$J_v = (\Psi_{\text{root}} - \Psi_{\text{stem}})/r_2, \tag{22.8}$$

$$J_v = (\Psi_{stem} - \Psi_{leaf})/r_3, \tag{22.9}$$

$$J_v = (\Psi_{leaf} - \Psi_{air})/r_4. \tag{22.10}$$

We now multiply the first equation (Eqn (22.7)) through by $r_1$; Eqn (22.8) through by $r_2$; Eqn (22.9) through by $r_3$; and Eqn (22.10) through by $r_4$:

$$J_v r_1 = (\Psi_{soil} - \Psi_{root}), \tag{22.11}$$

$$J_v r_2 = (\Psi_{root} - \Psi_{stem}), \tag{22.12}$$

$$J_v r_3 = (\Psi_{stem} - \Psi_{leaf}), \tag{22.13}$$

$$J_v r_4 = (\Psi_{leaf} - \Psi_{air}). \tag{22.14}$$

In Eqns 22.11–22.14, we add up the left sides and add up the right sides and then equate the resultant left and right sides to get one equation (Eqn (22.15)):

$$\begin{aligned} J_v r_1 + J_v r_2 + J_v r_3 + J_v r_4 = {} & (\Psi_{soil} - \Psi_{root}) + (\Psi_{root} - \Psi_{stem}) \\ & + (\Psi_{stem} - \Psi_{leaf}) + (\Psi_{leaf} - \Psi_{air}). \end{aligned} \tag{22.15}$$

We now cancel units in Eqn (22.15) and factor the left-hand side.

$$J_v(r_1 + r_2 + r_3 + r_4) = \Psi_{soil} - \Psi_{air}. \tag{22.16}$$

We divide each side of Eqn (22.16) by $(r_1 + r_2 + r_3 + r_4)$:

$$J_v(r_1 + r_2 + r_3 + r_4)/(r_1 + r_2 + r_3 + r_4) = (\Psi_{soil} - \Psi_{air})/(r_1 + r_2 + r_3 + r_4). \tag{22.17}$$

We simplify the left-hand side of Eqn (22.17) and get the equation as shown by Baker (1984):

$$J_v = (\Psi_{soil} - \Psi_{air})/(r_1 + r_2 + r_3 + r_4)\ \text{QED}.$$

(QED is used in mathematics, and it is Latin for “quod erat demonstrandum” or “which was to be proved”.)

## 22.8 APPENDIX: BIOGRAPHY OF GEORG OHM

Georg Simon Ohm (1789–1854) was an ingenious German investigator who, although removed from the influence of personal contact with the renowned physicists of his time and working independently and alone, discovered the great law bearing his name (Cajori, 1929, p. 234). He was born in Erlangen on March 16, 1787, and was educated at the university there (Preece, 1971, cited under Ohm). He then taught school at Gottstadt, Neufchâtel, and Bamberg. In 1817, he became teacher of mathematics and physics in the Jesuits’ college in Cologne, and taught there for nine years with great success. A pupil of that time, who later attained fame as a mathematician, was Lejene Dirichlet (1805–1859).

Ohm wanted to do research, but the want of leisure and books, as well as the lack of suitable apparatus, made progress difficult. The mechanical skill that he had acquired as a boy from his father, a locksmith, enabled him to construct much apparatus for himself (Cajori, 1929, p. 235).

Ohm's first experiments were on the relative conductivity of metals. In these tests, he was troubled by variations in his batteries ("Wogen der Kraft" or "surge in power"). He adopted thermoelectric elements as the sources of current that were free from this trouble. He published the experimental results that were the basis for his famous law in 1826. The following year he published a book entitled *Die galvanische Kette, mathematisch bearbeitet* (Mathematical Work on the Galvanic Chain) published in Berlin, 1827. It contained a theoretical deduction of his law, and became far more widely known than his article of 1826, giving the experimental deduction. There was unfavorable reception of his conclusions. In the Berlin *Jahrbücher für wissenschafliche Kritik*, Ohm's theory was "named a web of naked fancies, which can never find the semblance of support from even the most superficial observation of facts; he who looks on the world with the eye of reverence must turn aside from this book as the result of an incurable delusion, whose sole effort is to detract from the dignity of nature" (Cajori, 1929, p. 238).

Because Ohm's great ambition was to secure a university professorship, we can understand how this criticism affected him. To write his book of 1827, he had secured leave of absence and had gone to Berlin, where the library facilities were better than at Cologne. Not only did he fail to secure promotion by the publication of his book but he also incurred the ill will of a school official, who was a supporter of Hegelianism and, therefore, opposed to experimental research. In consequence, Ohm resigned his position in Cologne (Cajori, 1929, p. 238).

For six years, Ohm lived in Berlin, giving three mathematical lessons a week in the *Kriegsschule* for a small salary. In 1833, he obtained an appointment at the polytechnic in Nürnberg. Gradually, his electric researches called forth respect and admiration, particularly from foreigners, including Gustav Fechner (1801–1887) in Germany, Wheatstone in England (Section 22.9), Heinrich Lenz (1804–1865) in Russia, and Joseph Henry (1797–1878) in America. In 1841, the Royal Society of London awarded him its Copley Medal, and, in 1842, it made him a foreign member. Ohm's experience reminds us of the biblical saying, "A prophet is not without honor, save in his own country" (Matthew 13:57).

In 1849, at the age of 62, the ambition of Ohm's youth was finally attained. He was appointed extraordinary professor at the University of Munich and, in 1852, ordinary professor. His writings were numerous. In addition to a number of papers on mathematical subjects, Ohm wrote a textbook, *Grundzuge der Physik* (Main Features of Physics) (1854). He died in Munich on July 7, 1854 (Preece, 1971).

## 22.9 APPENDIX: BIOGRAPHY OF CHARLES WHEATSTONE

Sir Charles Wheatstone (1802–1875) was an English physicist whose name is associated with the Wheatstone bridge for measuring electrical resistance. He was born near Gloucester in February 1802. He became a manufacturer of musical instruments, but in 1834 accepted the chair of experimental physics at King's College, London. At about this time, Wheatstone measured (with a revolving mirror) the great speed of electric discharge in conductors. Applying this speed for sending messages, he and William Fothergill Cooke (1806–1879, an English inventor) patented an early form of electric telegraph in 1837. Wheatstone's inventions included a cryptographic machine, the concertina (a small musical instrument of the accordion type, with bellows and keys), and a form of stereoscope. He wrote papers on the transmission of sound in solids and on the physiology of vision, binocular vision, and color. Wheatstone showed that the electrical sparks from different metals give different spectra. He played a prominent part in the early development of electric generators and of telegraphy with submarine cables (Preece, 1971, cited under Wheatstone).

Wheatstone, a great admirer of Ohm, perceived the necessity of more accurate means of measuring resistances. The measurement of resistance had been brought to perfection chiefly by those interested in the development of the telegraph. Wheatstone invented the rheostat, but this had been superseded by the resistance box. The earlier methods of measuring resistance had the defect of depending on the constancy of the batteries used (Cajori, 1929, p. 239). Wheatstone overcame the trouble by adopting a method suggested in 1833 by Samuel Hunter Christie (1784–1865; British mathematician) (Marquis Who's Who, 1968). A footnote in a book by James Clerk Maxwell (1892, p. 495) states, "Sir Charles Wheatstone, in his paper on 'New Instruments and Processes,' *Phil. Trans.*, 1843, brought this arrangement [Wheatstone's bridge] into public notice, with due acknowledgment of the original inventor, Mr. S. Hunter Christie, who had described it in his paper on 'Induced Currents,' *Phil. Trans.*, 1833, under the name of a Differential Arrangement".

Wheatstone was an experimentalist of extraordinary skill, but disliked speaking in public. In fulfillment of his duties at King's College he delivered a course of eight lectures on sound, but his habitual (though unreasonable) distrust of his own powers of speech proved to be an invincible obstacle, and he soon discontinued his lectures. Nevertheless, he retained the professorship for many years. In private, people were charmed by his able and lucid exposition, but in public, including at the Royal Society, his attempt to repeat the same information invariably proved unsatisfactory (Cajori, 1929, p. 239). For this reason, some of his more important investigations were brought before the Royal Society by Faraday.

Wheatstone's *Scientific Papers* were collected and published by the Physical Society of London in 1879. Wheatstone retired to private life, living on the income from his inventions, particularly that of the telegraph. He died in Paris on October 19, 1987 (Preece, 1971, cited under Wheatstone).

## 22.10 APPENDIX: BIOGRAPHIES OF MEMBERS OF THE SIEMENS FAMILY

There were four important men in the Siemens family: Werner, William, Friedrich, and Alexander.

Werner von Siemens (1816—1892) was the chief founder of the electrical firm with his name. He was born on December 13, 1816, at Lenthe, Hanover, Germany. Between 1838 and 1848, he held a commission in the artillery, was entrusted with many specialized undertakings, and, in particular, became acquainted with the recently developed electric telegraph. In 1847, he founded, together with skilled mechanic J.G. Halske, the firm of Siemens and Halske for the manufacture of telegraphic apparatus. This firm, under Siemens's guidance, became one of the most important electrical companies in the world, with branches in different countries. The branches in England and Russia were particularly important. It carried out large telegraphic projects and expanded into other electrical fields, as new applications of electricity were developed (Weston, 1971).

Many of Werner von Siemens's inventions related to telegraphic apparatus. He used gutta-percha, a rubberlike substance from trees in Malaysia, as an insulator for telegraphic cable in 1847. This form of insulation was later widely used for electric-light cables. The Siemens armature, which he invented in 1856 for use in telegraphy, was used in large generators and has evolved into the modern armature. One of the most important of Siemens's discoveries was that of the dynamoelectric principle, which governs the self-excitation of the dynamo. He died at Charlottenburg, Berlin, on December 6, 1892 (Weston, 1971).

Sir William Siemens (Karl Wilhelm; 1823—1883) was Werner's brother and is known for his work in electricity and in the application of heat. In both fields, he combined the functions of innovator, manufacturer, and successful businessman. He was born at Lenthe, Hanover, on April 4, 1823. After attending the University of Göttingen, he entered, as a pupil, the manufacturing concern of Count Stolberg at Magdeburg. At the age of 19, he first visited England in the hope of introducing an electroplating process invented by himself and Werner, which he succeeded in selling. He returned to Germany, but in 1844 was again in England, this time with another invention, the "chronometric", or differential, governor. Finding that British patent law afforded the inventor a protection then lacking in Germany, he henceforth made England his home.

The next few years were spent in trying to develop his inventions, of which at this time his water meter was commercially the most successful. His activities made him a respected figure in scientific circles. His paper "On the Conservation of Heat Into Mechanical Effect", read to the Institution of Civil Engineers in 1853, gained him the Telford Medal, and in 1862, he was elected a member of the Royal Society. William's chief work in the field of heat was concerned with regenerative heating and consequent improvements in steelmaking processes.

In the field of electricity, William became an acknowledged authority and leader. From 1848 onward, he represented the firm of Siemens and Halske in London, and when in 1865 the separate firm of Siemens Brothers was established, he became a partner and director. At first, the chief business was the erection of overland telegraph lines and the laying of submarine telegraph cables. William was, however, in constant close liaison with all the ideas and projects of his brother Werner in Berlin and, when the latter discovered the dynamoelectric principle, William introduced it to England by reading a paper about it to the Royal Society in 1867. Gradually, in the late 1870s and 1880s, the electric-light side of the business grew. One of the last projects with which William was associated was the Portrush electric railway in the north of Ireland, opened in 1883, which utilized water turbines driving a Siemens dynamo. William Siemens was knighted in 1883, and he died in London the same year on November 19 (Weston, 1971).

Friedrich Siemens (1826—1904) was the brother of Werner and William. He was born in Mentzendorff, Germany, on December 8, 1826 (Marquis Who's Who, 1968). Friedrich, along with William, first tried to apply the regenerative condenser to the steam engine, using the heat from the regenerator to preheat the boiler feed water. When this did not succeed, other applications were sought and the idea occurred of applying the principle to furnaces, using the heat regained from the flue gases to heat the air supply to the furnace. This was patented by Friedrich in 1856 and met with great success for use both in glassmaking and in steel manufacture. Later, the use of gas instead of solid fuel greatly extended the use of the regenerative furnace (Weston, 1971). He died in May 26, 1904.

Alexander Siemens (1847—1928), William's nephew, was born in Hanover, Germany, on January 22, 1847. In 1867, he went to England, where he worked first in the workshops of Siemens Brothers at Woolwich, and then in the erection of the Indo-European telegraph line in Persia (1868) and in the laying of the Black Sea cable (1868). In 1878, he became a naturalized British subject. The following year he took over the management of the electric-light department of Siemens Brothers, and was responsible for the installation of electric light at Godalming, Surrey, the first English town to be so lighted.

Like many other members of the family, Alexander patented several inventions. After the death of Sir William, he became a director of the company, a position he retained until 1918. He took an active part in public activities associated with his profession, was a member of several important committees, and was twice president of the Institution of Electrical Engineers. He died at Milford-on-Sea, Hampshire, on February 16, 1928 (Weston, 1971).

Siemens is still an important name in business today, and the company is often noted in *The Wall Street Journal*.

## References

Baker, D.A., 1984. Water relations. In: Wilkins, M.B. (Ed.), Advanced Plant Physiology. Pitman, London, pp. 297–318.

Cajori, F., 1929. A History of Physics. Macmillan, New York.

Clerk Maxwell, J., 1892. A Treatise on Electricity and Magnetism, vol. II. Reprinted 1904. Oxford University Press, London (Reprinted photographically in Great Britain in 1937 by Lowe and Brydone, Printers, London, from sheets of the Third edition.).

Gradmann, H., 1928. Untersuchungen über die Wasserverhältnisse des Bodens als Grundlage des Pflanzenwachstums. Jahrbucher für Wissenschaftliche Botanik 69, 1–100.

Hausmann, E., Slack, E.P., 1948. Physics. D. Van Nostrand, New York.

Hodgman, C.D., 1959. Handbook of Chemistry and Physics, fortieth ed. Chemical Rubber Publishing, Cleveland, Ohio.

Huber, B., 1924. Die Beurteilung des Wasserhaushaltes der Pflanze. Ein Beitrag zur vergleichenden Physiologie. Jahrbucher für Wissenschaftliche Botanik 64, 1–120.

Ingersoll, L.R., Martin, M.J., Rouse, T.A., 1953. A Laboratory Manual of Experiments in Physics. McGraw-Hill, New York.

Kirkham, D., Powers, W.L., 1972. Advanced Soil Physics. Wiley, New York.

Kirkham, M.B., 1982. Water and air conductance in soil with earthworms: an electrical-analogue study. Pedobiologia 23, 367–371.

Kirkham, M.B., 2002. The concept of the soil–plant–atmosphere continuum and applications. In: Raats, P.A.C., Smiles, D., Warrick, A.W. (Eds.), Environmental Mechanics: Water, Mass and Energy Transfer in the Biosphere, Geophysical Monograph, vol. 129. American Geophysical Union in Cooperation with CSIRO, Australia, pp. 327–335 (American Geophysical Union: Washington, D.C).

Kramer, P.J., 1983. Water Relations of Plants. Academic Press, New York.

Marquis Who's Who, 1968. Who's Who in Science from Antiquity to the Present, first ed. Marquis-Who's Who, Chicago.

Nobel, P.S., 1974. Introduction to Biophysical Plant Physiology. W.H. Freeman, San Francisco.

Ohm, Georg Simon, 1971. In: Preece, W.E. (Ed.), Encyclopaedia Britannica, General ed., vol. 16, pp. 896–897.

Philip, J.R., 1957. The Physical Principles of Soil Water Movement during the Irrigation Cycle. International Commission on Irrigation and Drainage, Third Congress, Algiers. R. 7, Question 8, 8.125–8.154.

Philip, J.R., 1966. Plant water relations: some physical aspects. Annu. Rev. Plant Physiol. 17, 245–268.

Schaum, D., 1961. Schaum's Outline of Theory and Problems of College Physics, sixth ed. Schaum, New York.

Slichter, C.S., 1899. Theoretical investigations of the motion of ground-water. US Geol. Surv. Annu. Rep. 19, 295–384.

Smythe, W.R., 1950. Static and Dynamic Electricity, second ed. McGraw-Hill, New York.

United States Department of Agriculture, 1954. Diagnosis and Improvement of Saline and Alkali Soils. In: Richards, L.A. (Ed.), Agr Handbook No. 60. United States Department of Agriculture, Washington, DC.

van den Honert, T.H., 1948. Water transport in plants as a catenary process. Discuss. Faraday Soc. 3, 146–153.

Wheatstone, Sir Charles, 1971. In: Preece, W.E. (Ed.), Encyclopaedia Britannica, General ed., vol. 23, p. 473.

Weston, M.K., 1971. Siemens. Encyclopaedia Britannica vol. 20, 484–485.

C H A P T E R

# 23

# Leaf Anatomy and Leaf Elasticity

In this chapter we learn how to measure leaf elasticity and calculate moduli of elasticity for the leaves. But before we study elasticity, we need to look at leaf anatomy to understand the type of organ for which we are making the calculations.

## 23.1 LEAF ANATOMY

Plants are usually classified according to their water relations as follows: xerophytes, mesophytes, and hydrophytes (Esau, 1977; p. 351). Xerophytes are adapted to dry habitats. Mesophytes require abundant available soil water and a relatively humid atmosphere. Hydrophytes (or hygrophytes) depend on a large supply of moisture or grow partly or completely submerged in water. The structural features typical of plants of the different habitats are referred to as xeromorphic, mesomorphic, and hydromorphic, respectively. The characteristics that distinguish plants of the various habitats are most striking in leaves. Here we consider dicotyledonous and monocotyledonous leaves and focus mainly on mesophytes, and then we look at special adaptations of xerophytes.

### 23.1.1 Dicotyledonous Leaves

Figure 23.1 shows a dicotyledonous leaf. It is a leaf of the shrub, lilac (*Syringa vulgaris* L.) (Torres and Costello, 1963; p. 124). It is composed of an upper (adaxial) and lower (abaxial) epidermis. One stoma is evident in the lower epidermis. The thin, colorless layer deposited on the walls of the upper epidermal cells is called the cuticle and is composed of a waxy material called cutin (Torres and Costello, 1963; p. 43). The mesophyll is divided into an upper palisade mesophyll and a lower spongy mesophyll. One or two layers of columnar, compact cells lie beneath the upper epidermis. These cells make up the palisade mesophyll (also called the palisade parenchyma). Between the palisade tissue and the lower

http://dx.doi.org/10.1016/B978-0-12-420022-7.00023-9

Copyright © 2014 Elsevier Inc. All rights reserved.

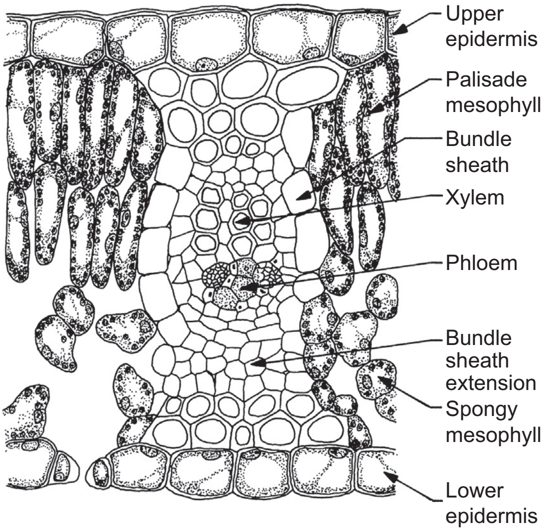

**FIGURE 23.1** A transverse section of a lilac leaf, a dicotyledonous leaf. *From Torres and Costello (1963), p. 124. This material is reproduced with permission of The McGraw-Hill Companies.*

epidermis, there is a layer of large, irregular, loosely packed cells with many intercellular spaces between them. This tissue is the spongy mesophyll (also called the spongy parenchyma). The stoma in Figure 23.1 is located near the intercellular spaces, which allows easy transport of carbon dioxide to the mesophyll. Chloroplasts, oval-shaped bodies, are present in the mesophyll cells. Dispersed throughout the mesophyll are the veins of the leaf. A vein is a strand of vascular tissue in a flat organ such as a leaf (Esau, 1977; p. 531). The largest central vein is known as the midrib. The vein is in the center of Figure 23.1, and the conducting tissue of the vein consists of xylem and phloem. The xylem tissue is closest to the adaxial surface, because, when the vascular tissue bends over from the stem into the leaf, the xylem, which is closer to the center of the plant in each vascular bundle than the phloem (see Chapter 17, Section 17.1, for stem anatomy), comes out on top of the vascular bundle. Thus, the xylem is on top of the phloem in the leaf vascular bundle. In the figure, the cells in the xylem are shown with thick walls and are empty because the vessel members are dead at maturity. A bundle sheath surrounds the vascular tissue. The bundle sheath extensions link the bundle sheath to both the upper and lower epidermis. The bundle sheath extensions have thick cell walls because they are made up of sclerenchyma.

In the dicotyledons, the supporting tissue in leaves may be collenchyma or sclerenchyma, which we defined in Chapter 17, Section 17.1. In the collenchyma tissue only one type of cell is identified, a collenchyma cell. It is living tissue closely related to parenchyma. In fact, it is usually regarded as a form of parenchyma specialized as supporting tissue in young organs (Esau, 1977; p. 4). The sclerenchyma tissue has two types of cells: sclereids and fibers. Both types of cells have thick, secondary, often lignified cell walls and may lack protoplasts at maturity. The sclereids vary in shape from polyhedral to elongated and may be much branched. Fibers are generally long, slender cells (Esau, 1977; p. 4) with a lignified or nonlignified secondary wall. A fiber cell may or may not have a living protoplast at maturity (Esau, 1977; p. 510). Sometimes it is hard to distinguish fibers and sclereids, so a third type of sclerenchyma cell is identified as a fiber sclereid, which is a sclerenchyma cell with characteristics intermediate between those of a fiber and a sclereid (Esau, 1977; p. 510). The vascular bundles themselves also contribute to the support of the blades. The collenchyma occurs along the larger veins, on one or both sides. Sclerenchyma occurs in the form of bundle sheaths and bundle sheath extensions, composed of fibrous cells, and as sclereids in the mesophyll.

Many herbaceous dicotyledons have leaves with a relatively undifferentiated mesophyll (Esau, 1977; pp. 355–357). The palisade tissue is absent or weakly developed, the intercellular volume is large, and the leaf is often thin. The epidermis bears a thin cuticle, and the stomata are more or less raised. Examples of leaves with relatively undifferentiated mesophyll are those of *Pisum sativum* (pea) and *Lactuca sativa* (lettuce). A thin, loosely organized mesophyll with a single row of palisade cells is found in *Raphanus sativus* (radish), *Solanum tuberosum* (potato), and *Lycopersicon esculentum* (tomato). Leaves of the species *Gossypium* (cotton) have long palisade cells that occupy approximately one-third to one-half of the blade thickness.

Various shrubby and woody species furnish examples of leaves with well-differentiated palisade parenchyma on the adaxial side of the leaf (e.g., *Vitis*, grape; *Syringa*, lilac, Figure 23.1; *Ligustrum*, privet; and *Pyrus*, pear) (Esau, 1977; pp. 356–357).

### 23.1.2 Monocotylendous Leaves

The leaves of the monocotyledons vary in form and structure, and some resemble those of the dicotyledons (Esau, 1977; p. 359). Monocotyledonous leaves may have petioles and blades, for example *Canna* (common name is also canna) and *Hosta* (plantain lily). But the majority is differentiated into blade and sheath, and the blade is relatively narrow. The venation is typically parallel. In contrast, dicotyledonous leaves normally show a reticulate pattern of venation (Bowes, 2000; p. 10).

The anatomic structure of monocotyledonous leaves ranges from hydromorphic to extreme xeromorphic. Hydrophytes in the monocotyledons show the same basic features as those in the dicotyledons, and both have an abundance of aerenchyma. Aerenchyma is parenchyma tissue containing particularly large intercellular spaces of schizogenous, lysigenous, or rexigenous origin. *Schizogenous* is a term applied to an intercellular space originating by separation of cell walls along the middle lamella (Esau, 1977; p. 524), *lysigenous* is a term applied to an intercellular space originating by the dissolution of cells (Esau, 1977; p. 514), and *rexigenous* is a term applied to an intercellular space originating by the rupture of cells (Esau, 1977; p. 524).

Numerous monocotyledonous leaves develop large amounts of sclerenchyma, which in some species serves as an important source of commercial hard leaf fibers. The fibers are associated with the vascular bundles or appear as independent strands (Esau, 1977; p. 360).

The grass leaf typically consists of a more or less narrow blade and a sheath enclosing the stem. Vascular bundles of different sizes alternate rather regularly with one another, as typified by the wheat leaf (Figure 23.2). The median bundle may be the largest (Esau, 1977; p. 360). The mesophyll of grasses shows, as a rule, no distinct differentiation into palisade and spongy mesophyll (parenchyma), although sometimes the cell rows beneath both epidermal layers are more regularly arranged than in the rest of the mesophyll. In some grasses, the mesophyll cells surround the vascular bundles in an orderly manner, each cell oriented with its longer diameter at right angles to the bundle so that in transverse sections the mesophyll cells appear to radiate from the bundles (Esau, 1977; p. 360).

The epidermis of grasses contains a variety of cells. The narrow guard cells of the stomata are associated with subsidiary cells (see Chapter 24,

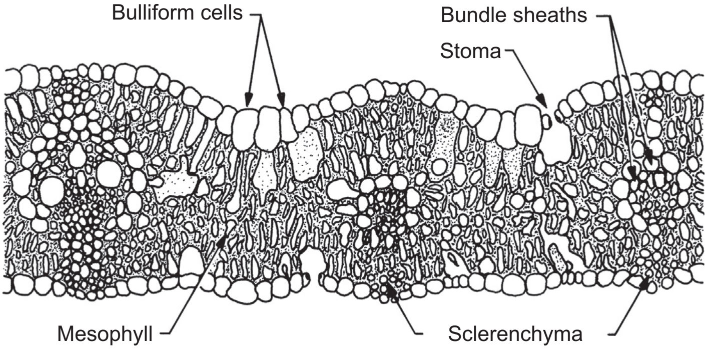

**FIGURE 23.2** A transverse section of a wheat leaf, a monocotyledonous leaf. The adaxial epidermis bears bulliform cells in grooved parts of the blade. Subepidermal cells are elongated like palisade cells. There is an inner thick-walled and an outer thin-walled bundle sheath. Sclerenchyma in the ribs is connected with the bundle sheath. *From* Esau (1965), *p. 700. This material is used by permission of John Wiley & Sons, Inc.*

Section 24.2, for stomatal anatomy). Silica cells, cork cells, and trichomes may be present. Enlarged epidermal cells, referred to as *bulliform cells* (Figure 23.2), are cells participating in folding movements of grass leaves. In a number of xeric grasses, enlarged epidermal cells line adaxial grooves between the vein ribs and are continuous with similarly enlarged mesophyll cells, called the *hinge cells.* During excessive loss of water, the bulliform cells or the hinge cells, or both, become flaccid and enable the leaf to fold or to roll. But the shrinkage of the various large, thin-walled cells is only one factor causing folding, because leaves without such cells also respond to loss of moisture by rolling. Differential shrinkage of other tissues, distribution of sclerenchyma, and cohesive forces among tissues also contribute to rolling and folding of leaves (Esau, 1977; p. 362).

Grass leaves have strongly developed sclerenchyma. Commonly, fibers extend from the large vascular bundles to the epidermis. The leaf margins may have fibers, as do leaves of wheat (not shown in Figure 23.2 because the figure shows only the center of the leaf; but see Figure 19.8C in Esau (1977), p. 363, for the sclerenchyma at the edge of a wheat leaf).

### 23.1.3 Grass Leaf Structure and Type of Photosynthesis

The bundle sheaths of grasses show variations that are significant taxonomically and indicators of the type of photosynthesis characteristic of the species (Esau, 1977; p. 362). After the discovery of the $C_4$ or Hatch and Slack (1966) pathway of photosynthesis in sugarcane [see Laetsch (1974) for a review of the history of the discovery of the $C_4$ photosynthetic pathway], comparative grass leaf anatomy became the object of intensive investigation in relation to photosynthesis (Esau, 1977; p. 364).

The most common photosynthetic cycle is the $C_3$ or Calvin—Benson pathway. In $C_3$ plants, carbon dioxide from the atmosphere is fixed as phosphoglyceric acid, a three-carbon compound. In $C_4$ plants, an additional mechanism is involved, in which atmospheric carbon dioxide is fixed as oxaloacetic acid, a four-carbon molecule. The leaves of $C_3$ and $C_4$ plants differ in morphology as well as in the chemical mechanisms of carbon dioxide fixation (Mellor and Jensen, 1986). In $C_3$ plants, chloroplasts are found in mesophyll cells throughout the leaf cross-sections. Bundle sheath cells that surround the vascular bundles in $C_3$ plants are lacking or essentially lacking in chloroplasts.

In leaves of $C_4$ plants, such as corn leaves, however, the chloroplasts that fix carbon dioxide by the $C_3$ mechanism are highly concentrated in the bundle sheath cells. In a $C_4$ leaf, the chloroplasts that fix carbon dioxide by the $C_4$ mechanism are located in the relatively large mesophyll cells that make up the body of the leaf. The four-carbon malic and aspartic acids (formed from the initial four-carbon product, oxaloacetic acid) produced by the chloroplasts in these mesophyll cells are transported to the $C_3$ chloroplasts in the bundle sheaths. Enzymes there split off carbon dioxide from the malic and aspartic acids, and this carbon dioxide is taken up by the $C_3$ mechanism to form phosphoglyceric acid, the compound that is metabolized to produce the various carbohydrates, proteins, and other compounds that make up the major components of the plant. The three-carbon molecule left after the splitting of carbon dioxide from malic and aspartic acid is pyruvic acid. The pyruvic acid is returned to the $C_4$ chloroplasts, where it is activated by transfer of a high-energy phosphate group from adenosine triphosphate to form phosphoenolpyruvate. The phosphoenolpyruvate in turn reacts with incoming carbon dioxide from the atmosphere to form oxaloacetic acid, with the loss of phosphate. This completes the $C_4$ cycle. Thus, in $C_4$ plants there are two connected carbon dioxide fixing cycles. The $C_4$ cycle feeds the $C_3$ cycle (Mellor and Jensen, 1986).

The $C_4$ cycle is characteristic of plants that require relatively high temperatures for growth. In the angiosperms, this cycle has been recorded in representatives of some 18 families, including the grass family, Poaceae (Ehleringer et al., 1991). This number is few compared to the total number of plant families, which is about 300 (Kirkham, 2011; p. 252). The $C_4$ plants are widely distributed in the various evolutionary arms of the angiosperms and are among the most recently evolved (Hatch, 1992). About half of the species of Poaceae are included among the $C_4$ plants (Esau, 1977; p. 364). The $C_4$ plants are of tropical origin and occur widely in xerophytic environments. In northern regions, few angiosperms are specialized for the $C_4$ photosynthetic cycle. Woolhouse (1978) shows a map with the percentage distribution of $C_4$ grasses in the flora of North America. In far northern regions of Canada and Alaska, 0% of the flora has the $C_4$ photosynthetic pathway; in the southern United States, high percentages occur (e.g., 80% in southern Florida).

## 23.1.4 Xerophytic Adaptations

Plants overcome adverse conditions of a particular environment in different ways (Esau, 1977; p. 351). In a habitat deficient in water, for example, some plants develop features protecting the aerial parts from excessive loss of water; others form underground water storage organs, or develop roots reaching great depths [e.g., the deep roots of sunflower; see Rachidi et al. (1993), who found depletion of water by sunflower roots at the 2.7 m depth]; and still others control the problem by having a short life span restricted to the time when water supply is most abundant. Availability of water is an especially important factor affecting the form and structure of plant leaves. Xeromorphic characteristics of leaves include:

1. Thick cuticle (wax)
2. Small intercellular spaces
3. A large proportion of mechanical tissue (sclereids, fibers)
4. Relatively small cells
5. Multiple epidermis
6. Several layers of palisade cells between the epidermis and the spongy parenchyma
7. Sunken stomata
8. Presence of hairs in stomatal pits (crypts)
9. Ledges of wall material on upper and lower sides of guard cells (appears as horns)
10. Presence of water storage cells
11. Spines
12. Lignified cells

Fahn and Cutler (1992) survey morphological and anatomical adaptations that enable plants to grow in arid and semiarid regions.

## 23.2 INTERNAL WATER RELATIONS

Plants have little storage capacity for water compared with the amounts that pass through them each day (Baver et al., 1972; p. 394). They must regulate their water status to survive. To understand this regulatory process, we must discuss the internal water balance of plants, including elasticity. Here we look at leaf elasticity from a physical point of view. We follow the analysis of Gardner and Ehlig (1965), which also has been partially reproduced in Baver et al. (1972, pp. 394–398).

As we saw in Eqn (17.1), under equilibrium conditions the state of the water in plant leaf cells may be written in terms of the various components of the potential energy, as follows

$$\Psi = \Psi_s + \Psi_p + \Psi_m + \Psi_g, \tag{23.1}$$

where $\Psi$ is the total water potential, $\Psi_s$ is the osmotic (solute) potential component, $\Psi_p$ is the pressure potential component (turgor pressure), $\Psi_m$ is the component due to adsorption forces such as those in the cell wall, and $\Psi_g$ is the component due to gravity. We usually ignore gravity, so Eqn (23.1) becomes

$$\Psi = \Psi_s + \Psi_p + \Psi_m, \tag{23.1a}$$

The partition of energy between the osmotic and adsorption components is somewhat arbitrary, because some of the water in the leaf tissue may be subject to both osmotic effects and adsorption forces, particularly at low leaf-water content. In the vacuole, the osmotic component is important.

If the cell solution were to behave ideally, the osmotic pressure would be directly proportional to the solute concentration (i.e., van't Hoff's law, which we discussed in Chapter 17, applies). There would exist, then, a simple relation between osmotic potential and cell water content:

$$\Psi_s = \Psi_s^o/\theta, \qquad (23.2)$$

where $\Psi_s^o$ is the osmotic pressure at full turgor and $\theta$ is the relative water content of the cell. $\theta$ is the ratio of the water content of the cell to the water content that it has when in equilibrium with free water at the same temperature and pressure. If the amount of bound water is appreciable, then this amount should be subtracted from $\theta$. Some investigators have found appreciable amounts of bound water (as much as 30%; Slavík, 1963). However, we shall consider the amount of bound water to be small, and we shall not subtract it from $\theta$.

The osmotic and pressure components of the potential are not independent. Because of the elastic nature of the cell wall, changes in turgor pressure cause changes in cell volume, due to changes in cell water content. An increase in the turgor pressure results in an expansion of the cell walls. This is accomplished by the uptake of water. Unless this uptake is also accompanied by a proportional uptake of solutes, the solute concentration decreases with a consequent increase in the osmotic potential. Solute transport across the membranes can and does occur, but at a rate that is generally slower than the rate of water movement, so that the immediate response of a cell to any change in water potential is a change in its water content or degree of hydration (Baver et al., 1972; p. 396).

As stated, the components of the water potential in a leaf cell are not completely independent. On a short-term basis, if the total water potential is specified, this determines both the osmotic and the turgor potential, as well as the degree of hydration. (We recognize that we can never *measure* zero water potential in a leaf, even when fully hydrated. The water potential is always slightly negative.)

As the relative water content decreases, the solute concentration must increase proportionately, if the solute content remains constant (Gardner and Ehlig, 1965). This results in a decrease in the osmotic potential. If it is assumed that the relation between the turgor pressure and the cell volume is linear, then

$$\Psi_p = e(\theta - \theta_o)/\theta_o, \qquad (23.3)$$

where $\theta_o$ is the relative water content at which the turgor potential becomes zero and $e$ is the modulus of elasticity. Substituting Eqns (23.2) and (23.3) into Eqn (23.1a), we get

$$\Psi = \Psi_s^o/\theta + e(\theta - \theta_o)/\theta_o + \Psi_m(\theta), \tag{23.4}$$

in which $\Psi_m$ is now a function of $\theta$. Equation (23.4) gives us a relation between the water potential and the relative water content of the cell. $\Psi_m(\theta)$ represents the relation between the water content and the matric potential. Growth can be expected to cause some departure from the expression used in deriving Eqn (23.4), but to the extent that the assumptions are valid, Eqn (23.4) gives a unique relation between the total water potential and the relative water content of the leaf.

In practice, it is easier to make the measurements needed to test Eqn (23.4) on tissue rather than on single cells. Therefore, Gardner and Ehlig (1965) used tissue [leaves of cotton (*Gossypium hirsutum* L.), bell pepper (*Capsicum frutescens* L.), sunflower (*Helianthus annuus* L.), and birdsfoot trefoil (*Lotus corniculatus* L.)]. The plants were grown in a greenhouse. To obtain different values of water potential, they withheld water from the plants until their leaves wilted to the desired extent. Water potential and osmotic potential were determined with thermocouple psychrometers. The relative water content was determined by using the method of Barrs and Weatherley (1962).

Figure 23.3 shows the relation between the relative water content and osmotic potential for the four plant species, as determined by Gardner and Ehlig (1965). The data are plotted on a logarithmic scale and the straight line has a slope of 45°, as would be predicted if the solute content were to remain constant and the amount of bound water were negligible.

If a plant is growing in a saline soil solution, then over a period of time, the solute content of the cells tends to adjust accordingly. The rate of adjustment varies from species to species. Figure 23.4 shows the relation between the total water potential and the osmotic potential for bell pepper on both saline and nonsaline substrates (Ehlig et al., 1968).

If we neglect the matric and gravitational potentials, we can use Eqn (23.1) to obtain the turgor potential by subtracting the osmotic potential from the total water potential. All three potentials are plotted as a function of relative water content for nonsaline plants (Figure 23.5). Of particular interest is the abrupt change in slope of the pressure potential (turgor potential) at a leaf relative water content of about 0.85. In pepper, for example, this corresponds to a total water potential of about −11 bars (−1.1 MPa) and coincides with the appearance of marked symptoms of visible wilting. The change in slope corresponds to a change in the elastic modulus of the leaf tissue and explains the wilting symptoms. This also corresponds roughly with the point at which the stomata are almost completely closed (Baver et al., 1972, p. 398).

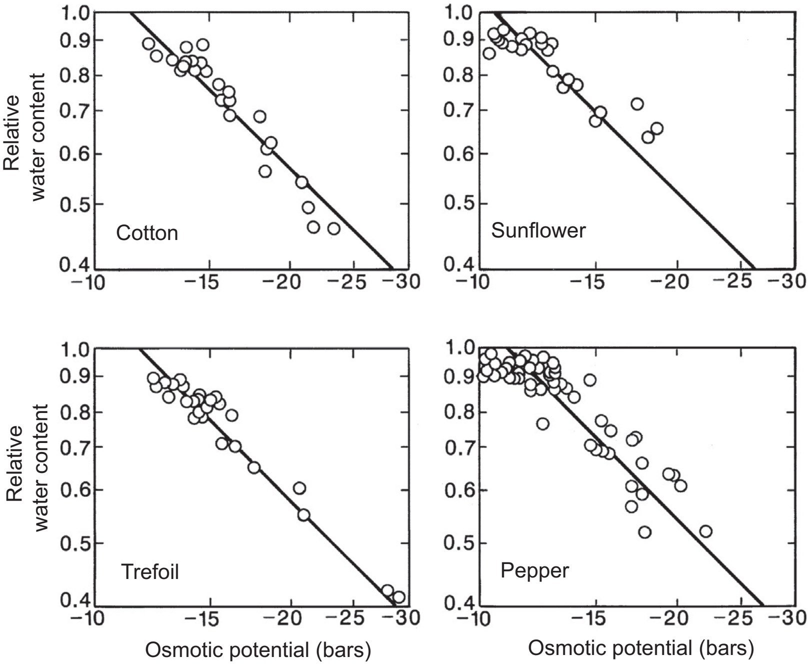

FIGURE 23.3 Leaf relative water content as a function of the average osmotic potential in the plant leaf. The straight lines represent the relation expected if the solutes behave ideally and there is no bound water. *From Gardner and Ehlig (1965), American Society of Plant Physiologists. Reprinted by permission of the American Society of Plant Biologists, Rockville, Maryland.*

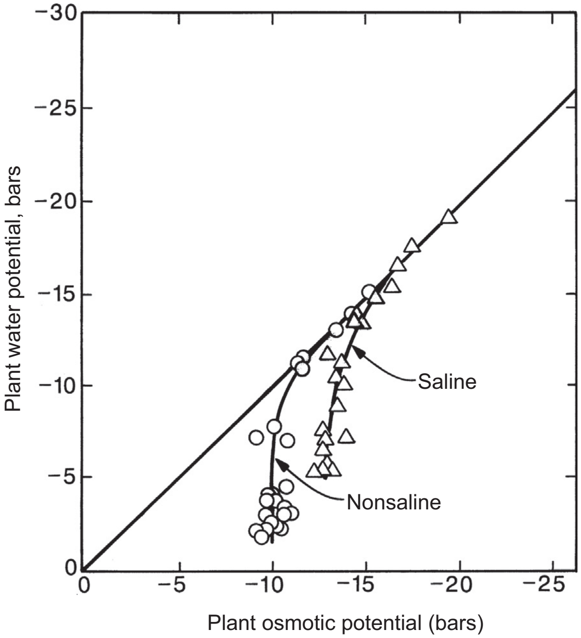

FIGURE 23.4 Plant leaf-water potential (total) as a function of the osmotic potential component. *From Ehlig et al. (1968), American Society of Agronomy: Madison, Wisconsin. Reprinted by permission of the American Society of Agronomy.*

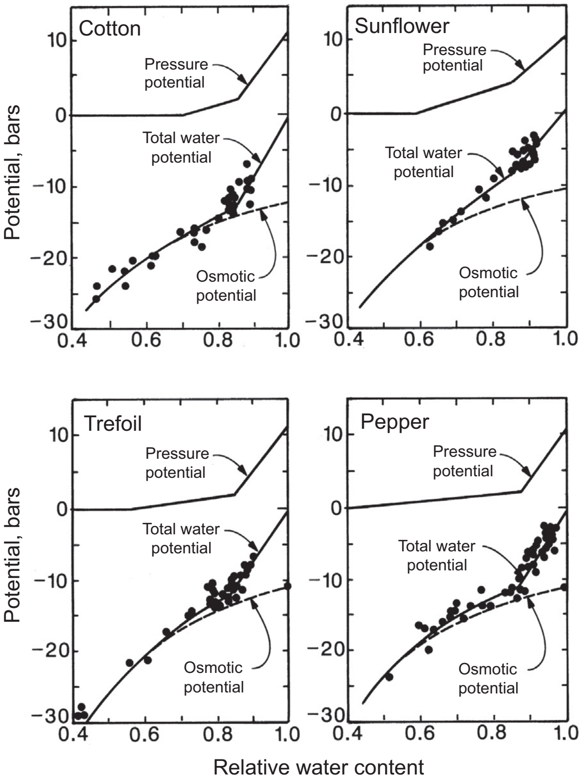

**FIGURE 23.5** The osmotic, pressure, and total water potential of the plant leaf as a function of the relative water content. The circles represent the experimentally determined values for the total water potential. The dashed line is the theoretically predicted osmotic potential. The osmotic and pressure potential components are added to give the calculated relation between total water potential and relative water content indicated by the smooth curve. *From Gardner and Ehlig (1965), American Society of Plant Physiologists. Reprinted by permission of the American Society of Plant Biologists, Rockville, Maryland.*

## 23.3 ELASTICITY

Before we look at the data that Gardner and Ehlig (1965) calculated for the moduli of elasticity of the plants they studied, let us define *modulus of elasticity*. To do this, we refer to a college physics book (Schaum, 1961; pp. 90—91). *Elasticity* is defined as the property by virtue of which a body tends to return to its original size or shape after a deformation and when the deforming forces have been removed. *Stress* is measured by the force applied per unit area that produces or tends to produce deformation in a body. It is expressed in such units as lb/ft$^2$, newton/m$^2$, and dyn/cm$^2$.

$$\text{Stress} = \text{force}/(\text{area of surface on which force acts}) = F/A. \qquad (23.5)$$

*Strain* is the fractional deformation resulting from a stress. It is measured by the ratio of the change in some dimension of the body to the total value of the dimension in which the change occurred (strain is a pure number and has no dimensions). Thus, if a wire of initial length $l$ experiences an elongation $\Delta l$ when a force is applied to the wire, the *longitudinal strain* is

$$\text{longitudinal strain} = (\text{change in length})/(\text{initial length}) = \Delta l/l. \qquad (23.6)$$

The *elastic limit* is the smallest value of the stress required to produce permanent strain in the body. Within the elastic limit of any body, the ratio of the stress to the strain produced is a constant. This constant is called the *modulus of elasticity* of the material of the body.

$$\begin{aligned}\text{Modulus of elasticity} &= \text{stress required to produce unit strain}\\ &= \text{stress/strain}\end{aligned} \qquad (23.7)$$

Equation 23.7 is called *Hooke's law.* (For a biography of Hooke, see the Appendix, Section 23.5.)

There are two types of elasticity: length elasticity and volume elasticity. We now define *length elasticity* or *Young's modulus, Y.* (For a biography of Young, see the Appendix, Section 23.6.) Consider that a wire or rod of length $l$ and cross-sectional area $A$ experiences an elongation $\Delta l$ when a stretching force $f$ is applied to it. Then

$$\begin{aligned}Y &= (\text{longitudinal stress})/(\text{longitudinal strain}) = (F/A)/(\Delta l/l)\\ &= (Fl)/(A\Delta l)\end{aligned} \qquad (23.8)$$

$Y$ may be expressed in lb/in$^2$, newton/m$^2$, or dyn/cm$^2$. $Y$ depends only on the material of the wire or rod and not on its dimensions.

We now define *volume elasticity* or *bulk modulus, B.* Consider that a body is subjected to a hydrostatic pressure, the same amount of force acting perpendicularly on each unit of surface area. The shape of the body remains the same but its volume decreases.

$$\begin{aligned}\text{Volume stress} &= F/A = \text{normal force per unit area}\\ &= \text{pressure increase } \Delta p\end{aligned} \qquad (23.9)$$

$$\text{Volume strain} = (\text{volume decrease } \Delta V)/(\text{initial volume } V) = \Delta V/V \qquad (23.10)$$

$$B = \text{volume stress/volume strain} = \Delta p/(\Delta V/V) = (V\Delta p)/\Delta V \qquad (23.11)$$

The reciprocal of the bulk modulus of a substance is called the *compressibility* of the substance.

## 23.4 ELASTICITY APPLIED TO PLANT LEAVES

Now let us return to the analysis of Gardner and Ehlig (1965). They wanted to determine the elasticity of plant cells. They first plotted turgor potential (pressure potential) versus relative water content (Figure 23.6). If the relative water content is taken as a measure of average cell size (volume) (i.e., they are calculating bulk modulus), it is obvious that cell size is not a simple linear function of turgor pressure. However, the data can be represented reasonably well by two straight line segments. One of the line segments is drawn so as to pass through the point of maximum turgor pressure corresponding to $\Psi_s^o$, as determined from Figure 23.3, when $\theta = 1$. It appears that Hooke's law is obeyed reasonably well, if a distinction is made between a condition of high turgor pressure and one of low turgor pressure and with a different (bulk)

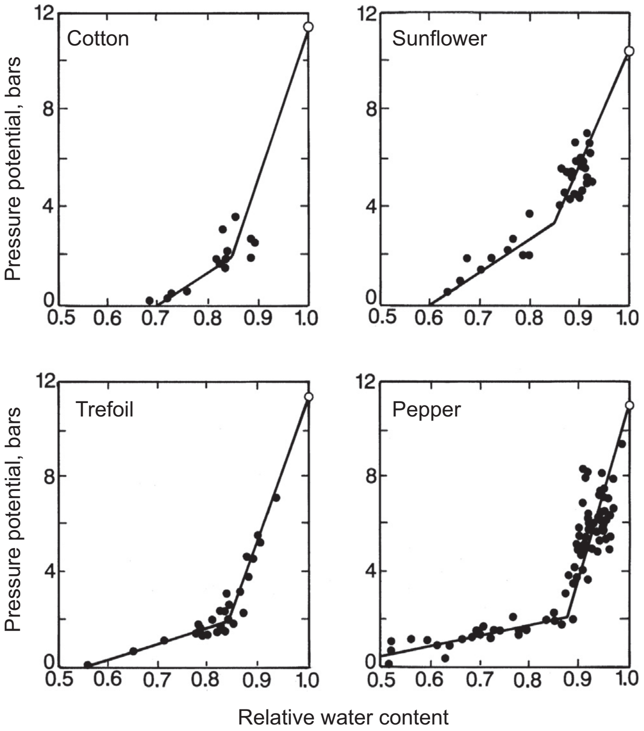

**FIGURE 23.6** Pressure potential of the plant leaf as a function of the relative water content. The pressure potential at a relative water content of unity was taken numerically equal to the osmotic potential at this water content in Figure 23.3. *From Gardner and Ehlig (1965), American Society of Plant Physiologists. Reprinted by permission of the American Society of Plant Biologists, Rockville, Maryland.*

modulus of elasticity for each range. The change in the elasticity occurs at about 2 bars for cotton, trefoil, and pepper, and at about 3.5 bars for sunflower.

Gardner and Ehlig (1965) then looked at the elastic properties of a leaf along different axes (in plane of the leaf and perpendicular to the plane of leaf) (length elasticity or Young's modulus). To investigate this, they determined the areas of the individual leaf disks as a function of relative water content (Figure 23.7). They divided the relative water content (as noted, an indication of volume) by the relative area to obtain the thickness of the leaf disks (Figure 23.8). Note that the data in Figure 23.8 fall on a straight line above a water content of about 0.4, but tend to curve toward the origin at lower water contents. The curvilinear part of the curve is explained by assuming that the water bound in the cell walls does not contribute to the expansion of the leaf. The straight line portion of the curve is displaced upward because of this water. On extrapolating the curves in Figure 23.8 back to zero relative water content, the quantity of water involved can be estimated. This turns out to be 15% for cotton and approximately 10% for sunflower, trefoil,

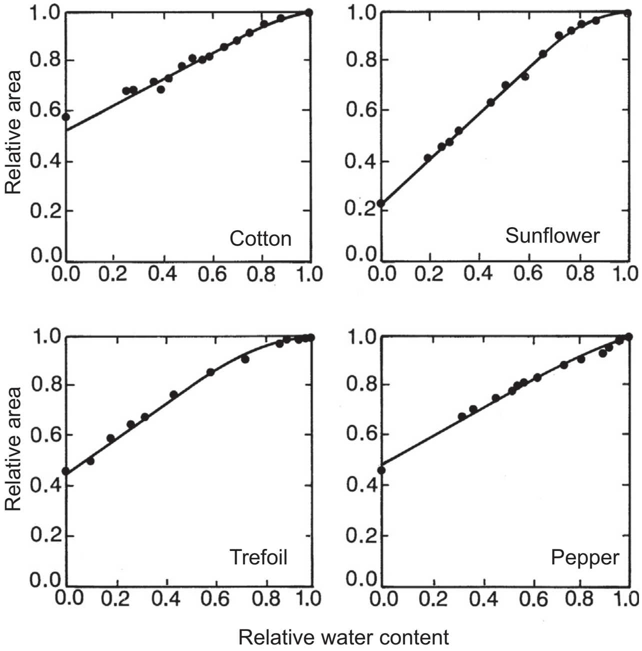

**FIGURE 23.7** Relative area of leaf disks as a function of relative water content. *From Gardner and Ehlig (1965), American Society of Plant Physiologists. Reprinted by permission of the American Society of Plant Biologists, Rockville, Maryland.*

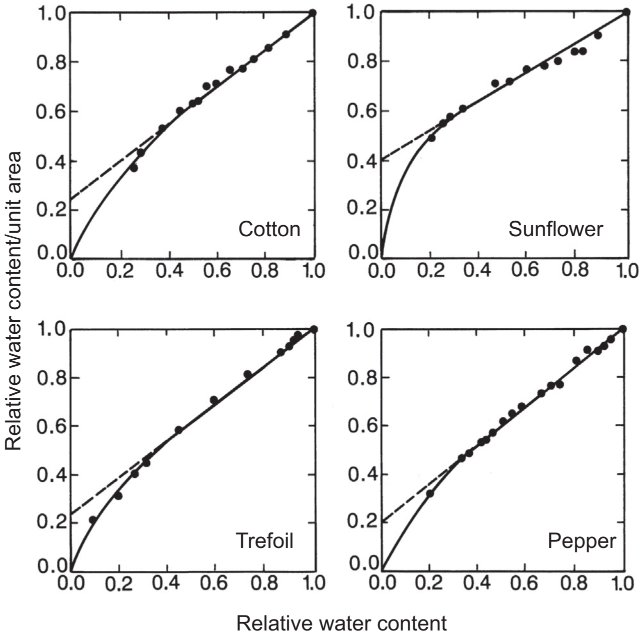

**FIGURE 23.8** Relative water content per unit area as a function of the relative water content. This ratio gives a measure of leaf thickness. *From Gardner and Ehlig (1965), American Society of Plant Physiologists. Reprinted by permission of the American Society of Plant Biologists, Rockville, Maryland.*

and pepper, relative to the fully turgid condition. (In Figure 23.8, read from the dashed line on the ordinate horizontally over to the solid line, and then read the corresponding relative water content on the abscissa.)

The relative diameter and the relative thickness are plotted in Figure 23.9 as a function of pressure potential (turgor pressure or turgor potential). Most of the increase in volume with increasing turgor pressure occurs in the leaf thickness with only a small increase occurring in the lateral dimensions of the leaf. All four species studied exhibited nearly the same moduli of elasticity in the high turgor pressure range, with more variation between species in the low-pressure range. Values for the elastic moduli taken from the slopes of the lines in Figures 23.6 and 23.9 are given in Table 23.1. Ordinarily, the elastic modulus is defined in terms of the increase in a dimension relative to that dimension when there is zero stress. However, it is much more difficult to fix precisely the point of zero turgor than the point of maximum turgor. For this reason, the moduli in Table 23.1 were calculated with respect to a relative water content of 1.0.

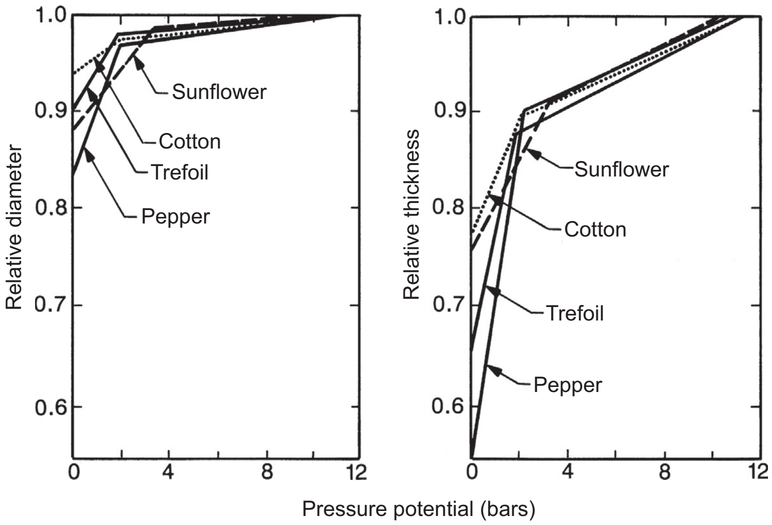

**FIGURE 23.9** Relative diameter and relative thickness of leaf disks as a function of the pressure potential. The slopes of these lines are proportional to the moduli of elasticity. *From Gardner and Ehlig (1965), American Society of Plant Physiologists. Reprinted by permission of the American Society of Plant Biologists, Rockville, Maryland.*

We can compare the values for moduli of elasticity in Table 23.1 to those of nonliving materials (Table 23.2). (To compare units in Tables 23.1 and 23.2, remember that $1\ \mathrm{N/m^2} = 10\ \mathrm{dyn/cm^2}$ because $1\ \mathrm{N} = 10^5\ \mathrm{dyn}$ and $1\ \mathrm{m^2} = 10^4\ \mathrm{cm^2}$. For example, brass has a bulk modulus of $10 \times 10^{10}\ \mathrm{N/m^2}$. This equals $10 \times 10^{11}\ \mathrm{dyn/cm^2}$.) Comparing Tables 23.1 and 23.2, we see

**TABLE 23.1** Moduli of Elasticity

| Species | Turgor Pressure Range (bars) | Bulk Modulus (dyn/cm$^2$) | In Plane of Leaf (dyn/cm$^2$) | Perpendicular to Plane of Leaf (dyn/cm$^2$) |
|---|---|---|---|---|
| Cotton | >2 | $6.0 \times 10^7$ | $42.0 \times 10^7$ | $8.1 \times 10^7$ |
| | <2 | $1.5 \times 10^7$ | $5.0 \times 10^7$ | $2.0 \times 10^7$ |
| Sunflower | >3.4 | $4.7 \times 10^7$ | $46.5 \times 10^7$ | $7.9 \times 10^7$ |
| | <3.4 | $1.4 \times 10^7$ | $3.3 \times 10^7$ | $2.3 \times 10^7$ |
| Trefoil | >2 | $6.0 \times 10^7$ | $48.0 \times 10^7$ | $7.7 \times 10^7$ |
| | <2 | $0.63 \times 10^7$ | $2.6 \times 10^7$ | $0.85 \times 10^7$ |
| Pepper | >2 | $7.1 \times 10^7$ | $35.5 \times 10^7$ | $9.9 \times 10^7$ |
| | <2 | $0.44 \times 10^7$ | $1.6 \times 10^7$ | $0.59 \times 10^7$ |

*From Gardner and Ehlig (1965), American Society of Plant Physiologists. Reprinted by permission of the American Society of Plant Biologists, Rockville, Maryland.*

**TABLE 23.2** Typical Elastic Constants

| Material | Young's Modulus ($N/m^2$) | Bulk Modulus ($N/m^2$) |
|---|---|---|
| Aluminum | $6.9 \times 10^{10}$ | ...[1] |
| Brass | $9.0 \times 10^{10}$ | $10 \times 10^{10}$ |
| Copper | $11 \times 10^{10}$ | $14 \times 10^{10}$ |
| Nickel | $21 \times 10^{10}$ | ... |
| Steel | $20 \times 10^{10}$ | $17 \times 10^{10}$ |
| Tungsten | $35 \times 10^{10}$ | ... |
| Glass | $5.4 \times 10^{10}$ | $3.6 \times 10^{10}$ |
| Ethyl ether | ... | $0.6 \times 10^{9}$ |
| Ethyl alcohol | ... | $1.1 \times 10^{9}$ |
| Water | ... | $2.1 \times 10^{9}$ |
| Mercury | ... | $28 \times 10^{9}$ |

[1] *Not given.*

*From Shortley and Williams (1971), p. 225. Reprinted by permission of Pearson Education, Inc: Upper Saddle River, New Jersey.*

that the bulk modulus of turgid plants is about $10^4$ times less than that of nonliving materials. The bulk modulus of wilted plants is about $10^5$ times less than that of nonliving materials. The modulus in the plane of a leaf of turgid plants is about $10^3$ times less than Young's modulus for nonliving materials. The modulus in the plane of a leaf of a wilted plant is about $10^4$ times less than Young's modulus for nonliving materials. A dry cotton fiber has a Young's modulus of $1 \times 10^{11}$ dyn/cm$^2$ (Nobel, 1974; p. 38). (A dry cotton fiber is almost entirely cellulose.) Young's modulus for cotton fibers is about 5% of that for steel. One can see that the moduli of elasticity for plants can be fairly large.

Some interesting conclusions concerning the phenomenon of wilting can be drawn from the data on elasticity (Table 23.1). It has generally been assumed that the permanent wilting point corresponds to zero turgor pressure in the plant leaf. The data (Figure 23.6 and Table 23.1) indicate that visible wilting symptoms occur at a turgor pressure of 2 or 3 bars. Therefore, the visible wilting associated with the permanent wilting point is due to a marked change in the elastic properties of the cell when the turgor pressure drops below a critical value, rather than the complete absence of turgor. This is logical from a physical standpoint. Disregarding the support given to the leaf blade by the veins, the bending of a leaf is similar to the bending of a beam. The extent to which the leaf will flex under its own weight should be inversely proportional to the appropriate modulus of elasticity and to the cube of the blade thickness (one cubes a leaf dimension to get a volume). When the turgor pressure is above 2 bars, the thickness is relatively constant and little variation in flexure with varying turgor pressure is to be expected. When the turgor pressure is reduced below the critical pressure of about 2 bars, the elastic modulus decreases markedly, allowing the leaf to sag. As the turgor pressure is further reduced, the reduction in leaf thickness tends to permit further bending. The cotton leaf, on one hand, is relatively rigid and is well supported by the veins, so that it exhibits only modest wilting. The pepper leaf, which, on the other hand, is quite elastic and undergoes a considerable change in thickness, shows extreme wilting as the turgor pressure approaches zero (Figure 23.9). The critical turgor pressure at which this change in elasticity is observed corresponds to a water potential of about −11 to −13 bars. This is in good agreement with the traditionally accepted permanent wilting point, which is reasonably well correlated with a soil water potential of −15 bars.

Pressure−volume curves have been used to determine modulus of elasticity of leaves (Melkonian et al., 1982). But we have focused in this chapter on the paper by Gardner and Ehlig (1965), because it relates the physical laws of elasticity (Hooke's law, Young's modulus, bulk modulus) to plant leaves.

## 23.5 APPENDIX: BIOGRAPHY OF ROBERT HOOKE

Robert Hooke (1635−1703) was an English experimental physicist, who discovered the first law of elasticity for solid bodies, known as Hooke's law. He was born on July 18, 1635, at Freshwater, Isle of Wight (Preece, 1971a).

In 1654, Robert Boyle (1627−1691; English physicist and chemist) settled at Oxford, where he erected a laboratory, kept several operators at work, and engaged, in 1655, Robert Hooke as his chemical assistant. After reading of the air pump of Otto von Guericke (1602−1686; German physicist), Boyle used Hooke's skill to make a less clumsy pump, which was completed in 1659 (Cajori, 1929; p. 78).

On November 12, 1662, Hooke was appointed curator of experiments to the Royal Society, of which he was elected a fellow in 1663, and filled the office during the remainder of his life. In 1665, he was appointed professor of geometry in Gresham College. He was secretary to the Royal Society between 1677 and 1683, publishing in 1681−1682 the papers read before that body under the title of *Philosophical Collections.*

Hooke's optical investigations led him to adopt in 1665 in an imperfect form the undulatory theory of light, which preceded the paper on the wave theory of light presented by Christian Huygens (1629−1695; Dutch physicist) at the meeting of the French Academy of Sciences in 1678 (Preece, 1971a). (Huygens was induced by Louis XIV to settle in Paris, where he remained from 1666 to 1681 and, like his great contemporaries Newton and Leibniz, Huygens never married.) Hooke was the first to state clearly that the motions of the heavenly bodies must be regarded as a mechanical problem, and he approached in a remarkable manner the discovery of universal gravitation (Preece, 1971a).

Hooke invented the wheel barometer, discussed the application of barometric indications to meteorologic forecasting, and put forward the idea of using the pendulum as a measure of gravity. He is credited with the invention of the anchor escapement for clocks and of the application of spiral springs to the balances of watches (1676) (Preece, 1971a). Hooke died on March 3, 1703, in London. His principal writings are *Micrographia* (1665), *Lectiones Cutlerianae* (1674–1679), and *Posthumous Works.*

## 23.6 APPENDIX: BIOGRAPHY OF THOMAS YOUNG

Thomas Young (1773–1829), an English physicist and physician, who gave his name to Young's modulus, was born at Milverton, Somersetshire, England, on June 13, 1773 (Preece, 1971b). This great scientist had an extraordinary childhood (Cajori, 1929; p. 148). He could read with fluency at the age of 2. When 4 years old he had read the Bible twice through; at the age of 6 he could repeat the whole of Goldsmith's *Deserted Village.* He devoured books, whether classical, literary, or scientific, in rapid succession. At about the age of 16 years, he abstained from using sugar on account of his opposition to the slave trade. At the age of 19 years, he entered upon a medical education, which was pursued first in London, then in Edinburgh (Scotland), Göttingen (Germany), and finally at Cambridge (England). He began medical practice in London in 1799 (Preece, 1971b). In 1801, he accepted the office of professor of natural philosophy in the Royal Institution, the metropolitan school of science established in the preceding year. He held this position for 2 years. In 1802, he was appointed foreign secretary of the Royal Society and held this office for the remainder of his life. He was elected fellow of the Society in 1794.

Young's earliest studies were on the anatomic and optical properties of the eye; then followed his first epoch of optical discovery, 1801–1804. In 1801, the paper that Young read before the Royal Society dealt with the color of thin plates, in which he supported the undulatory theory of light (Cajori, 1929; p. 149). He made crucial early researches that effectively established the wave theory and was the first to make a thorough application of it to sound and light. He gave the word *energy* its scientific significance (Preece, 1971b).

Young's observations were made with great exactness, but his mode of explaining them was condensed and somewhat obscure (Cajori, 1929; p. 149). His papers, containing the great principle of interference, constituted by far the most important publication on physical optics issued since the time of Newton, yet they made no impression on the scientific public. They were attacked by Lord Brougham in the *Edinburgh Review.* Young's articles were declared to contain "nothing which deserves the name either of experiment or discovery," to be "destitute of every species of merit." "We wish to raise our feeble voice," says Brougham, "against innovations that can have no other effect than to check the progress of science." After stating that the law of interference was "absurd" and "illogical," Brougham said, "We now dismiss, for the present, the feeble lucubrations of this author, in which we have searched without success for some traces of learning, acuteness, and ingenuity, that might compensate his evident deficiency in the powers of solid thinking, calm and patient investigation, and successful development of the laws of nature, by steady and modest observation of her operations." Young issued an able reply, published in the form of a pamphlet, which failed to turn public opinion in favor of this theory (Cajori, 1929; p. 150).

Because his wave theory was laughed at, Young proceeded to other studies. The 12 succeeding years after 1801 were given to medical practice and to the study of philology, especially the decipherment of Egyptian hieroglyphic writing. The Rosetta stone (black basalt, 114 cm long and 71 cm wide) is an ancient Egyptian stone bearing inscriptions in two languages and three scripts: hieroglyphics, demotic (another ancient Egyptian writing), and Greek. It was found in August 1799, by a French man, whose name is given variously as Bouchard or Boussard, during the execution of repairs to the fort of St Julien near the town of Rosetta, or Rashid, on the left bank of a branch of the Nile in the western delta, about 48 km from Alexandria. It passed into British hands with the French surrender of Egypt (1801) and is now in the British Museum, London. The inscription records the commemoration of the accession of Ptolemy V Ephiphanes to the throne of Egypt in the year 197–196 BC in the ninth year of his reign. The stone gave the key to the translation of Egyptian hieroglyphics hitherto undeciphered (Seton-Williams, 1971).

The decipherment of the hieroglyphic inscription was largely the work of Young and Jean François Champollion (1790–1832; French Egyptologist). Young was the decipherer of the demotic script (Robinson, 2005) and deduced that it was related directly to the hieroglyphics (Kassell, 2006). He discovered that the royal names were written within ovals known as cartouches, and he worked out the names of Ptolemy and Cleopatra. He also discovered in 1814 the way in which the hieroglyphic signs were to be read, by examining the direction in which the birds and animals in this pictorial script faced. The work of these two men established the basis for the translation of all hieroglyphic texts (Seton-Williams, 1971). One hieroglyph that we recognize today is the ankh, a cross with a loop at the top. It is the symbol for life.

When Augustin Fresnel (1788–1827; French physicist) began to experiment on light and to bring into prominence Young's theory, Young resumed his early studies, and entered into his second great epoch of optical investigation (Cajori, 1929; p. 149). Young died in London on May 10, 1829.

## References

Barrs, H.D., Weatherley, P.E., 1962. A re-examination of the relative turgidity technique for estimating water deficits in leaves. Aust. J. Biol. Sci. 15, 413–428.

Baver, L.D., Gardner, W.H., Gardner, W.R., 1972. Soil Physics, fourth ed. Wiley, New York.

Bowes, B.G., 2000. A Color Atlas of Plant Structure. Iowa State University Press, Ames.

Cajori, F., 1929. A History of Physics. Macmillan, New York.

Ehleringer, J.R., Sage, R.F., Flanagan, L.B., Pearcy, R.W., 1991. Climate change and the evolution of $C_4$ photosynthesis. Trends Ecol. Evol. 6, 95–99.

Ehlig, C.F., Gardner, W.R., Clark, M., 1968. Effect of soil salinity on water potentials and transpiration in pepper (*Capsicum frutescens*). Agron. J. 60, 249–253.

Esau, K., 1965. Plant Anatomy, second ed. Wiley, New York.

Esau, K., 1977. Anatomy of Seed Plants, second ed. Wiley, New York.

Fahn, A., Cutler, D.F., 1992. Xerophytes: Encyclopedia of Plant Anatomy vol. 13. Gebrüder Borntraeger, Berlin. Part 3.

Gardner, W.R., Ehlig, C.F., 1965. Physical aspects of the internal water relations of plant leaves. Plant Physiol. 40, 705–710.

Hatch, M.D., Slack, C.R., 1966. Photosynthesis by sugar-cane leaves. A new carboxylation reaction and the pathway of sugar formation. Biochem. J. 101, 103–111.

Hatch, M.D., 1992. $C_4$ photosynthesis: an unlikely process full of surprises. Plant Cell Physiol. 33, 333–342.

Kassell, L., 2006. The last true know-it-all. Book review of The Last Man Who Knew Everything: Thomas Young, the Anonymous Polymath Who Proved Newton Wrong, Explained How We See, Cured the Sick, and Deciphered the Rosetta Stone, Among Other Feats of Genius. By Andrew Robinson. Pi Press, New York, 288 pp. Am. Sci. 94, 378–379.

Kirkham, M.B., 2011. Elevated Carbon Dioxide: Impacts on Soil and Plant Water Relations. CRC Press, Boca Raton, Florida.

Laetsch, W.M., 1974. The $C_4$ syndrome: a structural analysis. Annu. Rev. Plant Physiol. 25, 27–52.

Melkonian, J.J., Wolfe, J., Steponkus, P.L., 1982. Determination of the volumetric modulus of elasticity of wheat leaves by pressure-volume relations and the effect of drought conditioning. Crop Sci. 22, 116–123.

Mellor, R.S., Jensen, R.G., 1986. Photosynthesis: nature's big green machine. Sci. Food Agr. 4 (1), 14–19.

Nobel, P.S., 1974. Introduction to Biophysical Plant Physiology. W.H. Freeman and Company, San Francisco.

Preece, W.E. (Ed.), 1971a. Hooke, Robert. Encyclopaedia Britannica, vol. 11, p. 669.

Preece, W.E. (Ed.), 1971b. Young, Thomas. Encyclopaedia Britannica, vol. 23, p. 909.

Rachidi, F., Kirkham, M.B., Stone, L.R., Kanemasu, E.T., 1993. Soil water depletion by sunflower and sorghum under rainfed conditions. Agric. Water Manage. 24, 49–62.

Robinson, A., 2005. A polymath's dilemma. Nature 438, 291.

Schaum, D., 1961. Theory and Problems of College Physics, sixth ed. Schaum, New York.

Seton-Williams, M.V., 1971. Rosetta Stone. In: Encyclopaedia Britannica, vol. 19, 629.

Shortley, G., Williams, D., 1971. Elements of Physics, fifth ed. Prentice-Hall, Englewood Cliffs, New Jersey.

Slavík, B., 1963. Relationship between the osmotic potential of cell sap and the water saturation deficit during the wilting of leaf tissue. Biol. Plant 5, 258–264.

Torres, A.M., Costello, W.L., 1963. A Laboratory Manual for General Botany. Wm. C. Brown, Dubuque, Iowa.

Woolhouse, H.W., 1978. Light-gathering and carbon assimilation processes in photosynthesis: their adaptive modifications and significance for agriculture. Endeavour (New Series) 2 (1), 35–46.

CHAPTER

# 24

# Stomatal Anatomy and Stomatal Resistance

The two main parts of a plant that control its water status are the roots, where water enters, and the stomata on the leaves, where water exits. We considered roots in Chapters 15 and 16. Here we consider stomata.

## 24.1 DEFINITION OF STOMATA AND THEIR DISTRIBUTION

The stomata are apertures in the epidermis, each bounded by two guard cells. In Greek, *stoma* means "mouth", and the term is often used with reference to the stomatal pore only. Esau (1965, p. 158) uses the term stoma to include the guard cells and the pore between them, and we will use her definition. The plural of stoma is *stomata*. There is no such word as "stomates".

Stomata occur in vascular plants. Vascular plants include the lower vascular plants such as horsetails (*Equisetum*), ferns (class Filicinae), gymnosperms, and angiosperms. As noted before, the angiosperms are the flowering plants and this group consists of the two large classes: Monocotyledoneae (monocotyledons) and Dicotyledoneae (dicotyledons) (Fernald, 1950).

By changing their shape, the guard cells control the size of the stomatal aperture. The aperture leads into a substomatal intercellular space, the substomatal chamber, which is continuous with the intercellular spaces in the mesophyll. In many plants, two or more cells adjacent to the guard cells appear to be associated functionally with them and are morphologically distinct from the other epidermal cells. Such cells are called *subsidiary*, or *accessory*, cells (Esau, 1965, p. 158).

The stomata are most common on green aerial parts of plants, particularly the leaves. They can also occur on stems, but less commonly than on leaves. The aerial parts of some chlorophyll-free land plants

http://dx.doi.org/10.1016/B978-0-12-420022-7.00024-0

Copyright © 2014 Elsevier Inc. All rights reserved.

(*Monotropa*, *Neottia*) and roots have no stomata as a rule, but rhizomes have such structures (Esau, 1965, p. 158). Stomata occur on some submerged aquatic plants and not on others. The variously colored petals of flowers often have stomata, sometimes nonfunctional. Fruits also can have stomata. Stomata are found on stamens and gynoecia.

Stomata can be distributed in the following ways on the two sides of a leaf:

- An *amphistomatous* leaf has stomata on both surfaces. Most plants have such a distribution.
- A *hypostomatous* leaf has stomata only on the lower surface. Many tree species are characterized by having hypostomatous leaves, such as horse chestnut (*Aesculus hippocastanum*) and basswood (*Tilia europaea*) (Meidner and Mansfield, 1968; see their Table 1.1). The leaf of poplar (*Populus* sp.) is an exception. It has stomata on both surfaces and a petiole that allows the leaf to turn readily in the wind. These adaptations may allow its fast growth rate. The fast growth rate of poplar is one reason it is widely used in phytoremediation (use of plants to remove pollutants from soil).
- An *epistomatous* leaf has stomata only on the upper surface of the leaf. Some floating plants are epistomatous.
- A *heterostomatous* leaf has stomata that occur with more than twice the frequency on the abaxial surface than on the adaxial surface. An *isostomatous* leaf has stomata that occur with approximately equal frequencies on both surfaces.

The *stomatal ratio* is the ratio of stomatal frequency on the adaxial surface to that on the abaxial surface.

## 24.2 STOMATAL ANATOMY OF DICOTS AND MONOCOTS

Figure 24.1 shows how the stomata develop differently in broad-leaved plants (mainly dicotyledons), which have elliptical shapes, compared to grass species (monocotyledons), which have dumbbell shapes. The most commonly occurring stomata are elliptical in shape and differentiate from a protodermal cell by division into two guard cells, which soon assume their typical shape—like a bean in surface view (Figure 24.1(A)). By separating slightly in the center, the guard cells form the stomatal pore between them. There is no radical change in the shape of the guard cells as they grow in size except that the early rounded shape changes into a more elongated, elliptical one. Adjacent epidermal cells may or may not be distinctive in appearance, but they usually function as subsidiary cells (Meidner and Mansfield, 1968, p. 6).

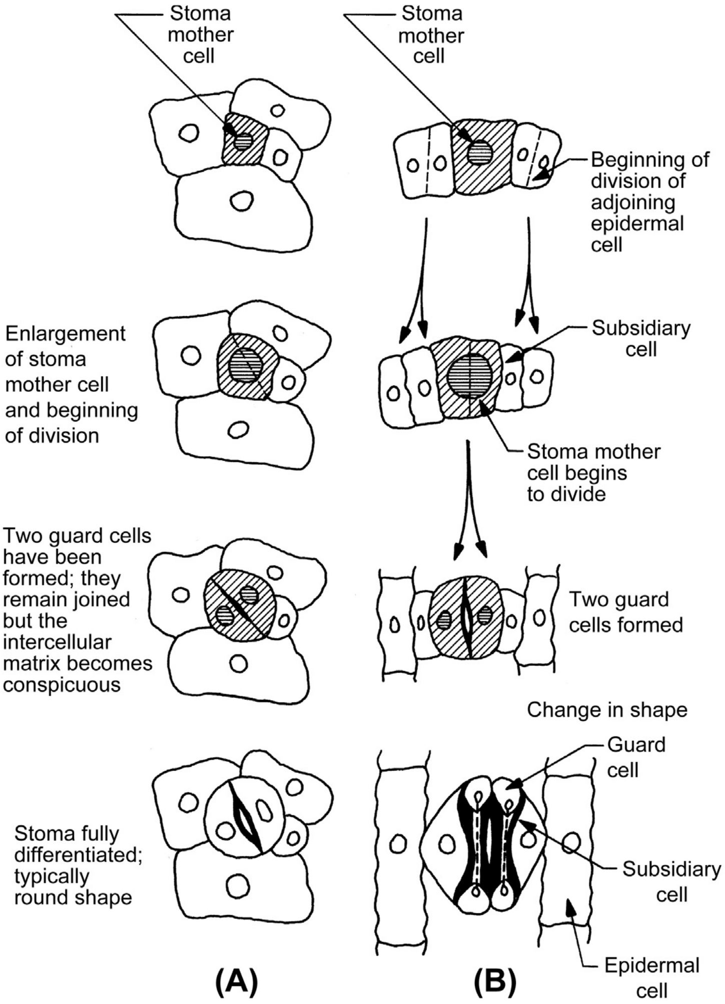
Stoma mother cell
Stoma mother cell
Beginning of division of adjoining epidermal cell
Enlargement of stoma mother cell and beginning of division
Subsidiary cell
Stoma mother cell begins to divide
Two guard cells have been formed; they remain joined but the intercellular matrix becomes conspicuous
Two guard cells formed
Change in shape
Guard cell
Stoma fully differentiated; typically round shape
Subsidiary cell
Epidermal cell
(A)
(B)

**FIGURE 24.1** Four stages in the differentiation of (A) elliptically shaped and (B) graminaceous stomata. *From Meidner and Mansfield (1968), p. 7. This material is reproduced with permission of The McGraw-Hill Companies.*

In most members of the Poaceae (formerly Gramineae) (grass family) and Cyperaceae (sedge family), differentiation of a stoma begins with the division of two protoderm cells on either side of a stoma mother cell. The two daughter cells resulting from these divisions, which lie adjacent to the stoma mother cell, are the two future subsidiary cells. They are clearly distinguishable in shape from the other epidermal cells. The stoma mother cell divides next to form the guard cells, between which the stomatal pore appears. At this stage, the graminaceous stoma resembles the elliptical one in shape, but a further stage in its development results in an elongation of the guard cells which finally assume the characteristic dumbbell shape (Figure 24.1(B)) (Meidner and Mansfield, 1968; pp. 6–8).

In leaves with parallel veins, such as those of monocotyledons and some dicotyledons, and in the needles of conifers, the stomata are arranged in parallel rows. In netted-veined leaves, which include most dicotyledons and a few monocotyledons, the stomata are scattered (Esau, 1965; p. 158). In leaves with parallel veins, which have the stomata in longitudinal rows, the developmental stages of the stomata are observable in sequence in the successively more differentiated portions of the leaf. This sequence is basipetal, that is, from the tip of the leaf downward. In the netted-veined leaves, the different developmental stages are mixed in mosaic fashion so that mature stomata occur side by side with immature ones (Esau, 1965; p. 166).

## 24.3 STOMATAL DENSITY

Esau (1965, p. 158) gives the density of stomata as between 100 and 300/mm$^2$ for leaves of many species. The number of stomata depends on the species. Meidner and Mansfield (1968; see their Table 1.1) give the frequency of stomata on leaves of different species, including the lower vascular plants (ferns), gymnosperms, and angiosperms. Most plants have more stomata on the lower (abaxial) surface than on the upper (adaxial) surface, but wheat (*Triticum* sp.) is an exception. It has more stomata on the upper surface than on the lower surface. The number of stomata per unit area changes as a leaf grows. It tends to be higher in earlier stages of development than in later stages (Meidner and Mansfield, 1968; p. 6). Stomata may grow in size and change shape as the leaf blade expands.

At maturity of a leaf, the number of stomata per unit leaf area may not be constant. It can be affected by environmental factors. More stomata per unit area occur in sun leaves than in shade leaves. More stomata per unit area occur in leaves of plants growing in moist soil and high humidity than in those growing in dry conditions. Stomatal density can be affected by leaf position. Liang et al. (1975) measured stomatal density on the 15 uppermost leaves of six varieties of the grain sorghum [*Sorghum bicolor* (L.) Moench] and their 15 $F_1$ hybrids. The second leaf from the top had the highest density, and leaf no. 15 had the lowest. Distribution can also vary with distance from the leaf base. Liang et al. (1975) found in their study with sorghum that stomatal density on the abaxial surface (which had more stomata than the adaxial surface) was highest at the basal portion of the leaves.

## 24.4 DIFFUSION OF GASES THROUGH STOMATAL PORES

The distribution of stomata affects the diffusion of gases through them. Early important investigations on the diffusion of gases and liquids through small openings were carried out by Brown and Escombe (1900). These investigations proved that the rates of diffusion through small single apertures are proportional to the diameters and not to the areas of the openings. This agreed with results previously established by Stefan for the converse case of evaporation from circular surfaces of water (Maximov, 1929; p. 172). He compared evaporation from large surfaces (e.g., lakes) and small surfaces. For surfaces of small dimension, diffusion is more rapid at the edges than at the center, because at the margins the molecules of water vapor can diffuse fanwise in all directions instead of only perpendicularly to the surface at the center. It follows that, in still air, the smaller the area of the evaporating surface, the more rapid the rate of evaporation. But for areas of such small dimensions as leaves or small bowls of water, it appears, as has been mathematically calculated by Stefan (1881), that evaporation is proportional not to the area of these objects but to their periphery or radius (Maximov, 1929; p. 136).

Brown and Escombe (1900) found that their "diameter law" holds good also for the case of diffusion through a number of small openings (i.e., through a "multiperforate septum"). From this it follows that more water vapor will diffuse in unit time through several small apertures than through a single larger opening with an area equal to the combined areas of the smaller ones. If, however, the perforations in a septum separating two mixtures of gases of different composition (e.g., dry and moist air) are very close together, the rate of diffusion is modified. The "lines of flow" of the diffusing molecules, which normally tend to diverge fanwise as they issue from the apertures (Figure 24.2), now interfere with one another and mutually hinder the spread of the diffusing particles, thus slowing down the rate of diffusion. Brown and Escombe (1900) showed experimentally that such interference begins when the distance between the apertures is somewhat less than 10 times the diameter of the holes. The fact that the rate of diffusion through small openings is proportional not to the area, but to the diameter of the opening, greatly increases the possible amount of diffusion that can take place through a multiperforate septum (Maximov, 1929; pp. 172–173).

Molecular biology research has been done to understand stomatal spacing (Shpak et al., 2005). An enzyme in the flowering plant *Arabidopsis thaliana*, called *YODA* (*YDA*), is crucial to the formation and arrangement of stomata. *YODA* is the name given to a mitogen activated protein (MAP) kinase kinase kinase (MAPKK kinase gene), which is an important

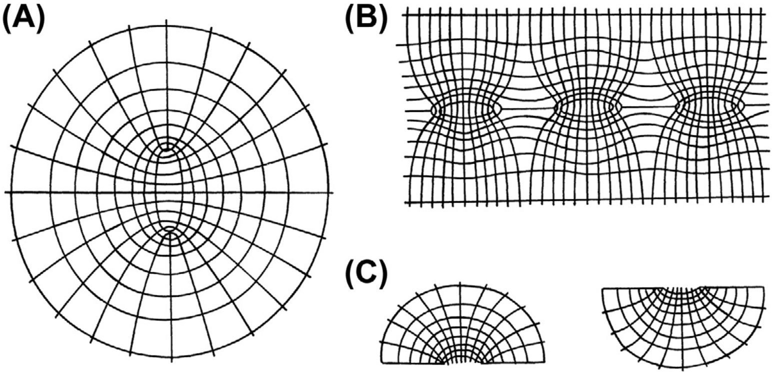

**FIGURE 24.2** Diagrammatic representation of the diffusion of water vapor through small openings. (A) Diffusion through a single opening in a vertical septum; the fanlike, diverging lines show the courses of the diffusing particles; perpendicular to them are concentric lines of equal vapor density. (B) Diffusion through a horizontal multiperforate septum (three openings are represented); (C) Diffusion through single openings of the same size. *From Maximov (1929), p. 173.*

regulator of stomatal development. Mutations in the *YDA* gene result in a plant in which almost all the cells at the plant surface are guard cells. This overproduction of stomata has severe consequences, and many of the mutant seedlings die (Bergmann et al., 2004; Serna, 2004). Mutations in three other genes—named *Too Many Mouths* (*TMM*), *Stomatal Density and Distribution1* (*SDD1*), and *Four Lips* (*FLP*)—also affect stomata, not only producing stomatal clusters but also allowing the formation of single stomata. The single stomata ensure correct gas exchange and so these three mutants develop normally (Serna, 2004).

## 24.5 GUARD CELLS

Guard cells may occur at the same level as the adjacent epidermal cells, or they may protrude above or be sunken below the surface of the epidermis (Figure 24.3). In some plants, stomata are restricted to the epidermis that lines depressions in the leaf, the stomatal crypts. Epidermal hairs may also be prominently developed in such crypts. Stomata are level with the epidermal cells in most mesophytic plants and plants that grow in moist habitats. Plants that grow in dry habitats often have stomata that are situated below the level of the epidermal cells.

The guard cells are generally crescent-shaped with blunt ends (kidney shaped) in surface view (Figure 24.3(D)) and often have ledges of wall material on the upper and lower sides. In sectional views such ledges appear like horns (Figure 24.3(E), (F) and (H)). Sometimes a ledge occurs only on the upper side (Figure 24.3(A), (G) and (I)), or none is present. If

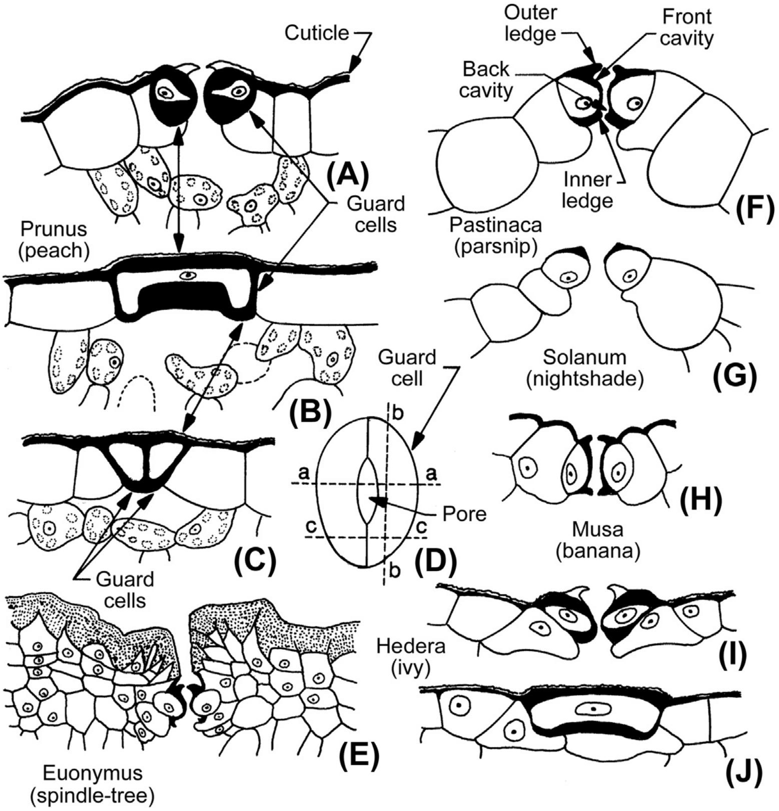
Cuticle
Outer ledge
Front cavity
Back cavity
Inner ledge
(A)
Guard cells
Prunus (peach)
Pastinaca (parsnip)
(F)
Solanum (nightshade)
(G)
Guard cell
(B)
b
a
a
Pore
c
c
b
(D)
(H)
Musa (banana)
(C)
Guard cells
Hedera (ivy)
(I)
(E)
(J)
Euonymus (spindle-tree)

**FIGURE 24.3** Stomata in abaxial epidermis of foliage leaves. (A–C) Stomata and some associated cells from each leaf sectioned along planes indicated in D by the broken lines *aa*, *bb*, and *cc*. (E–I) stomata from various leaves cut along the plane *aa*. (J) One guard cell of ivy cut along the plane *bb*. The stomata are raised in A, F, G. They are slightly raised in I, slightly sunken in H, and deeply sunken in E. The hornlike protrusions in the various guard cells are sectional views of ledges. Some stomata have two ledges (E, F, H); others only one (A, G, I). Ledges are cuticular in A, E, I. The *Euonymus* leaf has a thick cuticle; epidermal cells are partly occluded with cutin. *From Esau (1965), p. 159. This material is used by permission of John Wiley & Sons, Inc.*

two ledges are present, the upper delimits the front cavity above the stomatal pore, and the lower encloses the back cavity between the pore and the substomatal chamber (Figure 24.3(F)). The ledges are more or less heavily cutinized (Esau, 1965; p. 159).

The walls of the guard cells can be differentially thickened. The change in shape of the guard cells occurs because the wall that is turned away from the stomatal aperture, the so-called back wall, is thin and apparently elastic (Figure 24.3(A), (E–I)). When the turgor increases, the thin wall bulges away from the aperture, while the front wall (facing the pore) becomes straight or concave. The whole cell appears to bend away from the aperture, and the aperture increases in size. Reversed changes occur under decreased turgor (Esau, 1965; p. 161).

Another distinct type of stomatal mechanism is illustrated by the guard cells of Poaceae and Cyperaceae. These cells are bulbous at two ends and straight in the middle (Figure 24.1, right). The middle part has a strongly but unevenly thickened wall; the bulbous ends have thin walls, and the wall between the bulbous ends of two adjacent cells may be incomplete so that the protoplasts of the two guard cells are partially confluent. Increase in turgor causes a swelling of the bulbous ends and the consequent separation of the straight median portions from each other. The nucleus in a gramineous guard cell is extended and simulates the shape of the cell lumen. It has two enlarged ends connected by a thin threadlike middle part.

In addition to the nucleus, guard cells contain chloroplasts, which are not present in other epidermal cells. These chloroplasts are considered to be photoreceptors involved in the light-induced opening of stomata. Mitochondria are also present in guard cells. The osmotic pressure of guard cell sap of open stomata is higher than that of sap in neighboring epidermal cells. The increase in osmotic pressure is thought to be due, in large part, to the influx of potassium (see Section 24.6). Anthocyanin is absent in guard cells, but occurs in epidermal cells. Proteinaceous crystals and calcium oxalate crystals are absent in guard cells, but occur in epidermal cells. Guard cells are, in general, more resistant to adverse conditions such as low temperatures and drought. They do not senesce as rapidly as other epidermal cells.

## 24.6 MECHANISM OF STOMATAL OPENING

The outstanding feature of stomata, the unevenly thickened walls of the guard cells, is related to the changes in shape and volume (and the concomitant changes in the size of stomatal aperture), which are operated by turgor changes in guard cells (Esau, 1965; p. 160). Many factors control guard cell turgor, including carbon dioxide concentration, light, temperature, endogenous rhythms, atmospheric vapor pressure deficit, and soil water potential (Heath and Mansfield, 1969; see their summarizing Figure 9.9).

No matter what causes the opening, the basic mechanism underlying stomatal opening in light, in most cases, is thought to be related to the uptake of potassium by guard cells in amounts sufficient to lower significantly the solute potential. It has been known for a long time that potassium accumulates in guard cells. As early as 1905, Macallum (1905) observed accumulation of potassium in the guard cells of tulip. Imamura (1943) found an abundance of potassium in guard cells of open stomata, but little in closed ones. He also observed that the "suction force" of guard cells changed during opening and closing without any appreciable changes in their starch content. Imamura suggested that these changes in suction force were regulated by movement of solutes, particularly potassium, in and out of the guard cells. Two more Japanese workers, Yamashita (1952) and Fujino (1967), confirmed that the potassium content in guard cells is correlated with stomatal movement. Earlier papers by Fujino in Japanese, unknown in the United States, showed that guard cells contain large concentrations of potassium, but small quantities when closed in the dark. Fischer (1968) independently showed that potassium uptake was necessary for stomatal opening. When Fujino published his paper in English in 1967, his earlier work became known in America. Both Fujino and Fischer are attributed with proposing that stomatal opening and closing are the result of transport of potassium ions.

Many papers were published between the late 1960s and the 1990s confirming the role of potassium in the control of stomatal opening. The work was done at the leaf or cellular level. For example, Peaslee and Moss (1968) showed that K-deficient corn (*Zea mays* L.) leaves had smaller stomatal widths than control leaves. Stomata of normal corn leaves opened about 6.5 μm in diameter, while stomata in K-deficient leaves were less than 1 μm in diameter. Now, work focuses on the molecular biology of potassium transport into guard cells. Stomatal opening depends on blue and red light. Stomata open in response to weak blue light and the opening is enhanced by background red light. Blue light activates an enzyme (plasma membrane $H^+$-ATPase; ATPase stands for adenosine triphosphatase) and increases the inside negative electrical potential across the plasma membrane in guard cells. The potential drives $K^+$ uptake, and the accumulated positive $K^+$ charges are compensated mainly by malate$^{2-}$ formed in guard cells. Red light induces stomatal opening at high intensity. Red light likely mediates stomatal opening via reduction of the intercellular concentration of carbon dioxide by mesophyll photosynthesis (Shimazaki et al., 2007).

Even though much is known about stomata, stomatal movements cannot yet be reliably predicted (Brodribb and McAdam, 2011). The complexity that characterizes stomatal control in seed plants is absent in early-diverging vascular plant lineages. Ziegler (1987) reviews the evolution of stomata.

## 24.7 BOUNDARY LAYER

Above all objects is a thin layer of still air, called the laminar sublayer (Rosenberg, 1974; p. 78), or the boundary layer, which adheres to their

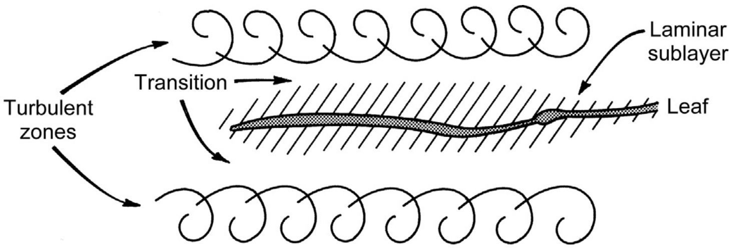

**FIGURE 24.4** Air structure near a small object (like a leaf) in an air stream. *From Rosenberg (1974), p. 79. This material is used by permission of John Wiley & Sons, Inc.*

surfaces. A plane with only one surface exposed, such as the soil surface, will have such a layer on one side. An object, like a leaf, within an air stream will have the layer on all surfaces (Figure 24.4). The thickness of the layer depends on the roughness of the surface, on the wind speed, and on the leaf dimension. A leaf with a hairy surface is rougher than a leaf with a smooth wax. The boundary layer will be thicker the rougher the surface is. Roughness is nearly zero over very smooth surfaces, like open water on a calm day. Roughness increases with increasing height of objects sticking above the surface (Rosenberg, 1974; p. 104). The boundary layer is thinner the more windy the conditions. In growth chamber experiments, it is important to have fans circulating air in the closed chambers, so that the boundary layer (or more specifically, boundary-layer resistance) is reduced and gas exchange (in particular, carbon dioxide uptake) is similar to natural conditions in the open environment. The thickness of the boundary layer depends on the linear dimension of the leaf in the downwind direction (Nobel, 1974; p. 305). Both boundary-layer resistance and stomatal resistance are important in controlling gas transport through leaves (see next section).

## 24.8 LEAF RESISTANCES

The resistances to water vapor transport in a leaf are the epidermal resistance, made up of the stomatal resistance and the cuticular resistance, and the boundary-layer resistance. The resistances to carbon dioxide transport in a leaf are the same as for water vapor (stomatal, cuticular, and boundary-layer resistances); a fourth resistance called the mesophyll resistance is discussed later in this section.

Water vapor diffuses through two of the resistances in a leaf acting in *series*: the stomatal aperture resistance (stomatal resistance) ($r_s$) and the boundary-layer (air) resistance ($r_a$), which results from the lengthening of the diffusion path outside of the stomata and which is an inverse function of wind and turbulence (Gale and Hagan, 1966). The resistance to cuticular water loss ($r_c$) is very large and is in *parallel* to $r_s$.

Let us now review our physics concerning resistors in series and parallel (Schaum, 1961; p. 156). In a series circuit (Figure 24.5, left), resistance is as follows:

$$R = R_1 + R_2 + R_3 + \ldots, \tag{24.1}$$

where $R$ = equivalent resistance of a series combination of conductors having resistances $R_1$, $R_2$, $R_3$, ... The total *potential difference* across several resistors connected in series is equal to the sum of the potential differences across the separate resistors. Current in every part of the series circuit is the same.

In a parallel circuit (Figure 24.5, right), resistance is as follows:

$$1/R = (1/R_1) + (1/R_2) + (1/R_3) + \ldots, \tag{24.2}$$

where $R$ = equivalent resistance of a parallel combination of conductors having resistances $R_1$, $R_2$, $R_3$, ... $R$ is always less than the smallest of the individual resistances. Connecting additional resistors in parallel decreases the joint resistance of the combination. The *potential difference* across several resistors in parallel is the same as that across each of the resistors. The potential difference is the same across all branches. The sum of the currents in the branches is equal to the value of the line current. Current values in the different branches vary inversely as the resistances of the different branches (Figure 24.5, right) (Schaum, 1961).

The conductance via the cuticle $r_c^{-1}$ is very small and may be neglected, unless $r_s$ is large, as when the stomata close. As noted, the epidermal resistance ($r_e$) is made up of the two resistances $r_c$ and $r_s$ in parallel (Waggoner, 1966):

$$r_e = 1/[(1/r_c) + (1/r_s)] = (r_c r_s)/(r_s + r_c). \tag{24.3}$$

The stream of water, $T$ (in units of g/cm$^2$/s, for example), transpired from a leaf is assumed in accordance with diffusion theory to be

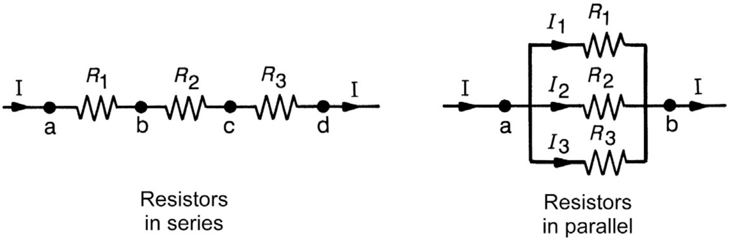

**FIGURE 24.5** Left: Resistors in series. Right: Resistors in parallel. *From Schaum, D., ©1961. Theory and Problems of College Physics. Schaum Publishing Co, New York, p. 158. This material is reproduced with permission of The McGraw-Hill Companies.*

proportional to the difference $\Delta X$ in water concentration (g/cm$^3$) between the surfaces of the mesophyll cells and the free air outside (Waggoner, 1966):

$$T = \Delta X/[r_a + (r_s r_c)/(r_s + r_c)] = \Delta X/(r_a + r_e). \tag{24.4}$$

Or Eqn (24.4) may be shown as follows (Gale and Hagan, 1966):

$$T = \left\{[H_2O]_{int} - [H_2O]_{ext}\right\}/(r_s + r_a), \tag{24.5}$$

where $T$ is transpiration, defined above; $[H_2O]_{int}$ is the water vapor concentration at the mesophyll surface and $[H_2O]_{ext}$ is the vapor concentration of the air (cm$^3$ vapor/cm$^3$ air); and $r_s$ and $r_a$ are the resistances as defined above (s/cm). We are neglecting $r_c$.

The diffusion theory, upon which Eqns (24.4) and (24.5) are based, is Fick's law. (For a biography of Fick, see the Appendix, Section 24.11.) In 1855, Adolf Fick discovered the linear flow law of diffusion, which is called Fick's law, to describe the diffusion of solutes in solution, and it is as follows (Kirkham and Powers, 1972; p. 75):

$$Q = DA(C_1 - C_2)/L, \tag{24.6}$$

where $Q$ is the quantity of solute per unit time, $D$ is the diffusion coefficient, $L$ is the length of the element through which the diffusion is occurring, $A$ is the cross-sectional area of the element, and $(C_1 - C_2)/L$ is the *concentration gradient*. We give Fick's law in Table 7.1, which lists linear flow laws used in soil—plant—water relationships.

Photosynthesis may be described similarly as a diffusion process of $CO_2$ from the outside air to the chloroplasts, but here a fourth resistance (in addition to $r_s$, $r_c$, and $r_a$) to diffusion of $CO_2$ is present in the liquid phase from the mesophyll wall to the chloroplast ($r_m{}'$). In addition to liquid phase $CO_2$ diffusion resistance, $r_m{}'$ also includes all the metabolic factors that affect the photosynthetic rate. Thus, photosynthesis may be expressed as follows (Gale and Hagan, 1966):

$$P = \left\{[CO_2]_{ext} - [CO_2]_{int}\right\}/\left(r'_s + r'_a + r'_m\right), \tag{24.7}$$

where $P$ is the photosynthetic rate (cm$^3$ $CO_2$/cm$^2$/s); $[CO_2]_{ext}$ is the concentration of the carbon dioxide in the outside air and $[CO_2]_{int}$ is the $CO_2$ concentration at the site of the $CO_2$ sink, that is, the chloroplast (cm$^3$ $CO_2$/cm$^3$ air); and $r_s{}'$, $r_a{}'$, and $r_m{}'$ are the resistances to $CO_2$ diffusion as defined above (s/cm). The primes denote resistance to flow of carbon dioxide, and no primes are used to denote resistance to flow of water vapor. Using Waggoner's (1966) analysis, we get:

$$P = \Delta X'/\left[r'_a + \left(r'_s r'_c\right)/\left(r'_s + r'_c\right) + r'_m\right] = \Delta X'/\left(r'_a + r'_e + r'_m\right), \tag{24.8}$$

where $P$ is the photosynthetic rate, as defined above, and $\Delta X'$ is the decrease in carbon dioxide concentration between the air and the site of chemical combination of carbon dioxide with a receptor.

The fact that there is a fourth resistance (mesophyll resistance) for carbon dioxide transport, which is not present for water vapor transport, has been the theoretical basis for the use of antitranspirants. When an antitranspirant is applied to a leaf, transpiration ($T$; Eqn (24.5)) should be reduced more than photosynthesis ($P$; Eqn (24.7)) is reduced. However, in practice, an antitranspirant reduces both $T$ and $P$ tremendously, so that photosynthesis is essentially stopped until the antitranspirant is removed. Figures 24.6 and 24.7 show circuits that illustrate resistances encountered in a leaf, as conceived by plant physiologists (Kramer, 1983; Baker, 1984).

The upper surface of a leaf (usually the adaxial surface) and the lower surface of a leaf (usually the abaxial surface) each have a resistance associated with them. If a leaf has no stomata on a surface, then there will be no stomatal resistance for that surface. Resistances of adaxial and abaxial stomata are assumed to act in parallel (Kramer, 1983; p. 302), or

$$1/R_{\text{total}} = (1/R_{\text{abaxial}}) + (1/R_{\text{adaxial}}). \tag{24.9}$$

However, this assumption means that the potential on the abaxial surface of the leaf is the same as the potential on the adaxial surface of the leaf (see the preceding paragraphs concerning resistance in a parallel

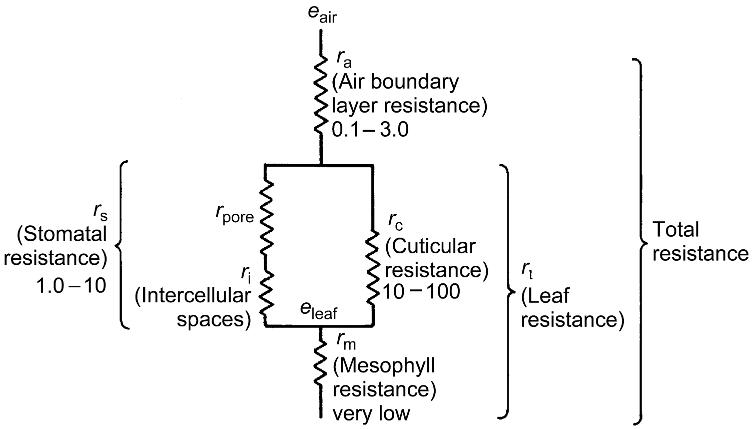

**FIGURE 24.6** Diagram showing resistances in seconds per centimeter to diffusion of water vapor from a leaf. Stomata and cuticular resistances vary widely among species and with leaf hydration and atmospheric humidity. The rate of transpiration is proportional to $\Delta e$, the water vapor pressure gradient, $e_{leaf}$ to $e_{air}$, and inversely proportional to the resistances in the pathway. *From Kramer (1983), p. 296. Reprinted by permission of Academic Press.*

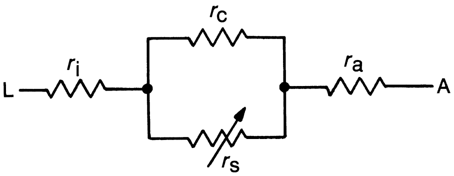

FIGURE 24.7 Resistances encountered by a water molecule diffusing from a leaf cell (L) into the surrounding air (A). $r_i$ is the resistance of the intercellular spaces, $r_c$ is the resistance of the cuticle, $r_s$ is the variable resistance of the stomata, and $r_a$ is the resistance of the boundary layer of unstirred air at the leaf surface through which water molecules must diffuse. *From Baker (1984). Reprinted by permission of Pearson Education Limited, Essex, United Kingdom and by permission of Dennis A. Baker.*

circuit). But this is not the case for plants (Kirkham, 1986). The adaxial surface of a leaf has a different water potential than the abaxial surface. So the limitation of Eqn (24.9), as applied to the total resistance of a plant leaf, should be recognized. However, it is the only equation we have to get the total resistance of a leaf, when the resistances on each surface are known. So we use it.

## 24.9 MEASUREMENT OF STOMATAL APERTURE AND STOMATAL RESISTANCE

Because water is lost mainly through the stomata on the surfaces of leaves, it is critical to know the extent of stomatal opening, to evaluate how much water a plant is losing. Kanemasu (1975a) enumerates different methods used to assess stomatal aperture. These methods include the following:

1. Observation under a microscope (Hsiao and Fischer, 1975a).
2. Use of cobalt–chloride paper (Teare et al., 1973; Kanemasu and Wiebe, 1975). Cobalt–chloride paper is prepared by dipping filter paper in a solution of $CoCl_2.6H_2O$ and then drying it. The paper is blue when dry, but pink when moist. The dry, blue paper, when placed on a leaf, covered with plexiglass, and held firmly by a small spring clamp, will turn pink from water vapor escaping from the leaf surface. This method can be used to compare the rates of transpiration from upper and lower leaf surfaces and from leaves of different plants under different environmental conditions.
3. Determination of resistance from leaf chamber (cuvette) transpiration, which can also incorporate the capability to monitor $CO_2$ assimilation for photosynthesis (Davenport, 1975). Work with the two models of the portable photosynthetic systems of Li-Cor, Inc (Lincoln, Nebraska) (Model LI-6200 and Model LI-6400) reports data

from cuvette measurements. In 1987, Model LI-6200 was put on the market and is a closed system; subsequently, Model LI-6400 was developed and it is an open system.

4. Mass-flow porometry: when stomata close, the permeability of the leaf to various gases (porosity) is greatly reduced. In mass-flow porometry, air is forced under pressure through the leaf, and the rate of flow or leaf resistance to flow is indicative of porosity (Figure 24.8) (Hsiao and Fischer, 1975b). The mass-flow porometer developed by Gregory and Pearse (1934) is the basis for most mass-flow porometers. Amphistomatous leaves are needed to use mass-flow porometers, because air must enter one side of the leaf and exit from the other side. If the resistance of one epidermis is high, the reading obtained with the porometer reflects mainly the opening of that epidermis. When using mass-flow porometers, it is assumed that the mesophyll resistance is constant and small compared to the resistance offered by the epidermis of a leaf with closed stomata. Mass-flow porometers are not available commercially.
5. Diffusion porometry: diffusion porometers measure diffusion of water vapor from the substomatal cavities through the stomata. Diffusion porometry includes both transient (dynamic)-state and steady-state methods (Kanemasu, 1975a). In the steady-state

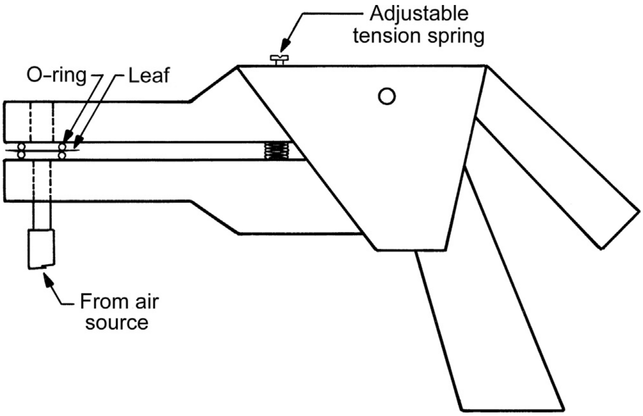

**FIGURE 24.8** A mass-flow porometer. The basic structural material consists of plexiglass cemented together. The critical aspect in construction is alignment of the two O-rings, both horizontally and vertically. Alignment of the two arms of the cup (cut from 1.3-cm-thick plexiglass sheets) is ensured by fixing, with a close-fitting metal pin, the upper arm snugly between the two large parallel trapezoidal plates glued to the lower arm. One O-ring is glued to an arm first. The other arm is then sanded to ensure good horizontal alignment of the O-rings. Vertical alignment is effected when the second O-ring is glued onto the arm. *From Hsiao and Fischer (1975b). Reprinted by permission of the Director of the Washington State University Agricultural Research Center, Pullman, Washington.*

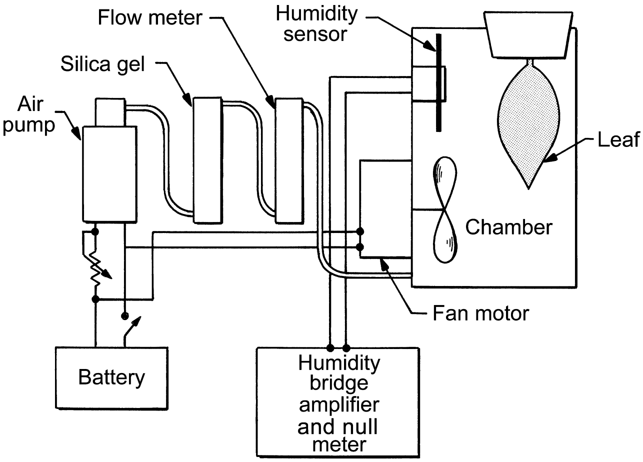

**FIGURE 24.9** Block diagram of steady-state porometer showing components and interconnections. *From Campbell (1975). Reprinted by permission of the Director of the Washington State University Agricultural Research Center, Pullman, Washington, and Gaylon S. Campbell.*

porometer, dry gas is passed over an enclosed leaf at a known flow rate and the humidity of the exhaust gas is measured (Figure 24.9) (Campbell, 1975). In the transient-state porometer, a sensor responsive to a change in humidity is clamped to a leaf (van Bavel et al., 1965; Kanemasu et al., 1969; Ehrler, 1975; Kanemasu, 1975b). Tan and Black (1978) describe a diffusion porometer for use on conifer needles.

Day (1977) and Parkinson and Day (1980) give theory associated with the steady-state porometer, and Chapman and Parker (1981) supply theory for the transient-state porometer. Of all the methods used to measure stomatal resistance only (i.e., photosynthetic rate is not measured), diffusion porometers (transient- and steady-state types) are most widely used for quantitative measurements (Livingston et al., 1984). They are commercially available. The transient-state one is made in Cambridge, England, by Delta-T Devices, Ltd, and imported for sale in the United States by Dynamax, Inc (Houston, Texas) (Figure 24.10). The only commercially available steady-state diffusion porometer is made by Decagon Devices (Model SC-1; Figure 24.11). An attached leaf is put into its sensor head, which contains two humidity sensors: one close to the leaf and one farther away from the leaf. Temperature is also recorded at these two locations. The readout gives four values (relative humidity at two locations; temperature at two locations), and the software of the porometer calculates stomatal resistance from these measured values. The porometer can be adjusted so it reads out stomatal conductance instead of

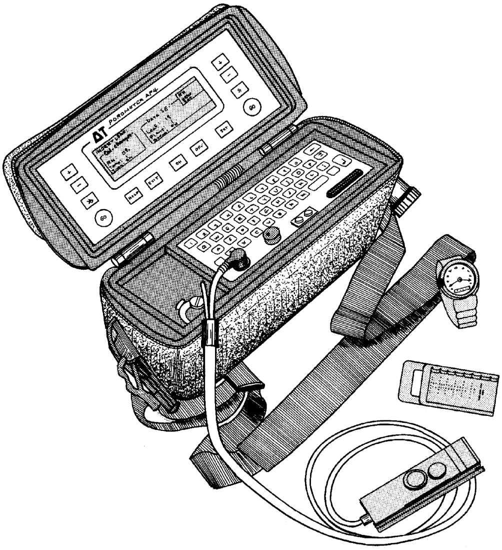

**FIGURE 24.10** A commercially available transient porometer. Automatic cycling ensures consistent results by repeating the measurement cycle (in typically 3—10 s) so that as soon as a repeatable value has been reached—usually after about four or five cycles—the next leaf can be sampled. The relative humidity level at which the instrument cycles can be set between 20% and 70% to match the ambient relative humidity as closely as possible, to avoid upsetting the stomata. The sensor head, shown in the lower right of the figure, weighs 80 g and incorporates a window for checking the alignment of the leaf with the sampling area—a slot 2.5 × 22.5 mm. The calibration plate, shown above the sensor head in the figure, has six values of diffusion resistance in the range 0—30 s/cm. The porometer comes with a rechargeable battery, padded carrying case, and a strap so one can put it around the neck while taking measurements in the field. The size of the porometer is 350 × 200 × 100 mm and it weighs 3.2 kg. *From a Dynamax, Inc, Houston, Texas, brochure. Reprinted by permission of Dynamax, Inc., Houston, Texas.*

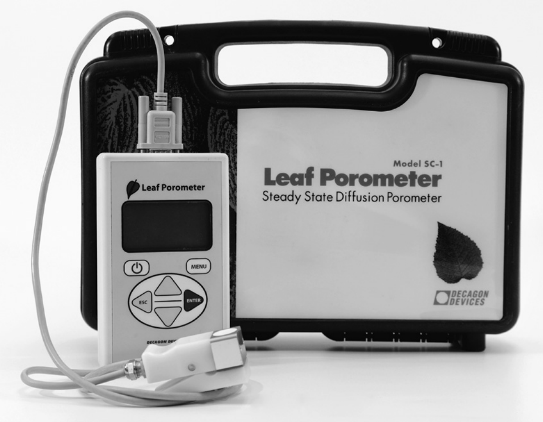

**FIGURE 24.11** The steady-state diffusion porometer sold by Decagon Devices, Pullman, Washington. *Photograph taken by Marsha K. Landis, Graphic Designer and Web Manager, Departments of Agronomy; Plant Pathology; and Horticulture, Forestry, and Recreation Resources, Kansas State University, Manhattan, Kansas. Used by permission of Marsha K. Landis.*

stomatal resistance. Kirkham (2007) gives further details about the operation of the porometer.

When taking measurements of stomatal resistance with a porometer, one must be aware of leaf angle because light intensity strongly affects stomatal opening. (We discuss interception of solar radiation by leaves at different angles in Chapter 30.) For example, stomatal resistance on corn (maize) can vary from less than 1 s/cm when stomatal are wide open and perpendicular to the sun's rays to more than 40 s/cm when a leaf is shaded (John M. Norman, Department of Soil Science, University of Wisconsin, personal communication, February, 1982).

## 24.10 THEORY OF MASS-FLOW AND DIFFUSION POROMETERS

As noted in Section 24.4, if stomata are spaced so that diffusion from one does not interfere with another, stomata can be considered to conduct water vapor more or less independently of each other. Hence, stomatal mass-flow and diffusive resistances per unit leaf area are inversely proportional to the number of stomata in that area (i.e., to stomatal frequency) (Hsiao, 1975).

The simplest physical model of a stomatal pore is that of a cylinder (Hsiao, 1975). Therefore, the relation between mass-flow resistance (in the mass-flow porometer) and stomatal opening tends to take on a form similar to that of the Poiseuille equation: resistance to flow is inversely proportional to the fourth power of the radius of the opening. This approximation becomes invalid, however, in the case of nearly closed stomata, because the term for interaction with the path wall becomes large and must be considered. In most cases, the stomatal pore is not circular and the length of the pore (normal to the conducting path) does not necessarily vary with the width of the pore. The mass-flow resistance then becomes inversely proportional to the third or even lower power of the width (Hsiao, 1975).

For diffusive resistance, the simplest approach is to apply Fick's law of diffusion to an assumed simple pore geometry. The result is that, to the first approximation, stomatal diffusive resistance is inversely proportional to the total pore area. For circular stomatal pores (Hsiao, 1975),

$$r_s = (A/nD)\left(4L_s/\pi d^2\right), \tag{24.10}$$

where $A$ is the leaf area being studied, $n$ is the number of stomata, $D$ is the diffusivity of water vapor in air, $L_s$ is the depth of the stomatal tube (i.e., of the stomatal pore), and $d$ is the stomatal pore diameter. If the so-called end correction (Monteith, 1973; p. 145) is applied to one end (outer end) of the stomatal tube, a factor, $1/2\,d$, is added, and the resulting equation is (Kanemasu, 1975b):

$$r_p = (A/nD)\left[4t/\left(\pi d^2 + 1/2d\right)\right] \tag{24.11}$$

where $r_p$ is the resistance of a calibration plate, $t$ is the thickness of the plate, $A$ is the aperture area, $n$ is the number of holes, $D$ is the diffusivity of water vapor in air, and $d$ is the diameter of the holes. Equation (24.11) is identical to the equation used for calculating the resistance of the calibration plate for the transient-state diffusion porometer (Kanemasu, 1975b).

## 24.11 APPENDIX: BIOGRAPHY OF ADOLF FICK

Adolf Eugen Fick (1829–1901), a physiologist, was born in Kassel, Hesse, Germany, on September 3, 1829, the son of Friedrich Fick and Marianne (Spousel) Fick. He got his MD at the University of Marburg in 1851 and married Emile von Cölln in 1862. He was an assistant to Carl Ludwig (1816–1895; German physiologist) in Zurich in 1852. Fick was a professor of physiology in Zurich beginning in 1862 and was a professor at the University of Würzburg from 1868. He was the author of *Die medizinische Physik* (1856) and *Untersuchungen über elektrischen nervenreizung* (1864).

He made important discoveries in every branch of physiology. He proved that carbohydrates rather than albumin are the source of muscle energy. He constructed the first plethysmography, which measured the pulse rate. In about 1864, he invented the myotonograph for measuring and recording muscle tension. In 1870, he developed a method to determine cardiac output by gasometry (Marquis Who's Who, 1968). He discovered the linear flow law of diffusion, named after him, to describe diffusion of solutes in solution, as in animal tissue (Fick, 1855). (He was a prosector; Kirkham and Powers, 1972; p. 429.) He died in Blankenberge, Belgium, on August 21, 1901.

## References

Baker, D.A., 1984. Water relations. In: Wilkins, M.B. (Ed.), Advanced Plant Physiology. Pitman, London, pp. 297–318.

Bergmann, D.C., Lukowitz, W., Somerville, C.R., 2004. Stomatal development and pattern controlled by a MAPKK kinase. Science 304, 1494–1497.

Brown, H.T., Escombe, F., 1900. Static diffusion of gases and liquids in relation to the assimilation of carbon and translocation in plants. Philos. Trans. R. Soc. Lond. 193B, 223–291.

Brodribb, T.J., McAdam, S.A.M., 2011. Passive origins of stomatal control in vascular plants. Science 331, 582–585.

Campbell, G.S., 1975. Steady-state diffusion porometers. In: Kanemasu, E.T. (Ed.), Measurement of Stomatal Aperture and Diffusive Resistance. Bulletin 809, College Agriculture Research Center, Washington State Univ, Pullman, Washington, pp. 20–23.

Chapman, D.C., Parker, R.L., 1981. A theoretical analysis of the diffusion porometer: steady diffusion through two finite cylinders of different radii. Agric. Meteorol. 23, 9–20.

Davenport, D.C., 1975. Stomatal resistance from cuvette transpiration measurements. In: Kanemasu, E.T. (Ed.), Measurement of Stomatal Aperture and Diffusive Resistance. Bulletin 809, College Agriculture Research Center, Washington State Univ, Pullman, Washington, pp. 12–15.

Day, W., 1977. Stomatal resistance in different gases. J. Appl. Ecol. 14, 643–647.

Ehrler, W.L., 1975. The porometer of van Bavel, Nakayama, and Ehrler. In: Kanemasu, E.T. (Ed.), Measurement of Stomatal Aperture and Diffusive Resistance. Bulletin 809, College Agriculture Research Center, Washington State Univ, Pullman, Washington, pp. 15–17.

Esau, K., 1965. Plant Anatomy, second ed. Wiley, New York.

Fernald, M.L., 1950. Gray's Manual of Botany, eighth ed. American Book, New York.

Fick, A., 1855. Über diffusion. Ann. Phys. Leipz. 170, 59–86 (Cited by Kirkham and Powers, 1972, p. 458).

Fischer, R.A., 1968. Stomatal opening: role of potassium uptake by guard cells. Science 160, 784–785.

Fujino, M., 1967. Adenosine triphosphate and adenosine triphosphatase in stomatal movement. Sci. Bull. Fac. Educ. Nagasaki Univ. 18, 1–47.

Gale, J., Hagan, R.M., 1966. Plant antitranspirants. Annu. Rev. Plant Physiol. 17, 269–282.

Gregory, F.G., Pearse, H.L., 1934. The resistance porometer and its application to the study of stomatal movement. Proc. R. Soc. B144, 477–493.

Heath, O.V.S., Mansfield, T.A., 1969. The movements of stomata. In: Wilkins, M.B. (Ed.), The Physiology of Plant Growth and Development. McGraw-Hill, New York, pp. 301–332.

Hsiao, T.C., 1975. Relationships among aperture, mass-flow resistance and diffusive resistance. In: Kanemasu, E.T. (Ed.), Measurement of Stomatal Aperture and Diffusive Resistance. Bulletin 809, College Agriculture Research Center, Washington State Univ, Pullman, Washington, pp. 24–25.

Hsiao, T.C., Fischer, R.A., 1975a. Microscopic measurements. In: Kanemasu, E.T. (Ed.), Measurement of Stomatal Aperture and Diffusive Resistance. Bulletin 809, College Agriculture Research Center, Washington State Univ, Pullman, Washington, pp. 2–5.

Hsiao, T.C., Fischer, R.A., 1975b. Mass flow porometers. In: Kanemasu, E.T. (Ed.), Measurement of Stomatal Aperture and Diffusive Resistance. Bulletin 809, College Agriculture Research Center, Washington State Univ, Pullman, Washington, pp. 5–11.

Imamura, S., 1943. Untersuchungen über den Mechanismus der Turgorschwankung der Spaltöffungsschliesszellen. Jpn. J. Bot. 12, 251–346.

Kanemasu, E.T. (Ed.), 1975a. Measurement of Stomatal Aperture and Diffusive Resistance. Bulletin 809, College Agriculture Research Center, Washington State Univ, Pullman, Washington.

Kanemasu, E.T., 1975b. The porometer of Kanemasu, Thurtell, and Tanner. In: Kanemasu, E.T. (Ed.), Measurement of Stomatal Aperture and Diffusive Resistance. Bulletin 809, College Agriculture Research Center, Washington State Univ, Pullman, Washington, pp. 17–20.

Kanemasu, E.T., Wiebe, H.H., 1975. Other methods. In: Kanemasu, E.T. (Ed.), Measurement of Stomatal Aperture and Diffusive Resistance. Bulletin 809, College Agriculture Research Center, Washington State Univ, Pullman, Washington, pp. 23–24.

Kanemasu, E.T., Thurtell, G.W., Tanner, C.B., 1969. Design, calibration and field use of a stomatal diffusion porometer. Plant Physiol. 44, 881–885.

Kirkham, D., Powers, W.L., 1972. Advanced Soil Physics. Wiley, New York.

Kirkham, M.B., 1986. Water relations of the upper and lower surfaces of maize leaves. Biol. Plant 38, 249–257.

Kirkham, M.B., 2007. Horizontal root growth: water uptake and stomatal resistance under microgravity. Vadose Zone J. 7, 1125–1131. http://dx.doi.org/10.2136/vzj2007.0097.

Kramer, P.J., 1983. Water Relations of Plants. Academic Press, New York.

Liang, G.H., Dayton, A.D., Chu, C.C., Casady, A.J., 1975. Heritability of stomatal density and distribution on leaves of grain sorghum. Crop Sci. 15, 567–570.

Livingston, N.J., Black, T.A., Beames, D., Dunsworth, B.G., 1984. An instrument for measuring the average stomatal conductance of conifer seedlings. Can. J. Res. 14, 512–517.

Macallum, A.G., 1905. On the distribution of potassium in animal and vegetable cells. J. Physiol. 52, 95–128.

Marquis Who's Who, 1968. Who's Who in Science from Antiquity to the Present, first ed. Marquis-Who's Who, Chicago.

Maximov, N.A., 1929. The Plant in Relation to Water. George Allen & Unwin, London.

Meidner, H., Mansfield, T.A., 1968. Physiology of Stomata. McGraw-Hill, New York.

Monteith, J.L., 1973. Principles of Environmental Physics. American Elsevier, New York.

Nobel, P.S., 1974. Introduction to Biophysical Plant Physiology. Freeman, San Francisco.

Parkinson, K.J., Day, W., 1980. Temperature corrections to measurements made with continuous flow porometers. J. Appl. Ecol. 17, 457–460.

Peaslee, D.E., Moss, D.N., 1968. Stomatal conductivities in K-deficient leaves of maize (Zea *mays* L.). Crop Sci. 8, 427–430.

Rosenberg, N.J., 1974. Microclimate: The Biological Environment. Wiley, New York.

Schaum, D., 1961. Theory and Problems of College Physics, sixth ed. Schaum, New York.

Serna, L., 2004. Good neighbours. Nature 430, 302–304.

Shimazaki, K-i., Doi, M., Assmann, S.M., Kinoshita, T., 2007. Light regulation of stomatal movement. Annu. Rev. Plant Biol. 58, 219–247.

Shpak, E.D., McAbee, J.M., Pillitteri, L.J., Torii, K.U., 2005. Stomatal patterning and differentiation by synergistic interactions of receptor kinases. Science 309, 290–293.

Stefan, J., 1881. Versuche über die Verdampfung. Sitzungsber. D.K. Akad. D. Wiss. Wien, Abt. II 85, 943 (cited by Maximov, 1929, p. 429).

Tan, C.S., Black, T.A., 1978. Evaluation of a ventilated diffusion porometer for the measurement of stomatal diffusion resistance of Douglas-fir needles. Arch. Met. Geoph. Biokl. Ser. B 26, 257–273.

Teare, I.D., Mohan Rao, M.R., Kanemasu, E.T., 1973. Correlation of transpiration rates by cobalt chloride method and stomatal-diffusion porometer. Indian J. Agr. Sci. 43, 639–642.

van Bavel, C.H.M., Nakayama, F.S., Ehrler, W.L., 1965. Measuring transpiration resistance of leaves. Plant Physiol. 40, 535–540.

Waggoner, P.E., 1966. Decreasing transpiration and the effect upon growth. In: Pierre, W.H., Kirkham, D., Pesek, J., Shaw, R. (Eds.), Plant Environment and Efficient Water Use. American Society of Agronomy and Soil Science Society of America, Madison, Wisconsin, pp. 49–72.

Yamashita, T., 1952. Influence of potassium supply upon various properties and movement of the guard cell. Sieboldia Acta. Biol. 1, 51–70.

Ziegler, H., 1987. The evolution of stomata. In: Zeiger, E., Farquhar, G.D., Cowan, I.R. (Eds.), Stomatal Function. Stanford University Press, Stanford, California, pp. 29–57.

CHAPTER

# 25

# Solar Radiation, Black Bodies, Heat Budget, and Radiation Balance

The sun is the battery that drives processes on earth, including evaporation, transpiration, and the ascent of water in plants. Therefore, it is essential to understand the sun's energy. In this chapter, we study solar radiation and the laws associated with a black body, because the sun can be considered to be a black body. We calculate the heat budget at the surface of the earth and define the radiation balance.

## 25.1 SOLAR RADIATION

All bodies emit radiant energy in the form of electromagnetic waves when they are at a temperature above absolute zero (−273.16 °C or −459.69 °F = hypothetical point at which a substance would have no molecular motion and no heat). The source of this *thermal radiation* or *temperature radiation* is the incessant molecular motion. During collisions, or more generally as a result of interactions between molecules, part of their energy is transformed into radiation. Conversely, radiation can be absorbed by the molecules and converted into kinetic and potential energy, thereby raising the temperature of the body (Van Wijk and Scholte Ubing, 1966; p. 62). (We ignore radiation from radioactive materials. This is another type of radiation.)

Solar radiation reaches the outer surface of the earth's atmosphere with an almost constant intensity of about 1400 $W/m^2$ or 2.0 $cal/cm^2/min$ measured perpendicularly to the solar beam (Johnson, 1954). About 98% is contained in the wavelength interval 0.2–4.5 μm, including about 40–45% in the 0.4–0.7 μm range (visible) (Figure 25.1), and about 2% at wavelengths shorter and longer than these limits. The distribution of the

http://dx.doi.org/10.1016/B978-0-12-420022-7.00025-2

Copyright © 2014 Elsevier Inc. All rights reserved.

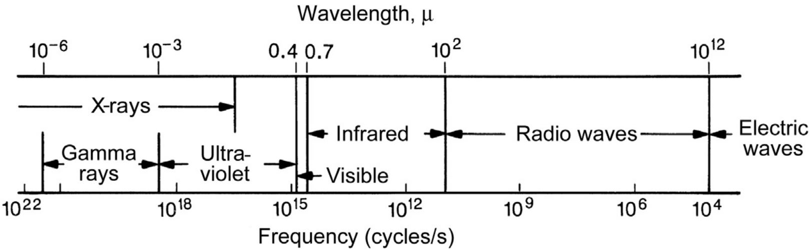
Wavelength, µ
$10^{-6}$
$10^{-3}$
0.4 0.7
$10^{2}$
$10^{12}$
X-rays
Gamma rays
Ultra-violet
Infrared
Visible
Radio waves
Electric waves
$10^{22}$
$10^{18}$
$10^{15}$
$10^{12}$
$10^{9}$
$10^{6}$
$10^{4}$
Frequency (cycles/s)

**FIGURE 25.1** Electromagnetic spectrum on logarithmic wavelength and frequency scales. *From Rosenberg (1974), p. 6. This material is used by permission of John Wiley & Sons, Inc.*

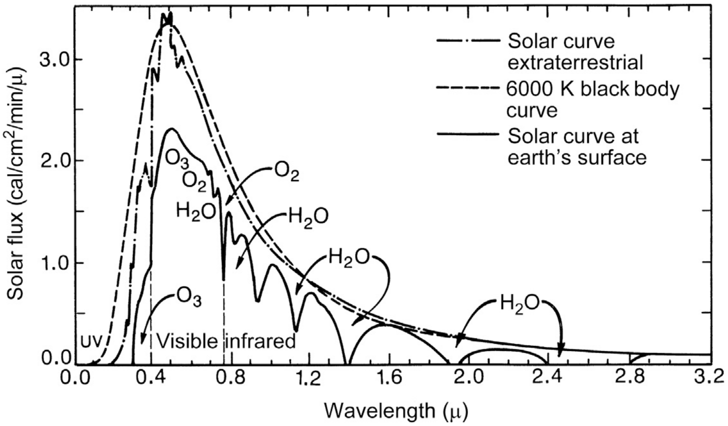

**FIGURE 25.2** Theoretical and actual spectra of solar radiation at the top of the atmosphere and the actual spectrum at the earth's surface. *From Rosenberg (1974), p. 9. This material is used by permission of John Wiley & Sons, Inc.*

incident flux with wavelength can be regarded as comparatively smooth, with few major gaps and a peak at the wavelength of green light (about 0.5 µm). Throughout the main region, the distribution of incident flux with wavelength corresponds roughly with that expected from radiation theory for a perfect absorber and emitter at a temperature of 6000 K (Figure 25.2) (Slatyer, 1967; p. 28). (We soon will define a perfect absorber and emitter.)

## 25.2 TERRESTRIAL RADIATION

In contrast to solar radiation, the earth's temperature is roughly 300 K. The black body radiation (which we will define soon), corresponding to this temperature, has its maximum spectral intensity at approximately

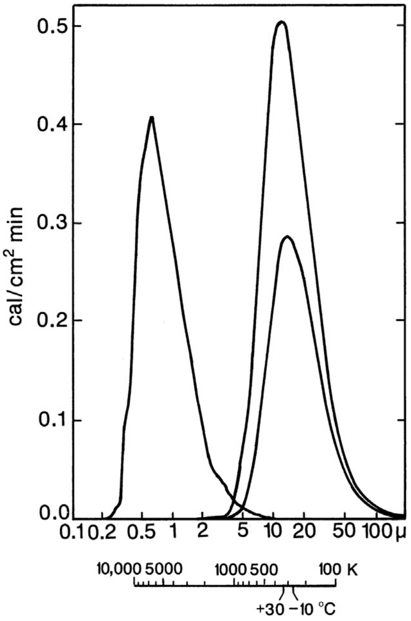

**FIGURE 25.3** Distribution of intensity of two bands of atmospheric radiation, according to wavelength. The curve on the left is for shortwave (solar) radiation and the two curves on the right are for long-wave (terrestrial) radiation. The taller curve on the right corresponds to earth temperature of 30 °C and the curve nested inside it is for earth temperature of −10 °C. *From Geiger (1965), p. 8. This material is used by the permission of the legal successor to Rudolph Geiger, Prof. Dr. Walter Geiger, Perlschneider Str. 18, 81241 Munich, Germany.*

10 μm and 98% of its energy is contained in the wavelength interval 0.5–80 μm (Van Wijk and Scholte Ubing, 1966; pp. 74, 92; Slatyer, 1967; p. 29). In consequence, the spectral range of solar radiation and terrestrial thermal radiation, although overlapping slightly, can be considered as completely separate (Figure 25.3). The former (solar radiation), although containing some infrared radiation, is commonly called short-wave radiation, and the latter (terrestrial thermal radiation) is called long-wave radiation (Slatyer, 1967; p. 29).

## 25.3 DEFINITION OF A BLACK BODY

Before we continue further, let us define black-body radiation, using the description of Shortley and Williams (1971, pp. 323–326). All materials at temperatures above absolute zero are continually emitting radiation. As the temperature of a solid is increased, the energy radiated from the solid increases rapidly. The amount of radiant power emitted by a solid depends significantly on the character of the surface of the solid.

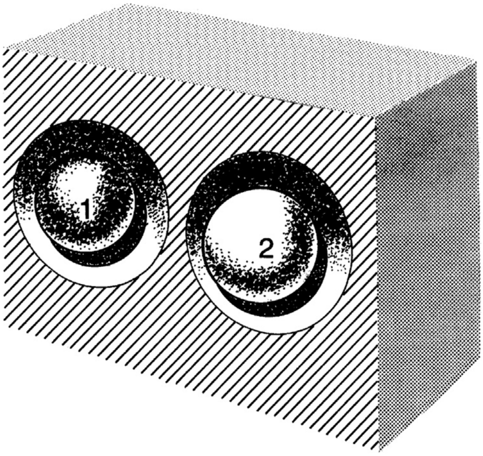

**FIGURE 25.4** Two spherical bodies of the same size but of different materials suspended within evacuated spherical cavities. *From Shortley, G. and Williams, D., ©1971. Elements of Physics, 5th ed., p. 323. Reprinted by permission of Pearson Education, Inc: Upper Saddle River, New Jersey.*

In beginning the discussion of radiation, it is helpful to define a "perfect radiator", whose rate of radiation is the maximum possible for its temperature. That such a maximum exists can be shown by considering the inverse process, *absorption*.

Figure 25.4 shows in cross section a solid object maintained at a uniform temperature $T$ throughout. Within this solid there are two identical evacuated spherical cavities containing opaque bodies of the same size but of different materials; for example, body 1 may be made of wood and body 2 may be made of polished metal. It is found by experiment that as a result of radiative interchanges of heat, the temperatures of bodies one and two eventually become equal to the temperature $T$ of the enclosing walls and remain at that temperature, in accordance with the general principle of thermal equilibrium.

We assume that the inner walls of the cavities are perfectly absorbing. Then the only radiation reaching bodies 1 and 2 is that *radiated* by the inner walls of the cavities; these cavity walls do not reflect any radiation and return it to the bodies. Under these circumstances, the radiant energy incident per second on unit area of each body will be the same; call it $E$, in W/m$^2$. Of the incident radiation $E$, a certain fraction will be reflected and the remainder will be absorbed. As indicated in Figure 25.5, let $\rho$ denote the fraction of the incident radiation that is reflected and $\alpha$ denote the fraction that is absorbed; $\rho$ is called the *reflectance* and $\alpha$ the *absorptance*. These quantities are dimensionless and their sum is unity for the surface of any opaque body; $\alpha + \rho = 1$. The product $\rho_1 E$ gives the radiant power reflected from unit area of body 1, while $\rho_2 E$ gives the radiant power reflected from unit area of body 2, in W/m$^2$. Similarly, $\alpha_1 E$ and $\alpha_2 E$ give the radiant power absorbed per unit area of bodies 1 and 2.

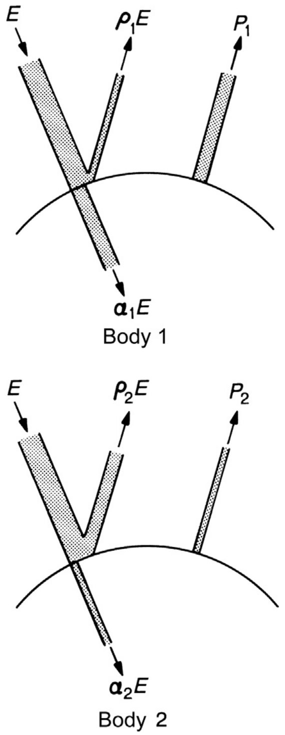

**FIGURE 25.5** Radiant energy incident per second on unit area, $E$ (W/m$^2$), of the two bodies illustrated in Figure 25.4. Of the incident radiation $E$, a certain fraction will be reflected, $\rho$, and the remainder will be absorbed, $\alpha$. The radiated power per unit area (W/m$^2$) is $P_1$ for body 1 and $P_2$ for body 2. The figure shows that the rate of absorption equals the rate of emission. *From Shortley, G. and Williams, D., ©1971. Elements of Physics, 5th ed., p. 324. Reprinted by permission of Pearson Education, Inc: Upper Saddle River, New Jersey.*

Now, let the radiated power per unit area, in W/m$^2$, be $P_1$ for body 1 and $P_2$ for body 2. If the temperatures of the bodies in Figures 25.4 and 25.5 are to remain constant, as much energy must be lost per second by radiant emission as is gained by absorption and we may write

$$\text{rate of absorption} = \text{rate of emission},$$

or

$$\alpha_1 E = P_1 \tag{25.1}$$

and

$$\alpha_2 E = P_2. \tag{25.2}$$

Dividing the first equation by the second, we find that

$$\alpha_1/\alpha_2 = P_1/P_2, \quad \text{or} \quad P_1/\alpha_1 = P_2/\alpha_2. \tag{25.3}$$

Equation 25.3, and the observed temperature equality, give *Kirchhoff's principle of radiation*, which states: *The ratio of the rates of radiation of any two surfaces at the same temperature is equal to the ratio of the absorptances of the two surfaces*. Qualitatively, we can say that good radiators are good absorbers. (For a biography of Kirchhoff, see the Appendix, Section 25.13.)

Now we return to the problem of defining a perfect radiator. There is a maximum value of the absorptance $\alpha$. Because no surface can absorb *more* than *all* of the incident radiation, the maximum value $\alpha$ can have is unity. In view of Eqn (25.3), we may say that a surface having the maximum rate of radiation is one that has the maximum absorptance and is, therefore, one that absorbs all radiation incident upon it. Such a surface is *black* to all types of radiation. Therefore, we may define a perfect radiator as follows: A *perfect radiator* is a body that absorbs all incident radiation and is, therefore, called a *black body.* A perfect radiator is a perfect absorber.

## 25.4 EXAMPLE OF A BLACK BODY

No material surface absorbs all of the radiation incident upon it. Even lampblack reflects about 1% of the incident radiation. In practice, a perfectly black surface can be most closely approximated by a very small opening in the wall of a large cavity such as the one shown schematically in Figure 25.6. Radiation may enter or leave the cavity through the opening. Of the radiation entering through the opening, a part is absorbed by the interior walls of the cavity and a part is reflected. Of the part reflected, only a small fraction escapes through the opening and the remainder is again partially absorbed and partially reflected by the walls. After repeated reflections, all of the entering radiation is absorbed except for the small portion that escapes through the opening. The opening, therefore, approximates a *black surface* or *perfect absorber.*

The inside walls of the cavity are radiating as well as absorbing, and a part of this radiation escapes through the opening. It can be shown that if the walls are at a uniform temperature *T*, the radiation that escapes is almost identical with the radiation that would be emitted by a perfect radiator at temperature *T*. The hole closely approximates the surface of a black body emitting so-called *black-body radiation*. To indicate the accuracy of this approximation, we note that computation shows that even if the interior surface of a sphere has an absorptance of only 1/2, a 25 cm sphere with a 5 cm hole will absorb 99% of diffuse radiation (coming equally from all directions) incident on the hole, and hence will radiate through the hole 99% of the radiation of a perfect radiator. A smaller hole will do correspondingly better (Shortley and Williams, 1971; p. 325).

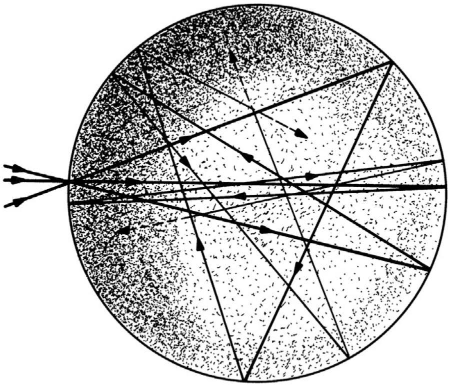

**FIGURE 25.6** A small hole in the wall of an enclosure, showing complete absorption of several representative rays. *From Shortley, G., and Williams, D., ©1971. Elements of Physics, 5th ed., p. 325. Reprinted by permission of Pearson Education, Inc: Upper Saddle River, New Jersey.*

## 25.5 TEMPERATURE OF A BLACK BODY

The total radiation emitted from the surface of a body increases rapidly as the temperature of the surface is increased. The quantitative relation between rate of radiation and surface temperature of an ideal radiator or black body is given by the *Stefan–Boltzmann law* and has the form

$$P_{\text{Black}} = \sigma T^4 (\text{black body}), \tag{25.4}$$

where $P$ is the radiated power per unit area. The rate of radiation increases as the *fourth power* of the absolute temperature $T$. The proportionality constant $\sigma$ is called the Stefan–Boltzmann constant and has the value $5.670 \times 10^{-8}$ W/m$^2$/K$^4$. (For a biography of Stefan, see the Appendix, Section 25.14, and for that of Boltzmann, see Section 25.15.)

## 25.6 GRAY BODY

The total radiation from many surfaces that are definitely not black also is very nearly proportional to the fourth power of the absolute temperature. This is true of surfaces composed of platinum, iron, tungsten, carbon, and many other materials. In every case, however, the proportionality constant is less than that for an ideal-radiator surface. Such a radiator is called a *gray body*. Because the absorptance $\alpha$ of a gray body is independent of its temperature, we see, by comparison with a black body in Eqns (25.3) and (25.4), that its rate of radiation is (Shortley and Williams, 1971; p. 326)

$$P = \alpha P_{\text{Black}} = \alpha\sigma T^4. \tag{25.5}$$

Because of this relation, $\alpha$ also is called the *emissivity* of the surface.

## 25.7 SPECTRUM OF A BLACK BODY

The Stefan–Boltzmann law gives the total rate of radiation of a perfect radiator (black body) at absolute temperature $T$, but gives no information concerning the *spectrum* of a perfect radiator (Shortley and Williams, 1971; p. 843). The spectrum of a perfect radiator is continuous. To discuss the relative amounts of energy in radiation of different wavelengths in the spectrum, we introduce the quantity $P_\lambda$, which gives the radiated power per unit area in a unit wavelength range at wavelength $\lambda$. This quantity, called the spectral radiance, can be determined by means of a spectrometer. What is observed in actuality is the amount of radiant power contained in a short wavelength interval between $\lambda$ and $\lambda + \Delta\lambda$. The radiant power per unit area of source, emitted in this wavelength range, is given by $P_\lambda\Delta\lambda$, represented by the shaded area in Figure 25.7. The unit in which $P_\lambda$ is measured is W/m$^2$ per unit wavelength interval; for example, W/m$^2$ per nanometer.

Plots of the distribution of power in the spectrum of a black body at different temperatures are shown by the solid lines in Figure 25.8. These curves all have two basic similarities in form:

1. They do not cross; the curves for higher temperatures are above the curves for lower temperatures at all wavelengths.
2. The maxima of the curves are displaced toward shorter wavelengths as the temperature of the black body is increased.

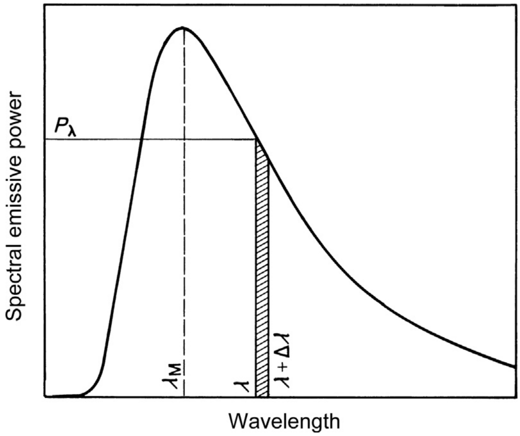

**FIGURE 25.7** Power radiated per unit area as a function of wavelength; definition of $P_\lambda$. *From Shortley, G., and Williams, D., ©1971. Elements of Physics, 5th ed., p. 844. Reprinted by permission of Pearson Education, Inc: Upper Saddle River, New Jersey.*

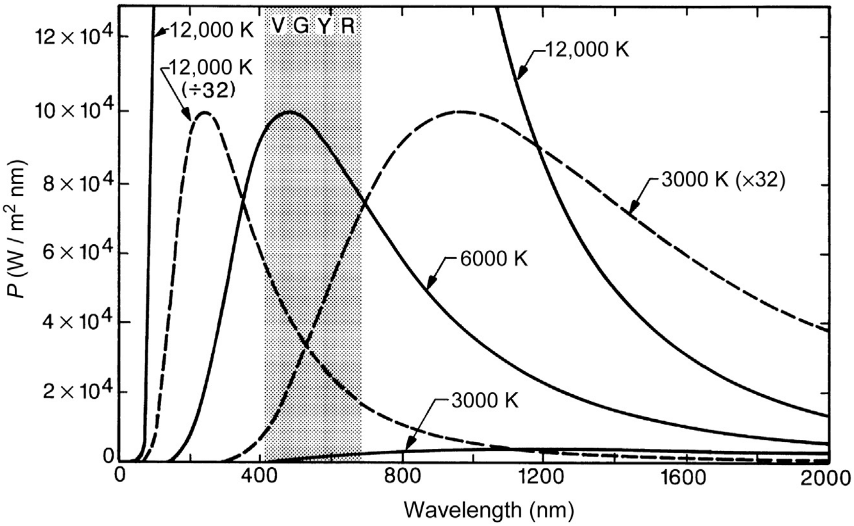

**FIGURE 25.8** The solid lines show plots of black-body radiation curves for temperatures of 3000, 6000, and 12,000 K. Broken lines show the 3000 K curve with ordinates multiplied by 32 and the 12,000 K curve with ordinates divided by 32; this adjustment brings the maxima of these curves to the same value as the maximum of the 6000 K curve. *From Shortley, G., and Williams, D., ©1971. Elements of Physics, 5th ed., p. 844. Reprinted by permission of Pearson Education, Inc: Upper Saddle River, New Jersey.*

The progressive shift of maximum toward the violet end of the spectrum accounts for the observed change in color of a radiating metal body from red through white to blue as its temperature is increased. Sunlight has the characteristics of black-body radiation corresponding to a temperature of about 6000 K and serves to define "white". Incandescent-lamp filaments are much cooler (about 3000 K) and give light that is more orange than daylight. Certain stars, such as Vega (12,000 K) are much hotter and appear blue. These points regarding color are illustrated by the broken curves in Figure 25.8, in which the ordinates of the 3000- and 12,000-degree curves have been scaled so that all three curves are plotted with the same maximum.

The wavelength $\lambda_M$ of the maximum of the curve (see Figure 25.7) is found experimentally to vary inversely as the absolute temperature, according to the law

$$\lambda_M = A/T \tag{25.6}$$

where $A$ is a constant whose value is $2.8978 \times 10^6$ nm K. This relation is called *Wien's displacement law*. (For a biography of Wien, see the Appendix, Section 25.16.) Thus with each doubling of temperature (see Figure 25.8), the value of $\lambda_M$ is divided by 2 (Shortley and Williams, 1971; pp. 843–845).

## 25.8 SUN'S TEMPERATURE

With our knowledge about black bodies, the Stefan–Boltzmann law, and Wien's displacement law, we now return to solar radiation. The sun's surface temperature $T_s$ can be calculated with the Stefan–Boltzmann law. The Stefan–Boltzmann constant can be expressed as $8.26 \times 10^{-11}$ cal/cm$^2$/min/K$^4$ (Geiger, 1965; p. 6). Geiger (1965, p. 7) says, since radiation decreases with the square of the distance, and the sun's radius is $s = 695{,}560$ km, the earth's radius $R$ is negligible in comparison with the distance $M$ of the sun from the earth,

$$\left(\sigma T_s^4\right)/k = M^2/s^2, \tag{25.7}$$

from which the value of $T_s$ is found to be 5793 K (Geiger, 1965; p. 7) ($M = 150 \times 10^6$ km; $R = 6370$ km).

## 25.9 EARTH'S TEMPERATURE

The Stefan–Boltzmann law also provides a conclusion about the earth's mean temperature, based on the assumption that the earth radiates like a black body. Because the earth's temperature is subject to variations in time, but remains unchanged on the whole over thousands of years, the amount radiated by the surface of the sphere of area $4\pi R^2$ must be equal to the quantity received by the cross-sectional area $\pi R^2$ multiplied by the solar constant $k$. The mean surface temperature of the earth $T_E$, calculated from the equation

$$\left(\sigma T_E\right)\left(4\pi R^2\right) = k\pi R^2 \tag{25.8}$$

is found to be 278 K = 5 °C. The surface temperature of the earth observed near the ground is higher (14 °C), because of the protective effect of the atmosphere, which is correspondingly cooler at higher levels (−50 to −80 °C) (Geiger, 1965; p. 7).

## 25.10 COMPARISON OF SOLAR AND TERRESTRIAL RADIATION

Even if the quantity of radiation received from the sun is equal to that radiated by the earth, the two types of radiation are fundamentally different in quality. The total intensity of solar radiation is spread over a wide range of wavelengths. According to Wien's displacement law (Eqn (25.6)), the product of the temperature $T$ of a radiating body and the wavelength corresponding to maximum intensity of radiation, $\lambda_M$, is constant. With $T$ in °K and $\lambda_M$ in microns (Geiger, 1965; p. 7)

$$T\lambda_M = 2880\ (^\circ\mathrm{K}, \mu). \tag{25.9}$$

As noted earlier, the higher the temperature of a body, the farther the radiation maximum is displaced toward shorter wavelengths. For the surface temperature of 5793 K (calculated temperature of sun; see earlier), $\lambda_M$ is 0.50 μm; the observed maximum is 0.47 μm, which means a higher temperature of the sun. The difference shows that the sun radiates only approximately as a black body. In either case, the most intense solar radiation occurs in the blue-green range of visible light. The wavelength of maximum intensity of radiation for the earth's actual surface temperature of 14 °C or 287 K is about 10.0 μm, which is well into the invisible infrared (Geiger, 1965; p. 7) (Figure 25.1).

Distribution of intensities over the spectrum is so asymmetric that 25% of the total radiation lies below $\lambda_M$, in the short-wavelength range, and 75% is above $\lambda_M$. It is therefore appropriate to introduce a wavelength $\lambda_s$ as a center of balance, such that 50% of the total intensity lies on either side of it; then $T\lambda_s = 4100(^\circ\mathrm{K}, \mu)$. In Figure 25.3, below the abscissa, which has a logarithmic wavelength scale, is shown a scale of temperature determined by this equation. For solar radiation, $\lambda_s$ is 0.7 μm, in the visible red. Forty percent of solar radiation lies within the infrared part of the spectrum (Geiger, 1965; p. 8). On the left in Figure 25.3 is the curve of solar radiation from observations. The area enclosed by the curve represents the total intensity, hence the solar constant, reduced to one quarter (for the reasons mentioned earlier) for comparison with the earth's radiation. The two distribution curves on the right correspond to earth temperatures of +30 °C and −10 °C. The figure makes it clear that in meteorology it is correct to distinguish between two fundamentally different streams of radiation. Solar radiation and diffuse sky radiation are in the range from 0.3 to 2.2 μm. Radiation emitted by the earth and its atmosphere lies between 6.8 and about 100 μm. The intervening range from 2.2 to 6.8 μm is used by both types of radiation to the extent of less than 5%. Hence there is a marked division between the two kinds of radiation, which we shall refer to as short-wavelength and long-wavelength radiations (Geiger, 1965; pp. 8–9).

## 25.11 HEAT BUDGET

Now let us turn to the heat budget at the surface of the earth. We shall use Geiger's description (1965, pp. 9–10). We assume an ideal case in which the earth's surface is entirely horizontal and extensive. In this case, the boundary between ground and atmosphere is a plane. The plane contains no heat, but under normal circumstances a considerable exchange of heat occurs across it. The quantities that determine this heat exchange will now be discussed.

Radiation *S* is the first (major) factor of heat exchange. Heat arrives at the earth's surface from the sun, the sky, and the atmosphere (insolation). Heat is sent back into space (outgoing or terrestrial radiation). Factors that add heat to the surface of the ground are considered positive; those that subtract heat from it are negative. The sum of insolation and outgoing radiation, that is, the balance, decides in individual cases whether *S* is positive or negative. In Geiger's (1965) book, the unit for *S*, as for all factors in the heat budget, is cal/cm$^2$/min, also called in English the langley per minute, abbreviated ly/min. These are not SI units. The SI unit is W/m$^2$ (1 W = 1 J/s = 0.239 cal/s).

The second factor *B* is determined by the flow of heat from the ground to the surface or in the reverse direction. During a cold winter night heat flows upward through the ground and *B* is, therefore, positive; on a summer afternoon, *B* is negative because heat is transported downward from the surface.

Third, the air above the ground plays a part in the exchange of heat *L*. This factor also may be positive or negative. Transport of heat to or from the ground depends not only on physical heat conduction, as within the ground, but also on mass exchange (eddy diffusion) because of the great mobility of the air.

Fourth, there is the effect of evaporation *V*. This is measured, like all the other heat-economy factors, in calories per square centimeter per minute (Geiger, 1965) or W/m$^2$. The quantity of heat in calories required to evaporate 1 g of water is called the latent heat of vaporization and varies with temperature. At 25 °C, it is 583 cal/g. If a round figure of 600 cal/g is used for temperatures above 0 °C, then *V* in cal/cm$^2$/min corresponds to the evaporation of a certain depth of water in millimeters per hour. Normally *V* is negative, but positive values are possible, as when dew or hoarfrost forms on the surface and heat of condensation or sublimation is released.

From the surroundings of the area under consideration, there can flow warmer or colder, moister or drier, air, a process that is called *advection*. This advection process has an effect on the heat economy of the area and upsets the assumption on which the previous discussion was based, namely that horizontal counter-influences are absent. We introduce the additional advection process by defining the factor *Q*.

Precipitation may entail a gain or a loss of heat for the ground, depending on its temperature, and this is given by the symbol *N*. Over oceans, lakes, and rivers, the factor *W*, for the exchange of heat between water and its surface, is used instead of *B*.

The complete equation for the heat exchange at a flat vegetation-free ground surface is:

$$S + B\ (\text{or}\ W) + L + V + Q + N = 0. \tag{25.10}$$

Note: Geiger was a German, so the letters stand for German words, as follows: $S =$ die Sonne (the sun); $B =$ der Boden (the soil); $W =$ das Wasser (the water); $L =$ die Luft (the air); $V =$ die Verdunstung or die Verdampfung (the evaporation); $Q =$ die Quer (*in die Quer* in German means "crosswise"); $N =$ der Niederschlag (the rain).

## 25.12 RADIATION BALANCE

Now let us consider specifically the factor $S$ in Eqn (25.10), because it is the most important factor taking part in the heat exchange at the surface of the earth. We continue with Geiger's (1965, pp. 12–13) analysis.

The symbol $S$ means the radiation balance or net radiation. If insolation is greater than outgoing (terrestrial) radiation, the balance is positive; if it is less, the balance is negative. A negative balance is described as a net loss of radiation. Sometimes the term "outgoing radiation" is used to designate the Stefan–Boltzmann radiation loss and sometimes for the negative radiation balance. Geiger (1965) uses the term "effective outgoing radiation" and avoids the ambiguous term "outgoing radiation."

The radiation balance consists of two radiation streams of different spectral ranges (Figure 25.3). There is a short-wavelength part only as long as the sun shines, that is, during the daytime. Radiation reaching the surface of the earth consists of that part of direct solar radiation $I$ that is not reflected by clouds, absorbed by the atmosphere, or scattered diffusely, and also that part of the nondirectional sky radiation $H$ that represents diffusely scattered radiation that has reached the ground and provides "daylight" within the visible spectrum. The value of $I + H$ reaching a horizontal surface is called *global radiation*. Part of this radiation is reflected by the earth's surface. This short-wavelength reflected radiation $R$ depends on the nature of the ground, in contrast to $I + H$. The reflection factor or *albedo* is the ratio of the reflected to the incident radiation, usually expressed as a percentage (Table 25.1).

Incoming long-wavelength radiation is of no significance in the radiation balance of the earth as a planet. It is, however, of great importance for the radiation balance of the earth's surface. The atmosphere of the earth contains water vapor, ozone, and other gases (Figure 25.2), all of which absorb radiation and emit it according to Kirchhoff's law (Eqn (25.3)). This long-wavelength atmospheric radiation $G$ is termed counterradiation, because it counteracts the terrestrial radiation loss. It

**TABLE 25.1** Albedo of Various Surfaces for Total Solar Radiation with Diffuse Reflection (Both Short Wavelength)

| Surface | Percent Reflected |
|---|---|
| Fresh snow cover | 75–95 |
| Compressed snow | 70 |
| Melting snow | 30–65 |
| Dense cloud cover | 60–90 |
| Old snow cover | 40–70 |
| Clean firn snow | 50–65 |
| Dry salt cover | 50 |
| Light sand dunes, surf | 30–60 |
| Clean glacier ice | 30–46 |
| Dirty firn snow | 20–50 |
| Lime | 45 |
| Granite | 15 |
| Quartz sand | 35 |
| Sandy soil | 15–40 |
| Meadows and fields | 12–30 |
| Prairie, wet | 22 |
| Prairie, dry | 32 |
| Stubble fields | 15–17 |
| Grain crops | 10–25 |
| Pine, spruce wood | 10–14 |
| Deciduous wood | 16–37 |
| Yellow leaves (autumn) | 33–36 |
| Desert, midday | 15 |
| Desert, low solar altitude | 35 |
| Bare fields | 12–25 |
| Wet plowed fields | 5–14 |
| Densely built-up areas | 15–25 |
| Woods | 5–20 |
| Grass, green | 16–27 |

**TABLE 25.1** Albedo of Various Surfaces for Total Solar Radiation with Diffuse Reflection (Both Short Wavelength)—cont'd

| Surface | Percent Reflected |
|---|---|
| Grass, dried | 16–19 |
| Dark clay, wet | 2–8 |
| Dark clay, dry | 16 |
| Sand, wet | 9 |
| Sand, dry | 18 |
| Dark cultivated soil | 7–10 |
| Water surfaces, sea | 3–10 |
| Water, 0–30 °C | 2 |
| Water, 60 °C | 6 |
| Water, 85 °C | 58 |

*From Geiger (1965), p. 15, and Van Wijk and Scholte Ubing (1966), p. 87. This material is used by the permission of Dr. Walter Geiger, legal successor to Prof. Dr. Rudolf Geiger, Perlschneider Str. 18, 81241 Munich, Germany.*

occurs both by day and by night, and, in fact, is somewhat greater during the day, because it is dependent on temperature.

It might be expected that part of this long-wavelength radiation would also be lost through reflection by the ground. However, the earth's natural surface cover can be considered to resemble a black body. In general, the albedo of natural surfaces is less than 5%. Snow cover, which reflects so strongly within the visible spectrum that newly fallen snow produces a striking improvement in light conditions, is practically an ideal black body for long waves, reflecting at the most 0.5% of the incident radiation.

According to the Stefan–Boltzmann law, the radiation emitted by the soil surface by day and by night would be exactly $\sigma T^4$ ($T$ is the surface temperature), if the ground were a black body. As just stated, this condition is largely fulfilled by natural surfaces. To the extent that it is not fulfilled, the outgoing radiation will be reduced according to Kirchhoff's law. But at the same time, the amount of outgoing long-wavelength reflected radiation would be increased, and it is not possible to distinguish it instrumentally from the terrestrial radiation.

The radiation balance $S$ is, therefore, given by the equation

$$S = I + H + G - \sigma T^4 - R \left(\text{cal/cm}^2/\text{min} \;\; \text{or} \;\; \text{W/m}^2\right) \qquad (25.11)$$

The last two factors in Eqn (25.11) depend on the nature of the ground surface, while the first three on the right-hand side of the equation are

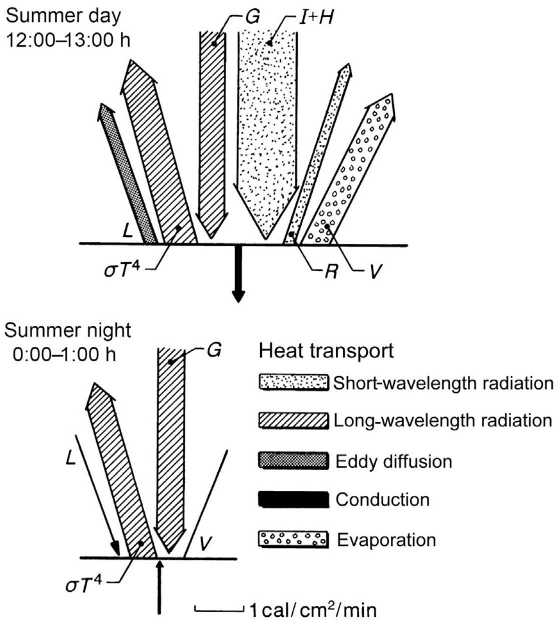
Summer day
12:00–13:00 h
G
I+H
L
$\sigma T^4$
R
V
Summer night
0:00–1:00 h
G
L
V
$\sigma T^4$
Heat transport
Short-wavelength radiation
Long-wavelength radiation
Eddy diffusion
Conduction
Evaporation
1 cal/cm²/min

**FIGURE 25.9** The importance of radiation as compared with the other factors in the heat budget. $I$, direct solar radiation; $H$, diffusely scattered radiation; $G$, long-wave atmospheric radiation; $\sigma T^4$, radiation emitted by soil surface; $R$, short-wave reflected radiation; $L$, heat; $V$, evaporation; $I + H$, global radiation. *From Geiger (1965), p. 14. This material is used by the permission of the legal successor to Rudolf Geiger Prof. Dr. Walter Geiger, Perlschneider Str. 18, 81241 Munich, Germany.*

independent of it. Figure 25.9 shows the magnitude of these factors for a summer day and a summer night.

## 25.13 APPENDIX: BIOGRAPHY OF GUSTAV KIRCHHOFF

Gustav Robert Kirchhoff (1824–1887), the German physicist who established spectroscopy on a sound theoretical basis and studied complex electrical circuits as well as radiation, was born at Königsberg (Kaliningrad) on March 12, 1824. He was educated at the university of his native town. After acting as *Privatdozent* in Berlin (1847–1850), he became extraordinary professor of physics in Breslau in 1850. Four years later he was appointed professor of physics in Heidelberg, and in 1875 he was transferred to Berlin, where he remained for the rest of his life.

Kirchhoff's contributions to experimental and mathematical physics were numerous and important. In his work in electricity, he modified the resistance bridge, brought to public attention by Wheatstone (see Chapter 22), and developed a theorem that gives the distribution of currents in a network. Kirchhoff extended Ohm's theory for a linear conductor (see Chapter 22) to the case of conductors in three dimensions, and so generalized the equations dealing with the flow of electricity in conductors. Another important piece of work was the demonstration that an electric disturbance is propagated along wire with the same velocity as light is propagated in free space (Preece, 1971a).

His name is best known for the researches, in conjunction with the great German chemist Robert Wilhelm Bunsen (1811–1899), on the development of spectrum analysis. The rich period of Kirchhoff's life was the 20 years he taught in Heidelberg and worked with Bunsen. It was during the years 1859–1862 that these great investigators together made the outstanding discoveries of spectrum analysis. At the time the physical laboratory in Heidelberg was unpretentious and was located in a house, the "Riesengebäude," then 150 years old. The memorable researches were carried on in a small room. In 1857 Bunsen and Henry E. Roscoe first described the Bunsen burner. This new burner furnished Bunsen and Kirchhoff with a nonluminous gas flame of fairly high temperature, in which chemical substances could be vaporized and a spectrum could be obtained, due purely to the luminous vapor (Cajori, 1929; p. 168).

To Kirchhoff belongs the merit of having enunciated a complete account of the theory of spectrum analysis. He established the method on a solid basis. He gave the explanation of the Fraunhofer lines and thus opened up to investigation a new field in spectrum analysis applied to the composition of celestial bodies (Preece, 1971a). Although spectrum analysis, as a terrestrial science, was due equally to Kirchhoff and Bunsen, its celestial applications belong to Kirchhoff alone. Kirchhoff's explanation of the Fraunhofer lines was epoch-making. Said Helmholtz (1821–1894; German physicist), "It has in fact most extraordinary consequences of the most palpable kind, and has become of the highest importance for all branches of natural science. It has excited the admiration and stimulated the fancy of men as hardly any other discovery has done, because it has permitted an insight into worlds that seemed forever veiled for us." In this connection, Kirchhoff frequently related the following story. The question of whether or not Fraunhofer's lines reveal the presence of gold in the sun was being investigated at the time. Kirchhoff's banker remarked on this occasion: "What do I care for gold in the sun if I cannot fetch it down here?" Shortly afterward Kirchhoff received from England a medal for his discovery, and its value in gold. While handing it over to his banker, he observed, "Look here, I have succeeded at last in fetching some gold from the sun" (Cajori, 1929; p. 169).

Kirchhoff's researches concerning radiation played a leading role. He defined a perfect black body, and, as to the experimental realization of it, he suggested a closed box with black walls inside, kept at a constant temperature and having a very small opening through which radiation may pass from the inside to the outside. He died in Berlin on October 17, 1887 (Preece, 1971a).

## 25.14 APPENDIX: BIOGRAPHY OF JOSEF STEFAN

Josef Stefan (1835–1893), the Austrian physicist who made original contributions to the kinetic theory of gases, hydrodynamics, and radiation, was born on March 24, 1835, at St. Peter near Klagenfurt. He was educated at the University of Vienna, where he became doctor of philosophy in 1858; then *Privatdozent* in mathematical physics; in 1863 professor ordinarius of physics; and in 1866 director of the Physical Institute. He was a distinguished member of the Vienna Academy of Sciences, of which he was appointed secretary in 1875. Before Stefan's work, Kirchhoff had already described the perfect radiator as the perfectly black body, namely, one that absorbed all the radiation that fell on it and reflected none, but emitted radiation of all wavelengths. Stefan showed empirically in 1879 that the radiation of such a body was proportional to the fourth power of its absolute temperature, a relationship since known as Stefan's law or as the Stefan–Boltzmann law after it had been deduced by Ludwig Boltzmann in 1884 from thermodynamic considerations. Stefan's law was one of the first important steps leading to the understanding of black-body radiation from which the quantum idea of radiation sprang. Stefan died on January 7, 1893, in Vienna (McKie, 1971).

## 25.15 APPENDIX: BIOGRAPHY OF LUDWIG BOLTZMANN

Ludwig Boltzmann (1844–1906), Austrian physicist, made important contributions to many branches of physics. His greatest achievements were the development of statistical mechanics and the statistical explanation of the second law of thermodynamics. He was born in Vienna on February 20, 1844, and studied at the university there, receiving his doctorate in 1866. He held professorships in mathematics (Vienna, 1873–1876), experimental physics (Graz, 1876–1889), and theoretical physics (Graz, 1869–1873; Munich, 1889–1893; Vienna, 1894–1900; Leipzig, 1900–1902; Vienna, 1902–1906). Despite his several professorships, theoretical physics was his real vocation (Klein, 1971).

In 1905, when he was professor of theoretical physics at the University of Vienna, Boltzmann was invited to give a course of lectures in the summer session at the University of California in Berkeley. His recollections of that summer survive in his popular essay, "Reise eines deutschen Professors ins Eldorado." An abridged translation is presented in *Physics Today* (Boltzmann, 1905). Boltzmann's great sense of humor is evident in this writing.

When Boltzmann began his scientific work, he attacked the problem, until then unconsidered, of explaining the second law of thermodynamics on the basis of the atomic theory of matter. In a series of papers published during the 1870s, Boltzmann showed that the second law could be understood by combining the laws of mechanics, applied to the motions of the atoms, with the theory of probability. In this way, he made clear that the second law is an essentially statistical law and that a system will approach a state of thermodynamic equilibrium, because the equilibrium state is overwhelmingly the most probable state. The entropy function of thermodynamics, whose behavior shows the trend to equilibrium and whose maximum value characterizes the equilibrium state, is itself a measure of the probability of the macroscopic state. (The equation relating entropy and probability is engraved on the monument at Boltzmann's grave in Vienna.) He built much of the structure of statistical mechanics, a structure later elaborated by the U.S. mathematical physicist Josiah Willard Gibbs (1839—1903) (Klein, 1971).

Apart from Boltzmann's work on statistical mechanics, he made extensive calculations in the kinetic theory of gases. He was also one of the first Europeans to recognize and to expound on the importance of James Clerk Maxwell's (1831—1879; Scottish physicist) theory of electromagnetism, a subject on which he published a two-volume treatise. Boltzmann also derived, using thermodynamics, Stefan's law for black-body radiation, a derivation that Hendrik Antoon Lorentz (1853—1928, Dutch physicist who got the Nobel Prize in physics in 1902) called "a true pearl of theoretical physics" (Klein, 1971).

Boltzmann's work in statistical mechanics was strongly attacked by Wilhelm Ostwald (1853—1932; German chemist who received the Nobel Prize in chemistry in 1909) and the energeticists who did not believe in atoms and wanted to base all of physical science on energy considerations only. Boltzmann also suffered from misunderstandings, on the part of others, about his ideas on the nature of irreversibility. They did not fully grasp the statistical nature of his reasoning. He was fully justified against both sets of opponents by the discoveries in atomic physics, which began shortly before 1900 and by the fluctuation phenomena, such as Brownian motion, which could be understood only by statistical mechanics (Klein, 1971). In 1905, Einstein explained Brownian motion (Isaacson, 2009; pp. 25, 27) by means of Boltzmann's ideas (Cercignani, 1998; p. 102), but Boltzmann died apparently before he knew about Einstein's confirmation of his work. Cercignani (1998) gives an in-depth discussion of the scientific world in which Boltzmann lived.

Depressed by the criticism of his work, Boltzmann took his own life by hanging on September 5, 1906, at Duino, near Trieste, Italy (Klein, 1971).

## 25.16 APPENDIX: BIOGRAPHY OF WILHELM WIEN

Wilhelm Wien (1864–1928), German physicist and Nobel Prize winner, was born January 13, 1864, at Gaffken, East Prussia. He studied at the universities of Göttingen, Heidelberg, and Berlin, and in 1890 entered the Physicotechnical Institute near Berlin as assistant to Helmholtz. In 1896, he was appointed professor at the technical high school in Aachen. In 1899 he went to Giessen; in 1900 to Würzburg; and in 1920 to Munich. He wrote on optical problems; on radiation, especially black-body radiation, for which in 1911 he was awarded the Nobel Prize; on water and air currents, on discharge through rarefied gases, cathode rays, and X-rays. Wien's most important contributions to black-body radiation are contained in three laws named after him, the most famous of these being known as Wien's displacement law. His autobiography was published posthumously under the title *Aus dem Leben und Wirken eines Physikers* (1930). Wien died on August 30, 1928, in Munich (Preece, 1971b).

## References

Boltzmann, L., 1905. A German professor's trip to El Dorado. Phys. Today 45 (1), 44–51, 1992. (Translated by Bertram Schwarzschild).

Cajori, F., 1929. A History of Physics. Macmillan, New York.

Cercignani, C., 1998. Ludwig Boltzmann: The Man Who Trusted Atoms. Oxford University Press, New York.

Geiger, R., 1965. The Climate Near the Ground, revised ed. Harvard University Press, Cambridge, Massachusetts. Translated by Scripta Technica, Inc.

Isaacson, W., 2009. Einstein. The Life of a Genius. HarperCollins, New York.

Johnson, F.S., 1954. The solar constant. J. Meteorol. 11, 431–439.

Klein, M.J., 1971. Boltzmann, Ludwig. Encyclopaedia Britannica 3, 893.

McKie, D., 1971. Stefan, Josef. Encyclopaedia Britannica 21, 198.

Preece, W.E. (Ed.), 1971a. Kirchhoff, Gustav. Encyclopaedia Britannica, vol. 13, p. 383.

Preece, W.E. (Ed.), 1971b. Wien, Wilhelm. Encyclopaedia Britannica, vol. 23, p. 499.

Rosenberg, N.J., 1974. Microclimate: The Biological Environment. Wiley, New York.

Shortley, G., Williams, D., 1971. Elements of Physics, fifth ed. Prentice-Hall, Englewood Cliffs, New Jersey.

Slatyer, R.O., 1967. Plant–Water Relationships. Academic Press, London.

Van Wijk, W.R., Scholte Ubing, D.W., 1966. Radiation. In: van Wijk, W.R. (Ed.), Physics of Plant Environment, second ed. North-Holland, Amsterdam, pp. 62–101.

CHAPTER

# 26

# Infrared Thermometers

Plant temperature and water use are related because, if a plant is well watered, the stomata are open, transpirational cooling occurs, and canopy temperature is cool. Conversely, as a plant becomes water stressed, stomata close, transpiration is reduced, and canopy temperature increases. Consequently, one can use canopy temperature to characterize the water status of a crop (Kirkham et al., 1983, 1984, 1985). In the 1970s, portable, commercially available infrared thermometers that measure thermal radiation were developed and refined (Jackson et al., 1980). They provide a means to measure remotely plant canopy temperatures, and measurements with them are easy because the instruments are hand-held and lightweight (Jackson et al., 1977). (Jackson and colleagues at the U.S. Water Conservation Laboratory in Phoenix, Arizona, did pioneering experiments with portable infrared thermometers. For a biography of Jackson, see the Appendix, Section 26.7.) In this chapter, we consider the theory and use of infrared thermometers.

## 26.1 INFRARED THERMOMETERS

Infrared thermometers have the advantage of measuring many leaves at one time. Before their development, it was difficult to determine the magnitude of the temperature difference either between plants or between plants and air, because there was no way of defining the temperature of a group of leaves. A leaf with the surface normal to incident solar radiation has a higher temperature than a leaf that has a surface parallel to the sun's rays or one that is shaded (Tanner, 1963). Severe sampling problems exist if one can make only a few measurements on individual leaves, such as one does when using thermocouples. The temperature that is measured depends on the location of the thermocouple (for example, base of leaf versus tip of leaf). Tanner (1963) said, "There is no single temperature value that represents the plant and which has been demonstrated to be useful for any given research problem".

http://dx.doi.org/10.1016/B978-0-12-420022-7.00026-4

Copyright © 2014 Elsevier Inc. All rights reserved.

The developments in infrared thermometry have provided instruments that surmount the sampling problem. The thermal radiation from all plant surfaces in the field of view (F.O.V.) of the instrument is integrated into a single measurement. A temperature measurement with an infrared thermometer gives a temperature with a particular definition: the black-body temperature that would produce the radiation entering the instrument from plant parts in the F.O.V. (Tanner, 1963). Because the thermal radiation emissivity of green plants is high (0.95—0.97) (Tanner, 1963), the measured (apparent) radiation temperature can be converted to the plant temperature with little error. Most natural surfaces have high emissivities, ranging between 0.90 and 0.98 (Campbell, 1977; p. 49). Measurements made with infrared thermometers are particularly useful in studies of transpiration (water loss from plants), because the temperature measured with the instrument (radiated from the upper part of the plant) gives weight to the plant portions participating most actively in transpiration (Tanner, 1963).

As we noted in Chapter 25, a good approximation of a black body is a small hole in the wall of a hollow body (Figure 25.6). A beam of radiation that enters the hole and hits the inside wall is partly reflected to another part of the wall, where again a fraction is absorbed and so on. After a number of reflections, little radiant energy is left and the chance that some of it is reflected outward through the hole is exceedingly small. For similar reasons, a dense vegetative cover in which part of the leaves are seen on edge when viewed from above is much darker (i.e., has a lower reflection factor) than the surface of a single leaf (van Wijk and Scholte Ubing, 1966; p. 66).

## 26.2 DEFINITIONS

In Chapter 25, we defined black body and emissivity. Here we define other terms that are used in association with radiation and in the literature dealing with infrared thermometers. We shall use the definitions provided by van Wijk and Scholte Ubing (1966, pp. 62—63). *Radiant energy* is the energy traveling in the form of electromagnetic waves. It has the dimension of energy so that it is measured in joule, erg, calorie, or an equivalent quantity. The amount of radiant energy emitted, transferred, or received per unit time is called *radiant flux* $\Phi$ (Greek letter, capital phi). It has the dimension of energy per unit time. In physical literature, the watt (W) ($1\ \mathrm{W} = 1\ \mathrm{J/s}$) and the erg/s are commonly used as units; in meteorology, the unit cal/min is frequently employed. *Radiant flux density* $H = \mathrm{d}\Phi/\mathrm{d}A$ is the flux per unit of surface; it is expressed as $\mathrm{W/m^2}$, $\mathrm{erg/cm^2/s}$, $\mathrm{cal/cm^2/min}$ (=langley/min) (one langley $= 1\ \mathrm{cal/cm^2}$), or equivalent units. The units of radiant flux density (van Wijk and Scholte Ubing, 1966; p. 63) are the same as those for radiated power per unit area (Shortley and Williams, 1971; p. 324). When it is desired to point out that the radiant flux is directed toward the surface of observation, the term *irradiancy* or *irradiance* is used. If one wants to stress that the radiation is emitted by a source, the radiant flux density is sometimes called *radiancy* or *emittancy.* Emittancy is also called *radiant emittance* (Campbell, 1977; p. 48).

As noted in Chapter 25, the amount of radiant energy contained in thermal radiation depends strongly on the wavelength $\lambda$ of the radiation that is emitted or received. It is often necessary to consider the energy, intensity, flux, etc. per unit of wavelength interval. Such quantities are called spectral quantities. They will be indicated by the subscript lambda ($\lambda$).

## 26.3 PRINCIPLES OF INFRARED THERMOMETRY

Let us now turn to the basic principles of infrared thermometers. We follow the analysis of Perrier (1971, p. 654). The energy emitted by a body that is not perfectly black is given by Eqn (25.5), $P = \alpha P_{\text{Black}} = \alpha\sigma T^4$. For a perfect black body, $\alpha = 1$ and Eqn (25.5) reduces to Eqn (25.4), the Stefan–Boltzmann law. We apply Eqn (25.5) to the surface temperature, $T_s$, of leaves. If $P$ is in units of W/m$^2$, the surface temperature will be in °$K$, and the Stefan–Boltzmann constant $\sigma$ will be $5.67 \times 10^{-8}$ W/m$^2$/K$^4$ (Campbell, 1977; p. 49). The term $\alpha$ (emissivity) is dimensionless. The emissivity, $\alpha$, is sometimes abbreviated $\varepsilon$, the abbreviation used by Perrier (1971). Surface temperature can be calculated from Eqn (25.5) if surface emissivity is known and the flux of thermal radiation emitted is measured. [Perrier (1971, p. 654) uses the term "emittance," but most publications use the term "emissivity" for $\varepsilon$.]

A radiometer has a sensor that receives energy from the measured surface through the optics of the radiometer, which define the F.O.V. by use of a diaphragm, lens, and sometimes a mirror, and bring localized surface areas into focus. It is necessary to select the waveband of thermal energy emitted by the surface from the total energy received by the sensor and originating at the surface. Therefore, a filter with a sharp bandpass in the infrared region (Table 26.1) is used generally to eliminate the short-wave radiation. The bandpass of 8–14 μm is particularly suitable (Figure 26.1). This selected bandpass includes the peak of black body emission at normal temperature (9–10 μm) so that the maximum energy is measured. Moreover, water does not absorb radiation in this band; thus, the effect of water vapor on the measurement is minimized. But that part of the long-wave radiation emitted by the surroundings and reflected by the surface in this waveband cannot be eliminated directly (Figure 26.2; $\phi_r$).

TABLE 26.1 The Electromagnetic Spectrum

| Type of Radiation | Frequency Range (cycles/s) | Wavelength Range (cm) |
|---|---|---|
| Electric waves | $0\text{–}10^4$ | Infinity–$3 \times 10^6$ |
| Radio waves | $10^4\text{–}10^{11}$ | $3 \times 10^6\text{–}0.3$ |
| Infrared | $10^{11}\text{–}4 \times 10^{14}$ | $0.3\text{–}7.6 \times 10^{-5}$ |
| Visible | $4 \times 10^{14}\text{–}7.5 \times 10^{14}$ | $7.6 \times 10^{-5}\text{–}4 \times 10^{-5}$ |
| Ultraviolet | $7.5 \times 10^{14}\text{–}3 \times 10^{18}$ | $4 \times 10^{-5}\text{–}10^{-8}$ |
| X-rays | $16 \times 10^{16}\text{–}3 \times 10^{22}$ | $10^{-6}\text{–}10^{-12}$ |
| Gamma rays | $3 \times 10^{18}\text{–}3 \times 10^{21}$ | $10^{-8}\text{–}10^{-11}$ |

*From Rosenberg (1974), p. 5. This material is used by permission of John Wiley & Sons, Inc.*

Theoretically, a simple integration of the relation representing the response of infrared thermometers can be written as follows:

$$A = \varepsilon\sigma T_s^4 + (1 - \varepsilon)B \quad \left[A \text{ in units of W/m}^2\right] \tag{26.1}$$

where $A$ is the flux of long-wave radiation from the surface; $T_s$ is the real temperature of the surface (leaves); $B$ is the total incident long-wave (or thermal) radiation in units of W/m$^2$; $(1 - \varepsilon)$ $B$ is the reflected component influencing the thermometer output; $\varepsilon$ is the surface emissivity; and $\sigma$ is the Stefan–Boltzmann constant.

It is supposed that $\varepsilon$ is independent of $T_s$ over a narrow range (−15 to 60 °C) and is independent of wavelength over a narrow waveband (8–14 µm). This condition is important only in the second term $(1 - \varepsilon)$ $B$. It

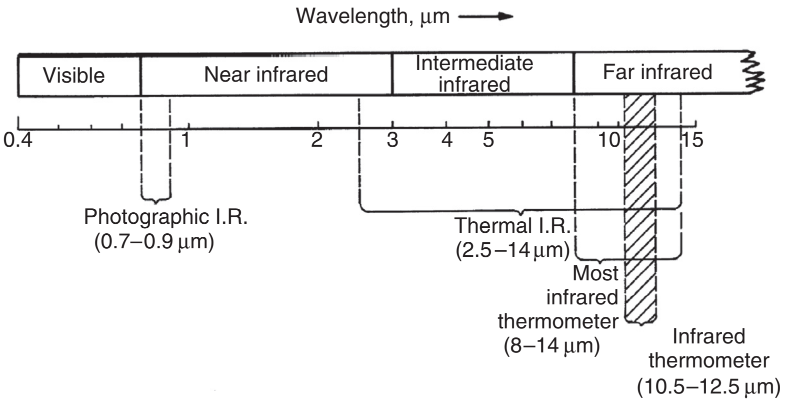
Wavelength, µm
Visible
Near infrared
Intermediate infrared
Far infrared
0.4
1
2
3
4
5
10
15
Photographic I.R. (0.7–0.9 µm)
Thermal I.R. (2.5–14 µm)
Most infrared thermometer (8–14 µm)
Infrared thermometer (10.5–12.5 µm)

FIGURE 26.1 A portion of the electromagnetic spectrum relating photographic infrared, thermal infrared, and infrared thermometer ranges to the visible and infrared regions. *From Jackson et al. (1980), p. 5.*

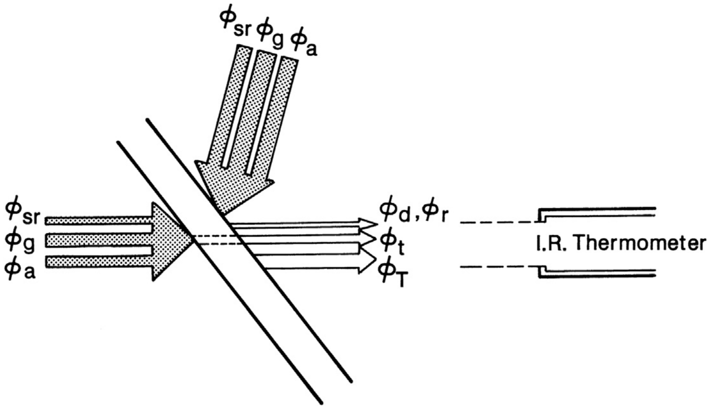

**FIGURE 26.2** Scheme of fluxes of energy on a surface like a leaf. $\phi_T$: energy emitted by the surface; $\phi_g$: part of global radiation received by the surface; $\phi_a$: part of long-wave radiation emitted by sky and received by the surface; $\phi_{sr}$: radiation from the surroundings received by the surface; $\phi_r$: reflected part of all these radiations; $\phi_d$: diffused part of all these radiations; $\phi_t$: transmitted part. *From Perrier (1971), Figure 17.7(C), p. 656. With kind permission of Kluwer Academic Publishers and Professor Alain Perrier.*

is supposed also that the filter function is practically independent of the temperature $T_s$ (0–40 °C) and the temperature of the filter is constant. As a first approximation, since $\varepsilon$ and $B$ are known, by assuming that $\varepsilon$ is close to unity (generally, for leaves $0.94 < \varepsilon < 0.98$), the real surface temperature ($T_s$) can be estimated ($T$) from the relation

$$A = \sigma T^4. \tag{26.2}$$

In Eqn (26.2) (compare with Eqn (26.1)), the calculated surface temperature ($T$) will be overestimated because the term containing $B$ is neglected and also underestimated because $\varepsilon$ is overestimated. This compensation between the two opposed deviations leads to a small overall error in the calculation of the surface temperature ($T$). Experience shows that $B$ is most often less than $A$, and the maximum of $B$ is reached in the evening (more scattering and reflection) or under a cloudy sky. The error generally varies between 0.5 and 1.5 °C.

## 26.4 USE OF A PORTABLE INFRARED THERMOMETER

Now let us turn to field use of infrared thermometers, following the description of Jackson et al. (1980, p. 52). To obtain representative canopy temperatures, it is desirable to point the infrared thermometer so that a maximum amount of vegetation is viewed by the sensor. This can be accomplished by viewing the target obliquely and at right angles to any structures which might be present in the field. It is best to take readings looking in several directions to minimize effects that the sun's angles (Kimes et al., 1980) (altitude angle; azimuth angle) may have on target temperature. The viewing angle used by Kirkham et al. (1984) was 30°, and they held the thermometer 1.2 m away from the crop (corn). Jackson et al. (1980) take measurements 1–2 h following solar noon, a time when a maximum difference between canopy and air temperature usually occurs. Routine weather observations, such as cloud cover, wind speed, precipitation, target conditions, and wet- and dry-bulb air temperatures, are recorded whenever canopy temperatures are measured. Wet- and dry-bulb air temperatures are essential in determining the Crop Water Stress Index (see Chapter 27). It is best to take measurements on cloud-free days to minimize errors due to reflection and scattering from clouds.

## 26.5 CALIBRATION OF INFRARED THERMOMETERS

Jackson et al. (1980) found that the readout temperature on most factory-calibrated instruments is not an accurate representation of apparent black-body temperatures. They calibrated all instruments under standardized conditions. Jackson et al. (1980) and Perrier (1971, p. 655) describe the calibration of an infrared thermometer. Let us use Perrier's description.

The unique relationship between the data supplied by the infrared thermometer ($A_0$) and the flux of long-wave radiation $A$ (Eqn (26.1)) reaching the apparatus from the surface is obtained in the laboratory by measuring $A_0$ for many different surface temperatures ($T$) of a reference black body. The temperature ($T$) gives the flux $A$ (Eqn (26.2)), so that it is possible to draw the curve relating $A_0$ to $A$ or directly to $T$. For these measurements, the infrared thermometer is put either close to the surface of a sphere immersed in a temperature-controlled bath (Figure 26.3(A)) (thus obtaining a very good black body at known temperature $T$) or at the top of a perfectly reflecting cone placed on a reference surface (anodized aluminum) (Figure 26.3(B)), the temperature of which is controlled and varied. Such calibration curves relating $A_0$ to $T$ are reproducible within a range of 0.3 °C. Some manufacturers provide a black-body plate with a thermometer imbedded in it to perform checks of the calibration. Sadler and van Bavel (1982) and Stigter et al. (1982) also describe calibration of infrared thermometers.

## 26.6 ADVANTAGES OF INFRARED THERMOMETERS

Infrared thermometers have three advantages. First, they are easy to use. The infrared thermometer is pointed at the canopy and a readout on

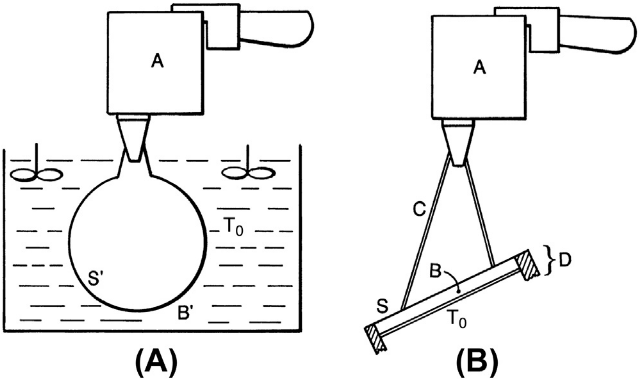

**FIGURE 26.3** Schematic diagram of infrared thermometer being calibrated either using (A) a controlled temperature bath, B′, or (B) an aluminum block, B. Other abbreviations: A, radiation thermometer; $T_0$, controlled temperature; S′, spherical surface (black surface); S, anodized aluminum surface; C, cone (reflecting surface); D, reference surface system. *From Perrier (1971), Figure 17.7(C), p. 656. With kind permission of Kluwer Academic Publishers and Professor Alain Perrier.*

the back of the instrument, facing the viewer, immediately displays the temperature. The instruments can give either the temperature of the canopy or the difference in temperature between the air and the canopy. The latter temperature usually is preferred, because it indicates how stressed a crop is. Canopies with temperatures below ambient temperature are less water stressed than those with temperatures above ambient temperature. (The air temperature can be measured separately with a thermometer.) Infrared thermometers have been used to schedule irrigations of crops such as corn (Clawson and Blad, 1982). In such work it is important to measure the canopy temperature of a well-watered control for a standard, local reference.

A second advantage of infrared thermometers is that they can rapidly measure temperatures remotely and nondestructively. A third advantage is that they can integrate temperatures over an area (the F.O.V.) and thus avoid the sampling problem of single-point measurements made, for example, with thermocouples. Note that thermocouples used to measure leaf temperature touch the leaf directly and measure a different temperature than that determined with an infrared thermometer. The infrared thermometer measures a black-body temperature. Measurements made with thermocouples and infrared thermometers cannot be compared directly.

Canopies must be well developed and covering the soil before data can be collected with commercially available infrared thermometers (Figure 26.4). Measurements cannot be made on individual plants, such as those in pots in controlled environments. Amiro et al. (1983) describe a

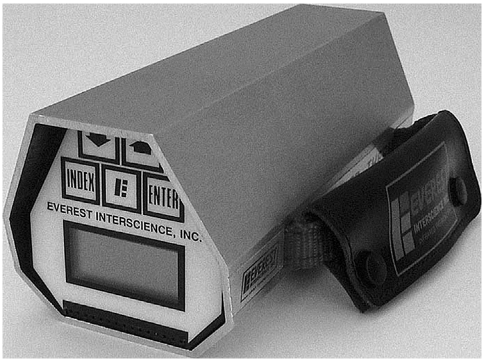

**FIGURE 26.4** A commercially available, hand-held infrared thermometer. *From a brochure of Everest Interscience, Tucson, Arizona. Picture courtesy of Everest Interscience.*

small infrared thermometer that can be used on broad or narrow leaves grown under controlled environment or field conditions. A focusing system must be implemented for narrow leaves.

Of all the instruments available to measure water in plants (thermocouple psychrometers, pressure chambers, diffusion porometers, infrared thermometers), the infrared thermometer might have the most immediate, practical value. It provides an easy way to measure canopy temperature and to schedule irrigations. An elevated canopy temperature indicates water stress and a need for irrigation. Baker et al. (2007) found that canopy temperature minus air temperature provided a good predictor of the degree of drought stress in cotton and could be used to schedule irrigations. Producers might use the infrared thermometer on crops to detect water stress before damage occurs. This would be particularly important on high-value crops, such as those grown by horticulturists. Canopy temperature measurements can be made at different locations in a field to identify stressed areas. Consequently, infrared thermometers are valuable as a means to determine remotely spatial variability due to drought or any other stress that reduces the transpiration rate.

## 26.7 APPENDIX: BIOGRAPHY OF RAY JACKSON

Ray Dean Jackson, a soil physicist at the U.S. Water Conservation Laboratory (retired), was born in Shoshone, Idaho, on September 28, 1929. He married in 1952 and 1968 and has seven children (American Men and Women of Science, 1994). He served in the U.S. Marine Corps before receiving his B.S. degree at Utah State University in 1956. He earned an M.S. in soil physics from Iowa State University in 1957, and a PhD from Colorado State University in 1960. From 1957 to 1960 he was a soil scientist with the Soil and Water Conservation Research Division, Agriculture Research Service (ARS) of the United States Department of Agriculture (USDA), in Colorado. In 1960, he joined the U.S. Water Conservation Laboratory of the USDA in Phoenix, Arizona, as a research physicist, where he worked until retirement in 1992. He was research leader and the technical advisor for soil—plant—atmosphere relations for the Western Region of the ARS. He was an adjunct professor of soil and water science at the University of Arizona, Tucson. In the summer of 1964 he was an Organization for Economic Cooperation and Development (OECD) fellow at Rothamsted Experimental Station, England.

Jackson published on subjects relating to diffusion in porous media, soil—water evaporation, soil—water movement, heat transfer, simultaneous heat and water transfer, atmospheric radiation, and infrared thermometry. He was perhaps the first researcher to publish measured soil—water diffusivity data for the relatively dry water contents of the western United States, a region where water vapor diffusion predominates, and he showed that diffusion theory held at these low water contents. This work formed the basis for the development of the "desert survival still" developed by Jackson and van Bavel (1965). They demonstrated that a transparent plastic sheet covering a hole in the soil could be used to collect potable water from desert soils and plants. This technique is taught in survival courses worldwide (American Society of Agronomy, 1975).

Jackson received the Superior Service Unit Award from the USDA in 1963. He is a fellow of the American Society of Agronomy, Soil Science Society of America, and the American Association for the Advancement of Science (American Men and Women of Science, 1994). In 1992, he won the Outstanding Scientist of the Year Award from the USDA-ARS. The award recognized his leadership skills and his research, which resulted in the commercialization of hand-held infrared thermometers to measure remotely plant leaf temperatures for determination of a crop's water needs (American Society of Agronomy, 1992).

## References

American Men and Women of Science, 1994. Nineteenth ed., vol. 4. J—L. R.R. Bowker, New Providence, New Jersey.

American Society of Agronomy, Jackson, Ray D., 1975. Agron. J. 67, 103.

American Society of Agronomy, 1992. People. USDA-ARS. Agronomy News December issue, 10.

Amiro, B.D., Thurtell, G.W., Gillespie, T.J., 1983. A small infrared thermometer for measuring leaf temperature in leaf chambers. J. Exp. Bot. 34, 1569—1576.

Baker, J.T., Gitz, D.C., Payton, P., Wanjura, D.F., Upchurch, D.R., 2007. Using leaf gas exchange to quantify drought in cotton irrigated based on canopy temperature measurements. Agron. J. 99, 637—644.

Campbell, G.S., 1977. An Introduction to Environmental Biophysics. Springer-Verlag, New York.

Clawson, K.L., Blad, B.L., 1982. Infrared thermometry for scheduling irrigation of corn. Agron. J. 74, 311–316.

Jackson, R.D., van Bavel, C.H.M., 1965. Solar distillation of water from soil and plant materials: simple desert survival technique. Science 149, 1377–1379.

Jackson, R.D., Reginato, R.J., Idso, S.B., 1977. Wheat canopy temperature: a practical tool for evaluating water requirements. Water Resour. Res. 13, 651–656.

Jackson, R.D., Pinter Jr, P.J., Reginato, R.J., Idso, S.B., 1980. Hand-held Radiometry. Agr Rev Manuals ARM-W-19. United States Department of Agriculture, Science and Education Administration, Western Region, Oakland, California.

Kimes, D.S., Idso, S.B., Pinter Jr, P.J., Reginato, R.J., Jackson, R.D., 1980. View angle effects in the radiometric measurement of plant canopy temperatures. Remote Sens. Environ. 10, 273–284.

Kirkham, M.B., Johnson, D.E., Kanemasu, E.T., Stone, L.R., 1983. Canopy temperature and growth of differentially irrigated alfalfa. Agr. Meteorol. 29, 235–246.

Kirkham, M.B., Suksayretrup, K., Wassom, C.E., Kanemasu, E.T., 1984. Canopy temperature of drought-resistant and drought-sensitive genotypes of maize. Maydica 29, 287–303.

Kirkham, M.B., Redelfs, M.S., Stone, L.R., Kanemasu, E.T., 1985. Comparison of water status and evapotranspiration of six row crops. Field Crops Res. 10, 257–268.

Perrier, A., 1971. Leaf temperature measurement. In: Šesták, Z., Čatský, J., Jarvis, P.G. (Eds.), Plant Photosynthetic Production. Manual of Methods. Dr W. Junk N.V, The Hague, The Netherlands, pp. 632–671.

Rosenberg, N.J., 1974. Microclimate: The Biological Environment. John Wiley and Sons, New York.

Sadler, E.J., van Bavel, C.H.M., 1982. A simple method to calibrate an infrared thermometer. Agron. J. 74, 1096–1098.

Shortley, G., Williams, D., 1971. Elements of Physics, fifth ed. Prentice-Hall, Englewood Cliffs, New Jersey.

Stigter, C.J., Jiwaji, N.T., Makonda, M.M., 1982. A calibration plate to determine performance of infrared thermometers in field use. Agr. Meteorol. 26, 279–283.

Tanner, C.B., 1963. Plant temperatures. Agron. J. 55, 210–211.

van Wijk, W.R., Scholte Ubing, D.W., 1966. Radiation. In: van Wijk, W.R. (Ed.), Physics of Plant Environment, second ed. North-Holland, Amsterdam, The Netherlands, pp. 62–101.

CHAPTER

# 27

# Stress-Degree-Day Concept and Crop Water Stress Index

The stress-degree-day (SDD) procedure and crop water stress index (CWSI) are methods to evaluate water stress in plants. They were developed in the 1970s by scientists at the United States Department of Agriculture (USDA) Water Conservation Laboratory in Phoenix, Arizona (Jackson, 1982). The CWSI has been used widely since then (Anda, 2009; Agam et al., 2013). We now define SDD and the CWSI and show their application.

## 27.1 SDD PROCEDURE

The work of the Phoenix scientists began in 1976 (Dean, 1976). The SDD concept was developed before the CWSI. Let us follow the description of its development by Jackson et al. (1977). The water status of a plant is a primary determinant of grain yield. A means for evaluating water status by remote measurement could open the way to improved yield predictions and, in irrigated areas, to improved scheduling times. The temperature of a plant canopy can be measured remotely with lightweight, handheld infrared (IR) thermometers (see Chapter 26). The difference between the temperature of a plant canopy and the temperature of the surrounding air ($T_c - T_a$) may be an indicator of the water status of a crop because water stress causes partial stomatal closure, thus reducing transpiration and allowing sunlit leaves to warm above ambient air temperature. The Phoenix scientists introduced the concept of a stress-degree-day. SDD is a daily value of $T_c - T_a$ measured at the time of maximum surface temperature (generally 1–1.5 h after solar noon). SDD is defined as follows:

$$\mathrm{SDD} = \sum_{n=i}^{N} (T_c - T_a)_n, \tag{27.1}$$

which is the plant canopy temperature $T_c$ minus the air temperature $T_a$ 150 cm above the soil, summed over $N$ days beginning at day $i$.

*Principles of Soil and Plant Water Relations*
http://dx.doi.org/10.1016/B978-0-12-420022-7.00027-6

Copyright © 2014 Elsevier Inc. All rights reserved.

(The SDD concept is similar to the growing-degree-day concept: $\mathrm{GDD} = \Sigma\{[(T_\mathrm{M} + T_\mathrm{m})/2] - T_\mathrm{t}\}$, where GDD is growing-degree-day; $T_\mathrm{t}$ is the threshold temperature for growth; $T_\mathrm{M}$ and $T_\mathrm{m}$ are the daily maximum and minimum air temperatures, respectively, and the GDD values are summed over $N$ days, the number of days under consideration (Lowry, 1969, p. 194). The threshold temperature varies with different crops.)

Jackson et al. (1977) evaluated water stress in plants (durum wheat, *Triticum durum* Desf. var. Produra) by using the SDD concept. They differentially irrigated the wheat. Plot 1 was the dry treatment (only enough irrigation water added to permit survival, a stressful condition in arid Phoenix, Arizona, where crops are usually amply watered, so they will grow). Plot 6 was the wet plot and was overwatered. Plots 2—5 received amounts of irrigation water that varied between the amounts added to Plots 1 and 6. Figure 27.1 shows their results. The greater the stress (lack of water), the greater was the value of the SDD. They began the summation of the SDD on day 83 (February 24, 1976), the day on which differential irrigation treatments were started. They ended the SDD summation on the day of harvest. Plot 6, which received an excessive

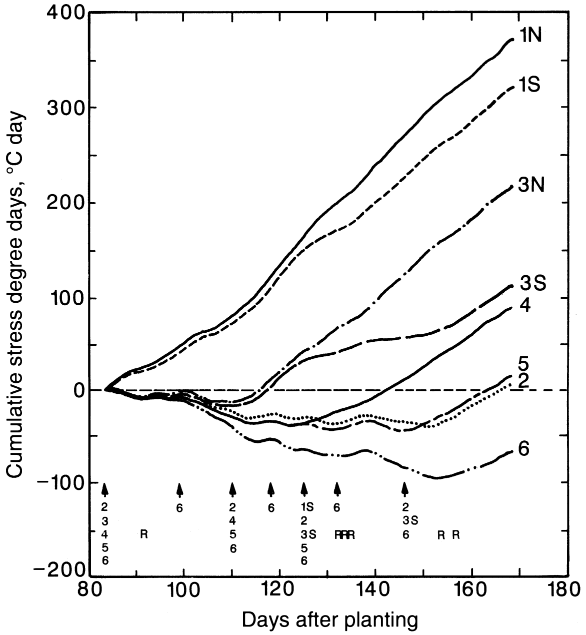

**FIGURE 27.1** Stress-degree-days versus days after planting. Plot numbers are shown at the right. Arrows indicate irrigations, the numbers of the plots receiving the irrigation being shown below the arrows. R indicates rain. N indicates north side of a plot. S indicates south side of a plot. *From Jackson et al. (1977). American Geophysical Union. Reproduced by permission of American Geophysical Union.*

amount of irrigation water, had canopy temperatures that were consistently less than air temperatures, and the SDD became less than −100 during the latter part of the season.

In general, if a plant has adequate water, $T_c - T_a$ will be near zero or negative; if it is water stressed, $T_c - T_a$ will be greater than zero. Thus, the sum of the positive values of $T_c - T_a$ may serve as an index of when to irrigate. Jackson et al. (1977) defined a positive SDD as follows:

$$\mathrm{SDD_{pos}} = \sum_{n=i}^{N} (T_c - T_a)_n \tag{27.2}$$

in which values of $T_c - T_a$ less than zero are set equal to zero. The index $i$ is the first day after irrigation, and $N$ is the number of days required for $\mathrm{SDD_{pos}}$ to reach a prescribed value.

Figure 27.2 shows $\mathrm{SDD_{pos}}$ and soil water depletion (measured using a neutron probe) for two of the plots in the experiment of Jackson et al. (1977). Cloudiness and other climatic conditions can cause abrupt changes in the slope of the $\mathrm{SDD_{pos}}$ versus time graph (Figure 27.2) during the first few days after irrigation. As water depletion increases, $T_c - T_a$ is always positive, the slope rapidly increases, and the effect of climatic factors diminishes.

Jackson et al. (1977) proposed an $\mathrm{SDD_{pos}}$ 10 as an index for the time to irrigate wheat in Arizona. They recognized that this value is somewhat

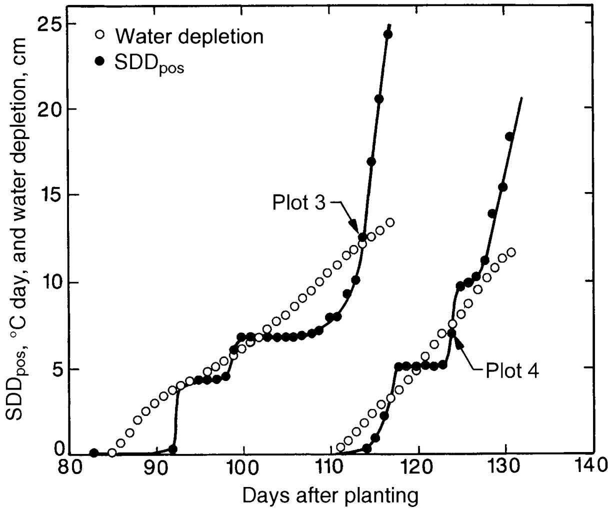

**FIGURE 27.2** Positive stress-degree-days and water depletion for two plots, beginning after the last irrigation. Numerical values on the ordinate are the same for both factors. *From Jackson et al. (1977). American Geophysical Union. Reproduced by permission of American Geophysical Union.*

dependent on the means used to measure $T_c$ and $T_a$ (for example, the height at which $T_a$ is measured), that it may be soil and crop specific (they used a loam soil), and that it may be different under other climatic conditions. Nevertheless, the $\mathrm{SDD_{pos}}$ appears to provide a possible means to develop irrigation scheduling based on remotely sensed plant canopy temperatures.

## 27.2 CANOPY-MINUS-AIR TEMPERATURE AND EVAPOTRANSPIRATION

Let us now turn to the relation between $T_c - T_a$ and evapotranspiration. One approach to estimating the amount of water depleted from the root zone is to use an evapotranspiration equation based on the temperature difference $T_c - T_a$, such as the following equation (Jackson et al., 1977):

$$\mathrm{ET} = R_n - G - f(u)C(T_c - T_a), \tag{27.3}$$

in which ET is evapotranspiration, $R_n$ is net radiation, $G$ is soil heat flux, $f(u)$ is a function of wind speed, and $C$ is the volumetric heat capacity of air. This equation is a reliable predictor of crop evapotranspiration (Stone and Horton, 1974). Stone and Horton (1974) used Eqn (27.3) for the same purpose that Jackson et al. (1977) were concerned with—to develop a method of predicting water use over large areas by using remotely sensed parameters.

To use Eqn (27.3), Jackson et al. (1977) made some simplifying assumptions. They found that for their experimental conditions, wind was not of major importance in the calculation of ET using Eqn (27.3). (This may not be true for locations with persistent winds and higher wind speeds than those recorded in Phoenix, Arizona.) They were not concerned with hourly values of ET, but wanted to calculate daily values of actual ET, using a minimum of input data and a one-time-of-day measurement of $T_c - T_a$. For 24-h periods, it is safe to assume that the soil heat flux $G$ is negligible. With Jackson et al.'s (1977) simplifying assumptions, Eqn (27.3) becomes

$$\mathrm{ET} = R_n - \mathrm{B}(T_c - T_a), \tag{27.4a}$$

in which B is a composite constant that must be determined.

The parameter B in Eqn (27.4a) was evaluated by using daily values for ET from a lysimeter, daily values of $R_n$ over the lysimeter, and one-time-of-day (taken between 13:30 and 14:00 h) measurements of $T_c - T_a$ for every day for which ET, $R_n$, and $T_c - T_a$ data were available, from day 60 until harvest of the wheat. These data are shown in Figure 27.3. Figure 27.3(A) shows the relation for $\mathrm{ET} - R_n$ versus $T_c - T_a$. A statistical value for B was obtained by forcing Eqn (27.4a) through the

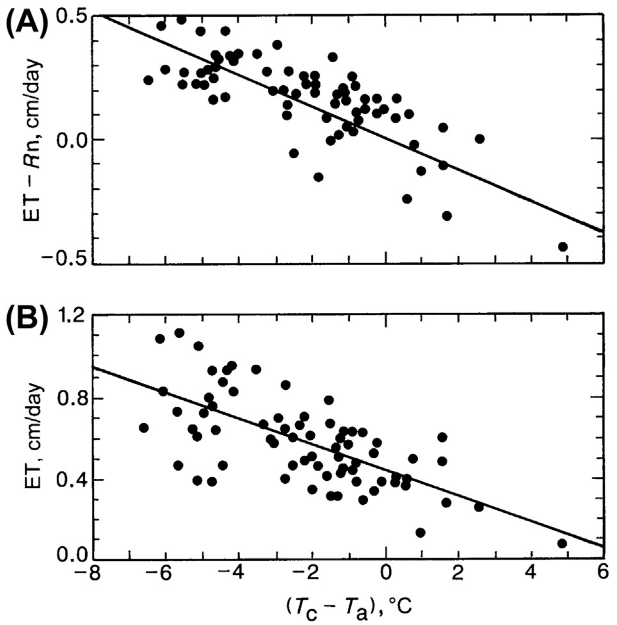

**FIGURE 27.3** Evapotranspiration and net radiation as a function of canopy—air temperature difference. *From Jackson et al. (1977). American Geophysical Union. Reproduced by permission of American Geophysical Union. See text for explanation of parts A and B.*

origin, since Eqn (27.4a) indicates that for $T_c - T_a = 0$, $\text{ET} - R_n = 0$. This yielded

$$\text{ET} = R_n - 0.064(T_c - T_a). \tag{27.4b}$$

In Figure 27.3(B), the dependence of ET on $T_c - T_a$ alone was determined. The relation is

$$\text{ET} = 0.438 - 0.064(T_c - T_a). \tag{27.5}$$

The constants in Eqn (27.4b) and Eqn (27.5) were evaluated by using ET data from lysimeters. To test their applicability, ET was calculated by using $R_n$ and $T_c - T_a$ data from the wheat plots. Water depletion was also calculated. The measured and calculated data are compared in Figure 27.4. In Figure 27.4(A), ET was calculated from Eqn (27.4b) by using net radiation measured over the north sides of each plot. In Figure 27.4(B), the net radiation was averaged over the six plots for each day, and the average was used in Eqn (27.4b). In Figure 27.4(C), the seasonal average of $R_n$ was used in Eqn (27.4b), whereas in Figure 27.4(D), $R_n$ was taken as the statistically derived constant from Figure 27.3(B) (i.e., from Eqn (27.5)). The data in Figures 27.4(A) and (B) indicate that if daily estimates of $R_n$ are available, water use can be estimated reasonably well by using Eqn (27.4a).

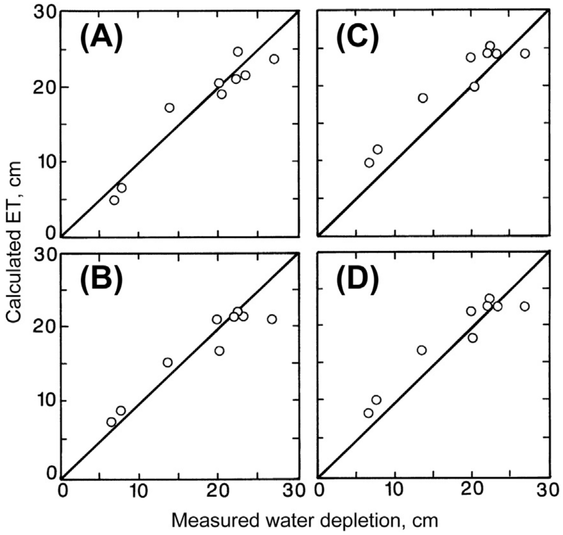

FIGURE 27.4 Calculated evapotranspiration and measured water depletion. The lines indicate a 1:1 relation. See text for explanation of different parts of figure. *From Jackson et al. (1977). American Geophysical Union. Reproduced by permission of American Geophysical Union.*

The data of Jackson et al. (1977) indicate that air temperature could be determined on the ground and airborne scanners could measure $T_c$, enabling water use by crops to be evaluated over large areas. In sum, the work by Jackson et al. (1977) showed that (1) the SDD concept can be used as an indicator for determining the times and amounts of irrigation; and (2) because predicted ET, from an expression relating ET to net radiation and $T_c - T_a$, and measured water used agreed reasonably well, the expression may be useful in determining amounts of irrigation water to apply.

## 27.3 CROP WATER STRESS INDEX

Now let us consider the CWSI, which was developed by the Phoenix scientists 4 years after the SDD concept was developed (Idso et al., 1982). The CWSI is also called the plant water stress index (PWSI). Only the difference between canopy temperature and air temperature is considered in the SDD concept. However, SDD may be influenced by factors such as air vapor pressure, net radiation, and wind speed (Idso et al., 1981). It is important to determine the significance of these other factors and to devise a means for adjusting for them. Consequently, the Phoenix

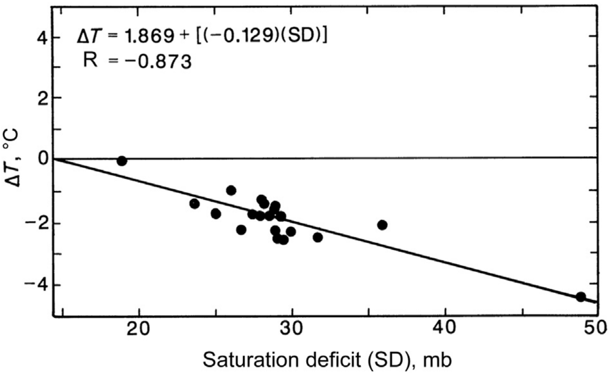

**FIGURE 27.5** The regression of cotton leaf—air temperature difference (Δ*T*, °C) on the saturation deficit of the air (mb). Air temperature and vapor pressure were measured 1 m above the cotton crop. The data are restricted to the period 08:00—18:00 h (Mountain Standard Time) on predominantly sunny days when the crop was fully hydrated, i.e., from 2 to 6 days after a heavy irrigation. *From Ehrler, (1973). American Society of Agronomy, Madison, Wisconsin. Reprinted by permission of the American Society of Agronomy.*

workers developed a plant-(crop-) water-stress index that essentially normalizes the SDD value.

The basis for the PWSI was established by the work of Ehrler (1973). He used thermocouples to measure the leaf temperature of four varieties of cotton (*Gossypium hirsutum* L. 'Deltapine SL', 'Deltapine-16', and 'Hopicala', and *Gossypium barbadense* L. 'Pima-S4'). He found that for clear, sunny days, the difference between leaf and air temperatures from 08:00 to 18:00 h was a linear function of air vapor pressure deficit (VPD), as long as the plants were well supplied with water (Figure 27.5).

Working with IR thermometers, Idso et al. (1981) extended Ehrler's (1973) data to include alfalfa (*Medicago sativa* L.), soybeans (*Glycine max* L. Merr.), and squash (*Cucurbita pepo* L.). They plotted values of $T_c - T_a$ versus VPD (Figures 27.6—27.8) and found that crop-specific linear relationships prevailed throughout the greater portion of the daylight period (i.e., from about 2—3 h after sunrise to about 2—3 h before sunset). They also found these relationships to be essentially undisturbed by variations in other environmental parameters, such as wind speed or the normal course of insolation through the day. Only shading by clouds seemed to have a significant influence, reducing foliage (canopy) temperature relative to that of the air by several degrees (Idso, 1982a).

Figure 27.9 provides a generalized representation of these results and a framework for describing the development of the PWSI (Idso, 1982a). The lower limit of this graph, which represents a state of potential evaporation, is referred to as the *non-water-stressed* baseline. It is crop specific and must be obtained by experimentation as described in the preceding paragraphs. Once established, it is used to define the other limiting condition that prevails when water stress is a maximum and transpiration completely suppressed, which is accomplished as follows (Idso, 1982a).

Consider a well-watered plant transpiring at the potential rate. A plot of $T_c - T_a$ versus VPD ($T_c$, canopy temperature, is also called $T_f$, foliage temperature) for this plant will fall somewhere on the non-water-stressed baseline; and as the air VPD decreases to zero, it will move along this baseline to achieve the $T_f - T_a$ value representative of the linear relationship's intercept. If this term is positive, as it has proven to be (Idso, 1982a) (value $a$ in Figure 27.9), there will still be a small evaporative flux from the plant to the air, even though the air at that point is saturated, due to the positive vapor pressure gradient (VPG) that exists between the plant and the air as a result of the plant's higher temperature.

This driving force for evaporation is easily evaluated as VPG $= \rho_s(T_f) - \rho_s(T_a)$, where $\rho_s(T_f)$ is the saturated vapor pressure at the temperature of the foliage and $\rho_s(\mathrm{T_a})$ is the saturated vapor pressure at the temperature of the air; for transpiration to be reduced to zero, VPG must be reduced to zero. One way by which this may be accomplished is to supersaturate the

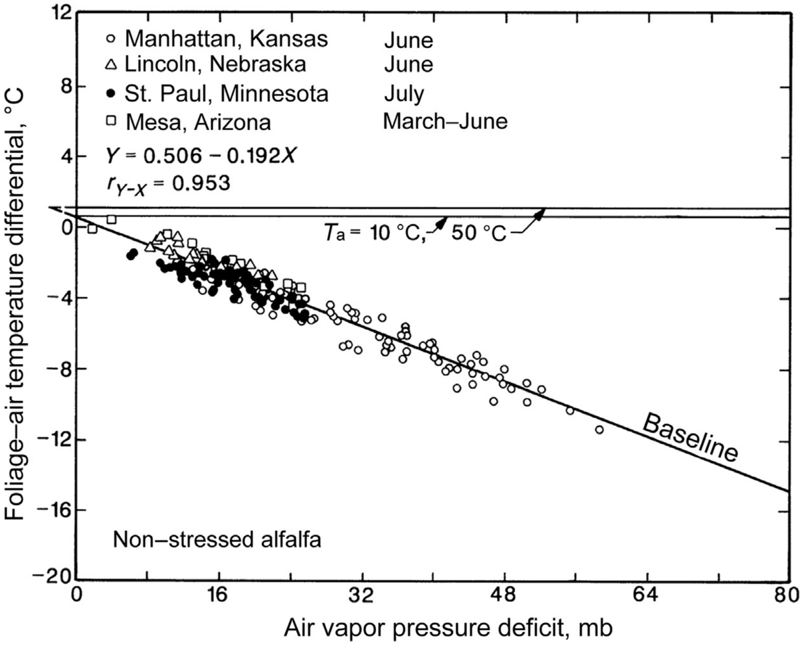

**FIGURE 27.6** Foliage–air temperature differential versus air vapor pressure deficit for well-watered alfalfa grown at the specified sites and dates during 1980. *From Idso et al. (1981). Elsevier Scientific Publishing Company, Amsterdam. Reprinted by permission of Elsevier, Amsterdam.*

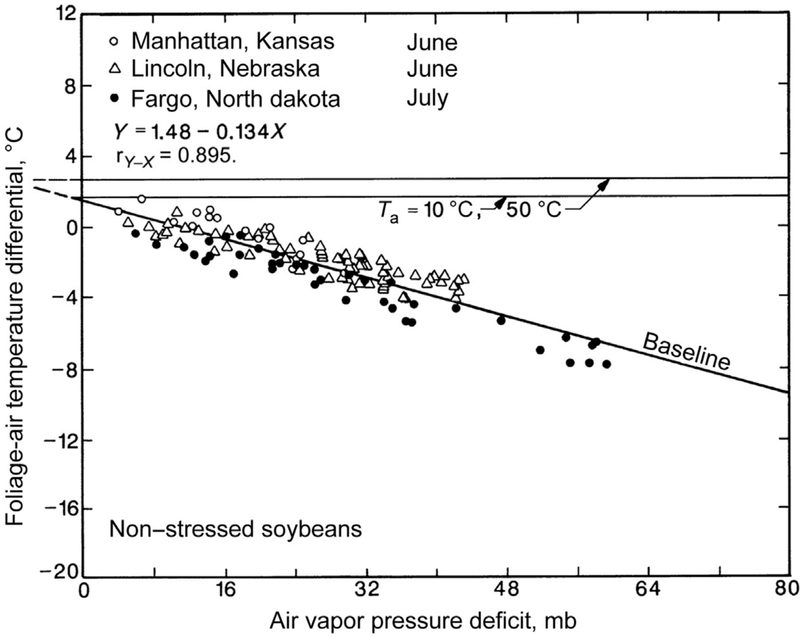

**FIGURE 27.7** Foliage—air temperature differential versus air vapor pressure deficit for well-watered soybeans grown at the specified sites and dates. *From Idso et al. (1981). Elsevier Scientific Publishing Company: Amsterdam. Reprinted by permission of Elsevier, Amsterdam.*

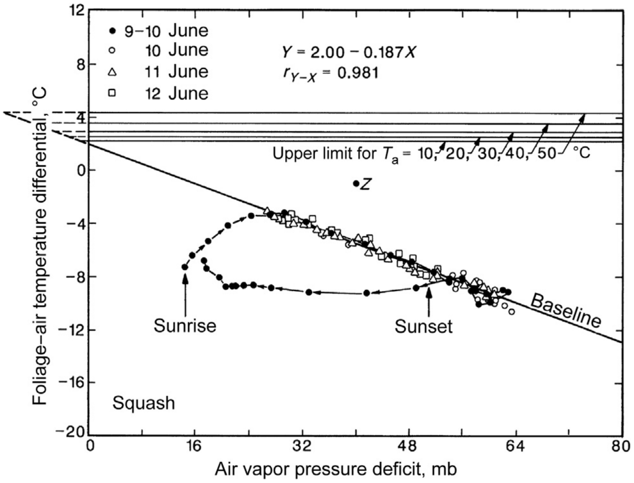

**FIGURE 27.8** Foliage—air temperature differential versus air vapor pressure deficit for well-watered squash grown at Tempe, Arizona, in June, 1980. *From Idso et al. (1981). Elsevier Scientific Publishing Company: Amsterdam. Reprinted by permission of Elsevier, Amsterdam.*

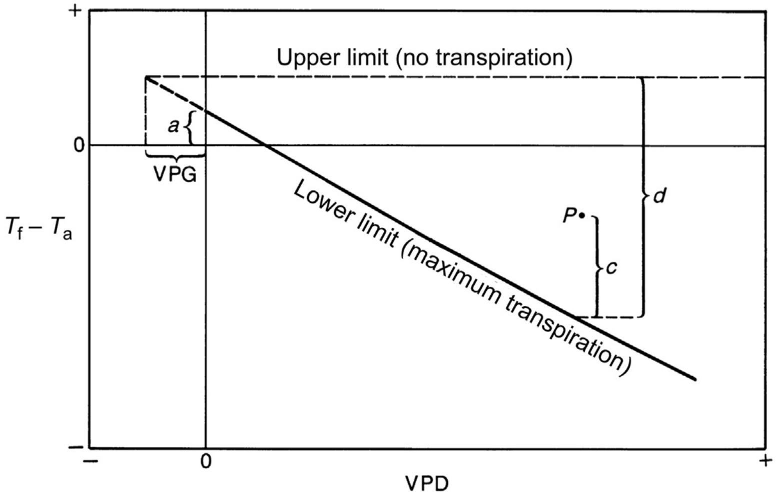
Upper limit (no transpiration)
Lower limit (maximum transpiration)
$T_f - T_a$
VPD
VPG
a
c
d
P
+
0
−
−
0
+

**FIGURE 27.9** The general form of the relationship between foliage–air temperature differential ($T_f - T_a$) and air vapor pressure deficit (VPD) for a stand of vegetation sufficiently supplied with water to transpire at the potential rate, i.e., the lower limit (maximum transpiration line), plus an illustration of how the upper limit (no transpiration line) is derived using the vapor pressure gradient (VPG). The values $c$ and $d$ are used to define the plant water stress index. See text for explanation. *From Idso et al. (1982). American Geophysical Union. Reproduced by permission of American Geophysical Union.*

air, that is, to create a negative VPD equivalent in absolute magnitude to the VPG. Then, following the non-water-stressed baseline back into the negative VPD region by this amount will specify the upper limit to which $T_f - T_a$ may rise at the particular air temperature in question. This latter point of emphasis is made to underscore the fact that there is not a unique upper limit for a given species, as is the case with the non-water-stressed baseline, but rather a variety of limits corresponding to the variety of air temperatures that may prevail. For plants with a small baseline intercept (i.e., less than 0.5 °C), this upper limit dependency on air temperature is weak and can sometimes be ignored (Idso, 1982a).

Consider now a data point representative of a stressed plant that locates it at position $P$ in Figure 27.9. In this format, Idso et al. (1981) defined the PWSI (or CWSI) as the ratio of the vertical distance between the data point and the non-water-stressed baseline and the total vertical distance between the baseline and the upper limit (i.e., PWSI $= c/d$). Thus defined, it can be seen that as a plant goes from a condition of maximum transpiration to one of no transpiration, the index goes from a value of zero to unity; Jackson et al. (1981) have demonstrated that actual transpiration ($E$) at any point $P$ in this range is specified as $E = E_p(1-\text{PWSI})$, where $E_p$ is the potential evaporation rate that could be sustained in the given circumstances, but with a nonlimiting supply of soil moisture (Idso, 1982a). (The PWSI or CWSI has sometimes been referred to as the IJ index after Idso and Jackson, the two scientists who developed the concept. For a biography of Idso, see the Appendix, Section 27.8. A biography of Jackson appears in Chapter 26, Section 26.7.)

## 27.4 HOW TO CALCULATE THE CROP WATER STRESS INDEX

Let us now take a specific example that shows how to obtain the PWSI (or the CWSI). Let us refer to Figure 27.8 (Idso et al., 1981). Suppose at a time when the air VPD is 40 mb, the value of $T_f - T_a$ is −1 °C, so that the point $Z$ on Figure 27.8 represents the status of the crop, which in this case is squash. Now, if the crop had been sufficiently supplied with water to evaporate at the potential rate, $T_f - T_a$ would have been −5.5 °C, as obtained from intersecting the non-water-stressed baseline at VPD = 40 mb. Conversely, if the crop had not been transpiring at all, and $T_a$ was 30 °C (for example), then $T_f - T_a$ would be expected to have been about 3 °C. With this information, we can define the PWSI (or CWSI) to be the ratio of the vertical distance above the non-water-stressed baseline that the point $Z$ has conceptually traveled in falling below the potential evaporation rate to the total possible distance that it could conceptually travel, which in this example is −1 °C − (−5.5 °C) divided by 3 °C − (−5.5 °C) or 4.5 °C/8.5 °C = 0.53. Thus, we see that as the ratio of actual to potential evaporation goes from 1 to 0, the CWSI goes from 0 to 1.

## 27.5 CROP WATER STRESS INDEX FOR ALFALFA, SOYBEANS, AND COTTON

Idso et al. (1981) did not determine $T_c - T_a$ versus VPD for water-stressed squash, so no measured points in Figure 27.8 lie around point $Z$ in the figure. They did, however, determine $T_c - T_a$ versus VPD for water-stressed alfalfa and soybeans (Figures 27.10 and 27.11). Note that for water-stressed alfalfa and soybeans points lie between the baseline or lower limit (maximum transpiration) and the upper limit (no transpiration). In Figure 27.12, Idso et al. (1981) have converted the data from Figures 27.10 and 27.11 into the format of the CWSI. The soybeans, in this instance, were still fairly young, and covered only about 10% of the ground. Thus, with their rather limited rooting volume, they experienced a dramatic rate of stress development as the hot and dry day, on which the data were obtained, progressed (maximum air temperature was 39 °C and minimum relative humidity was 17%). But the alfalfa, with its

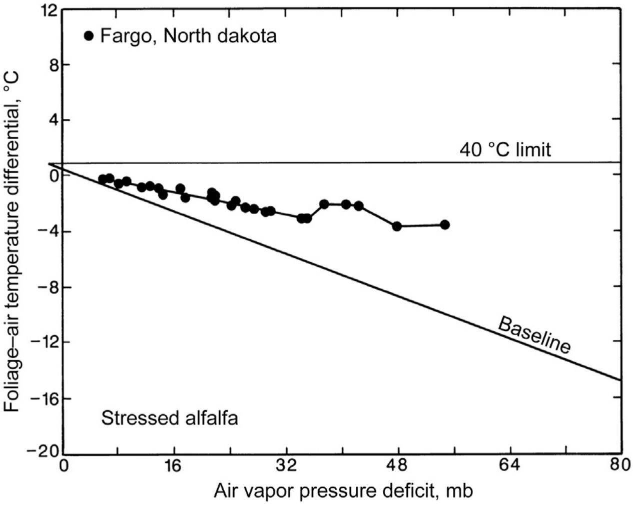

**FIGURE 27.10** Foliage–air temperature differential versus air vapor pressure deficit for stressed alfalfa growing at Fargo, North Dakota. *From Idso et al. (1981). Elsevier Scientific Publishing Company: Amsterdam. Reprinted by permission of Elsevier, Amsterdam.*

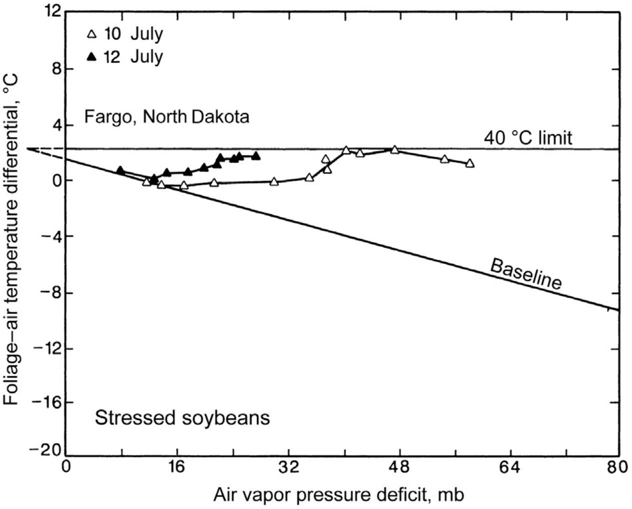

**FIGURE 27.11** Foliage–air temperature differential versus air vapor pressure deficit for stressed soybeans growing at Fargo, North Dakota. *From Idso et al. (1981). Elsevier Scientific Publishing Company: Amsterdam. Reprinted by permission of Elsevier, Amsterdam.*

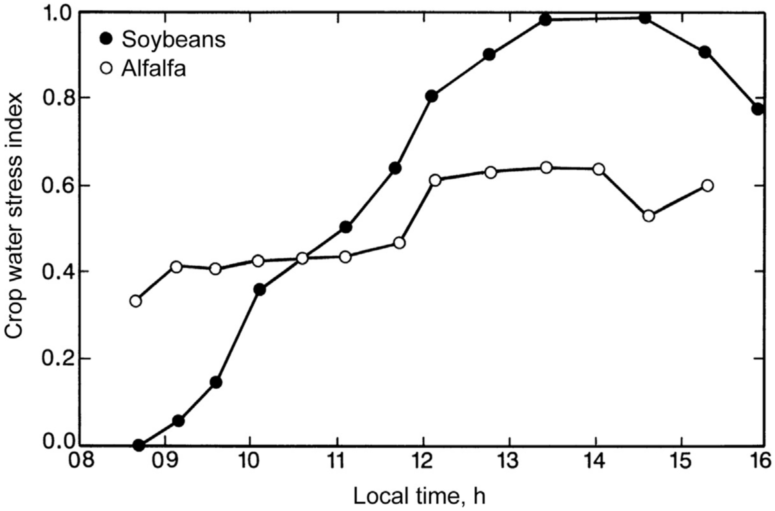

**FIGURE 27.12** The crop water stress index as a function of time for severely stressed soybeans and less severely stressed alfalfa at Fargo, North Dakota. *From Idso et al. (1981). Elsevier Scientific Publishing Company: Amsterdam. Reprinted by permission of Elsevier, Amsterdam.*

well-developed root system, showed a much greater buffering capacity to stress development, although it too showed a significant increase in stress in the afternoon. Maximum stress for both crops occurred about 1–2 h after solar noon, indicating that this was a good time for a once-a-day measurement, as was used by Jackson et al. (1981), to quantify the stress history of several differently irrigated wheat plots. Figure 27.13

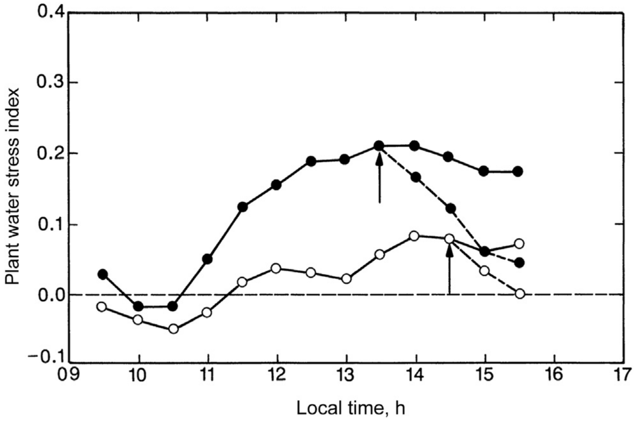

**FIGURE 27.13** The plant water stress index for mildly and moderately stressed cotton preceding and following irrigations shown by arrows. *From Idso et al. (1982). American Geophysical Union. Reproduced by permission of American Geophysical Union.*

shows the crop-(plant-) water-stress index plotted for mildly stressed cotton (lower line) and moderately stressed cotton (upper line) before and after irrigation (Idso et al., 1982).

## 27.6 IMPORTANCE OF A WIDE RANGE OF VAPOR PRESSURE DEFICIT VALUES

Plots of $T_c - T_a$ versus VPD for well-watered plants appear to yield a unique linear relationship under a specific climatic condition. The Phoenix scientists postulate that the existence of such linear relationships provides a simple criterion for identification of a potential evaporation (Idso et al., 1981). Their findings also provide a means for normalizing the SDD value for environmental variability, by converting it into the CWSI. It is evident, however, that defining stress in this fashion limits the ability to quantify, with confidence, the CWSI under conditions of low VPD, where the variability of $T_c - T_a$ approaches the degree of scatter inherent in the data (see Figures 27.6 and 27.7). Therefore, it is important to have a wide range of VPD values to obtain meaningful CWSIs.

## 27.7 NORMALIZED DIFFERENCE VEGETATION INDEX

What the CWSI measures should not be confused with what the normalized difference vegetation index (NDVI) measures. Light from the sun, reflected from plants, can show approximately how much plant material is present in a field (Jackson et al., 1980). Jackson et al. (1980) present a vegetation index, now called the NDVI, as follows:

$$\text{NDVI} = [(\text{IR} - \text{red})]/[(\text{IR} + \text{red})]. \tag{27.6}$$

The NDVI is obtained from the ratio between the red and near-red IR reflectance bands, which are measured with radiometers (Hillel and Rosenzweig, 2005). Tucker et al. (1981) found that the band 0.63—0.69 μm in the red region and the band 0.76—0.90 μm in the IR region give reliable results to analyze natural materials in situ. These two bands are sensitive to the chlorophyll density and the green leaf density, respectively, of a plant canopy. Their results were confirmed by Stone and Kirkham (1983). Chlorophyll absorbs in the red and blue bands (see Chapter 3, Section 3.2, Part 6 for the exact wavelengths), but the NDVI is based on the red band, not the blue band. The reflectance data can be obtained on land by handheld radiometers (Stone and Kirkham, 1983) or remotely by aircraft or satellites (Hillel and Rosenzweig, 2005). The CWSI measures the difference between canopy and air temperatures and cannot be monitored by aircraft or satellites. How far into the sky a temperature differential occurs due to evaporational cooling needs to be determined (Kirkham, 2013). Turbulence of the atmosphere mixes canopy temperature with ambient air temperature, so the difference between canopy and air temperatures should occur only over a short distance. As noted in Chapter 26, Kirkham et al. (1984) measured canopy temperature at a distance 1.2 m away from the crop.

However, scientists who obtain reflectance data remotely are trying to take measurements of canopy temperature from aircraft. Drones are now being used to obtain reflectance data for monitoring of crop health. A drone is a pilotless airplane whose flight is controlled by an operator in an accompanying craft or on the ground (Webster's New World Dictionary of the American Language, 1959). Drones measure the NDVI, which tells that a crop is stressed, but not the reason for the stress. It can be stressed due to drought, flooding, cold, heat, or insects. We need ground truth to tell the reason for the stress. The CWSI can tell us that a crop is water stressed and can be used for irrigation scheduling. Drones are either fixed-wing aircraft or helicopters. When helicopters are used, the blades stir up the air and affect the plant temperature. However, drones are being equipped with temperature sensors that can measure within 1/100th of a degree centigrade (Kevin P. Price, Department of Agronomy, Kansas State University, personal communication, August 15, 2013). It is hoped that the air mixing problem from the aircraft can be overcome, so that drones eventually could measure a CWSI. Temperature data from drones may soon be able to detect how far above a crop the temperature differential exists.

## 27.8 APPENDIX: BIOGRAPHY OF SHERWOOD IDSO

Sherwood B. Idso was born on June 12, 1942, in Thief River Falls, Minnesota, where he lived until graduating from high school in 1960. He then enrolled in the Institute of Technology at the University of Minnesota, where he received a bachelor's degree in physics with distinction in 1964, an M.S. degree in 1966, and a Ph.D. in 1967. He moved to the US Water Conservation Laboratory of the USDA in Phoenix, Arizona, in 1967, where he worked as a research physicist. He also was an adjunct professor in the Departments of Geology and Geography at Arizona State University in Tempe. Much of his work at the US Water Conservation Laboratory related to the study of the effects of elevated carbon dioxide on plant growth, often done in collaboration with Bruce A. Kimball. See Kirkham (2011) for citations of their work. Since stopping doing research with the USDA, Idso has been actively involved in disseminating information, through a Web site, about the climatic and biological effects of elevated carbon dioxide in the atmosphere. Idso and his wife have seven children (Idso, 1982b). Two of his children, Craig D. Idso and Keith E. Idso, also work to disseminate information about carbon dioxide in the atmosphere.

Sherwood Idso has published numerous scientific papers. In addition to his publications on carbon dioxide, he has studied heat and moisture transfer in the soil-plant-atmosphere continuum (SPAC). He developed methods for evaluating evaporative water losses from soil, plants, and open water, along with a number of techniques for the remote sensing of soil- and plant-water status. He has an abiding interest in severe weather phenomena and is a dedicated investigator of dust storms and dust devils (Idso, 1982b). He is well known for his writings related to climate change.

In 1977, Idso received the Arthur S. Flemming Award “for his innovative research into fundamental aspects of agricultural-climatological interrelationships affecting food production and the identification of achievable research goals whose attainment could significantly aid in assessment and improvement of world food supplies”. The Flemming Award is presented annually to people under the age of 40 years who work in civilian or military capacities in the federal government. The Downtown Jaycees of Washington, D.C., sponsor the award (American Meteorological Society, 1978).

## References

American Meteorological Society, 1978. About our members. Bull. Am. Meteor. Soc. 59, 747.

Agam, N., Cohen, Y., Berni, J.A.J., Alchanatis, V., Kool, D., Dag, A., Yermiyahu, U., Ben-Gal, A., 2013. An insight to the performance of crop water stress index for olive trees. Agr. Water Manage. 118, 79–86.

Anda, A., 2009. Irrigation timing in maize by using the crop water stress index (CWSI). Cereal Res. Commun. 37, 603–610.

Dean, J.P., 1976. Sensing soil moisture—remotely. Agr. Res. 25 (4), 7–9.

Ehrler, W.L., 1973. Cotton leaf temperatures as related to soil water depletion and meteorological factors. Agron. J. 65, 404–409.

Hillel, D., Rosenzweig, C., 2005. Desertification. In: Hillel, D. (Ed.), Encyclopedia of Soils in the Environment, vol. 1. Elsevier, Amsterdam, pp. 382–389.

Idso, S.B., 1982a. Non-water-stressed baselines: a key to measuring and interpreting plant water stress. Agric. Meteorol. 27, 59–70.

Idso, S.B., 1982b. Carbon Dioxide: Friend or Foe? IBR Press, Tempe, Arizona (Available from the Institute for Biospheric Research, Inc., 631 E. Laguna Drive, Tempe, Arizona 85282).

Idso, S.B., Jackson, R.D., Pinter Jr, P.J., Reginato, R.J., Hatfield, J.L., 1981. Normalizing the stress-degree-day parameter for environmental variability. Agric. Meteorol. 24, 45–55.

Idso, S.B., Reginato, R.J., Farah, S.M., 1982. Soil- and atmosphere-induced plant water stress in cotton as inferred from foliage temperatures. Water Resour. Res. 18, 1143–1148.

Jackson, R.D., 1982. Canopy temperature and crop water stress. In: Hillel, D. (Ed.), Advances in Irrigation, vol. 1. Academic Press, New York, pp. 43–85.

Jackson, R.D., Reginato, R.J., Idso, S.B., 1977. Wheat canopy temperature: a practical tool for evaluating water requirements. Water Resour. Res. 13, 651–656.

Jackson, R.D., Pinter Jr, P.J., Reginato, R.J., Idso, S.R., 1980. Hand-held Radiometry. Agr Rev Manuals ARM-W-19. United States Department of Agriculture, Science and Education Administration, Western Region, Oakland, California.

Jackson, R.D., Idso, S.B., Reginato, R.J., Pinter Jr, P.J., 1981. Canopy temperature as a crop water stress indicator. Water Resour. Res. 17, 1133–1138.

Kirkham, M.B., 2011. Elevated Carbon Dioxide: Impacts on Soil and Plant Water Relations. CRC Press, Boca Raton, Florida.

Kirkham, M.B., 2013. Research needs for agriculture under elevated carbon dioxide. In: Hillel, D., Rosenzweig, C. (Eds.), Handbook of Climate Change and Agroecosystems. Global and Regional Aspects and Implications. Imperial College Press, London, pp. 225–234.

Kirkham, M.B., Suksayretrup, K., Wassom, C.E., Kanemasu, E.T., 1984. Canopy temperature of drought-resistant and drought-sensitive genotypes of maize. Maydica 29, 287–303.

Lowry, W.P., 1969. Weather and Life: An Introduction to Biometeorology. Academic Press, New York.

Stone, J.M., Kirkham, M.B., 1983. Water content of sludge-injected soil growing wheat. Environ. Conserv. 10, 337–342.

Stone, L.R., Horton, M.L., 1974. Estimating evapotranspiration using canopy temperatures: field evaluation. Agron. J. 66, 450–454.

Tucker, C.J., Jones, W.H., Kley, W.A., Sundstrom, G.J., 1981. A three-band hand-held radiometer for field use. Science 211, 281–283.

Webster's New World Dictionary of the American Language, College ed., 1959. World Publishing, Cleveland.

# CHAPTER

# 28

# Potential Evapotranspiration

The term *potential evapotranspiration* (PET) must be defined when we talk of evapotranspiration (ET). *Evapotranspiration*, as defined by the Soil Science Society of America (2008), is the "combined loss of water from a given area, and during a specified period of time, by evaporation from the soil surface and by transpiration from plants". The concept of PET was put forth by Thornthwaite (1948), an American, and Penman (1948), an Englishman. We will use the definition of Rosenberg (1974, p. 172), noting that his definition is similar to that of Penman. (For a biography of Penman, see the Appendix, Section 28.5.)

## 28.1 DEFINITION OF POTENTIAL EVAPOTRANSPIRATION

Rosenberg says that potential evapotranspiration (abbreviated as ETP by him, but as PET by most others) is "the evaporation from an extended surface of [a] short green crop which fully shades the ground, exerts little or negligible resistance to the flow of water, and is always well supplied with water. Potential evapotranspiration cannot exceed free water evaporation under the same weather conditions".

In fact, we know that real (actual) ET differs from the potential under most circumstances. The reasons for these differences are best explained by reference to the conditions imposed by the definition of PET and by an analysis of the reality of these conditions. We follow the discussion of (Rosenberg 1974, pp. 172–178), even though we could use other references (e.g., Chang, 1968; pp. 129–144).

## 28.2 FACTORS THAT AFFECT POTENTIAL EVAPOTRANSPIRATION

First, let us look at the influence of *extended surfaces* (or what is called the influence of *fetch*) on PET. An extended surface has great

http://dx.doi.org/10.1016/B978-0-12-420022-7.00028-8

Copyright © 2014 Elsevier Inc. All rights reserved.

(if unspecified) fetch. Fields should be at least 20 m from their centers in any direction from which the wind blows. However, in some experiments, it has been found that temperature profiles to 5 m, even at 200 m from the edge of a field, are not fully adjusted to the new surface. Any visible difference in plant growth along the border of a field is evidence of inadequate field size for measuring PET within the meaning of the phrase "extended surface" (Rosenberg, 1974, p. 172).

Second, let us look at the influence of crop height. Many of the important crops grown worldwide are not short: corn, sorghum, winter and spring grains, cotton, and trees. The taller the crop, the more effective is its exchange of energy with the ambient air. Alfalfa (called lucerne in England) should fit the definition of a "short crop", but studies have shown that the quantities of water evaporated by this crop increase with increasing crop height (Figure 28.1). We know also that the type of leaf influences the ET rate and that, all things being equal, broad-leaved plants will transpire more than the grasses (Rosenberg, 1974, p. 172).

Third, let us look at the influence of crop cover. Row crops do not normally shade the ground fully except in some cases at advanced stages in their development. Nor do the broadcasted crops such as alfalfa shade the ground for some time after periodic cuttings. We know that water use may continue to increase with increasing leaf area, even when leaf area great enough to shade the ground completely has been achieved. Brun et al. (1972), for example, showed that in soybean and sorghum fields the

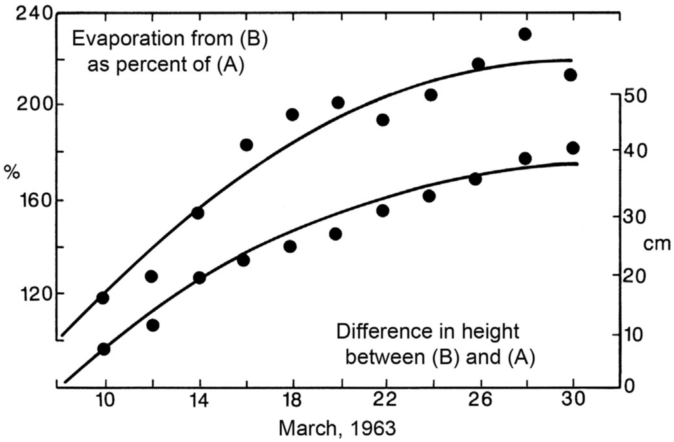

**FIGURE 28.1** Evapotranspiration from lysimeters, with similar exposures, but where crop of alfalfa (lucerne) was kept clipped short in one (A), but allowed to grow in height in other (B). Evaporation rates from (B) increased to more than double those from (A) as crop in (B) grew to 42 cm higher than in (A). Both lysimeters were surrounded by areas of alfalfa of similar heights to crops growing in them. *From Chang (1968), Figure 81. Reproduced by permission of Dr Jen-Hu Chang.*

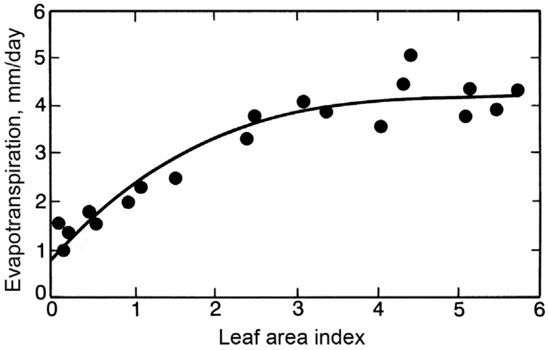

**FIGURE 28.2** Relationship between leaf area index and evapotranspiration. *From Chang (1968), Figure 71, p. 130. Reproduced by permission of Dr Jen-Hu Chang.*

proportion of water lost, as transpiration increases, is closely correlated to leaf area index, with transpiration being approximately 50% of the total ET at a leaf area index of two. This proportion increases to 95% of the total ET at a leaf area index of four. [*Leaf area index* is defined as the area of leaves above a unit area of ground taking only one side of each leaf into account (Monteith, 1973, p. 52).] Figures 28.2 and 28.3 show relationships between ET and leaf area index (Chang, 1968, p. 130; Ritchie, 1972).

Fourth, let us look at the influence of the internal plant resistance to water flow. The concept of PET assumes that plants behave passively as wicks for the transport of water from the soil to the air. However, plants can close their stomata and increase the resistance to water flow. Under well-watered conditions, some plants appear to have low resistances.

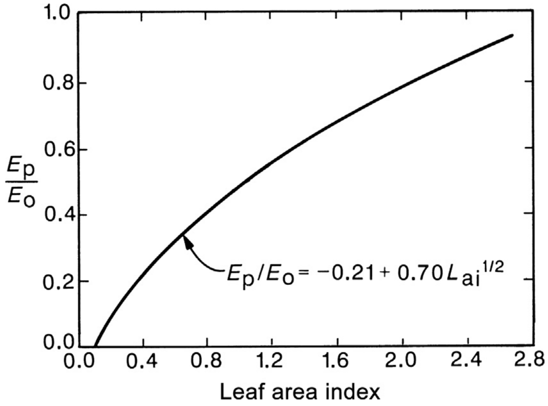

**FIGURE 28.3** The plant evaporation, $E_p$, relative to the potential evaporation, $E_o$, as influenced by leaf area index, when the soil-water is not limited. *From Ritchie (1972), American Geophysical Union. Reproduced by permission of American Geophysical Union.*

Alfalfa is one of these plants. Cold weather, however, has an interesting effect on the resistance of the alfalfa crop, as shown in Figures 28.4 and 28.5 for two days, April 21 and 22, respectively. Evapotranspiraton (LE) was greatly reduced on April 22 (Figure 28.5) after a cold night. Thus, even if alfalfa is well watered, its stomata appear to close when temperatures fall (Rosenberg, 1974).

Fifth, let us look at the influence of soil-water availability. Obviously, in the case of range-land and dry-land agriculture, plants are not always well supplied with water. This can be the case in irrigated agriculture also, inadvertently or by intention. When the water supply becomes limited, it

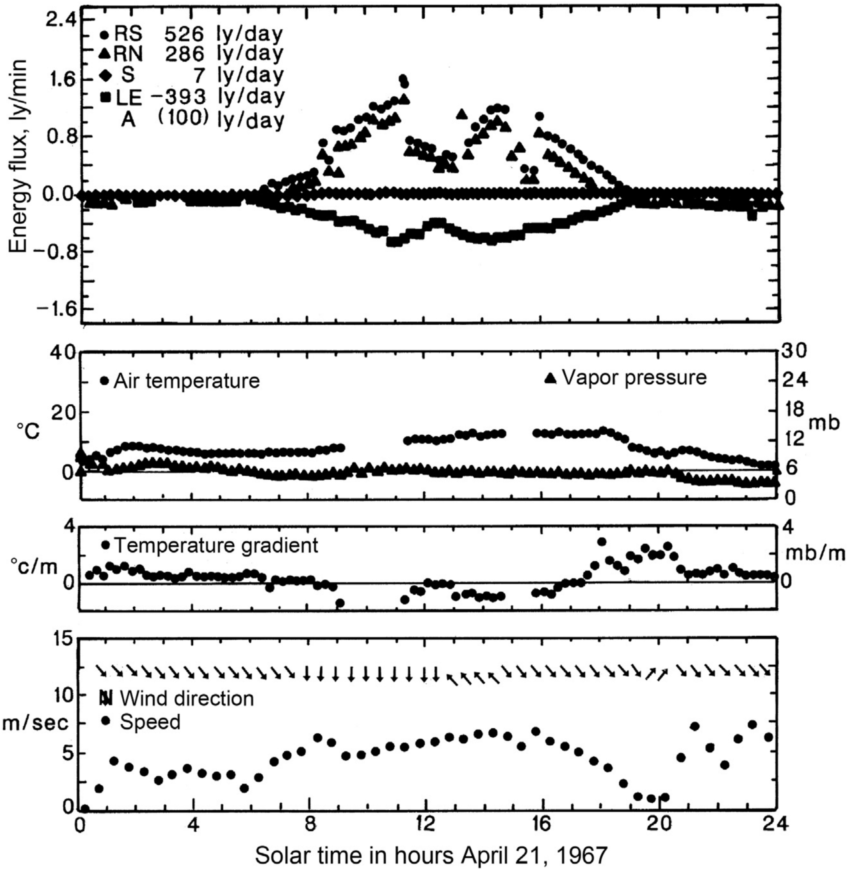

**FIGURE 28.4** Energy balance with lysimetrically measured evapotranspiration from alfalfa at Mead, Nebraska, April 21, 1967. Air temperature and vapor pressure measured at 100 cm; gradients between 45 and 100 cm; wind speed at 200 cm. RS = solar radiation; RN = net radiation; S = soil heat flux; LE = evaporation; A = sensible heat flux. *From Rosenberg (1974), p. 174. This material is used by permission of John Wiley & Sons, Inc.*

is important to get the greatest yield per unit of water expended. For this reason, water is often added at critical stages of growth. Most annual crops are especially sensitive to water shortage from the time of flower initiation, during flowering, and to a lesser extent, during fruit and seed development (Salter and Goode, 1967, p. 192). We know that strategic irrigation at certain periods in the growth cycle of a crop, such an anthesis, may lead to great increases in yield.

The definition of PET states that the crop is "well supplied with water". Therefore, with decreasing soil moisture availability, ET will be reduced below the potential (Figures 28.6, 28.7, 28.8, 28.9, and 28.10).

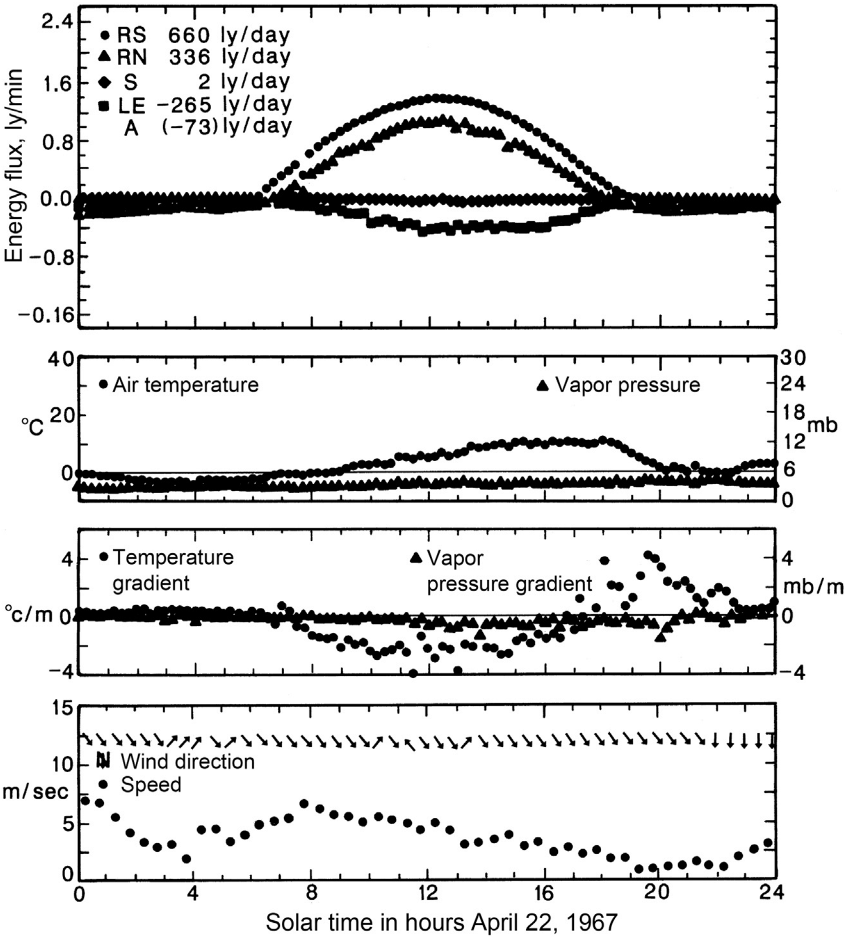

**FIGURE 28.5** Same as Figure 28.4 except for April 22, 1967. *From Rosenberg (1974), p. 175. This material is used by permission of John Wiley & Sons, Inc.*

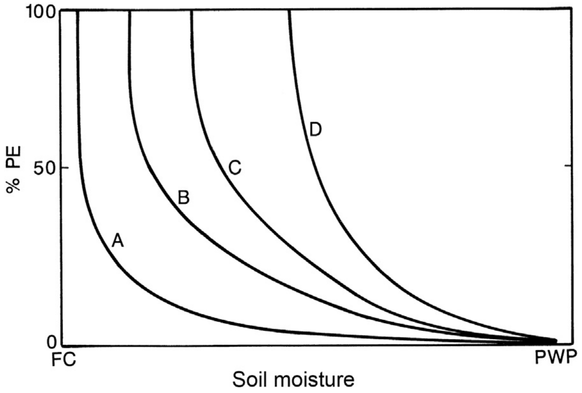

**FIGURE 28.6** Adjustment of potential evapotranspiration for soil dryness and rooting depth of crops. Curves A to D correspond to increases in rooting depth of crop. FC = field capacity; PWP = permanent wilting point. *From Chang (1968), Figure 79, p. 139. Reproduced by permission of Dr Jen-Hu Chang.*

van Bavel (1967) suggested that the transpiration rate in alfalfa begins to diminish after a soil-water potential of about −4 bars is reached and cites other works in which this breaking point has ranged from −0.2 to −10 bars for corn and cotton, respectively. Ritchie (1972) said that the evaporation from the soil surface is a two-stage process. The first stage is the constant-rate stage in which the evaporation is limited only by the supply of energy to the surface of the soil. The second stage is the falling-rate stage in which water movement to the evaporating sites near the surface is controlled by the hydraulic properties of the soil.

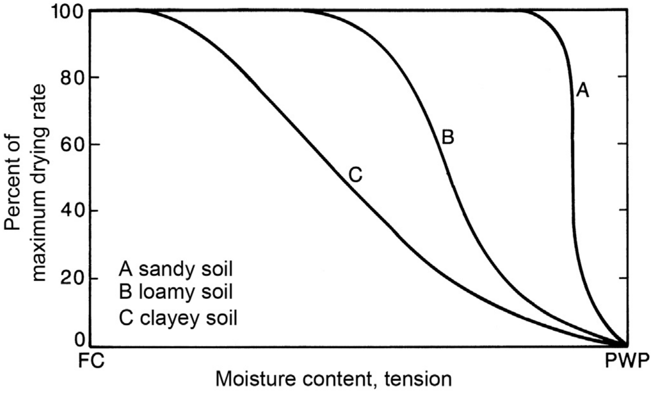

**FIGURE 28.7** Drying rate of three types of soil. FC = field capacity; PWP = permanent wilting point. *From Chang (1968), Figure 78, p. 13. Reproduced by permission of Dr Jen-Hu Chang.*

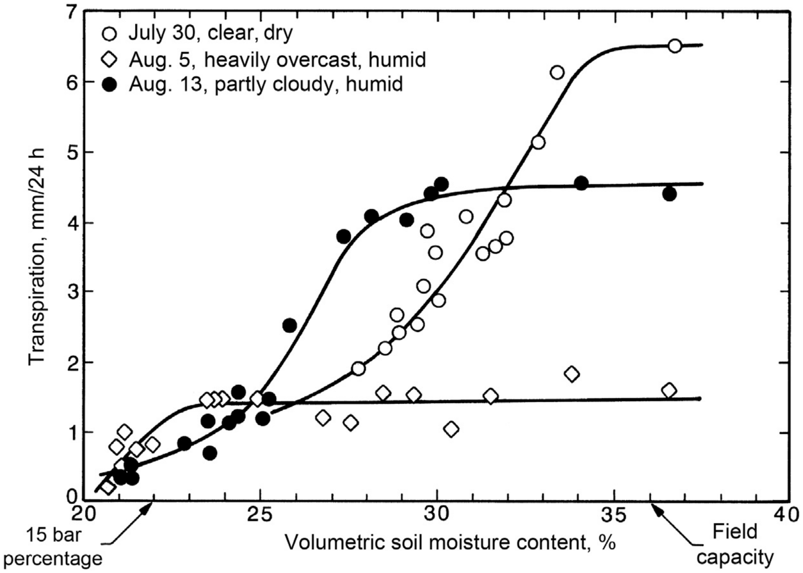

**FIGURE 28.8** Actual transpiration rate as a function of soil moisture content. *From Chang (1968), Figure 75, p. 136. Reproduced by permission of Dr Jen-Hu Chang.*

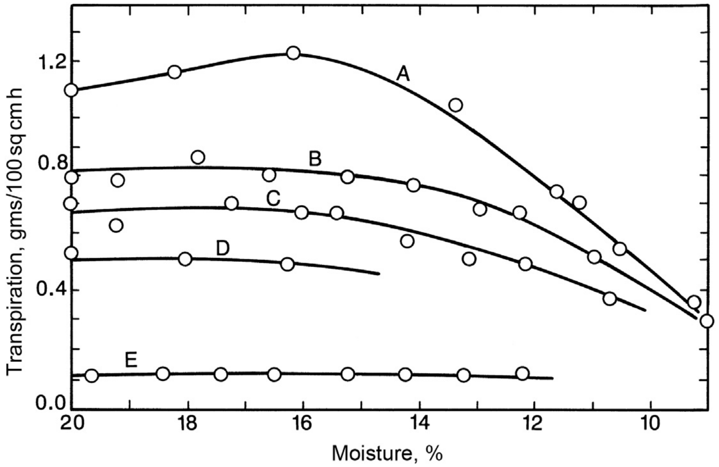

**FIGURE 28.9** The transpiration of kidney beans in grams 100 cm$^2$/h versus the moisture percentage of the soil at various light intensities at a temperature of 20 °C and a relative humidity of 40%. A: light intensity $4.5 \times 10^4$ erg/cm$^2$/s; B: 2.4; C: 1.4; D: 0.66; E: results from Veihmeyer and Hendrickson (undated). *Data from Bierhuizen (1958), Chang (1968), Figure 74, p. 135. Reproduced by permission of Dr Jen-Hu Chang.*

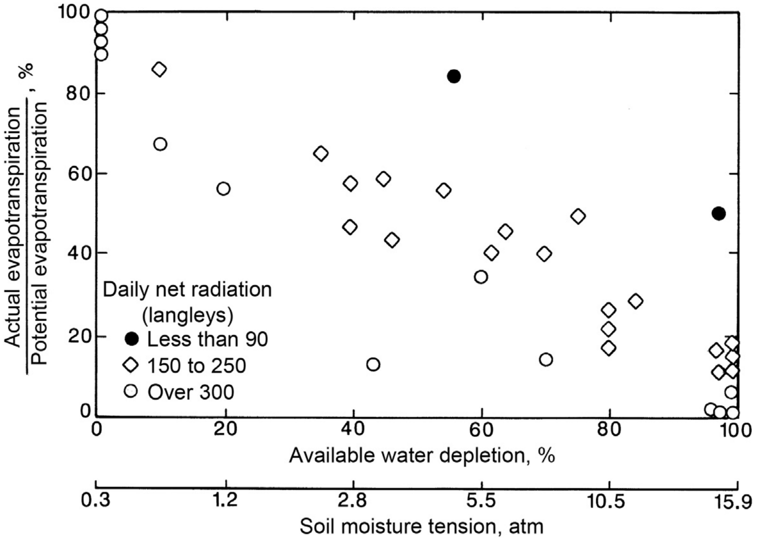

**FIGURE 28.10** Relative daily actual evapotranspiration rate from short grass as function of moisture depletion from the root zone and soil moisture tension averaged over the total root depth. *From Chang (1968), Figure 76, p. 137. Reproduced by permission of Dr Jen-Hu Chang.*

These studies relating soil-water to ET show that the potential rate of ET cannot prevail unless the soil is kept well supplied with water.

Sixth, let us look at the relation of free water evaporation and plant water use (Rosenberg, 1974, p. 176). The condition that PET cannot exceed free water evaporation under the same weather conditions probably applies well in humid regions. For example, the amount of water used by rye and fescue grass is about 80% of that evaporated from open water in evaporation pans, except when winds are strong and the air is hot and dry. Then the ratio drops, apparently because hot and dry conditions cause an increase in stomatal resistance.

However, in the Great Plains of the United States and in yet more arid regions, well-watered crops that exert little canopy resistance and that are tall or aerodynamically rough can consume more energy and transpire more water than is evaporated from free water surfaces. If the free water surfaces are extensive and the crop areas are not, the differences may be pronounced. A case in point occurred during the period of strong regional advection of sensible heat into eastern Nebraska during May, 1967 (Rosenberg, 1974, p. 177). Evaporation from evaporation pans with land exposures and with lake exposures showed lower daily evaporation than was measured with precision weighing lysimeters in an irrigated alfalfa field (Table 28.1). The data in Table 28.1, and other data, show that free water evaporation need not always show the upper limit or the PET in

**TABLE 28.1** Lysimetrically Measured Alfalfa Evapotranspiration (ET) Compared with Pan Evaporation in Nebraska

| Location | May 17–22, 1967 (5 days Total) Alfalfa about 25 cm Tall (mm) |
|---|---|
| Alfalfa in lysimeters at Mead, Nebraska | 51.91 |
| Alfalfa ET due to advection | 19.10 |
| Land exposure pans | 45.66 |
| Lake exposure pans | 36.08 |

*Data extracted from Rosenberg, 1974, p. 177.*

subhumid and arid regions as it does, apparently, in humid regions (Rosenberg, 1974, p. 178).

## 28.3 ADVECTION

In the preceding paragraph, we used the term *advection*. Advection is defined as the exchange of energy, moisture, or momentum as a result of horizontal heterogeneity (Chang, 1968, p. 140). If an area upwind of an irrigated field is hot and dry, then sensible (measurable) heat will be transferred to the irrigated field and its ET rate will be increased. However, if the advected air is colder than the vegetation, then the ET rate will be relatively low. Advection is a serious problem in arid and semiarid climates.

Advected energy involves the *clothesline effect* (Chang, 1968, p. 140). When warm air blows through a small plot with little or no guard area, a severe horizontal heat transfer occurs. The clothesline effect represents either the experimental bias because of the small size of the field or the border conditions unrepresentative of the large field as a whole. The clothesline effect cannot be tolerated in agronomic or climatological investigations. Where advection is important, plant growth may be improved by having larger irrigated fields to minimize the clothesline effect.

Advected energy also involves an *oasis effect* (Chang, 1968, p. 140). Inside a large field, the vertical energy transfer from the air above to the crop is called the oasis effect. The oasis effect must be reckoned with as a climatic characteristic, because it affects the ET rates many kilometers into an irrigated field (unlike the clothesline effect).

## 28.4 EXAMPLE CALCULATION TO DETERMINE POTENTIAL EVAPOTRANSPIRATION

Let us now follow an easy method developed by Kanemasu (1977) that we can use to estimate PET. Farmers who irrigate need to know how much moisture is being used by their crops. By estimating PET, they can tell the amount of water lost by plants. As we have said, PET is evaporation from a wet surface. It is limited by the energy that the surface can absorb. The more energy it absorbs, the higher the evaporation is. So evaporation is much higher on a sunny day than on a cloudy day, and PET depends primarily on the energy from the sun. Various methods of estimating PET require data on solar radiation, temperature, humidity, and wind speed. [We will not discuss the various methods used to measure ET, but the interested reader is referred to the following publications for a discussion of methods: Rose (1966, pp. 78–87); Slatyer (1967, pp. 56–64); Tanner (1967); Rosenberg (1974, pp. 159–205); Kanemasu et al. (1979); and Allen et al. (1998), who use the term "reference evapotranspiration" instead of potential evapotranspiration. Reference evapotranspiration is more specifically defined than PET. It is in reference to a particular surface, which has a grass crop with an assumed height of 0.12 m, a fixed surface resistance of 70 s/m, and an albedo of 0.23. The reference surface closely resembles an extensive surface of a green, well-watered grass of uniform height, actively growing, and completely shading the ground. The fixed surface resistance of 70 s/m implies a moderately dry soil surface resulting from about a weekly irrigation frequency (Allen et al., 1998). Pereira et al. (1997) also define PET and reference evapotranspiration.] To estimate PET, Kanemasu (1977) chose the Priestley–Taylor method, because it requires relatively easy-to-obtain information (solar radiation and average temperature).

Figures 28.11 and 28.12 show the relationship between the daily solar radiation and daily PET at various mean temperatures. In Kansas, solar radiation on a clear summer day would typically be about 650 cal/cm$^2$/day; on a cloudy day, it would be about 450 cal/cm$^2$/day; and, on an overcast day, it would be about 150 cal/cm$^2$/day.

*Example calculation*: Suppose that one wanted to know the PET for corn in Kansas. The solar radiation is 600 cal/cm$^2$/day; maximum temperature is 30 °C (86 °F); and minimum temperature is 25 °C (77 °F). One would calculate the average temperature as $(30 + 25)/2 = 27.5$ °C (81.5 °F). One then looks at Figure 28.11 (for wheat and corn) and selects the appropriate point between the 30 and 20 °C lines. The PET value is about 0.24 inch of water per day (0.61 cm/day). If maximum and minimum temperatures are not available, one can use the noon temperature.

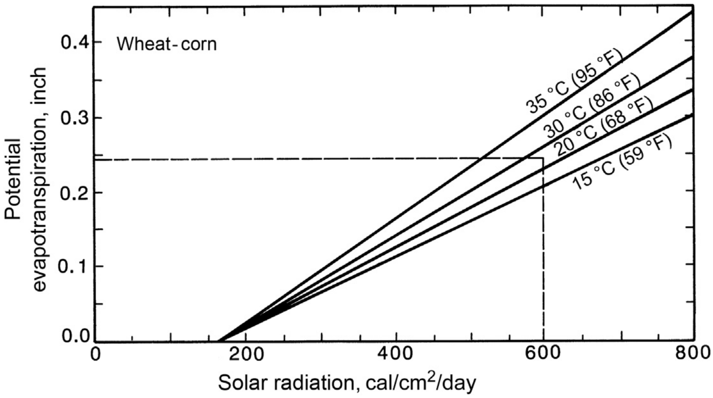

**FIGURE 28.11** Potential evapotranspiration for winter wheat and corn as a function of solar radiation and mean temperature. 1 inch = 2.54 cm. *From Kanemasu (1977). Reproduced by permission of the Publications Coordinator, Department of Communications, College of Agriculture, Kansas State University.*

Under a full crop cover and when water is not limiting (plants are not severely stressed), actual ET and PET are approximately equal (Kanemasu, 1977). Therefore, under normal cropping conditions, ET would equal PET for an extended period during the summer, for example, from pretasseling to blister stages in corn. Under situations of little crop cover (e.g., poor stand development, early and late in the growing season), actual ET can be less than PET. Then, evaporation from the soil surface is important.

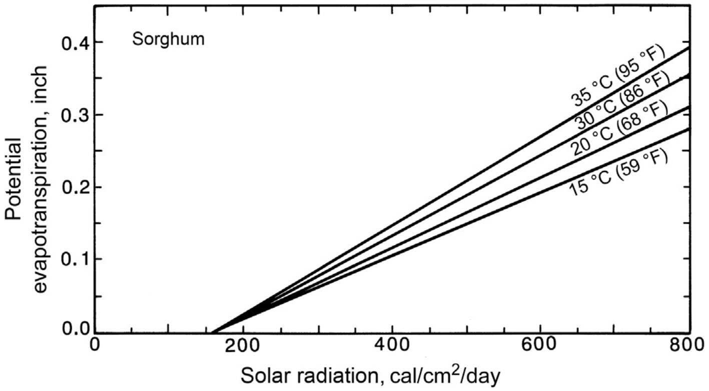

**FIGURE 28.12** Potential evapotranspiration for sorghum as a function of solar radiation and mean temperature. 1 inch = 2.54 cm. *From Kanemasu (1977). Reproduced by permission of the Publications Coordinator, Department of Communications, College of Agriculture, Kansas State University.*

Although the procedure outlined by Kanemasu (1977) gives only an approximation of daily PET, it allows quick estimates of daily water loss from several crops during a major portion of their growing season when irrigation is often necessary to avoid stress. To maintain the root zone at optimum soil-water content, ET losses must be matched by rain or irrigation. In Kansas, for example, a 2 inch (5 cm) irrigation on corn can be used up in eight hot days (8 × 0.25 inches = 2 inches). Thus, it is important to estimate the amount of water lost by ET, to know when to irrigate.

## 28.5 APPENDIX: BIOGRAPHY OF HOWARD PENMAN

Howard Latimer Penman (1909—1984), an English agricultural physicist, was born in 1909 at Dunston-on-Tyne in County Durham. He was raised in modest circumstances and was the son of a master carpenter employed by a shipbuilding company in Tyneside, a coastal area in northeast England (Ratcliffe, 1994). Because of his outstanding ability and interest in science, he qualified for a first-class honors degree in physics at Armstrong College, then part of Durham University (which is now called the University of Newcastle on Tyne), where he did his earliest research (van Bavel, 1985). Later, he was awarded an M.S, in physics for research concerning the absorption of sound by porous bodies. For his PhD research, done at Durham University, he studied the temperature dependence of the dispersion of sound in gases (Ratcliffe, 1994). In 1937, he took a position in the Physics Department of the Rothamsted Experimental Station, where he remained until his retirement in 1974, with a three-year interruption during the war to work with the Admiralty (van Bavel, 1985). His work during the war was with the Mine Design Department, and he measured the output of sound from ships and submarines to aid in the development of acoustic mines. He had distinguished physicists working with him during the war, including Francis H.C. Crick, who won the Nobel Prize in 1962. In 1944, he returned to Rothamsted, where he published his classic paper "Natural evaporation from open water, bare soil and grass" (1948). He was head of the physics department at Rothamsted Experimental Station from 1954 to 1974 and was president of the Royal Meteorological Society from 1961 to 1963 (Royal Meteorological Society, 1985). The Royal Meteorological Society awarded him the Darton Prize in 1952 for his paper on "Evaporation over the British Isles" and in 1966 he was awarded the Hugh Robert Mill Prize for work on "The water balance of the earth's surface and its practical application to agriculture". He was elected Fellow of the Royal Society and awarded the Officer of the Order of the British Empire (OBE) in 1962. He was a founding member of the British Soil Science Society (Ratcliffe, 1994). He and his wife had no children.

Internationally known among soil scientists, agricultural meteorologists, and hydrologists for his classic work on evaporation under natural conditions, he did equally innovative research on the movement of gases and vapors in soil, and, in cooperation with R.K. Schofield, on diffusive gas exchange by plant leaves (van Bavel, 1985). This last work is less well known, but it anticipated by decades later work by others that clarified the linkage between plant transpiration and photosynthesis through the stomatal mechanism. Algorithms now used in models of crop growth and water use differ little from the original equations given by Penman and Schofield.

Penman's writings on the relation between evaporation from agricultural lands and atmospheric conditions established his wide reputation, and he had scientific contacts on every continent. He was unremittingly dedicated to the idea that physics had a significant contribution to make in agriculture (van Bavel, 1985). In public, he was a stern lecturer and acrimonious debater, but, on the personal level he was a kind, gentle, and helpful person. His interests included gardening and music. He was passionate about music and was a faithful member of choral groups in London. It was his habit to take the train after work into the city, rehearse all night, and then return around midnight to his home in Harpenden. He died on October 13, 1984, at St. Alban's City Hospital after a brief illness (van Bavel, 1985).

## References

Allen, R.G., Pereira, L.S., Raes, D., Smith, M., 1998. Crop Evapotranspiration. Guidelines for Computing Crop Water Requirements. FAO Irrigation and Drainage Paper 56. Food and Agriculture Organization of the United Nations, Rome.

Bierhuizen, J.F., 1958. Some observations on the relation between transpiration and soil moisture. Neth. J. Agr. Sci. 6, 94–98.

Brun, L.J., Kanemasu, E.T., Powers, W.L., 1972. Evapotranspiration from soybean and sorghum fields. Agron. J. 64, 145–148.

Chang, J.-H., 1968. Climate and Agriculture. An Ecological Survey. Aldine, Chicago.

Kanemasu, E.T., 1977. An Easy Method of Estimating Potential Evapotranspiration. Keeping up with Research. No. 30. Kansas Agricultural Experiment Station, Manhattan, Kansas.

Kanemasu, E.T., Wesely, M.L., Hicks, B.B., Gerber, J.F., 1979. Techniques for calculating energy and mass fluxes. In: Barfield, B.J., Gerber, J.F. (Eds.), Modification of the Aerial Environment of Plants. American Society of Agricultural Engineering, St. Joseph, Michigan, pp. 156–182.

Monteith, J.L., 1973. Principles of Environmental Physics. American Elsevier, New York.

Penman, H.L., 1948. Natural evaporation from open water, bare soil and grass. Proc. Roy. Soc. A193, 120–145.

Pereira, A.R., Villa Nova, N.A., Sediyama, G.C., 1997. Evapo(transpir)ração. Fundação de Estudos Agrários Luiz de Queiroz (FEALQ), Piracicaba, Brazil (in Portuguese).

Ratcliffe, R.A.S., 1994. Pen portraits of presidents—Howard penman, MSc, PhD, OBE, FRS. Weather 49, 425–427.

Ritchie, J.T., 1972. Model for predicting evaporation from a row crop with incomplete cover. Water Resour. Res. 8, 1204–1213.

Rose, C.W., 1966. Agricultural Physics. Pergamon Press, Oxford.

Rosenberg, N.J., 1974. Microclimate: The Biological Environment. Wiley, New York.

Royal Meteorological Society, 1985. Howard Penman, OBE, FRS. Weather 40 (3), 97.

Salter, P.J., Goode, J.E., 1967. Crop Responses to Water at Different Stages of Growth. Res. Rev. No. 2. Commonwealth Bureau of Horticulture and Plantation Crops, East Malling, Maidstone, Kent. Commonwealth Agricultural Bureaux, Farnham Royal, Bucks, England.

Slatyer, R.O., 1967. Plant–Water Relationships. Academic Press, London.

Soil Science Society of America, 2008. Glossary of Soil Science Terms. Soil Science Society of America, Madison, Wisconsin.

Tanner, C.B., 1967. Measurement of evapotranspiration. In: Hagan, R.M., Haise, H.R., Edminster, T.W. (Eds.), Irrigation of Agricultural Lands. American Society of Agronomy, Madison, Wisconsin, pp. 534–574.

Thornthwaite, C.W., 1948. An approach toward a rational classification of climate. Geogr. Rev. 38, 55–94.

van Bavel, C.H.M., 1967. Changes in canopy resistance to water loss from alfalfa induced by soil water depletion. Agr. Meteorol. 4, 165–176.

van Bavel, C.H.M., 1985. In memoriam. H.L. Penman. Soil. Sci. 139, 385–386.

CHAPTER

# 29

# Water and Yield

In this chapter we look at water and yield and, in particular, the relationship between evaporation (or transpiration) and yield. If we could develop a reasonably simple relation (equation), we could predict the effect of water deficits on field yields, a desirable goal. To assess the relation between water and yield, Tanner and Sinclair (1983, pp. 7–11) looked at five different analyses done by the following investigators: de Wit (1958); Arkley (1963); Bierhuizen and Slatyer (1965); Stewart (1972); and Hanks (1974). Here we present only de Wit's analysis, the earliest one and basis for subsequent work. (For a biography of de Wit, see the Appendix, Section 29.7.) We consider water-use efficiency, which is defined as the "biomass production per unit cropped area for a unit of water evaporated and transpired (*ET*) from the same area" (Tanner and Sinclair, 1983; p. 2). Water-use efficiency can be based on either the evapotranspiration (*ET*), called the *ET* efficiency, or on the crop transpiration, called the *T* efficiency. The difference is important because suppression of soil evaporation and prevention of weed transpiration can improve the *ET* efficiency, but it need not improve the *T* efficiency. These two water-use efficiencies may be based on either the total dry matter production or the marketable yield, and the yield base should be given.

## 29.1 DE WIT'S ANALYSIS

de Wit (1958) showed that for dry, high-radiation climates, yield and transpiration were related as

$$Y/T = m/T_{\max}, \tag{29.1}$$

where $Y$ = total dry matter mass per area, $T$ = total transpiration per area during growth to harvest, and $T_{\max}$ = mean daily free water evaporation

http://dx.doi.org/10.1016/B978-0-12-420022-7.00029-X
Copyright © 2014 Elsevier Inc. All rights reserved.

for the same period. The constant $m$ is related to the WR/pan used by Briggs and Shantz (1917) ($1/m \simeq$ WR/pan) where WR = water requirement. de Wit showed that $m$ was governed mainly by species and, for a first approximation, it was independent of soil nutrition and water availability unless there was a serious nutrition deficiency or unless soil water was too high (e.g., due to inadequate aeration).

de Wit proposed that this relation should hold until $T$ approaches a maximum production governed by the growing conditions. The relation in Eqn (29.1) could be simplified for humid regions because, when water was not limiting, fluctuations in intercepted radiation, although reflected in transpiration and growth, would not affect appreciably the ratio $T/T_{\mathrm{max}}$. de Wit found under these conditions that

$$Y/T = n, \qquad (29.2)$$

where $n$ is a constant, gave a better description than does Eqn (29.1).

The value of $m$ in Eqn (29.1) can be approximated with Eqn (29.3) from water-use efficiency and mean daily pan evaporation ($E_{\mathrm{pan}}$):

$$m = (Y/T)E_{\mathrm{pan}}. \qquad (29.3)$$

In the Great Plains of the United States, de Wit (1958) found, using data of Briggs and Shantz and a number of other sources, that $m$ was equal to 55, 115, and 207 kg/ha/day for Grimm alfalfa, Kubanka wheat, and Red Amber sorghum, respectively (Tanner and Sinclair, 1983; pp. 8–9) [or 5.5, 11.5, and 20.7 g dry matter per kilogram water per day, respectively (Chang, 1968; p. 128)]. In the Netherlands, the value for $n$ for beets, peas, and oats was 6.1, 3.4, and 2.6 g per kilogram water per day, respectively (Chang, 1968; p. 128). The value of $m$ and $n$ are more dependent on the climatic conditions than on the nutrient level of the soil and the availability of water, provided that the nutrient level is not too low and the availability of water is not too high. These values are also independent of the degrees of mutual shading, if the leaf mass is not too dense. Where these conditions are not fulfilled, the $m$ and $n$ values are larger (Chang, 1968; p. 128).

Table 29.1 compares the values of $m$ derived from the experiments of Briggs and Shantz (1914) and subsequent field observations (Tanner and Sinclair, 1983; p. 8). In Table 29.1, the $m$'s developed from the data of Briggs and Shantz (1914) and Hanks et al. (1969) do not include root dry matter, whereas an estimate of root yield was made for the other data. Also, pan evaporation was used directly with no correction to free water evaporation, as made by de Wit. [According to LeGrand and Myers (1976), readings taken of pan evaporation tell how much water evaporates from lakes, if one applies a pan coefficient of about 0.70.]

Except for the Wisconsin data, corn, sorghum, and millet give the highest values of $m$, followed by the grain cereals, potatoes, and then the

**TABLE 29.1** Experimental Estimates of $m$ (kg/ha/d) From Data of Briggs and Shantz (1914) and Subsequent Field Experiments

| Crop | Briggs and Shantz | Subsequent Field Data | Source |
|---|---|---|---|
| Corn | 213 ± 14 | 215 ± 20 | UT, Stewart et al. (1977) |
| | | 258 ± 1 | CO, Stewart et al. (1977) |
| | | 262 ± 46 | AZ, Stewart et al. (1977) |
| | | 314 ± 12 | CA, Stewart et al. (1977) |
| Grain sorghum | 240 ± 10 | 141 ± 6 | Great Plains, Hanks et al. (1969) |
| Millet | 260 ± 35 | 150 ± 18 | Great Plains, Hanks et al. (1969) |
| Wheat | 158 ± 10 | 125 ± 15 | Great Plains, Hanks et al. (1969) |
| Potato | 160 ± 8 | 217 ± 24 | WI, Tanner, 1976 (unpublished) |
| Alfalfa | 90 ± 11 | 214 ± 26 | WI, Tanner, 1977 (unpublished) |
| Soybean | 102 ± 7 | 128 ± 34 | KS, Teare et al. (1973) |

*From Tanner and Sinclair (1983). Reprinted by permission of the American Society of Agronomy, Crop Science Society of America, and Soil Science Society of America.*

legumes. The data for corn indicate a high level of variability in $m$, even though the corn crops were subjected to nearly the same experimental treatments. The high $m$ for potato and alfalfa in Wisconsin may indicate that Eqn (29.2) rather than Eqn (29.1) is applicable to this humid region. If so, it is difficult to know whether to use Eqn (29.1) or Eqn (29.2), because gradations in humidity occur not only between locations, but also seasonally at one location. Table 29.1 also shows that there is no consistent improvement in $m$ between the crops grown in 1912–1913 (Briggs and Shantz, 1914) and more recently, excluding the Wisconsin data for the reasons discussed above. Thus, to the extent that $m$ is a measure of $T$ efficiency for total biomass production, it appears that there has been no increase in $T$ efficiency since Briggs and Shantz did their work at the beginning of the 1900s.

## 29.2 RELATIONSHIP BETWEEN YIELD AND TRANSPIRATION AND YIELD AND EVAPOTRANSPIRATION

Let us look at figures showing the relationship between yield and transpiration and yield and ET. Figures 29.1 and 29.2 show the relationship between yield and transpiration as determined by Arkley (1963), who used data from Briggs and Shantz (1913a). The classic work by Briggs and Shantz demonstrated a close relation between transpiration and dry matter production. That is, dry matter is decreased by water deficits. In their experiments, the linear relationship held for different varieties of oats (Figure 29.1) and barley (Figure 29.2).

For the same plant species, the efficiency of water use may vary according to the climate (Chang, 1968; p. 220). Stanhill (1960) compared measurements of pasture growth and potential ET at seven localities in

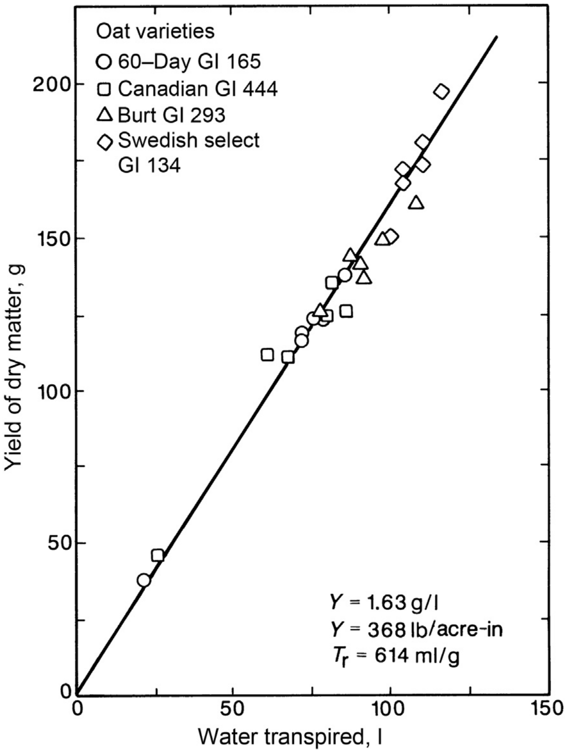

**FIGURE 29.1** Relationship between yield of dry matter and amount of water transpired by oat varieties. *Data obtained by Briggs and Shantz (1913a, 1913b) and shown by Arkley (1963). From Chang (1968), Figure 69, p. 126. Reproduced by permission of Dr Jen-Hu Chang.*

different parts of the world. In Figure 29.3, the cumulative measured dry-weight yields are plotted against cumulative measured transpiration. A linear relationship exists at each site, but the slope of the line changes with latitude. In general, the growth rate per unit of water used is higher at high latitudes. This is a result of the increased respiration rate in the tropics.

The relationship between ET and dry matter production may or may not be linear. This is partly because the fraction of evaporation that does not contribute to plant growth varies throughout the crop life cycle. Figures 29.4–29.6 show the relationship between yield and ET as determined by Allison et al. (1958) and Staple and Lehane (1954). Even when dry matter production does increase linearly with ET, the regression line seldom passes through the zero point. In other words, ET in the field might be appreciable when the yield is still zero (Chang, 1968; pp. 211–212). Allison et al. (1958) analyzed the yields of a number of crops grown in a lysimeter near Columbia, South Carolina, for a

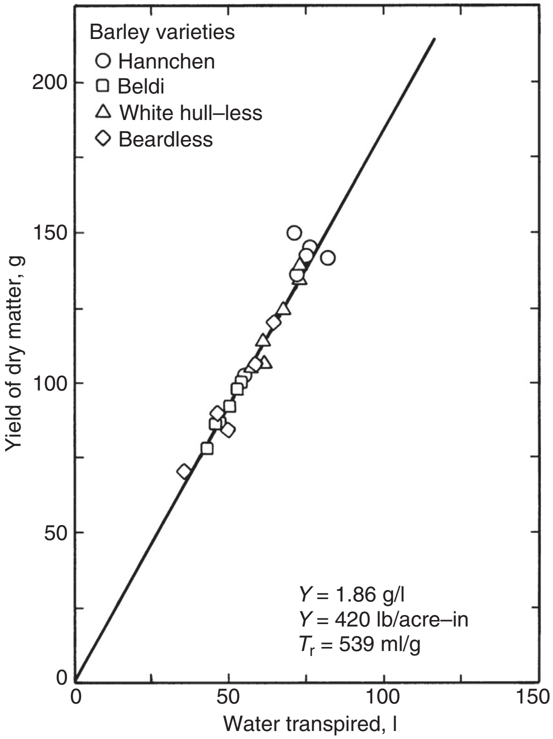

**FIGURE 29.2** Relationship between yield of dry matter and amount of water transpired by barley varieties. *Data obtained by Briggs and Shantz (1913a, 19193b) and shown by Arkley (1963). From Chang (1968), Figure 70, p. 127. Reproduced by permission of Dr Jen-Hu Chang.*

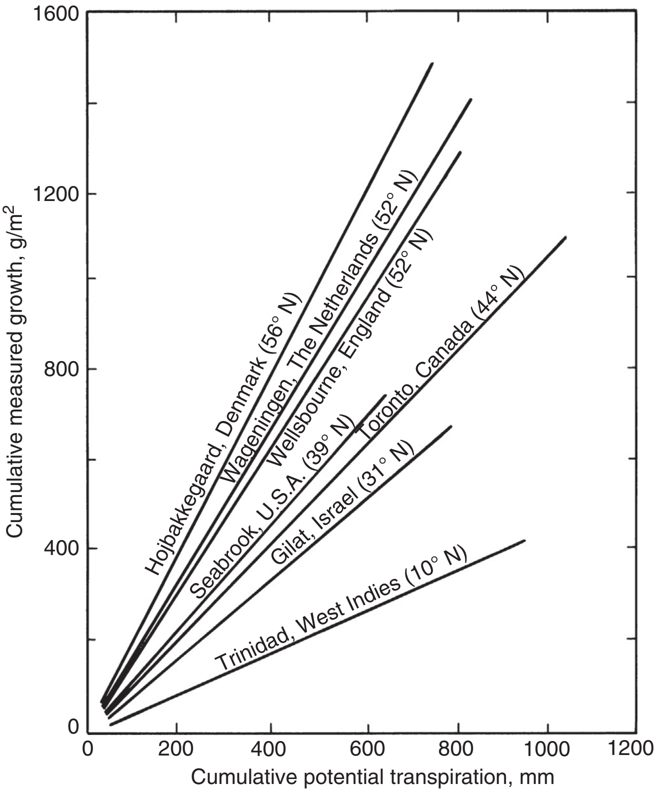

**FIGURE 29.3** Measurements of potential evapotranspiration and dry matter production from pastures. *Data of Stanhill (1960). From Chang (1968), Figure 114, p. 222. Reproduced by permission of Dr Jen-Hu Chang.*

period of more than 5 years. Their data indicated that the first 18 in (46 cm) of evapotranspired water was required to produce only enough for plant survival (Figure 29.4). The increase in dry matter was almost linear with increasing amounts of water used from 18 to 22 inches (46–56 cm). Staple and Lehane (1954) studied the use of water by spring wheat grown in tanks and in the open field in Swift Current, Canada. They reported that 4.9 in (12 cm) of water for tanks and 5.64 in (14 cm) for the field were necessary to establish the plants (Figures 29.5 and 29.6). Beyond this, the yield in the tanks increased nearly linearly. But in the field the yield increased curvilinearly. In either case, the maximum production potential was not realized because of the shortage of water.

Before concluding this section on the relationship between water and yield, let us briefly look at the situation of an individual leaf. Up to

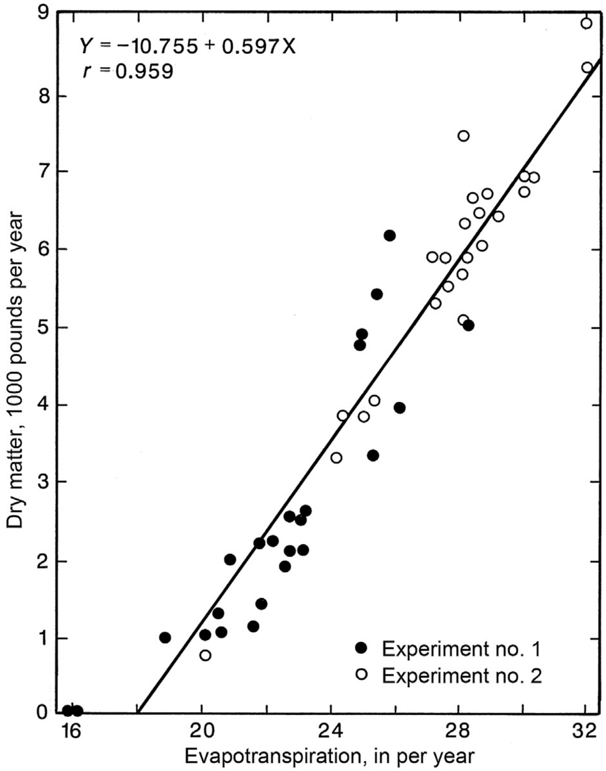

**FIGURE 29.4** Relationship between crop yields and water use. *Data of Allison et al. (1958). From Chang (1968), Figure 105, p. 212. Reproduced by permission of Dr Jen-Hu Chang.*

now, we have been considering groups of leaves as they might exist under field conditions. For a single leaf, the net assimilation, or net photosynthesis, increases with light intensity to the saturation point and then levels off. The transpiration rate will, however, increase linearly with radiation to a much higher intensity. Thus, the ratio between transpiration and photosynthesis will vary according to the radiation intensity in a manner postulated by de Wit (1958) (Figure 29.7). This same relationship was later quantitatively presented by Bierhuizen (1959) (Figure 29.8). The high ratio occurring at extremely low radiation intensity is because transpiration has some value, whereas photosynthesis first has to compensate for the respiration. This high ratio is of little significance because of the low rates of both processes. The lowest ratio is reached at a radiation intensity of 0.1—0.2 langleys per minute. Such low radiation intensities are observed only in the early morning and late afternoon. As the radiation intensity increases, beyond 0.2 langleys per minute, the ratio of transpiration to photosynthesis for a

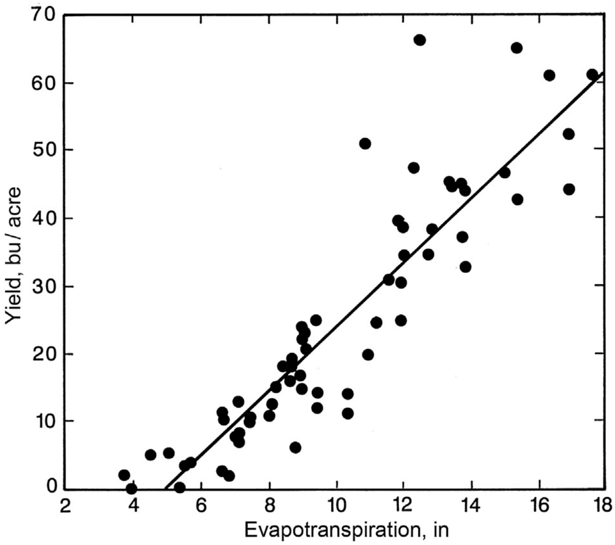

**FIGURE 29.5** Relationship between wheat yield and evapotranspiration in tanks, 1922–1952. *Data from Staple and Lehane (1954). From Chang (1968), Figure 106, p. 213. Reproduced by permission of Dr Jen-Hu Chang.*

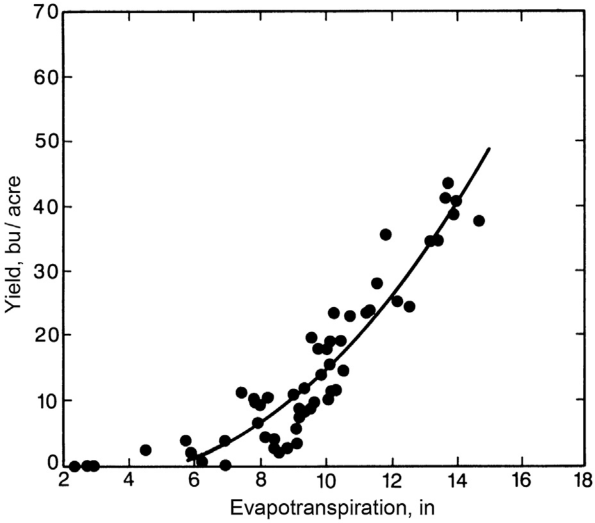

**FIGURE 29.6** Relationship between wheat yield and evapotranspiration on field plots. *Data from Staple and Lehane (1954). From Chang (1968), Figure 107, p. 213. Reproduced by permission of Dr Jen-Hu Chang.*

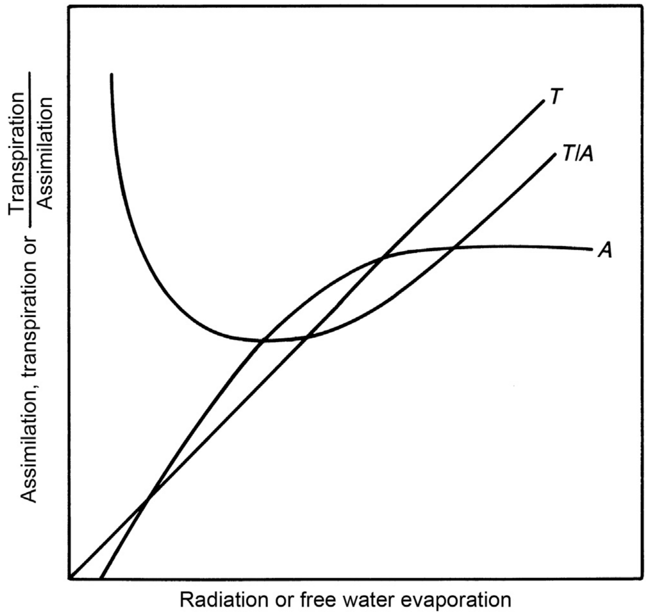

**FIGURE 29.7** Relationship between net assimilation (*A*), transpiration (*T*), and the transpiration to assimilation ratio ($T/A$) for leaves of plants as a function of the radiation or free water evaporation. *Figure from de Wit (1958). From Chang (1968), Figure 67, p. 124. Reproduced by permission of Dr Jen-Hu Chang.*

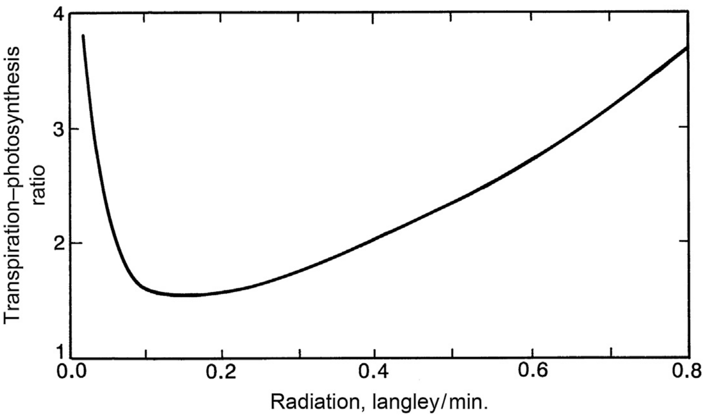

**FIGURE 29.8** Relationship between radiation and the transpiration–photosynthesis ratio. *Figure from Bierhuizen (1959). From Chang (1968), Figure 68, p. 124. Reproduced by permission of Dr Jen-Hu Chang.*

single leaf increases nearly linearly. Thus, for a single leaf, the efficiency of water use in the production of dry matter will be lower in areas of high radiation, such as in the arid tropics.

## 29.3 WATER AND MARKETABLE YIELD

In many instances, the reductions of yields of grain and other marketable parts of crops are roughly in proportion to the decreases in transpiration induced by water deficits (Tanner and Sinclair, 1983; p. 18). However, often there are stages of development, such as pollination, at which marketable yield may be extraordinarily affected. Figure 29.9 shows a generalized relation between yield and adequacy of water at different stages of growth. The curve was developed for sugar cane in Hawaii, but can be applied, in general, to other crops (Chang, 1968; pp. 214–215). Table 29.2 summarizes moisture-sensitive periods for selected crops during which a water deficit depresses the economic yield much more than at other periods (Chang, 1968; p. 216). Varieties (cultivars) may also respond differently under drought conditions. A drought-resistant variety may follow the upper broken curve in Figure 29.9, whereas a variety less resistant to drought may follow the lower broken curve.

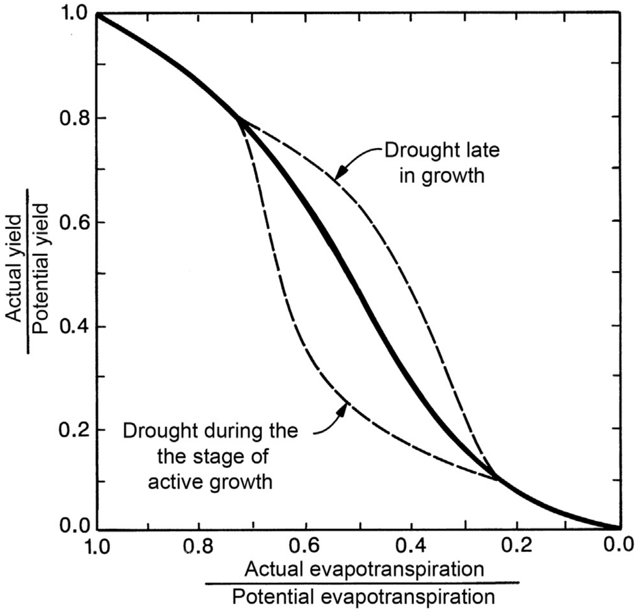

**FIGURE 29.9** Generalized relationship between yield and adequacy of water application. *From Chang (1968), Figure 108, p. 214. Reproduced by permission of Dr Jen-Hu Chang.*

**TABLE 29.2** Moisture-Sensitive Stages (from Chang, 1968, p. 216)

| **Crop** | **Critical Stage** |
|---|---|
| Cauliflower | No critical moisture-sensitive stage; frequent irrigation required from planting to harvest |
| Lettuce | Just before harvest when the ground cover is complete |
| Cabbage | During head formation and enlargement |
| Broccoli | During head formation and enlargement |
| Radishes and onions | During the period of root or bulb formation |
| Snap beans | During flowering and pod development |
| Peas | At the start of flowering and when the pods are swelling |
| Turnips | From the time when the size of the edible root increases rapidly until harvest |
| Potatoes | After the formation of tubers |
| Potatoes (White Rose) | From stolonization to the beginning of tuberization |
| Soybeans | Period of major vegetative growth and blooming |
| Oats | Commencement of ear emergence |
| Wheat | During heading and filling |
| Barley | Effects of water stress on grain yield and protein content shown to be greater at the early boot stage than at the soft dough stage, and shown to be greater at the soft dough stage than at the onset of tillering or ripening stages |
| Corn | Period of silking and ear growth |
| Cotton | At the beginning of flowering |
| Apricots | Period of floral bud development |
| Cherries and peaches | Period of rapid growth prior to maturity |
| Olives | Later stages of fruit maturity |

*Table reproduced with the permission of Dr J.-H. Chang.*

## 29.4 WATER AND QUALITY

We need to note also that water deficits may be necessary to increase the quality of a crop. So far, we have been concerned only with the relationship between water and dry matter (or marketable yield) production. The quality of an agricultural product, however, is not necessarily related to the yield. In analyzing the relationship between water and crop quality, one must differentiate between natural rainfall and controlled irrigation water. Rainfall usually is accompanied by high cloudiness and low radiation, but the application of irrigation water is not complicated by a change of unfavorable weather conditions.

The effects of irrigation on crop quality are summarized in Table 29.3 from Chang (1968, pp. 223–224). In general, adequate irrigation throughout periods of active vegetative growth results in an improvement in crop quality. However, during the ripening period, moderate moisture stress often has been found to be desirable, especially in the case of certain compounds such as rubber, sugar, and tobacco. For example, the rubber content of guayule is increased by a slight moisture stress. The withdrawal of irrigation water several weeks before harvest is a common practice in sugar cane culture. Late water stress also has been found to increase the sucrose concentration of sugar beets. The aroma of Turkish tobacco is improved by water stress late in the crop cycle. The flavor and taste of most fruits also can be enhanced by the same means (Chang, 1968; p. 224).

## 29.5 CROP WATER-USE EFFICIENCY

Here are a few final comments on crop water-use efficiency (Tanner and Sinclair, 1983; pp. 18–21). Experimentally, we need to do three things: (1) be able to distinguish transpiration (*T*) from evaporation (*E*) in studies of *ET*; (2) be able to make estimates of vapor pressure deficit (*VPD*) because data on yield and transpiration are normalized by using *VPD* to account for differences in years and locations; and (3) improve our understanding of dry matter partitioning into roots, shoots, and marketable yield.

When increased water-use efficiency is found as a result of improved management, the increases result from increased transpiration as a fraction of the *ET*. *ET* efficiency is increased, although *T* efficiency is changed little, if any (Tanner and Sinclair, 1983; p. 20). Conditions such as low fertility, water stress, plant disease, or insects that lower the leaf area so that the canopy is no longer closed will increase soil evaporation and thereby lower $Y/\mathrm{ET}$. Factors such as poor growing temperatures and extreme infertility can lower both $Y/T$ and $Y/\mathrm{ET}$. Nevertheless, a decrease

**TABLE 29.3** Effect of Irrigation on Crop Quality

| Crop | Effect |
|---|---|
| Pasture | Irrigation increased the protein and decreased the fat contents of the herbage but had little effect on the crude fiber and ash content. |
| Vegetables | Maintaining a low moisture stress during the whole growth period generally resulted in the highest yield and quality. |
| Snap beans | Irrigation decreased the percentage of pods that were badly crooked or severely malformed. Fibrous content of beans was generally reduced. |
| Sweet corn | Irrigation increased the number of marketable ears per plant, the average weight per ear and the gross yield of unhusked ears, and the percentage of usable corn cut from these ears for canning or freezing. |
| Soybeans | Irrigated soybeans had slightly lower oil content and slightly higher protein content. |
| Barley | Irrigation increased the yield of grain and improved malting quality, mainly by increasing extract. |
| Potatoes | Irrigation that gave good increase in yield of potatoes very seldom reduced the specific gravity and was more likely to increase it. |
| Tobacco | Irrigated tobacco had lower nicotine and protein, but higher carbohydrate content. |
| Fruits | Canned peaches that were tough and leathery in texture, pears that remained green and hard a week or more after the ripening season, prunes that were sunburned, and walnuts with partly filled shells were some of the results of a relatively long time without readily available moisture. |
| Olives | The higher yield obtained by irrigation was due to an increase in fruit size, rather than in the number of fruits. Irrigated groves had a higher oil content than unirrigated ones. |

*For references for the results, see Chang (1968, pp. 223—224). Table reproduced with the permission of Dr J.-H. Chang.*

in leaf area index has to be severe before substantial changes in $Y/T$ will be observed. Changes in ET efficiency occur more readily than changes in $T$ efficiency.

Changing plant architecture is not likely to change $T$ efficiency significantly in canopies achieving a leaf area index of about three. However, canopy structure and population can modify the loss due to evaporation relative to the loss due to transpiration, and, therefore, can affect ET efficiency more than $T$ efficiency. Crop breeding can change rates of maturation to take advantage of seasonal water availability and perhaps change rooting habits to increase soil water supply or change the timing of withdrawal. Such changes may aid in the efficient use of water and ET efficiency without changing the $T$ efficiency.

The crop can be managed (e.g., population and fertility) to increase or decrease leaf area index, thus changing the partitioning of $E$ and $T$ and ET efficiency. Preventing evaporation from the soil and transpiration from weeds also modifies the partitioning of $E$ and $T$. However, there is a limit to the improvement in water-use efficiency that such manipulations can provide. The ET efficiency can only approach the $T$ efficiency as the upper limit.

To summarize, it appears that there are two ways to modify the $T$ efficiency based on total dry matter of crops (Tanner and Sinclair, 1983; p. 20). First, crops can be grown in humid climates where the VPD is small and advection is minimal. However, in these regions, sunlight is usually less and total yields may be smaller. Second, the partitioning of total dry matter can be changed to create more marketable products. This would increase the $T$ efficiency of the marketable yield. This option means changing the chemistry of the plant. The changes would have to be large, and, consequently, are unlikely. Therefore, changing the $T$ efficiency of the marketable yield seems improbable. Tanner and Sinclair (1983, p. 25) conclude that transpiration efficiency is a relatively difficult to manipulate variable. Transpiration efficiencies of different crops have changed little since Briggs and Shantz did their work at the beginning of the 1900s. Even though the likelihood of large improvements in $T$ efficiency is small, crop water-use efficiency can be improved, as was noted in the preceding section (e.g., changing rooting habits, increasing leaf area index, minimizing soil evaporation, and preventing transpiration from weeds).

## 29.6 WATER-USE EFFICIENCY UNDER ELEVATED CARBON DIOXIDE

As noted by Tanner and Sinclair (1983), it is difficult to increase crop water-use efficiency unless there is a basic change in the chemistry of the plants. One way would be to change photosynthetic systems. Crops with the $C_4$ type of photosynthesis have a higher water-use efficiency than crops with the $C_3$ type of photosynthesis. This is due to two facts. First, under the same environmental conditions, $C_4$ plants keep their stomata more closed than $C_3$ plants, thereby losing less water than $C_3$ plants. Second, due to their efficient cycling of carbon dioxide in the plant, $C_4$ plants are more productive than $C_3$ plants. [For further discussion, see the following chapters in Kirkham (2011): Chapter 8 on stomatal conductance; Chapter 11 on water-use efficiency, and Chapter 12 on $C_3$ and $C_4$ plants.] Therefore, both biomass and water use are different in $C_4$ plants, and each contributes to increased water-use efficiency of $C_4$ plants compared to $C_3$ plants. But changing $C_3$ plants into $C_4$ plants has not been successful. $C_3$—$C_4$ intermediates do not show the whole spectrum of components of the $C_4$ pathway and have shown little or no advantages in terms of productivity (Kirkham, 2011; p. 112).

However, all plants, both $C_3$ and $C_4$, have increased productivity under elevated carbon dioxide, and all plants close their stomata when the carbon dioxide in the atmosphere is increased (Kirkham, 2011; p. 353). Therefore, as the carbon dioxide concentration in the atmosphere has increased, we are inadvertently increasing the water-use efficiency. We can calculate this increase in water-use efficiency. Let us look at the increase in water-use efficiency since 1958, when the carbon dioxide concentration in the atmosphere was first carefully measured (Kirkham, 2011; p. 1). In 1958, the carbon dioxide concentration in the atmosphere was 316 ppm. Based on data from experiments done with grain sorghum [*Sorghum bicolor* (L.) Moench] under different carbon dioxide concentrations (Kirkham, 2011; p. 234), we can calculate that in 2011, when the carbon dioxide concentration in the atmosphere was 390 ppm, it took 55 ml less water to produce a gram of sorghum grain than it did in 1958. We shall work in English units for our calculations, because producers in the United States use English units. However, our answer will be a percentage increase in water-use efficiency, which does not require knowledge of English units. We know that 1 bushel (abbreviated bu) of sorghum grain weighs 56 pounds. Let us consider the 55 ml/g: (55 ml/g) × (453.6 g/lb) × (56 lb/bu) = 1,397,088 ml/bu. Rounding and converting to liters we get 1397 l/bu. We convert this number to gallons (abbreviated gal) per bushel, as follows: (1397 l/bu) × (1 gal/3.8 lL) = 367 gal/bu. We remember this number, because we shall return to it. We know 1 acre = 43,560 ft$^2$. We divide this number by 12 in, and we get 3630 ft$^3$ of $H_2O$ per inch per acre. (Think of this as the equivalent of 1 in of water standing on 1 acre.) We know 1 ft$^3$ = 7.48 gal. This is given in textbooks or we can calculate it. Therefore, 1 in $H_2O$/acre = 27,152.4 gal. In Kansas, grain sorghum requires 22 in of ET (Loyd R. Stone, Department of Agronomy, Kansas State University, personal communication, April 1, 2013). The water can come from irrigation or rain.

We then multiply, as follows: 22 in × 27,152.4 gal = 597,352.8 gal to raise 22 in of ET. The average yield of grain sorghum in Kansas between the years 2000 and 2011 has been 62 bu/acre, so we get 9634.7 gal/bu. We return to the number we remembered from before (367 gal/bu) and then do the following division to get our water savings: (367 gal/bu)/(9634.7 gal/bu) = 0.038 savings ratio per bushel. Due to the increase in carbon dioxide, we saved 3.8% water to raise sorghum in 2011 compared to 1958. This water savings will increase as the carbon dioxide concentration in the atmosphere increases.

## 29.7 APPENDIX: BIOGRAPHY OF CORNELIUS DE WIT

Cornelius ("Kees") Teunis de Wit (1924–1993), professor at the Agricultural University, Wageningen, The Netherlands, was born east of Arnhem. His introduction to agriculture was while he worked as a farm laborer during World War II (Rabbinge, 1995). His thesis at Wageningen was notable for its theoretical nature and foreshadowed his founding of the department of theoretical production. Early in his career, he worked in Burma. Later, he developed strong ties with Mali, Israel, and the United States. In the 1950s, after writing his dissertation on fertilizer placement, he wrote classic monographs on competition, on the relation between transpiration and crop yields, and on the photosynthesis of leaf canopies. He calculated the population that the earth's photosynthesis could feed. In the 1960s and 1970s, de Wit and his colleagues at Wageningen took up the dynamic simulation of crop growth, incorporating biochemistry, development from seeds to grain, the soil and atmosphere around the crop, and its pests (American Society of Agronomy, 1994). His countrymen elected him a senator in the parliament of Gelderland, and, in The Hague during the 1980s, he served on the Netherlands Scientific Council for Governmental Policy. Afflicted by diabetes, he retired in February, 1989, and was honored by ceremonies attended by scientists from many countries. Undaunted, he continued to work and advised the Consultative Group on International Agricultural Research and suggested research that should be carried out on crops in different regions.

He was a Knight of the Order of The Netherlands Lion and Foreign Associate of the National Academy of Sciences of the United States. In 1984, he was cowinner, with Don Kirkham, of the Wolf Prize in agriculture; Kirkham was recognized for theoretical work and de Wit for development of numerical models. The citation read, "for their innovative contributions to the quantitative understanding of soil water and other environmental interactions influencing crop growth and yield".

de Wit and his wife had two children. He died at age 69 years on December 8, 1993 (American Society of Agronomy, 1994).

# References

Allison, F.E., Roller, E.M., Raney, W.A., 1958. Relationship between evapotranspiration and yields of crops grown in lysimeters receiving natural rainfall. Agron. J. 50, 506–511.

American Society of Agronomy, 1994. Deaths. Cornelius T. de Wit. Agronomy News. February issue. American Society of Agronomy, Madison, Wisconsin, p. 25.

Arkley, R.J., 1963. Relationships between plant growth and transpiration. Hilgardia 34, 559–584.

Bierhuizen, J.F., 1959. Plant growth and soil moisture relationships. In: Plant-water Relationships in Arid and Semiarid Conditions. United Nations Educational, Scientific and Cultural Organization, Paris (Cited by Chang, 1968, p. 251).

Bierhuizen, J.F., Slatyer, R.O., 1965. Effect of atmospheric concentration of water vapor and $CO_2$ in determining transpiration-photosynthesis relationships of cotton leaves. Agr. Meteorol. 2, 259–270.

Briggs, L.J., Shantz, H.L., 1913a. The Water Requirement of Plants. I. Investigations in the Great Plains in 1910 and 1911. US Dep Agr Bur Plant Industry, Bull. No. 284. United States Department of Agriculture, Washington, DC.

Briggs, L.J., Shantz, H.L., 1913b. The Water Requirement of Plants. II. A Review of the Literature. US Dep Agr Bur Plant Industry, Bull. No. 285. United States Department of Agriculture, Washington, DC.

Briggs, L.J., Shantz, H.L., 1914. Relative water requirement of plants. J. Agr. Res. 3, 1–63.

Briggs, L.J., Shantz, H.L., 1917. The water requirement of plants as influenced by environment, 3. In: Proc. 2nd Pan-Am Sci. Congr., pp. 95–107.

Chang, J.-H., 1968. Climate and Agriculture: An Ecological Survey. Aldine, Chicago.

de Wit, C.T., 1958. Transpiration and Crop Yields. Verslag Landbouwkundig Onderzoek No. 64.6. Institute for Biological and Chemical Research on Field Crops and Herbage, Wageningen, The Netherlands.

Hanks, R.J., 1974. Model for predicting plant yield as influenced by water use. Agron. J. 66, 660–665.

Hanks, R.J., Gardner, H.R., Florian, R.L., 1969. Plant growth-evapotranspiration relations for several crops in the central Great Plains. Agron. J. 61, 30–34.

Kirkham, M.B., 2011. Elevated Carbon Dioxide: Impacts on Soil and Plant Water Relations. CRC Press, Taylor and Francis Group, Boca Raton, Florida.

LeGrand, F.E., Myers, H.R., 1976. Weather Observation and Use. OSU Extension Facts No. 9410. Oklahoma State University, Stillwater, Oklahoma.

Rabbinge, R., 1995. Prof. Dr Ir. Cornelius Teunis de Wit (1924–93). J. Ecol. 83, 345–346 (The same obituary by R. Rabbinge appears in Agr Systems 47; I–III, 1995.).

Stanhill, G., 1960. The relationship between climate and the transpiration and growth of pastures. In: Proceedings, Eighth International Grassland Congress (Cited by Chang, 1968, p. 281.).

Staple, W.J., Lehane, J.J., 1954. Weather conditions influencing wheat yields in tanks and field plots. Can. J. Agr. Sci. 34, 552–564.

Stewart, J.I., 1972. Prediction of Water Production Functions and Associated Irrigation Programs to Minimize Crop Yield and Profit Losses due to Limited Water. Ph.D. Thesis. University of California, Davis, California. University Microfilms #73–16, 934. (Cited by Tanner and Sinclair, 1983, p. 27.).

Stewart, J.I., Hagan, R.M., Pruitt, W.O., Hanks, R.J., Riley, J.P., Danielson, R.E., Franklin, W.T., Jackson, E.B., 1977. Optimizing Crop Production through Control of Water and Salinity

Levels in the Soil. Pub. no. PRWG151-1. Utah Water Research Lab, Utah State University, Logan, Utah (Cited by Tanner and Sinclair, 1983, p. 27.).

Tanner, C.B., Sinclair, T.R., 1983. Efficient water use in crop production: research or research. In: Taylor, H.M., Jordan, W.R., Sinclair, T.R. (Eds.), Limitations to Efficient Water Use in Crop Production. American Society of Agronomy, Crop Science Society of America, Soil Science Society of America, Madison, Wisconsin, pp. 1–27.

Teare, I.D., Kanemasu, E.T., Powers, W.L., Jacobs, H.S., 1973. Water-use efficiency and its relation to crop canopy area, stomatal regulation, and root distribution. Agron. J. 65, 207–211.

CHAPTER

# 30

# Solar Time and Interception of Direct-Beam Solar Radiation

As we saw in Chapter 25, the Sun is the battery that drives processes on earth, including evapotranspiration (Chapter 28). The amount of water lost by evapotranspiration is central to plant–water relations. Another key process driven by interception of the Sun's rays is photosynthesis, which provides the light necessary for the photosynthetic reaction, as follows:

$$6CO_2 + 6H_2O \xrightarrow[\text{Chlorophyll}]{\text{light}} C_6H_{12}O_6 + 6O_2$$

In this reaction, carbon dioxide ($CO_2$) and water ($H_2O$) join in the presence of light and chlorophyll to form sugar ($C_6H_{12}O_6$) and oxygen ($O_2$). Life on earth would not be possible without photosynthesis.

How do plant leaves intercept the rays from the Sun? Before we consider that question, we first need to understand basic principles of astronomy. We begin with the concept of time, which is related to the Sun. We rely on the description of this topic by Abell (1975).

## 30.1 TIME OF DAY

As we look up to the sky at night, we get the impression that the sky is a great hollow spherical shell with the earth at the center. The early Greeks regarded the sky as just such a *celestial sphere* (Abell, 1975; p. 13). The dictionary (Webster's New World Dictionary of the American Language, 1959) defines the celestial sphere as "the infinite sphere of the heavens hypothecated from the half visible from a point on the earth". The *ecliptic* is the apparent path of the sun on the celestial sphere (Abell, 1975; p. 678). The point on the celestial sphere directly above an observer (defined as opposite the direction of a plumb bob) is the observer's *zenith*. Straight down, 180° from the zenith, is the observer's *nadir*. Halfway between, and 90° from each, is the observer's *horizon* (Abell, 1975; p. 114).

*Principles of Soil and Plant Water Relations*
http://dx.doi.org/10.1016/B978-0-12-420022-7.00030-6

Copyright © 2014 Elsevier Inc. All rights reserved.

A *great circle* is any circle on the surface of a sphere (any sphere and not specifically the celestial sphere) whose center is at the center of the sphere (Abell, 1975; p. 113). The earth's equator is a great circle on the earth's surface halfway between the North Pole and the South Pole. The Sun's ecliptic is great circle on the celestial sphere. We can also imagine a series of great circles that pass through the North and South Poles. These circles are called *meridians*. They intersect the equator at right angles. A meridian can be imagined passing through an arbitrary point on the surface of the earth. The great circle passing through the celestial poles and the zenith (and also through the nadir) is called the observer's *celestial meridian* (Abell, 1975; p. 114). This meridian specifies the east–west location of that place. The longitude of the place is the number of degrees, minutes, and seconds of arc along the equator between the meridian passing through the place and the one passing through Greenwich, England, the site of the old Royal Observatory (Abell, 1975; p. 113). The meridian passing through Greenwich, which is a borough of London, also is called the Prime Meridian (Webster's New World Dictionary of the American Language, 1959), and its longitude is $0^\circ\, 0'\, 0''$. [For the difficulty in determining longitude, and the person (John Harrison) who finally figured out how to measure it by making a precise clock that worked at sea, see Sobel (2007).] My globe [Cram's Scope-O-Sphere, 12 in (30 cm) World Globe, The George F. Cram Co., Inc., Indianapolis, Indiana] designates the meridian 180° away from the Prime Meridian or Meridian of Greenwich as the *equinoctial colure*. The word colure comes from the Greek *kolouroi*, which literally means dock-tailed (ones) and this word comes from *kolos*, docked, plus *oura*, tail; so named because the "tail" (i.e., the lower part) is always cut off from view by the horizon—at least in Greece and comparable latitudes (Webster's New World Dictionary of the American Language, 1959). *Colure* means either of two imaginary circles of the celestial sphere intersecting each other at right angles at the poles: one passes through the ecliptic at the solstice, the other at the equinox (Webster's New World Dictionary of the American Language, 1959). The *solstice* is either of two points on the Sun's ecliptic at which it is farthest north or farthest south of the equator; it is also the time at which the Sun reaches either of these two points, called the *summer solstice* and the *winter solstice*. The *equinox* is the time when the Sun crosses the equator, making night and day of about equal length in all parts of the earth (Webster's New World Dictionary of the American Language, 1959). We shall discuss the solstice and equinox later in this chapter.

The most obvious coordinate system is based on the horizon and zenith of the observer. Great circles passing through the zenith (*vertical circles*) intersect the horizon at right angles. Imagine a vertical circle through a particular star (Figure 30.1). The *altitude* of that star is the number of degrees along this circle from the horizon up to the star. It is

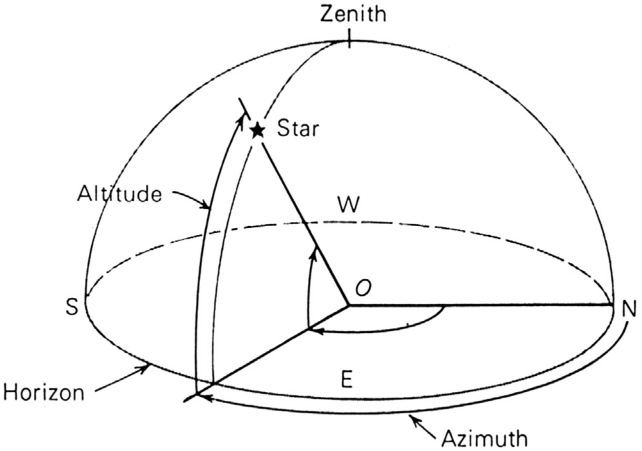

**FIGURE 30.1** Altitude and azimuth. *From Abell (1975), p. 115. This material is used by permission of Brooks/Cole, a Division of Cengage Learning.*

also the angular "height" of the star as seen by the observer (Abell, 1975; p. 115).

The *azimuth* is the number of degrees along the horizon to the vertical circle of the star from some reference point on the horizon. In astronomical tradition, azimuth formerly was measured from the south point on the observer's horizon, but in modern practice azimuth is measured from the north point, in conformity with the convention of navigators and engineers (Figure 30.1). (However, as we shall see in the next section, physicists measure azimuth from the east.) In either case, azimuth is measured (from the north or south) to the east (clockwise to one looking down from the sky) along the horizon from 0 to 360°. The altitude and azimuth system is called the *horizon system* (Abell, 1975; p. 115). Latitude and longitude, permanently attached to the earth, are a horizon system.

We now turn to the definition of the *hour angle*. The measurement of time is based on the rotation of the earth. As the earth turns, objects in the sky appear to move around us, crossing a local meridian each day. Time is determined by the position in the sky, with respect to the local meridian, of some reference object on the celestial sphere. The interval between successive meridian crossings or *transits* of that object is defined as a *day*. The actual length of a day depends on the reference object chosen. Several different kinds of days, corresponding to different reference objects, are defined. Each kind of day is divided into 24 equal parts, called *hours* (Abell, 1975; pp. 130–131).

Time is reckoned by the angular distance around the sky that the reference object has moved since it last crossed the meridian. The motion of that point around the sky is like the motion of the hour hand on a 24-h clock. The angle measured to the west along the celestial equator from the local meridian to the *hour circle* passing through any object (for example, a star) is that object's *hour angle*. An hour circle is a great circle on the celestial sphere running north and south through the celestial poles. *Time* can be defined as the *hour angle of the reference object* (Abell, 1975; p. 131).

As an example, suppose that the star Rigel is chosen as the reference for time. Then when Rigel is on the meridian it is $0^h0^m0^s$, "Rigel time". Twelve Rigel hours later, Rigel is halfway around the sky, at an hour angle of 180°, and the Rigel time is $12^h0^m0^s$. When Rigel is only 1° east of the meridian, and one Rigel day is nearly gone, the star is at an hour angle of 359°, and the Rigel time is $23^h56^m0^s$ (Abell, 1975; p. 131).

Time can be represented graphically by means of a time diagram, as in Figure 30.2. Here we imagine ourselves looking straight down on the north celestial pole from outside the celestial sphere. The pole appears at a point in the middle of the diagram, and the celestial equator (not the earth's equator) appears as a circle centered on the pole. As the earth turns to the east, the local meridian of an observer on earth sweeps around the sky, so that its intersection with the celestial equator would move counterclockwise around the circle in the time diagram. However, it is customary to represent the observer's meridian as fixed, intersecting the celestial equator, say, at the top of the diagram. Then the celestial sphere

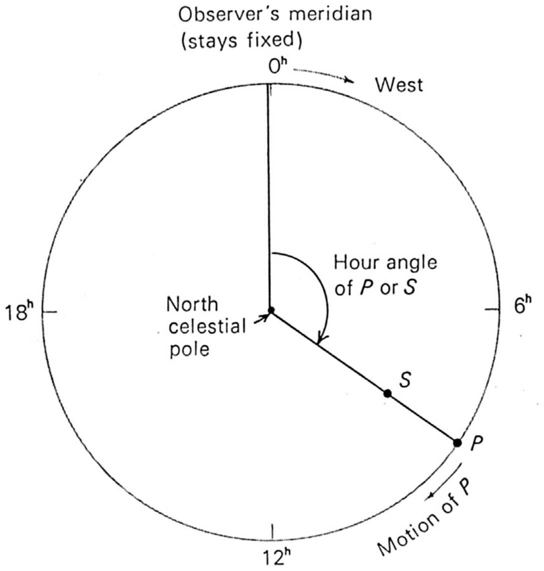

**FIGURE 30.2** Time diagram. *From Abell (1975), p. 131. This material is used by permission of Brooks/Cole, a Division of Cengage Learning.*

must be regarded as rotating clockwise with respect to the meridian. Let the reference object be denoted by *S* (e.g., a star). Its (*S*'s) hour circle intersects the equator (great circle) at *P* (*P* for "point"), and as the celestial sphere rotates, the point *P* moves clockwise around the circle, like the hour hand of a clock. The hour angle of *S* (or *P*) increases uniformly with the rotation of the celestial sphere. In the diagram (Figure 30.2), it is shown as about 120°. The time would then be about $8^{h}$ (Abell, 1975; p. 131), as we shall see in the next paragraph.

Because of the relation between hour angle and time, it is often convenient to measure angles in time units. In this notation, 24 h corresponds to a full circle of 360°, 12 h to 180°, 6 h to 90°, and so on. One hour equals 15° and 1° is 4 min of time. Here we must distinguish between minutes and seconds of time (subdivisions of an hour), denoted by $^{m}$ and $^{s}$, respectively, and minutes and seconds of *arc* (subdivisions of a degree), denoted by $'$ and $''$, respectively (Abell, 1975; p. 131). The conversion between units of time and arc is given in Table 30.1.

We can measure time by solar (Sun) time and by sidereal (star) time (Abell, 1975; pp. 132–133). *Sidereal* means "of the stars" (Webster's New World Dictionary of the American Language, 1959). Sidereal time is based on the sidereal day with its subdivisions of sidereal hours, minutes, and seconds. It is defined as the hour angle of the *vernal equinox*. The vernal equinox is defined as the point on the celestial sphere where the Sun in its apparent path around the sky (ecliptic) crosses the celestial equator from south to north. Another way to consider the vernal equinox is as follows. The north and south halves of the celestial sphere are separated by the celestial equator, halfway between the north and south celestial poles, and the place where the Sun crosses it on the first day of spring is called the vernal equinox (Abell, 1975; p. 30). It is one of the points on the celestial sphere where the celestial equator and the ecliptic intersect (Abell, 1975;

**TABLE 30.1** Conversion between Units of Time and Arc

| Time Units | Arc Units |
|---|---|
| $24^{h}$ | 360° |
| $1^{h}$ | 15° |
| $4^{m}$ | 1° |
| $1^{m}$ | $15'$ |
| $4^{s}$ | $1'$ |
| $1^{s}$ | $15''$ |

*From Abell (1975), p. 132. This material is used by permission of Brooks/Cole, a Division of Cengage Learning.*

p. 115). The sidereal day begins at sidereal noon, $0^h0^m0^s$ sidereal time, with the vernal equinox on the meridian (Abell, 1975; p. 133).

*Vernal* means "belonging to spring." In the northern hemisphere, the vernal equinox occurs on about March 21 and the *autumnal* (fall) *equinox* occurs on about September 23 (Abell, 1975; p. 124). On the date of the *summer solstice*, which is about June 22 in the northern hemisphere, the Sun shines down most directly upon the northern hemisphere of the earth and the Sun appears 23½° *north* of the equator. (We shall see later why the angle is 23½° is important.) To a person at a latitude 23½° N, the Sun is directly overhead, and this latitude on the earth, at which the Sun can appear at the zenith at noon on the first day of summer, is called the *Tropic of Cancer*. The situation is reversed six months later, about December 22, the date of the *winter solstice*, which occurs about December 22 in the northern hemisphere. At latitude 23½° S, the *Tropic of Capricorn*, the Sun passes through the zenith at noon. It is winter in the northern hemisphere, summer in the southern (Abell, 1975; pp. 122–124). As we shall discuss later, the plane of the earth's equator is inclined at about 23½° (23°27′) to the plane of the ecliptic.

Sidereal time is useful in astronomy and navigation. The common coordinate system used to denote positions of stars and planets on the celestial sphere is referred to the celestial equator and the vernal equinox, much as latitude and longitude on the earth are referred to the earth's equator and meridian of Greenwich, England. Therefore, the position of a star in the sky with respect to the observer's meridian is directly related to the sidereal time. Every observatory maintains clocks that keep accurate sidereal time (Abell, 1975; p. 133).

However, sidereal time is not useful for daily living. We regulate our day by the Sun, not the vernal equinox (Abell, 1975; p. 133). The solar day is the period of the earth's rotation with respect to the Sun. As noted, the sidereal day is the time required for the earth to make a complete rotation with respect to a point in space, the vernal equinox (Abell, 1975; p. 132). A solar day is slightly longer than a sidereal day, as a study of Figure 30.3 shows. Suppose we start a day when the earth is at *A*, with the Sun on the meridian of an observer at point *O* on the earth. The direction from the earth to the Sun, *AS*, if extended, points in the direction *C* among the stars on the celestial sphere. After the earth has made one rotation with respect to the stars, the same stars in direction *C* will again be on the local meridian to the observer at *O*. However, because the earth has moved from *A* to *B* in its orbit about the Sun during its rotation, the Sun has not yet returned to the meridian of the observer but is still slightly to the east. The vernal equinox is so nearly fixed among the stars that the earth has completed, essentially, one *sidereal day*, but to complete a *solar day* it must turn a little more to bring the Sun back to the meridian. In other words, a solar day is slightly *longer* than a sidereal day, or one complete rotation

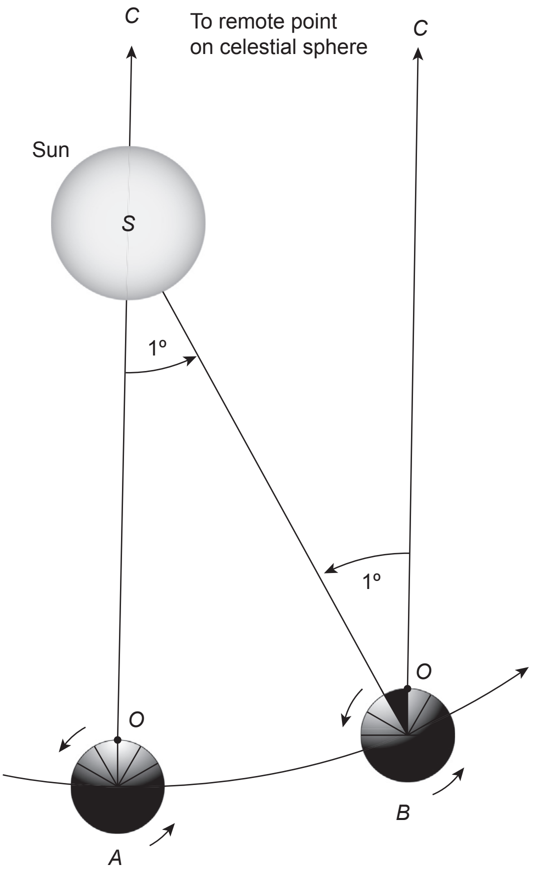

**FIGURE 30.3** Sidereal and solar day. *From Abell (1975), p. 132. This material is used by permission of Brooks/Cole, a Division of Cengage Learning.*

of the earth. There are about 365 days in a year and 360° in a circle; thus the daily motion of the earth in its orbit is about 1° in relation to the Sun. This 1° angle, *ASB* (Figure 30.3), is nearly the same as the additional angle over and above 360° through which the earth must turn to complete a solar day. It takes the earth about 4 min to turn through 1°. A solar day, therefore, is about 4 min longer than a sidereal day (Abell, 1975; pp. 132–133).

On about September 23, the Sun passes through the autumnal equinox, halfway around the sky from the vernal equinox. On that date, at midnight, when the day begins, the vernal equinox is on the meridian, and so solar time and sidereal time are in agreement. With each succeeding day, however, sidereal time gains $3^{m}56^{s}$ on solar time, and the two kinds of time do not agree again until the daily difference between them accumulates to a full 24 h one year later (Abell, 1975; p. 133).

Sidereal time is reckoned by the hour angle of the vernal equinox, and *apparent solar time* is determined by the hour angle of the Sun. At midday, apparent solar time, the Sun is on the meridian. The hour angle of the Sun is the time *past midday* (*post meridiem* or P.M.). It is convenient to start the day not at noon, but at midnight. Therefore, the elapsed apparent solar time since the beginning of a day is the hour angle of the Sun plus 12 h. During the first half of the day, the Sun has not yet reached the meridian. We designate those hours as *before midday* (*ante meridiem*, or A.M.). We customarily start numbering the hours after noon over again, and designate them by P.M. to distinguish them from the morning hours (A.M.). But it is often useful to number the hours from 0 to 24, starting from the beginning of the day at midnight. For example, in various conventions, 7:46 P.M. may be written as $19^h46^m$, 19:46, or simply 1946 (Abell, 1975; p. 133). *Apparent solar time*, defined as the hour angle of the Sun plus 12 h, is the most obvious and direct kind of solar time. It is the time that is kept by a sundial. In a sundial, the raised marker, or *gnomon*, casts a shadow whose direction indicates the hour angle of the Sun. Apparent solar time was the time kept by man through many centuries (Abell, 1975; p. 133).

The exact length of an *apparent solar day*, however, varies slightly during the year. Recall that the difference between an apparent solar day and a sidereal day, if time is counted from noon on one day, is the extra time required, after one rotation of the earth with respect to the vernal equinox to bring the Sun back to the meridian. The length of this extra time depends on how far east of the meridian the Sun is after the completion of one sidereal day. The earth rotates to the east at a nearly constant rate of 1° every 4 sidereal minutes. Thus, if the Sun were exactly 1° east of the meridian, about four sidereal minutes would be needed to bring it the rest of the way to the meridian (Abell, 1975; p. 134).

The length of the apparent solar day would be constant, if the eastward progress of the Sun, in its apparent annual journey around the sky, were precisely constant. However, there are two reasons why the amount by which the Sun shifts to the east is not the same every day of the year. The first reason is that the earth's orbital speed varies. In accordance with Kepler's second law—the law of areas—the earth moves fastest when it is nearest the Sun (perihelion) in early January and slowest when it is farthest from the Sun (aphelion) in July. (For Kepler's three laws of planetary motion and his biography, see the Appendix, Section 30.4.) However, the earth's rate of rotation is nearly constant. Consequently, it (the earth) moves farther in its orbit during a sidereal day in January than in July (Figure 30.4). The Sun's apparent motion along the ecliptic is just the reflection of the earth's revolution, so the Sun's daily progress to the east reflects the inequalities of the earth's daily progress in its orbit. We see, then, that the extra amount by which the earth must turn after a

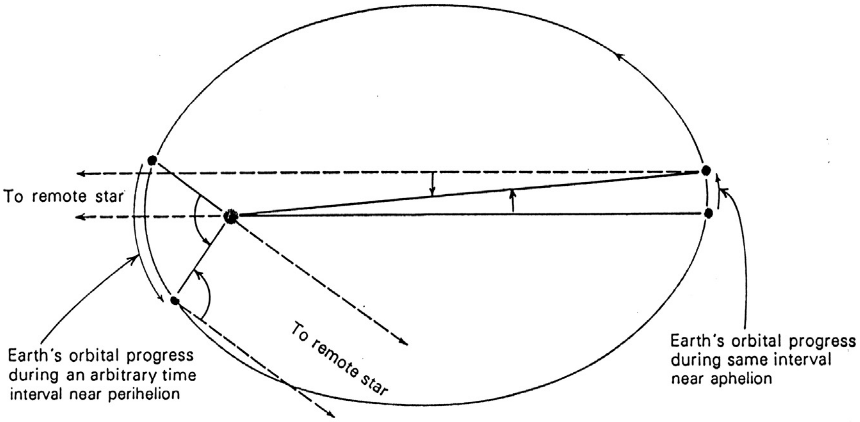
To remote star
To remote star
Earth's orbital progress during an arbitrary time interval near perihelion
Earth's orbital progress during same interval near aphelion

**FIGURE 30.4** Variation in the length of an apparent solar day because of the earth's variable orbital speed. (The effect, of course, is grossly exaggerated.) *From Abell (1975), p. 134. This material is used by permission of Brooks/Cole, a Division of Cengage Learning.*

sidereal day to complete a rotation with respect to the Sun is not always exactly the same (Abell, 1975; p. 134).

The second reason for the variation in the rate of the Sun's eastward progress, and the consequent nonuniformity in the length of the apparent solar day, is that the Sun's path—the ecliptic—does not run exactly east and west in the sky, along the celestial equator, but is inclined to the equator by 23½°. [Globes of the earth are usually mounted with the earth's axis tilted from the vertical. This tilt is the same angle of 23½°, for that is the angle the earth's axis must make with the perpendicular to the plane of its orbit around the Sun (Abell, 1975; p. 121).] Even if the earth's orbit were circular, so that the Sun moved uniformly along the ecliptic, the amount by which it moved to the east would vary slightly throughout the year. The situation is illustrated in Figure 30.5, which shows the celestial sphere, the celestial equator, and the ecliptic. To make the effect more obvious, the obliquity of the ecliptic is exaggerated. Now suppose the Sun moved equal distances along the ecliptic near March 21 and June 22; such equal distances are marked off on the ecliptic in the figure. Near the vernal equinox, part of the Sun's motion is northward, and it progresses less to the *east* than it does along other points of the ecliptic. But, at the solstice, the Sun is moving not only due east, but it is also north of the equator where the hour circles converge, so that a 1° advance on the ecliptic is more than a 1° advance to the east. A similar analysis shows the Sun would also make more eastward progress near the winter solstice than near the autumnal equinox. With the actual 23½° obliquity, it turns out that a 1° advance on the ecliptic corresponds to 0.92° advance to the east at the equinoxes and 1.08° advance to the east at the solstices. Thus,

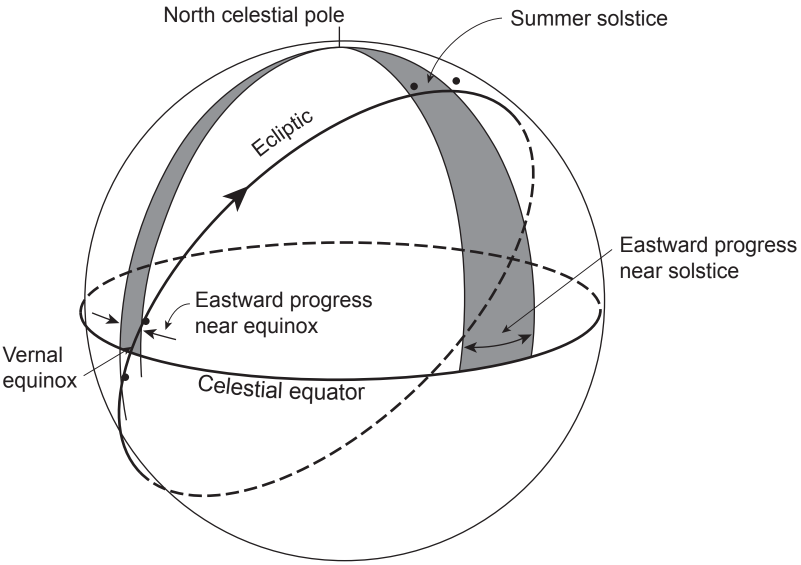

**FIGURE 30.5** The Sun's apparent eastward daily progress varies because of the obliquity of the ecliptic. *From Abell (1975), p. 135. This material is used by permission of Brooks/Cole, a Division of Cengage Learning.*

even if the Sun did move uniformly on the ecliptic, its eastward progress would be variable (Abell, 1975; pp. 134–135).

The apparent solar day is always about 4 min longer than a sidereal day, but because of the Sun's variable progress to the east, the precise interval varies by up to one-half minute one way or the other. The variation can accumulate after a number of days to several minutes. After the invention of clocks that could run at a uniform rate, it became necessary to abandon the apparent solar day as the fundamental unit of time. Otherwise, all clocks would have to be adjusted to run at a different rate each day.

*Mean solar time* is based on the *mean solar day*, which has a duration equal to the *average* length of an apparent solar day. Mean solar time is defined as the hour angle of the mean Sun plus 12 h, where the *mean Sun* is a fictitious point along the celestial equator with the same average eastern rate as the true Sun. In other words, mean solar time is just apparent solar time averaged uniformly (Abell, 1975; p. 135).

The irregular rate of apparent solar time causes it to run alternately ahead of and behind mean solar time. The difference between the two kinds of time can accumulate to about 17 min. The difference between apparent solar time and mean solar time is called the *equation of time*, shown graphically in Figure 30.6. One can read from the plot, for any date of the year, the correction to apply to mean solar time to obtain apparent

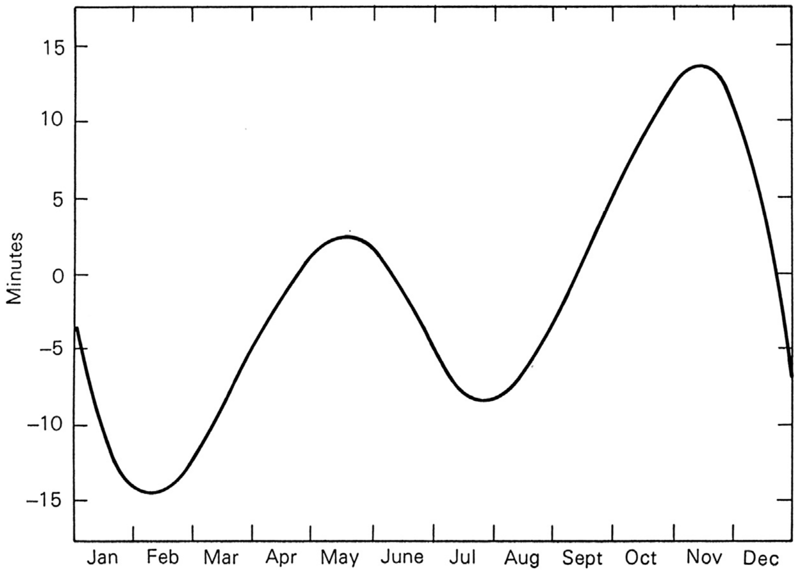

**FIGURE 30.6** Equation of time (apparent minus mean solar time). *From Abell (1975), p. 136. This material is used by permission of Brooks/Cole, a Division of Cengage Learning.*

solar time. When the equation of time is positive, apparent time is ahead of mean time. Often the equation of time is plotted on globes of the earth as a nomogram, shaped like the figure eight and placed in the region of the South Pacific Ocean.

Although mean solar time has the advantage of progressing at a uniform rate, it is still inconvenient for practical use. Recall that it is defined as the hour angle of the mean Sun. But hour angle refers to the local celestial meridian, which is different for every longitude on earth. Thus, observers on different north—south lines on the earth have a different hour angle of the mean Sun and hence a different mean solar time. If mean solar time were strictly observed, people traveling east or west would have to reset their watches continually as their longitude changed, if it were always to read the local mean time correctly (Abell, 1975; p. 136).

Until the end of the nineteenth century, every city and town in the USA kept its own local mean time. With the development of railroads and telegraph, however, the need for standardization became necessary. In 1883, the nation was divided into four time zones (Abell, 1975; p. 136). Within each zone, all places keep the same time, the local mean solar time of a standard meridian running more or less through the middle of each zone. Now travelers reset their watches only when the time change has amounted to a full hour. In the USA for local convenience, the boundaries between the four time zones are chosen to correspond, as much as possible, to divisions between states. Mean solar time, so standardized, is called standard time. The standard time zones in the USA (not including Alaska and Hawaii) are Eastern Standard Time (EST), Central Standard Time (CST), Mountain Standard Time (MST), and Pacific Standard Time (PST), which, respectively, keep the mean times of the meridians of 75°, 90°, 105°, and 120° west longitude. Hawaii and Alaska both keep the time of the meridian 150° west longitude, 2 h less advanced than Pacific Standard Time (Abell, 1975; p. 136).

In 1884, an international conference was held in Washington, DC, in which 26 nations were represented (Abell, 1975; pp. 136–137). At that conference it was agreed to establish a system of 24 international time zones around the world. Each time zone, on the average, is 15° wide in longitude, although the zone divisions are usually irregular over land areas to follow international boundaries. At sea, the zone time of any place is the mean time of the standard meridian running through the center of the zone of that place. The zones are numbered consecutively from the Greenwich meridian. Those west of Greenwich are denoted (+) and those east are denoted (−). The EST time zone is zone number +5 (Abell, 1975; p. 137). Manhattan, Kansas, is zone number +6.

The procedure for determining standard time from apparent solar time, as read say, from a sundial, is illustrated in the following example (Abell, 1975; p. 139). At Los Angeles (118° west longitude), the apparent solar (sundial) time on March 16 was 11:30 a.m. From the equation of time (Figure 30.6), we note that on March 16 apparent solar time is 9 min behind mean solar time. Thus the local mean time is 11:39 a.m. Now Los Angeles is in the Pacific Standard Time zone, which keeps the time of the meridian at 120° west longitude. Los Angeles is 2° east of that meridian, so its local time is 8 min *more advanced* than that of the 120° meridian. Pacific Standard Time is thus 11:31 a.m.

## 30.2 INTERCEPTION OF DIRECT-BEAM SOLAR RADIATION

We now have an understanding of the Sun and its relation to earth to determine time. We need to know time to determine the how much of the Sun's energy is intercepted by plant leaves at each moment during the day. Because almost no information exists in textbooks demonstrating the interaction of leaf angles and Sun angles, the objective of this section is to describe Sun and leaf geometry to determine direct-beam solar radiation on a leaf at any time, angle, orientation, and location in the world. Direct-beam solar radiation is represented by $I$ in the radiation-balance equation (Eqn (25.11)). It is the light that strikes us when the Sun is out and there are no clouds in the sky. We shall focus on the sloping surface of a plant leaf, but the procedure can be used for any inclined surface, including the sloping side of soil tilled up in a ridge.

To determine the light interception on a sloping surface, we need to know four angles. Two of the angles are the Sun's angles and two of the angles are the leaf's angles. For a theoretical consideration of these angles, see Kirkham (1986). Here we shall consider practical application of the theory.

Let us first look at the Sun's angles. Following along with what we learned in the previous section about altitude and azimuth (Figure 30.1), we can designate the Sun's position by two angles, *solar altitude* and *solar azimuth*. Solar altitude is the angle measured from the horizon up to the Sun. We shall abbreviate this angle $A$. It equals 0° when the Sun is on the horizon and 90° when the Sun is at the zenith directly overhead. The Sun is only directly above the earth, i.e., at 90° at solar noon, at two times. As noted in the previous section, these two times are about June 22 at the Tropic of Cancer, located at 23°27′ north of the equator, and about December 22 at the Tropic of Capricorn, located 23°27′ south of the equator. These times occur at the solstices. A solstice is defined as either of the two points on the Sun's apparent annual path where it is displaced farthest, north or south, from the earth's equator, that is, a point of greatest deviation of the ecliptic from the celestial equator (Glickman, 2000). An object would not cast a shadow if the Sun were 90° above it (i.e., at the Tropic of Cancer on about June 22 or the Tropic of Capricorn on about December 22). All other objects cast shadows when the Sun shines on them. In Manhattan, Kansas, during the entire year, the Sun is never directly above us (i.e., at an altitude of 90°). However at solar noon, it is at its zenith—the highest point the Sun rises during the day.

*Solar azimuth* is the angle measured clockwise from north (usually from north, but not always; see the next paragraph) to the projection of the Sun on the horizon. We shall abbreviate the solar azimuth with the Greek letter, lower case omega, $\omega$. When measured from north, it equals 0° at north, 90° at east, 180° at south, 270° at west, and 360° at north to complete the full circle. Solar azimuth is measured from "true" or "geographic" north. True north is the direction toward the North Pole of the earth's axis. Although surveyors often use "magnetic" north, the direction toward which a magnetic compass points, solar designers must use true north, the basis of the Sun-angle charts. As a magnetic variation map shows (Vestine, 1971; Bennett, 1978, p. 7), the difference between magnetic and geographic north can be substantial. For example, in the USA it can be as much as 20° in Oregon.

Solar azimuth is not always measured from north, although it often is. It appears that meteorologists and architectural designers measure solar

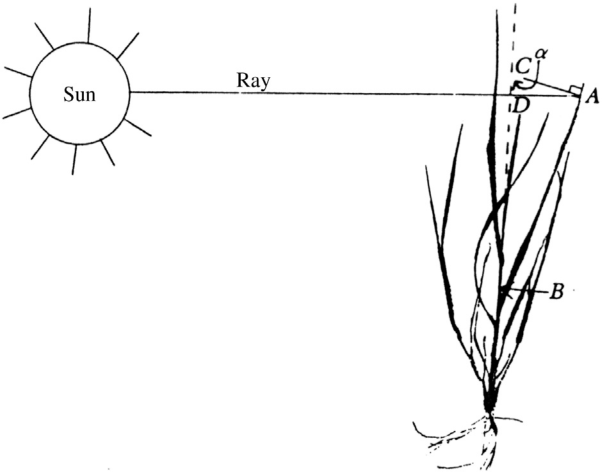

**FIGURE 30.7** Solar ray on a wheat leaf. Angle ABC was measured. To calculate solar intensity on the leaf surface, the angle alpha ($\alpha$) or angle ACB is needed. $\alpha = (90-\text{measured angle})°$. The dotted line shows the extension of the vertical culm. The line CA is perpendicular to the leaf. *From Kirkham (1982), American Society of Agronomy. Reprinted by permission of the American Society of Agronomy.*

azimuth from north, such as Bennett (1978). East is sometimes used as the reference direction, especially by physicists. One needs to know from what direction (north or east) azimuth is measured.

Now let us turn to the two leaf angles that we need to know. The first angle we abbreviate with the Greek letter alpha, $\alpha$, which is the "slope" angle of the leaf surface with respect to the vertical (Figure 30.7), and $\alpha$ is equal to 90° minus the slope measured from the horizontal. However, when we measure a leaf's angle (which we do with a protractor), we measure the angle between the vertical (e.g., stem or culm) and the leaf surface (angle ABC in Figure 30.7). So the measured angle is thus $(90-\alpha)°$ (Figure 30.7). The other leaf angle is called the aspect angle, which we abbreviate by the Greek letter beta, $\beta$. These aspect angles are shown in Table 30.2. For example, if the direction that the leaf points is north, then the direction that the leaf faces is south, and $\beta$ is 180°.

Now that we know the four angles, we use the direct-beam solar radiation equation to determine the light interception on the sloping surface. The equation used to determine light intensity on inclined surfaces, like a plant leaf, has been published in several sources (Fons et al., 1960; Lee, 1963; ASHRAE, 1967, p. 475; Kondratyev, 1977). The equation has been in the literature for hundreds of years. My father, Don Kirkham, sought the origin of the equation. He traced it back to the 1700s, but could trace it no further. So the first scientist to derive the equation is apparently

**TABLE 30.2** Relation between Leaf Orientation and the Angle $\beta$ Used to Determine Direct-Beam Solar Radiation on a Leaf

| Direction Leaf Points | Direction Leaf Faces | $\beta$, Degrees |
|---|---|---|
| N | S | 180 |
| S | N | 0 |
| E | W | 270 |
| W | E | 90 |
| NE | SW | 225 |
| NW | SE | 135 |
| SE | NW | 315 |
| SW | NE | 45 |

*From Kirkham (1986), Institute of Agrophysics, Polish Academy of Sciences, Lublin, Poland. Reproduced by permission of Prof. Dr. Jan Gliński, Editor-in-Chief,* International Agrophysics, *Institute of Agrophysics.*

unknown (Don Kirkham, personal communication, c.1978). The form of the equation used here is given by Fons et al. (1960; see p. 4, Eqn 5 and p. 5, Eqn 8) as:

$$I/I_o = \sin A \cos \alpha - \cos A \sin \alpha \sin(Z - \beta), \tag{30.1}$$

where

$I/I_o$ = intensity of received direct-beam radiation to incident direct-beam radiation ($I'$ used by Fons et al. is $I_o$ here)
$A$ = solar altitude
$Z = \omega - 90°$, where $\omega$ is solar azimuth measured from north
$\alpha$ = angle between a vertical and a normal to the leaf; the angle measured with a protractor is between the leaf surface and the vertical (stem); the measured angle is therefore $(90-\alpha)°$, and $(90-\alpha)°$ is subtracted from 90° to get $\alpha°$
$\beta$ = aspect angle of the leaf surface (direction leaf faces; N = 0°; NE = 45°; E = 90°, etc.) (Table 30.2)

Values of solar azimuth $\omega$ and solar altitude $A$ are given by Bennett (1978).

Let us take an example, as given by Kirkham (1986). The measurement was taken in Stillwater, Oklahoma, on March 11, 1980. The second-to-the-top leaf of the winter wheat (*Triticum aestivum* L.) cultivar "Priboy" was measured. The leaf pointed southeast, and, therefore, faced northwest. The angle $\beta$ was 315°. Angle $\alpha$, the angle between the stem (culm) and the normal to the leaf, was 10°. The leaf was nearly horizontal. The measurement was taken at local solar noon, so the Sun was at its zenith; the azimuth angle $\omega$ was 180°, and $Z = 180° - 90° = 90°$. (To get local solar time, one's watch should read 12 noon when the Sun is at its maximum height for the day.) The solar altitude angle was 50° and it was obtained from Bennett (1978, p. 51). So $Z = 90°$; $\alpha = 10°$; $A = 50°$; $\beta = 315°$. Putting these values in Eqn (30.1), we get:

$$\begin{aligned} I/I_o &= \sin 50° \cos 10° - \cos 50° \sin 10° \sin(90 - 315)° \\ &= (0.766)(0.985) - (0.643)(0.174)(0.707) \\ &= 0.754 - 0.079 = 0.675. \end{aligned}$$

As a check, we can read a similar $I/I_o$ value of 0.6873 on p. 77 of Fons et al. (1960).

Kirkham (1984) measured the interception of direct-beam solar radiation of two cultivars of winter wheat: 'KanKing', a drought-resistant cultivar, and 'Ponca', a drought-sensitive cultivar. KanKing as developed by Earl G. Clark, a Kansas farmer and wheat breeder, during the drought years of the 1950s in Kansas (Heyne, 1956). They were grown under well watered conditions. However, the drought-resistant cultivar had its leaves prostrate on the ground during the winter, while the drought-sensitive cultivar had erect leaves. The horizontal leaves of KanKing intercepted more direct-beam solar radiation than the erect leaves of Ponca (Figure 30.8). The leaves of KanKing were wider during the winter than those of Ponca, perhaps because it intercepted more direct-beam solar radiation during the winter than Ponca. KanKing's leaf orientation may be one reason why it is drought-tolerant. It can intercept more solar radiation and grow more during the winter, putting its roots down deeper and thus allowing a deeper root zone for water extraction

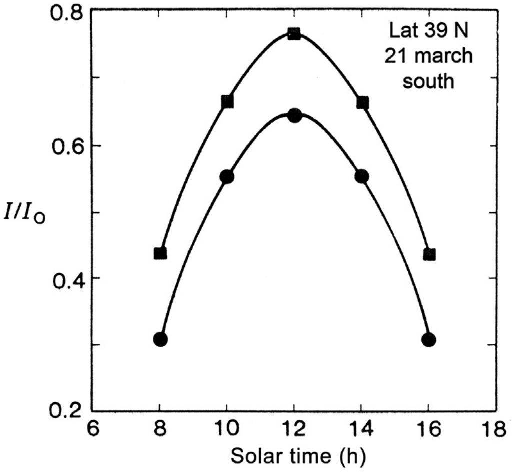

**FIGURE 30.8** Calculated ratio of intensity of received direct-beam radiation to intensity of incident direct-beam radiation ($I/I_o$) for south-facing leaves of a winter wheat cultivars with horizontal leaves (e.g. 'KanKing') (squares) and a winter wheat cultivar with erect leaves (e.g. 'Ponca') (circles). *From Kirkham (1984), Crop Science Society of America. Reprinted by permission of the Crop Science Society of America.*

during the spring growing season. Kirkham (1984) did not measure the root depth of Ponca and KanKing, but the relation between $I/I_0$ and root depth needs to be determined.

We now have a way to quantify the amount of solar energy intercepted by plant leaves. Just as buildings and solar-powered installations can be placed to maximize interception of the Sun's rays, cultivars of different plants can be developed for improved efficiency of solar energy use (Kirkham and Smith, 1984). We could orient plant rows so that leaves would intercept more solar energy and, thereby, increase photosynthesis and plant production (Kirkham, 1982).

We have applied the direct-beam solar radiation equation to a plant leaf. For its application to the sloping surface of soil, see Affleck et al. (1976), who worked in Iowa, where it is important to orient seed beds so they can warm up early in the spring and corn (*Zea mays* L.) can get a good start on growth. If the corn is planted on the south-facing side of a sloped surface, it will warm up more than if it is planted on a flat surface.

## 30.3 HOW TO MEASURE ALTITUDE AND AZIMUTH ANGLES OF SUN

We can determine solar altitude and azimuth if we do not have tables or graphs, such as those in Bennett (1978). To use this method of getting altitude and azimuth, we do not need to know solar time. However, we do need tables of tangents and sines or a calculator that can calculate them. A freshman astronomy student might be more interested in this method than a crop scientist. However, the Sun and its angles are important in crop growth, so students of crop science also need to know the information. The procedure comes from Don Kirkham (personal communication, February 3, 1983) and is illustrated in Figure 30.9.

We have a vertical rod of height $h$ that casts a shadow of length $s$. The rod could be a meter stick. We draw an East–West line through the end of the shadow. We can get the East–West line from a compass or know it from hedgerows, fences, highways, etc. The abbreviations in Figure 30.9 are as follows:

$L$ = length of the perpendicular from the E–W line to the bottom of the rod; $L$ is the shortest walking distance from the bottom of the rod to the E–W line.
$x$ = projection of a point at the bottom of the rod on the E–W line, which goes through the end of the shadow of the rod
$\alpha$ = altitude (angle) of the Sun
$\omega$ = azimuth (angle) of Sun measured from east

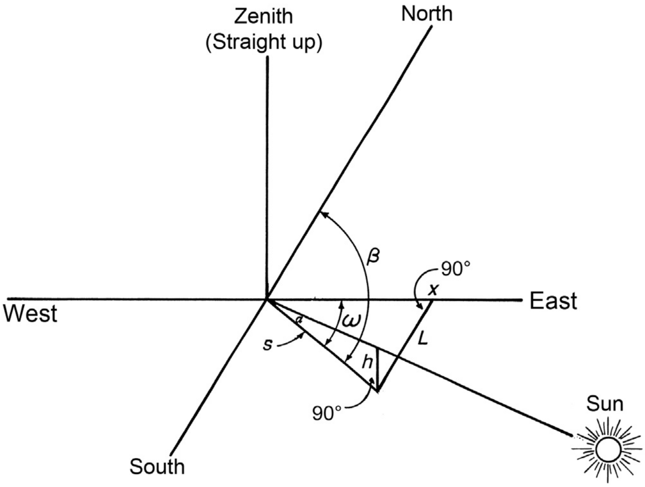

**FIGURE 30.9** Illustration of how to measure altitude and azimuth angles of the Sun. See text, Section 30.3, for explanation of the symbols. *Figure drawn by Don Kirkham, Iowa State University, Ames, Iowa.*

$\beta = \omega + 90° =$ azimuth (angle) of Sun measured from north
$\tan \alpha = h/s$
$\alpha = \tan^{-1} h/s$
$\sin \omega = L/s$
$\omega = \sin^{-1} L/s$

While the meter stick is in the vertical position, the shadow could be scratched in the soil. Then the length of the scratch could be measured with the meter stick. After drawing an East–West line through the end (furthest from the rod) of the shadow, one could use the meter stick to measure $L$.

Example:

$h = 100$ cm
$s = 99$ cm
$L = 95$ cm
$\tan \alpha = h/s = 100/99$
$\alpha = \tan^{-1} 100/99$
$\alpha = 45.3°$ or $45°$ (altitude angle of Sun)
$\sin \omega = L/s = 95/99$
$\omega = \sin^{-1} 95/99$
$\omega = 74°$ (azimuth angle of Sun measured from east)
$74° + 90° = 164°$ (azimuth angle of Sun measured from north).

Bennett (1978, p. 6) gives a method of determining true north. When beginning work at a specific site, a designer can read true north from a map, such as those drawn by the United States Geological Survey, or determine it through the following procedure. Developed by Vitruvius (Roman architect and engineer of the first century BC), the process relies upon the fact that the Sun's motion is symmetrical around true south. On a sunny day, do the following:

1. In the morning, place a stake in a clearing on the site.
2. Mark the end of its shadow.
3. With the shadow as the radius, draw a circle on the ground around the stake.
4. In the afternoon, when the end of the shadow again falls exactly on the circle, mark its end point a second time.
5. Divide in half the distance between the two marks (that made in the morning and that in the afternoon). A line from the stake to this spot points due north.

## 30.4 APPENDIX: BIOGRAPHY OF JOHANNES KEPLER

Unless noted, all the following biographical material on Kepler comes from Ronan (1971).

Johannes Kepler (1571—1630) was a German astronomer whose studies of the motions of the planets helped to lay the foundations of modern astronomy. He was born on December 27, 1571, at Weil in Württemberg. His father was a petty officer in the duke of Württemberg's army and his mother, Catherine (née Guldenmann), came from a family of once noble standing. Johannes was born premature by two months and was a delicate child. With his younger brother Heinrich, he lived with his grandparents while his father was engaged in the Dutch wars and his mother accompanied her husband to the Netherlands. When about four years of age, he contracted small-pox and nearly went blind with the result that his eyesight was permanently impaired.

He first attended school in Weil, then in Leonberg on the return of his parents, and finally in the convent schools of Adelberg (1584) and Maulbronn (1586). In September, 1588, he obtained his bachelor's degree and entered the University of Tübingen the following year. There, in August 1591, he obtained his master's degree. He had hoped to enter the ministry but instead was persuaded to accept the post of professor of mathematics at Graz in 1594.

At Tübingen, Kepler came under the influence of Michael Maestlin (an astronomer) who became a lifelong friend. Maestlin was a protagonist of the views of Copernicus, which he had to teach privately to his young pupil, because the Ptolemaic system was still the picture of the universe that was held in official circles. Kepler absorbed the heliocentric concept of Copernicus and later developed it with brilliance. [We remember that the Ptolemaic system, named after Ptolemy, an Alexandrian astronomer, mathematician, and geographer, who lived in the second century AD, held that the earth was the center of the universe, around which the heavenly bodies moved. The Copernican system was the theory of Nicolaus Copernicus, a Polish astronomer (1473–1543), which held that the planets revolve around the Sun and that the turning of the earth on its axis accounts for the apparent rising and setting of the stars. The Copernican system is the basis of modern astronomy (Webster's New World Dictionary of the American Language, 1959).]

As professor at Graz, Kepler lectured on mathematics and also, at the request of the university, on Virgil (Roman poet; 70–19 BC) and rhetoric. He was also expected to prepare annual almanacs giving astronomical and astrological predictions. Kepler, was, however, primarily interested in the problems of the planetary system. He believed that there must be some regularity in the relationship between the orbits of the planets, and he spent his major efforts in seeking this relationship. The first fruits of his labors were published in 1596 under the title *Prodromus Dissertationum Mathematicarum continens Mysterium Cosmographicum*. The publication of this work brought him fame, and he began corresponding on friendly terms with Tycho Brahe (1546–1601), a Danish astronomer, and Galileo Galilei, known as Galileo (1564–1642), an Italian astronomer and physicist, two of the most eminent astronomers of the day.

In April of 1597, Kepler married the wealthy Barbara von Mühleck, whom he had met in Graz, but by September all Protestant theologians were expelled from the city. He left, but his wife's influence allowed him to return after a month. However, the situation remained unfavorable and in 1600 Kepler and his wife had to leave Graz. The Roman Catholic Hensart von Hohenberg, who was an old pupil of Maestlin's and with whom Kepler had been in correspondence, suggested that Tycho Brahe might help. Tycho himself had been forced to leave the island of Hveen, but when he was appointed court mathematician to Emperor Rudolf II in Prague, he invited Kepler to join him there, and Kepler and his wife made their home in Prague.

Tycho died a year after Kepler's arrival in Prague, and he was thereupon appointed by the emperor to succeed his late patron as court mathematician, although at a reduced salary. All the observations which Tycho had made were at Kepler's disposal, and as later events proved, these were a veritable storehouse of information to which astronomy will ever be in debt.

In 1604, he published *Astronomiae pars optica*. This book contained Kepler's fundamental ideas on the nature of vision and a definition of a ray of light, which later became generally adopted in geometrical optics. He also offered an explanation of the reflection of light and an approximation to the law of refraction. (It is interesting to note that a man with limited eyesight made these important contributions to the understanding of vision and light.)

Unlike Tycho, Kepler had no talent for experimentation (Cajori, 1929; p. 33). But he was a great thinker and excelled as a mathematician. He absorbed Copernican ideas and early grappled with the problem of determining the real paths of the planets. He studied observations on the planets recorded by his master. He took the planet Mars and found that no combinations of circles would give a path which could be reconciled with the actual observations. In one case the difference between the observed and his computed values was 8 min, and he knew that an accurate observer like Tycho could not make such an error so great. He tried an ellipse for the orbit of Mars, and it fitted. Thus, after more than four years of assiduous computation, and after trying 19 imaginary paths and rejecting each because it was more or less inconsistent with observation (Cajori, 1929; p. 34), Kepler at last discovered that the planets revolved round the Sun in elliptical paths with the Sun at one focus, and this formed his first law. It was his efforts to reconcile the observations with the Copernican system that Kepler was led to take this bold step, making a complete break with the traditions of more than 2000 years, and it had a profound effect on future astronomy.

Next, with his belief in the order and regularity of the heavens, he sought some kind of regular motion which would describe the behavior of the planets in paths of elliptical form. Such work entailed much labor, but finally he discovered that the radius vector of each planet described equal areas of the ellipse in equal times (his second law). This new and fundamentally important work, the *Astronomia nova*, was published in Prague in 1609, and the book made public his two laws to date of planetary motion.

In 1612, he was appointed mathematician to the states of upper Austria. In 1613, with a new emperor, he advocated the introduction of the Gregorian calendar, but was frustrated by antipapal prejudice. During this year, he married Susanna Reutlinger, his first wife having died two years earlier.

Kepler extended his planetary laws to the satellites of Jupiter in the *Epitome astronomiae Copernicanae* published in parts between 1618 and 1620−1621. He published his third planetary law connecting the periods and mean distances of the planets in 1619 in his *De Harmonice Mundi* with which his great contributions to astronomy were completed.

In sum, Kepler's three laws are as follows (Cajori, 1929; p. 34): (1) Each planet moves in an ellipse, having the Sun in one of its foci; (2) The radius vector joining the Sun with a planet moves over equal areas in equal times; (3) The square of the times of revolution of any two planets are proportional to the cubes of their mean distance from the Sun, i.e., $T^2 : T_1^2 = D^3 : D_1^3$. It was conjectured by Newton, and also by Hooke and others, that if Kepler's third law was true, then the attraction between the earth and other members of the solar system varied inversely as the square of the distance. The accuracy of Kepler's third law was doubted at that time. To show that the above conjecture was true required the genius of Newton (Cajori, 1929; p. 64).

In 1628, Kepler and his family moved to Silesia, where he continued to work. On November 15, 1630, in Ratisbon (Regensburg), Kepler died while visiting a meeting of imperial electors (Voelkel, 1999; p. 135), leaving behind him achievements that changed astronomy and ensured his permanent fame.

## References

Abell, G.O., 1975. Exploration of the Universe, third ed. Holt, Rinehart, and Winston, New York. 738 pages.

Affleck, S.B., Kirkham, D., Buchele, W.F., 1976. Seedbed preparation for optimum temperature, moisture, aeration and mechanical impedance. In: Proceedings of the 7th Conference of the International Soil Tillage Research Organization, ISTRO. Report No. 45. Division of Soil Management, Agricultural College of Sweden, Uppsala, Sweden. S-750 07.

ASHRAE, 1967. Handbook of Fundamentals. American Society of Heating, Refrigerating and Air-Conditioning Engineers, New York, NY, 544 pp.

Bennett, R., 1978. Sun Angles for Design. Robert Bennett Architect and Engineer, Bala Cynwyd, Pennsylvania, 76 pp.

Cajori, F., 1929. A History of Physics. Macmillan, New York.

Fons, W.L., Bruce, H.D., McMasters, A., 1960. Tables for Estimating Direct Beam Solar Irradiation on Slopes at 30°–46° Latitude. Pacific Southwest Forest and Range Experiment Station, Forest Service, United States Department of Agriculture, Berkeley, California, 298 pp.

Glickman, T.S., 2000. Glossary of Meteorology, second ed. American Meteorological Society, Boston, Massachusetts. 855 pp.

Heyne, E.G., 1956. Earl G. Clark, Kansas farmer wheat breeder. Trans. Kans. Acad. Sci. 59, 391–404.

Kirkham, M.B., 1982. Orientation of leaves of winter wheat planted in north-south or east-west rows. Agron. J. 74, 893–898.

Kirkham, M.B., 1984. Leaf orientation, light reception, and growth of winter wheat. Crop Sci. 24, 925–928.

Kirkham, M.B., 1986. Theoretical consideration of direct-beam solar radiation on plants leaves. Int. Agrophys. 2, 53–58.

Kirkham, M.B., Smith, E.L., 1984. Solar intensity on winter wheat leaves. Field Crop. Res. 8, 297–306.

Kondratyev, K. Ya, 1977. Radiation Regime of Inclined Surfaces. Tech. Note 152, WMO No. 467. World Meteorological Organization, Geneva, 82 pp.

Lee, R., 1963. Evaluation of Solar Beam Irradiation as a Climatic Parameter of Mountain Watersheds. Colorado State University Hydrology Paper 2, Fort Collins, Colorado, 50 pp.

Ronan, C.A., 1971. Kepler, Johannes. Encyclopaedia Britannica 13, 309–311.

Sobel, D., 2007. Longitude. The True Story of a Lone Genius Who Solved the Greatest Scientific Problem of His Time. Walker Pub. Co, New York.

Vestine, E.H., 1971. Geomagnetism. Encyclopaedia Britannica 10, 179–185.

Voelkel, J.R., 1999. Johannes Kepler and the New Astronomy. Oxford University Press, New York and Oxford.

Webster's New World Dictionary of the American Language, college ed., 1959. World Publishing, Cleveland.

# Index

*Note*: Page numbers followed by "f" indicate figures; "t", tables; "b", boxes.

A
Abaxial phloem, 282
Abaxial side of leaf, 443–444
Abrasion of cuticle, for in situ hygrometer, 323
Abrasion of soil, to reduce soil repellency, 216
Absolute zero, 311–312
Absorptance, 456
Absorption, 455–456
  gravity-free, 205
  representative rays, 459f
  water, 270
Accessory cells, 431
Acoustic waves, 97
Acquired immune deficiency syndrome, 3
Actual evapotranspiration, 508f
Actual velocity, 88, 230
Adaxial phloem, 282
Adaxial side of leaf, 411
Adsorption, 38
  errors, 318–319
Advection, 464, 509
Adventitious roots, 260
Aerenchyma, 280–282, 411–412
Agriculture Research Service (ARS), 480–481
*Agrostis palustris* (creeping bent grass), effect of soil aeration and temperature on, 195
AIDS (acquired immune deficiency syndrome), 3
Air pressure potential, 46–47
Air-entry value for tensiometer, 54
Air, components of, 187t
Albedo factor, 465, 466t–467t
Alfalfa (Lucerne), 502
  crop-water-stress index, 488–489
  de Wit analysis, 516, 517t
  definition of potential evapotranspiration, 501
  evapotranspiration, 502f
  osmotic potential of, 294
  root water uptake rate, 140
Ampere (amp) (unit), 21
Amphistomatous leaf, 432
Analogues, electrical, 5
Analogy, 392–394
Anatomy
  of root, 262–263
  of stem, 250–251
  of stomatal, 432–434
Angiosperm, families with 4 photosynthetic pathway, 414
Angle of contact, 75–76
Ångstrom (unit), 29–30
Ångström, Anders Jons, 29–30
Anions, 188–189
Anode, 188
Antecedent soil water content, 212–213
Anthocyanin, 438
Antitranspirants, 443
Apollonian curves, 94–95
Apollonius of Perga, 97–98
Apoplast, 248
Apparent dielectric constant of soil, 108
Apparent probe length, in time domain reflectometry, 108
Apparent solar time, 540
  irregular rate of, 542–543
  standard time from, 544
Aquatic plants, 431–432
*Arabidopsis thaliana*, 435–436
Army Corps of Engineers, U.S., cone penetrometer, 175
ARS. *See* Agriculture Research Service
Ascent of water in plants, 347
  barometric height, 347
  cohesion theory, 349–352
  soil–plant–atmosphere continuum, 365–368
  tall buildings and animals, 347–348
    electrical pumping systems, 348
    gravitational gradient, 348

Ascent of water in plants (*Continued*)
    net filtration pressure, 349
    peripheral circulation features, 348–349
    pressure measurements, 348
Aspartic acid, 413–414
Astronauts on moon, weight of, 178
Astronomical unit (AU), 21–22, 30
Available water (AW), 153, 160
  influenced on potential evapotranspiration, 155
  lower limit, 157
  soil moisture contents, 161t
  upper limit, 153
  volume of bulk soil, 160
Average pore velocity, 230
Axial system of cells in secondary xylem, 283
Azimuth, 535

B
Back wall, 437–438
Balancing pressure, 289, 334–335
Balun (time domain reflectometry), 111–112
Bandpass (filter), infrared thermometers, 518
Bar (unit), definition of, 19
Barley, transpiration and yield, 518, 519f
Barrow, Isaac, 25
Barrs and Weatherley, method to determine relative water content, 298–299
Base units, 21, 21t
Basswood (*Tilia europaea*), 432
Bazin, Henri Émile, 100
Beets, water use, 160–161
Bell pepper (*Capsicum frutescens* L.), 417
Bicollateral arrangement of vascular bundles, 282
Birch, water content of, 255
Bird's foot trefoil, stem anatomy, 279–280, 280f
Birdsfoot trefoil (*Lotus corniculatus* L.), 417
Bismuth thermocouple, thermoelectric power, 315
Black body, 455–458
  absorbing, 456
  example, 458
  hole in wall, 459f
  power radiation, 460f
  radiant energy, 457f
  solid lines, 461f
  spectrum, 460–461
  spherical bodies, 456f
  temperature, 459
Black death, 2
Black surface, 458
Black-body radiation, 458
Blackman growth curve, 8, *see also* Soil-plant-water relation
  dry weight *vs*. time logarithm, 10–11
  efficiency index, 9
  exponential equation, 9
  factors, 8
  logarithmic dry matter accumulation curve, 10f–11f
Blunt, 23
Bodleian library, 98
Boltzmann, Ludwig, 470–472
Bordered pit, 361
Bose, Satyendra Nath, 364–365
Bose, Sir Jagadis Chunder, 364–365
Bose–Einstein condensation, 364–365
Bound water, 158–159
  plant, 158–159
  soil, 217–218
Boundary layer, 439–440
Boundary-layer resistance, 440–441
Bovine spongiform encephalopathy (BSE), 3
Boyer, John Strickland, 343–344
Boyle, Robert, 426
Breakthrough curve, 230–231
  characteristic of unsaturated soil, 233f
  chloride
    for Aiken clay loam, 234f
    for Oakley sand, 234f
  flow in tube, 233f
  for piston flow, 232f
  pore velocities, 233f
  tritium, 234f
Briggs, Dr Lyman James, 164–167
Briggs and Shantz, 153, 156, 164–167
British thermal unit (Btu), 20
Bromide, as tracer, 219
Brown and Escombe, diffusion through small openings, 435
BSE. *See* Bovine spongiform encephalopathy
Bubonic plague. *See* Black death
Buck formula, 316
Bulk density, limitations for plant growth, 161

Bulk modulus, 420
Bulliform cells, 412–413
Bundle sheath, type of photosynthesis, 413
Bundle sheath extension, 409–410
Bunsen, Robert Wilhelm, 469

## C

$C_3$ plants. *See* Three-carbon compound plants
$C_4$ plants. *See* Four-carbon compound plants
Cactus, determination of wilting point, 156
Calcium sulfate, 63–64
Calibration, 134–135, 317–318
Calorie (cal), 19–20
Calvin-Benson pathway, 413
Cambium, importance in cohesion theory, 378
Campbell Scientific (company), 113, 182
Canny's theory, 360
Canopy temperature, 490
Canopy-minus-air temperature, 486–488
Capacitor, 103–104
Capillary attractiveness, to keep chemicals near soil surface, 220–221
Capillary fringe, 82–83
Capillary potential, 42
Capillary rise equation, 207–208
Capillary tube
  height of rise, 74
  Poiseuille's law, 95
  rise and fall of water in, 79
*Capsicum frutescens* (pepper), diurnal cycle of water potential, 417
  potentials of, 417
Carbon dioxide fixation, 413
Cardinal properties, 302
Casparian strip, 245–246, 248f
  in cortex, 282
  endodermis characterization, 249
Cathode, 188
Cations, 188–189
Cauchy, Baron Augustin, 99–100
Cavitation
  in cohesion theory, 356
  definition of, 54, 362–363
  monitored by acoustical method, 357
  with pressure probe, 360
Celestial equator, 538
Celestial sphere, 533
Cell membrane, pressure gradient, 257
Cell phones, frequency of, 106–107
Cell wall, importance in cohesion theory
  leaf xylem, 356
  matric potential, 356
  unevenly thickened in guard cells, 282
Center of gravity, 44–45
Center of mass. *See* Center of gravity
Centimeter-gram-second (CGS), 42–43
  absolute system, 16
  dyne-s in, 174
Central Standard Time (CST), 543–544
Centrifugation, to measure tensile strength of water, 354–356
CGPM. *See* General Conference on Weights and Measures
CGS. *See* Centimeter-gram-second
Champollion, Jean François, 428–429
Chloride breakthrough curves, 234f
Chlorophyll a, wavelengths of, absorption, 238
Chlorophyll b, wavelengths of, absorption, 238
Chloroplasts, 409–410, 413–414, 438
Chord, 91
Christie, Samuel Hunter, 403
CI. *See* Cone index
Circle, equation of, 92
Citrus (orange), 245
Clausius, Rudolf Julius Emanuel, 307
Clausius–Clapeyron equation, 302–303, 316
Clay, effect on field capacity, 318
Clothesline effect, 509, *see also* Oasis effect
Coaxial cable, 109–111, 110f
Cobalt-chloride paper, 444
Cohesion theory, 349
  alternative theories, 360
    cavitation, 362–363
    long-distance water transport, 361
    pit cavity, 361
    pit membrane, 361
    pressure probe, 361
    watergates, 361
  ascent of sap, 351–352, 351f
  controversy about, 364–365
  diffusion of water, 352
  hydrogel, 364
  limitations, 352–353
    air blockage, 357
    dead xylem tissue, 356
    differences in hydrostatic pressure, 355f
    dye experiments, 356–357

Cohesion theory (*Continued*)
    heat of fusion, 353
    hydrogen bonds, 353–354
    root pressure, 358–360
    Scholander's experiments, 358f
    structure of ice, 353
    tensile strength, 353
    Ursprung's values, 354–356
    water columns in xylem tissue, 356
    Z-tube, 354, 355f
  mangroves, 349, 350f
  plant–atmosphere continuum, 363–364
  SEM technique, 364
  xylem tissue, 349–350
Colding equation, *see also* Ellipse equation
Collateral arrangement of vascular bundles, 282
Collenchyma, 282
Colligative property, 302
Commelinaceae (spiderwort family), 280–281
Commercial cable tester (time domain reflectometry), 108, 111
Compensating-pressure theory, 360
Compressibility of substance, 420
Concentration gradient, in Fick's law, 442
Condenser, 103–104
Conductance, 397, 441
Cone index (CI), 175
Cone penetrometer, 175, 177f, *see also* Penetrometers
  applications, 179
  CI readings, 175
  conversion factors, 177
  dial gauge, 176–177
  differences in readings, 179
  gravity constant, 178
  military training, 180
  parts of, 175–176
  physical soil degradation, 179–180
  uses, 179
  value in kilograms, 178
Conifer, 300
Constant-heating method, 382
Constant-rate stage, 505–508
Constantan-chromel thermocouple, thermoelectric power, 315
Contact angle, 74
Contact sand, 209
Continuous wave, 104–105
Convection, 135–136
Cooke, William Fothergill, 403
Copernican system, 551–552
Coriolis effect, 44–45
Corn
  growth, 9
  de Wit analysis, 516–517
  and potential evapotranspiration, 505–508
  stem anatomy, 282
Cortex
  of root, 248
  of stem, 282
Cotton
  crop-water-stress index, 493–496
  leaf mesophyll, 411
  and potential evapotransprition, 505–508
  water potentials of, 318–319
  Young's modulus of fiber, 425–426
Coulomb (unit), 189
Coulomb, Charles Augstin de, 189
Council for Industrial and Scientific Research (CSIRO), 223–224
Counterradiation, 465
Creeping bentgrass, effect of soil aeration and temperature, 196f
Creutzfeldt-Jacob disease. *See* Bovine spongiform encephalopathy (BSE)
Creutzfeldt-Jakob disease. *See* Bovine spongiform encephalopathy (BSE)
Critical stages of growth, 504–505
Crop water stress index (CWSI), 483
  for alfalfa, soybeans, and cotton, 493–496
  calculation, 493
  canopy temperature, 490
  environmental parameters, 489
  leaf–air temperature difference, 489f
  non-water-stressed baseline, 489–490
  ratio of vertical distance, 492–493
  saturated vapor pressure, 490–492
  SDD, 488–489
Crop water-use efficiency, 526
  conditions, 526–528
  crop breeding, 528
  under elevated carbon dioxide, 529–530
  partitioning, 528
  photosynthetic systems, 528–529
  transpiration efficiency, 528
Crushing tissue to determine osmotic potential, 285–286
Cryoscanning electron microscope (SEM), 364
Cryptopores, 206–207

CSIRO. *See* Council for Industrial and Scientific Research
CST. *See* Central Standard Time
Cucurbitaceae (squash family), 282
Cultivar, definition of, 259
Cumulative infiltration, 202–203
Cuticle cells, 409–410
Cuticular resistance, 440
Cutin material, 409–410
CWSI. *See* Crop water stress index
Cycle, 104
Cylinder, hollow, flow in (Gardner's root equation), 268
Cyperaceae (sedge family), 433–434

## D

Darcy, Henry Philibert Gaspard, 98–100
Darcy velocity, 88, 229
Darcy's law, 87–88, 87f
  from Laplace's equation, 89–90
Davy, Sir Humphry, 197
de Wit, Cornelius Teunis, 530–531
de Wit's analysis, 515–516
  experimental estimation, 517t
  mean daily pan evaporation, 516
  nutrient level, 516
  water-use efficiency, 516
Decagon Devices (company), 143–144, 210, 216
*Déficit de saturation hydrique* (DSH), 298
Deficit irrigation, scheduled with pressure chamber, 341
Density, of stomata, of water, 434
Derived units, 21, 22t
Dermal tissue system, 279
Desert survival still, 481
Dew point temperature depression, 302–303
Dew-point technique, 325f
Dew-point temperature, calculation of, 302–303
Dew, 464
Dewpoint hygrometers, 321–322, 325f, *see also* In situ hygrometers
Diameter law, 435
Dicots, 432–434, 433f
Dicotyledonous
  leaves, 409–411, 410f
  roots, 245–246, 246f
Dicotyledons
  leaf anatomy, 410–412
  root anatomy, 245–246
  stem anatomy, 282
  stomatal anatomy, 432, 434
Dielectric
  characterization of, 106
  in coaxial cable, 109–110
  definition of, 37
Dielectric constant, 37, 103–104, 106–107
  soil water content measurement, 107–109
Dielectric constant, definition of, 37, 103–104, 106
Diffuse porous wood, 255
Diffuse radiation, 250
Diffusion, 97
  of gases, 435–436, 436f
  porometer, 448–449
  porometry, 445–446
  theory, 442
Diffusion coefficient of oxygen in air, 186–187
Diffusion coefficient of oxygen in water, 186–187
Diffusion porometry, 445–446
  theory, 446–448
Diffusion pressure deficit (DPD), 284, 367f, 400
Diffusion through small pores (stomata), 435
Diffusivity
  Gardner's root equation, 267–268
  Green and Ampt model, 204
Dijon, France, 98
Dipole, 28
Direct solar radiation, 465
Direct-beam solar radiation
  altitude and azimuth angles of Sun, 549–551
  interception, 544–545
    leaf angles, 546
    leaf orientation and angle relation, 547t
    plant leaf, 549
    sloping surface, 545
    solar altitude angle, 547–548
    solar azimuth, 545
    Sun's angles, 545
    winter wheat cultivar, 548–549
  principles of astronomy, 533
  Sun's rays, 533
Disc permeameter. *See* Tension infiltrometer
Discontinuous emptying of soil pores, 81–82
Diurnal cycle of water potential, 366–367

Dixon, Henry Horatio, 368
Dixon and Joly, cohesion theory, 352
Douglas fir, measured with pressure chamber, 355f
DPD (diffusion pressure deficit), 284, 367f, 400
DPHP technique. *See* Dual-probe heat-pulse technique
Drainage equation (ellipse equation), 93–94
Drought, terminal, 258
DSH. *See Déficit de saturation hydrique*
Dual thermal probe technique. *See* Dual-probe heat-pulse technique
Dual thermal probes, 123
  gravimetric method, 124
  Jaeger and, 145–148
  soil hydraulic character, 123
  soils thermal properties, 126–127
Dual-probe heat-pulse technique (DPHP technique), 123–125, 125f
  advantages, 133–134
  calibration, 134–135
  commercially available equipment, 143–145
  convection, 135–136
  de Vries's equation, 130
  electrical conductivity measurement, 136–137
  errors, 132–133
  example calculation, 130–131
  hydraulic lift, 143
  meaning of Q, 131
  particle density, 129
  roots in soil, 139–140
    drying cycles, 142f
    fibrous root system, 140
    plant physiological, 143
    temperature in soil, 141f
    turf grass study, 140
    volumetric water content, 141f
  soil surface measurement, 135
  soil water movement determination, 137–139
  temperature sensor, 127
  thermal conductivity, 127
  volumetric heat capacity, 128, 130
  water content measurement, 132
Dye experiment, in cohesion theory, 356–357
Dynagages, 382
Dynamax (company), 388
Dynamic diffusion porometer, 446–448
Dynamic penetration test, 172
Dyne unit, 16
Dyne-cm, 18

## E

Early wood, 284
Earth
  crust formation, 369–370
  equator, 538
  population, 1
  spins, 44–45
  temperature, 462
Eastern Standard Time (EST), 543–544
Echo from waveguide, 108
Efficiency index, 9
Elastic limit, 420
Elasticity, 97
Electrical analog, 397–398, 398f
Electrical conductivity units, 397
Electrical resistance sensors, 63–64
Electrode poisoning, 195–196
Electrodynamics, 97
Electrolysis, 188, *see also* Oxygen diffusion rate (ODR)
  anions, 188–189
  cations, 188–189
  Faraday's laws, 189
Electromagnetic waves, 97, 118–119
Electrostatics, 97
Ellipse equation, 90, *see also* Laplace's equation
  Apollonian curves, 95
  ellipsoid, 92, 93f
  homogeneous soil, 94f
  line segment, 91
  modified Colding equation, 94
  oblate ellipse, 91, 92f
  prolate ellipse, 91, 92f
  soil drainage need, 93–94
  in soil-water relation, 94
  subsurface drain problem, 93f
Emissivity of surface, 460
Emittancy, 474–475
End correction, stomatal resistance measurements, 448–449
Endodermis, 248–249, 249f
Energy, 18
English gravitational system, 16
Epidermal resistance, 440–441
Epidermis
  of grass leaf, 412–413

- of leaf, 445
- or stem, 281
- of root, 245
- xerophytes, 409

Epistomatous leaf, 432
Equation of continuity, 89–90
Equation of time, 542–543, 543f
Equilibrium condition, heads in a column of soil, 49
Equilibrium pressure, 288
Equinox, 534
Equivalent weight, 189
Erg, definition of, 18
Ergastic substances, 250–251
Ergmeter, 53, *see also* Tensiometer
Esau, Katherine, 262–263
- Certificate of Merit, 264
- electron microscopy, 263
- phloem in dicotyledons, 263
- textbooks, 263–264

*Escherichia coli* (*E. coli*), 6
EST. *See* Eastern Standard Time
Euler's constant, 267–268
Evaporation, 435
- in cohesion theory, 360
- in heat budget, 464

Evapotranspiration (ET), 155, 501, *see also* Potential evapotranspiration (PET)
- energy balance, 504f
- equation, 486
- leaf area index and, 503f
- from lysimeters, 502f

Evapotranspiration, 155
- related to canopy-minus-air temperature, 486–488

Extended surface, for potential evapotranspiration, 501–502

## F

F.O.V. *See* Field of view
Falling water table, 80–81
- maximum tension exerted on water in soil pore, 81
- variable diameter soil pores, 82f

Falling-rate stage, 505–508
False endpoints, pressure chamber, 339
Faraday (unit), 189
Faraday, Michael, 196
- chemical discovery, 198
- connection with scientific work, 198
- Davy's jealous opposition, 197
- electric and magnetic force, 198
- electricity, 198
- fundamental relations, 199
- journeyman bookbinder, 197
- scientific books, 197

Faraday's laws of electrolysis, 189
Fascicular (vascular) tissue system, 279
- interfascicular region, 248

FC. *See* Field capacity
Fechner, Gustav, 402
Fescue grass, and evaporation, 508
Fetch, 501–502
Fiber-tracheid, 250
Fiber, 410–411
- Young's modulus, 424–425

Fick, Adolf Eugen, 449
Fick's law, 442
Field capacity (FC), 153, 154f
- influencing factors, 154–155
- matric potential, 156
- moisture equivalent, 153
- obsolete, 155
- pot capacity, 155

Field of view (F.O.V.), 474
Filter, infrared thermometer, 475
First permanent wilting point, 156–157
Flowering plants, 349–350
Flowers, stomata on, 431–432
FLP. *See* Four Lips
Fluid flow, 97
Flux, 229–230
Flux density. *See* Flux per unit cross-section
Flux per unit cross-section, 88, 137, 230
Focal chord, 91
Foci point, 90–91
Foliage temperature. *See* Canopy temperature
Foot-pound (ft-lb), 18
Force, 15
- Newton's laws of motion, 15–16
- units of, 16

Forest soils, repellency of, 216
Four Lips (FLP), 435–436
Four-carbon compound plants ($C_4$ plants), 413–414
Fourier's heat flow law, 34
Frankel, Otto, 223–224
Free water evaporation, and potential evapotranspiration, 501
Freezing, 36–37
Freezing tissue to determine osmotic potential, 294
Frequency domain, 106–107

Fresnel, Augustin, 429
Frost protection, 33
Fruit, stomata on, 431–432
ft-lb. *See* Foot-pound
Fundamental tissue system, 279
Fungi, water potential of, 354

G
Galvanometer, 394–395
Gardner, Wilford Robert, 275
  memoirs in volumes, 276
  recognitions, 276
  seminal work, 275
  University of Wisconsin, 275
Gardner soil, 275
Gardner, Walter H., 275
Gardner, Willard, 275–276
Gardner's equation, 267–268
  assumptions, 269
  examples, 270–271
  matric potential, 269, 273
  Richards equation, 268f
  root distribution effect on wilting, 274
  root radius effect, 272
  steady-state solution for flow, 268
  suction at root–soil boundary, 273f
  values for rate of water uptake, 269–270
  wet and dry soil effect, 271, 272f
Gauss's law, 95
GDD. *See* Growing-degree-day
GED. *See* General equivalency degree
General Conference on Weights and Measures (CGPM), 20
General equivalency degree (GED), 52
Gibbs, Josiah Willard, 471
Gigahertz (GHz), 106
Giraffe, rise of fluids in, 349
Global radiation, 465
*Gossypium* (cotton), leaf meosphyll, 411
  water potentials of, 493–496
Gradmann, H., 391–392, 398–399
Gram-equivalent weight, 189
Gramineae (obsolete term), grass family, 433–434. *See* Poaceae
Grand period of growth, 7–8
Grape, hydrostatic pressure, 354–356
  leaf palisade, 411–412
Grass leaf, 413–414
Gravimetric heat capacity, 126
Gravimetric method, 124
Gravitation head, 48–49, 210
Gravitational potential, importance in infiltration, in plants, 45
Gravitational potential energy, 45
Gray body, 459–460
Greek tetraedros, 28
Green and Ampt equation, 203–205, *see also* Lewis equation
Ground tissue system, 250–251, 279–280
Growing-degree-day (GDD), 484
Growth layers of wood, 284
Growth, critical stages of
  exponential, 5–7
  importance to measure, 5–7
Guard cells, 436–438
Gymnosperm, 357–358

H
Hales, Stephen, 351–352
Hatch-Slack photosynthetic pathway, 413–414
Head, definition of, 48
  used to determine hydraulic conductivity with tension infiltrometer, 211–215
Heads in column of soil, 48–50
Heart pump, 348–349
Heartwood, 378
Heat
  budget, 463–465
  capacity, 126
  conduction, 33–34, 97
  of fusion, 32–33
  physical unit, 19–20
  of vaporization, 32
Heat-balance method, 381
  heat down, 383–384
  heat up, 383
  of heated stem segment, 382f
  radial flow, 384–386
  uses for herbaceous plants, 382
  uses for trees, 381–382
Heat-pulse method, 375–376, 376f
  advantages, 379–381
  in apple tree, 379f
  compensation, 377
  disadvantages, 381
  heat-pulse velocity, 377–378
  in kiwifruit vine, 380f
  miniature sap-flow sensor, 381f
  sap velocity, 378
  T-max heat-pulse method, 379
  thermistors, 377
Heat, definition of, 19–20

Hegelianism, 402
Height of plant, influence on potential evapotranspiration, 502–504
  on roughness, 508–509
Height of rise in a capillary tube, 74–76, 75f, 79–83
*Helianthus annuus* (sunflower), use to determine wilting point, 156
  water potentials of, 156, 417
Helmert's equation, 43
Helmholtz, Hermann Ludwig Ferdinand von, 118–119
Henry, Joseph, 402
Herbaceous plants, 375, 381
  constant-heating method, 382
Hertz (Hz), 104
Hertz, Heinrich Rudolf, 118–119
Hertzian waves, 104
Heterostomatous leaf, 432
Hieroglyphics, 428–429
High-pressure gas, danger of, 340
High-voltage engineering, 95
Hinge cells, 412–413
Höfler diagram, 285f–286f
Hooghoudt's modification of the ellipse equation, 94
Hooke, Robert, 426–427, *see also* Newton, Isaac
Hooke's law, 420
Horizon system, 535
Horse chestnut (*Aesculus hippocastanum*), 432
Horsepower-hour (hph), 19
Horton equation, 203
Hour angle, 535, 543
HP. *See* Hydrostatic pressure
hph. *See* Horsepower-hour
Huygens, Christian, 426–427
Hydraulic
  conductivity, 87–89, 201
  gradient, 66–67, 88
  head, 47–49
  lift, 143
  press, 340–341
Hydraulic conductivity, unsaturated, 123, 203–204, 211
  Gardner's root equation, 124, 127, 130, 272f
  measured with tension infiltrometer, 123, 207–208
Hydraulic resistance of roots, 258
Hydrogen bonding, 28–29, 29f
Hydrophyte, 245, 409
Hydrophyte, stem anatomy, 280–281
Hydrostatic pressure (HP), 253, 287
  changes in xylem, 367
  development in vascular cylinder, 246–248
  differences in, 355f
  potential, 46–48
Hydrostatics, 253
Hygrometer, 311–312, 323f
Hypodermis, 245
Hypostomatous leaf, 432
Hysteresis, 81

I

Ideal gas constant, 289–290, 311
Idso, Sherwood B., 497–498
Immobile water, 217–218, 218f
Impedance matching transformer, 111–112
Impulse, 174
In situ hygrometers, 322, 322f
Incident radiation, 456, 458
Incoming radiation, 465
Infiltration
  downward movement, 201
  Green and Ampt equation, 203–205
  Horton equation, 203
  Lewis equation, 202–203
  minidisk infiltrometer, 210–211
  Philip infiltration model, 205
  rate, 201
  redistribution, 206
  two and three-dimensional, 205–206
  water content profiles, 204f
  wetting front, 201–202, 202f
Infiltrometer, 123, 201
Influenza, 3
Infrared thermometers
  advantages, 478–479
    black-body temperature, 479
    canopies, 479–480
    high-value crops, 480
  black body, 474
  calibration, 478, 479f
  canopy temperature, 473
  hand-held, 480f
  leaves, 473
  using portable, 477–478
  principles, 475
    electromagnetic spectrum, 476t
    fluxes of energy, 477f

Infrared thermometers (*Continued*)
    radiometer, 475
    response, 476
    surface temperature calculation, 477
  radiant energy, 474–475
  spectral quantities, 475
  temperature measurement with, 474
Instrument for Reflectometry Analysis of Moisture in Soil (IRAMS), 117
Interfascicular tissue, 279–280
Internal plant resistance, related to potential evapotranspiration, 503–504
Internal water relations, 415
  cell solution, 416
  leaf relative water content, 418f
  matric and gravitational potentials, 417
  osmotic, pressure and water potential, 419f
  plant leaf-water potential, 418f
  solute concentration, 416–417
International System of Units (SI units). *See* Le Système International d'Unités
Intracellular solute concentration, 287
Intracellular water, 288f, 289
Intrinsic permeability, 89
Invisible college, 25
Ionization of water, 37
IRAMS. *See* Instrument for Reflectometry Analysis of Moisture in Soil
Irradiancy, 474–475
Irrigation frequency, Kansas, 510
Irrigation scheduling, based on stress-degree day, 484–485, 484f–485f
  with infrared thermometer, 478–480, 483
  with pressure chamber, 488–490
  with relative water content, 301
Irrigation, effects on crop quality, 526, 527t
Isopiestic thermocouple psychrometer, 319–320, 319f
Isostomatous leaf, 432
Isothermal conditions, measurements with thermocouple psychrometers, 318–319
Isotropic soil, 89

## J

Jackson, Ray Dean, 480–481
Jaeger, John Conrad, 145–148
Jensen Instruments, 193
Jet fill tensiometer, 59f
Joly, John, 369–370
Joly's theory of crust formation, 369–370
Joule, James Prescott, 326–327
  flow of electricity, 327
  Joule heating, 313–315
  paddle-wheel experiment, 327
Joule, definition of, 313–315

## K

KanKing winter wheat cultivar, 548–549
kcal. *See* Kilocalorie
KD2 PRO instrument, 143–144
Kekulé von Stradonitz, Friedrich August, 306
Kelvin, Baron William Thomson, 327
  dynamical theory of heat, 328
  experimental science, 327–328
  Kelvin equation, 311
  physical science, 328–329
  sounding apparatus, 328
Kepler, Johannes, 551
  *Astronomiae pars optica*, 552–553
  Copernican ideas, 553
  education, 551
  Maestlin influence, 551–552
  mathematics, 552
  planetary laws, 553
  regular motion, 553
Kilocalorie (kcal), 20
Kilogram-calorie (kg-cal). *See* Kilocalorie (kcal)
Kilowatt-hour (kWh), 19
Kirchhoff, Gustav Robert, 468
  contributions to experimental and mathematical physics, 468–469
  principle of radiation, 458
  radiation, 469–470
  theory of spectrum analysis, 469
Kiwifruit vine (*Actinidia deliciosa*), 378–379, 380f
Kostiakov equation for infiltration, 202–203
Krilium, 78–79
kWh. *See* Kilowatt-hour

## L

L.A. Richards Kids (Lark), 68
Laboratory-built tensiometer, 57–58
*Lactua sativa* (lettuce), leaf mesophyll, 411
Laminar flow, 89, 253–254
Laminar sublayer. *See* Boundary layer
Langley (unit), 4

Langley, Samuel Pierpont, 4
Laplace, Pierre Simon, 83–84
  equation, 89–90
  theory, 72–73, 73f
Late wood, 255, 284
Latent heat, 32
  of fusion, 32
  of vaporization, 464
Latitude, effect on transpiration and yield, 518–519
Latus rectum, 91
Law of resistance, 395–397, 396f
Le Bel, Joseph Achille, 306
*Le Système International d'Unités*, 20
  base units, 20, 21t
  CGPM goal, 20
  derived units, 21, 22t
  normalization, 23
  for pressure, 19
  supplementary units, 21–22
Leaf anatomy, 409
  dicotyledonous leaves, 409–411, 410f
  grass leaf, 413–414
  monocotylendous leaves, 411–413, 412f
  photosynthesis, 413–414
  xerophytic adaptations, 414–415
Leaf area index, 502–503
Leaf elasticity, 419–420
  elastic limit, 420
  Hooke's law, 420
  to plant leaves, 421–422
    elastic constants, 425t
    moduli of, 424t
    pressure potential, 421f
    pressure-volume curves, 426
    relative area of leaf disks, 422f
    relative diameter, 423, 424f
    relative water content, 423f
    wilting, 425–426
Leaf resistances, 440
  antitranspirant, 443
  diffusion theory, 442
  parallel circuit, 441
  photosynthesis, 442–443
  resistances in seconds, 443f–444f
  resistors in series, 441f
Least limiting water range (LLWR), 162–164, *see also* Nonlimiting water range (NLWR)
Leaves of cotton (*Gossypium hirsutum* L.), 417
Leibniz, Wilhelm, 25–26
Length elasticity, 420
Lenz, Heinrich, 402
Lettuce, leaf mesophyll, 411
Lewis equation, 202–203
Leyden jar, 118f
Lianas, Scholander's measurements, 357
Libriform fiber, 250
*Ligustrum* (privet), leaf palisade, 411
Lilac, leaf anatomy, 409–410, 410f
Linear flow laws, 95–97
Lines of flow, 435
Linnaeus, Carolus (von Linné, Karl), 6
Liquid water, 31t
LLWR. *See* Least limiting water range
Log period of growth, 7–8
Logarithms
  inventor of, 6–7
  rules of, 7
Lone-pair electrons, 28
Long-wave radiation, 454–455
Longitudinal strain, 420
Lorentz, Hendrik Antoon, 471
*Lotus corniculatus* (birdsfoot trefoil)
  stem anatomy, 417
  water potentials of, 417
Lower limit of available water, 157
Lower vascular plant, 282, 431, 434
Lucerne. *See* alfalfa
Ludwig, Carl, 449
*Lycopersicon esculentum* (tomato), leaf mesophyll, 411
Lysigenous, 411–412

**M**
Macropores, 206–207
Mad-cow disease, 3
Magnetostatics, 95
Malate, 439
Malic acid, 413–414
Mangrove, 349
Marketable yield, and water, 524
Mass, 16–17
Mass-flow
  porometer, 448
  porometry, 445, 445f
Massachusetts Institute of Technology (MIT), 77
Matric potential
  associated with nonlimiting water range, 161–164
  associated with tension infiltrometer, 138–139

Matric potential (*Continued*)
  associated with wilting point, 156–160
  Gardner's root equation, 157, 269
  for Green and Ampt infiltration, 203–205
  importance in infiltration, 201–204
  importance of cell wall's in cohesion theory, 356, 360
Matric potential energy, 42
  acceleration, 45
  CGS system of units, 42–43
  Coriolis effect, 44–45
  Helmert's equation, 43–44
  osmometer, 46f
  tensiometer, 42
  universal gravitation principle, 44
Matric suction, 42
Maximum dimensionless temperature difference (MDTD), 137
Maxwell, James Clerk, 198, 471
mb. *See* millibars
MDTD. *See* Maximum dimensionless temperature difference
Mean solar time, 542
Mechanical resistance, limitation for plant growth, 161–163
Megahertz (MHz), 106
MegaPascal (MPa), definition of, 42–43
Meniscus, 75–76
  in cohesion theory, 288
  concave, 75–76
  convex, 75–76
  of sap in pressure chamber, 289
Mercury manometer, 57, 58f
Mercury, density of, 54
Meridians, 534
Meristematic region of root, 243–245
Mesophyll. *See* palisade mesophyll; spongy mesophyll
Mesophyll resistance, 440, 443, 445
Mesophyte, 409
Mesopores, 206–207
Metaxylem, of wheat root, 246, 247f, 260
Meter-kilogram-second absolute system (mks absolute system), 16
Mho (unit), 397
Micropores, 206–207, 220–221
Microvoltmeter, 317–318
Middle lamella, 361
Midrib vein, 409–410
millibars (mb), 58–59
Minidisk infiltrometer, 210, *see also* Tension infiltrometer
  advantage, 211
  base, 210
  forces, 210
  water in under tension, 211
Miscible displacement, 238–239
MIT. *See* Massachusetts Institute of Technology
mks absolute system. *See* Meter-kilogram-second absolute system
Mobile water, 217f, 239
Mobility measurement, 216–217
  dry soil effect, 220–221
  hydraulic properties, 217
  longitudinal mobility, 220
  mobile fraction, 219f
  mobile–immobile water soil, 217–218
  pure water, 219
  tracer solution, 218
Modulus of elasticity, 420
Moisture characteristic curve, 79–80
Moisture equivalent, 153
Momentum, relation to impulse, 175
Monocots, 432–434, 433f
Monocotyledonous root, 246
Monocotyledons
  stem anatomy, 280–281
  stomatal anatomy, 432–434
Monocotylendous leaves, 411–413, 412f
Moon
  gravity on, 178
  weight on, 147
Mountain Standard Time (MST), 543–544
Multidimensional infiltration theory, 205
Multiperforate septum, 435
Multiplexer (time domain reflectometry), 112–113
Muscle pump, 349
Muskat, K., 89

## N

NaCl (sodium chloride)
  breakthrough curve, 230–232
  calibration solutions for thermocouple psychrometers, 317–318
Napier, John, 11–12
National Academy of Engineering, 224–225
National Academy of Sciences, 67, 181, 264, 276, 343–344, 530
Natural system, 7
NDVI. *See* Normalized difference vegetation index

Net radiation, 465–468
Netted-veined leaves, 434
Neutron-probe technique, 124
Newton (nt or N), 16
Newton, Isaac, 24
  arguments with Leibniz, 25
  building telescope, 25
  early life, 24–25
  last years, 26
  laws of motion, 15–16
  as president of Royal Society, 25–26
Newton-meter (Nm), 18
Nielsen, Donald Rodney, 239–240
  awards, 240
  professional program, 240
  soil-science research, 240
  water resources research, 240
  workshops, 240
Nighttime water potential, 285–286, 366–367, 503–504
NLWR. *See* Nonlimiting water range
Nm. *See* Newton-meter
Non-water-stressed baseline, 489–490
Nonlimiting water range (NLWR), 155, 161
  pedotransfer function, 164
  soil water content relationship, 162f
Normalized difference vegetation index (NDVI), 496
  drones, 497
  red and near-red IR reflectance bands, 496–497
Nuclear magnetic resonance imaging, 363–364
Null point, 319–320
Nutrition, and relation between transpiration and yield, 515–516

O

Oasis effect, 509
Oats, transpiration and yield, water use, 518, 518f
OBE. *See* Order of the British Empire
Oblate ellipse, 91, 92f
ODR. *See* Oxygen diffusion rate
OECD. *See* Organization for Economic Cooperation and Development
Ohm (unit), 95, 392–393, 398–399, 399f
Ohm, Georg Simon, 401–403
Ohm's law, 392–393, 399, 399f
Oil, effects on surface tension, 77–78
One-dimensional infiltration, 202–205
Opaqueness to infrared radiation, 34–35
Orchard soils, repellency of, 216
Order of the British Empire (OBE), 512
Organic matter, 154
  effect on field capacity, 128
  effect on time-domain reflectometry measurements, 109, 124
Organic soils
  repellency of, 215–216
  water content of, 297
Organization for Economic Cooperation and Development (OECD), 480–481
Osmolality, related to osmotic pressure, 302
Osmometer, 46, 46f, 302, *see also* Piezometer
  cardinal properties of solvent, 302
  colligative property, 302
  dew point depression, 302–303
  equation, 304
  vapor pressure depression, 303
  Wescor osmometer, 302–303, 302f
Osmosis, 289
Osmotic adjustment, 368
Osmotic potential, 45–46, 285–286, *see also* Turgor potential
  determination of in plants, 47, 285–286
  determined from pressure-volume curve, 287–291
  at full turgor, 292–293, 292f, 416
  xylem sap, 334–335, 349
  at zero turgor, 292–294, 292f
Osmotic pressure, 45–46, 289–290
  of guard cells, 438
  related to osmolality, 302
Ostwald, Wilhelm, 306–307, 471
Outgoing radiation, 465, 467
Overburden potential, 47
Oxaloacetic acid, 413–414
Oxidation, 188–189, 193
Oxygen diffusion rate (ODR), 162, 185
  bulk density *vs.*, 195f
  components of air, 187, 187t
  diffusion of gases, 186f
  electrical current, 191–192
  electrode poisoning, 195–196
  governing equations, 190
  Jensen Instruments, 193
  measurement system, 193
  microelectrode behavior, 190f
  model, 190

Oxygen diffusion rate (ODR) (*Continued*)
  oxidation potentials, 193
  oxygen availability, 187–188
  oxygen flux, 192
  phases, 186
  respiration by plant roots, 185–186
  *in situ* soil measurement, 194f
  soil aeration status, 195, 196f
  space in soil, 185f
  effect of tortuosity, 191

**P**

Pacific Standard Time (PST), 543–544
Palisade mesophyll, 409–410
Palisade parenchyma. *See* Palisade mesophyll
Palisade tissue, 411
Palm tree, 246
PAM. *See* Polyacrylamide
Pan evaporation, 516
Parallel resistance law, 262
  application to stomata, 434
Parallel resistors, 441, 441f
Parenchyma, 249–252
Partial derivatives, 253
Partial pressure of water vapor in air, 311, 315–316
  calculation of, 315–316
Pathological anatomy, 262–263
PE. *See* Potential energy
Peat soils, 216
Pedotransfer function, 164
Peltier, Jean Charles Athanase, 326
  Peltier effect, 313
  Peltier thermocouple psychrometer, 320, 320f
Penetrometers, 171
  measurements, 173–175
  relation of water content of soil, 174f
  spra-tainer can, 172f
  static and dynamic test, 172
  tilth, 171–172
  types of tests, 172–173
Penman, Howard Latimer biography, 512–513
Penman's concept of potential evapotranspiration, 501
Pepper
  diurnal cycle of water potential, 366–367
  water potentials of, 417
Perfect absorber, 458
Perfect radiator, 458
Perforation plate, 250
Period, definition of, 104
Periodic motion, 104
Permanent wilting point, 353–354
Permeability. *See* Hydraulic conductivity
PET. *See* Potential evapotranspiration
Petals, stomata on, 431–432
Pfeffer, Wilhelm Friedrich Philipp, 304–305
  awards, 305
  botanical institute in Leipzig, 305
  physiology lecture, 305–306
  plant physiology, 305
Philip, John Robert, 223
  American Geophysical Union, 225
  CSIRO, 223–224
  governmental science, 224
  Pye Lab, 224
  SPAC, 224
Philip infiltration model, 205
*Philosophiae Naturalis Principia Mathematica*, 25
Philosophimur, 25–26
Phloem, 250–251, 282
Photosynthesis, 413–414, 442–443
Physical units
  energy, 18
  force, 15–16
  heat, 19–20
  mass, 16–17
  power, 18–19
  pressure, 19
  weight, 16–17
  work, 17–18, 17f
Phytoremediation, 235–236, 432
Piezometer, 46–47, 53–54, *see also* Tensiometer
Piezometric potential, 46–47
Piston flow, 231–232, 232f
*Pisum sativum* (Pea)
  leaf mesophyll, 411
  water use, 516
Pit cavity, 361
Pit membrane, 361
Pit pair, 361
Pith
  of root, 245–246, 247f
  of stem, 245–246, 282, 386
Plagues, 3
Plant growth curve, 8, *see also* Soil-plant-water relation
  Blackman growth curve, 8–11
  exponential growth, 5–7

  - measurement, 5–7
  - sigmoid growth curve, 7–8, 8f
- Plant Moisture Stress (PMS), 341
- Plant water content, 297
- Plant water potential, 296–297
- Plant water stress index (PWSI). *See* Crop water stress index (CWSI)
- Plasmalemma, 257
- Plasmodesmata, 248
- Platinum microelectrode method to measure oxygen availability, 193
- PMS. *See* Plant Moisture Stress
- Poaceae (grass family), 280
  - photosynthetic pathway, 414
- Poise (unit), 38
- Poiseuille, Jean Leonard Marie, 261
- Poiseuille's law, 252
  - agronomic applications, 258
    - cultivar and variety, 259
    - limitations, 260–261
    - pressure drop in crops, 259
    - wheat breeding program, 260
    - wheat root, 258
  - assumptions, 253
    - fluid in Poiseuille, 254
    - mathematics, 254
    - Reynolds number, 253–254
  - calculations of flow, 254
    - cell membranes, 258
    - dilute solution, 257
    - interfibrillar spaces in cell wall, 256
    - pressure gradient in tree, 255
    - ring-porous wood, 255
    - vessel member, 257
    - xylem sap, 255
  - flux, 253
  - hydrostatic pressure, 253
  - partial derivatives, 253
  - viscosity, 252
- Polyacrylamide (PAM), 78–79
- Polyvinyl chloride (PVC), 125–126
- Ponca winter wheat cultivar, 548–549
- Poplar, contraction of trunk, 235–236, 379
  - phytoremediation, 432
  - stomata, 432
- Population (world), 1–3
- Pore space, 229
- Pore volume, 229
  - actual flow in tube, 231f
  - actual velocity of water, 230
  - average pore velocity, 230
  - breakthrough curve, 230–231
  - calculation of, 235–236
  - Darcy velocity, 229
  - flow in unsaturated soil, 232f
  - flux, 229–230
  - on length units, 237–238
  - mathematical analysis, 235
  - miscible displacement, 238–239
  - mobile water content and, 239
  - piston flow, 231f
  - saturated soil flow, 232f
  - soil column outflow experiment, 237f
- Porometer, 387–388
- Porosity, 88
- Portable infrared thermometer, 477–478
- Portable photosynthetic systems, 444–445
- Portsmouth collection, 26
- Pot capacity, 155
- Potamogetonaceae (pondweed family), 280–281
- Potassium chloride, calibration solutions for thermocouple psychrometers, 317
- Potassium, importance in stomatal opening, 438–439
- Potato
  - de Wit analysis, 515–517
  - leaf mesophyll, 282
  - phloem anatomy, 282
  - water potential of, 160–161, 161t, 181
- Potential difference (in resistors), 399, 441
- Potential energy
  - of air, 356
  - gradient in soil-plant-atmosphere, 498
  - gradient, 301
- Potential energy (PE), 18
- Potential evapotranspiration (PET), 501
  - actual transpiration rate, 507f–508f
  - alfalfa ET, 509t
  - constant-rate stage, 505–508
  - drying rate, 506f
  - example calculation, 510
  - extended surfaces, 501–502
  - falling-rate stage, 505–508
  - influence of crop height, 502
  - internal plant resistance, 503–504
  - leaf area index, 502–503
  - reference ET, 510
  - Rosenberg definition for, 501
  - for soil dryness and rooting depth, 506f
  - soil-water availability, 504–505
  - for sorghum, 511f
  - for winter wheat and corn, 511f

Pounds per square inch, changed to metric units, 175–176
Power, physical unit, 18–19
  units of, 18–19
Powers, William LeRoy, 51–52
Precipitation, in heat budget, 464
Preferential flow, 123, 206–207, 216–217
Pressure, 19
  plate, 56–57, 57f
  potential energy, 46–47
  to root, 23–24
  transducer, 64f
Pressure chamber, 333
  advantages and disadvantages, 336–337
    using high-pressure gas, 340
    low pressurization rates, 339
    rubber grommets, 340
    thermocouple hygrometers, 339
  commercially available, 338f
  and constant supply of gas, 340
  hydraulic press, 340–341
  leaf water potential, 334f
  pump-up, 341
  sap pressure in xylem of twig, 333f
  thermocouple psychrometer method, 333–334
  tuber water potential, 336
  xylem and leaf water potentials, 335f
Pressure head, 48–50, 53–54
Pressure membrane apparatus. *See* Pressure plate
Pressure potential, 46–47
Pressure probe, 295–296, 361
Pressure, definition of, 19
Pressure–volume curves, 279, 292f
  modulus of elasticity, 294
  osmotic potential, 292–293
  sap in dead cells, 294
  thawed tissue, 294
  upper graph, 293–294, 293f
Pressurization rate, pressure chamber, 339
Priestley-Taylor method to determine potential evapotranspiration, 510
Principle of divided circuit (Wheatstone bridge), 394–395
Prions, 3
Privet, leaf palisade, 411
Probes. *See* Waveguides
Prolate ellipse, 91, 92f
Protoxylem, 246
PST. *See* Pacific Standard Time
Pulse, 104–105
Pump-up pressure chamber, 341, 342f
PVC. *See* Polyvinyl chloride
*Pyrus* (pear), leaf palisade, 411
Pyruvic acid, 413–414

## Q

Quality, and water, 526
Quick draw tensiometer, 60f

## R

R (ideal gas constant), 289–290, 311
R (resistance)
  law of, 395–397
  measurement with Wheatstone bridge, 394–395
Radial flow, 384–386
Radial section of wood, 283, 378
Radian, 21–22
Radiancy, 474–475
Radiant
  energy, 474–475
  flux, 474–475
    density, 474–475
Radiant emittance. *See* Emittancy
Radiated power, in unit wavelength range, 460
Radiation balance, 465
  Albedo of surfaces, 465, 466t–467t
  importance of, 468f
  long-wavelength, 465
  negative balance, 465
  short-wavelength, 465
  Stefan-Boltzmann law, 467
Radiation transmission, 35f
Radiation, 458, 463–464, 476t
Radio waves, 146–147, 476t
Radiometer, 475
Radish, leaf mesophyll, 411
*Raphanus sativus* (radish), leaf mesophyll, 411
Rationale for studying plant-water relations, 311, 315, 318, 498
Ray system of cells of secondary xylem, 250t, 252, 283
Rectangular hyperbola, 290–291
Redistribution, 206
Reduction, 156, 188–189, 203, 524
Reference evapotranspiration, 510
Reflectance, 456
Reflected radiation, 465, 467, 468f
Reflection coefficient (membrane), 257, 295–296

Reflection, laws of, 76–77
Regnault, Henri Victor, 327–328
Regular wave train, 104–105
Relative humidity (RH), 316
Relative humidity, 311
  calculation of, 311
  relation to water potential, 311–312
Relative saturation deficit, 298
Relative turgidity (obsolete term), 298–299
Relative water content (RWC), 298–299
Remote sensing with infrared thermometers, 498
Repellency measurement, 215
  peat soils, 216
  sieved soil, 215–216
  sorptivity tube, 216
  temporal changes, 216
Residual water content, 158–159
Resistance
  law of, 395–397
  measurement with Wheatstone bridge, 394–395
  of plant related to potential evapotranspiration, 81
Resistivity, 396–397, 396f
Resistors in parallel, 262, 441, 441f
Resistors in series, 384, 440–441, 441f
Respiration, by roots, 185–186
Reverse flow, 363–364
Rexigenous, 411–412
Reynolds, Osborne, 261–262
Reynolds number, 253–254
RH. *See* Relative humidity
Rhizome, stomata on, 431–432
*Rhododendron roseum* (rhododendron), water potential of, 334–335
Richards, Lorenzo Adolph, 67–68
Richards-and-Ogata thermocouple psychrometer, 320
Richards's equation, 67
Rigel time, 536, *see also* Sidereal time
Ring-porous wood, 255
Rise and fall of water in soil pores, 79–83
Rising water table, variable diameter soil pores, 82–83, 83f
RMSE. *See* Root mean square error
Röntgen, Wilhelm Konrad, 119
Root
  hairs, 245
  pressure, 358–360
  in soil, 139–140
    drying cycles, 142f
    fibrous root system, 140
    plant physiological, 143
    temperature in soil, 141f
    turf grass study, 140
    volumetric water content, 141f
  soil air-filled pore space needed, 185–186, 220, 229
  water movement to (Gardner's equation), 267–269
  water uptake, 115, 133–134, 139–140
    depthwise pattern, 115
    sample problem, 115–117
    TDR measurement, 116f
  work done pushing in soil, 23
Root anatomy, *see also* Stem anatomy
  cell types in xylem tissue, 249–252, 250t
  dicotyledonous roots, 245–246, 246f
  elongating roots regions, 243–245
  endodermis, 248–249
  monocotyledonous root, 246, 247f
  movement of water, 246–248
  root hairs, 245
  tobacco root tip, 244f
  transection of wheat root, 248f
Root cap, 243–245
Root mean square error (RMSE), 132–133
Root radius, effect on water uptake, 272
Rosetta stone, 428
Roughness, 439–440
Royal Meteorological Society, 512
Royal Society (Institution) (London), 224–225
Rubber, increased quality with water, 526
RWC. *See* Relative water content
Rye grass, and evaporation, 508

S
Sachs, Julius von, 351–352
Saline soil
  electrical conductivity of, 397
  plant solute adjustment, 417
Sandemanian religion of Faraday, 198
Sap
  definition of, 349
  solute (osmotic) potential of, 334–335
Sap flow, 375
  heat-balance method, 381
    heat down, 383–384
    heat up, 383
    of heated stem segment, 382f

Sap flow (*Continued*)
    radial flow, 384–386
    used for herbaceous plants, 382
    used for trees, 381–382
  heat-pulse method, 375–376, 376f
    advantages, 379–381
    in apple tree, 379f
    compensation, 377
    disadvantages, 381
    heat-pulse velocity, 377–378
    in kiwifruit vine, 380f
    miniature sap-flow sensor, 381f
    sap velocity, 378
    T-max heat-pulse method, 379
    thermistors, 377
  van Bavel and, 386–389
Sap-tension theory. *See* Cohesion theory
Sapwood, 378
Saturated hydraulic conductivity, Wooding's equation, 205–206
Saturated soil
  pores under tension, 79–80
  water movement in, 87
Saturation vapor pressure over water, 316
Scattered vascular bundles, 281–282
Schelkunoff, Sergei A., 119–120
Schizogenous, 411–412
Scholander, Per Fredrik, 341–343
Scholander pressure chamber, 336–337
Scholander pressure–volume curve theory, 287
  equilibrium pressure, 288
  hydrostatic pressure, 287
  pressure chamber, 287
  pressure–volume–absolute temperature relation, 290f
  semipermeable membrane, 289
  turgor pressure, 287
  van't Hoff law, 290
Sclereid, 410–411
Sclerenchyma tissue, 282, 410–411, 412f
Screen cage psychrometer, 323, 324f
SDD procedure. *See* Stress-degree-day procedure
SDD1. *See* Stomatal Density and Distribution1
Secondary xylem, 246, 250–251, 255, 283–284
Seebeck effect, 312–313
SEM. *See* Cryoscanning electron microscope
Seminal roots, wheat, 258–259
Series resistors, 441, 441f
Shantz, Dr Homer LeRoy, 166
  in American Society of Agronomy, 166
  importance, 167
  research interests, 167
Shoot, 279
Short-wave radiation, 454–455
Sidereal day, 538–539
Sidereal time, 537–538
Siemen (unit), 397
Siemens family, 404–406
Sieve tubes, in root, 245
Sigmoid growth curve, 7–8, 8f
Sinusoidal transverse wave, 105f
Slichter, Charles S., 90
Slide-wire Wheatstone bridge, 395
Slug unit, 16
Small opening in a cavity
  approximating a black surface, 458
  to calibrate an infrared thermometer, 478
  similar to dense vegetation, 474
Smithsonian Meteorological Tables, 316
SMS. *See* Soil measurement system
Sodium chloride
  breakthrough curve, 231–232
  calibration solution of thermocouple psychrometers, 317
Soil
  head of steam, 48
  heads in column, 48, 49f
  surface measurement, 135
  texture and structure, 154
  thermal properties, 126–127
Soil aeration, 196f
  limitation for plant growth, 161
Soil conditioners, 78–79
Soil matric potential, 53
Soil measurement system (SMS), 58–59, 61f, 209–210
Soil moisture characteristic, 79–80
Soil moisture suction, 42
Soil moisture tension, 41–42
Soil physical factors affecting growth, 1
Soil plant analysis development meter (SPAD meter), 20
Soil psychrometer, 2, 124
Soil Science Society of America (SSSA), 388–389
Soil water
  diffusivity, 203–204
  flux density, 137
  movement, 137–139

Soil water budget, 153
Soil water characteristic curve. *See* Moisture characteristic curve
Soil water content, 124—125, 297
  convection effect on, 135—136
  with DPHP, 144
  drying cycle, 139—140
  measurement
    dielectric constant using, 107—109
    using TDR, 111—113
Soil-plant-atmosphere continuum (SPAC), 5, 53, 224, 365, 391, 392f, 498
  analogy, 392—394
  daily changes in water potentials, 366—367
  decrease in suction force, 393f
  diurnal fluctuation of suction, 367f
  electrical analog, 392, 397—398, 398f
  electrical conductivity units, 397
  formulation, 391—392
  hydrostatic pressure, 367
  law of resistance, 395—397, 396f
  Ohm's law, 399, 399f
  osmotic adjustment, 368
  Siemens family and, 404—406
  strain gauges, 367
  van den Honert's equation, 398—401
  water potential, 366
  Wheatstone bridge, 394—395, 394f—395f
Soil-plant-water relation
  black death, 2
  BSE, 3
  human population growth, 2f
  two-square-yard rule, 3—5
  water, 1
Soil-water relation
  ellipse equation in, 94
  linear flow laws in, 96t
Soil-water terminology
  heads in column of soil, 48—50
  water content, 41
  water movement, 50—51
  water potential, 41
    gravitational potential energy, 45
    matric potential energy, 42—45
    overburden potential, 47
    pressure potential energy, 46—47
    solute potential energy, 45—46
    tensiometer pressure potential, 47
    total soil moisture, 42
    water potential gradient, 47—48
Soilmoisture equipment corporation, 57—58
  jet fill, 59f
  quick draw, 60f
Solanaceae (nightshade family), 282
*Solanum tuberosum* (potato), 336
  leaf mesophyll, 411
  water potential of, 336
Solar altitude, 545
Solar azimuth, 545
Solar constant, 4
Solar radiation, 453
  actual spectra, 454f
  earth's atmosphere, 453—454
  electromagnetic spectrum, 454f
  and terrestrial radiation, 462—463
Solar survival still, 387—388
Solstice, 545
Solute front, depth of, 220
Solute potential, 45—46
Solvent
  for electrolytes, 37, 38f
  for nonelectrolytes, 37
Sorghum, 280
  application of Poiseuille's law, 260
  de Wit analysis, 516
  evapotranspiration, 516
  measurement of water potential, 502
  and potential evapotranspiration, 502—503
  stomata, 434
Sorptivity tube, 207—208, 207f
Soybeans
  crop-water-stress index, 489
  de Wit analysis, 517t
  evapotranspiration, 516
  growth, 10—11
  use of strain gauge on, 367
SPAC. *See* Soil-plant-atmosphere continuum
Space in a soil, 185f
SPAD meter. *See* Soil plant analysis development meter
Spanner thermocouple psychrometer. *See* Peltier thermocouple psychrometer
Specific gravity, 54—55
Specific heat, 30—32
Spectral quantities, 475
Spectral radiance, 460
Spectrum, of perfect radiator, 460
Spines, 415

Spongy mesophyll, 409–410
Spongy parenchyma. *See* Spongy mesophyll
Spra-tainer (spray-tainer), use in penetration test, 172
Sprinkling, 33
SSSA. *See* Soil Science Society of America
Standard time, 543–544
Static penetration test, 172
Static water in soil, 71
  rise and fall, 79
    falling water table in soil pore, 82f
    hysteretic curve, 81
    soil moisture characteristic curve, 79–80, 80f
    soil pore conditions, 83f
    subirrigation water, 83
  surface tension, 71–72, 71f
    angle of incidence, 76–77, 76f
    angles of contact, 76f
    in capillary tube, 74
    coefficient, 72
    examples, 77–79
    Laplace's theory, 72–73, 73f
    liquid height of rise, 75f
    meniscus, 75–76
    in sheet, 72–73, 72f
    wire pulling, 73, 73f
Steady-state
  diffusion porometer, 447f
  porometer, 445–448, 446f
Steel, Young's modulus, 425t
Stefan, Josef, 470
Stefan-Boltzmann law, 459, 462
Stele, of root, 245–246
Stem anatomy, 279
  bird's foot trefoil, 280f
  dicotyledonous stem, 279–280
  monocotyledonous stem, 280–281
  primary xylem
    cortex, 282
    pith of stems, 282
    stomata, 281
    vascular bundles, 282
  secondary xylem, 283–284
Stem flow. *See* Sap flow
Steradian, 21–22
Stoma, 431
Stomata, 281, 431
  in abaxial epidermis, 437f
  air structure, 440f
  anatomy
    dicots, 432–434, 433f
    monocots, 432–434, 433f
  aperture, 444–448
  boundary layer, 439–440
  density, 434
  diffusion of gases, 435–436, 436f
  diffusion porometer, 448–449
  guard cells, 436–438
  leaf resistances, 440
    antitranspirant, 443
    diffusion theory, 442
    parallel circuit, 441
    photosynthesis, 442–443
    resistances in seconds, 443f–444f
    resistors in series, 441f
  mass-flow porometer, 448
  opening, 438–439
  ratio, 432
  resistance, 444–448
Stomatal Density and Distribution1 (SDD1), 435–436
Stomatal resistance, 444–446
  diffusion porometry, 445–446
  mass-flow porometry, 445, 445f
  with porometer, 448
  steady-state
    diffusion porometer, 447f
    porometer, 445–448, 446f
  transient porometer, 447f
Strain, 420
Strain gauge, 367
Strasburger, Eduard, 351–352
Streamlines, 89
Stress
  definition of, 71–72
  water stress determined with acoustical method, 357
Stress-degree-day procedure (SDD procedure), 483
  days after planting *vs.*, 484f
  evapotranspiration equation, 486
  GDD, 484
  positive values, 485
  soil water depletion, 485, 485f
  water status of plant, 483
Suberin, 248
Suberization, effect on water potential of potato tuber, 336
Subirrigation, 83
Subsidiary cells, 431
Sugar-cane, increased quality with stress, 526

Summer solstice, 534
Sun
  apparent solar time, 540
  equinox, 534
  temperature, 462
Sunflower (*Helianthus annuus* L.), 417
Sunflower plant (*Helianthus annuus*), 140
Supercapillary size soil pores, 82–83
Supplementary units, 21–22
Surface tension, 35–36
Symplasm, 248
Symplast. *See* Symplasm
*Syringa vulgaris* (lilac), leaf anatomy, 409–410

**T**
T-max heat-pulse method, 379
Tangential section of wood, 283
Tanner, Champ Bean, 180
  accomplishments, 182
  American Meteorological Society, 181
  biophysical measurements, 182
  education, 180
  instrumentation, 180–181
  plant–water relations, 181
Tanner, Bertrand, 180
*Taxus cuspidata* (yew), water potential of, 334–335
TDR. *See* Time domain reflectometry
Telescoping of tillers, pressure chamber
Temperature, 154
  effect on dielectric constant, 106
  effect on field capacity, 154
  effect on penetration tests, 173
  effect on relative water content, 298
  effect on stomatal resistance, 446–448
  effect on tensiometers, 64–65
  effect on wilting point, 156–157
  influence on soil water percentage, 157t
  psychrometric constant, 315–316
  radiation, 453
  relative to vapor pressure, 302–303
  in soil column with turf grass, 141f
Tensile strength, 353
Tensiometer, 53, 54f
  applications, 65–67
  electrical resistance sensors, 63–64
  equivalent water and mercury, 55f
  in field using, 62f
  jet fill, 59f
  laboratory-built, 57–58
  matric potential, 61–63
  mercury manometer, 57, 58f
  pores in, 54
  porous cup, 53–54
  porous plate, 56f
  pressure apparatus, 56–57, 56f
  pressure plate, 57f
  pressure potential, 47
    water movement, 50–51, 50f
  pressure transducer, 64f
  quick draw, 60f
  with septum stopper, 63f
  in soil, 61–63
  soil measurement system, 58–59, 61f
  soil-water theory, 54
  temperature effects, 64–65
  tension height, 55
  transducer, 58–59
  vacuum dial gauge, 57–58
Tension
  in cohesion theory, 361
  definition of, 71–72
Tension head, 48
Tension infiltrometer, 123, 206–207, *see also* Infiltration
  antecedent volumetric water content, 212–213
  Darcy's law, 213
  ellipsoidal description, 221
    advantage, 223
    flux of water into soil, 222f
    tillage situations, 222–223
    volume of water, 221–222
    wet fronts, 221
  hydraulic conductivity, 211
    unsaturated, 213
  macropore flow, 207–208
  maximum tension, 209
  mobility measurement, 216–217
    dry soil effect, 220–221
    hydraulic properties, 217
    longitudinal mobility, 220
    mobile fraction, 219f
    mobile–immobile water soil, 217–218
    pure water, 219
    tracer solution, 218
  ready reckoner, 208
  repellency measurement, 215
    peat soils, 216
    sieved soil, 215–216
    sorptivity tube, 216
    temporal changes, 216
  SMS, 209–210

Tension infiltrometer (*Continued*)
  sorptivity, 211–212
    tube, 207–208, 207f
  towers, 208–209
  vadose zone, 209
  vegetation, 209
  Wooding's equation, 215
Terminal drought, 258
Terrestrial radiation, 454–455, 455f
  and solar radiation, 462–463
Tetens formula, 316
Tetrahedral charge structure of water, 27f
Thermal conductivity, 33–34, 126
Thermal currents, 315
Thermal diffusivity, 126–127
Thermal emfs, 315
Thermal radiation, 453
Thermistor thermometer, 377
Thermo-TDR probe, 136–137
Thermocouple hygrometers, 311
Thermocouple psychrometers, 311
  calibration, 317–318
  isothermal conditions, 318–319
  joule heating, 313–315
  Peltier system, 314f
  relative vapor pressure, 312
  thermoelectric
    effects, 312–313, 313f
    power, 315
  triple point, 311–312
  types, 319–326
  vapor pressure and temperature relation, 315–317
  water potential, 311
Thermoelectric effects, 312–313
Thermoelectric power, 315
Thermopile, 384
Thomson effect, 315
Three-carbon compound plants ($C_3$ plants), 413
Three-dimensional infiltration, 317–318
Tillage, to increase infiltration, 222–223
Tilth, 171–172
Time, 535–536, 536f
Time domain, 106–107
Time domain reflectometry (TDR), 103, 109f, 111f, 123–124
  circuit, 112f
  coaxial cable, 109–111
  commercially available equipment, 117
  dielectric constant, 103–104, 106–107
  frequency domain, 106–107
  Hertzian waves, 104
  Leyden jar, 118f
  periodic motion, 104
  practical information, 113–114
  root water uptake, 115
    depthwise pattern, 115
    sample problem, 115–117
    TDR measurement, 116f
  sinusoidal transverse wave, 105f
  soil water content measurement, 107–109, 111–113
  time domain, 106–107
  wave motion, 104–105
  waveguides, 109–111
  wavelengths and frequencies, 107f
Time of day, 533, *see also* Direct-beam solar radiation
  altitude of star, 534–535
  apparent solar day, 540, 541f
  apparent solar time, 540, 544
  azimuth, 535
  celestial equator, 538
  hour angle, 535, 543
  hour circle, 535–536
  mean solar time, 542
  meridians, 534
  Rigel time, 536
  sidereal day, 538–539, 539f
  Sidereal time, 537–538
  standard time, 543–544
  Sun's eastward progress, 541–542, 542f
  time and arc units, 537t
  vernal equinox, 537–539
  zone time, 544
Tissue pressure, 360
TMM. *See* Too Many Mouths
TNT. *See* 2,4,6-trinitrotoluene
Tobacco, increased quality with stress, 526
Tolman, Cyrus Fisher, 82–83
Tomato, leaf mesophyll, 411
Too Many Mouths (TMM), 435–436
Topp equation, 124
Tortuosity, 191
Torus, 361
Total water potential, 41
Tracheary elements, 249–250
Tracheids, 250
Trafficability, in relation to penetration, 171–172
Transient porometer, 447f
Transparency to visible radiation, 34

Transpiration
  in cohesion theory, 351–352
  infrared thermometers to monitor, 473
  in Ohm's law analogy, 392f
  as proportion of evapotranspiration, 502–503
  rate of a tree, 301
  ratio with photosynthesis, 520–524
  and yield, 518
Transpiration efficiency, 528, *see also* Water-use efficiency
Transverse section of wood, 283
Tree, contraction of trunk, 367
Triage system, 5
Trichome (leaf hair), influence on roughness, 412–413
2,4,6-trinitrotoluene (TNT), 51–52
Triple point, 311–312
*Triticum aestivum* (wheat), 34, 294
Tritium breakthrough curve, 234f
Tropic of Cancer, 538
True pearl of theoretical physics, 471
Tuber water potential, 336
Turf grass study, 140
Turgor potential, 47–48, 295
  using probes, 295
  tensions in xylem, 295–296
  veraison, 296
  wiltmeter, 296
Turgor pressure, 298–299
Two-dimensional infiltration, 205–206
Two-square-yard rule, 3
  calculations, 4
  SPAC, 5
  triage system, 5
Two-stage evaporation, 505–508

U
Ultimate permanent wilting point, 156–157
Ultramicropores, 206–207
United States Army Corps of Engineers, cone penetrometer, 175
United States Department of Agriculture (USDA), 164–165, 343–344, 397, 480–481, 483
Units of force, 16
Units of potentials, 42–43
Universal gravitation principle, 44
Unsaturated hydraulic conductivity
  Gardner's root equation, 41
  measured with tension infiltrometer, 211–215
Unsaturated zone in soil, 209
Upper chamber, 58–59
Upper limit of available water, 153
Uptake of water by root, 269, 274
USDA. *See* United States Department of Agriculture

V
Vacuole, water potential of, 368
Vacuum dial gauge tensiometer, 57–58
Vadose zone, 209
Valve
  in animal, 361
  in plant, 361
Valve, cohesion theory, 349
van Bavel, Cornelius H. M., 386–389
van den Honert's equation, 398–401
van der Waals, Johannes Diderik, 38–39
van der Waals-London force, 29–30
van't Hoff, Jacobus Hendricus, 306
  asymmetric carbon atom, 306
  chemical kinetics principles, 306–307
  van't Hoff law, 290
Vapor pressure deficit (VPD), 316, 489, 496, 526
Vapor pressure depression, 303
Vapor pressure gradient (VPG), 490
Vascular bundles, 282
Vascular plants, 431
Vascular tissue system, 279
Veihmeyer and Hendrickson, concept of available water, 160–161
Vein, 349, 409–410
Velocity of propagation, 108
Velocity of water in soil, 89–90
Veraison, 296
Vernal equinox, 537–538
Vertices, 90–91
Vessel member (vessels), 250
  cohesion theory, 349–350
  in leaf, 256
Vines, 251
  cohesion theory, 354–356
  diameter and length of vessel in, 375–376
  hydrostatic pressure, 354–356
  Scholander's measurements, 358f
Viscosity, 38, 252
*Vitis* (grape), 296
  hydrostatic pressure, 287
  leaf palisade, 411
Volt, 399
Volume elasticity, 420

Volume of ice, 127–128
Volumetric heat capacity, 126
Volumetric water content, 131
  importance of expressing, 107
  measured with time domain reflectometry, 103
VPD. *See* Vapor pressure deficit
VPG. *See* Vapor pressure gradient

**W**

Water, 1, 27–28
  hydrogen bonding, 28–29, 29f
  lone-pair electrons, 28
  molecule, 27–28
  properties, 30
    adsorption, 38
    change in temperature, 36f
    density, 36
    dielectric constant, 37
    freezing, 36–37
    heat conduction, 33–34
    heat of fusion, 32–33
    heat of vaporization, 32
    ionization, 37
    liquid water, 31t
    opaqueness to infrared radiation, 34–35
    radiation transmission, 35f
    solvent for electrolytes, 37, 38f
    solvent for nonelectrolytes, 37
    specific heat, 30–32
    surface tension, 35–36
    transparency to visible radiation, 34
    viscosity, 38
  table, 155
  between tensiometers, 50–51, 50f
  tetrahedral charge, 27f
  van der Waals and, 38–39
  van der Waals-London force, 29–30
Water and yield, 515
  crop water-use efficiency, 526–528
  de Wit's analysis, 515–517
  dry matter, 518, 518f
    PET and, 520f
  and ET, 519–520
  irrigation effects on crop quality, 526, 527t
  moisture-sensitive stages, 525t
  stages of development, 524
  transpiration and photosynthesis, 520–524
  water content, 41
  water deficits, 526
Water content (plant)
  compared to water potential measurements, 296–301
  in yellow birch, 359f
Water content (soil)
  antecedent, 212–213
  definition of, 113–114
  dry-weight base, 518–519
  effect on penetration tests, 180–181
  measured with time domain reflectometry, 103
  volumetric, 107
Water deficit (WD), 297
Water density, 36
Water movement in saturated soil
  Darcy's law, 87–88, 87f
  ellipse equation, 90
    Apollonian curves, 95
    ellipsoid, 92, 93f
    homogeneous soil, 94f
    line segment, 91
    modified Colding equation, 94
    oblate ellipse, 91, 92f
    prolate ellipse, 91, 92f
    soil drainage need, 93–94
    in soil-water relation, 94
    subsurface drain problem, 93f
  hydraulic conductivity, 87–89
  Laplace's equation, 89–90
  linear flow law, 95–97, 96t
Water potential, 41
  adaxial and abaxial leaves, 443
  in cohesion theory, 349–352
  components of, 42
  definition of, 42
  difference, 47–48
  diurnal cycle, 366–367
  gradient, 47–48
  gravitational potential energy, 45
  importance of measurement, 284–285
  matric potential energy, 42–45
  in Ohm's law analogy, 400
  overburden potential, 47
  pressure potential energy, 46–47
  relation to relative humidity, 311–312
  solute potential energy, 45–46
  tensiometer pressure potential, 47
  total soil moisture, 42
  water potential gradient, 47–48
Water release curve. *See* Moisture characteristic curve

Water retention curve. *See* Moisture characteristic curve
Water saturation deficit. *See Déficit de saturation hydrique* (DSH)
Water storage cells, 415
Water table
  effect on field capacity, 153–156
  falling, 80–81
  rising, 82–83
Water-filled porosity, 230, 235–236, 238
Water-use efficiency, 515
Wave speed, 104–105
Waveguides, 109–112
Wavelength, 104–105
Weeds, effect on crop-water use efficiency, 528
Weight, 16–17
Wesely, Marvin L., 181
Wet front. *See* Wetting—front
Wetting
  angle, 74
  depth of, 155
  front, 201–202
Wheat
  anatomy of leaf, 409–415
  anatomy of root, 243–252
  application of Poiseuille's law for water flow, 252–253
  de Wit analysis, 515–517
  diameter of vessels, 260
  evapotranspiration, 518–524
  measurement of osmotic potential of leaf, 284
  potential evapotranspration, 501
  stomata, 436
  stress-degree day, 483–486
  water use, 347
Wheat breeding program, 260
Wheatstone, Sir Charles, 403–404
Wheatstone bridge, 394–395, 394f–395f
Wiclicenus, Johannes, 306
Wien, Wilhelm, 472
Wien's displacement law, 461
Wilting coefficient, 156
Wilting point (WP), 153, 156
  average water percentage, 158f
  like FC, 156–157
  negative pressure potential, 159–160
  permanent WP, 156
  residual water content, 158–159
  temperature influence, 157t
  wilting coefficient, 156
Wiltmeter, 296
Wind, 32–33
  effect on boundary layer, 439–440
  effect on evaporation, 508
  effect on pressure chamber readings, 337–339
Winter solstice, 534
Wood, sections of, 283
Wooding's equation, 215
Woody plants, 375, 386
Work, 17, 17f
  to root, 23–24
  units of, 18
World wheat collection, 259
Wormhole, water and air conductance through, 397–398
WP. *See* Wilting point

X
Xerophyte, 409
Xerophytic adaptations, 414–415
Xylem sap, 255
Xylem tissue, 349–350, 409–410
  cell types, 249–252
  cohesion theory, 349–352
  evolution of, 258
  hydrostatic pressure in, 367
  in leaf, 409–410
Xylem vessel, 250–251

Y
YDA gene. *See* YODA gene
Yellow birch, water content of, 359f
Yew, water potential of, 335f
Yield, and water, 515
YODA gene, 435–436
Young, Thomas, 427–429
Young's modulus, 420

Z
Z-tube, 354, 355f
*Zea mays* (corn), 9, 59–61, 281f, 296, 549
Zone time, 544